Final
Report

September 1974

Space Tug
Thermal Control

MARTIN MARIETTA

MCR-74-147
Contract NAS8-29670

Final
Report

September 1974

**SPACE TUG
THERMAL
CONTROL**

Prepared for:
National Aeronautics and Space Administration
George C. Marshall Space Flight Center
Marshall Space Flight Center,
Alabama 35812

Approved

Terry L. Ward
Program Manager

MARTIN MARIETTA CORPORATION
P.O. Box 179
Denver, Colorado 80201

FOREWORD

This document is the Final Report submitted by the Martin Marietta
Corporation, Denver Division, under Contract NAS8-29670.

This study was performed for the National Aeronautics and Space
Administrations George C. Marshall Space Flight Center under the
technical direction of the Astronautics Laboratory, Thermal En-
gineering Branch, with Mr. Jack D. Loose serving as Technical
Monitor.   The work described herein was performed from 1 July 1973
to 30 April 1974.

The work of the following major contributors to the study is
acknowledged: J. Michael Connolly and Solomon H. Eichenbaum.

CONTENTS

Figure
----

1. INTRODUCTION AND SUMMARY

The introduction of a full capability Tug into the Shuttle mission spectrum in the 1980s will significantly broaden Shuttle's capability. To fully realize that capability it will be essential that the Tug be designed to perform its mission within a broad range of thermal environments with currently planned mission durations up to 7 days. The primary objective of this study was to develop a thermal design for the forward and intertank compartments and fuel cell heat rejection system that satisfy Tug requirements for low inclination geoschynronous deploy and retrieve missions. Key to this design was to evolve to a system that was reusable and minimized ground refurbishment requirements. Figure 1-1 presents baseline Tug configuration used in the study.

Passive concepts were demonstrated analytically for both the forward and intertank compartments. Each compartment used an external paint pattern tailored to the mission environments. The forward compartment, which contains the majority of the avionics equipment, was thermally designed with circumferential heat pipes to reduce the wide variance of skin temperatures resulting from constant attitudes. In addition, the forward shield (beta cloth) was modified to include a multilayered insulation blanket. Results indicated that the equipment used for rendezvous and docking, such as the television, laser radar, and its associated electronics, present one of the more severe thermal control problems. The most promising solution appears to be to mount the equipment on the thermal conditioning panels. The panels can be used to reduce heater power requirements. The fuel cell electrical power subsystem required an active heat rejection concept in the form of a pumped fluid radiator. Continued development of heat pipe radiators could result in their future application to thermal control of the fuel cell.

· Worst-case external heating environments were determined and used in the study. All mission phases were incorporated into study with the most significant one being the heating of the Tug in the orbiter after reentry and landing. Cargo bay purging was found to be required to maintain both operating and nonoperating equipment temperature limits.

A series of three catalogues were created to provide representative equipment data for use in the thermal study. Internal distribution of the catalogues resulted in a rather wide acceptance and a desire for additional categories of information to expand their usefulness.

Key thermal control systems derived in the study were carried an additional step to preliminary sets of design and performance specifications. Three specifications were developed covering the forward compartment thermal design, battery louvers, and fuel cell heat rejection system.

A follow-on plan was developed highlighting breadboard testing of the above key areas which were advanced to the preliminary specification phase. Tests also include a honeycomb conductivity test. In addition, several areas of analytical concern were identified that were beyond the original scope of the study.
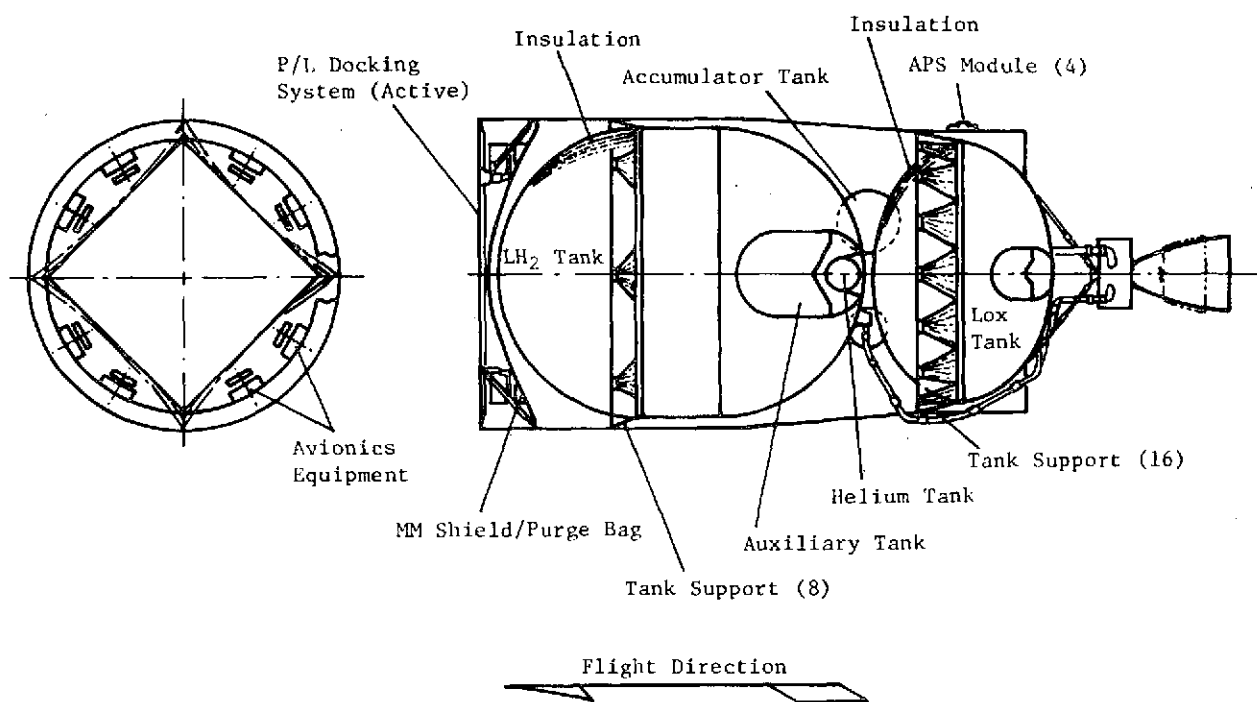
Figure 1-1 Baseline Tug Overall Configuration

2. EQUIPMENT THERMAL REQUIREMENTS, CHARACTERISTICS AND CONSTRAINTS CATALOGUES

New spacecraft designs generally start with studies oriented toward satisfying mission requirements. Systems-level studies of this nature generally result in identifying performance requirements, allowable system weights, power budgets, etc. New equipment (or revised existing equipment) designed to satisfy specific requirements is inherent in each new spacecraft. After some basic studies are completed the thermal designer translates the preliminary design one step further to evolve the design into thermal environments and anticipated equipment temperatures. Often the thermal designer is faced with new equipment and associated thermal data are lacking. To avoid this problem, this study began by identifying the thermal requirements, characteristics, and constraints of candidate equipment items.

The approach chosen to identify, handle, and document these data was to develop a generalized data bank containing thermal and general information for each component catalogued. The data bank was written to be dynamic in nature, allowing components to be added or deleted without affecting output of other components. A FORTRAN IV program containing four major subroutines was written to compile two catalogues using the data bank data as input data. The two catalogues contain equipment thermal requirements, and equipment physical characteristics and constraints, respectively. The data bank, catalogues, and a catalogue user's guide were published in two documents, (Ref 1 and 2).

The program and data bank provide the user a means of cataloging components for potential application to Tug or any other spacecraft in a standardized manner, while maintaining visibility to the source of the information. The data bank was organized by major system (such as the Avionics System), describing each subsystem followed by the components included within each subsystem. Table 2-1 describes the data that were catalogued and the reference used in identifying the subsystem descriptive information. Table 2-2 describes the subsystems included within the Avionics System, while Table 2-3 expands upon the Guidance Navigation and Control Subsystem describing the types of equipment, requirements, timelines, and notes. Table 2-4 presents the first component catalogued and shows the generalized and standard format used in cataloging all components.

TABLE 2-1

SPACE TUG EQUIPMENT DATA BANK

THE SPACE TUG EQUIPMENT DATA BANK HAS BEEN PREPARED
FOR NASA/MSFC UNDER CONTRACT NUMBER NAS 8-29670.

THIS DOCUMENT CONTAINS THE RAW DATA OF ALL EQUIPMENT
ITEMS IDENTIFIED FOR POTENTIAL APPLICATION TO THE
SPACE TUG SYSTEM.

THE FOLLOWING DATA IS INCLUDED IN THIS DOCUMENT

EQUIPMENT THERMAL REQUIREMENTS

EQUIPMENT PHYSICAL CHARACTERISTICS

EQUIPMENT CONSTRAINTS

THIS DOCUMENT WAS PREPARED BY THE MARTIN MARIETTA
AEROSPACE CORPORATION AND WAS SUBMITTED TO NASA/
MSFC ON 1 MAY 1974.

QUESTIONS CONCERNING THE DATA CONTAINED HEREIN
SHOULD BE DIRECTED TO
MR. TERRY L. WARD
PHONE 303-794-5211
EXTENSION 4702

THE SYSTEMS AND SUBSYSTEMS DESCRIBED HEREIN ARE DEFINED
BY AND IN ACCORDANCE WITH
BASELINE TUG DEFINITION DOCUMENT
REVISION A
DATED JUNE 26, 1972
RELEASED BY
PRELIMINARY DESIGN OFFICE
PROGRAM DEVELOPMENT
GEORGE C. MARSHALL SPACE FLIGHT CENTER
NATIONAL AERONAUTICS AND SPACE ADMINSTRATION

TABLE 2-2

AVIONICS SYSTEM
****

THE DATA CONTAINED IN THE AVIONICS SYSTEM SECTION PRETAINS TO THOSE CANDIDATE EQUIPMENT ITEMS WHICH HAVE BEEN IDENTIFIED FOR APPLICATION TO THE FOLLOWING SUBSYSTEMS

GUIDANCE, NAVIGATION AND CONTROL

DATA MANAGEMENT

COMMUNICATIONS

INSTRUMENTATION

ELECTRICAL POWER

TABLE 2-3

GUIDANCE NAVIGATION AND CONTROL SUBSYSTEM

EQUIPMENT ITEM	QUANTITY	WEIGHT (POUNDS)	POWER (WATTS)	REMARKS	1 2 3 (EARTH)
IMU	2	80.	40.	MOUNTED AT POSITION 1 WITH STAR TRACKER.	
STAR TRACKER	2	50.	18.	POSITION 1	
ELECTRONICS	2	26.			
HORIZON SCANNER	2	70.	38.	POSITION 3, POSSIBLY	
ELECTRONICS	2	10.		DEPLOYED.	
LASER RADAR (A)	2	70.	155.	POSITION 2, W/3 POSITION	
ELECTRONICS (A)	2	20.		MIRROR YAG	
TELEVISION (A)	2	20.	10.	POSITION 2, FORWARD LOOKING , ZOOM, ONE GIMBAL.	
ACS ELECTRONICS	2	28.	18.5		
SUN SENSOR	2	0.8	0.0	MOUNTED ON EXTERIOR AT POSITION 2 AND 4	
TOTALS		**372.8**	**279.5**		

NOTES   (A) INCLUDED IN RENDEZVOUS AND DOCKING CATEGORY OF MASS
         PROPERTIES.

TIMELINES

     CONTINUOUS OPERATION
          IMU
          ACS

HORIZON SCANNER*
STAR TRACKER   *
SUN SENSOR   *
                    15.31 TO 16.06. 18.45 TO 19.20, 23.40 TO 24.25
                    36.60 TO 37.35. 60.60 TO 61.35, 82.28 TO 83.03
                    87.54 TO 88.29, 90.59 TO 91.34
LASER RADAR   *   60.35 TO 61.35
TELEVISION   *   60.85 TO 61.35

AUTOCOLLIMATOR WAS EXCLUDED FROM CATALOG SINCE IT APPEARS THAT HORIZON
SCANNER CAN BE ATTACHED DIRECTLY TO IMU THERE BY AVOIDING THE NEED FOR
THE AUTOCOLLIMATOR.

RATE GYROS WHERE INCLUDED IN CATALOG HOWEVER NO FIRM REQUIREMENT HAS
BEEN ESTABLISHED.

TABLE 2-4

```
        SPACE TUG EQUIPMENT DATA BANK    RAW DATA
     THERMAL REQUIREMENTS, PHYSICAL CHARACTERISTICS, AND CONSTRAINTS
-----------------------------------------------------------------------
     AVIONICS SYSTEM
     GUIDANCE NAVIGATION AND CONTROL SUBSYSTEM
     ***********************************************************
 IMU  1 CAROUSEL 5B            DELCO ELECTRONICS      P/N 7886091-011
   DESIGN OPERATING CASE TEMPERATURE               60. TO 115. DEG. F
   NON-OPERATING AND STORAGE CASE TEMPERATURE      -35. TO 160. DEG. F
   ACCEPTANCE TEST TEMPERATURE REQUIREMENTS         57. TO 115. DEG. F
   QUALIFICATION TEST TEMPERATURE REQUIREMENTS      56. TO 118. DEG. F
   PACKAGE SHAPE        RECTANGULAR
   PACKAGE SIZE * LENGTH  22.7 * WIDTH  11. * HEIGHT  12.   (INCHES)
   CASE MATERIAL        ALUMINIUM
   CASE WEIGHT             20.     POUNDS
   TOTAL WEIGHT           80.     POUNDS
   SURFACE PROPERTIES       ALPHA = 0.900  * EMISSIVITY = 0.900
   INPUT STEADY STATE POWER   95.  WATTS **
    21.  AT  75. DEG,   94.  AT -80. DEG (WATTS AT DEG. FAHRENHEIT)
   OUTPUT POWER                0.  WATTS ** MILLI-WATT OUTPUT
   THERMAL DESIGN           ACTIVE    * PASSIVE
   ***********************************************************
 PHYSICAL CHARACTERISTICS AND CONSTRAINTS REMARKS
    NON MISSION ON-TIMES *PRELAUNCH YES* ASCENT YES* REENTRY OFF
    MISSION ON-TIMES * SHUT/TUG  ON* TUG/ORBIT  ON* TUG/PAY  ON
   MARRIED WITH MAGIC 352 COMPUTER
   MOUNT WITH Z-AXIS ALONG LONGITUDNIAL AXIS
   MAX CABLE LENGTH 1.8 METERS (6.0 FEET)
   QUALIFIED FOR 9 HOUR MISSION
   OPERATIONAL IN 8 HOURS
   ***********************************************************
     THE CAROUSEL 5B IMU IS DESIGNED AND BUILT BY
         DELCO ELECTRONICS DIVISION OF GENERAL MOTORS CORPORATION
         6767 HOLISTER AVE.   GOLTA, CALIFORNIA  93017
   THE DATA CONTAINED HEREIN WAS OBTAINED FROM
    MR. BILL CATTOI                  PHONE 805-968-1011 EXTENSION 623
   THIS IMU IS CURRENTLY IN A PRODUCTION PHASE AND IS BEING
   PROCURED BY SAMSO FOR USE ON THE TITAN 3C TRANSTAGE AS THE SINGLE
   GUIDANCE SENSOR FOR THIS SYSTEM IT IS MARRIED TO THE MAGIC 352
   COMPUTER ALSO BUILT BY DELCO AND SUPPLIED AS A TWO PACKAGE SYSTEM.
   THE IMU IS A 4 GIMBAL SYSTEM AND IS QUALIFIED FOR A 9 HOUR MISSION
   THIS IMU IS SCHEDULED TO FLY FOR THE FIRST TIME IN 1973. A SINGLE
   28 VDC SOURCE IS REQUIRED INTERCONNECTING CABLE WITH THE COMPUTER
   IS LIMITED TO 1.8 M ( 6 FT). THE GIMBAL SET IS INTERNALLY SHOCK
   MOUNTED. THE CASE IS PRESSURIZED TO 11.7 N/CM SQ (17 PSIA) AND THE
   UNIT IS DESIGNED WITH  AN INTERNAL ACTIVE THERMAL CONTROL SYSTEM
   COMPRISED OF A FAN AND THERMOSTATICLY CONTROLLED HEATERS. THE UNIT
   IS DESIGNED TO FUNCTION WITHIN A MAXIMUM POWER BUGET OF 205 WATTS.
   APPROXIMATELY 8 HOURS ARE REQUIRED FROM POWER ON TO GO-INERTIAL.


    REF. BROCHURE, UNIVERSAL SPACE GUIDANCE SYSTEM, DELCO ELECTRONICS
END***********************************************************************
```

Each component was catalogued in raw data form, identifying the appropriate system and subsystem. Preprinted keypunch sheets were used to reduce the amount of information to be written and correspondingly prepunched cards were used to reduce the key-punch task. This also limited the number of errors found in the review and editing of each component data sheet. One additional means of reducing errors was also applied. The data were assembled in the familiar set units and the program was used to convert the data to the International Units as shown in Table 2-5, the final data form.

Three major blocks of information were set aside for describing each component as shown separated by asterisk lines. The first block describes the component identifier (used by the program), name, manufacture, and part number. The remaining data in this block describe pertinent thermal design information of the component. Operating, nonoperating, and test box temperature limits are presented. The box shape and size, case material, and weights are specified. The exterior surface radiation properties, input power, variable power, and output power are presented. The last item describes the basic box thermal design for ground and flight operations. The word "active" to the left of the asterisk refers to a need of forced air cooling or a fluid loop on the ground, while "passive" refers to no special considerations required. The word "active" to the right of the asterisk refers to the need of special considerations in flight such as a fluid loop or other means beyond the mounting conduction and radiation capability of the box.

The second block of data contains information relative to the required on-times during the mission and pertinent characteristics and constraints remarks. The prelaunch, ascent, and reentry periods of flight were described as nonmission periods of flight because the Tug is attached to the Shuttle during these periods.

The third data block was set aside as a general narrative block to further identify the manufacturer, source of the material, expand the description of the component, development status, etc.

The first two data blocks were used by the program to build the two catalogues required by contract. The first catalogue, the Equipment Thermal Requirements Catalogue, is a summary of the data bank information in terms of allowable component temperatures as they relate to the various Tug mission phases. This summary was organized by subsystem and type of component as shown in Table 2-6. In addition, the thermal design and power dissipation are also presented. "Yes" was used to indicate that the component is on during mission phases while the Tug is attached to Shuttle, but not required to satisfy Tug mission requirements. "Int" indicates an intermittant usage during the mission.

2-6

TABLE 2-5

SPACE TUG EQUIPMENT DATA BANK   FINAL DATA
THERMAL REQUIREMENTS, PHYSICAL CHARACTERISTICS, AND CONSTRAINTS

AVIONICS SYSTEM
GUIDANCE NAVIGATION AND CONTROL SUBSYSTEM
****

IMU 1 CAROUSEL 5B   DELCO ELECTRONICS   P/N 7886091-011
   DESIGN OPERATING CASE TEMPERATURE   289. TO 319. DEG. K
                                                  (60. TO 115. DEG. F)
   NON-OPERATING AND STORAGE CASE TEMPERATURE   236. TO 344. DEG. K
                                                  (-35. TO 160. DEG. F)
   ACCEPTANCE TEST TEMPERATURE REQUIREMENTS   287. TO 319. DEG. K
                                                  (57. TO 115. DEG. F)
   QUALIFICATION TEST TEMPERATURE REQUIREMENTS   286. TO 321. DEG. K
                                                  (56. TO 118. DEG. F)

   PACKAGE SHAPE   RECTANGULAR
   PACKAGE SIZE * LENGTH 57.7 * WIDTH 27.9 * HEIGHT 30.5 CENTIMETERS
                  LENGTH 22.7 * WIDTH 11.0 * HEIGHT 12.0 INCHES
   PACKAGE AREA   8440.0 SQ. CENTIMETERS * 1308.2 SQ. INCHES
   PACKAGE VOLUME   49102.2 CU. CENTIMETERS * 2996.4 CU. INCHES
   CASE MATERIAL   ALUMINIUM
   CASE WEIGHT   9.1 KILOGRAMS *   20.0 POUNDS
   TOTAL WEIGHT   36.3 KILOGRAMS *   80.0 POUNDS
   SURFACE PROPERTIES   ALPHA = 0.900 * EMISSIVITY = 0.900
   INPUT STEADY STATE POWER   95. WATTS **
    21.0 AT 297. DEG, 94.0 AT 211. DEG (WATTS AT DEG. KELVIN)
    21.0 AT 75. DEG, 94.0 AT -80. DEG (WATTS AT DEG. FAHRENHEIT)
   OUTPUT POWER   0. WATTS ** MILLI-WATT OUTPUT
   THERMAL DESIGN   ACTIVE   * PASSIVE
   ****
   PHYSICAL CHARACTERISTICS AND CONSTRAINTS REMARKS
      NON MISSION ON-TIMES *PRELAUNCH YES* ASCENT YES* REENTRY OFF
      MISSION ON-TIMES * SHUT/TUG ON* TUG/ORBIT ON* TUG/PAY ON
   MARRIED WITH MAGIC 352 COMPUTER
   MOUNT WITH Z-AXIS ALONG LONGITUDNIAL AXIS
   MAX CABLE LENGTH 1.8 METERS (6.0 FEET)
   QUALIFIED FOR 9 HOUR MISSION
   OPERATIONAL IN 8 HOURS
   ****
      THE CAROUSEL 5B IMU IS DESIGNED AND BUILT BY
         DELCO ELECTRONICS DIVISION OF GENERAL MOTORS CORPORATION
         6767 HOLISTER AVE.   GOLTA, CALIFORNIA 93017
   THE DATA CONTAINED HEREIN WAS OBTAINED FROM
    MR. BILL CATTOI   PHONE 805-968-1011 EXTENSION 623
   THIS IMU IS CURRENTLY IN A PRODUCTION PHASE AND IS BEING
   PROCURED BY SAMSO FOR USE ON THE TITAN 3C TRANSTAGE AS THE SINGLE
   GUIDANCE SENSOR FOR THIS SYSTEM IT IS MARRIED TO THE MAGIC 352
   COMPUTER ALSO BUILT BY DELCO AND SUPPLIED AS A TWO PACKAGE SYSTEM.
   THE IMU IS A 4 GIMBAL SYSTEM AND IS QUALIFIED FOR A 9 HOUR MISSION
   THIS IMU IS SCHEDULED TO FLY FOR THE FIRST TIME IN 1973. A SINGLE
   28 VDC SOURCE IS REQUIRED INTERCONNECTING CABLE WITH THE COMPUTER
   IS LIMITED TO 1.8 M (6 FT). THE GIMBAL SET IS INTERNALLY SHOCK
   MOUNTED. THE CASE IS PRESSURIZED TO 11.7 N/CM SQ (17 PSIA) AND THE
   UNIT IS DESIGNED WITH AN INTERNAL ACTIVE THERMAL CONTROL SYSTEM
   COMPRISED OF A FAN AND THERMOSTATICLY CONTROLLED HEATERS. THE UNIT
   IS DESIGNED TO FUNCTION WITHIN A MAXIMUM POWER BUGET OF 205 WATTS.
   APPROXIMATELY 8 HOURS ARE REQUIRED FROM POWER ON TO GO-INERTIAL.

   REF. BROCHURE* UNIVERSAL SPACE GUIDANCE SYSTEM* DELCO ELECTRONICS

TABLE 2-6

TABLE 2-6

EQUIPMENT THERMAL REQUIREMENTS CATALOGUE

GUIDANCE NAVIGATION AND CONTROL SUBSYSTEM

EQUIPMENT ITEM   STAR TRACKERS

REF. NO.	DESCRIPTION AND MANUFACTURE	THERMAL DESIGN GROUND/ORBITAL	POWER WATTS MIN/MAX	MISSION PHASE THERMAL REQUIREMENTS AND TEMPERATURE LIMITS DEGREES KELVIN / (FAHRENHEIT) - MIN / MAX		MANEUVERS				REMARKS
				PRELAUNCH	SHUTTLE CARRY	SHUTTLE TUG	TUG ORBITAL	PAYLOAD TUG	REENTRY AND LANDING	
ST 1	CT-401 SENSOR BBRC	PASSIVE PASSIVE	5/ 5	OFF 243/333 (-22/140)	OFF 243/333 (-22/140)	OFF 243/333 (-22/140)	ON 243/333 (-22/ 0)	ON 243/333 (-22/140)	OFF 243/333 (-22/140)	ON DURING PRELAUNCH FOR CHECKOUT
ST 2	STAR TRACKER HONEYWELL	PASSIVE PASSIVE	3/ 3	OFF 255/302 (0/ 85)	OFF 255/302 (0/ 85)	OFF 255/302 (0/ 85)	INT 255/ 50 (-22/ 50)	INT 255/233 (0/ 50)	OFF 255/302 (0/ 85)	ON DURING PRELAUNCH FOR CHECKOUT
ST 3	M40S ITT GILFILLAN	PASSIVE PASSIVE	20/ 20	YES 293/323 (68/122)	OFF 288/323 (60/122)	OFF 288/323 (60/122)	ON 293/323 (68/122)	ON 293/323 (68/122)	OFF 288/323 (60/122)	ON DURING PRELAUNCH FOR CHECKOUT
ST 4	569B STAR TRACKER EMR PHOTOELECTRIC	PASSIVE PASSIVE	3/ 3	OFF 218/348 (-67/167)	OFF 218/348 (-67/167)	OFF 218/348 (-67/167)	INT 218/113 (68/113)	INT 218/318 (-67/113)	OFF 218/348 (-67/167)	ON DURING PRELAUNCH FOR CHECKOUT
ST 5	574 STAR CAMERA EMR PHOTOELECTRIC	PASSIVE PASSIVE	4/ 4	OFF 218/343 (-67/158)	OFF 218/343 (-67/158)	OFF 218/343 (-67/158)	INT 218/104 (68/104)	INT 218/313 (-67/104)	OFF 218/343 (-67/158)	ON DURING PRELAUNCH FOR CHECKOUT
ST 6	OAO STAR TRACKER BENDIX CORPORATION	PASSIVE PASSIVE	6/ 6	OFF 238/327 (-30/130)	OFF 238/327 (-30/130)	INT 238/310 (-30/100)	INT 238/100 (68/100)	INT 238/310 (-30/100)	OFF 238/327 (-30/130)	ON DURING PRELAUNCH FOR CHECKOUT
ST 7	OMA ATM STAR TRKR. BENDIX CORPORATION	PASSIVE PASSIVE	18/ 28	OFF 233/327 (-40/130)	OFF 233/327 (-40/130)	OFF 233/327 (-40/130)	INT 233/ 90 (68/ 90)	INT 233/305 (-40/ 90)	OFF 233/327 (-40/130)	ON DURING PRELAUNCH FOR CHECKOUT
ST 8	KS-199 STAR TRKR KOLLSMAN INSTR.	PASSIVE PASSIVE	8/ 18	OFF 272/310 (30/100)	OFF 272/310 (30/100)	OFF 272/310 (30/100)	INT 272/ 70 (68/ 70)	IN 272/310 (30/100)	OFF 272/310 (30/100)	ON DURING PRELAUNCH FOR CHECKOUT

The second catalogue, Equipment Physical Characteristics and Constraints Catalogue, presents the thermal characteristics of the components as derived from the data contained in the first data block and constraints remarks from the second block. Surface area and volume, power density, radiation time constant, adiabatic rise rate, thermal mass, and allowable sink temperature are presented. The data are presented in International units and English units. Some of the components were unable to meet their temperature limits in a 100% radiation environment, hence, the quantity of heat required to be removed via conduction was calculated and printed if the sink environment requirements were less than $0°K$. Within limits, the use or need of conduction to cool a component is usually an open issue for the thermal designer. Hence, the results indicate emphasis to be placed on a given component and the potential need for special considerations such as the use of heat pipes. Table 2-7 presents an example of the catalogue.

The catalogues proved to be a valuable asset during the study. We used various groups within the Denver Division to test the applicability of the data to other disciplines and projects and found a general acceptance and desire for additional data to be included. In general, the data in the catalogues were complete within the intended scope, however, several areas for expansion are apparent. For example, each component designer in the aerospace industry compiles component information relative to the needs of his particular technical discipline, but it is rarely a complete compilation of information. The data bank approach could easily be expanded to include the functional characteristics and requirements of the components tailored to meet specific component types and a complete description of testing and test requirements. The resultant catalogues would be extremely useful to the aerospace industry and would reduce the time required by those who attempt to maintain component files while limiting the amount of misinformation that is passed along by work of mouth. Follow-on work in this area is desirable and appropriate with direct benefits to the government.

TABLE 2-7

EQUIPMENT PHYSICAL CHARACTERISTICS AND CONSTRAINTS CATALOGUE

GUIDANCE NAVIGATION AND CONTROL SUBSYSTEM

EQUIPMENT ITEM STAR TRACKERS

REF. NO.	DESCRIPTION MANUFACTURER AND REMARKS	WEIGHT KG (LBS)	PACKAGE SHAPE	SURFACE AREA SQUARE CM (FT)	VOLUME CUBIC CM (FT)	RAD. ALPHA/ EMISS	POWER WATTS MIN/ MAX	POWER DENSITY O/A W/M2 (W/FT2)	TIME CONST. HOURS MIN MAX	ADIABATIC RISE RATE DEG K/HR DEG F/HR MIN MAX	THERMAL MASS W-HR/K BTU/F	ALLOWABLE TEMP. DESIGN MIN MAX	SINK DEG K/(F) QUAL MIN MAX	OPERATION MODE
ST 6	OAO STAR TRACKER BENDIX CORPORATION	7.3 (16.0)	RECT	2877 (3.1)	3832 (.35)	.70/ .85	6/ 6 (1/ 1)	20/ 20	1.00 1.00	1 1 / 2 2	5.3 2.6	236 307 / -33 93	236 307 / -33 93	INT

THE OAO-IV STRAPDOWN STAR TRACKER HAS A PASSIVE THERMAL CONTROL
HEAT IS REJECTED BY CONDUCTION TO A RADIATION SHIELD HAVING A PER-
MISSIBLE TEMPERATURE EXCURSION OF -29 TO 38 DEG.C(-20 TO 100 DEG
F). NO HEATERS ARE REQUIRED WITHIN THIS RANGE. UNIT IS HARD
MOUNTED TO VEHICLE MOUNTING FLANGE. UNIT REQUIRE CLEAR UNOBSTRACT-
ED VIEW TO OPERATE PROPERLY

REF. NO.	DESCRIPTION MANUFACTURER AND REMARKS	WEIGHT KG (LBS)	PACKAGE SHAPE	SURFACE AREA SQUARE CM (FT)	VOLUME CUBIC CM (FT)	RAD. ALPHA/ EMISS	POWER WATTS MIN/ MAX	POWER DENSITY O/A W/M2 (W/FT2)	TIME CONST. HOURS MIN MAX	ADIABATIC RISE RATE DEG K/HR DEG F/HR MIN MAX	THERMAL MASS W-HR/K BTU/F	ALLOWABLE TEMP. DESIGN MIN MAX	SINK DEG K/(F) QUAL MIN MAX	OPERATION MODE
ST 7	OMA ATM STAR TRKR. BENDIX CORPORATION	19.1 (42.0)	RECT	11211 (12.1)	77677 (2.74)	.25/ .90	18/ 28 (1/ 2)	16/ 25	.62 .61	1 2 / 2 4	12.9 6.8	238 302 / -30 84	247 302 / -14 84	INT

THE OMA ATM STAR TRACKER IS A GIMBALLED UNIT. THE ABOVE DIMENSIONS
ARE EXTERIOR LIMITS SEE REF FOR MORE DETAIL DESCRIPTION. UNIT IS
MARRIED TO ATM STAR TRACKER ELECTRONICS UNIT. UNIT HAS 3 INTERNAL
HEATERS OF 10 WATTS EACH TWO OF THE HEATERS HAVE SET POINTS OF -23
.3 TO -15.0 (-9.9 TO 5.0 DEG.F) AND THE THIRD HEATER HAS SET POIN
OF -15.3 TO -6.7 DEG C (5.5 TO 22.5 DEG.F). UNIT IS THERMALLY ISO
LATED, PAINTED WHITE, AND HAS A SUPERINSULATION BLANKET COVERING.

REF. NO.	DESCRIPTION MANUFACTURER AND REMARKS	WEIGHT KG (LBS)	PACKAGE SHAPE	SURFACE AREA SQUARE CM (FT)	VOLUME CUBIC CM (FT)	RAD. ALPHA/ EMISS	POWER WATTS MIN/ MAX	POWER DENSITY O/A W/M2 (W/FT2)	TIME CONST. HOURS MIN MAX	ADIABATIC RISE RATE DEG K/HR DEG F/HR MIN MAX	THERMAL MASS W-HR/K BTU/F	ALLOWABLE TEMP. DESIGN MIN MAX	SINK DEG K/(F) QUAL MIN MAX	OPERATION MODE
ST 8	KS-199 STAR TRKR KOLLSMAN INSTR.	9.1 (20.0)	RECT	4842 (5.2)	22184 (.78)	.20/ .75	8/ 18 (1/ 3)	17/ 38	.43 .42	3 6 / 5 11	3.0 1.6	247 290 / -14 62	226 307 / -51 93	INT

THE KS-199 STAR TRACKER WAS BUILT FOR THE MOL PROGRAM. ONE ENGINE-
ERING MODEL WAS BUILT AND FUNCTIONAL TESTED. THE GIMBAL SENSOR IS
COUPLED TO AN ELECTRONIC UNIT. THE TRACKER HAS INTERNAL HEATERS
TOTALING 10 WATTS AND ARE SUED FOR FAST WARM UP WHEN UNIT IS BELOW
-11.8 DEG C(10 DEG. F). THE UNIT THERMAL DESIGN IS PASSIVE WITH
UNIT THERMALLY ISOLATED FROM MOUNTING, AND COVERED BY SUPER-INSULA
TION BLANKET TO MAINTAIN PROPER OPERATING TEMPERATURE.

TABLE 2-7

Essential to the thermal analysis of the Space Tug and its associated equipment is an adequate definition of the expected environments to be encountered by the Tug. Many environments had to be evaluated as to their impact on the thermal design of the Tug vehicle. Both minimum and maximum heating conditions were defined. An environments timeline was generated in accordance with a major events timeline given in Table 3-1 and used for the transient mission analysis.

The thermal environments used early in the study to determine worst-case environments are summarized in Table 3-2. These environments were generated using the Tug flux model shown in Figure 3-1. The maximum on-orbit heating condition occurs in the Case 4 park orbit shown in Table 3-2. The planetary and albedo heating contributions of the park orbit and the vehicle's solar orientation make this case's heating slightly higher than other cases considered. Also from the environments study, the minimum heating condition occurs in the Case 7 geosynchronous orbit. The minimal planetary heating in the shadow portion of the orbit led to this case being selected to evaluate cold conditions using the steady-state sink temperature model.

In addition to the hot and cold environments used in the steady-state model, additional environments were needed for the initial orbital insertion and transfer to park orbit for the mission analysis transient model. From liftoff to cargo bay door opening, the cargo bay temperature was assumed to be constant at 294°K (70°F) for the first 10 minutes and was then increased to 80°F in a linear manner to 300°K (80°F) at 0.533 hours per Reference 3. A worst-case hot environment was simulated with the Tug in the orbiter cargo bay with the radiator doors deployed with the orbiter Z-axis solar oriented as shown in Figure 3-2.

The environments timeline used in the transient mission analysis is described in Table 3-3. These environments were input to the model for the mission simulation in the form of array tables. The launch and landing environments were simulated by driving the orbiter cargo bay liner and radiator door temperatures to the values taken from Reference 3. The reentry temperatures are shown in Figure 3-3. These temperatures represent a worst-case maximum heating condition with an assumed adiabatic payload in the cargo bay.

Table 3-1

Table 3-1   Space Tug Thermal Control Study Mission Sequence

NO.	EVENT START TIME (HOURS)	DURATION (HOURS)	EVENT DESCRIPTION
1	0	0	LIFTOFF
2	.133	0	INSERT INTO 104 x 195 KM (56 x 105 N. MILE) ORBIT @ 111 KM (60 N. MILE) ALTITUDE 28.5° INCLINATION
3	.533	.05	OPEN CARGO BAY DOORS AND DEPLOY SHUTTLE RADIATORS
4	.717	.0333	INSERTION INTO 185 KM (100 N. MILE) ORBIT
5	2.1835	.0333	INSERTION INTO 185 x 296 KM (100 x 160 N. MILE) TRANSFER ORBIT
6	2.9		INSERT INTO 296 KM (160 N. MILE) CIRCULAR ORBIT AND COAST
		.917	TUG/PAYLOAD DEPLOYMENT PREPARATION
7	3.06	.0833	MAN PAYLOAD HANDLING STATION AND TUG/PAYLOAD CONSOLE

Table 3-1 (cont)

NO.	START TIME (HOURS)	DURATION (HOURS)	
8	3.143	.0833	CHECKOUT TUG/PAYLOAD CONSOLE
9	3.227	.25	CHECKOUT TUG/PAYLOAD (ELECTRICAL CONTINUITY)
10	3.477	.0833	CHECKOUT PAYLOAD HANDLING STATION
11	3.56	.0833	CHECKOUT MANIPULATOR ARMS (ELECTRICAL CONTINUITY)
12	3.644	.0667	DEPLOY ARMS TO STANDBY POSITION
13	3.71	.0	MULTILAYER PURGE OFF
14	3.71	.0333	GN & C SYSTEM ACTIVATION/TUG THRUSTER INHIBIT
15	3.744	.0667	APS AND TUG PRESSURIZATION CHECKS
16	3.808	.0667	FUEL CELL POWER SYSTEM CHECKOUT
17	3.877	.0333	FUEL CELL ACTIVATION
18	3.91	0	DEMATE SATELLITE UMBILICALS
19	3.91	0	DEMATE TUG GROUND UMBILICALS (EXCEPT VENTS)
20	3.91	.0333	GUIDANCE INITIATION
21	3.943	.0333	RELEASE TUG HOLD DOWNS

Table 3-1 (cont)

Table 3-1 (cont)

Table 3-1 (cont)

NO.	START TIME (HOURS)	DURATION (HOURS)	
		1.167	TUG/PAYLOAD DEPLOYMENT
22	3.977	.0333	ROTATE TUG/PAYLOAD 50° OUT OF CARGO BAY (ASSUME TILT TABLE REMAINS IN THIS POSITION UNTIL TUG RETRIEVAL)
23	4.0	.0333	GRASP TUG WITH MANIPULATOR ARMS
24	4.0333	.0333	DEMATE REENTRY HELIUM UMBILICAL
25	4.067	.0167	POWER SWITCH INTERNAL
26	4.083	.0333	DEMATE VENT AND POWER UMBILICALS
27	4.117	.0333	DEMATE DATA AND C&W UMBILICALS
28	4.15	.0167	RELEASE TUG ADAPTER LATCHES
29	4.167	.0667	EXTEND TUG/PAYLOAD WITH ARMS
30	4.234	.0667	ROTATE TUG/PAYLOAD AWAY FROM CARGO BAY
31	4.30	.0333	RELEASE TUG/PAYLOAD
32	4.333	0	TUG CONTROL TRANSFERRED TO GROUND
33	4.333	.0833	STOW MANIPULATOR ARMS AND POWER DOWN

Table 3-1 (cont)

Table 3-1 (cont)

NO.	START TIME (HOURS)	DURATION (HOURS)	
34	4.417	.0833	ORBITER APS BURN; MANEUVERS TO SAFE DISTANCE FROM TUG/PAYLOAD
35	4.5	.0833	VISUALLY INSPECT TUG PAYLOAD
36	4.583	.0500	POWER DOWN PAYLOAD HANDLING STATION AND TUG/PAYLOAD CONSOLE
37	4.633	.43	MONITOR GROUND ACTIVITY AND VISUALLY OBSERVE TUG DEPARTURE
			PAYLOAD DELIVERY AND RETRIEVAL
39	5.06	0 - 11.0	PHASE IN SHUTTLE ORBIT
40	16.06	0 - 137	PHASING/PLANE CHANGE BURN 26.5° INCLINATION
41	16.20	0 - 3.0	COAST ONE REV. IN PHASING ORBIT
42	19.20	094 - .221	PERIGEE BURN 296 x 35800 KM (160 x 19300 N. MILE)
43	19.29	1.0	COAST IN TRANSFER ORBIT
44	20.29	0	MIDCOURSE CORRECTION

Table 3-1 (cont)

Table 3-1 (cont)

NO.	START TIME (HOURS)	DURATION (HOURS)	
45	20.29	3.96	COAST TO 35800 KM (19,300 N. MILE) APOGEE
46	24.25	.095	APOGEE BURN CIRCULARIZE 35,800 KM (19,300 N. MILE) ORBIT 0° INCLINATION
47	24.35	12.0	COAST AND ORBIT TRIM
48	36.35	1.0	DEPLOY PAYLOAD
49	37.35	0	PHASING BURN
50	37.35	24	COAST IN PHASING ORBIT
51	61.35	0	PHASING ORBIT CIRCULARIZATION BURN
52	61.35	12.0	RENDEZVOUS AND DOCKING
53	73.35	9.68	PHASE IN ORBIT FOR NODAL CROSSING
54	83.03	.062	DEBOOST BURN 315 x 35800 KM (170 x 19,300 N. MILE TRANSFER ORBIT) 26.5° INCLINATION
55	83.09	1.0	COAST
56	84.09	0	MIDCOURSE CORRECTION
57	84.09	4.2	COAST TO 315 KM (170 N. MILE) PERIGEE

Table 3-1 (cont)

| NO.	START TIME (HOURS)	DURATION (HOURS)	
58	88.29	.028 - .051	INJECT INTO RETURN PHASING ORBIT
59	88.34	0 - 3.0	COAST 1 REV. IN PHASING ORBIT
60	91.34	0 - .023	CIRCULARIZE INTO 315 KM (170 N. MILE) ORBIT 28.5° INCLINATION
61	91.34	0	ORBIT TRIM
			TERMINAL PHASE INITIATION AND TUG CAPTURE
62	91.34	.333	SEARCH AND ACQUISITION OF TUG BY ORBITER
63	91.38	3.0	VENT TUG MAIN TANKS AND CLOSE VENTS
64	91.67	3.78	COELLIPTIC WINDOW
65	91.68	0	CONTROL OF TUG TRANSFERRED TO CREW
66	94.77	1.5	PLANE CHANGE WINDOW
67	96.29	.58	ORBITER TPI BURN AND COAST
68	96.867	.0167	ORBITER TPF BURN
69	96.883	.33	ORBITER COAST TO AND ARRIVAL AT CAPTURE POSITION

Table 3-1 (cont)

Table 3-1 (cont)

Table 3-1 (cont)

NO.	START TIME (HOURS)	DURATION (HOURS)	
70	97.217	.667	TUG INTERIAL HOLD
71	97.217	25	MAN AND RECHECK PAYLOAD HANDLING STATION AND TUG CONSOLES AND RECHECK MANIPULATOR ARMS
72	97.55	.0833	TUG CAPTURE BY ARMS
73	97.634	0	SHUTTLE RCS INHIBIT
			TUG SAFING SEQUENCE
74	97.634	0	TUG APS INHIBIT AND POWER SWITCH TO BATTERY
75	97.634	.75	VENT TUG TANKS (APS), FUEL CELL AND ACCUMULATORS
76	98.383	0	CLOSE VENTS
77	98.383	.133	RETRACT TUG TILT TABLE
78	98.517	0	SECURE TUG TO TILT TABLE
79	98.517	.05	REMAKE POWER, C & W, AND DATA UMBILICALS
80	98.566	.0333	REMAKE VENT AND PURGE UMBILICALS
81	98.60	.05	CHECKOUT POWER AND DATA INTERFACES

Table 3-1 (concl)

Table 3-1 (concl)

NO.	START TIME (HOURS)	DURATION (HOURS)	
82	98.65	.0	TUG POWER AND DATA SWITCH TO SHUTTLE
83	98.65	.0333	UMBILICAL INTERFACE CHECKS
84	98.683	.0333	PRESSURIZE AND VENT MAIN TANKS
85	98.717	.0333	PRESSURIZE MAIN TANKS FOR LANDING
			TUG STOWAGE SEQUENCE
86	98.75	.0667	ROTATE TUG BACK INTO CARGO BAY
87	98.817	.10	SECURE TUG
88	98.917	.0333	POWER DOWN TUG SUBSYSTEMS
89	98.95	.05	RETURN MANIPULATOR ARMS TO STOWED POSITION
90	99.0	.0167	POWER DOWN MANIPULATOR ARMS
91	99.0167	.05	RETRACT RADIATORS AND CLOSE CARGO BAY DOORS
92	99.067	.0167	SECURE CARGO BAY DOORS
			DEBOOST AND LANDING
93	99.067	1.1	COAST TO ENTRY INTERFACE
94	100.2	.65	BEGIN REENTRY
95	100.85		LANDING

Table 3-2

Table 3-2 Tug Natural Environments Case Summary
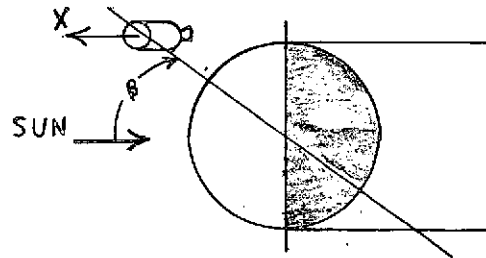
| CASE NO.	CONFIG-URATION	PARK		PHASING		TRANSFER		GEOSYNCHRONOUS	
		β	ORIENTATION	β	ORIENTATION	β	ORIENTATION	β	ORIENTATION
1	TUG/ ORBITER	52	-ZLV (DEPLOY MODE)	—		—		—	
2	TUG/ ORBITER	52	+ZLV (RETRIVE MODE)	—		—		—	
3	TUG	52	X-AXIS VELOCITY VECTOR	50	X-AXIS VELO-CITY VECTOR	50	X-AXIS VELO-CITY VECTOR	23.5	X-AXIS VELO-CITY VECTOR
4	TUG	52	X-AXIS ⊥ TO SUN VECTOR	50	X-AXIS ⊥ TO SUN VECTOR	50	X-AXIS ⊥ TO SUN VECTOR	23.5	X-AXIS ⊥ TO SUN VECTOR
5	TUG	52	X-AXIS 11 TO SUN VECTOR	50	X-AXIS 11 TO SUN VECTOR	50	X-AXIS 11 TO SUN VECTOR	23.5	X-AXIS 11 TO SUN VECTOR
6	TUG	0	X-AXIS VELO-CITY VECTOR	0	X-AXIS VELO-CITY VECTOR	0	X-AXIS VELO-CITY VECTOR	0	X-AXIS VELO-CITY VECTOR
7	TUG	0	X-AXIS ⊥ TO SUN VECTOR	0	X-AXIS ⊥ TO SUN VECTOR	0	X-AXIS ⊥ TO SUN VECTOR	0	X-AXIS ⊥ TO SUN VECTOR
8	TUG	0	X-AXIS 11 TO SUN VECTOR	0	X-AXIS 11 TO SUN VECTOR	0	X-AXIS 11 TO SUN VECTOR	0	X-AXIS 11 TO SUN VECTOR
9	TUG	-		—		52	X-AXIS ⊥ TO SUN SLOW ROLL	23.5	X-AXIS ⊥ TO SUN SLOW ROLL
10	TUG	-		—		0	X-AXIS ⊥ TO SUN SLOW ROLL	0	X-AXIS ⊥ TO SUN SLOW ROLL
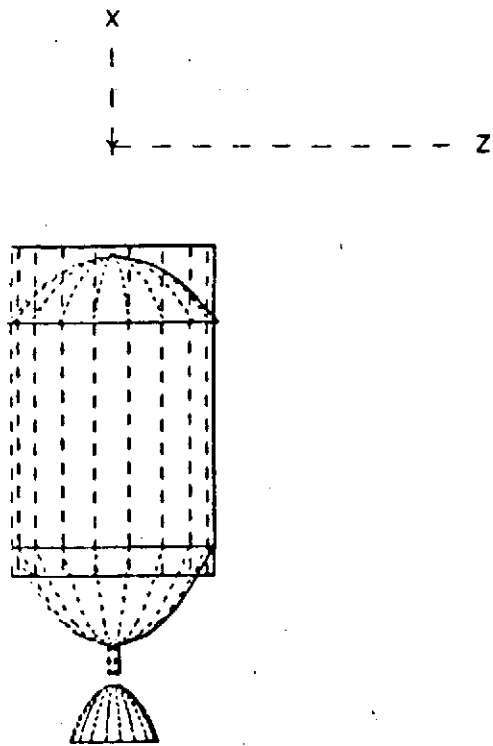
Figure 3-1 Tug Flux Model Y-Axis View
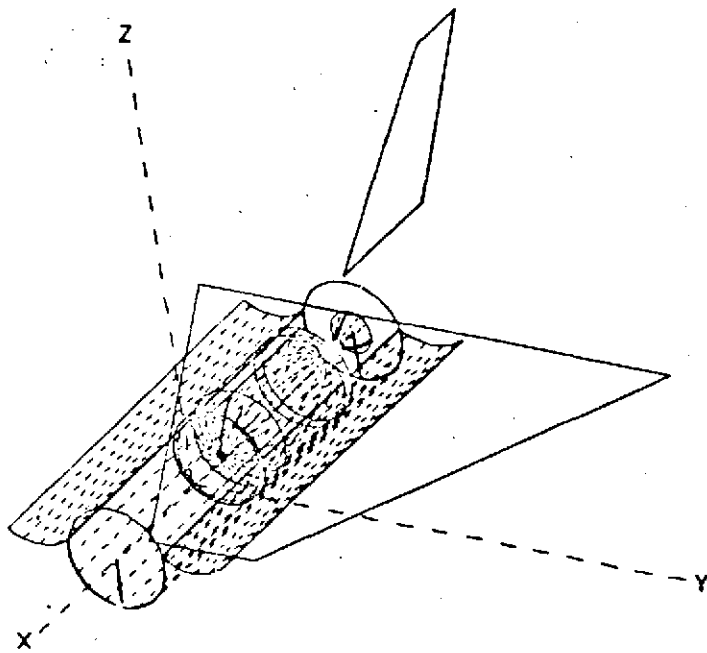
Figure 3-2 Predeployment Flux Model 3-D View

Table 3-3

Table 3-3   Tug/Orbiter Mission Environments

PHASE/ORBITS	MISSION TIME (HOURS)	DESCRIPTION
Launch	0 to 0.593	Radiator doors closed, cargo bay wall environment being boundary temperatures.
100 NM Circular	0.593 to 2.061	Radiator doors deployed, fluxes calculated using TRASYS (1 orbit)*
100 x 160 NM Transfer	2.061 to 2.805	Same as above (0.5 orbits)*
160 NM Circular	2.805 to 4.310	Same as above (1 orbit)*
160 NM Circular	4.310 to 19.360	Tug deployed - orbiter continues in circular orbit until 98.917 hours - fluxes from Case 4 park orbit.*
160 x 19300 NM Transfer	19.360 to 24.350	Tug transfer to geosynchronous-fluxes calculated using TRASYS.*
19300 NM Circular	24.350 to 84.353	Tug at geosynchronous fluxes from Case 7 geosynchronous (2.5 orbits).*
19300 x 160 Transfer	84.353 to 89.343	Tug return transfer from geosynchronous-fluxes calculated using TRASYS.*
160 NM Circular	89.343 to 98.917	Tug phasing-fluxes from Case 4 park (6.4 orbits).*
160 NM Circular	98.917 to 100.13	Tug retrieved, radiator doors open (1.3 orbits).*
Landing	100.13 to 110.0	Radiator doors closed, cargo bay wall environments being boundary temperatures.

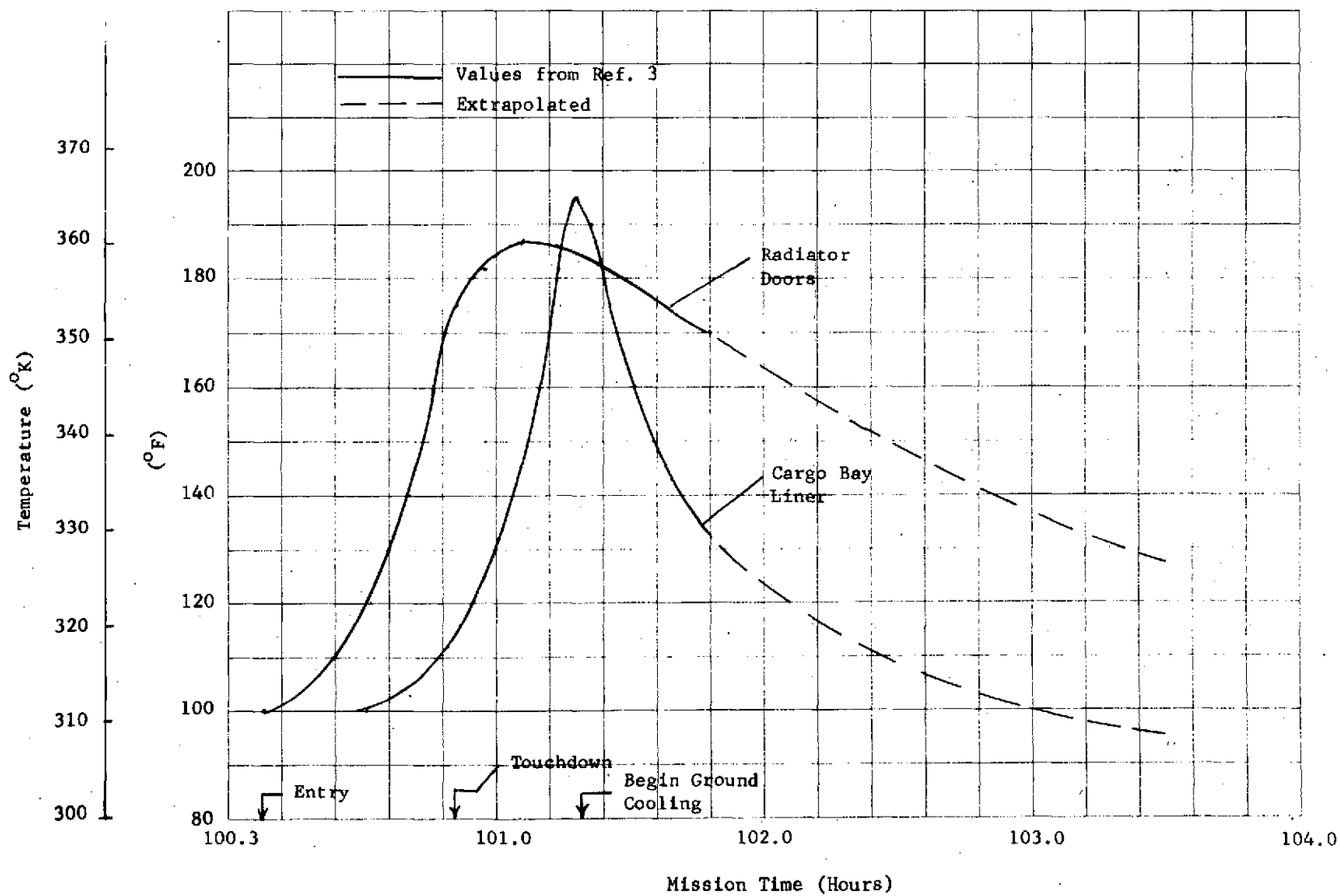*Incident orbital fluxes calculated with vehicle x-axis perpendicular to sun vector for the hot case (see Table 3-2).

Figure 3-3   Boundary Temperatures Used for Landing Environments

4. STEADY-STATE PARAMETRIC STUDIES

Studies were performed to evaluate the influence of various parameters on the thermal design of Tug. These studies were essential in assuring adequate thermal performance of the vehicle throughout its mission and were concerned with both active and passive means of providing thermal control to the Tug and its associated equipment. The studies relied heavily on minimum and maximum heating environments. The areas investigated as part of the study are tabulated in the order they occurred in Table 4-1. A description of each thermal model that was developed and the particular studies that it was used for is discussed in the following sections. The results of each of the studies are also presented.

Table 4-1 Parametric Studies Performed

Multilayer Insulation Concepts
Thermal Control Coatings
Forward Compartment Heat Pipe
Honeycomb Wall Structure Conductance
Influence of Component Spacing
Component Contact Conductance
Component Heater Sizing
Transient Mission Analysis
Simplified Louver System Operations

The parametric studies began early in the program with the development of a steady-state MITAS (Ref 4) thermal math model to generate compatmental sink temperatures. This model consists of 34 nodes as shown in Figure 4-1. The Tug compartment, tank insulation, and engine are simulated by 31 arithmetic nodes (zero mass nodes) and the boundaries consisting of the LH_2 node, the LOX node, and space. There were 117 radiation conductors and 12 linear conductors. Radiation conductors were calculated by the model from the configuration factors and node optical properties data with the use of the SCRPFA subroutine. Also, the absorbed environmental fluxes were calculated within the model from the incident flux tables and the surface optical properties. This technique allowed for parametric variation of the surface optical properties to investigate their influence on compartment sink temperatures. The maximum and minimum incident heating conditions from Table 3-2 for Case 4 park orbit and Case 7 geosynchronous orbit, respectively, were used in the model.
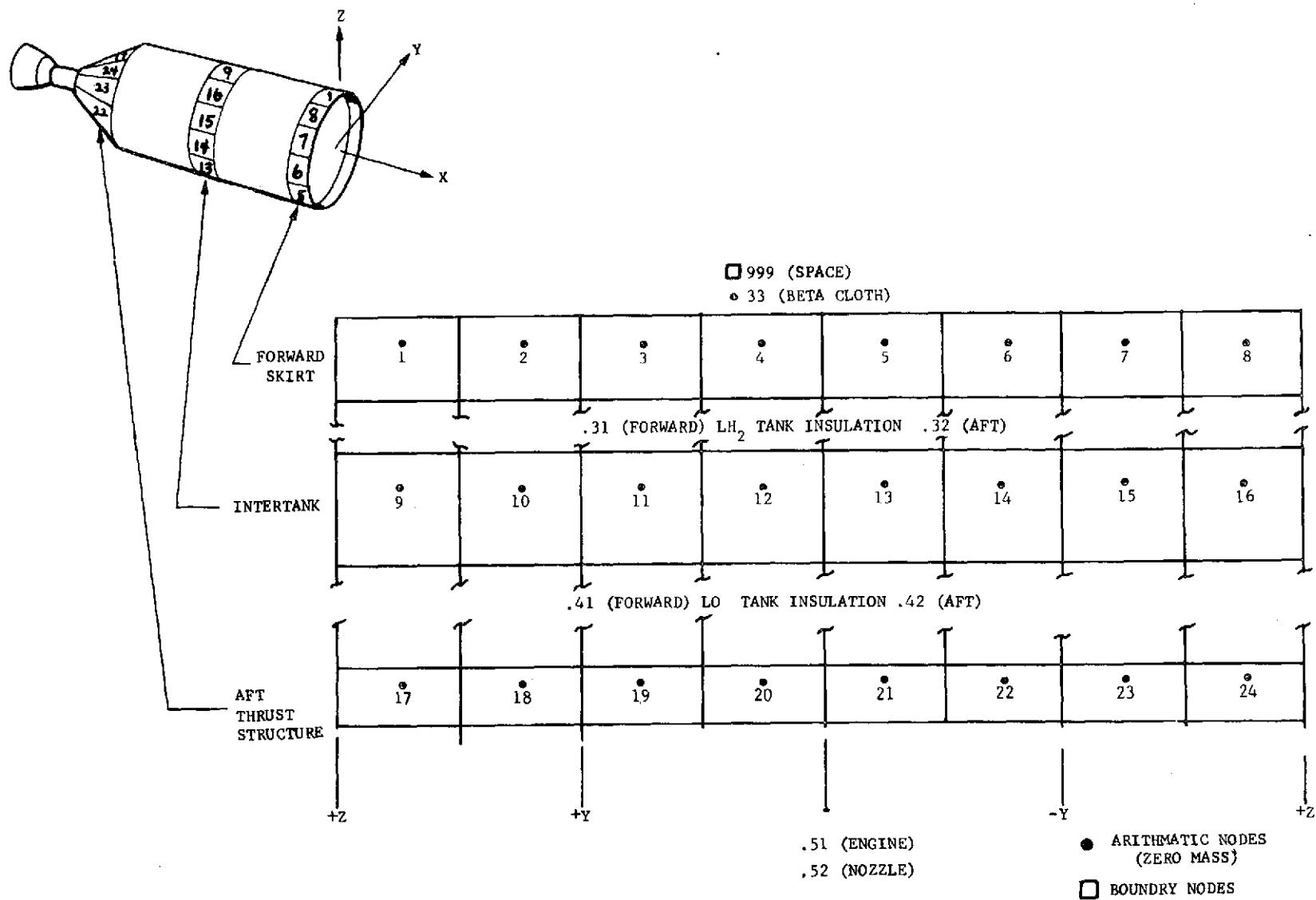
Figure 4-1

Figure 4-1 Compartmental Sink Temperature Model

4.1   INITIAL COATING STUDIES

Tradeoff studies to select the external surface coatings were per-
formed using the hot and cold environmental heating rates. The
optical coating parameters α and ε were varied along with the
compartmental average power dissipation.

Figure 4-2 presents the hot-case average radiation sink temperature
as a function of optical properties and selected power dissipations
for the forward compartment. The specific optical property ratios
used to generate the curves correspond to white paint (α/ε = .2/.9),
aluminum paint (α/ε = .26/.26), and a 50% mixture of white and
aluminum paint (α/ε = .23/.58). Forward compartment average sink
temperature data are presented in Figure 4-3 for the shadow portion
of Case 4 park orbit to show the effect of coating emissivity.
The same parametric runs were repeated using the cold-case envir-
onments and the results are presented in Figures 4-4 and 4-5 for
the sun and shadow portions of the orbit, respectively.

4.2   INSULATION AND COATING SELECTION

Figure 4-5 indicates that coatings by themselves will be inadequate
to maintain thermal control. This is based on maintaining the for-
ward compartment average sink temperature above a minimum of 200°K
(-100°F). This criterion (200°K) was chosen based on past exper-
ience on a similar system and a survey of minimum temperatures
obtained from Reference 2. Before pursuing coating selection
further, an investigation of vehicle heat leaks was conducted in
an effort to raise compartmental sink temperatures. It was found
that a significant heat leak existed at the forward compartment
beta cloth shield. By using a 24-layer Mylar insulation blanket
with gold on one side of each Mylar sheet, the effective emissivity
across the blanket was reduced to 0.025 per Reference 5. Using
the insulation, the forward compartment heat leak was reduced to
a point where selective coatings were adequate in controlling in-
ternal compartment sink temperatures.

The hot and cold cases were reanalyzed using the multilayer in-
sulation blanket and the results are shown in Figures 4-6 thru
4-8. Figure 4-6 presents the forward compartment maximum sink
temperatures versus α/ε ratio and shows the influence of the in-
sulation blanket. Figure 4-7 shows similar results for the sun
portion of Case 7 geosynchronous orbit. Minimum forward compart-
ment sink temperatures are shown in Figure 4-8 for shadow portion
of the Case 7 geosynchronous orbit. This curve shows an emittance
of 0.475 which gives the desired minimum operating sink temperature
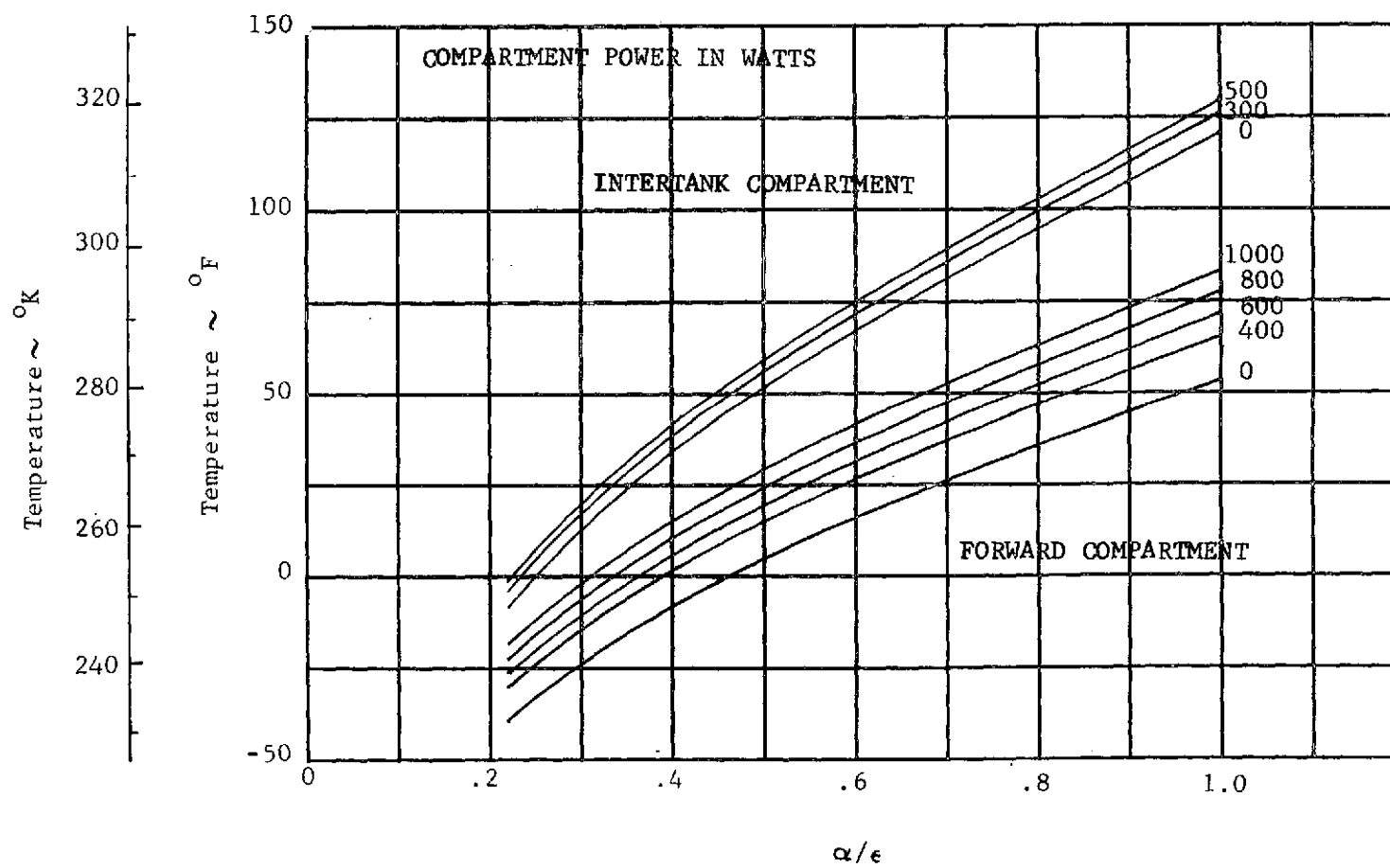200°K (-100°F) for nominal power dissipations of 800 to 1000 watts.

Figure 4-2
Parametric Runs, Hot Case Compartment Average Sink Temperature Park Orbit Case 4 (Full Sun)
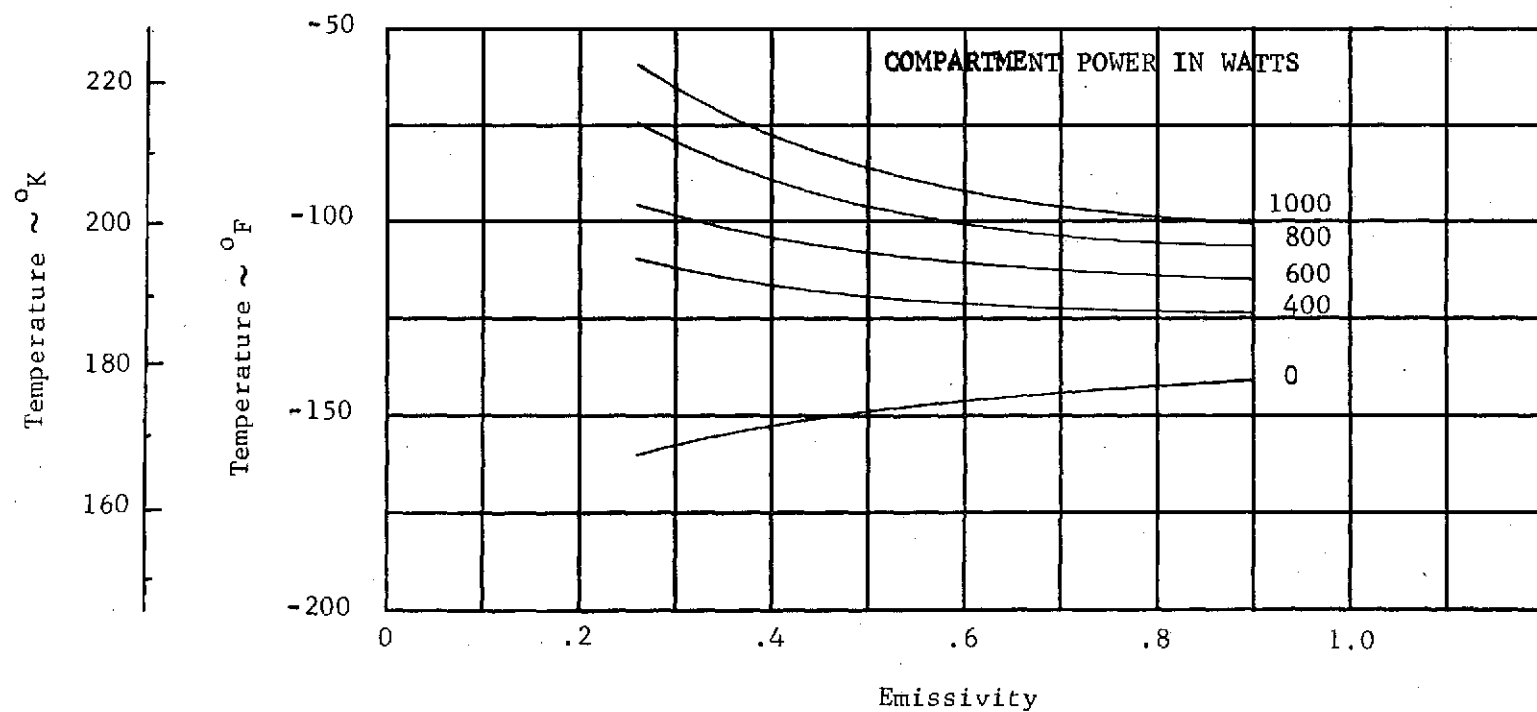
Figure 4-3
Parametric Runs, Forward Compartment Average Sink Temperature, Park Orbit Case 4 Earth Shadow Temperatures
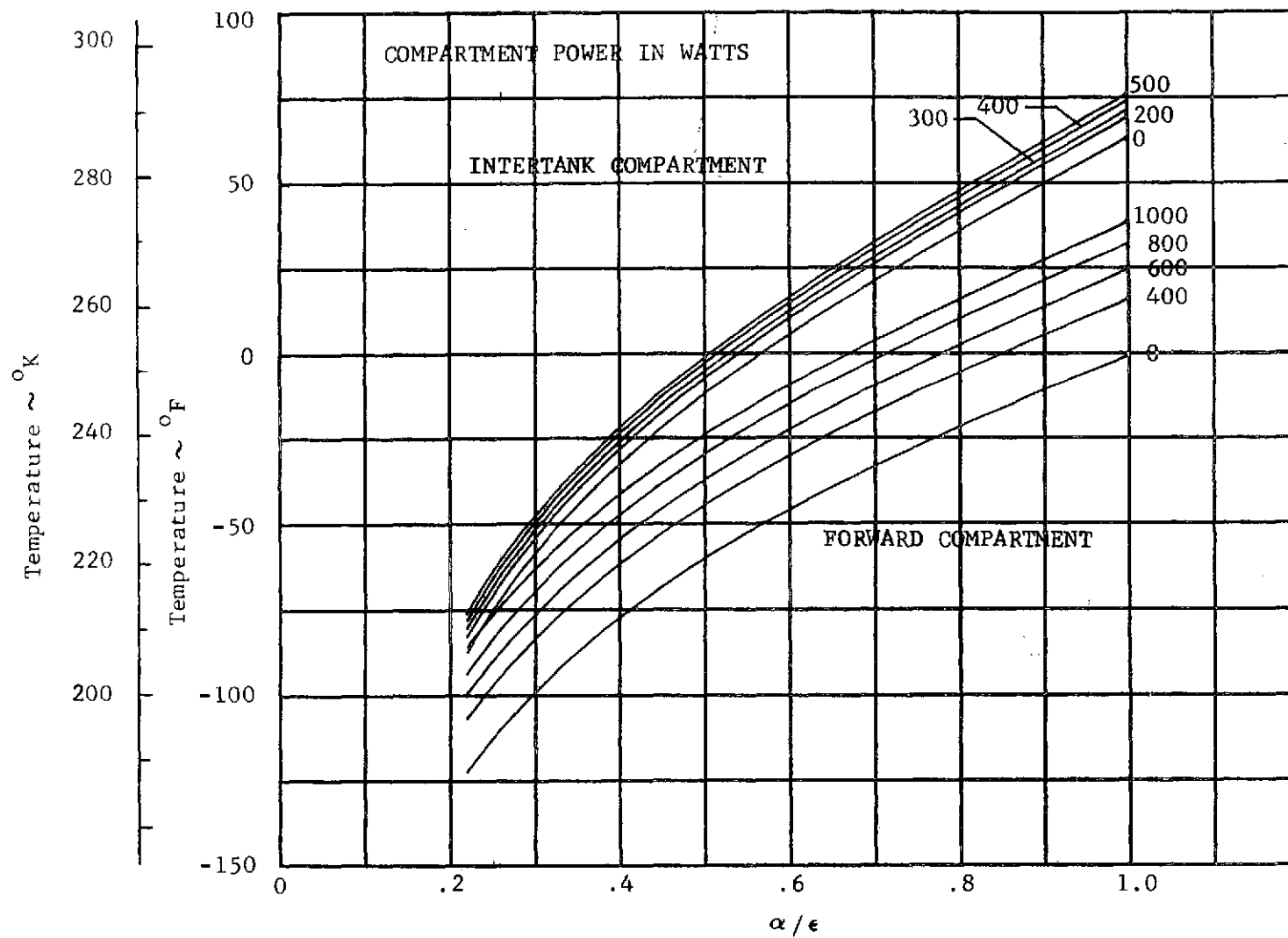
Figure 4-4
Parametric Runs, Compartment Average Sink Temperature, Synchronous Orbit Case 7 (Full Sun)

Figure 4-5
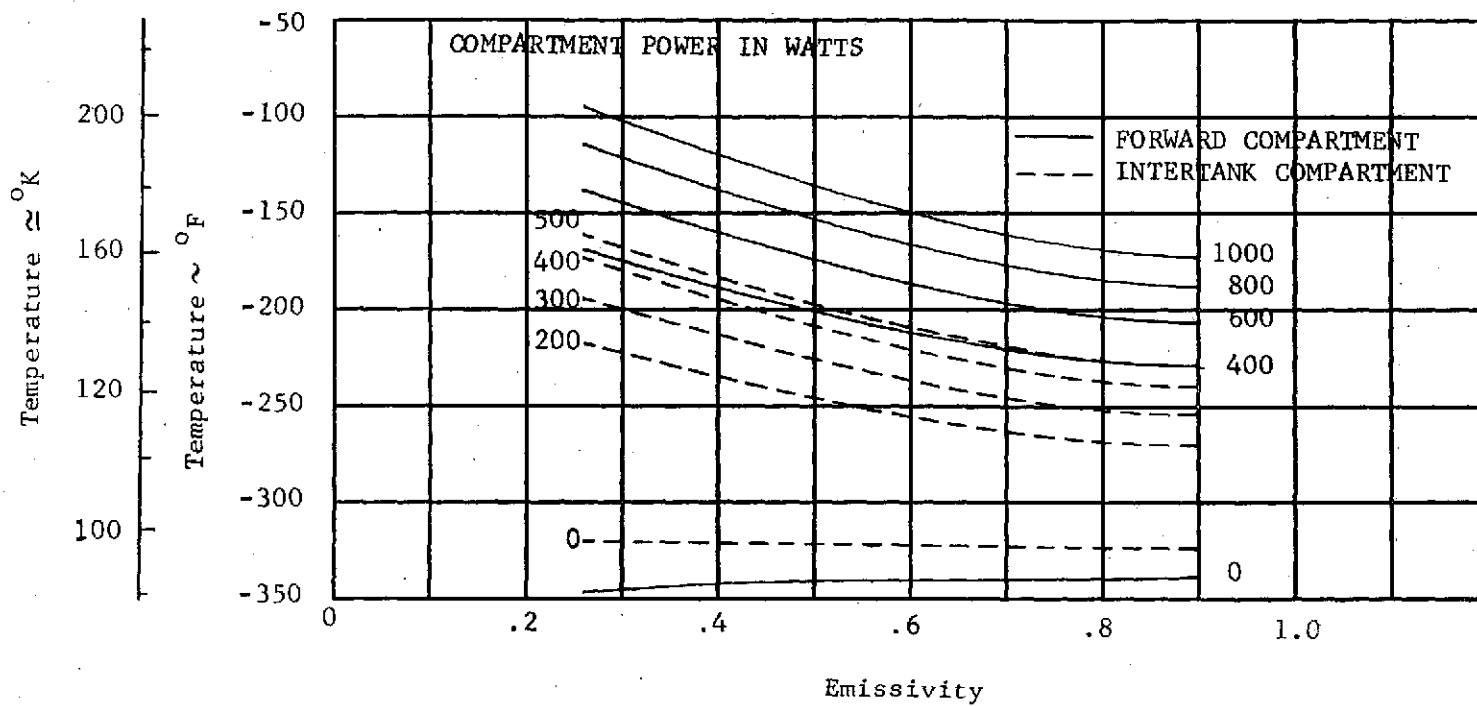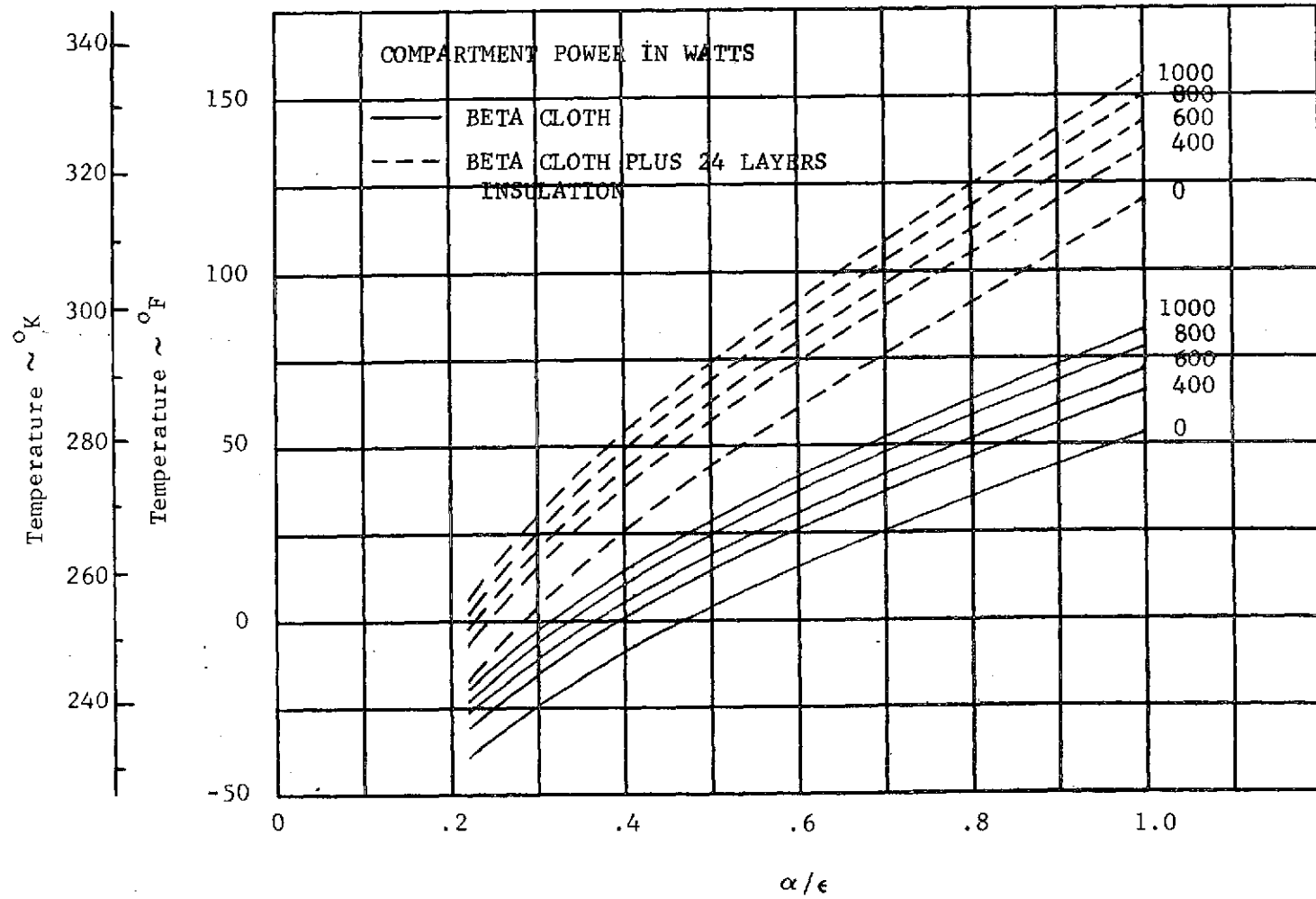*Parametric Runs, Compartment Average Sink Temperature, Synchronous Orbit Case 7, Earth Shadow Temperatures*

Figure 4-6
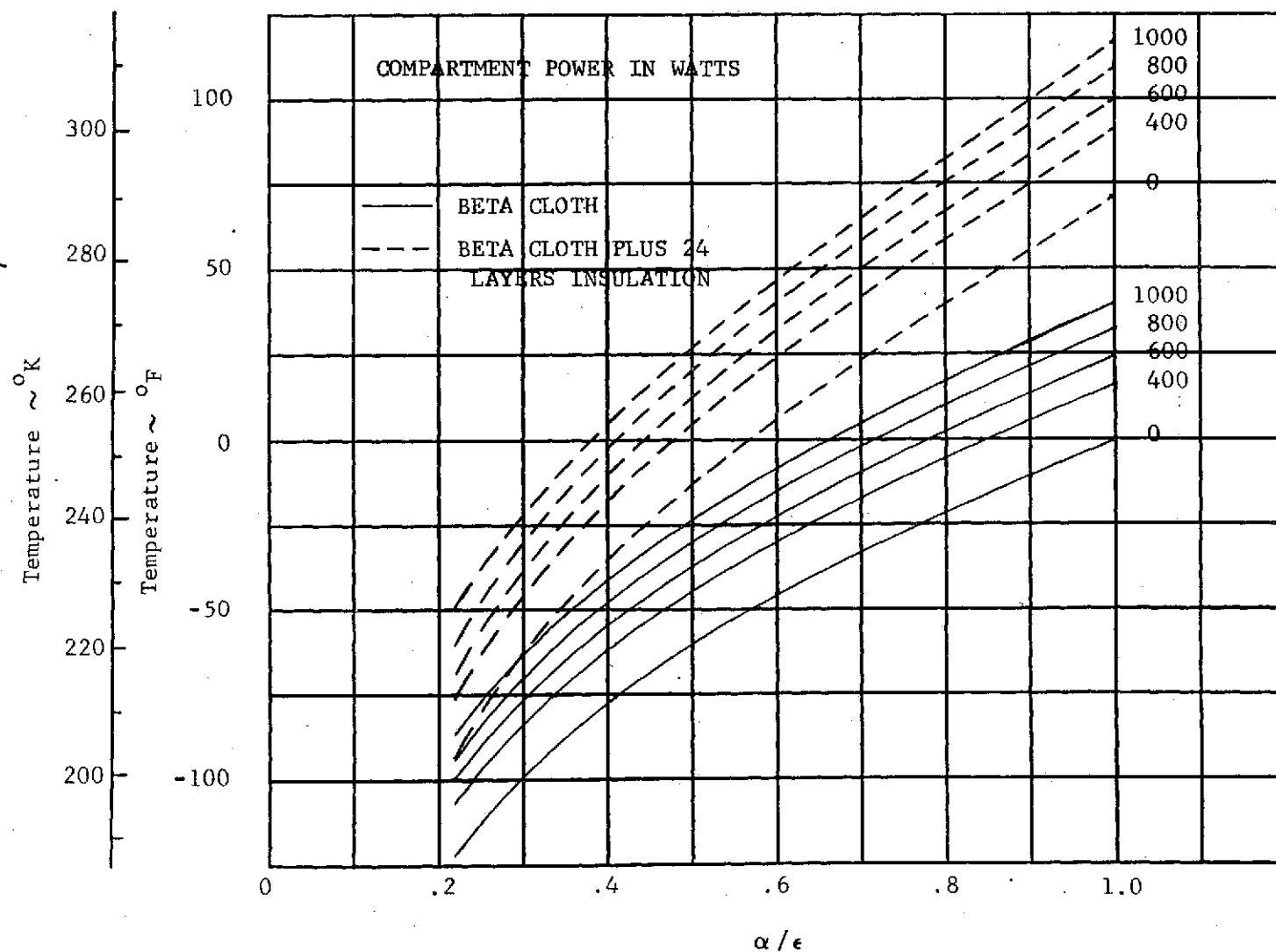Parametric Runs, Forward Compartment Average Sink Temperature, Park Orbit Case 4

Figure 4-7
Parametric Runs, Forward Compartment Average Sink Temperature, Sunchronous Orbit Case 7
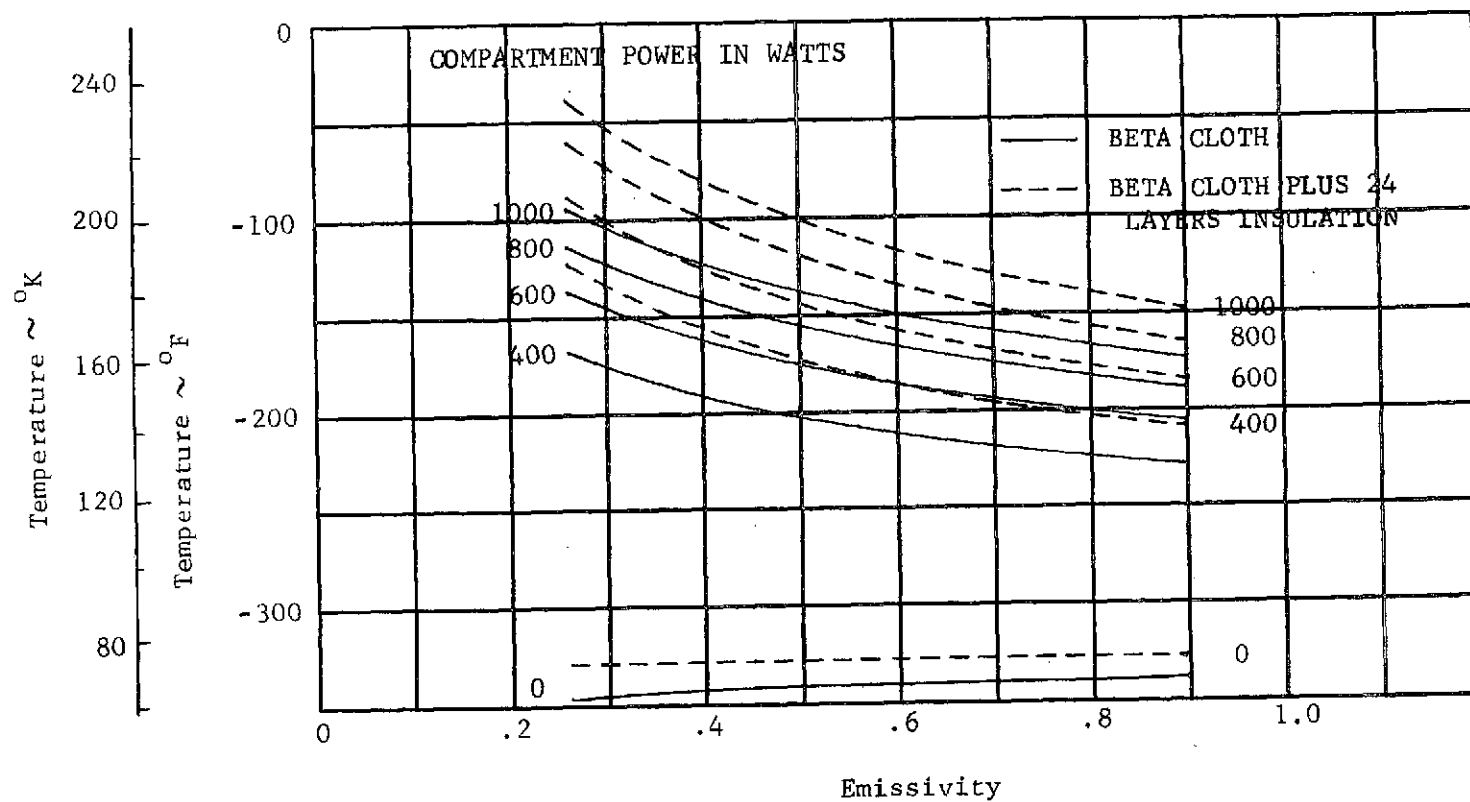
Figure 4-8
Parametric Runs, Forward Compartment Average Sink Temperature, Synchronous Orbit Case 7

Establishing a maximum sink temperature of 297°K (75°F), from Figure 4-6 dictates an α/ε value of 0.50. The previous emittance value of 0.475 fixes an α value of 0.2375. A similar analysis on the intertank compartment indicated an α/ε value of 0.60 was needed with $\alpha = 0.246$ and $\varepsilon = 0.41$.

The paint pattern needed to simulate the necessary optical properties is derived from Figure 4-9. The α and ε for all-white paint and all-aluminum paint are plotted on the left and right abscissas, respectively, and connected by straight lines. Finding the optical property on the graph fixes the percentages of aluminum to white paint needed for a mosaic pattern. For the forward compartment 63.5% aluminum paint and 36.5% white paint is needed, and for the intertank compartment 75% aluminum paint and 25% white paint is needed.

4.3 FORWARD COMPARTMENT HEAT PIPES

Upon completion of the thermal coating studies, heat pipes were simulated in the forward compartment to isothermalize the compartment walls. This was necessary because hot-case wall temperature gradients in excess of 72°K (130°F) existed between the sun and shadowed side of the vehicle. The average compartment sink temperature was unaffected by the heat pipes as shown in Figures 4-10 and 4-11. These curves compare directly with those of the coating study, Figures 4-6 and 4-8. Heat pipe performance data for a typical high capacity heat pipe was taken from Reference 6. The pipe operates at a 2 kW load over a temperature drop of 3.89°K (7°F). Based on the performance data, six parallel circumferential heat pipes were integrated into the compartment walls for simulation in the model.

Using a fin effectiveness of 0.85 and a joint conductance of $12.1 \frac{W}{m^2 \, °K}$ (800 Btu/hr-°F-ft²) Reference 7, a conductance value of 467 W/°K (2870 Btu/hr-°F) was calculated between each wall and each heat pipe node. The heat pipe performance data were reduced to an effective conductance between each heat pipe node of 879 W/°K (5400 Btu/hr-°F). The large heat pipe conductance caused oscillations when running the math model, resulting in excessive machine time for temperature convergence. A more efficient technique was then employed that replaced the original heat pipe nodes and network with an equivalent series network connecting adjacent compartment wall nodes with a conductance of 184.6 W/°K (1134 Btu/hr-°F). A reduction in the number of iterations was also achieved by first solving the network without the heat pipes and calculating a fourth power temperature average of the wall nodes. This temperature was applied to the wall nodes as starting wall temperatures for the heat pipe simulation.

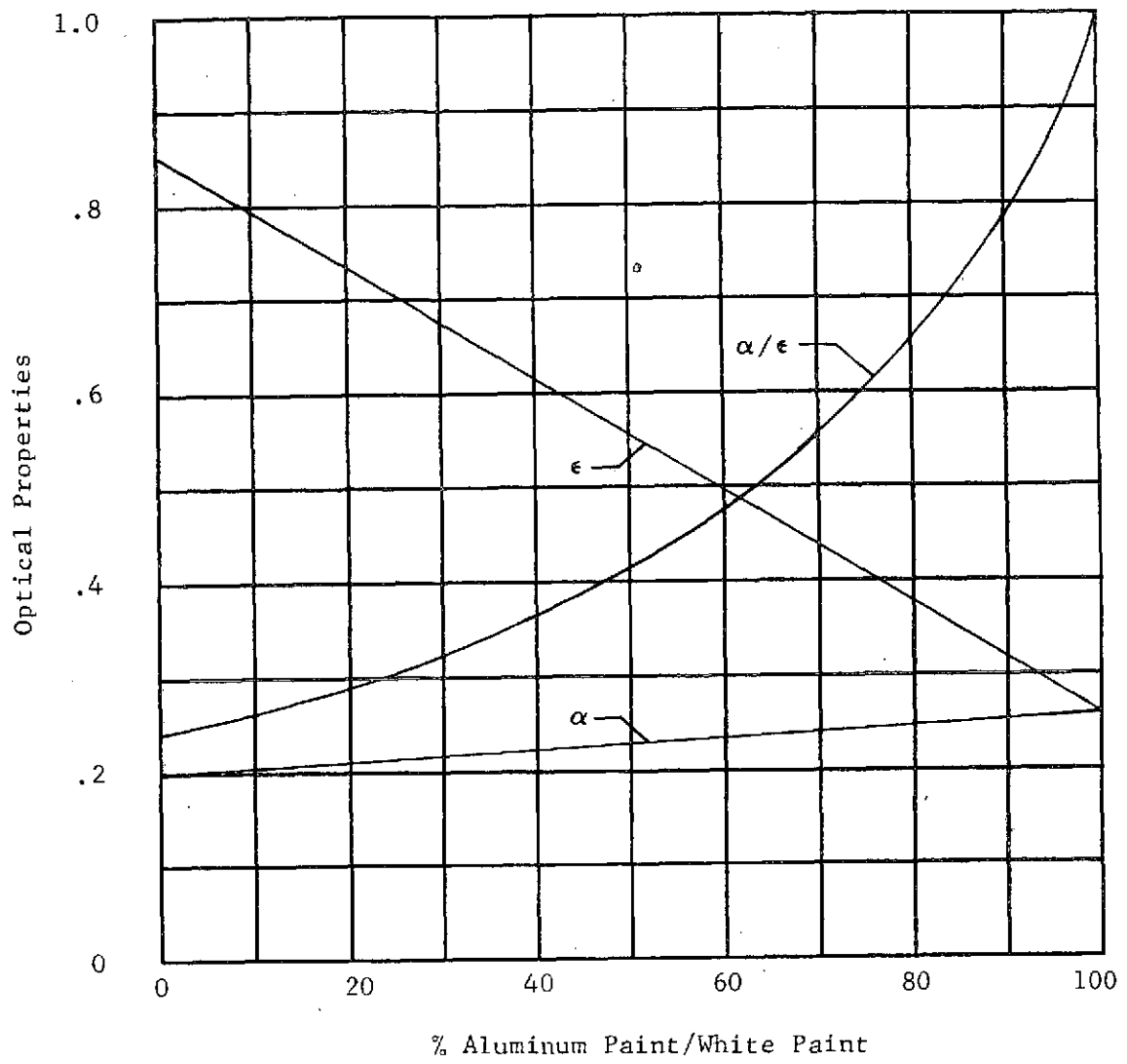Figure 4-9   Parametric Runs, Surface Properties

HEAT PIPES IN FORWARD COMPARTMENT

BETA CLOTH PLUS 24 LAYERS OF INSULATION
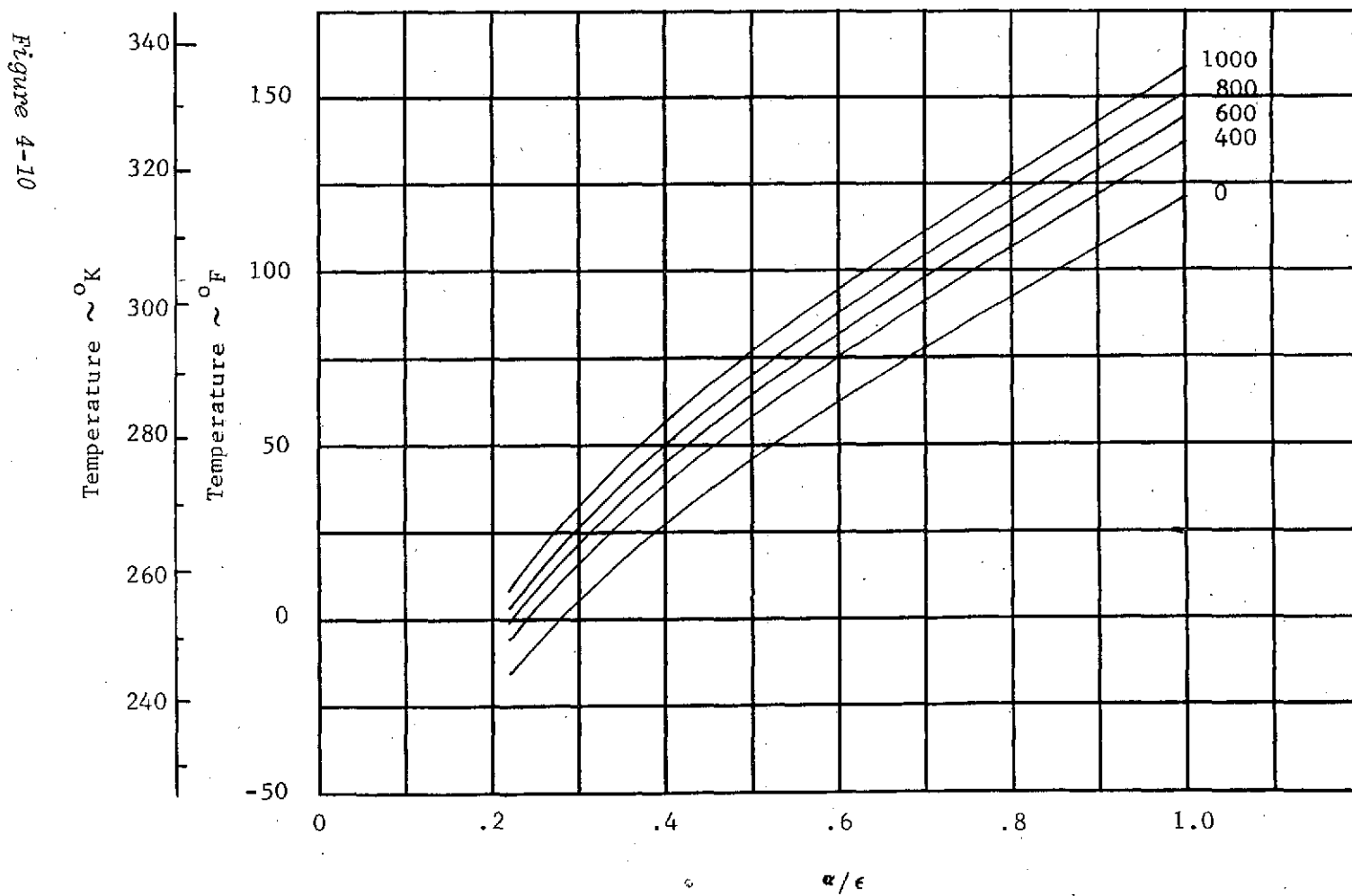

Figure 4-10
Parametric Runs, Forward Compartment Average Sink Temperatures Park Orbit Case 4

HEAT PIPES IN FORWARD COMPARTMENT

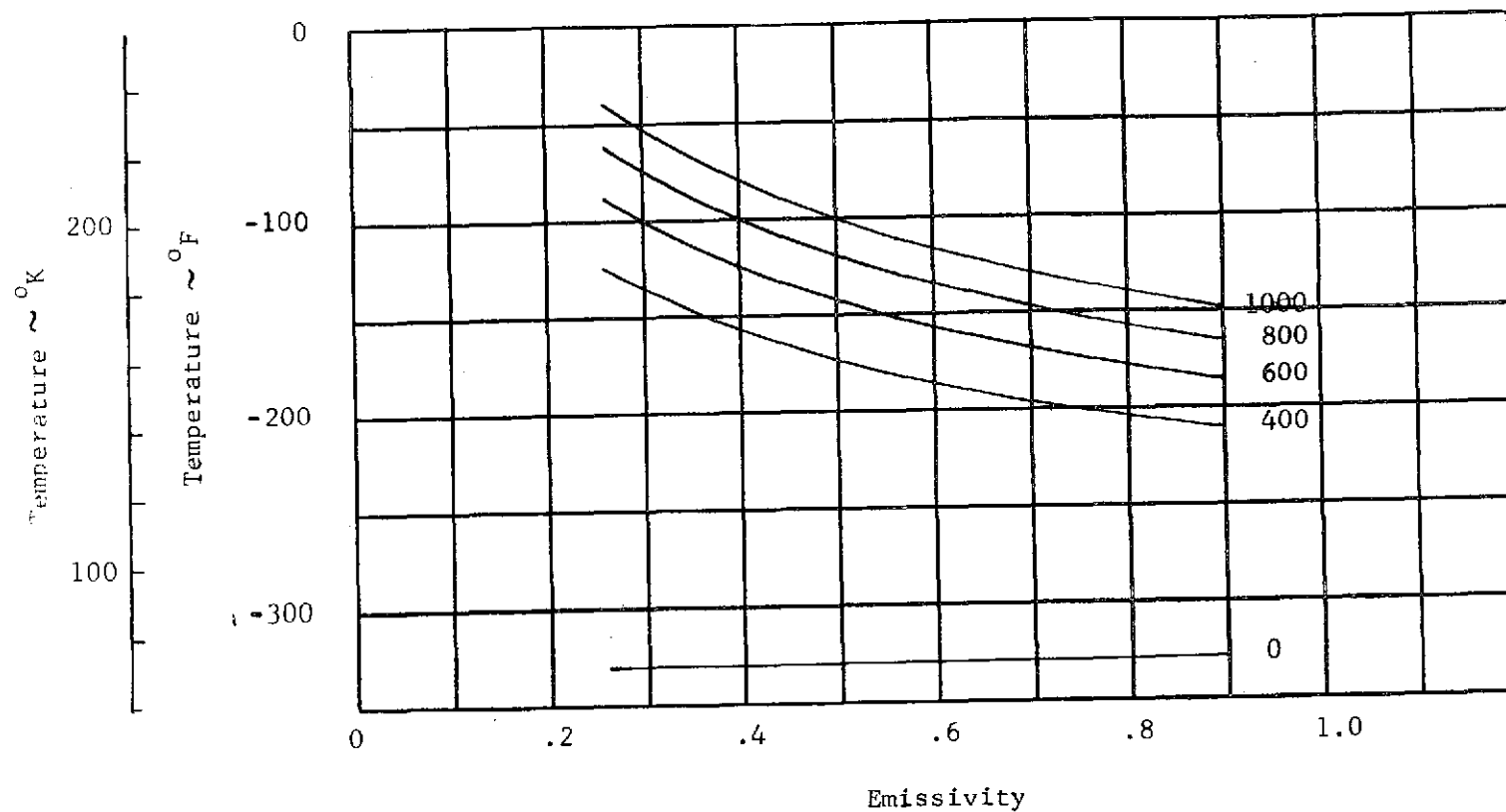BETA CLOTH PLUS 24 LAYERS OF INSULATION

EARTH SHADOW

Figure 4-11
Parametric Runs, Forward Compartment Average Sink Temperatures, Synchronous Orbit Case 7

The effectiveness of the heat pipe in reducing circumferential gradients is shown in Figures 4-12 and 4-13 for Case 7 geosychronous and Case 4 park orbits, respectively. The forward compartment wall temperature gradient is reduced from 50 to 2.8°K in geosychronous orbit and from 36 to 2.2°K in park orbit.

4.4 HONEYCOMB STUDIES

A study was performed to determine the influence of the honeycomb structure on compartmental temperatures. A duplicate set of forward compartment wall nodes were added to the model simulating the fiberglass epoxy, aluminum core honeycomb structure. Figures 4-14 and 4-15 show the influence of the honeycomb conductance on the forward internal sink temperature for the hot and cold cases, respectively. The ΔTs from the above curves should be added to Figures 4-6 and 4-8, respectively, to obtain the internal sink temperatures for the honeycomb structure. The maximum conductance value of 1 watt/°K (1.94 but/°F) per 0.093 m² (1 ft²) results in a compartment sink temperature 3.3°K (6°F) warmer than no honeycomb for the hot case. The conductance valve was obtained assuming an infinite value for the joint conductances. A more realistic value for the joint conductances would result in lower overall conductance values, thus increasing the effect on compartment sink temperatures. The use of a nonmetallic core, such as fiberglass would further increase the ΔT by reducing the conductivity as shown in the curves. Hence, the choice of the honeycomb structure for Tug will have an influence on the thermal design and could impact the basic passive concept chosen. A further discussion of the honeycomb structure is included in Section 7.
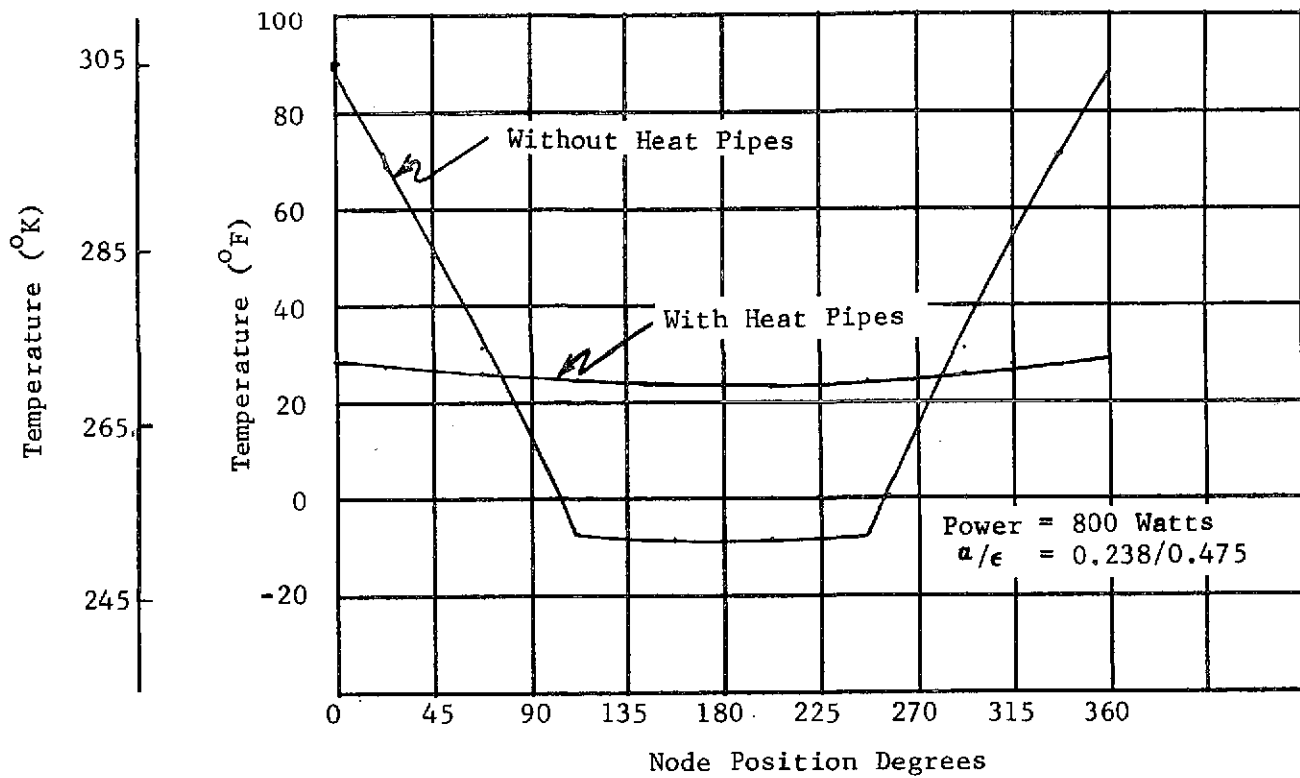
Figure 4-12
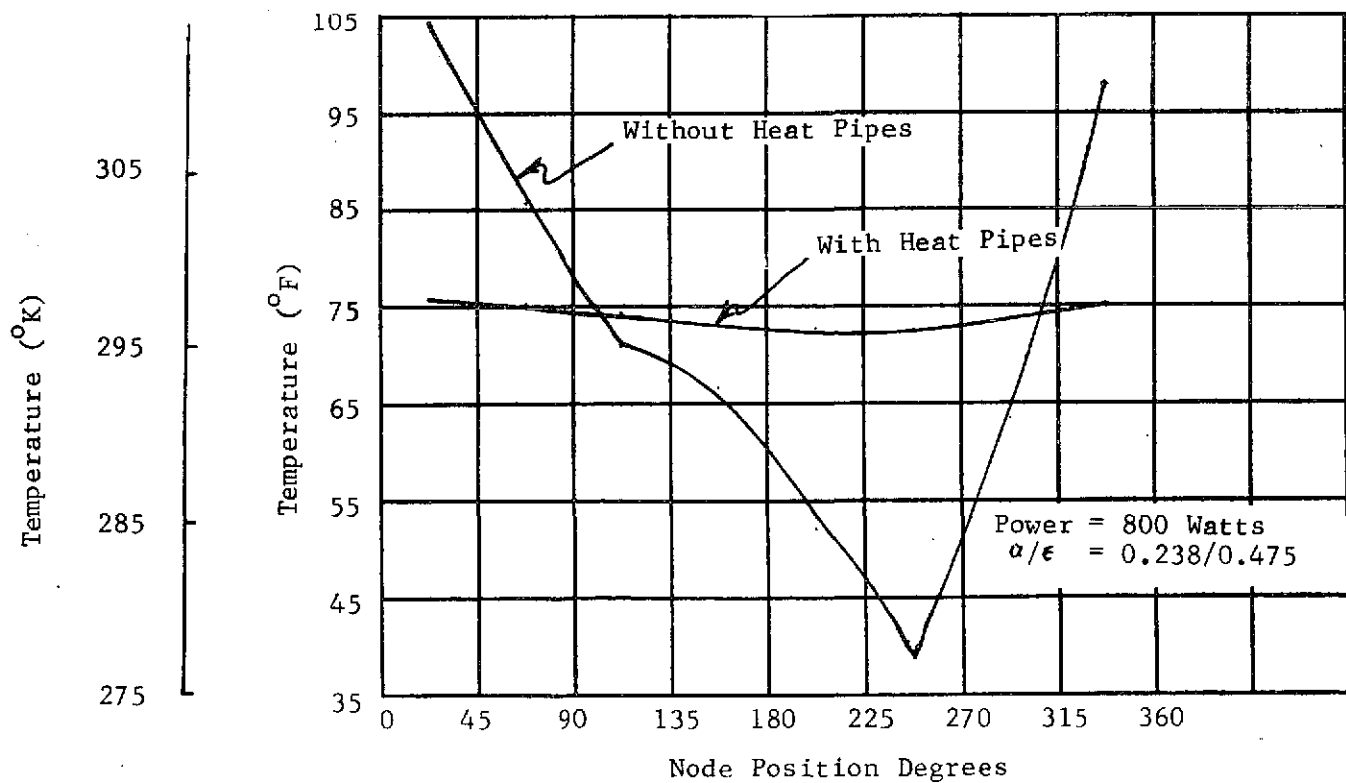*Forward Compartment Wall Temperatures, Geosynchronous (Vehicle in Sun)*

Figure 4-13
Forward Compartment Wall Temperature, Hot Case (Vehicle in Sun)
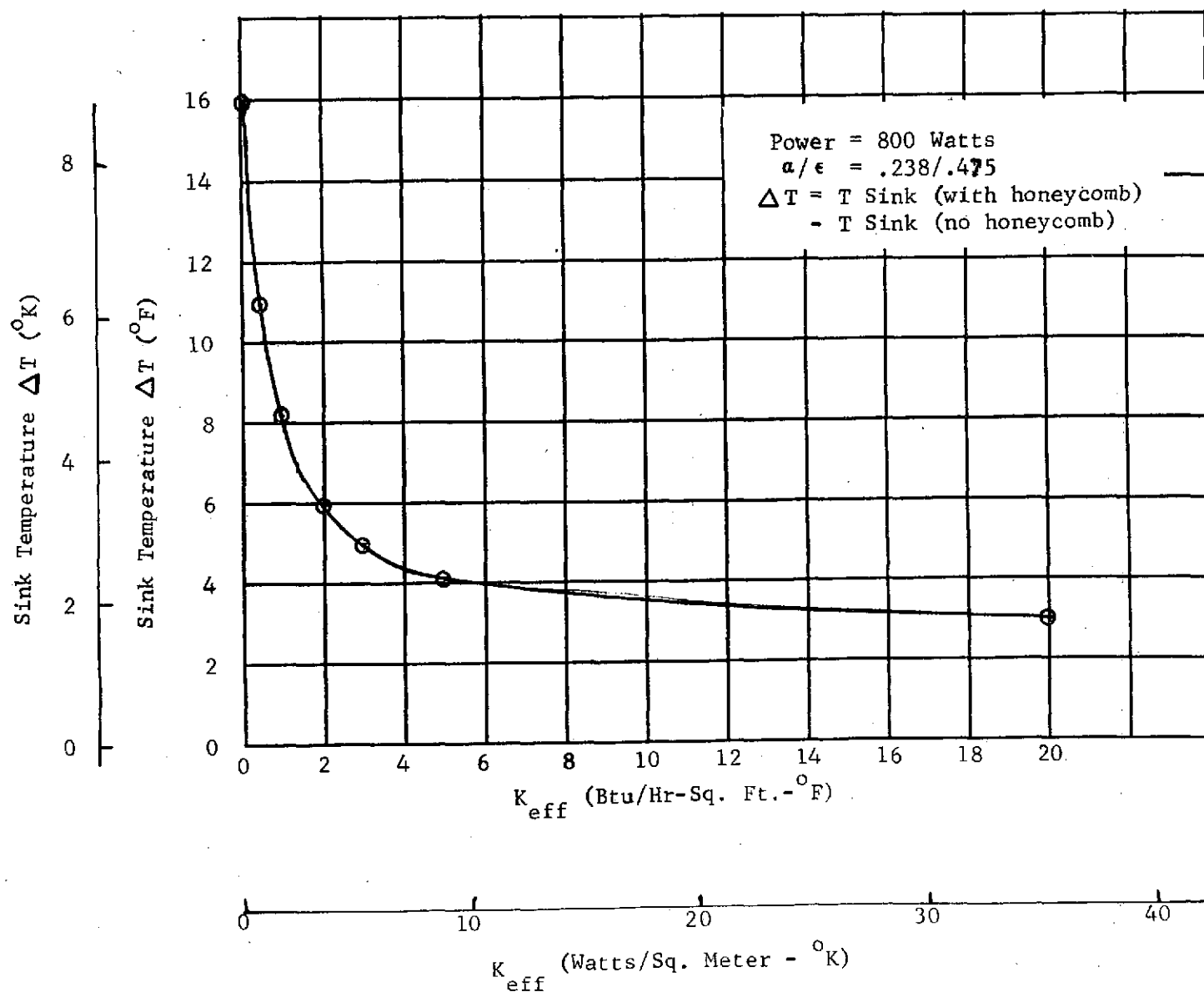
Figure 4-14

Figure 4-14
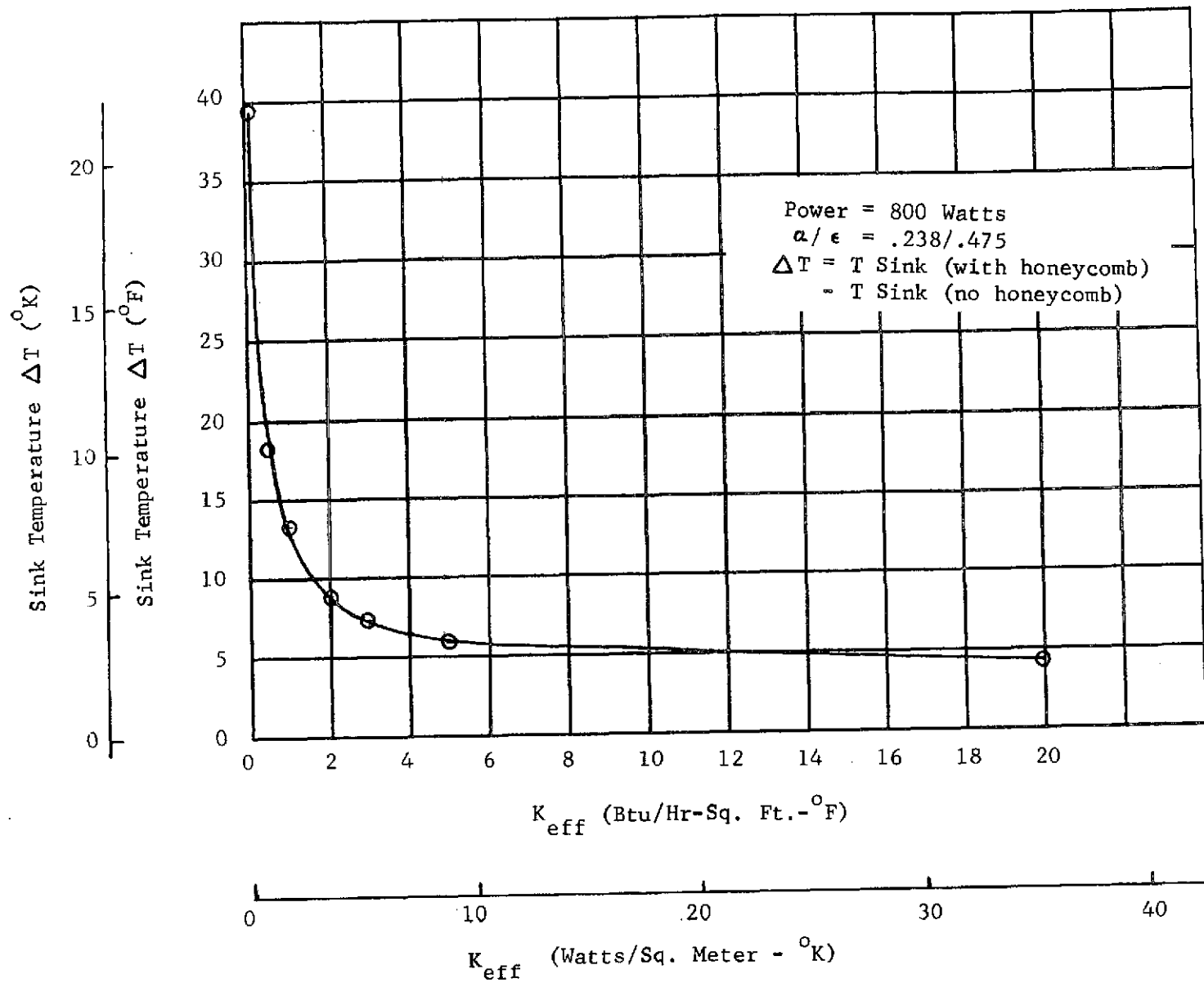Effect of Honeycomb Conductance on Compartment Sink Temperature, Hot Case

Figure 4-15
Effect of Honeycomb Conductance on Compartment Sink Temperature, Cold Case

5. TRANSIENT ANALYSIS

5.1 MODEL DESCRIPTION AND ASSUMPTIONS

A transient mission model was constructed to simulate an actual
Tug mission from liftoff through landing and subsequent cooldown.
This model was used to predict individual component temperature
histories along with the structural temperatures of the Tug vehicle.
The model incorporated the thermal control features resulting from
the previous studies using the steady-state sink temperature model.
These features include the use of heat pipes in the forward com-
partment, multilayer insulation on the forward compartment beta
cloth shield, and the external paint pattern determined from the
optical properties tradeoff studies. The transient model takes
both the thermal capacitance and a realistic power distribution
for each component into account in arriving at temperatures.

The overall transient mission model consists of two separate sub-
models for the forward and intertank compartments. The forward and
intertank compartment equipment is listed and described in Tables
5-1 and 5-2, respectively. Figure 5-1 is a TRASYS (Ref 9) computer
plot showing the forward compartment equipment, equipment identi-
fiers, node numbers, and their locations. An expanded rollout
view of the forward compartment is shown in Figure 5-2 and top view
is shown for clarity in Figure 5-3. The intertank equipment, equip-
ment location, and node numbers are shown in Figures 5-4 and 5-5.

The radiation network for the forward compartment consisted of 214
surfaces comprised of eight forward compartment cylinder walls, the
beta cloth shield, LH_2 forward dome, and 204 component surfaces.
The 214 original surfaces were reduced to 44 nodes for inclusion in
the thermal model. The radiation model for the intertank consists
of 56 surfaces condensed into 28 nodes. These include eight inter-
ior wall nodes, LH_2 and LOX domes, and 18 equipment nodes.

The six sides of each component were used in calculating the black-
body view factors using the TRASYS program. The view factors were
used to calculate the grey-body exchange factors also using TRASYS,
and were then condensed to single node components using the program
radiation condenser option.

Many thermal aspects of the mission analysis are common to both the
forward compartment and the intertank compartment models. The time
sequence of environments used is shown in Figure 5-6 and is presented
in Table 3-3. The liftoff and landing environments are controlled by
time varying boundary temperatures for the radiator doors and the

Table 5-1 Forward Compartment Equipment

Subsystem Equipment	Identifier	Quantity	Node Numbers	Data Reference Equipment Data Bank	Baseline* Document	Comments
Guideance, Navigation & Control						
Inertial Measurement Unit	IMU-11	1	300	x		Redundant unit
Star Tracker	ST-1	2	310, 320	x		Includes electronics
Horizon Scanner	HS-6	1	330	x		Redundant unit
Horizon Scanner Electronics	HSE-2	1	340	x		Redundant unit
Laser Radar	LR-2	2	350, 360	x		
Laser Radar Electronics	LRE-2	2	370, 380	x		
Television	TV-2	2	390, 400	x		
Data Management						
Computer	COMP-4	2	410, 420	x		
Data Acquisition Unit	--	6	530, 540		Page 67	Grouped in pairs in the thermal model.
Telemetry Formatter	--	2	560, 570		Page 67	
Data Bus Controller	--	2	580, 590		Page 67	
Tape Recorder	TR-1	1	490	x		
Communications						
Transponder, PM	TPM-1	2	430, 440	x		
Transmitter, FM	TFM-1	2	450, 460	x		
Decoder	DEC-1	2	470, 480	x		
Power Amplifier	PA-1	2	500, 510			
RF Multiplexer	RFM-1	1	520	x		
Hybrid Junction	--	1	600		Page 70	
Filter	--	1	610		Page 70	
Modulation processor	--	2	620, 630		Page 70	

*Reference 7 Baseline Tug Definition Document

Table 5-2 Intertank Compartment Equipment

System/Subsystem Equipment	Quantity	Node Numbers	Data Reference Equipment Data Bank	Baseline* Document	Comments
Auxiliary Propulsion System					
APS Tanks	8	201, 206, 221, 226 241, 246, 261, 266	X		
Valve Amplifier	1	290	X		
Main Propulsion System					
Helium Pressurization Spheres	4	231, 236, 251, 256	X		
Data Management Subsystem					
Data Acquisition Unit	2	280		Page 67	Grouped in pairs
Electrical Power Subsystem					
Fuel Cell FC1	1	300	X		
Battery	1	270	X		
LH$_2$ Sphere	1	211	X		
LOX Sphere	1	216	X		

*Reference 7 Baseline Tug Definition Document

5-2

TWO DATA ACQUISITION UNITS (540) (470, 480)
HYBRID JUNCTION DEC-1 (600)
FILTER (610)
TR-1 (490)
TELEMETRY FORMATTER (560, 570)
DATA BUS CONTROLLERS (580, 590)
MODULATION PROCESSORS (620, 630)
TWO DATA ACQUISITION UNITS (530)

IMU-11 (300)
ST-1 (310, 320)
TPM-1 (430, 440)
TFM-1 (450, 460)
RFM-1 (520)
PA-1 (500, 510)
LRE-2 (370)
TV-2 (390, 400)
LR-2 (350, 360)
LRE-2 (380)
COMP-4 (410, 420)
TWO DATA ACQUISITION UNITS (550)
HSE-2 (340)
HS-6 (330)

(300) Node Numbers
IMU-11 Equipment Identifier

Figure 5-1 Tug Forward Compartment Equipment

5-3

DATA ACQUISITION UNITS

TELEMETRY FORMATTER

DATA BUS CONTROLLER

DEC-1

TR-1

30"x 30"
ACCESS
DOOR

FILTER

HYBRID JUNCTION

ANTENNA

ST-1

IMU-11

TFM-1

TFM-1

RFM-1

PA-1

LRE-2

TV-2

ANTENNA

LR-2

VIEW A-A

VIEW LOOKING AFT

DATA ACQUISITION UNITS

DATA ACQUISITION UNITS

TELEMETRY FORMATTER

LRE-2

COMP-4

TV-2

LR-2

ANTENNA

HS-6

HSE-2

MODULATION
PROCESSOR

ANTENNA

DATA BUS CONTROLLER

SECTION C-C

VIEW B-B
ROTATED 180°

Figure 5-2   Tug Forward Compartment Equipment Locations

XX5 (TOP-TOWARD BETA CLOTH)
XX6 (BACK-TOWARD SKIRT)
XX4

TYPICAL COMPONENT
SURFACE NUMBERING
SYSTEM, NODE XXO
USED IN TRASYS
MODEL

XX2
XX1
XX3 (BOTTOM-TOWARD DOME)

540
300
430 TOP
450 MIDDLE
520 BELOW
8
310
320
500
510
440 TOP
460 BELOW
470 TOP
480 BELOW
370
7
2
600
490
390
610
31 (TANK DOME)
350
570 TOP
590 BELOW
560 TOP
580 BELOW
360
33 (BETA CLOTH)
400
6
3
380
410
630
420
620
550
530
340
4
5
330

Node Numbers are Used in MITAS

Figure 5-3 Tug Forward Compartment Interior Nodes

BATTERY (270)

DATA ACQUISITION
UNIT (280)

VALVE AMPLIFIER
UNIT (290)

FUEL CELL
(300)

(206)

APS TANKS
(201)

(261)
APS TANKS

(266)

(256)

HELIUM PRESSURIZATION
SPHERES

(251)

(246)
APS TANKS

(241)

FUEL CELL
LH$_2$ SPHERE (211)

FUEL CELL
LO$_2$ SPHERE (216)

(236)
HELIUM PRESSURIZATION
SPHERES

(231)

(226)
APS TANKS

(221)
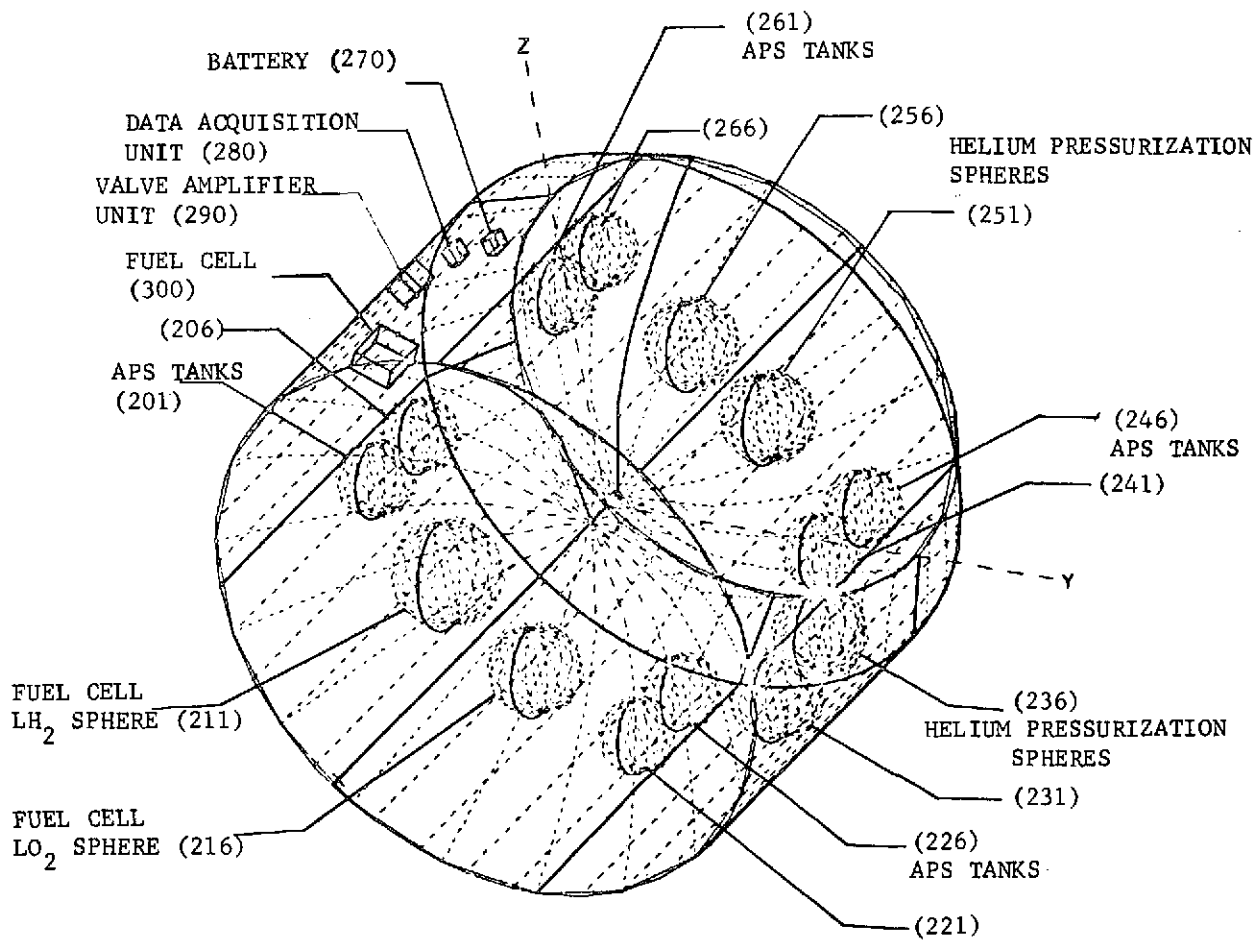
(226) Equipment Identifiers

Figure 5-4   Tug Intertank Compartment Equipment Nodes

( ) Indicates Nodes On Back Side
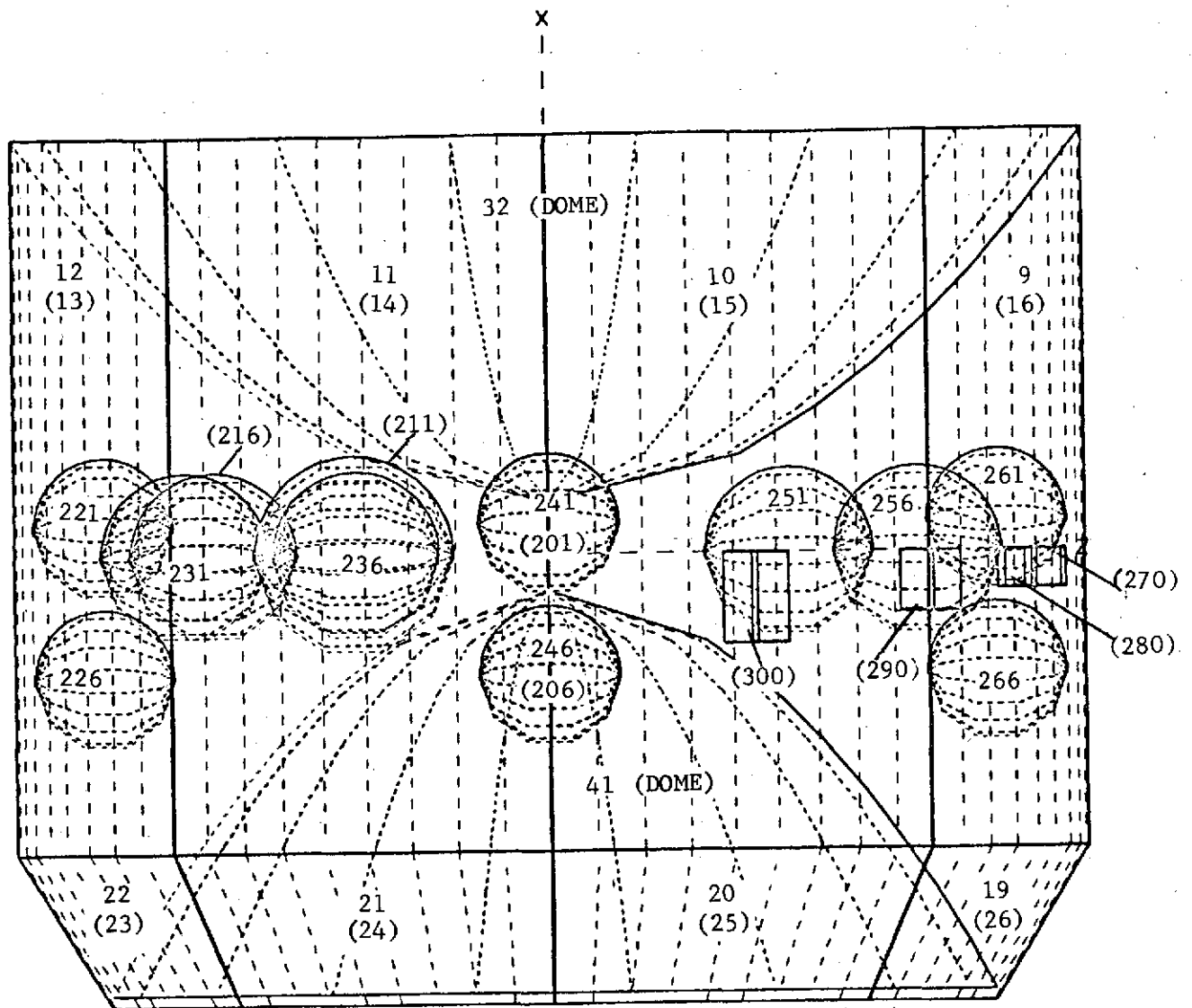
Figure 5-5 Tug Intertank Interior Nodes

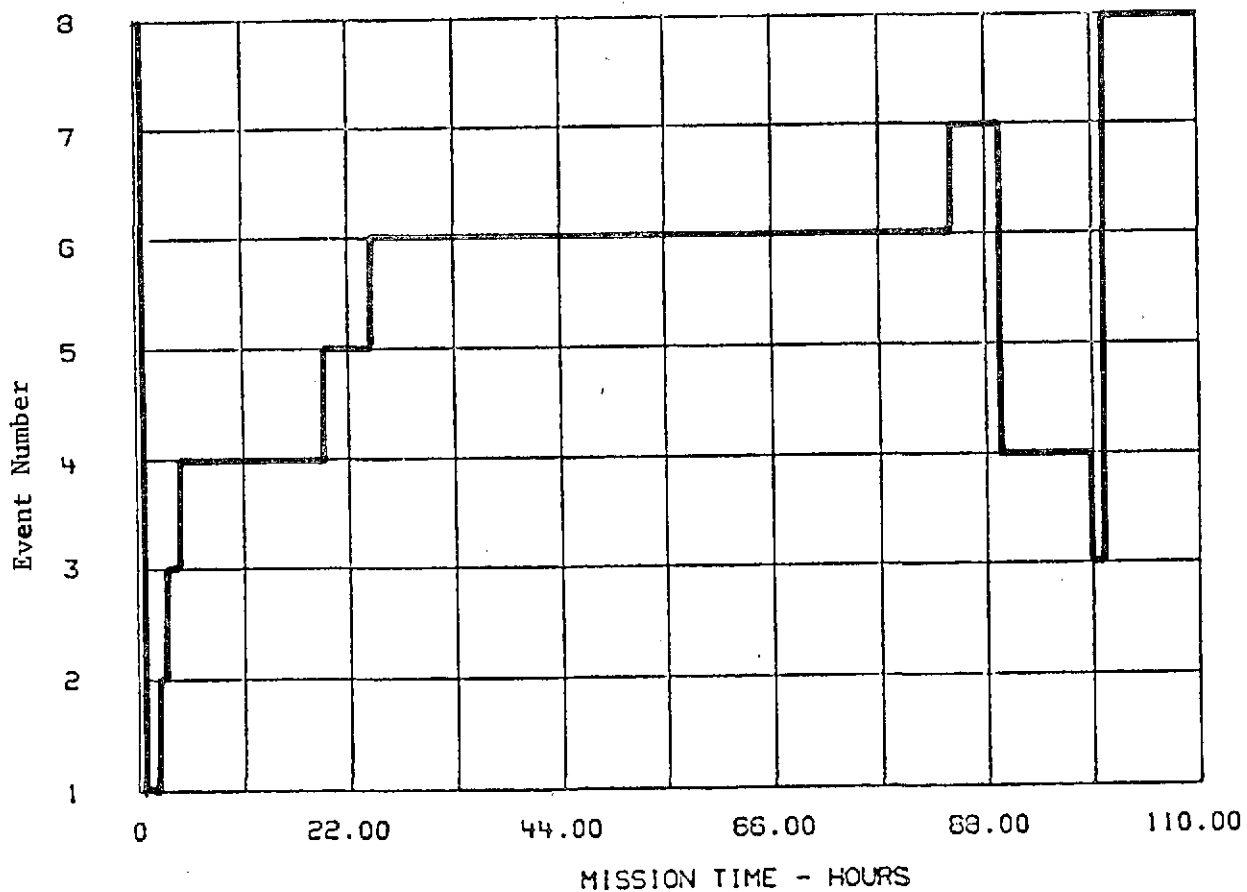| Event No.	Description
1	185 km Circular Orbit (Tug + Orbiter)
2	185 km x 296 km Transfer Orbit (Tug + Orbiter)
3	296 km Circular Orbit (Tug + Orbiter)
4	296 km Circular Orbiter (Case 4 – Tug Only)
5	296 km x 35,800 km Transfer Orbit (Tug Only)
6	35,800 km Geosynchronous Orbit (Tug Only)
7	35,800 km x 296 km Transfer Orbit (Tug Only)
8	Liftoff/Landing - Cooldown (Tug + Orbiter)

Figure 5-6   Tug Mission Event Sequence

cargo bay liner (ref 3). All on-orbit environments consist of the natural absorbed solar, albedo, and planetary heating, and were calculated using TRASYS in conjunction with the surface optical properties that were determined from the steady-state trade-off studies.

The Tug and orbiter radiation interchange was accounted for and depends on the vehicle configuration, which follows the events timeline shown in Figure 5-7. Additionally, convection interaction between the orbiter and the Tug was accounted for at liftoff and landing. A natural convection coefficient (h) was calculated with the use of the following correlation from Reference 10 for a horizontal wall.

$$N_u = 0.35 \left[G_r P_r \right]^{\frac{1}{4}}$$

where

N_u = Nusselt Number,

G_r = Grashof Number,

P_r = Prandtl Number.

Evlauating the properties of air at a temperature of 311°K (100°F) and assuming a constant acceleration of 2 g results in the following expression for

$$h = K \left[\rho^2 \Delta T \right]^{\frac{1}{4}}$$

where

$$K = 0.92278 \frac{watts}{meter^2 \, °K} = 0.5267 \frac{Btu}{hr \, ft^2 \, °F}$$

ρ = air density,

ΔT = temperature difference between orbiter cargo bay air temperature and the Tug skin

The air density is a function of altitude (taken from Reference 3), and input to the model as a time varying array. Also the quantity used for ΔT assumes that the entering air will be heated to the average cargo bay temperature as it passes through the orbiter structure. The resulting h value used in the model is shown in Figure 5-8.

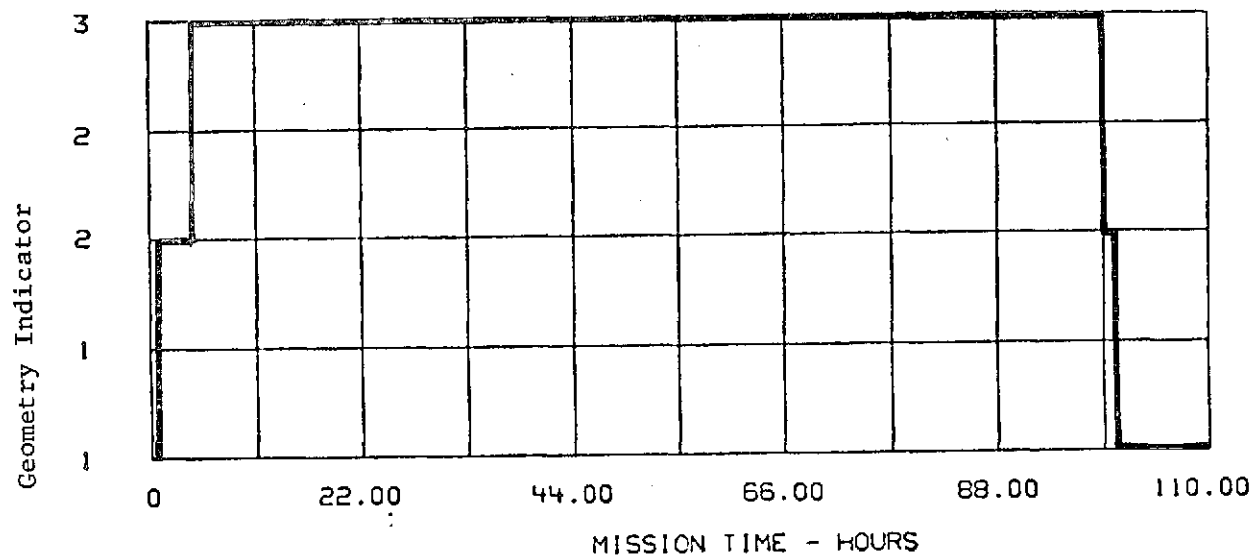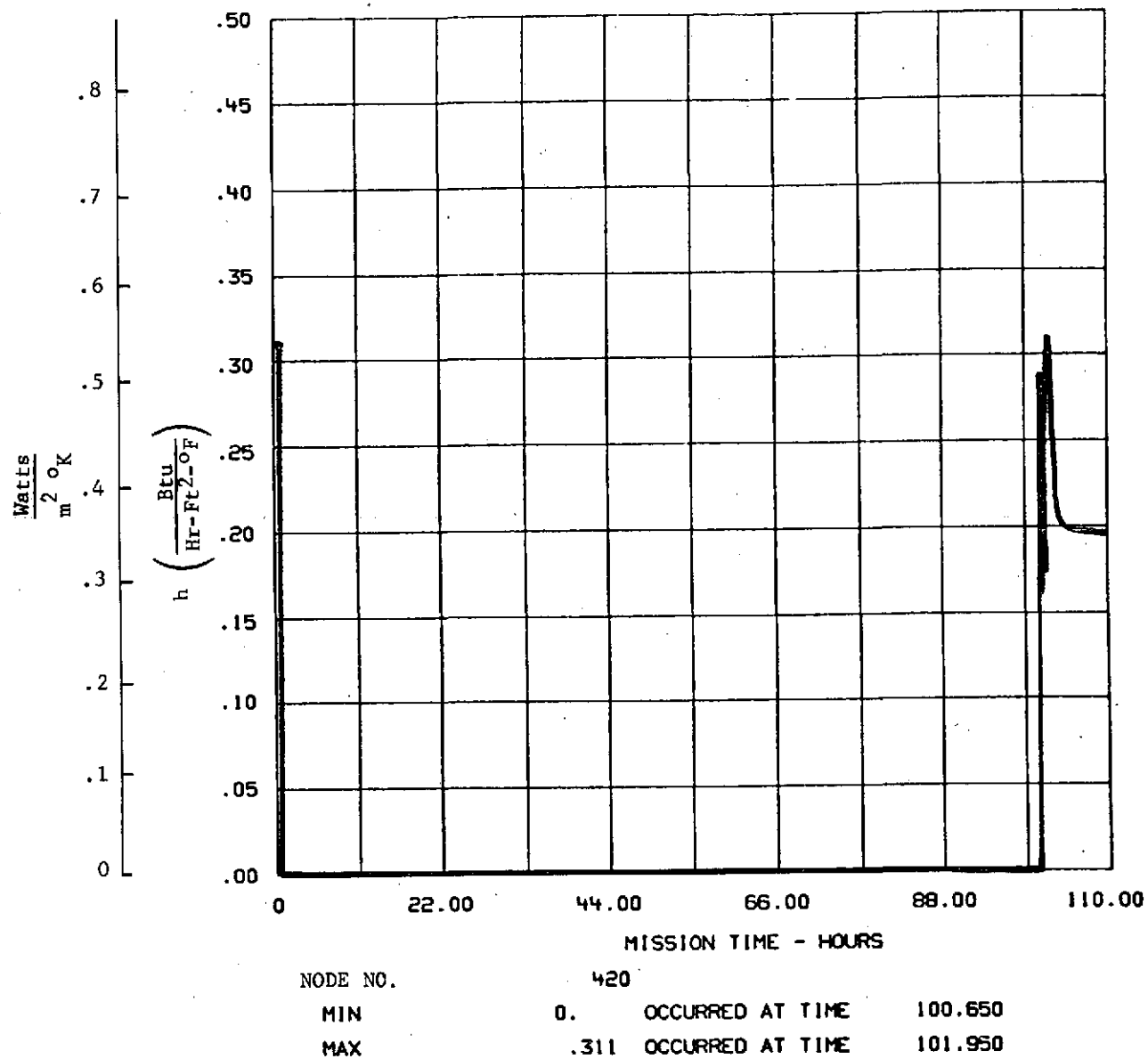| Indicator No.	Description
1	Tug in Orbiter, Doors Closed
2	Tug in Orbiter, Doors Open
3	Tug Deployed

Figure 5-7 Mission Geometry Sequence

Figure 5-8 Free Convection Heat Transfer Coefficient

A circumferential heat pipe was simulated in the forward compartment similar to the heat pipe used in the steady-state model. The major difference was that the fourth power average of the eight wall node temperatures was substituted for the calculated wall node temperature at the beginning of each time step. This technique saved computer time by reducing the number of iterations needed for each transient time step.

The emergency battery used in the intertank model also included a simulated louver system as shown in Figure 5-9. The battery was modeled assuming five of the sides were insulated with an integral 5 watt thermostatically controlled heater to maintain its storage temperature at 290.3°K (62.5°F) ± 1.39°K (2.5°F). The base of the battery was assumed to be coupled to a louver system whose blades were fully closed at 292°K (65°F) and fully open at 303°K (85°F). The louver system radiated to the external skin of the intertank. This assumed inner honeycomb paneling was removed from the louvered area. The effective emittance of the louver system was input to the model as function of the baseplate temperature and is shown in Figure 5-10. The battery was activated at 97.63 hours at which time 45 watts of internal energy were assumed to be generated within the battery for 0.5 hours.

The fuel cell was modeled as an insulated component that operated at a continuous boundary temperature of 356°K (180°F) until it is deactivated at 97.63 hours. At this time the fuel cell temperature was allowed to respond like any normal diffusion node.

A contact conductance value between the component and the mounting surface was calculated based on the number of bolted contacts assuming a $0.60 \frac{watts}{°K}$ $\left(1.13 \frac{Btu}{hr-°F} \right)$ conduction coupling per bolt for individual clip or rail mounts. This nominal value was taken from Reference 11 and based on aluminum bolted joints used in spacecraft application. In the final analysis, the original value had to be reduced for most of the components because the contact conductance couplings were dominating all other couplings. The component contact conductance used in the model along with other component thermal characteristics are given in Tables 5-3 and 5-5 for the forward compartment model and intertank compartment models respectively.

Transient analyses were run for two environment conditions designated "hot case" and "cold case." The hot case uses the environments time line described in Table 3-3 and shown in Figure 5-7 and the configuration time line shown in Figure 5-8. Component power dissipation cycles are indexed in Tables 5-3 thru 5-6. The hot case represents a mission consisting of a hot biased park orbit (Table 3-2, Case 4 park) and landing environment coupled with a hot geosynchronous orbit which included a cyclic shadow period (Table 3-2, case 7 geosynchronous).
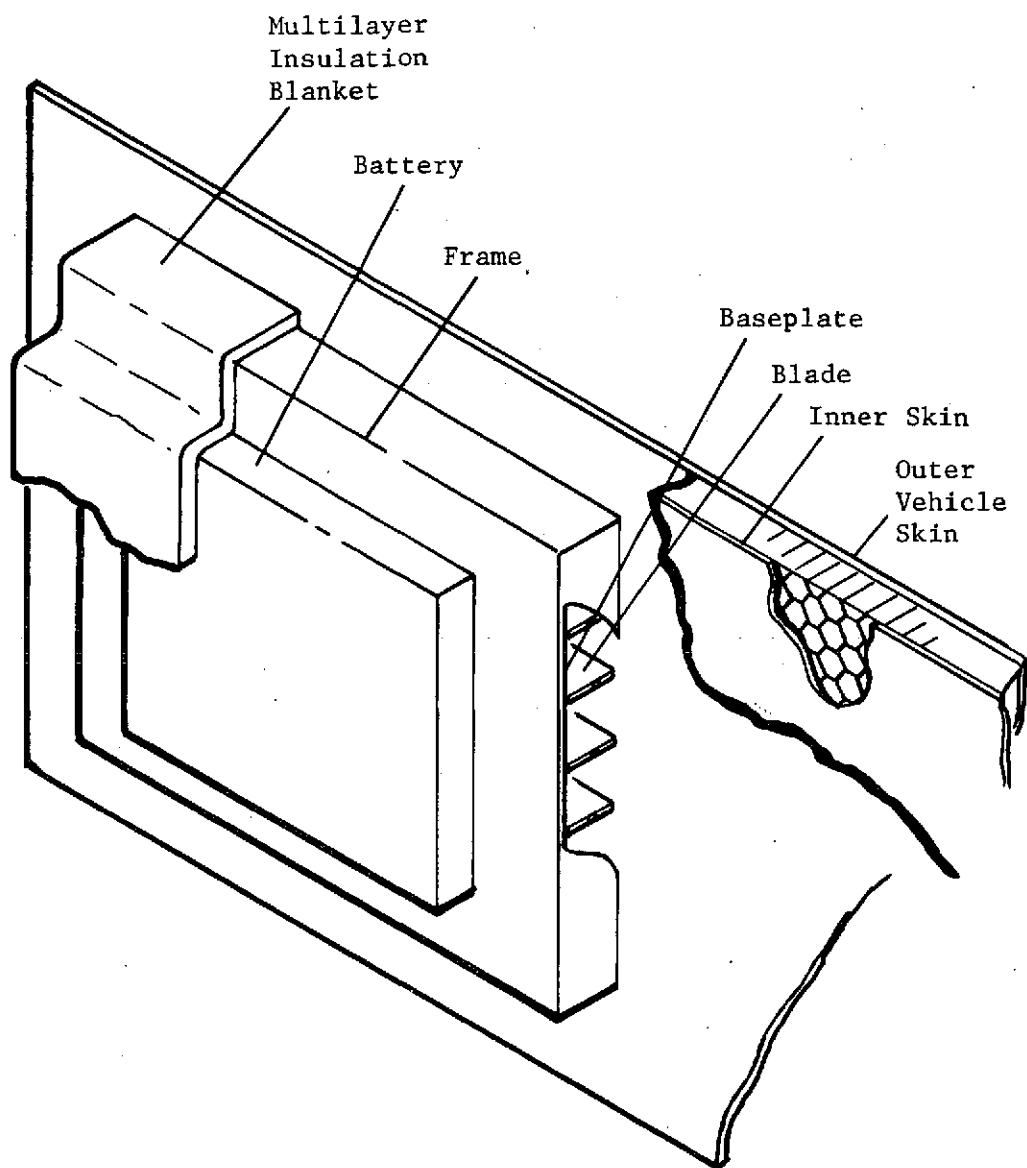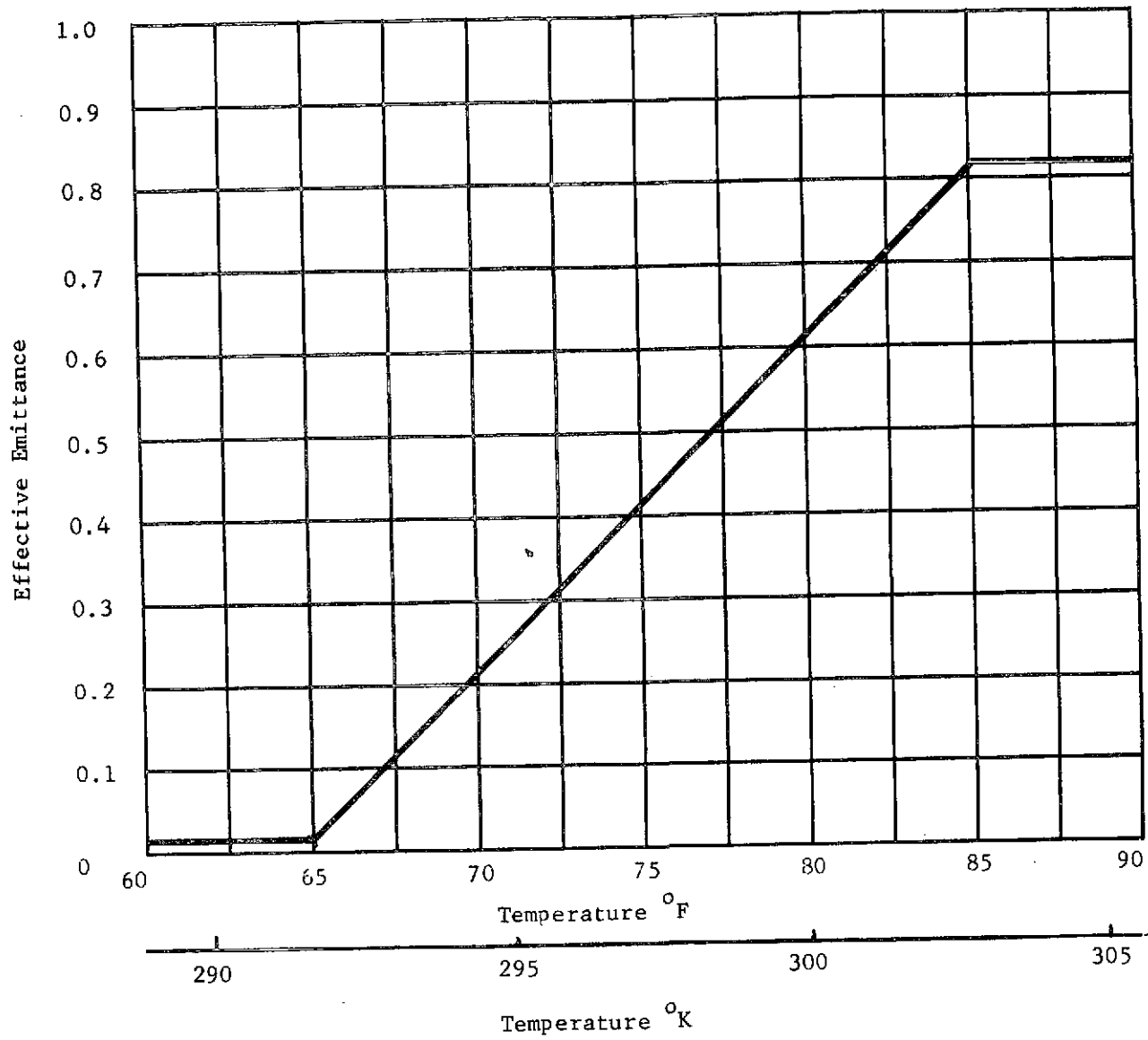
Figure 5-9 Louver System/Mounting Configuration

Figure 5-10   Louver System Effective Emittance Versus Battery Baseplate Temperature

Table 5-3   Forward Compartment Component and Hot-Case Summary

System/Component Name	Node No.	Surface Area, m²	ε	Contact Conductance, Watts °K	Thermal Mass, Watt-hr °K	Dissipated Power, watts	Power Time Line	Temperature History (Fig.)	Heater Duty Cycle (Fig.)	Heater Size, watts	Avg Heater Power Consumption watts
Guidance Navigation and Control											
Inertial Meas. Unit	300	0.544	0.90	3.57	6.91	144.0*	(1)	5-46	N/A	·	N/A
Star Tracker Pri	310	0.215	0.90	1.19	1.16	5.0	(2)	5-48	5-114	20	0.58
Star Tracker Sec	320	0.215	0.90	1.19	1.16	5.0	(2)	5-50	5-116	20	0.56
Horizon Scanner	330	0.218	0.90	1.79	0.79	10.0	(2)	5-52	5-118	15	0.40
Horizon Scanner Elec.	340	0.454	0.05	2.98	3.69	5.0	(2)	5-54	5-120	25	0.47
Laser Radar Pri	350	0.836	0.90	0.72	7.44	70.0	(3)	5-56	5-122	150	82.57
Laser Radar Sec	360	0.836	0.90	0.72	7.44	70.0	(3)	5-58	5-124	150	84.61
Laser Radar Elec Pri	370	0.557	0.90	0.47	2.11	30.0	(3)	5-60	5-126	150	65.32
Laser Radar Elec Sec	380	0.557	0.90	0.47	2.11	30.0	(3)	5-62	5.128	150	65.80
Television Pri	390	0.277	0.05	1.19	1.37	14.8	(4)	5-64	5-130	20	0.62
Television Sec	400	0.277	0.05	1.19	1.37	14.8	(4)	5-66	5-132	20	0.67
Data Management System											
Computer Pri	410	0.075	0.90	1.19	0.63	16.0	(1)	5-68	5-134	20	0.0
Computer Sec	420	0.075	0.90	1.19	0.63	16.0	(1)	5-70	5-136	20	0.0
Data Acc Unit 1,2	530	0.078	0.90	1.19	0.90	5.2	(5)	5-72	N/A	N/A	N/A
Data Acc Unit 3,4	540	0.078	0.90	1.19	0.90	5.2	(5)	5-74	N/A	N/A	N/A
Data Acc Unit 4,5	550	0.078	0.90	1.19	0.90	5.2	(5)	5-76	N/A	N/A	N/A
Tlmtry Frmtr Pri	560	0.139	0.90	1.19	0.63	7.0	(1)	5-78	N/A	N/A	N/A
Tlmtry Frmtr Sec	570	0.139	0.90	1.19	0.63	7.0	(1)	5-80	N/A	N/A	N/A
Data Bus Cont (Pri)	580	0.121	0.90	1.19	0.63	6.5	(1)	5-82	N/A	N/A	N/A
Data Bus Cont (Sec)	590	0.121	0.90	1.19	0.63	6.5	(1)	5-84	N/A	N/A	N/A
Tape Recorder	490	0.138	0.50	0.63	1.63	8.40	(1)	5-86	N/A	N/A	N/A
Communications System											
Transponder, PM Pri	430	0.122	0.85	1.79	0.42	6.2	(1)	5-88	N/A	N/A	N/A
Transponder, PM Sec	440	0.122	0.85	1.79	0.42	6.2	(1)	5-90	N/A	N/A	N/A
Transmitter, FM Pri	450	0.196	0.85	3.57	1.00	60.5	(1)	5-92	N/A	N/A	N/A
Transmitter, FM Sec	460	0.196	0.85	3.57	1.00	60.5	(1)	5-94	N/A	N/A	N/A
Decoder Pri	470	0.060	0.10	1.19	0.32	2.8	(1)	5-96	N/A	N/A	N/A
Decoder Sec	480	0.060	0.10	1.19	0.32	2.8	(1)	5-98	N/A	N/A	N/A
Power Amplifier Pri	500	0.018	0.90	0.60	0.05	16.2	(1)	5-100	N/A	N/A	N/A
Power Amplifier Sec	510	0.018	0.90	0.60	0.05	16.2	(1)	5-102	N/A	N/A	N/A
RF Multiplexer	520	0.130	0.85	0.60	0.47	0.0	N/A	5-104	N/A	15	0.0
Hybrid Junction	600	0.045	0.90	1.19	0.42	0.0	N/A	5-106	N/A	N/A	N/A
Filter	610	0.027	0.90	1.19	0.42	0.0	N/A	5-108	N/A	N/A	N/A
Modulation Proc Pri	620	0.153	0.90	1.79	1.47	7.5	(1)	5-110	N/A	N/A	N/A
Modulation Proc Sec	630	0.153	0.90	1.79	1.47	7.5	(1)	5-112	N/A	N/A	N/A

(1) Continuous power from liftoff to 98.92 hours.
(2) ON for 0.5 hours prior to each main engine burn per Table 3-1.
(3) Power on at 60.83 hours. Power off at 61.83 hours.
(4) Power on at 61.33 hours. Power off at 61.83 hours.
(5) Continuous power from liftoff through landing.

* Contains an internal heater.

Table 5-4

Table 5-4   Forward Compartment Cold-Case Summary

System Component Name	Node No.	Temp History (Fig.)	Heater Duty Cycle (Fig.)	Heater Size, watts	Average Heater Power Consumed, watts	System Component Name	Node No.	Temp. History (Fig.)	Heater Duty Cycle (Fig.)	Heater Size, watts	Average Heater Power Consumed, watts
Guidance Navigation & Control						Communications System					
Inertial Meas. Unit	300	5-47				Transponder, PM Pri	430	5-89			
Star Tracker Pri	310	5-49	5-115	20	20	Transponder, PM Sec	440	5-91			
Star Tracker Sec	320	5-51	5-117	20	20	Transmitter, FM Pri	450	5-93			
Horizon Scanner	330	5-53	5-119	15	15	Transmitter, FM Sec	460	5-95			
Horizon Scanner Elec.	340	5-55	5-121	25	25	Decoder, Pri	470	5-97			
Laser Radar Pri	350	5-57	5-123	150	150	Decoder, Sec	480	5-99			
Laser Radar Sec	360	5-59	5-125	150	150	Power Amplfr. Pri	500	5-101			
Laser Radar Elec Pri	370	5-61	5-127	150	150	Power Amplfr. Sec	510	5-103			
Laser Radar Elec Sec	380	5-63	5-129	150	150	RF Multiplexer	520	5-105		15	15
Television Pri	390	5-65	5-131	20	20	Hybrid Junction	600	5-107	N/A	N/A	N/A
Television Sec	400	5-67	5-133	20	20	Filter	610	5-109	N/A	N/A	N/A
Data Management						Modulation Processor, Pri	620	5-111	N/A	N/A	N/A
						Modulation Processor, Sec	630	5-113	N/A	N/A	N/A
Computer Pri	410	5-69	5-135	20	20						
Computer Sec	420	5-71	5-137	20	20						
Data Acc Unit 1,2	530	5-73	N/A	N/A	N/A						
Data Acc Unit 3,4	540	5-75	N/A	N/A	N/A						
Data Acc Unit 4,5	550	5-77	N/A	N/A	N/A						
Tlmtry Frmtr Pri	560	5-79	N/A	N/A	N/A						
Tlmtry Frmtr Sec	570	5-81	N/A	N/A	N/A						
Data Bus Cont Pri	580	5-83	N/A	N/A	N/A						
Data Bus Cont. Sec	590	5-85	N/A	N/A	N/A						
Tape Recorder	490	5-87	N/A	N/A	N/A						

Table 5-5 Intertank Compartment Component and Hot-Case Summary

System/ Component Name	Node No.	Surface Area, m^2	ε	Contact Conductance, Watts $^\circ K$	Thermal Mass, Watt-hr $^\circ K$	Oper. Power, watts	Power Time Line	Temp- erature History (Fig.)	Heater Size, watts	Average Heater Power Consump- tion, watts
Auxiliary Propulsion System										
APS Tanks	601*	1.028	$0.10^{(1)}$	Isolated	Heater Node	N/A	N/A	5-178**	1	0.04
Valve Amplifier	290	0.225	0.90	0.36	1.33	38.0	(2)	5-180	N/A	N/A
MainPropulsion Sys.										
Helium Press Spheres	231*	1.487	$0.10^{(1)}$	Isolated	Arithmetic Nodes	N/A	N/A	5-182	N/A	N/A
Data Management Sys.										
Data Acc Unit	280	0.078	0.90	0.24	0.89	5.2	(3)	5-184	N/A	N/A

(1) Represents emissivity of insulation blanket.
(2) Continuous power from liftoff to 98.92 hours.
(3) Continuous power from liftoff through landing.
 * 601 is representative of the eight APS tanks.
    231 is representative of the 4 helium pressurization spheres.
** Represents the temperature of outside insulation blanket.

Table 5-5 (concl)

System Component Name	Node No.	Surface Area m^2	ε	Contact Conductance, Watts $^\circ$K	Thermal Mass Watt-hr $^\circ$K	Oper. Power, watts	Power Time, watts	Temperature History (Fig.)	Heater Duty Cycle (Fig.)	Heater Size, watts	Average Heater Power Consumption, watts
Electrical Power Subsystem											
LH$_2$ Sphere	211	2.088	0.10(1)	Isolated	Arithmetic Node	N/A	N/A	5-186*	N/A	N/A	N/A
LOX Sphere	216	1.487	0.10(1)	Isolated	Arithmetic Node	N/A	N/A	5-188*	N/A	N/A	N/A
Battery**	275	0.140	0.10(1)	Louvered	1.11	45W		5-190	5-194	5	0.02
Fuel Cell***	433	0.445	0.10(1)	0.234	0.64	N/A	N/A	5-192	N/A	N/A	N/A

(1) Represents emissivity of insulation blanket.
*   Represents temperature of outside of insulation blanket.
**   Five sides of the battery are insulated 0.11 m^2 (1.19 ft^2), = 0.1. The base 0.29 m^2 (0.3125 ft^2) is covered by louvers (ε shown in Figure 5-10).
*** The fuel cell temperature is held at a constant 356°K (180°F) until 97.63 hours when its temperature is calculated normally.

Table 5-5 (concl)

Table 5-6 Intertank Compartment Cold-Case Summary

System/ Component Name	Node No.	Temperature History (Fig.)	Heater Duty Cycle (Fig.)	Heater Size, watts	Average Heater Power Consumed, watts
Aux. Propulsion System					
APS Tanks	601*	5-179**	N/A	.2	.16
Valve Amplifier	290	5-181**	N/A		N/A
Main Propl'sn System					
Helium Press Sphere	231*	5-183	N/A		N/A
Data Mgmt System					
Data Acc. Unit	280	5-185	N/A		N/A
Elec. Power Subsys.					
LH$_2$ Sphere	211	5-187	N/A		N/A
LOX Sphere	216	5-189	N/A		N/A
Battery	275	5-191	5-195		N/A
Fuel Cell	433	5-193	N/A		N/A

*   601 is representative of the eight APS tanks; 231 is representative of the four helium spheres.

**   Represents temperature of outside insulation blanket.

***   Represents net heat transfer to maintain fluid at 278°K (40°F).

The cold case used environments consistent with the hot case until 24.35 hours, corresponding to the first shadow point in geosynchronous orbit. At this time the Tug was reoriented with the longitudinal axis parallel to the solar vector (Table 3-2, Case 8 geosynchronous) to minimize external orbital heating. Component power dissipation cycles continued as in the hot case. The cold-case simulation was terminated at 45 hours.

5.2   FORWARD COMPARTMENT RESULTS

The results of the hot and cold cases for the forward compartment analyzed are summarized in Tables 5-3 and 5-4. Many of the forward compartment components had simulated thermostatically controlled heaters to maintain their temperature limits.

Each component was reviewed after the initial hot case run for compatibility with its allowable temperature limits while the compartment power was at the 800-watt level. Energy balances were performed on the components that dropped below their lower temperature limits to determine major heat leaks and heater sizing requirements. As previously discussed, the mounting conduction was reduced and heaters added where required. The heaters were sized to maintain the lower temperature limit of each component in the hot case. During this exercise, it became apparent that excessive heater power was being consumed for the hot case and this was expected to be significantly worst in the later cold-case run. The cold-case run was performed to further determine heater requirements. These runs pointed to the need for an alternative thermal control concept to avoid the excessive heater power consumption.

The total heater energy required by these components was calculated by time integrating the instantaneous heater power over the total mission duration. Individual component heater powers are tabulated in Table 5-3 and the total integrated heater energy for the entire forward compartment is shown in Figures 5-11 and 5-12 for the hot and cold cases, respectively. The hot-case mission resulted in an average of 275 watts of heater power over most of the mission. The cold-case mission consumed an average of 774 watts of heater power after 25 hours in the mission. This was not sufficient to maintain the component lower temperature limits. This emphasizes the need to alter the thermal control concept originally chosen. The transient model wall nodes are shown in Figure 5-13 and the hot and cold case temperature results for these nodes are given in Figures 5-14 thru 5-45. Figures 5-46 thru 5-137 present the forward component temperatures.

The remaining areas of the forward compartment are presented in Figures 5-138 thru 5-143. Figures 5-138 and 5-139 present the outer layer of insulation on the LH_2 tank dome temperature for the hot and cold cases. Figures 5-140 and 5-141 present the forward shield inner surface temperatures and Figures 5-142 and 5-143 present the outer surface (beta cloth) temperatures for the hot and cold cases respectively. Figures 5-144 and 5-145 present the forward compartment internal sink temperatures derived from each case. Comparison of these data with the previous steady-state results accounts for the honeycomb ΔT and should be compared only where steady-state conditions exist.

5.3 INTERTANK COMPARTMENT RESULTS

The intertank compartment results are presented beginning with the outer and inside skin temperatures in Figures 5-146 through 5-177. Tables 5-5 and 5-6 summarize the component data and refer to the appropriate figures for the hot and cold case temperature results. This compartment contains several tanks as shown in Figures 5-4 and 5-5, hence the data presented in the report is representative of each of the various types of tanks. Figure 5-178 presents the insulation temperature for one of the eight APS tanks where each tank was controlled to 278°K (40°F). Node 231, Figure 5-182, presents representative data for the four helium pressurization spheres. The fuel cell LH_2 and LOX tank plots represent the insulation temperatures. Each tank was held at its liquid temperature during the mission simulations. Insulation properties derived from Reference 5 were used on the LH_2, LOX, and APS tanks, assuming the configuration is as applied to the forward shield.

The LH_2 tank lower dome insulation and LOX tank upper dome insulation temperatures are presented in Figures 5-196 thru 5-199. The intertank compartment sink temperature is presented in Figures 5-200 and 5-201.

NODE NO.   115   Forward Compartment   Integrated Power

MIN   OF   0.   OCCURRED AT TIME   0.

MAX   OF   113227.128   OCCURRED AT TIME   110.000
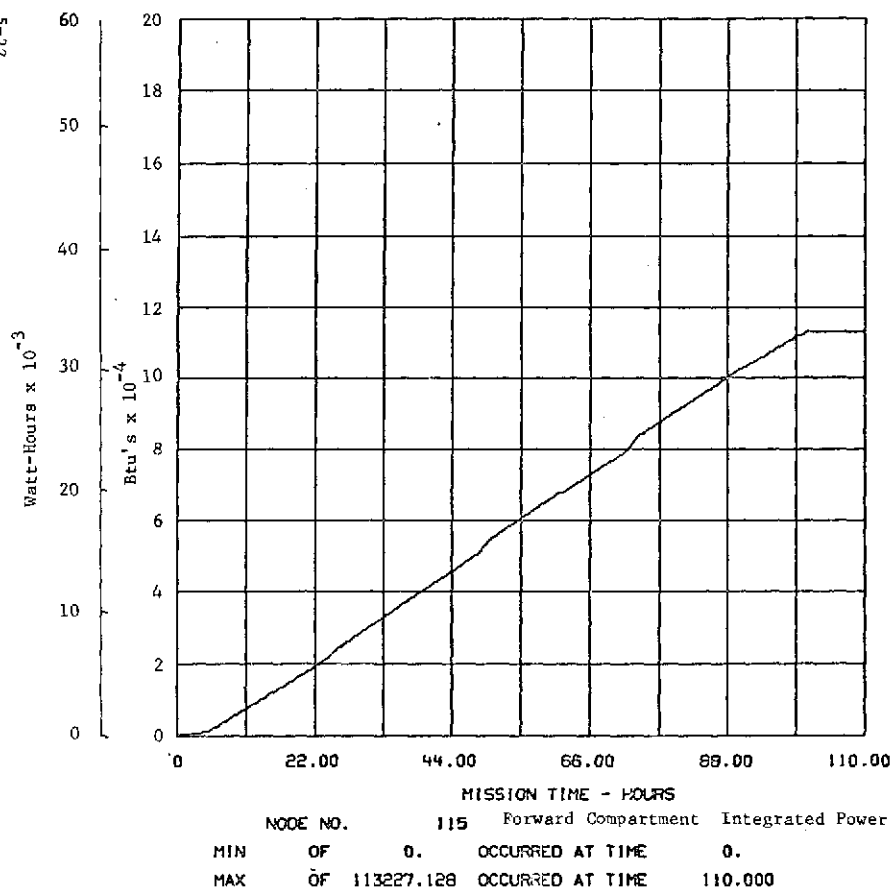
FIGURE 5-11.   ANALYSIS OF TUG FWD. COMP. + COMPONENTS WITH HEAT PIPES

NODE NO.   115   Forward Compartment   Integrated Power

MIN   OF   0.   OCCURRED AT TIME   0.

MAX   OF   75830.034   OCCURRED AT TIME   45.000
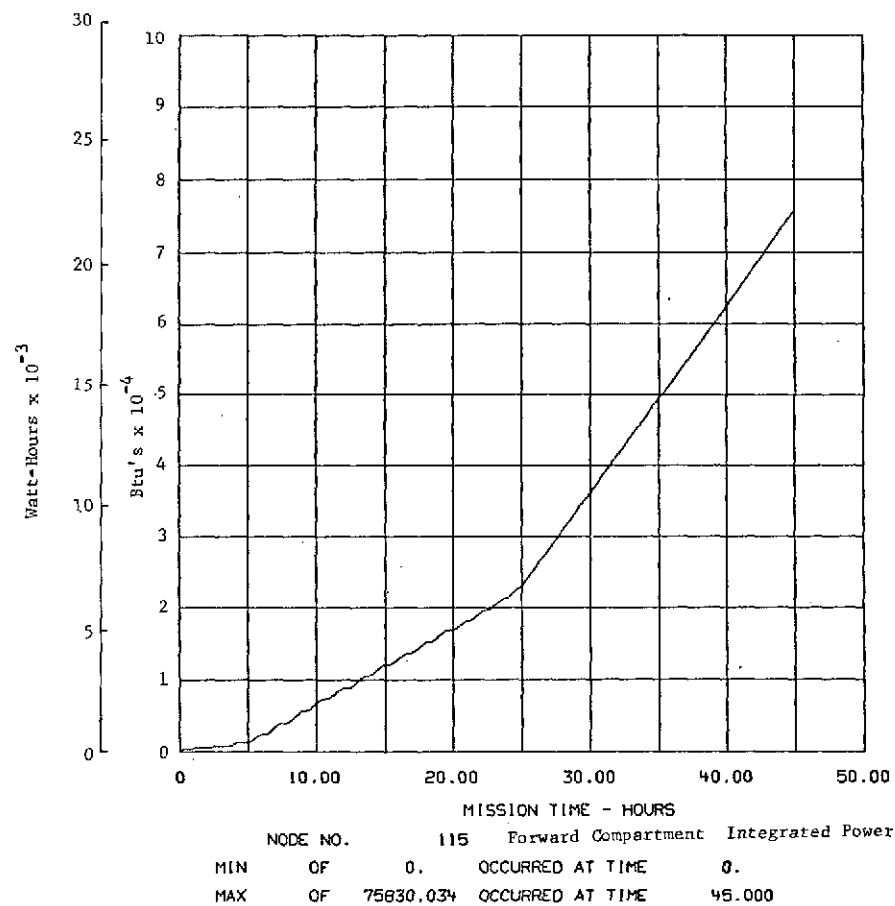
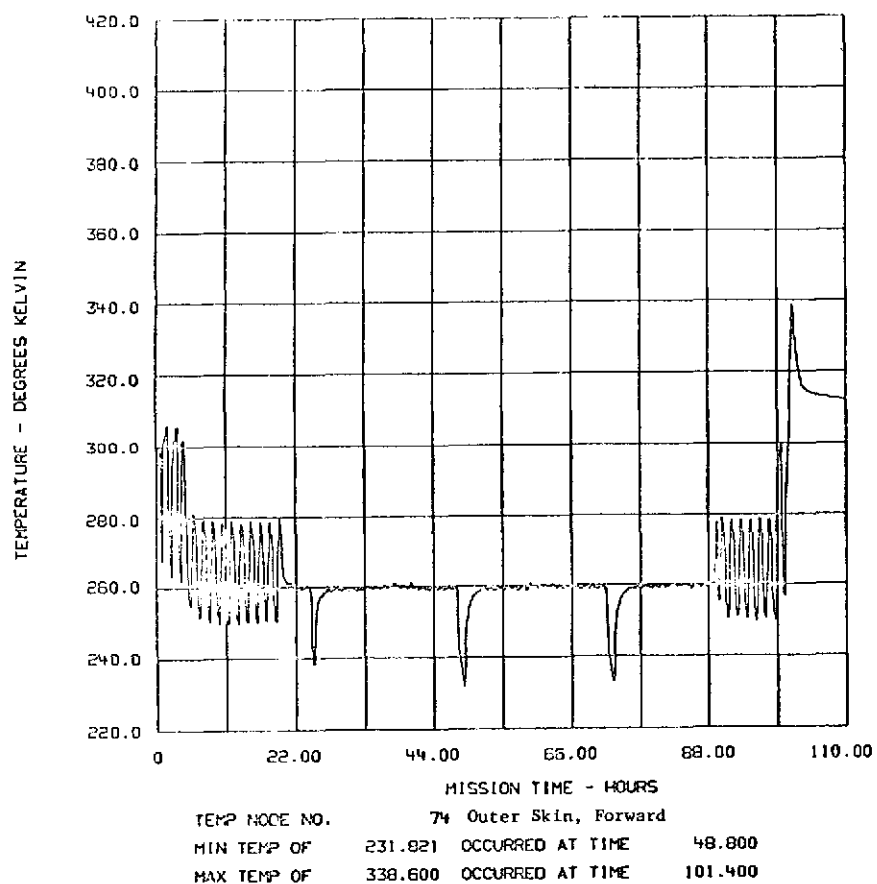FIGURE 5-12 .   ANALYSIS OF TUG FWD. COMP. STATIONED AT GEO. SHADOW PT.

Forward Comp.	71 (1)	72 (2)	73 (3)	74 (4)	75 (5)	76 (6)	77 (7)	78 (8)

Intertank Comp.	81 (9)	82 (10)	83 (11)	84 (12)	85 (13)	86 (14)	87 (15)	88 (16)

+Z   +Y   -Z   -Y   +Z

(   ) Interior Nodes
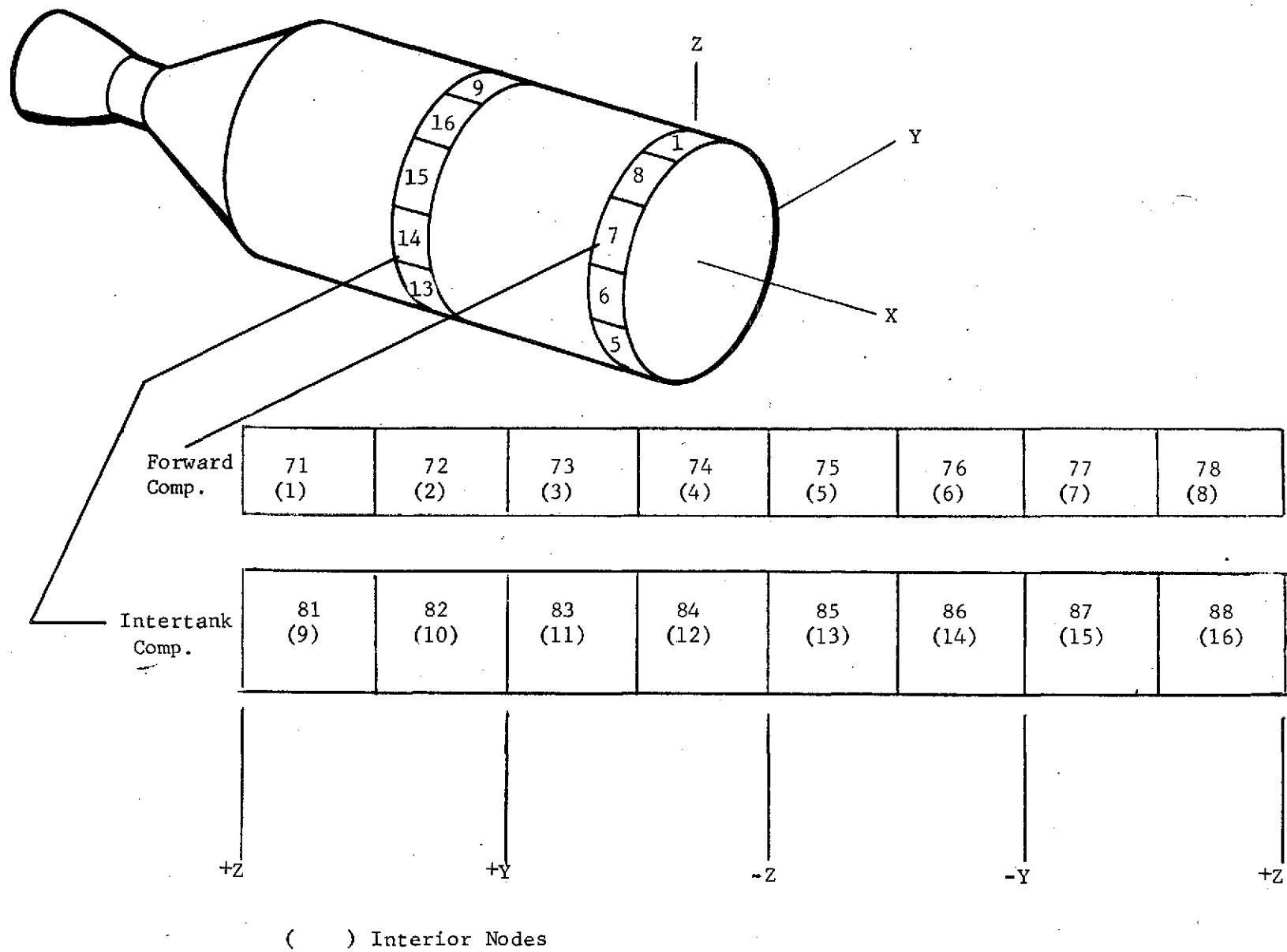
Figure 5-13. Transient Modal Skin Nodes
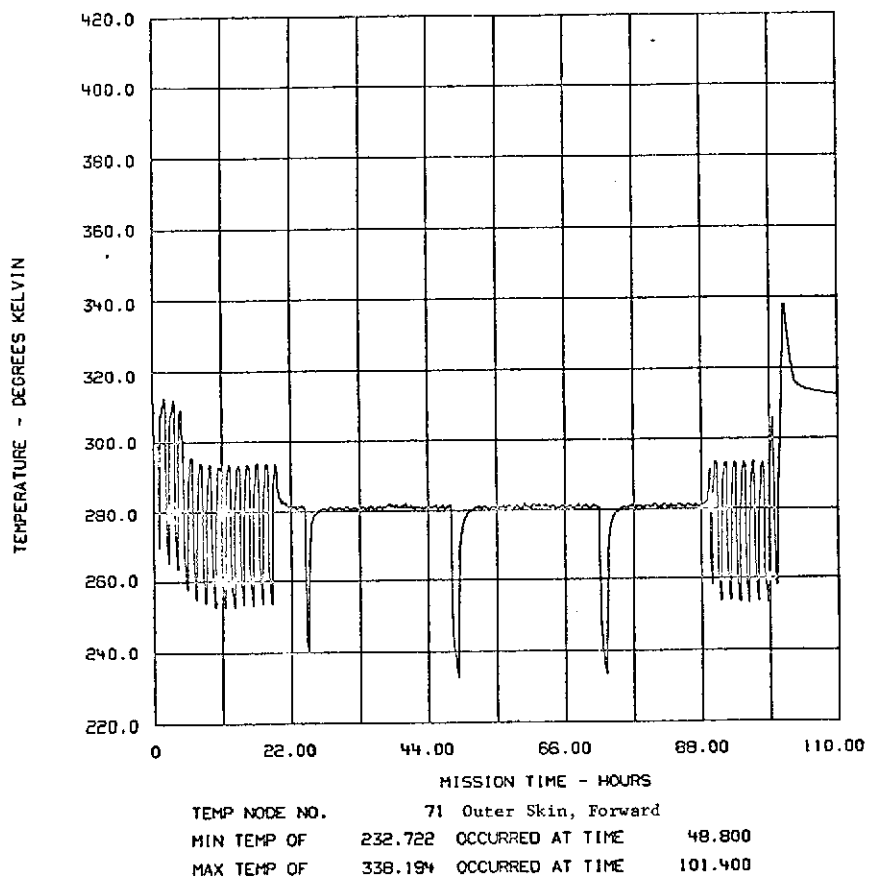
FIGURE 5-14 .   ANALYSIS OF TUG FWD. COMP. + COMPONENTS WITH HEAT PIPES

TEMP NODE NO.   71 Outer Skin, Forward
MIN TEMP OF   232.722 OCCURRED AT TIME   48.800
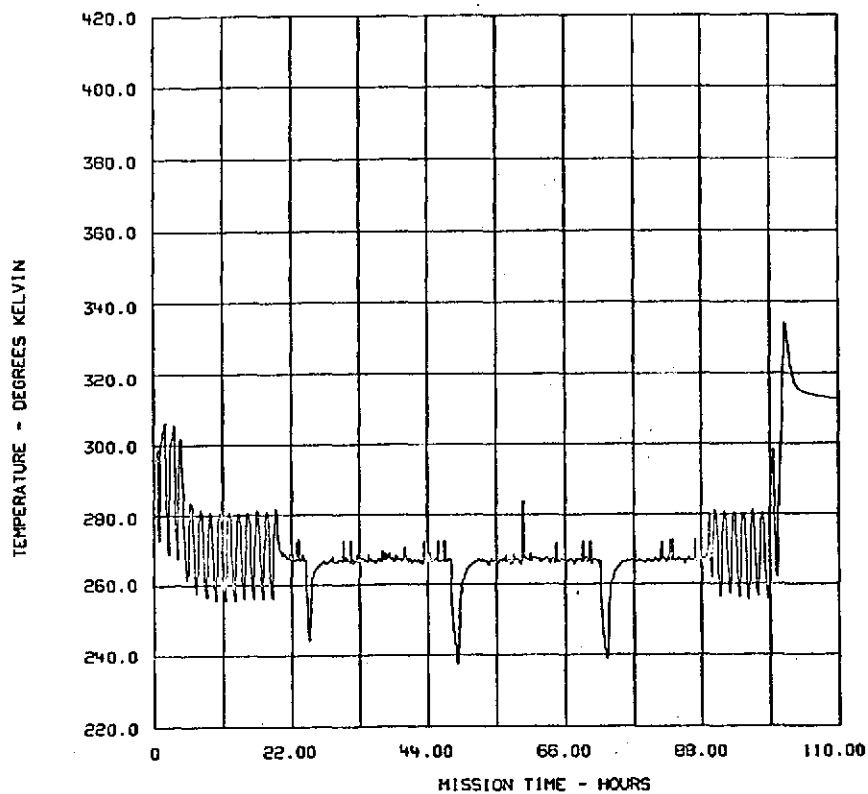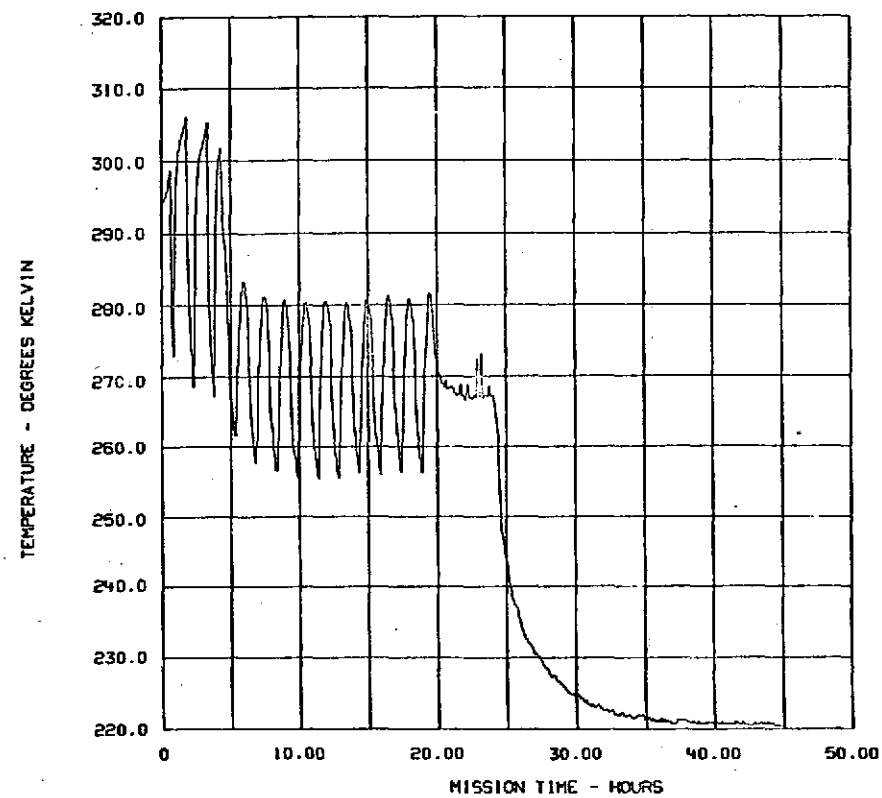MAX TEMP OF   338.194 OCCURRED AT TIME   101.400
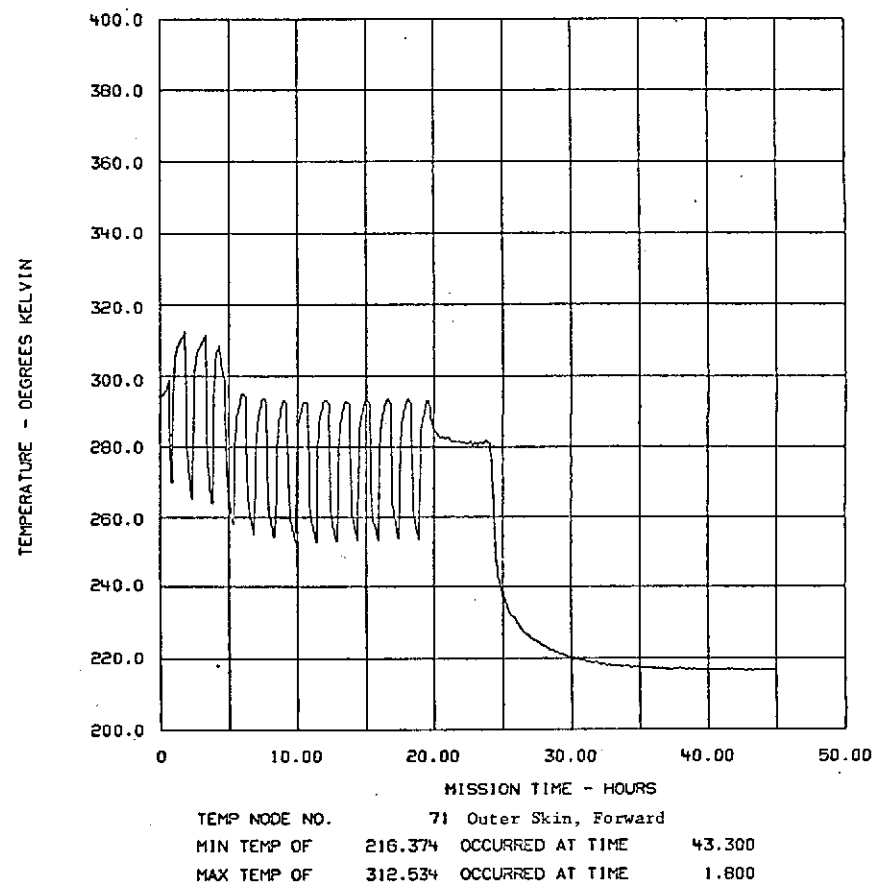
FIGURE 5-15 .   ANALYSIS OF TUG FWD. COMP. STATIONED AT GEO. SHADOW PT.

TEMP NODE NO.   71 Outer Skin, Forward
MIN TEMP OF   216.374 OCCURRED AT TIME   43.300
MAX TEMP OF   312.534 OCCURRED AT TIME   1.800
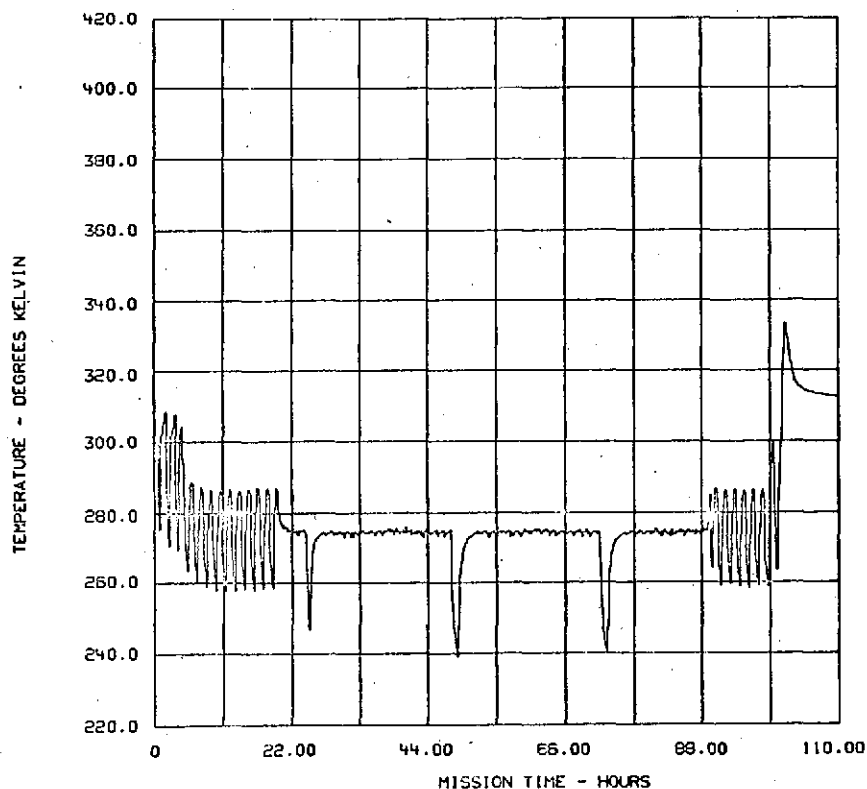
FIGURE 5-16 . ANALYSIS OF TUG FWD. COMP. + COMPONENTS WITH HEAT PIPES

TEMP NODE NO.   1 Inner Skin, Forward
MIN TEMP OF   239.889   OCCURRED AT TIME   49.800
MAX TEMP OF   333.599   OCCURRED AT TIME   101.400
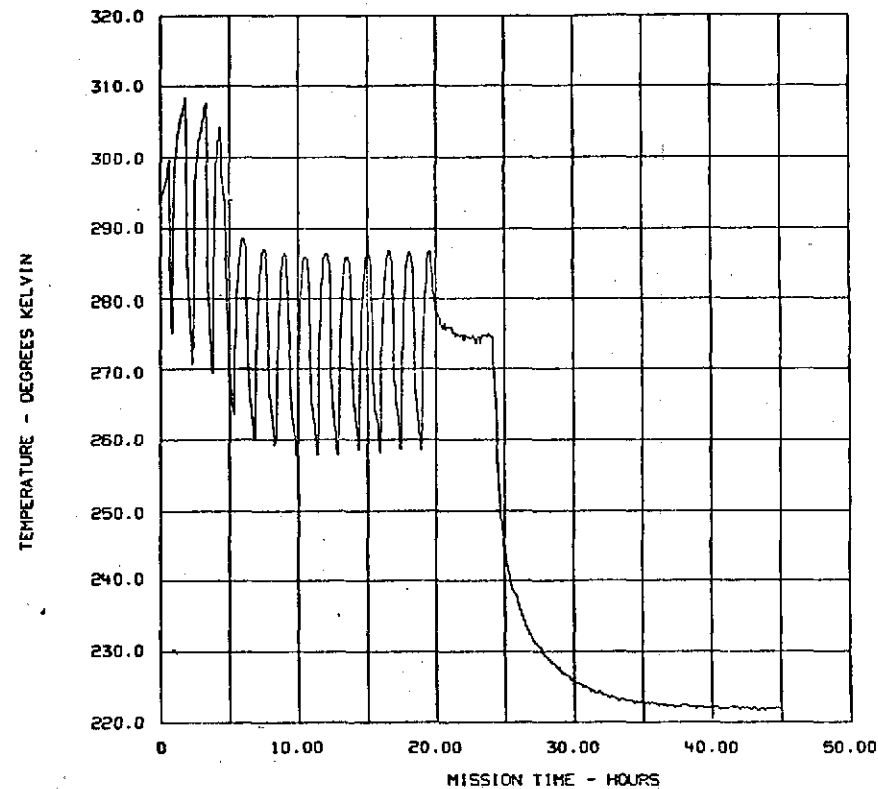
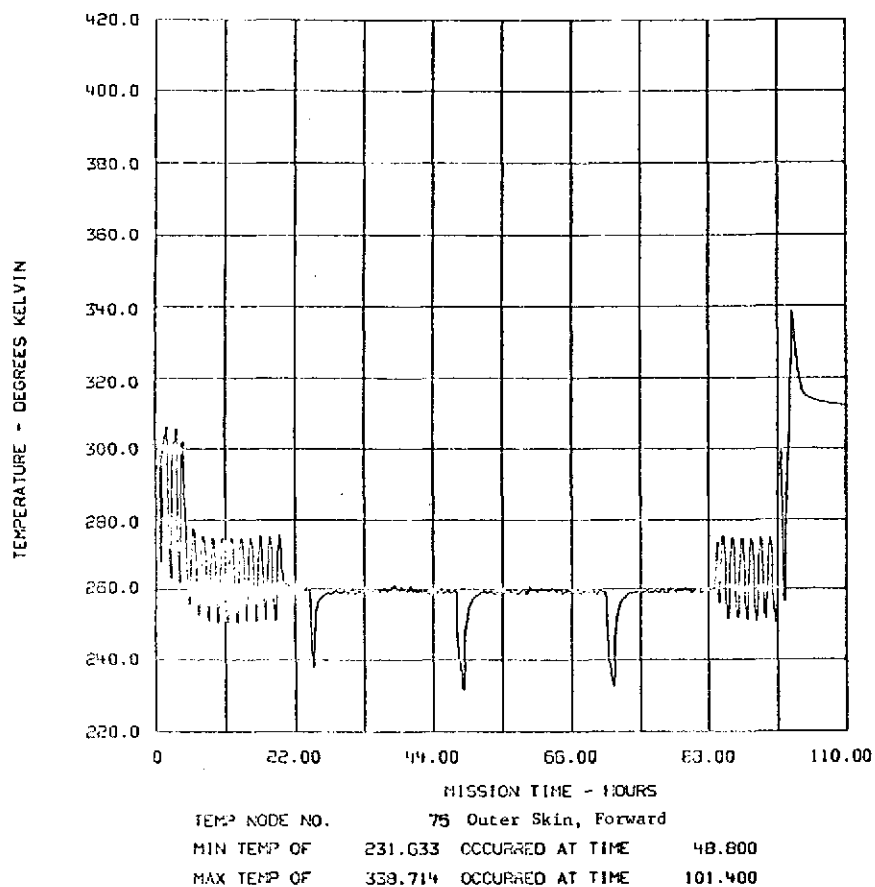FIGURE 5-17 . ANALYSIS OF TUG FWD. COMP. STATIONED AT GEO. SHADOW PT.

TEMP NODE NO.   1 Inner Skin, Forward
MIN TEMP OF   221.588   OCCURRED AT TIME   43.300
MAX TEMP OF   308.466   OCCURRED AT TIME   1.800

TEMPERATURE - DEGREES KELVIN

420.0
400.0
330.0
250.0
310.0
220.0
300.0
280.0
260.0
240.0
220.0

0   22.00   44.00   66.00   88.00   110.00
MISSION TIME - HOURS

TEMP NODE NO.   72 Outer Skin, Forward
MIN TEMP OF   232.435 OCCURRED AT TIME   48.800
MAX TEMP OF   338.113 OCCURRED AT TIME   101.400
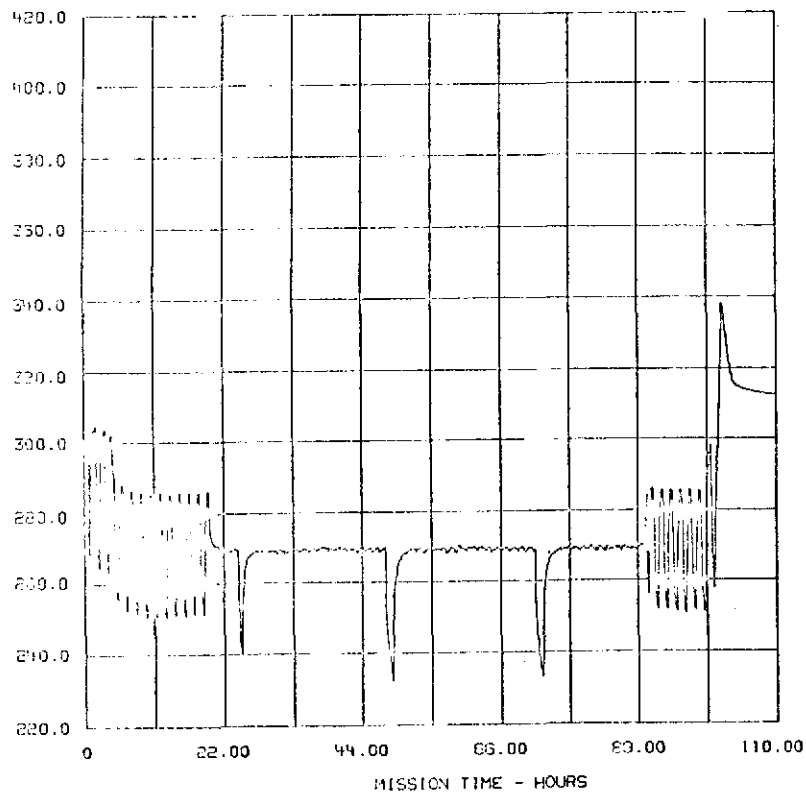
FIGURE 5-18 .   ANALYSIS OF TUG FWD. COMP. + COMPONENTS WITH HEAT PIPES
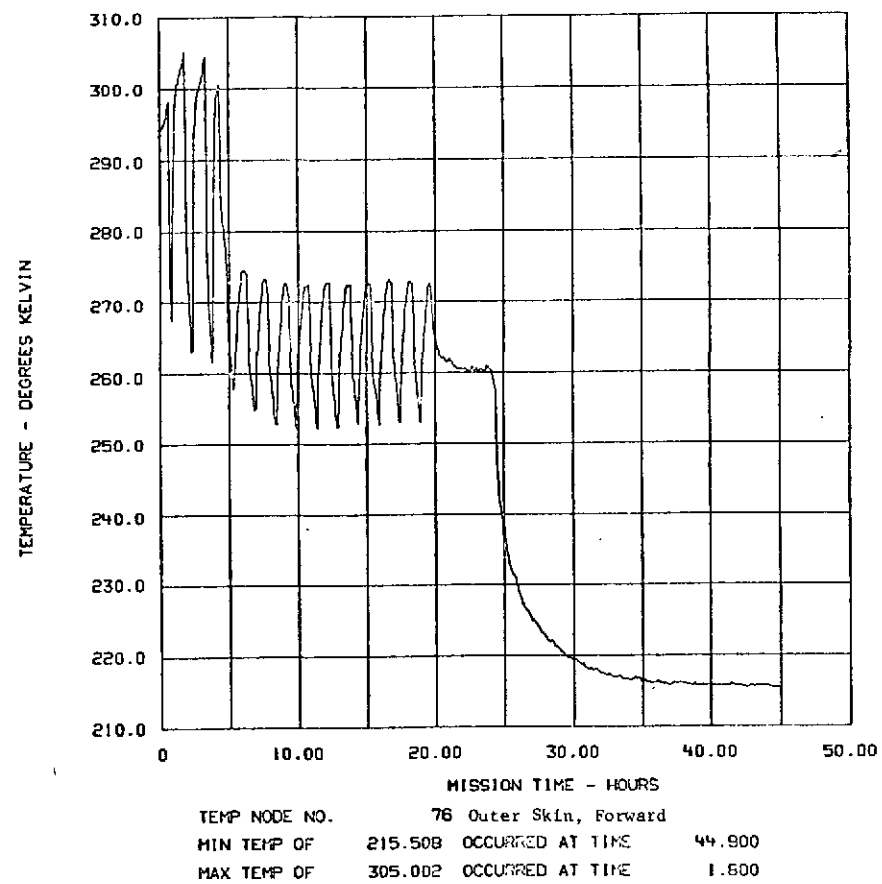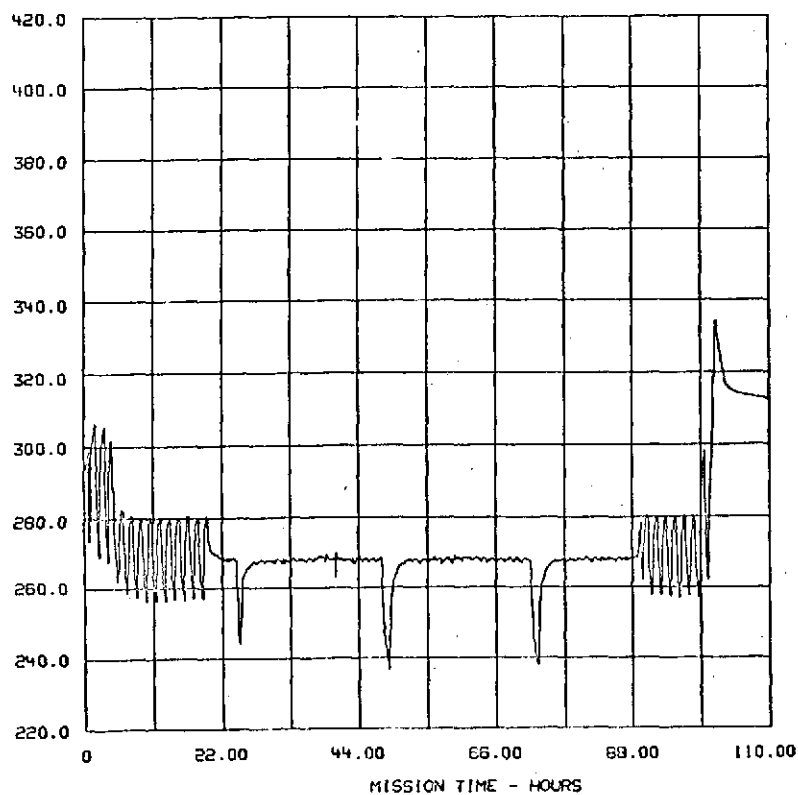

TEMPERATURE - DEGREES KELVIN

310.0
300.0
290.0
280.0
270.0
260.0
250.0
240.0
230.0
220.0
210.0

0   10.00   20.00   30.00   40.00   50.00
MISSION TIME - HOURS

TEMP NODE NO.   72 Outer Skin, Forward
MIN TEMP OF   216.393 OCCURRED AT TIME   43.300
MAX TEMP OF   304.630 OCCURRED AT TIME   1.800
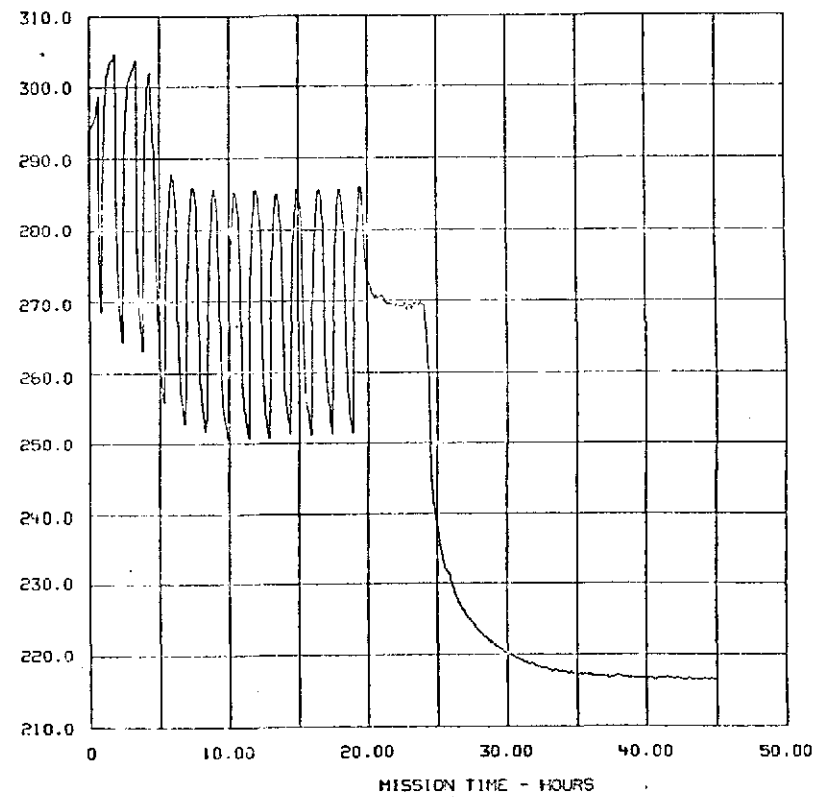
FIGURE 5-19 .   ANALYSIS OF TUG FWD. COMP. STATIONED AT GEO. SHADOW PT.

TEMPERATURE - DEGREES KELVIN

MISSION TIME - HOURS

TEMP NODE NO.	2 Inner Skin, Forward	
MIN TEMP OF	238.474 OCCURRED AT TIME	48.800
MAX TEMP OF	333.812 OCCURRED AT TIME	101.400
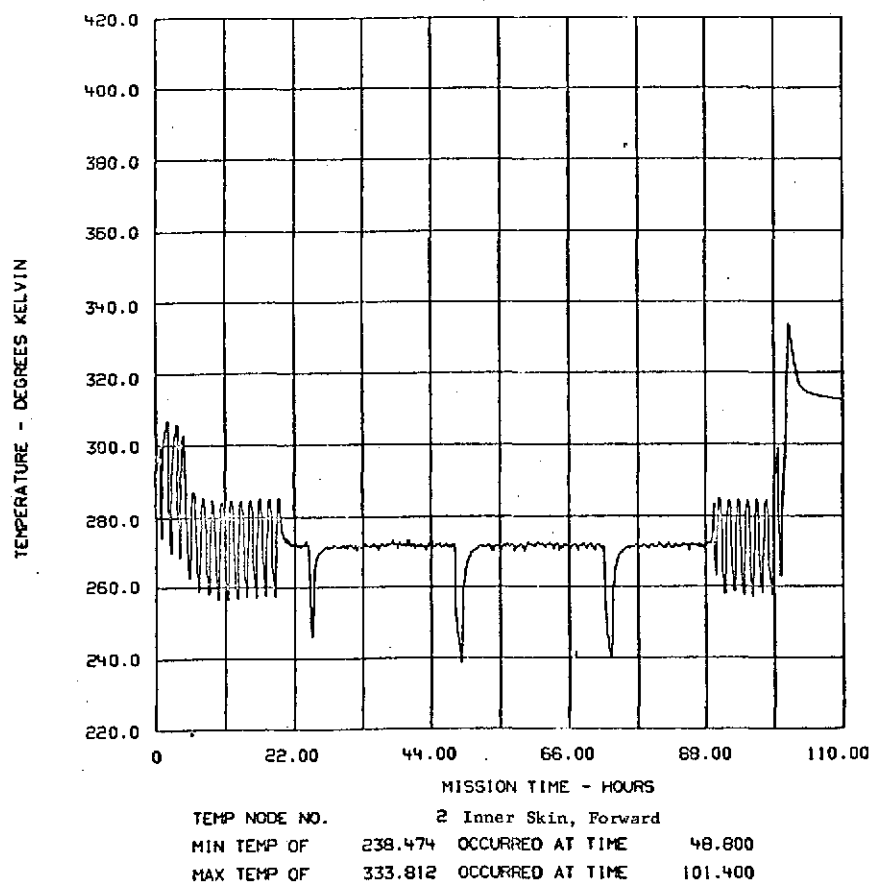
FIGURE 5-20 . ANALYSIS OF TUG FWD. COMP. + COMPONENTS WITH HEAT PIPES

TEMPERATURE - DEGREES KELVIN

MISSION TIME - HOURS

TEMP NODE NO.	2 Inner Skin, Forward	
MIN TEMP OF	221.456 OCCURRED AT TIME	43.300
MAX TEMP OF	306.830 OCCURRED AT TIME	1.800
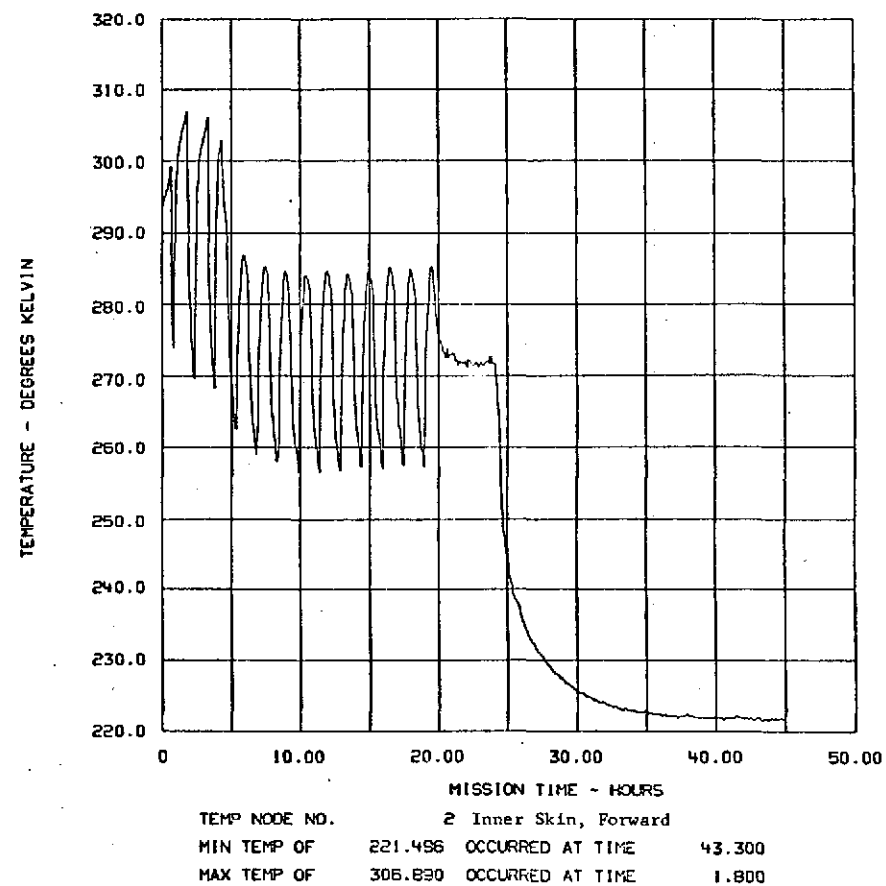
FIGURE 5-21 . ANALYSIS OF TUG FWD. COMP. STATIONED AT GEO. SHADOW PT.

TEMPERATURE – DEGREES KELVIN

MISSION TIME – HOURS

TEMP NODE NO.   73 Outer Skin, Forward
MIN TEMP OF   232.114   OCCURRED AT TIME   48.800
MAX TEMP OF   338.449   OCCURRED AT TIME   101.400
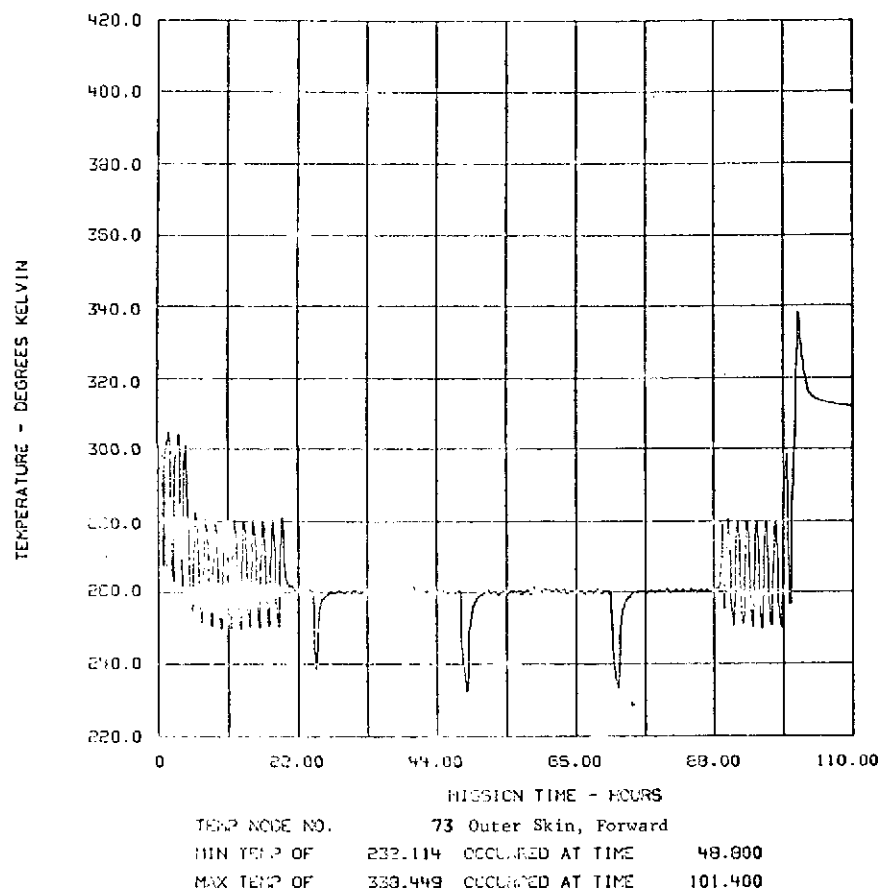
FIGURE 5-22 .   ANALYSIS OF TUG FWD. COMP. + COMPONENTS WITH HEAT PIPES

TEMPERATURE – DEGREES KELVIN

MISSION TIME – HOURS

TEMP NODE NO.   73 Outer Skin, Forward
MIN TEMP OF   216.180   OCCURRED AT TIME   44.900
MAX TEMP OF   305.104   OCCURRED AT TIME   1.800
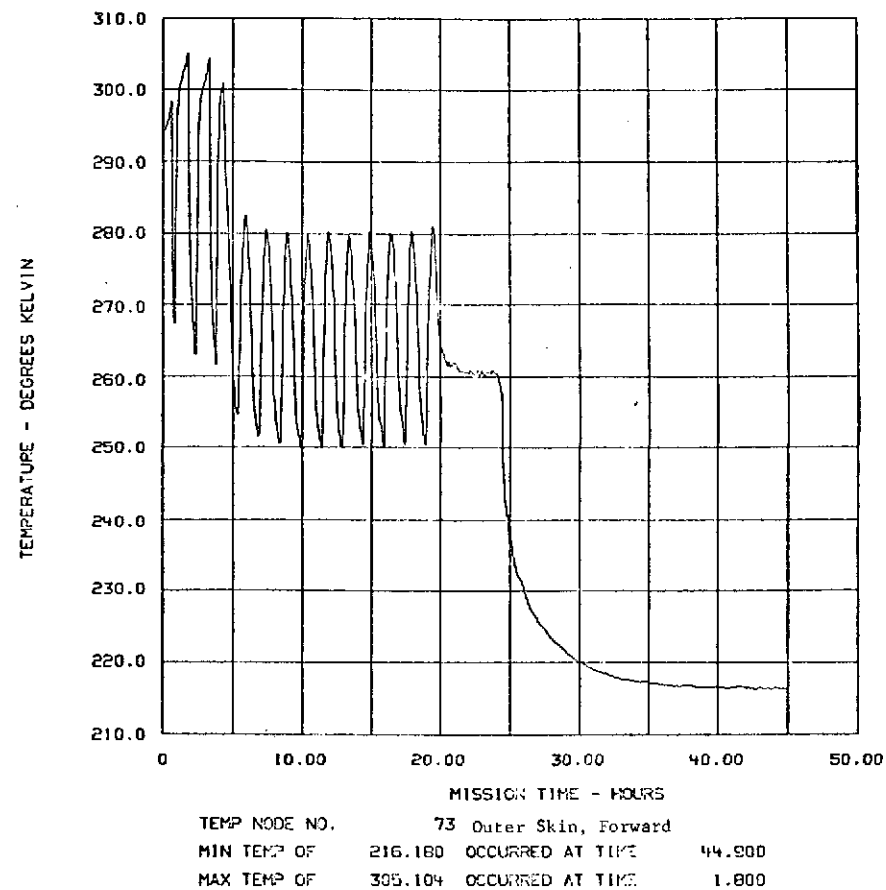
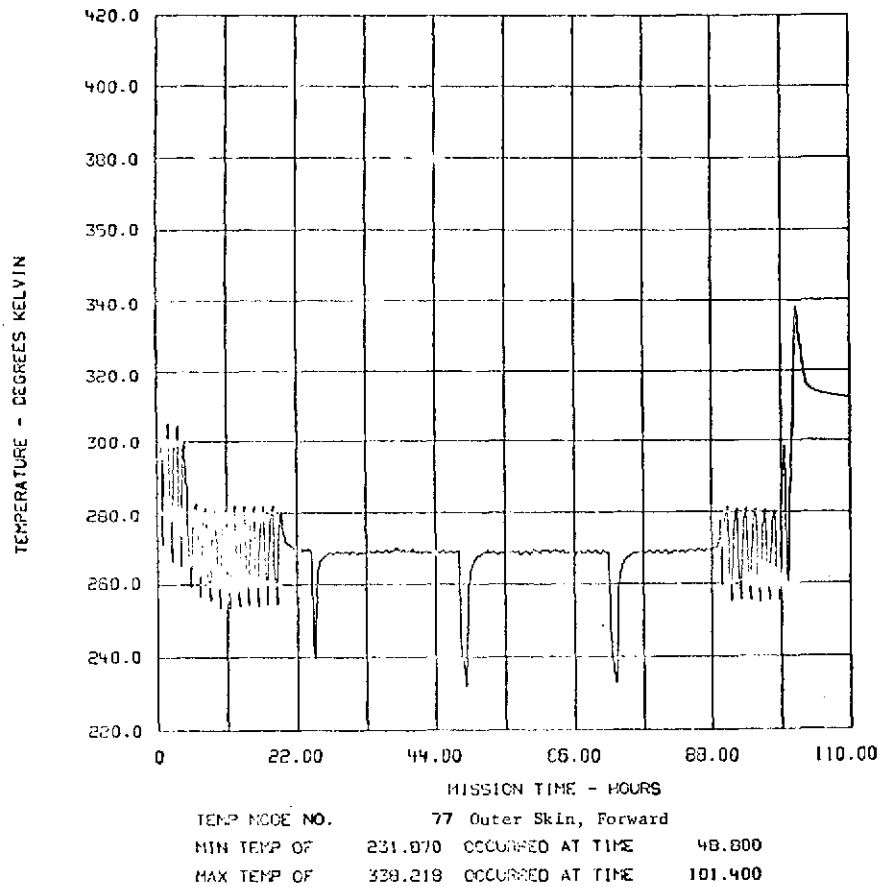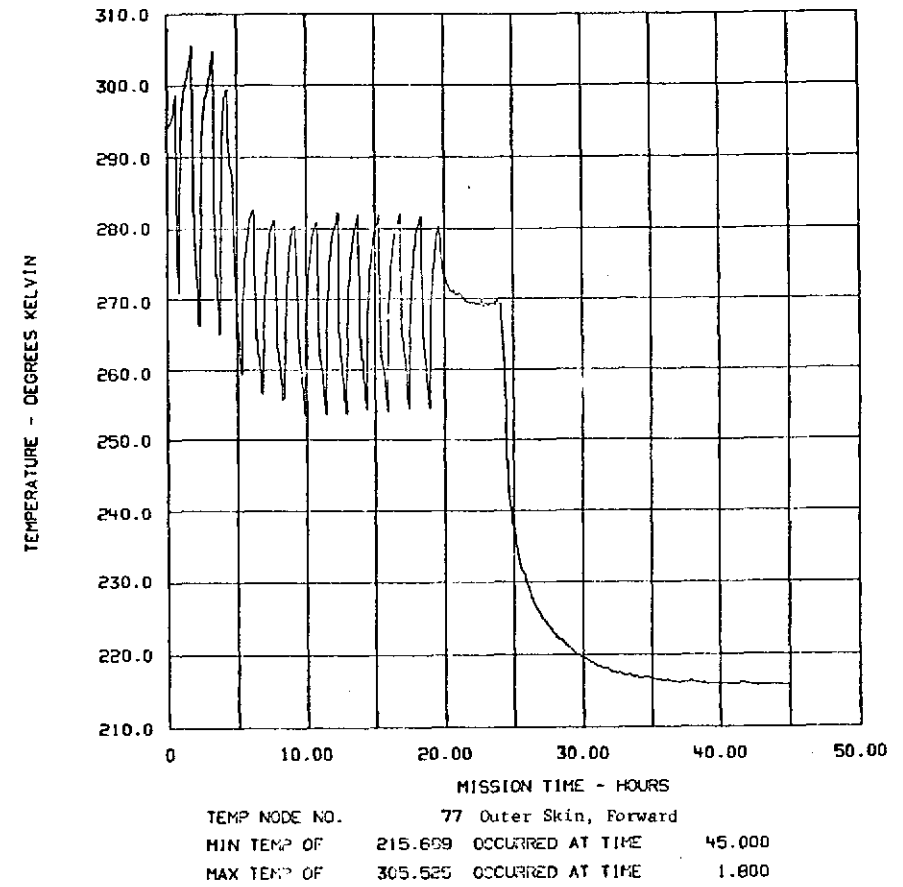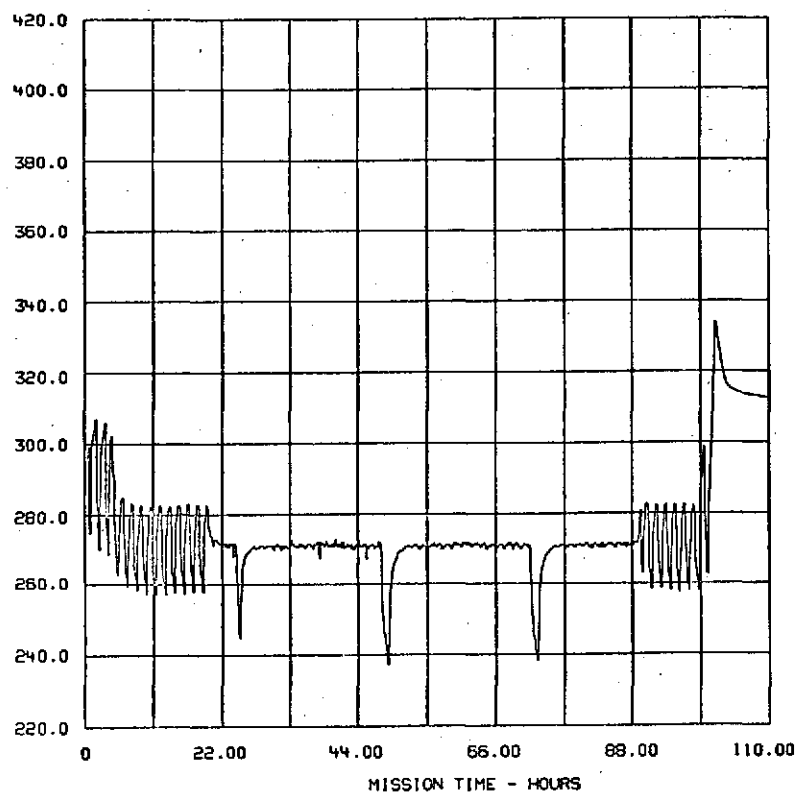FIGURE 5-23 .   ANALYSIS OF TUG FWD. COMP. STATIONED AT GEO. SHADOW PT.
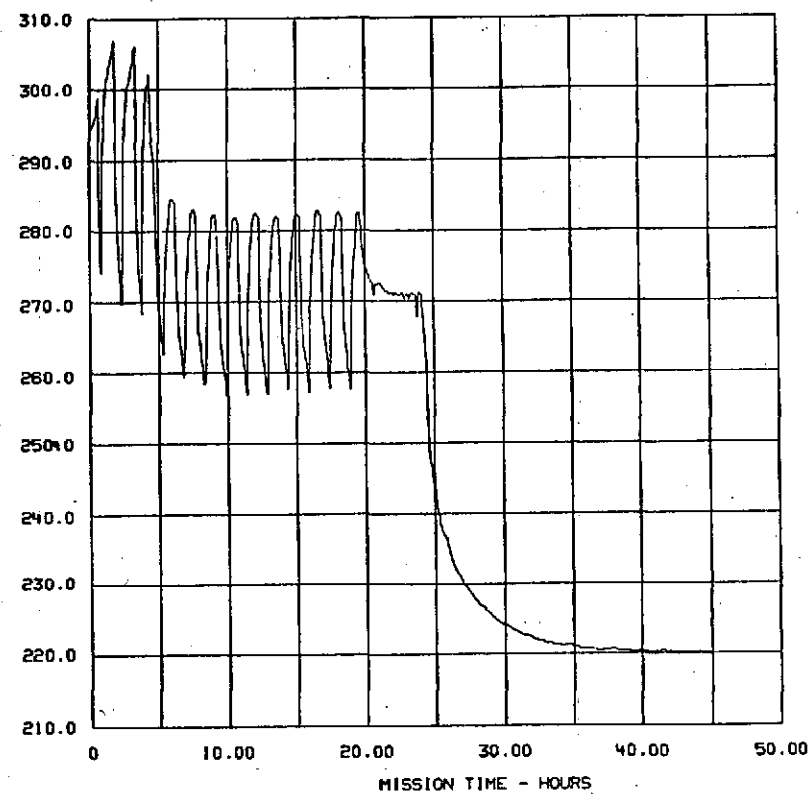
TEMPERATURE - DEGREES KELVIN

MISSION TIME - HOURS
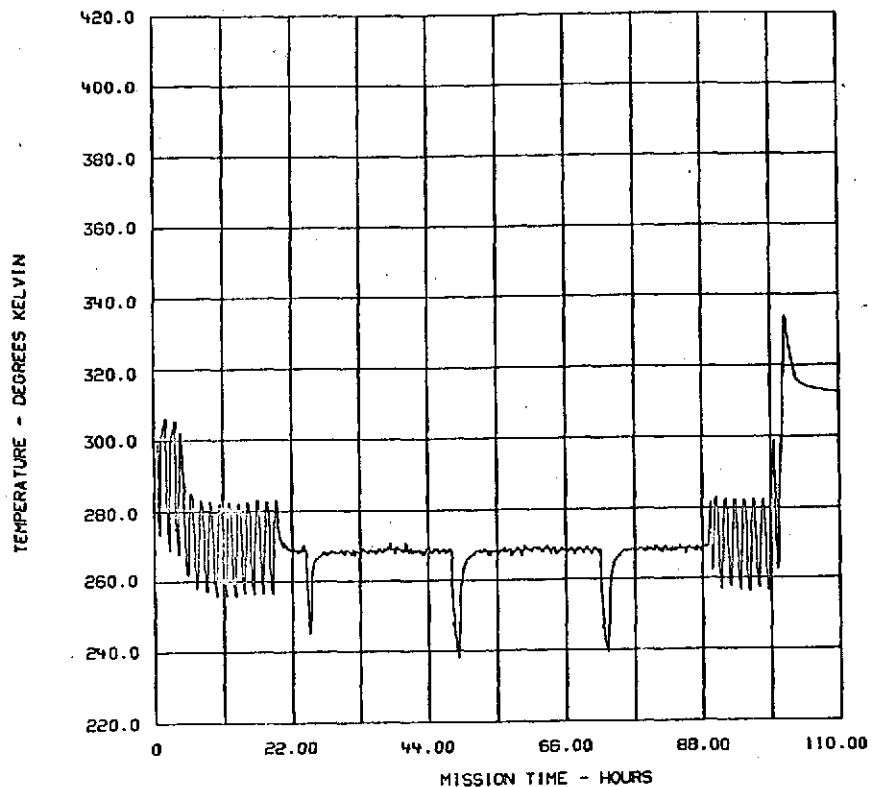
TEMP NODE NO.   3 Inner Skin, Forward
MIN TEMP OF   237.894   OCCURRED AT TIME   48.800
MAX TEMP OF   334.066   OCCURRED AT TIME   101.400

FIGURE 5-24 .   ANALYSIS OF TUG FWD. COMP. + COMPONENTS WITH HEAT PIPES

TEMPERATURE - DEGREES KELVIN

MISSION TIME - HOURS
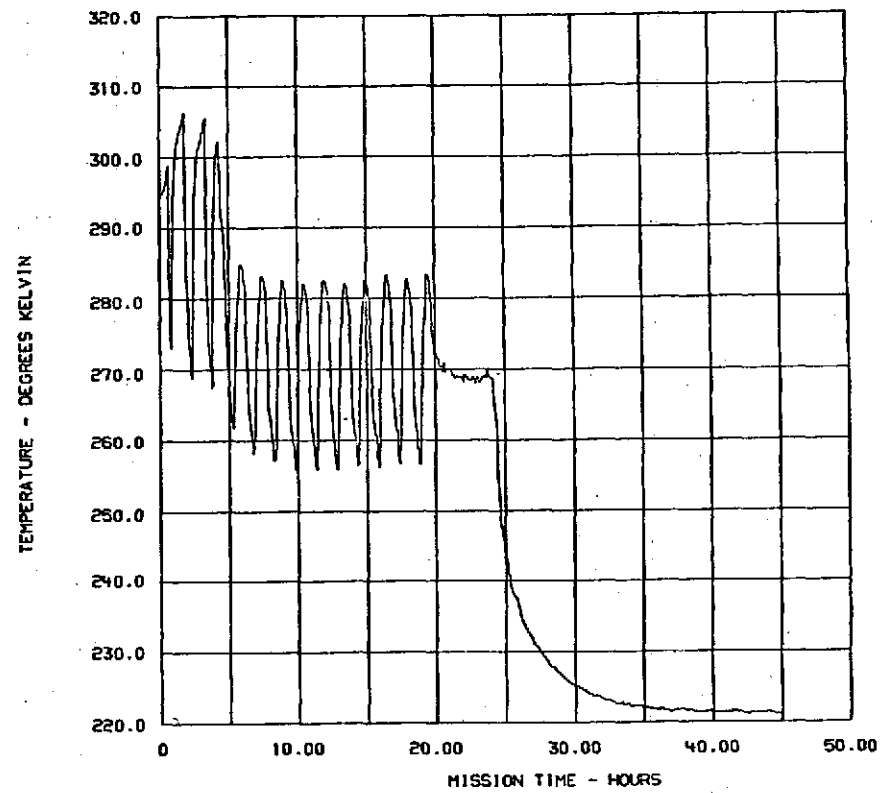
TEMP NODE NO.   3 Inner Skin, Forward
MIN TEMP OF   221.058   OCCURRED AT TIME   44.900
MAX TEMP OF   306.266   OCCURRED AT TIME   1.800

FIGURE 5-25 .   ANALYSIS OF TUG FWD. COMP. STATIONED AT GEO. SHADOW PT.

FIGURE 5-26 . ANALYSIS OF TUG FWD. COMP. + COMPONENTS WITH HEAT PIPES

TEMP NODE NO.   74 Outer Skin, Forward
MIN TEMP OF   231.821 OCCURRED AT TIME   48.800
MAX TEMP OF   338.600 OCCURRED AT TIME   101.400
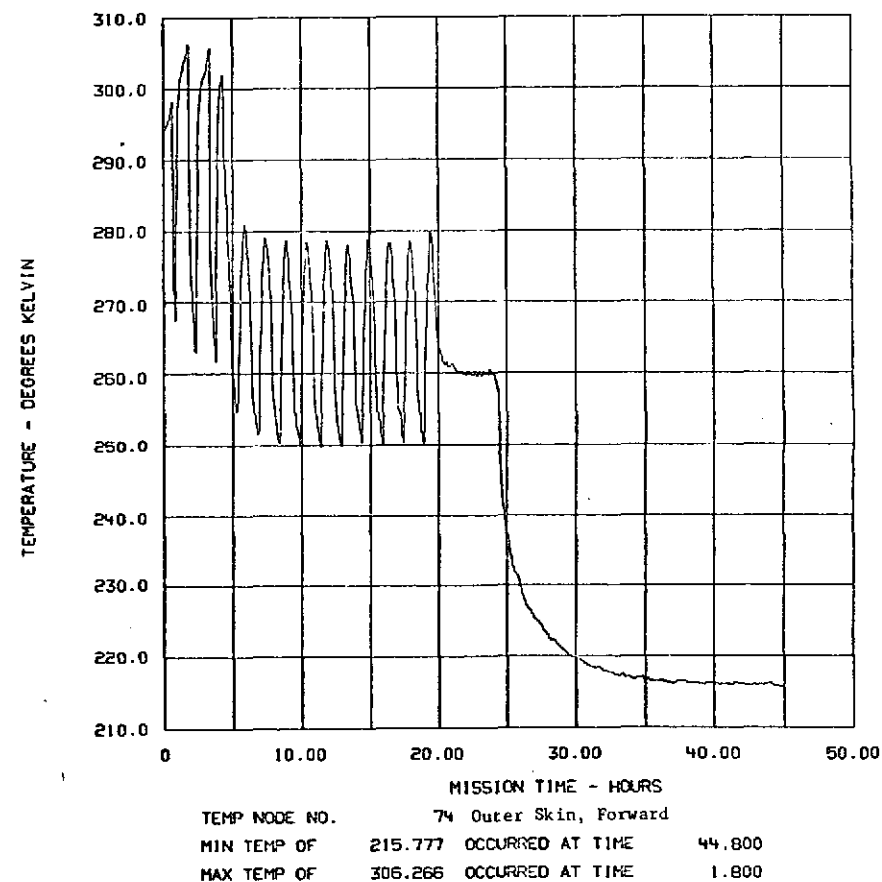
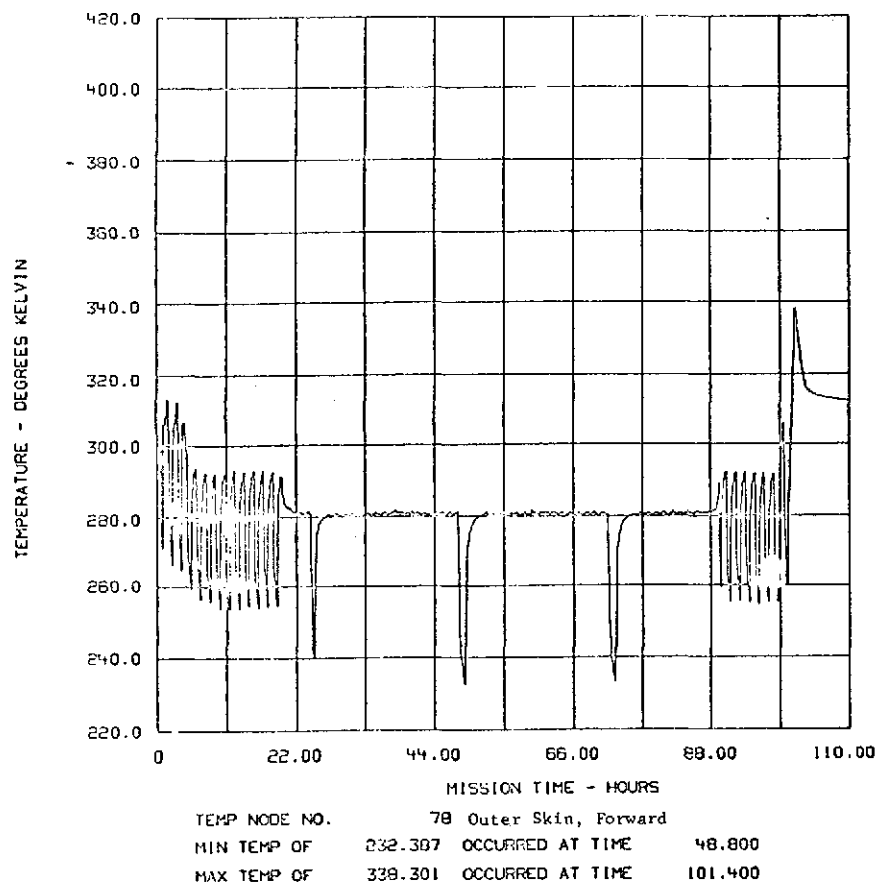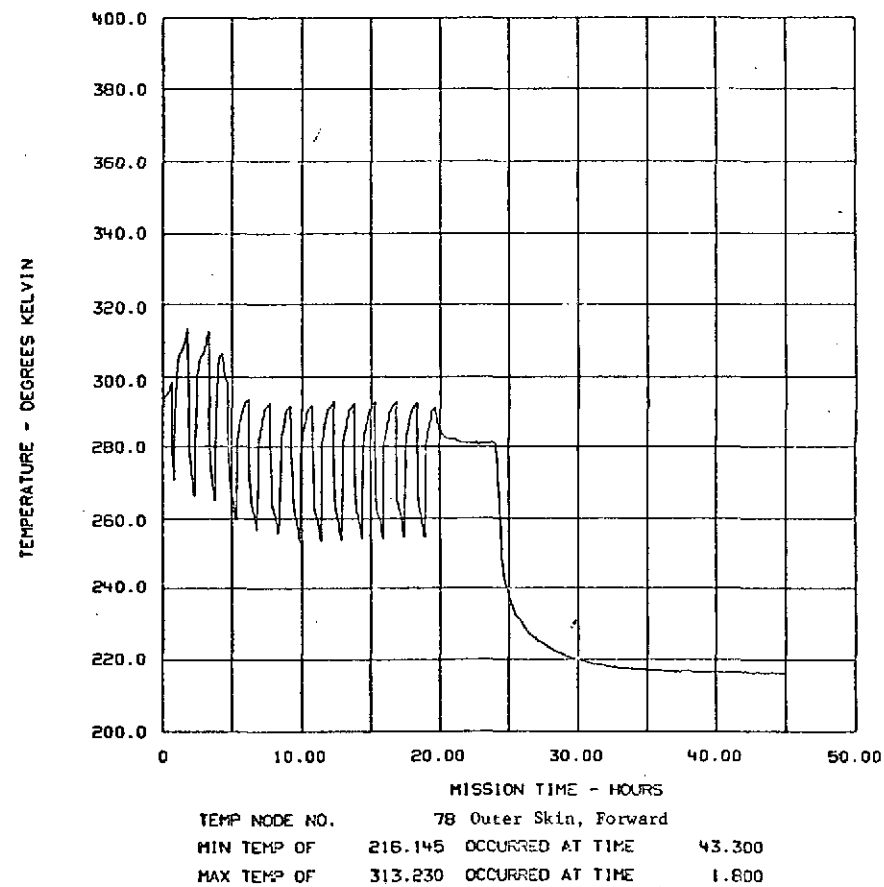FIGURE 5-27 . ANALYSIS OF TUG FWD. COMP. STATIONED AT GEO. SHADOW PT.

TEMP NODE NO.   74 Outer Skin, Forward
MIN TEMP OF   215.777 OCCURRED AT TIME   44.800
MAX TEMP OF   306.266 OCCURRED AT TIME   1.800

FIGURE 5-28 . ANALYSIS OF TUG FWD. COMP. + COMPONENTS WITH HEAT PIPES

TEMP NODE NO.   4 Inner Skin, Forward
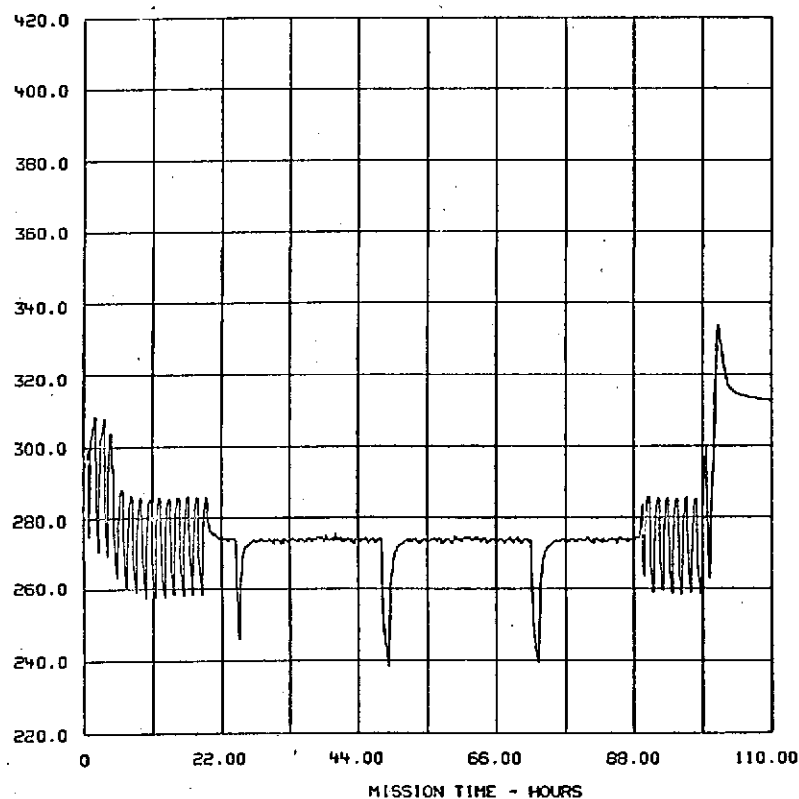MIN TEMP OF   237.246 OCCURRED AT TIME   48.800
MAX TEMP OF   334.193 OCCURRED AT TIME   101.400

FIGURE 5-29 . ANALYSIS OF TUG FWD. COMP. STATIONED AT GEO. SHADOW PT.

TEMP NODE NO.   4 Inner Skin, Forward
MIN TEMP OF   220.310 OCCURRED AT TIME   44.800
MAX TEMP OF   306.194 OCCURRED AT TIME   1.800

TEMPERATURE – DEGREES KELVIN

MISSION TIME – HOURS

TEMP NODE NO.		75 Outer Skin, Forward	
MIN TEMP OF	231.633	OCCURRED AT TIME	48.800
MAX TEMP OF	338.714	OCCURRED AT TIME	101.400

FIGURE 5-30 . ANALYSIS OF TUG FWD. COMP. + COMPONENTS WITH HEAT PIPES

TEMPERATURE – DEGREES KELVIN

MISSION TIME – HOURS

TEMP NODE NO.		75 Outer Skin, Forward	
MIN TEMP OF	215.550	OCCURRED AT TIME	44.800
MAX TEMP OF	306.225	OCCURRED AT TIME	1.800
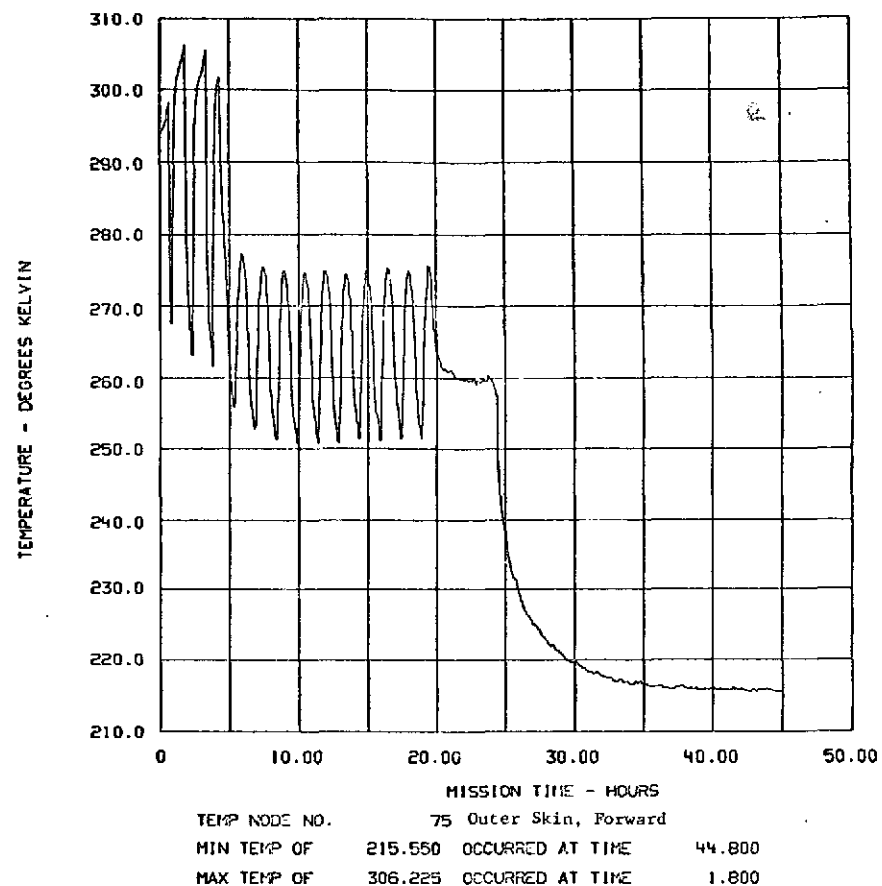
FIGURE 5-31 . ANALYSIS OF TUG FWD. COMP. STATIONED AT GEO. SHADOW PT.
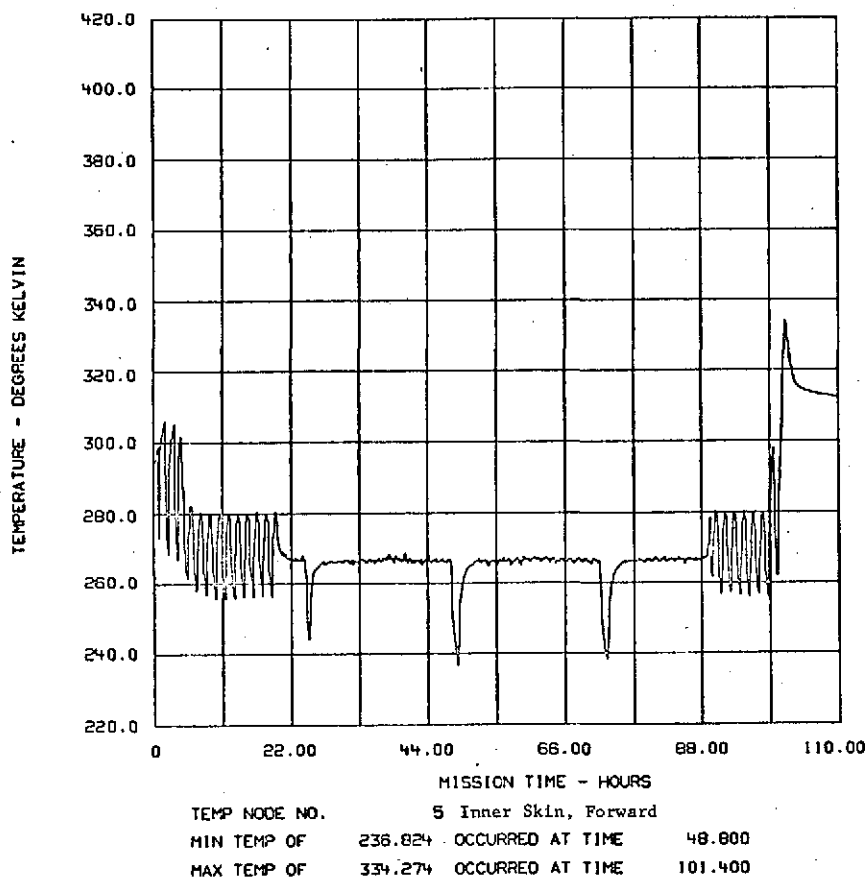
FIGURE 5-32 .   ANALYSIS OF TUG FWD. COMP. + COMPONENTS WITH HEAT PIPES

Left chart:

TEMPERATURE - DEGREES KELVIN

MISSION TIME - HOURS

TEMP NODE NO.   5 Inner Skin, Forward
MIN TEMP OF   236.824   OCCURRED AT TIME   48.800
MAX TEMP OF   334.274   OCCURRED AT TIME   101.400
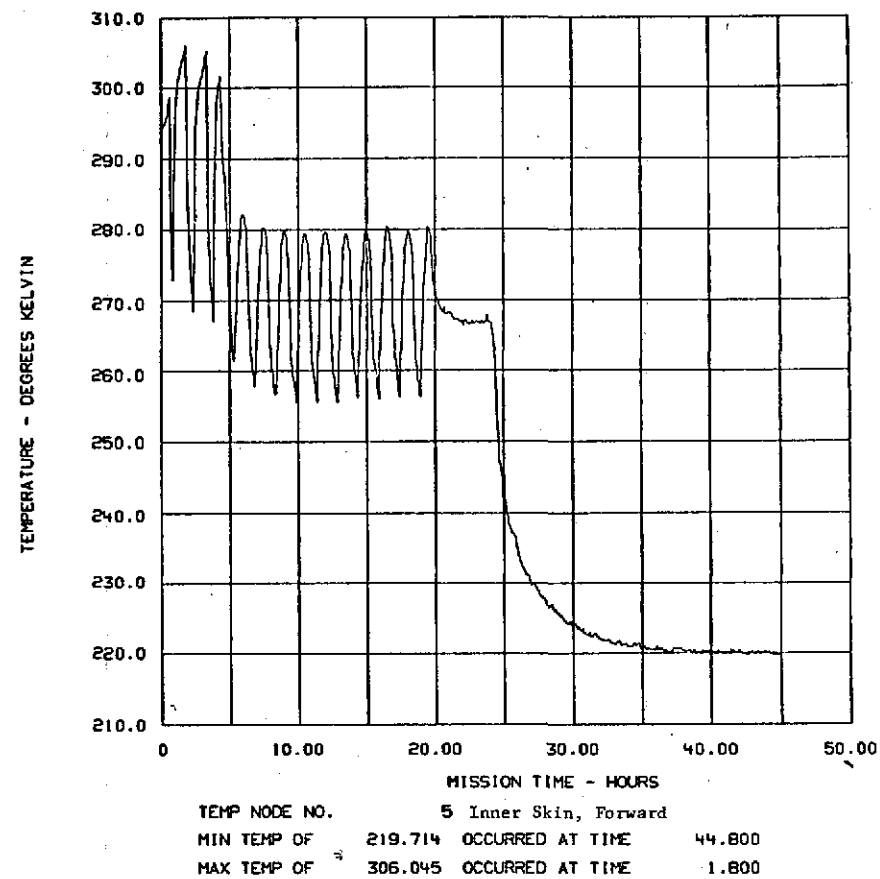
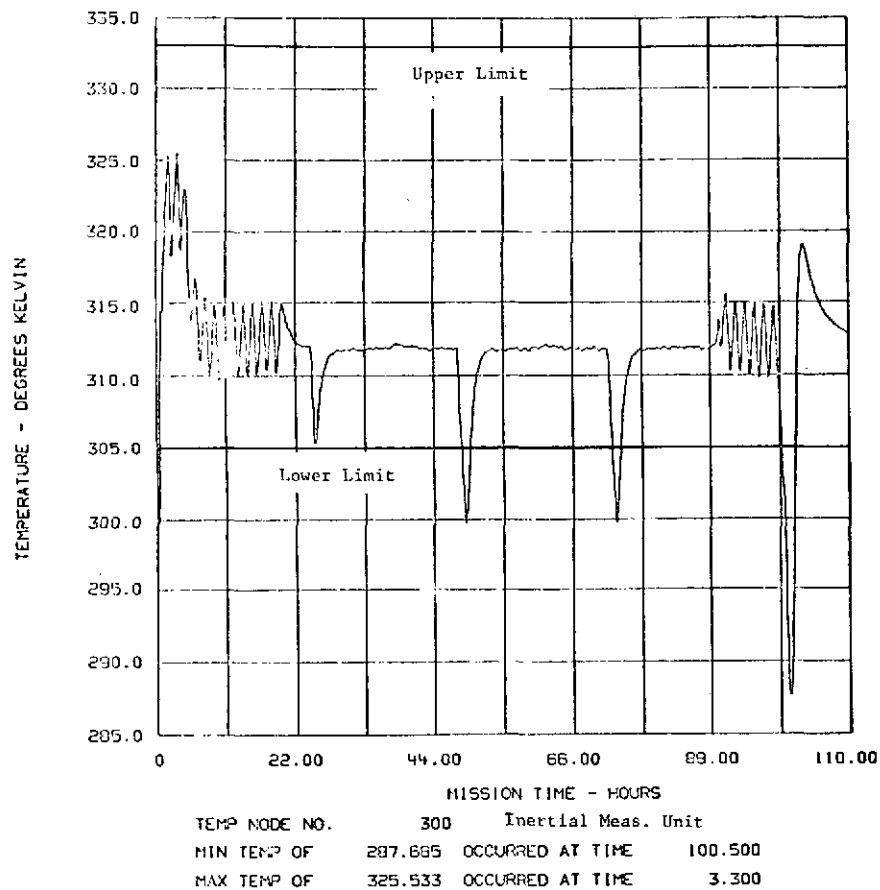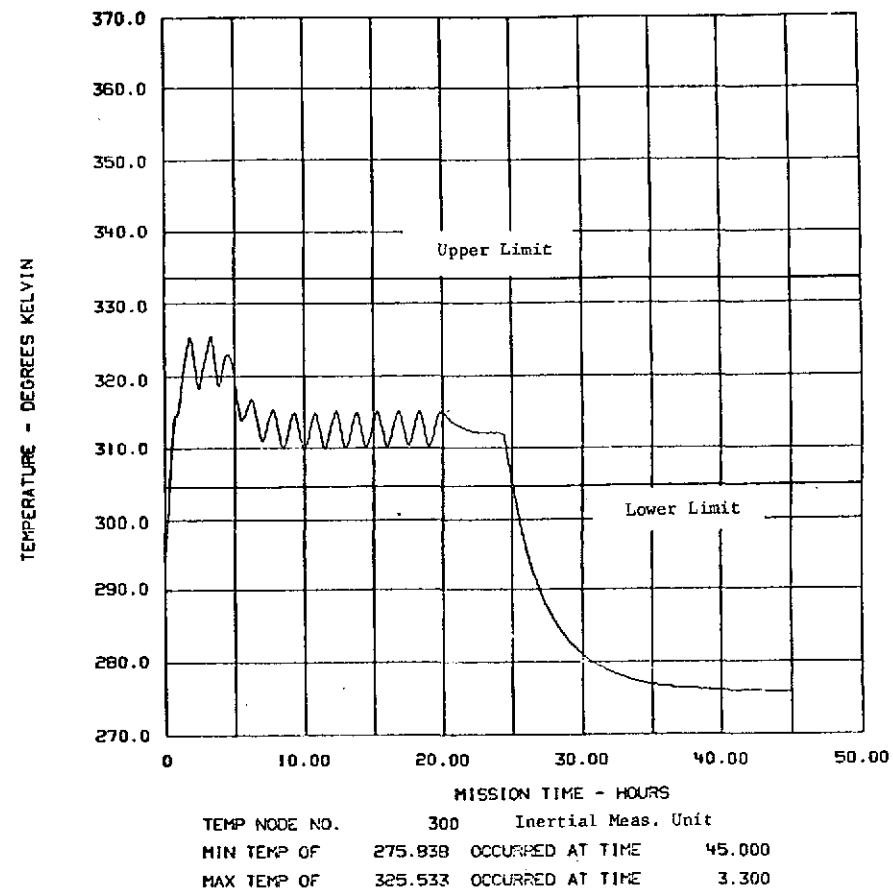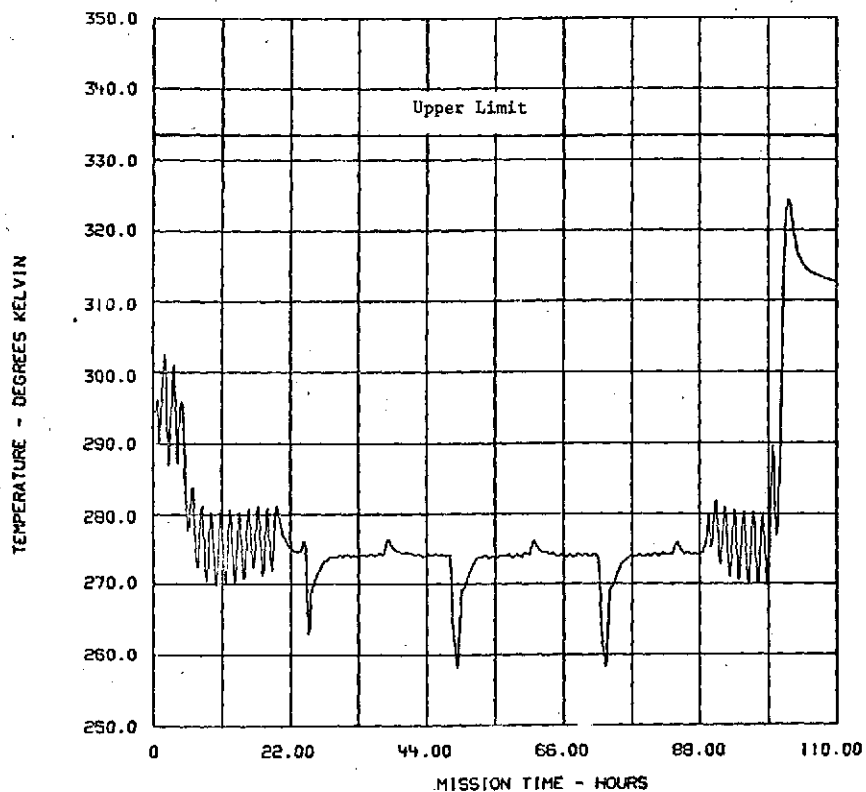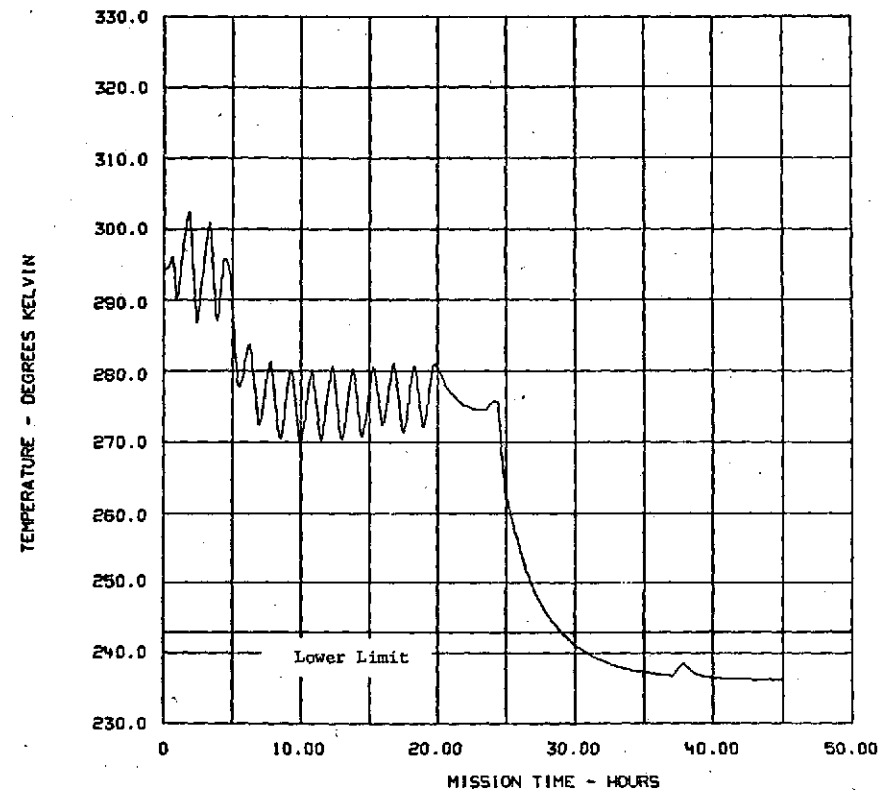FIGURE 5-33 .   ANALYSIS OF TUG FWD. COMP. STATIONED AT GEO. SHADOW PT.

Right chart:

TEMPERATURE - DEGREES KELVIN

MISSION TIME - HOURS

TEMP NODE NO.   5 Inner Skin, Forward
MIN TEMP OF   219.714   OCCURRED AT TIME   44.800
MAX TEMP OF   306.045   OCCURRED AT TIME   1.800

TEMPERATURE – DEGREES KELVIN

MISSION TIME – HOURS

TEMP NODE NO.   76 Outer Skin, Forward

MIN TEMP OF   231.624 OCCURRED AT TIME   48.800

MAX TEMP OF   330.520 OCCURRED AT TIME   101.400
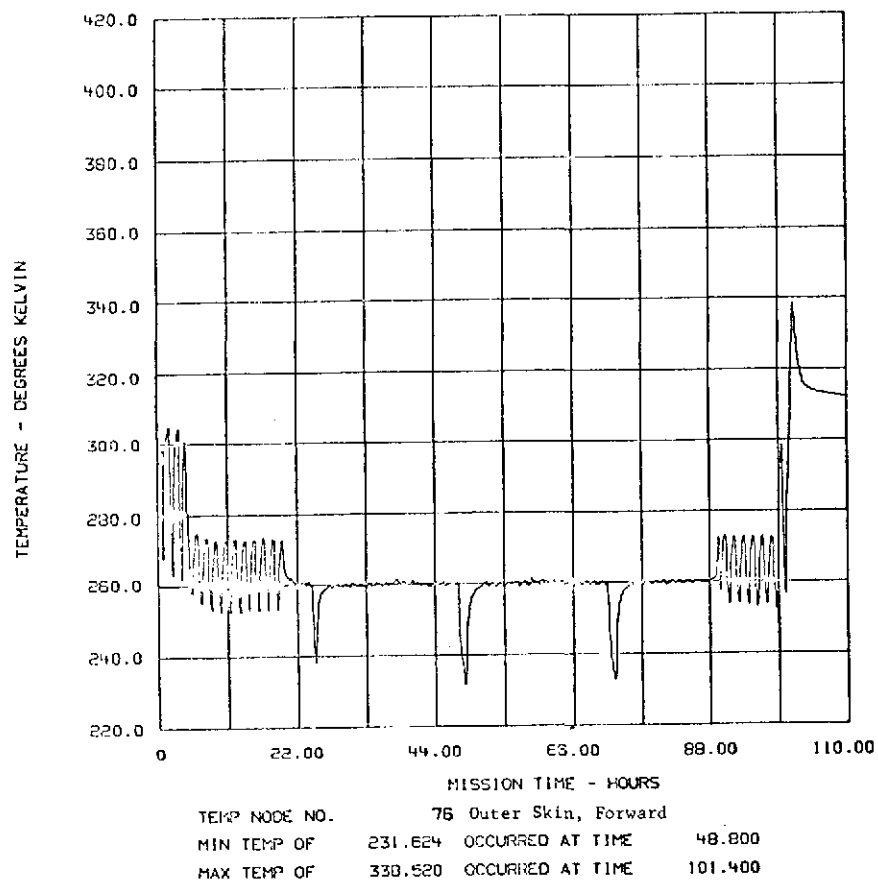
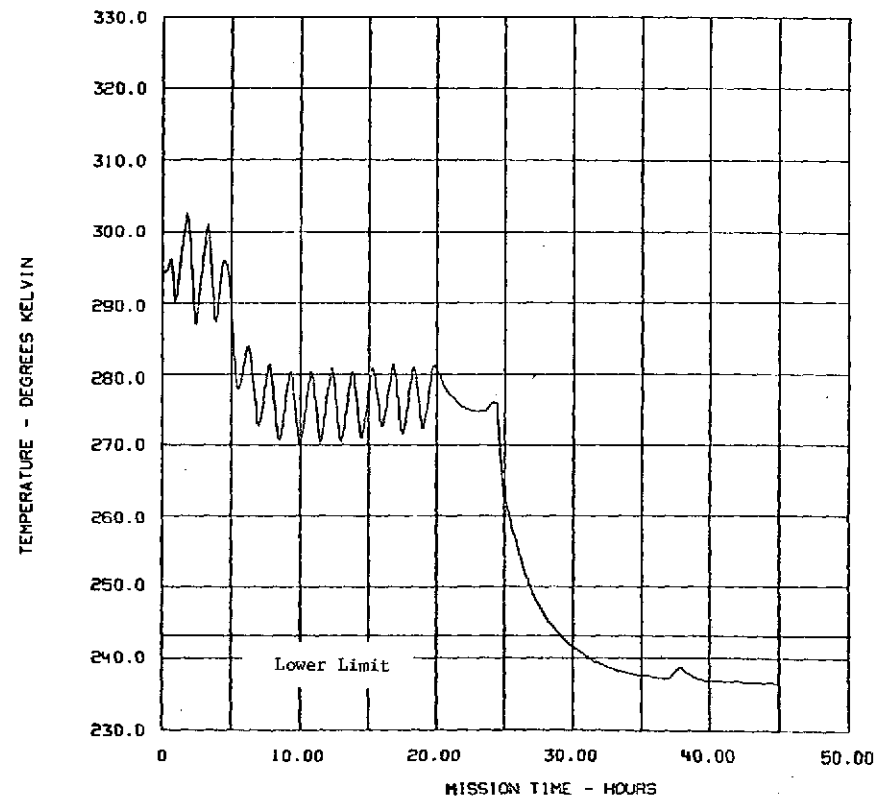FIGURE 5-34 .   ANALYSIS OF TUG FWD. COMP. + COMPONENTS WITH HEAT PIPES

TEMPERATURE – DEGREES KELVIN

MISSION TIME – HOURS

TEMP NODE NO.   76 Outer Skin, Forward

MIN TEMP OF   215.508 OCCURRED AT TIME   44.900

MAX TEMP OF   305.002 OCCURRED AT TIME   1.600

FIGURE 5-35 .   ANALYSIS OF TUG FWD. COMP. STATIONED AT GEO. SHADOW PT.

FIGURE 5-36 . . ANALYSIS OF TUG FWD. COMP. + COMPONENTS WITH HEAT PIPES

TEMP NODE NO.   6   Inner Skin, Forward
MIN TEMP OF   236.810   OCCURRED AT TIME   48.800
MAX TEMP OF   334.235   OCCURRED AT TIME   101.400

FIGURE 5-37 .   ANALYSIS OF TUG FWD. COMP. STATIONED AT GEO. SHADOW PT.
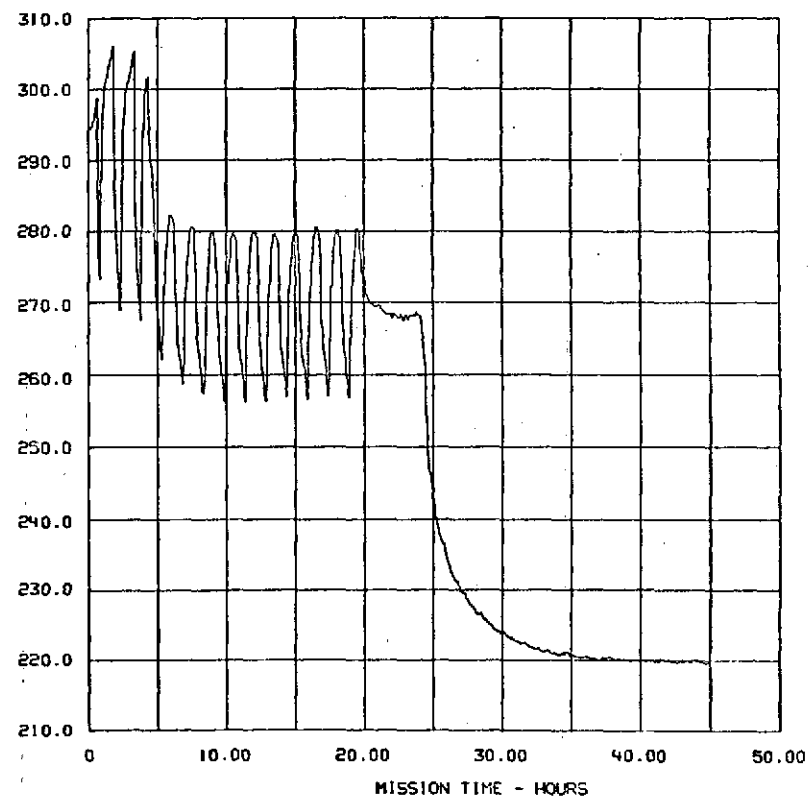
TEMP NODE NO.   6   Inner Skin, Forward
MIN TEMP OF   219.605   OCCURRED AT TIME   44.900
MAX TEMP OF   306.115   OCCURRED AT TIME   1.800

FIGURE 5-38 . ANALYSIS OF TUG FWD. COMP. + COMPONENTS WITH HEAT PIPES

TEMP NODE NO.   77 Outer Skin, Forward
MIN TEMP OF   231.070 OCCURRED AT TIME   48.800
MAX TEMP OF   338.219 OCCURRED AT TIME   101.400

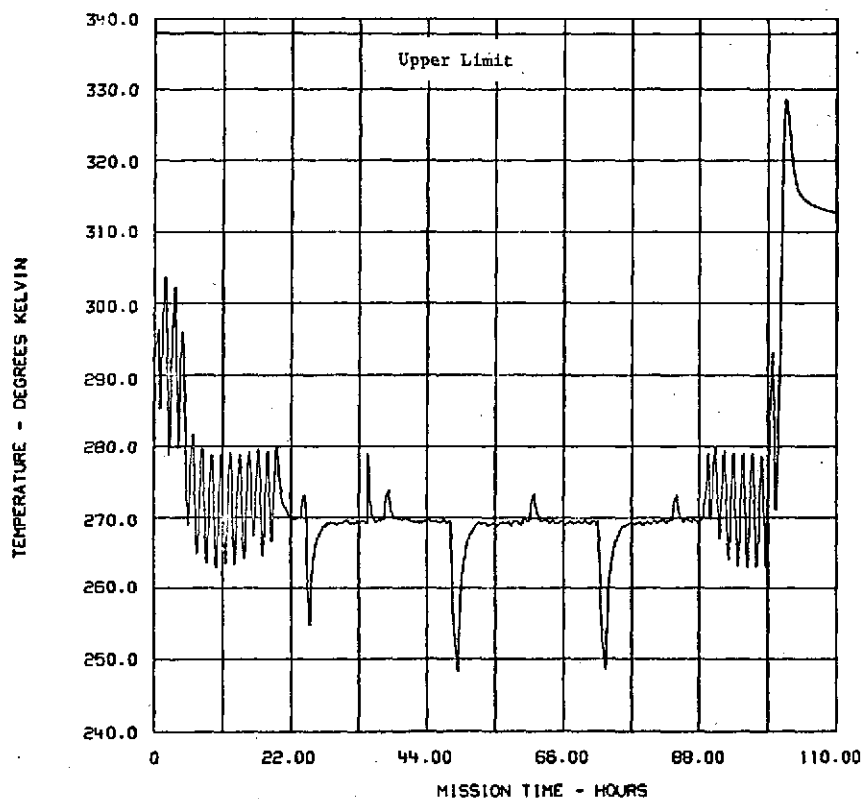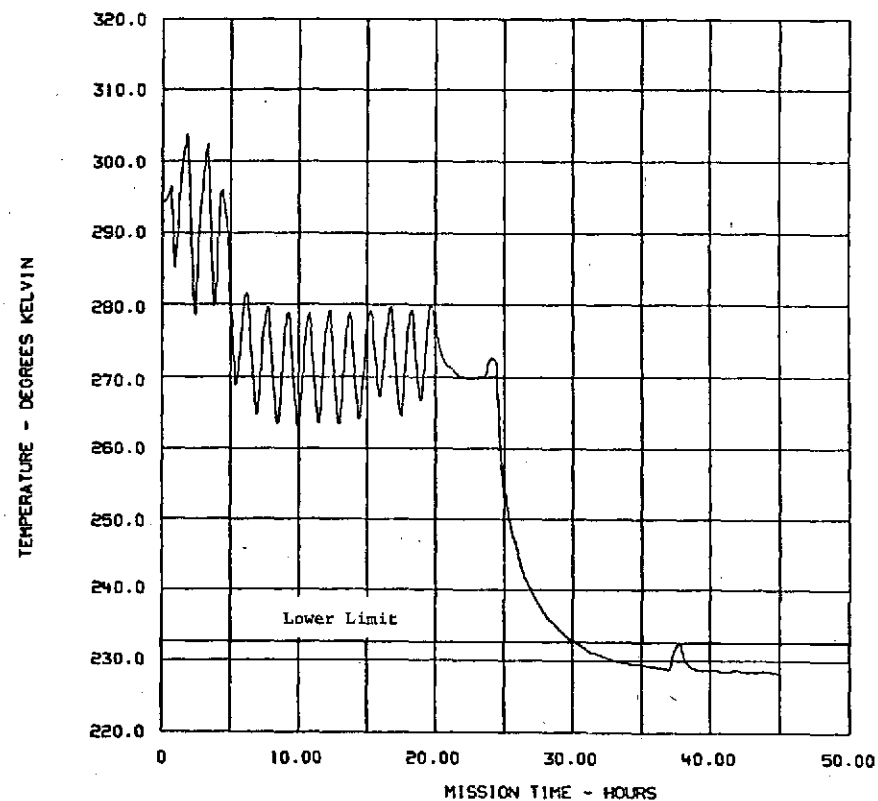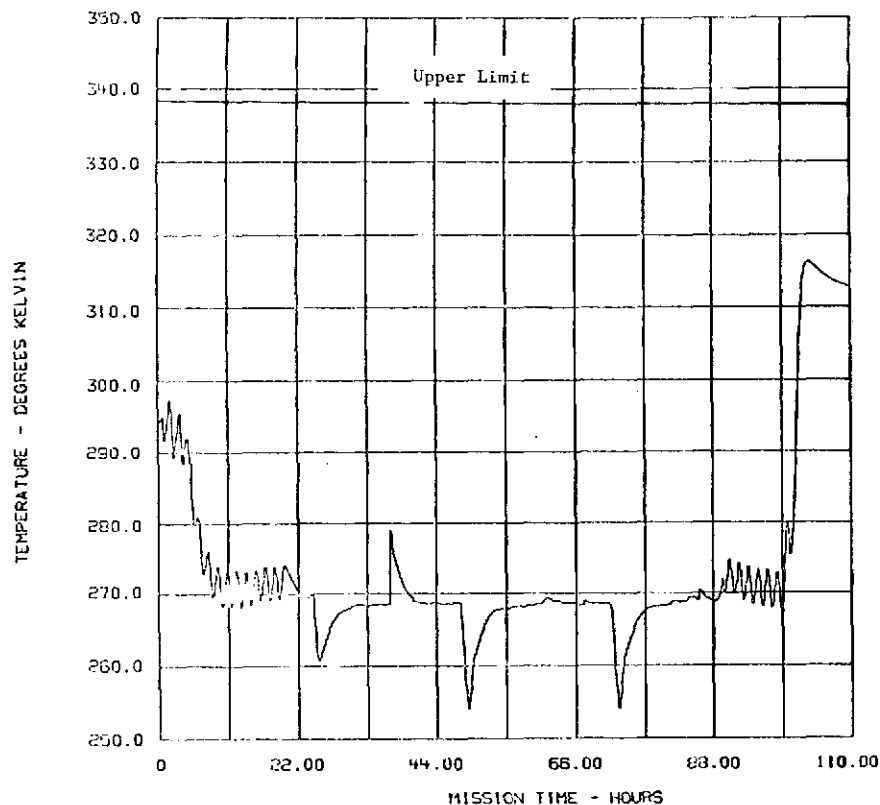FIGURE 5-39 . ANALYSIS OF TUG FWD. COMP. STATIONED AT GEO. SHADOW PT.

TEMP NODE NO.   77 Outer Skin, Forward
MIN TEMP OF   215.699 OCCURRED AT TIME   45.000
MAX TEMP OF   305.525 OCCURRED AT TIME   1.800

FIGURE 5-40 . ANALYSIS OF TUG FWD. COMP. + COMPONENTS WITH HEAT PIPES

TEMP NODE NO.   7 Inner Skin, Forward
MIN TEMP OF   237.217 OCCURRED AT TIME   48.800
MAX TEMP OF   334.061 OCCURRED AT TIME   101.400

FIGURE 5-41 . ANALYSIS OF TUG FWD. COMP. STATIONED AT GEO. SHADOW PT.

TEMP NODE NO.   7 Inner Skin, Forward
MIN TEMP OF   219.972 OCCURRED AT TIME   45.000
MAX TEMP OF   306.854 OCCURRED AT TIME   1.800

TEMPERATURE - DEGREES KELVIN

MISSION TIME - HOURS

TEMP NODE NO.   78 Outer Skin, Forward
MIN TEMP OF   232.387 OCCURRED AT TIME   48.800
MAX TEMP OF   339.301 OCCURRED AT TIME   101.400

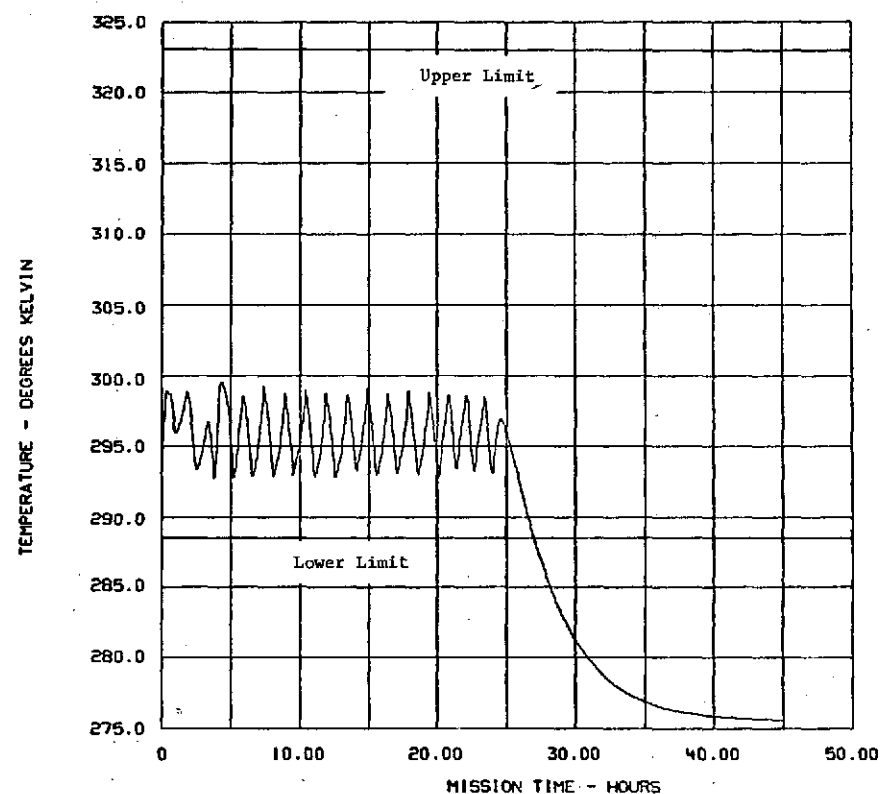FIGURE 5-42 .   ANALYSIS OF TUG FWD. COMP. + COMPONENTS WITH HEAT PIPES

TEMPERATURE - DEGREES KELVIN

MISSION TIME - HOURS

TEMP NODE NO.   78 Outer Skin, Forward
MIN TEMP OF   216.145 OCCURRED AT TIME   43.300
MAX TEMP OF   313.230 OCCURRED AT TIME   1.800

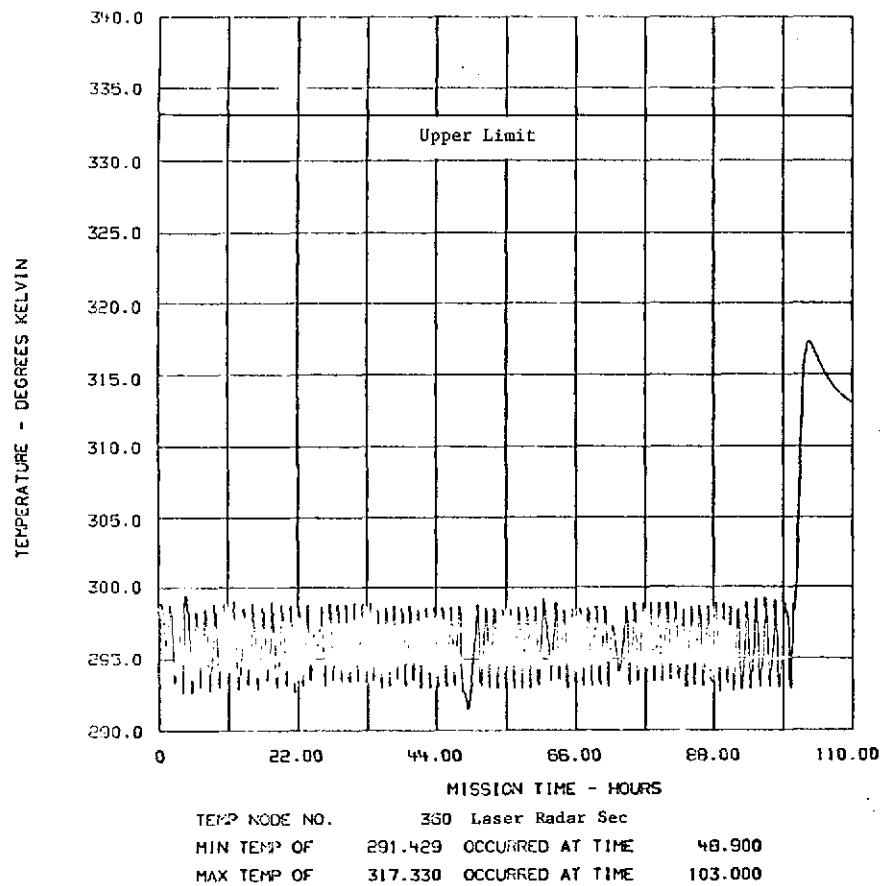FIGURE 5-43 .   ANALYSIS OF TUG FWD. COMP. STATIONED AT GEO. SHADOW PT.

FIGURE 5-44 . ANALYSIS OF TUG FWD. COMP. + COMPONENTS WITH HEAT PIPES
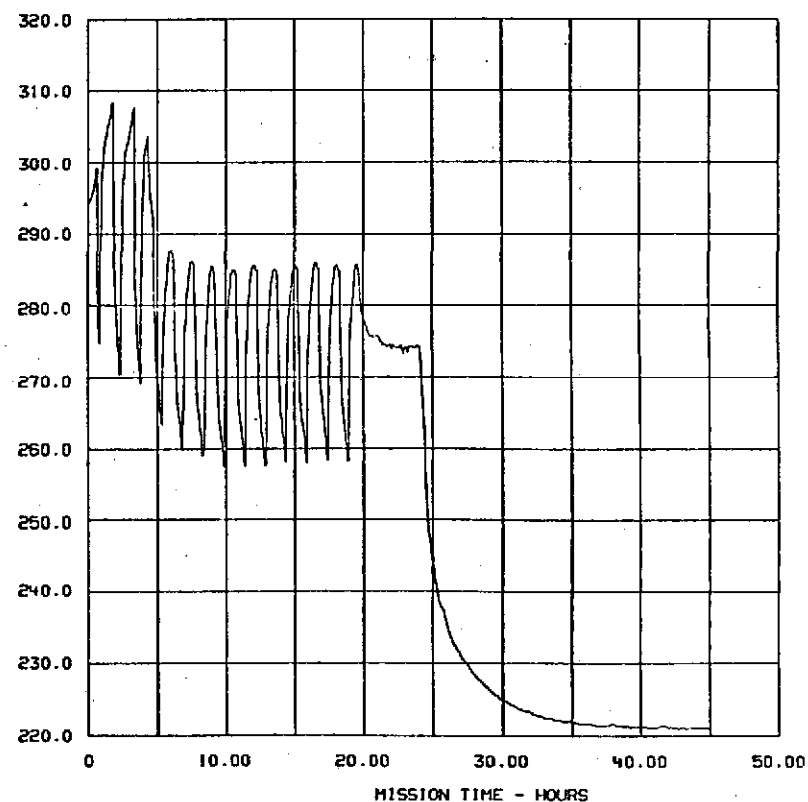
FIGURE 5-45 . ANALYSIS OF TUG FWD. COMP. STATIONED AT GEO. SHADOW PT.

FIGURE 5-46 . ANALYSIS OF TUG FWD. COMP. + COMPONENTS WITH HEAT PIPES

TEMP NODE NO.   300   Inertial Meas. Unit
MIN TEMP OF   287.685 OCCURRED AT TIME   100.500
MAX TEMP OF   325.533 OCCURRED AT TIME   3.300

FIGURE 5-47 . ANALYSIS OF TUG FWD. COMP. STATIONED AT GEO. SHADOW PT.

TEMP NODE NO.   300   Inertial Meas. Unit
MIN TEMP OF   275.838 OCCURRED AT TIME   45.000
MAX TEMP OF   325.533 OCCURRED AT TIME   3.300

FIGURE 5-48 . ANALYSIS OF TUG FWD. COMP. + COMPONENTS WITH HEAT PIPES

TEMP NODE NO.   310 Star Tracker Pri
MIN TEMP OF   259.123 OCCURRED AT TIME   48.900
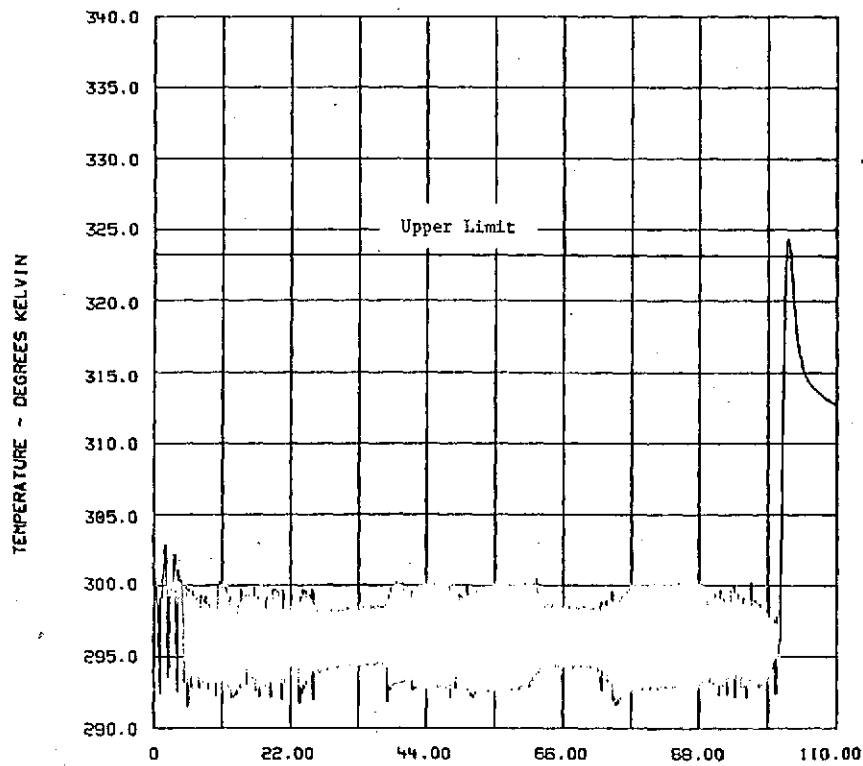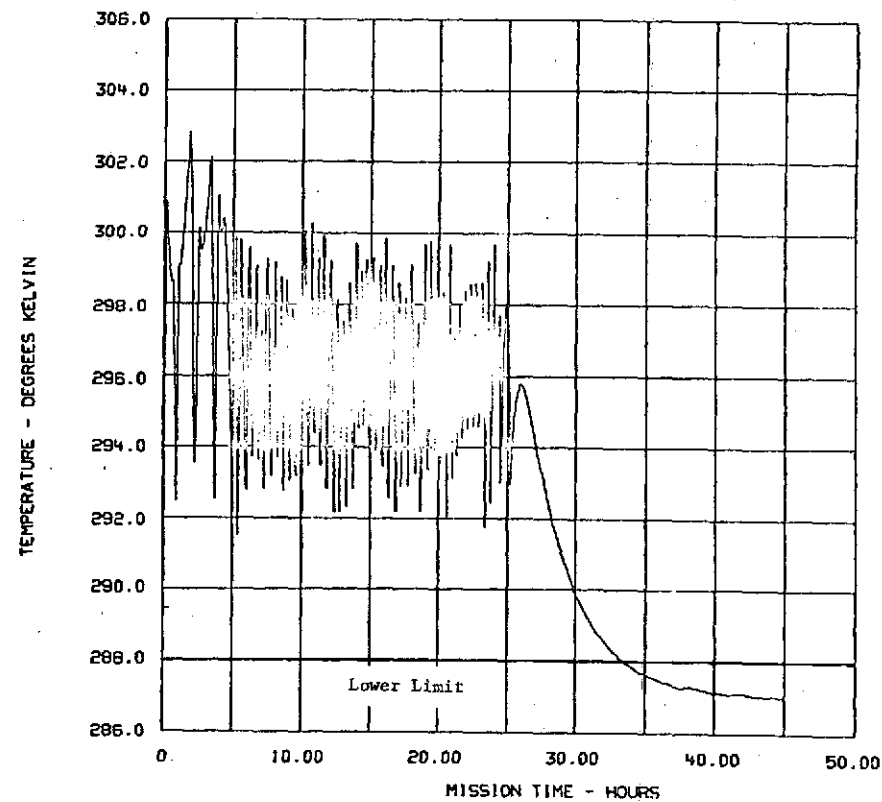MAX TEMP OF   324.259 OCCURRED AT TIME   102.200

FIGURE 5-49 . ANALYSIS OF TUG FWD. COMP. STATIONED AT GEO. SHADOW PT.

TEMP NODE NO.   310 Star Tracker Pri
MIN TEMP OF   236.182 OCCURRED AT TIME   45.000
MAX TEMP OF   302.516 OCCURRED AT TIME   1.800

FIGURE 5-50 . ANALYSIS OF TUG FWD. COMP. + COMPONENTS WITH HEAT PIPES
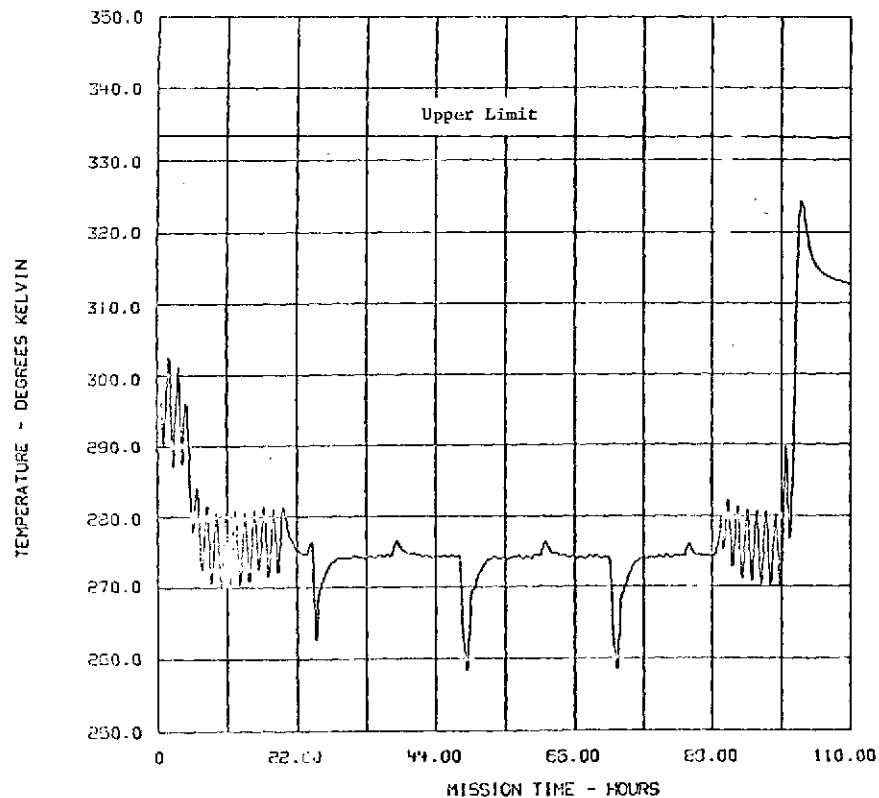
TEMP NODE NO.	320 Star Tracker Sec	
MIN TEMP OF	250.379 OCCURRED AT TIME	48.900
MAX TEMP OF	324.213 OCCURRED AT TIME	102.200

FIGURE 5-51   ANALYSIS OF TUG FWD. COMP. STATIONED AT GEO. SHADOW PT.

TEMP NODE NO.	320 Star Tracker Sec	
MIN TEMP OF	236.501 OCCURRED AT TIME	45.000
MAX TEMP OF	302.583 OCCURRED AT TIME	1.800

FIGURE 5-52 . ANALYSIS OF TUG FWD. COMP. + COMPONENTS WITH HEAT PIPES

TEMP NODE NO.   330 Horizon Scanner
MIN TEMP OF   248.259 OCCURRED AT TIME   48.900
MAX TEMP OF   328.487 OCCURRED AT TIME   101.800

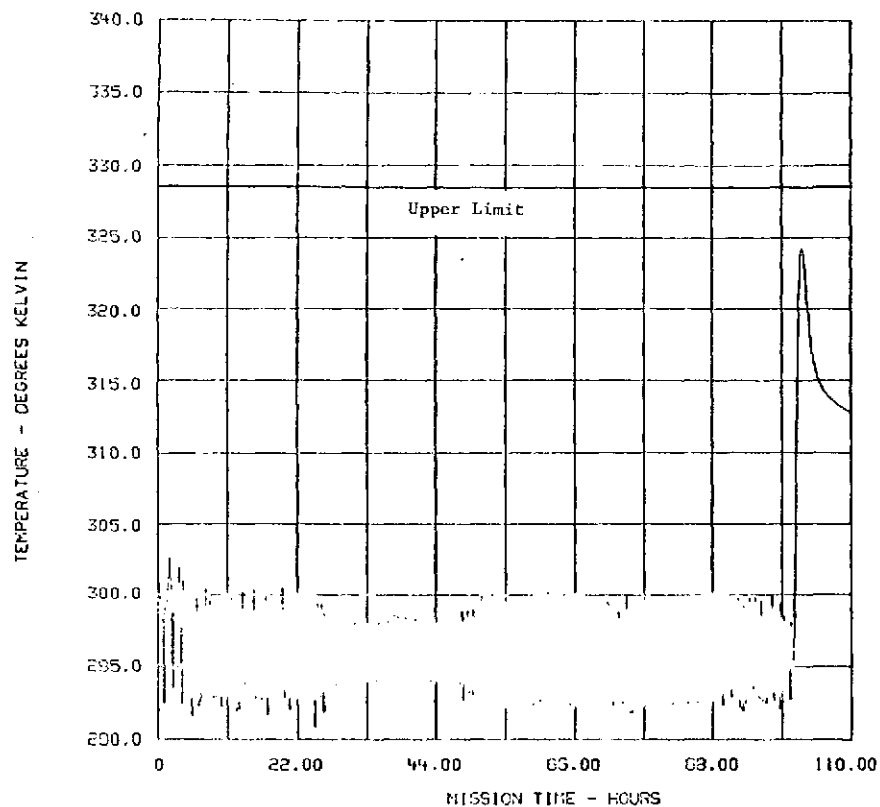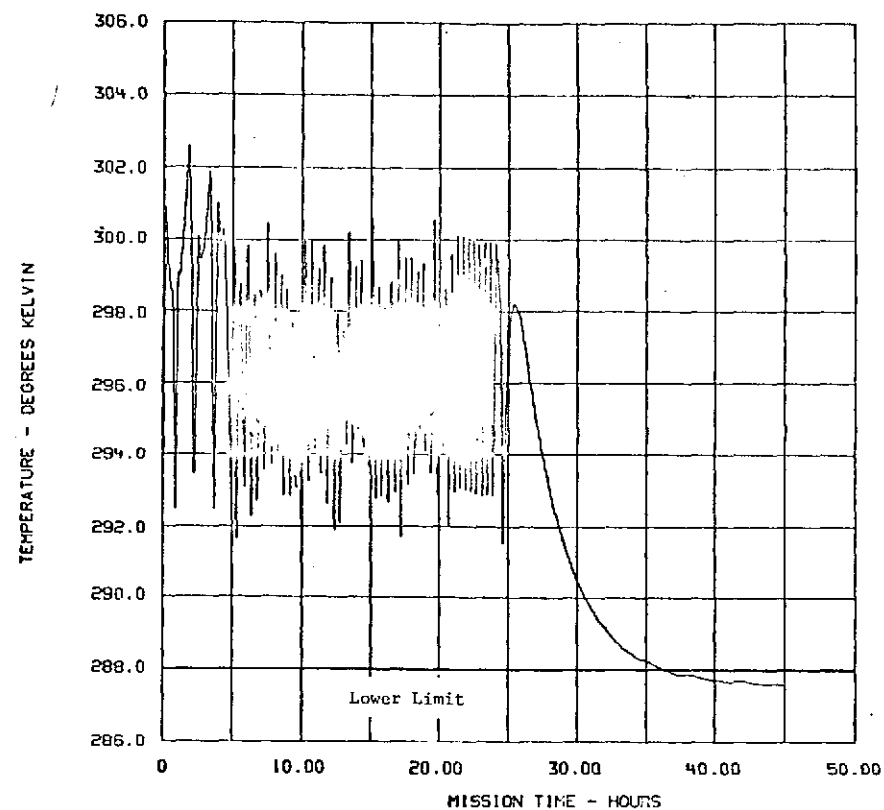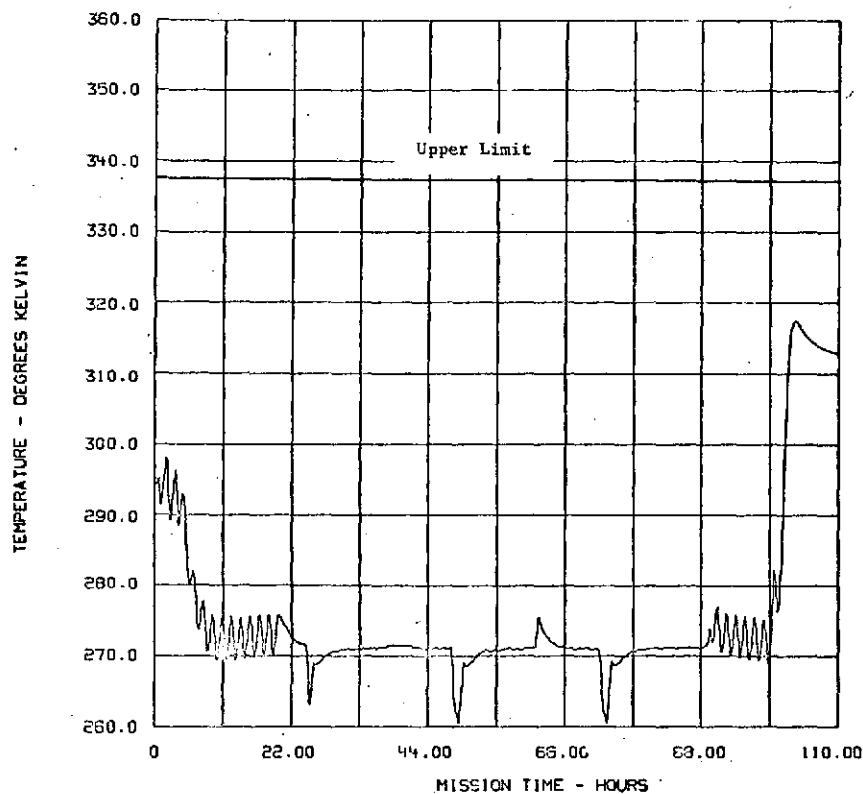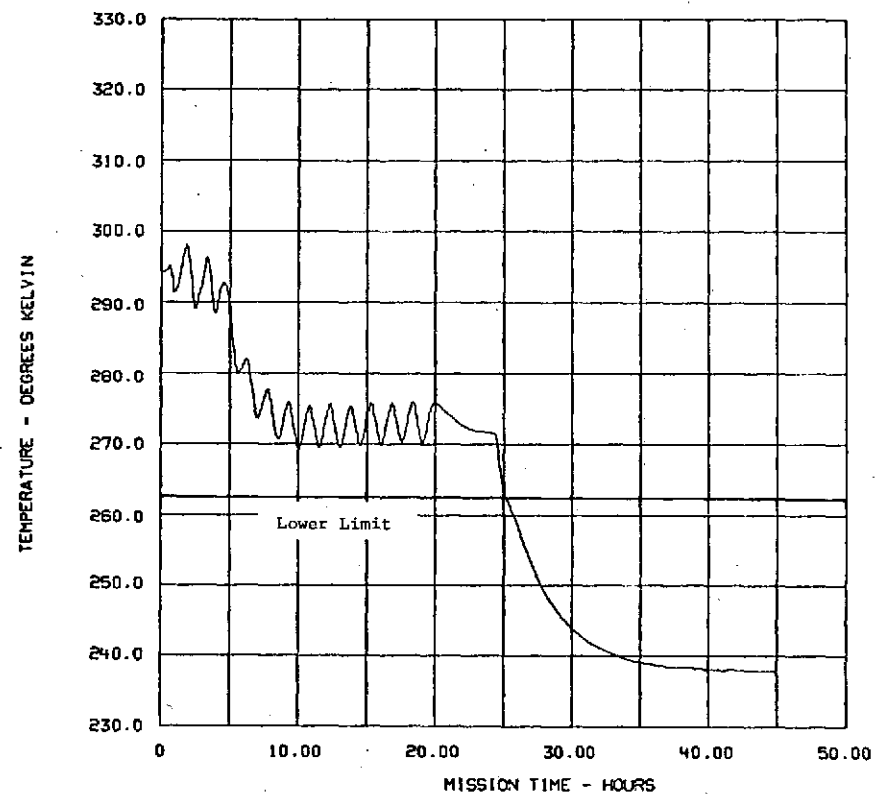FIGURE 5-53 . ANALYSIS OF TUG FWD. COMP. STATIONED AT GEO. SHADOW PT.

TEMP NODE NO.   330 Horizon Scanner
MIN TEMP OF   228.270 OCCURRED AT TIME   44.900
MAX TEMP OF   303.737 OCCURRED AT TIME   1.800

5-43

FIGURE 5-54 . ANALYSIS OF TUG FWD. COMP. + COMPONENTS WITH HEAT PIPES

TEMP NODE NO.   340 Horizon Scanner Elec.

MIN TEMP OF   253.963   OCCURRED AT TIME   48.900

MAX TEMP OF   316.263   OCCURRED AT TIME   103.300

FIGURE 5-55 . ANALYSIS OF TUG FWD. COMP. STATIONED AT GEO. SHADOW PT.
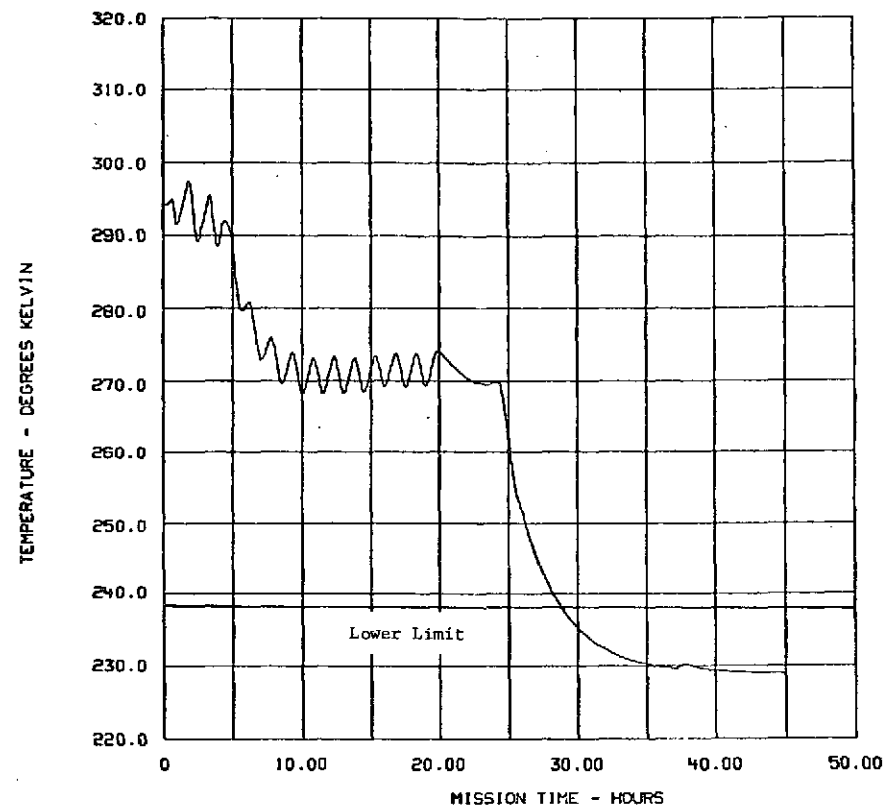
TEMP NODE NO.   340 Horizon Scanner Elec.

MIN TEMP OF   228.905   OCCURRED AT TIME   45.000

MAX TEMP OF   297.399   OCCURRED AT TIME   1.800
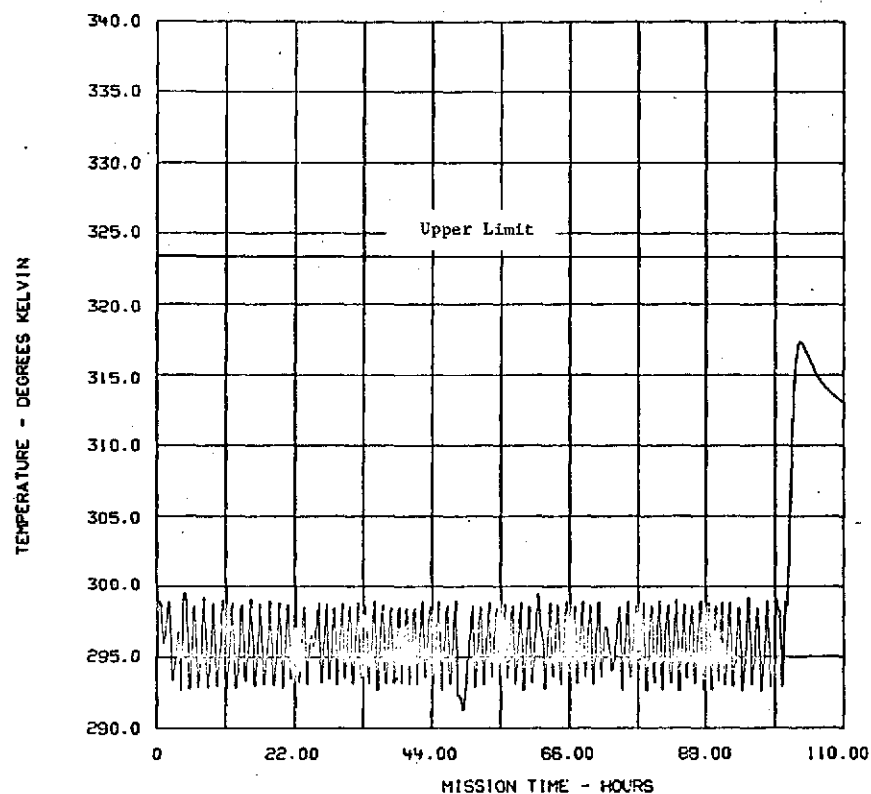
TEMP NODE NO. 350 Laser Radar Pri
MIN TEMP OF 291.207 OCCURRED AT TIME 48.900
MAX TEMP OF 317.372 OCCURRED AT TIME 103.000

FIGURE 5-56 . ANALYSIS OF TUG FWD. COMP. + COMPONENTS WITH HEAT PIPES

TEMP NODE NO. 350 Laser Radar Pri
MIN TEMP OF 275.599 OCCURRED AT TIME 45.000
MAX TEMP OF 299.523 OCCURRED AT TIME 4.300

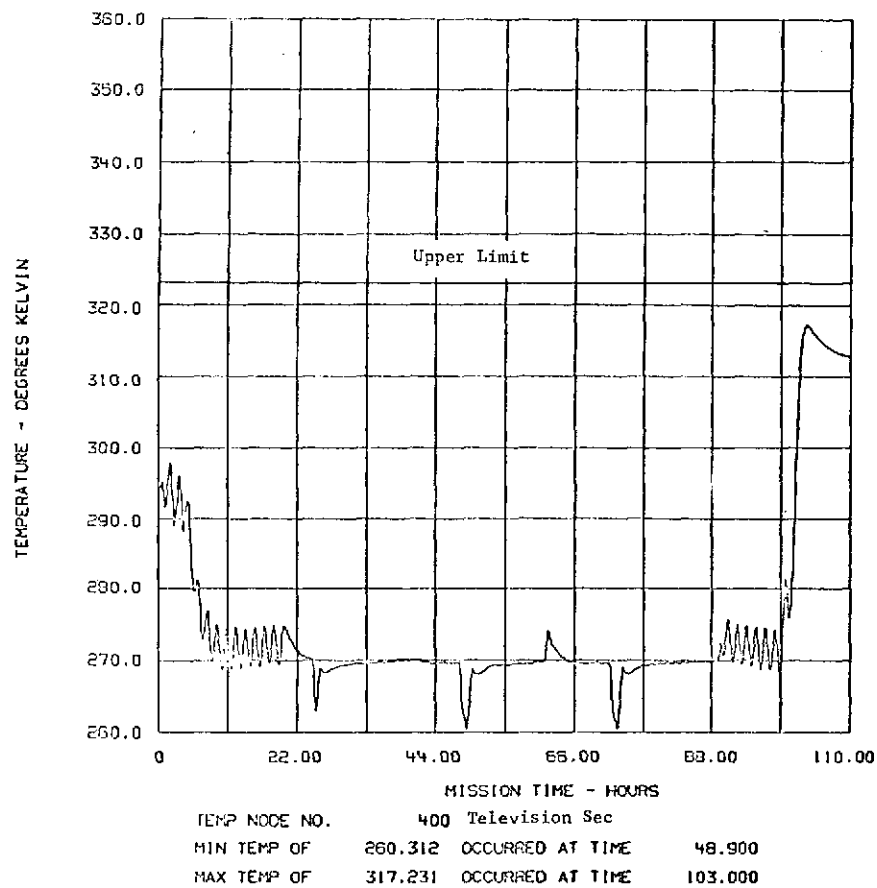FIGURE 5-57 . ANALYSIS OF TUG FWD. COMP. STATIONED AT GEO. SHADOW PT.

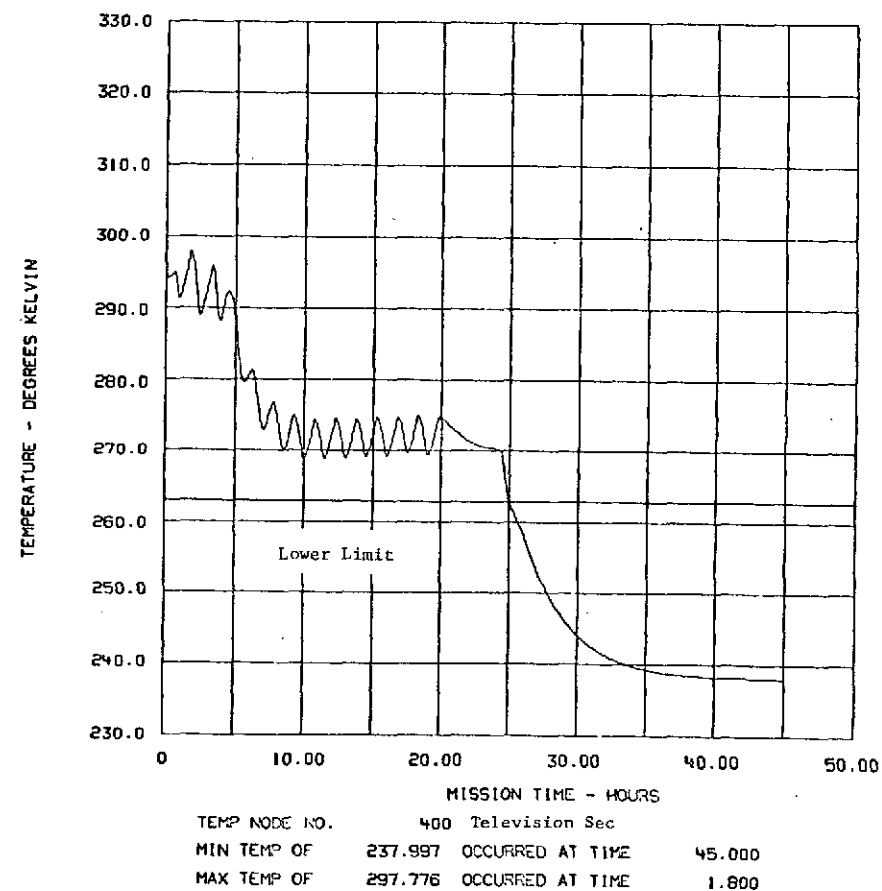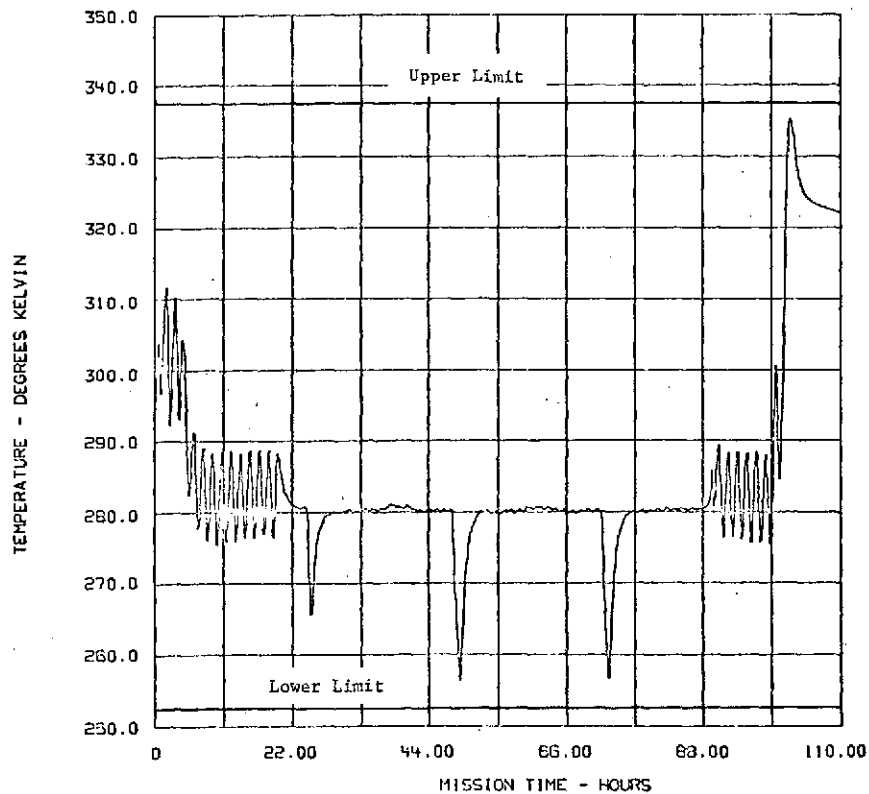FIGURE 5-58 .   ANALYSIS OF TUG FWD. COMP. + COMPONENTS WITH HEAT PIPES
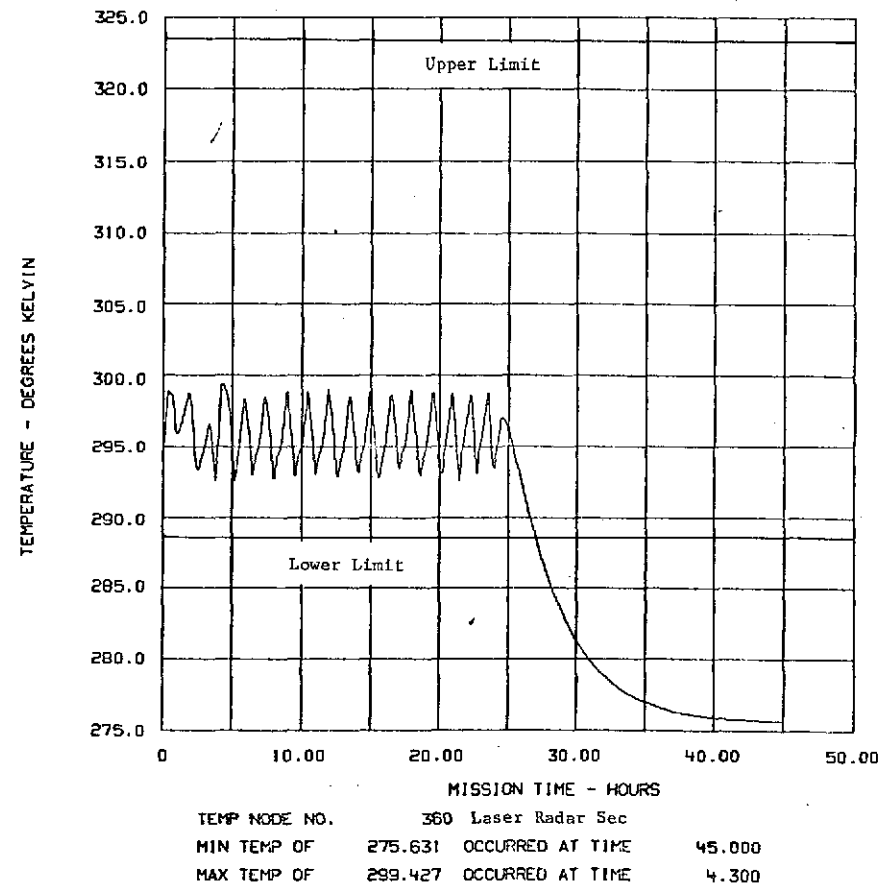
FIGURE 5-59 .   ANALYSIS OF TUG FWD. COMP. STATIONED AT GEO. SHADOW PT.

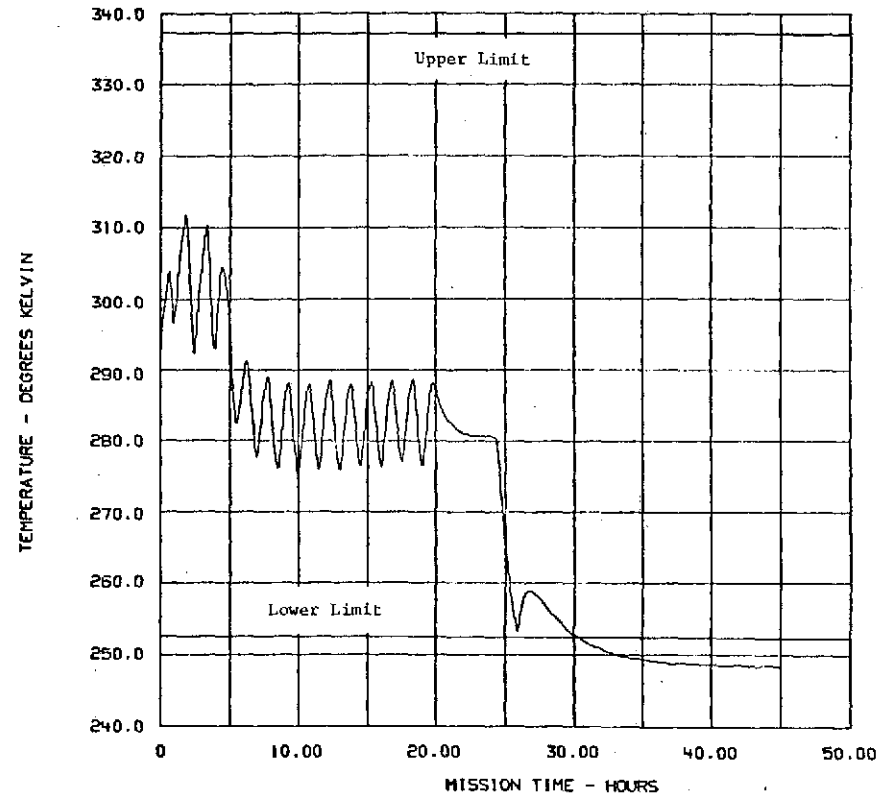FIGURE 5-60 .   ANALYSIS OF TUG FWD. COMP. + COMPONENTS WITH HEAT PIPES

TEMP NODE NO.	370	Laser Radar Elec Pri	
MIN TEMP OF	291.508	OCCURRED AT TIME	5.400
MAX TEMP OF	324.355	OCCURRED AT TIME	102.200

FIGURE 5-61 .   ANALYSIS OF TUG FWD. COMP. STATIONED AT GEO. SHADOW PT.

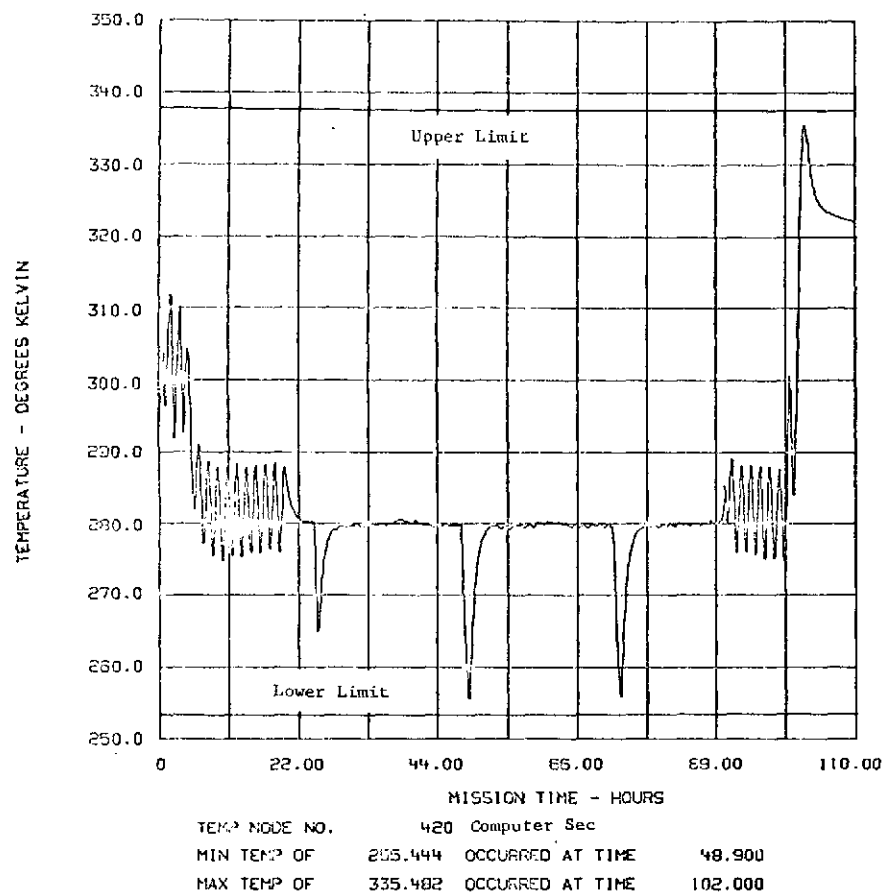| TEMP NODE NO.	370	Laser Radar Elec Pri	
MIN TEMP OF	287.003	OCCURRED AT TIME	45.000
MAX TEMP OF	302.818	OCCURRED AT TIME	1.800

FIGURE 5-62 . ANALYSIS OF TUG FWD. COMP. + COMPONENTS WITH HEAT PIPES

FIGURE 5-63 . ANALYSIS OF TUG FWD. COMP. STATIONED AT GEO. SHADOW PT.

TEMP NODE NO.   390 Television Pri
MIN TEMP OF   260.393 OCCURRED AT TIME   48.900
MAX TEMP OF   317.485 OCCURRED AT TIME   103.000

FIGURE 5-64 .   ANALYSIS OF TUG FWD. COMP. + COMPONENTS WITH HEAT PIPES

TEMP NODE NO.   390 Television Pri
MIN TEMP OF   237.861 OCCURRED AT TIME   45.000
MAX TEMP OF   298.045 OCCURRED AT TIME   1.800

FIGURE 5-65 .   ANALYSIS OF TUG FWD. COMP. STATIONED AT GEO. SHADOW PT.

5-149

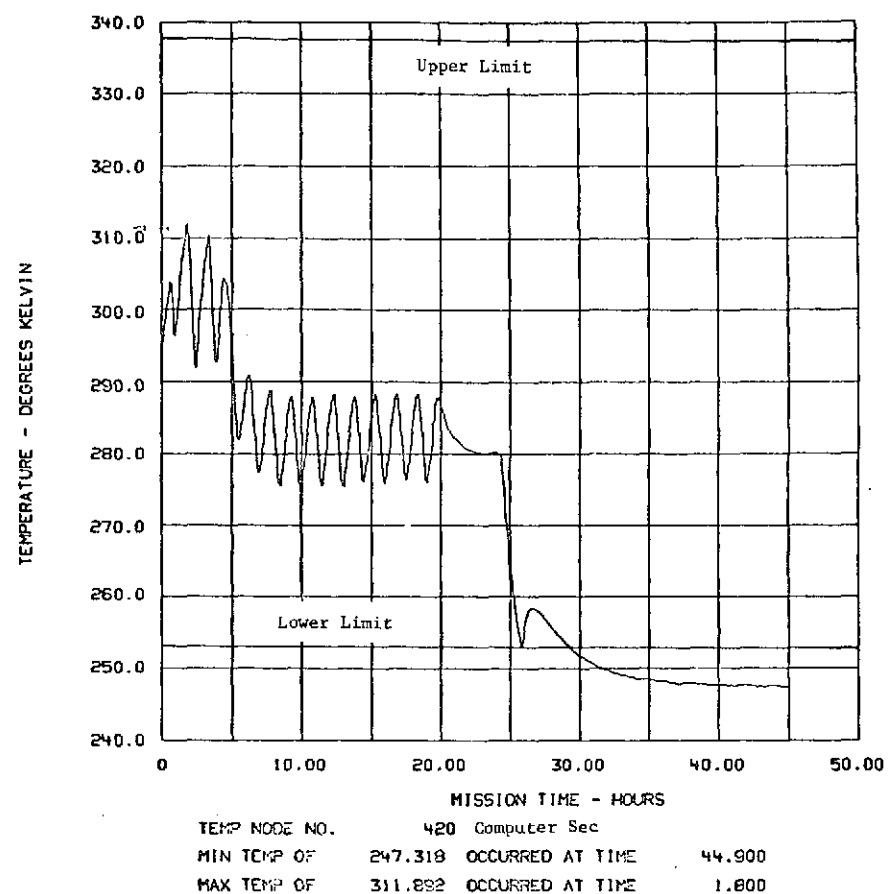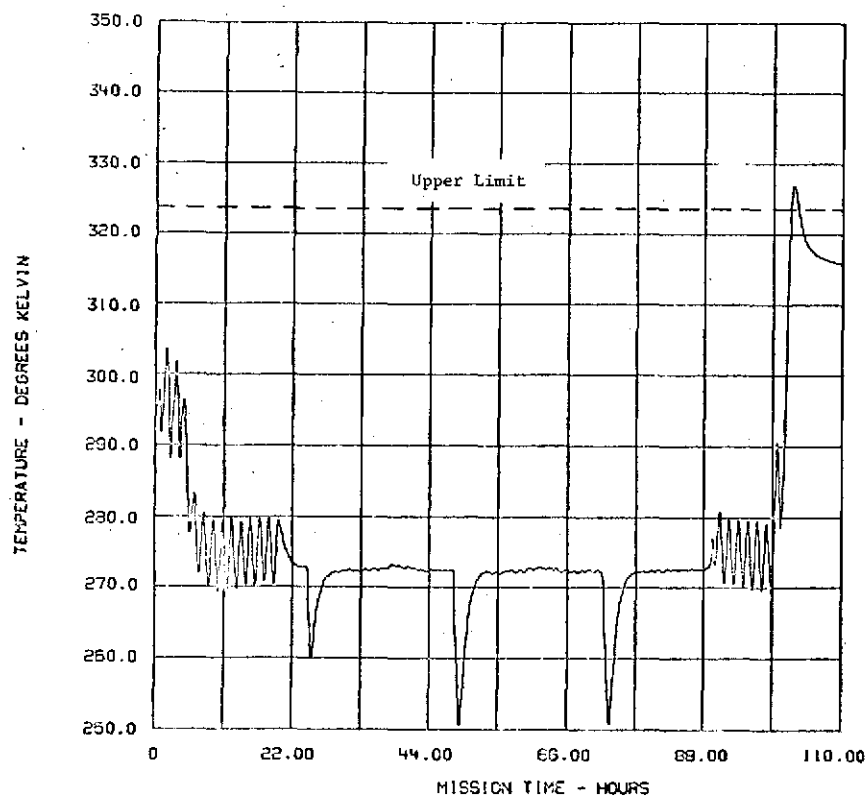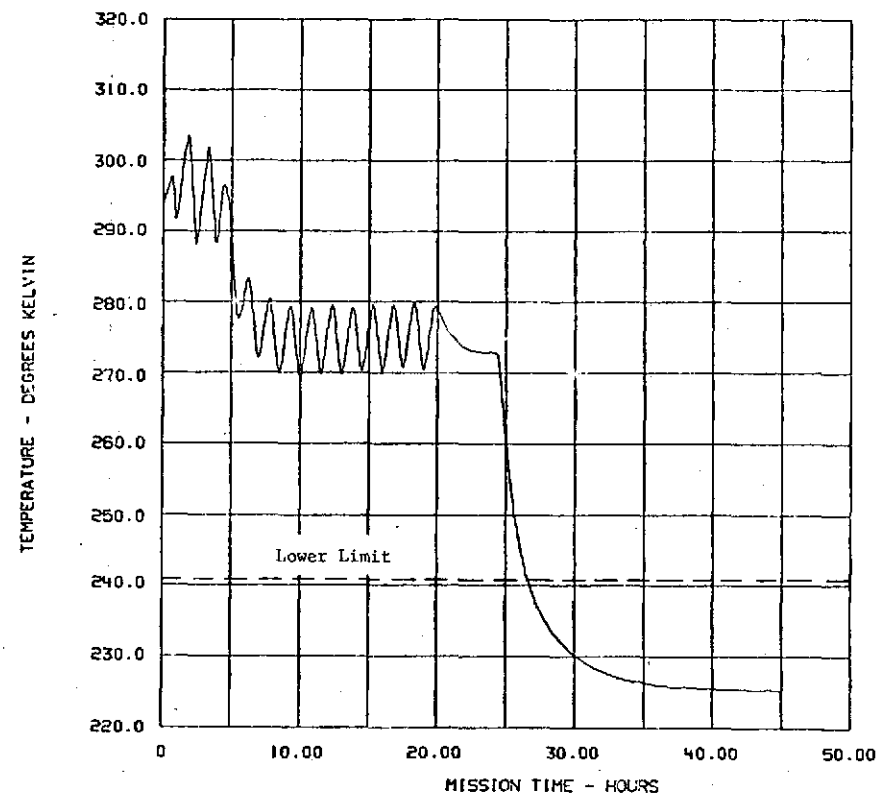FIGURE 5-66 .   ANALYSIS OF TUG FWD. COMP. + COMPONENTS WITH HEAT PIPES

TEMP NODE NO.   400   Television Sec
MIN TEMP OF   260.312   OCCURRED AT TIME   48.900
MAX TEMP OF   317.231   OCCURRED AT TIME   103.000

FIGURE 5-67 .   ANALYSIS OF TUG FWD. COMP. STATIONED AT GEO. SHADOW PT.

TEMP NODE NO.   400   Television Sec
MIN TEMP OF   237.997   OCCURRED AT TIME   45.000
MAX TEMP OF   297.776   OCCURRED AT TIME   1.800

TEMP NODE NO.   410 Computer Pri
MIN TEMP OF   256.315 OCCURRED AT TIME   49.900
MAX TEMP OF   335.281 OCCURRED AT TIME   102.000

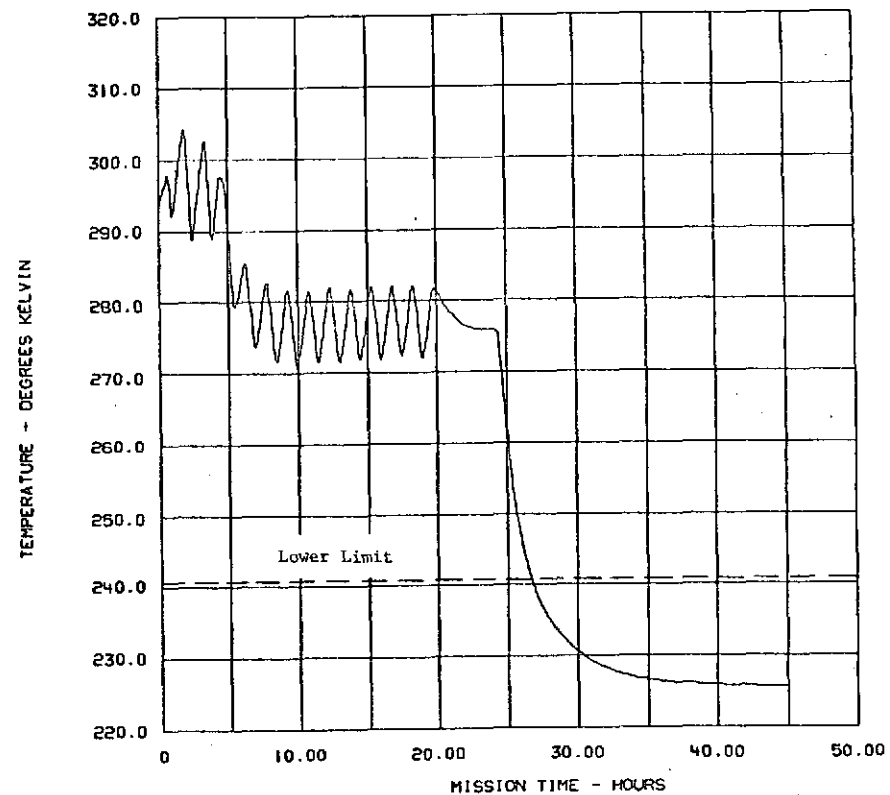FIGURE 5-68 .   ANALYSIS OF TUG FWD. COMP. + COMPONENTS WITH HEAT PIPES

TEMP NODE NO.   410 Computer Pri
MIN TEMP OF   248.304 OCCURRED AT TIME   44.900
MAX TEMP OF   311.855 OCCURRED AT TIME   1.800

FIGURE 5-69.   ANALYSIS OF TUG FWD. COMP. STATIONED AT GEO. SHADOW PT.

FIGURE 5-70 . ANALYSIS OF TUG FWD. COMP. + COMPONENTS WITH HEAT PIPES

FIGURE 5-71 . ANALYSIS OF TUG FWD. COMP. STATIONED AT GEO. SHADOW PT.

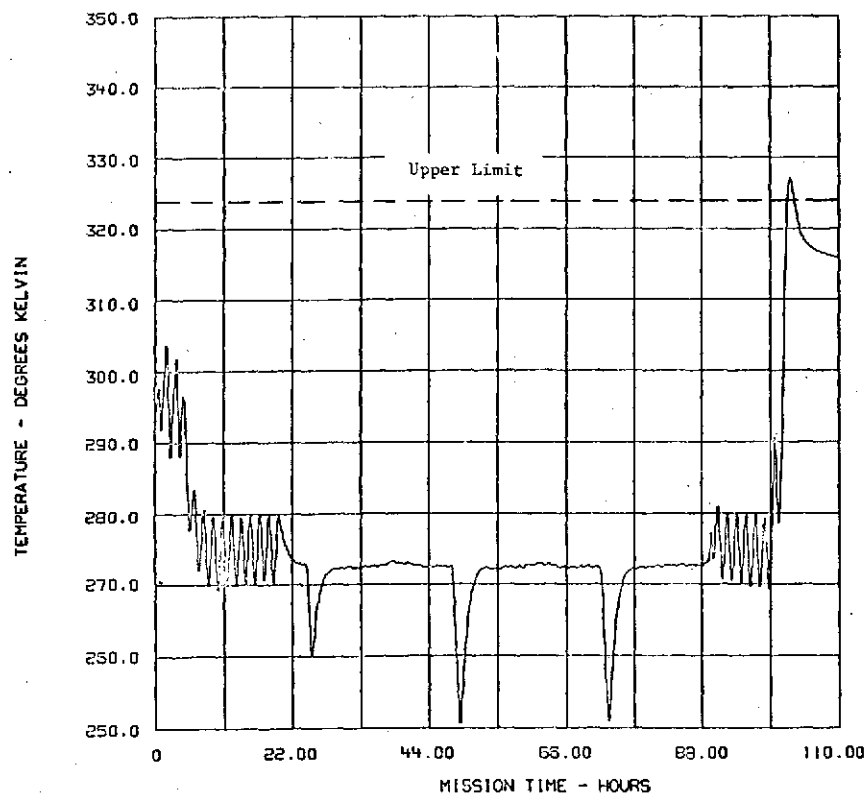FIGURE 5-72 . ANALYSIS OF TUG FWD. COMP. + COMPONENTS WITH HEAT PIPES

TEMP NODE NO. 530 Data Acc Unit 1, 2
MIN TEMP OF 250.615 OCCURRED AT TIME 48.900
MAX TEMP OF 326.882 OCCURRED AT TIME 102.200

FIGURE 5-73 . ANALYSIS OF TUG FWD. COMP. STATIONED AT GEO. SHADOW PT.

TEMP NODE NO. 530 Data Acc Unit 1, 2
MIN TEMP OF 225.139 OCCURRED AT TIME 44.900
MAX TEMP OF 303.659 OCCURRED AT TIME 1.800

5-53

TEMPERATURE - DEGREES KELVIN

Upper Limit

MISSION TIME - HOURS
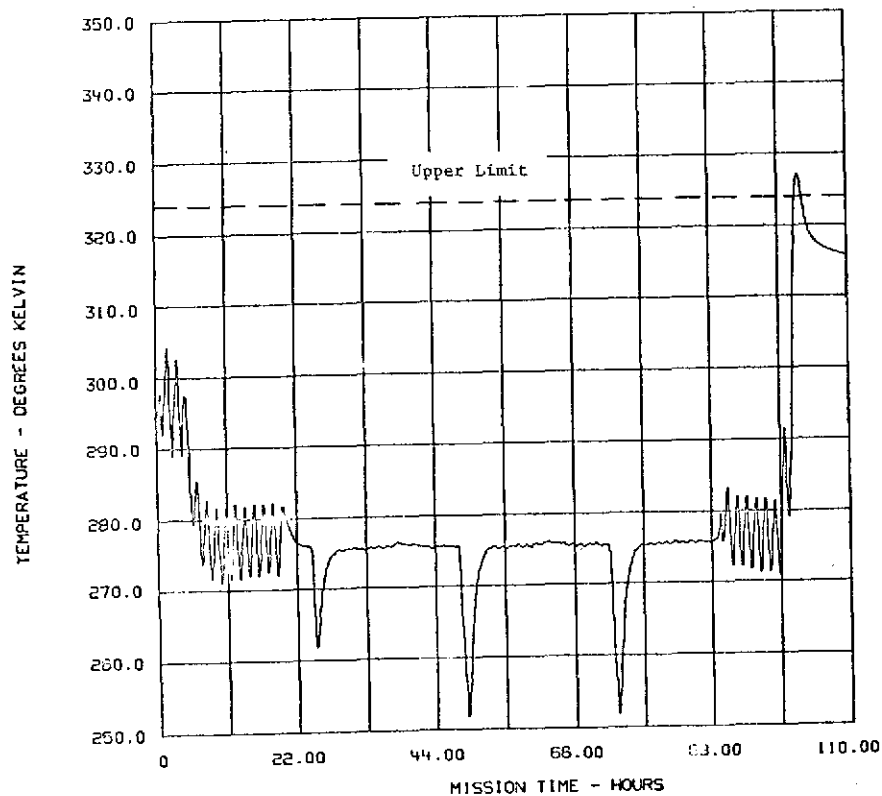
TEMP NODE NO.	540 Data Acc Unit 3, 4	
MIN TEMP OF	251.667 OCCURRED AT TIME	48.900
MAX TEMP OF	327.082 OCCURRED AT TIME	102.200

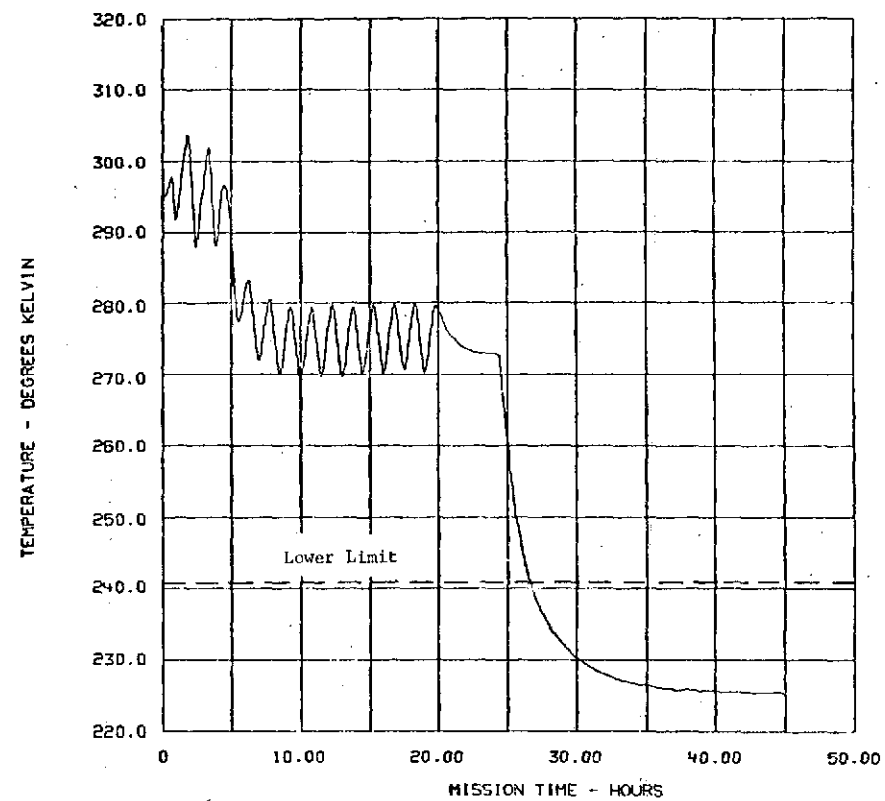FIGURE 5-74. ANALYSIS OF TUG FWD. COMP. + COMPONENTS WITH HEAT PIPES

TEMPERATURE - DEGREES KELVIN

Lower Limit

MISSION TIME - HOURS

TEMP NODE NO.	540 Data Acc Unit 3, 4	
MIN TEMP OF	225.569 OCCURRED AT TIME	45.000
MAX TEMP OF	304.313 OCCURRED AT TIME	1.800

FIGURE 5-75. ANALYSIS OF TUG FWD. COMP. STATIONED AT GEO. SHADOW PT.

FIGURE 5-76. ANALYSIS OF TUG FWD. COMP. + COMPONENTS WITH HEAT PIPES

TEMP NODE NO. 550 Data Acc Unit 4, 5
MIN TEMP OF 250.615 OCCURRED AT TIME 48.900
MAX TEMP OF 326.942 OCCURRED AT TIME 102.200

FIGURE 5-77. ANALYSIS OF TUG FWD. COMP. STATIONED AT GEO. SHADOW PT.
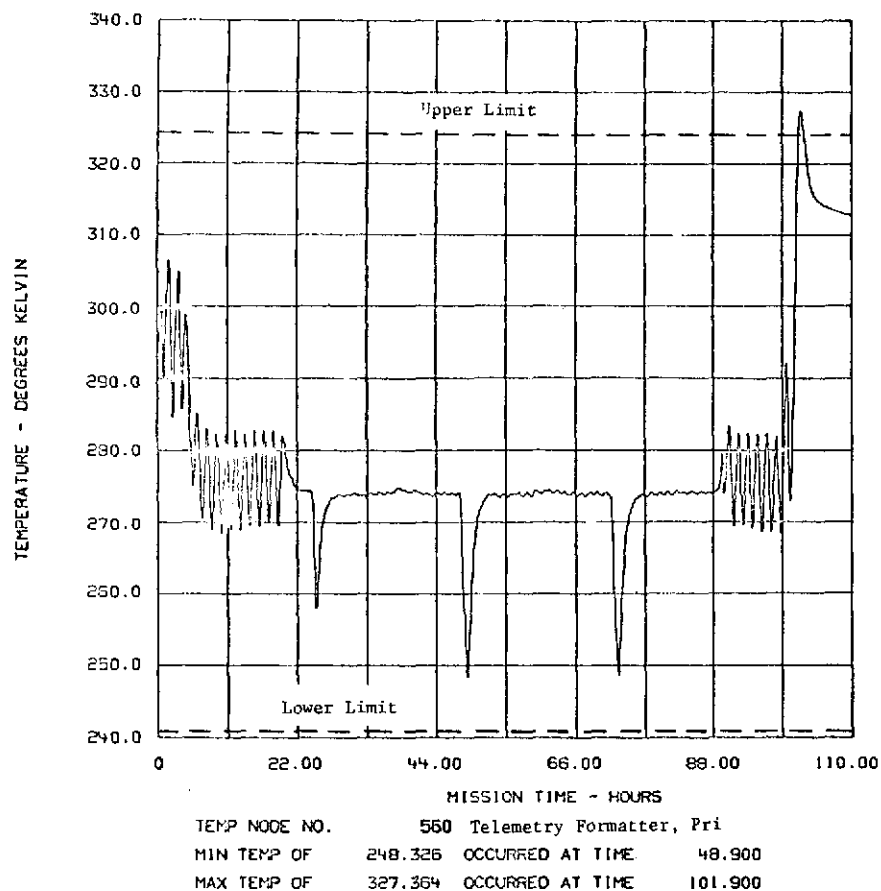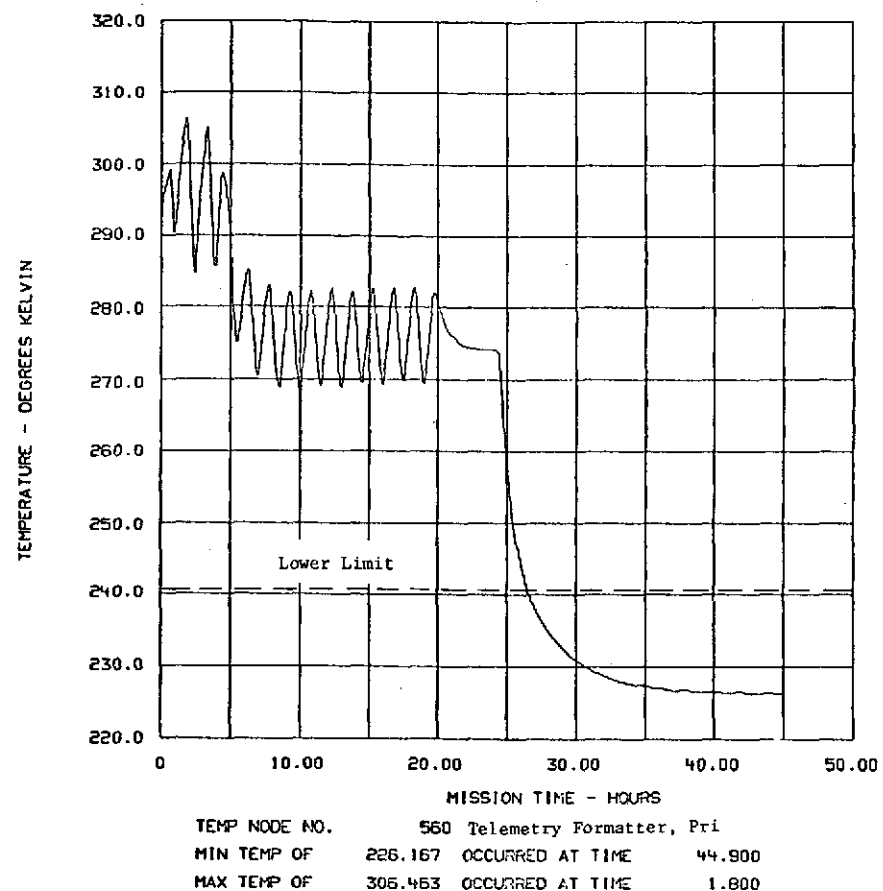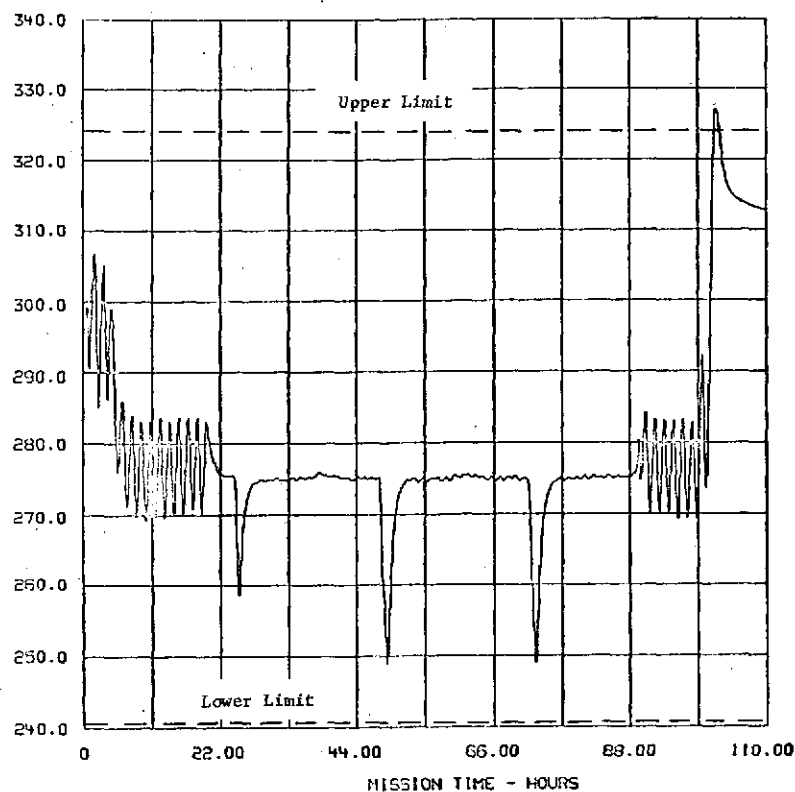
TEMP NODE NO. 550 Data Acc Unit 4, 5
MIN TEMP OF 225.242 OCCURRED AT TIME 45.000
MAX TEMP OF 303.706 OCCURRED AT TIME 1.800

FIGURE 5-78 . ANALYSIS OF TUG FWD. COMP. + COMPONENTS WITH HEAT PIPES

TEMP NODE NO.		560	Telemetry Formatter,	Pri
MIN TEMP OF	248.326	OCCURRED AT TIME	48.900	
MAX TEMP OF	327.364	OCCURRED AT TIME	101.900	

FIGURE 5-79 . ANALYSIS OF TUG FWD. COMP. STATIONED AT GEO. SHADOW PT.

TEMP NODE NO.		560	Telemetry Formatter,	Pri
MIN TEMP OF	226.167	OCCURRED AT TIME	44.900	
MAX TEMP OF	305.463	OCCURRED AT TIME	1.800	

FIGURE 5-80 . ANALYSIS OF TUG FWD. COMP. + COMPONENTS WITH HEAT PIPES
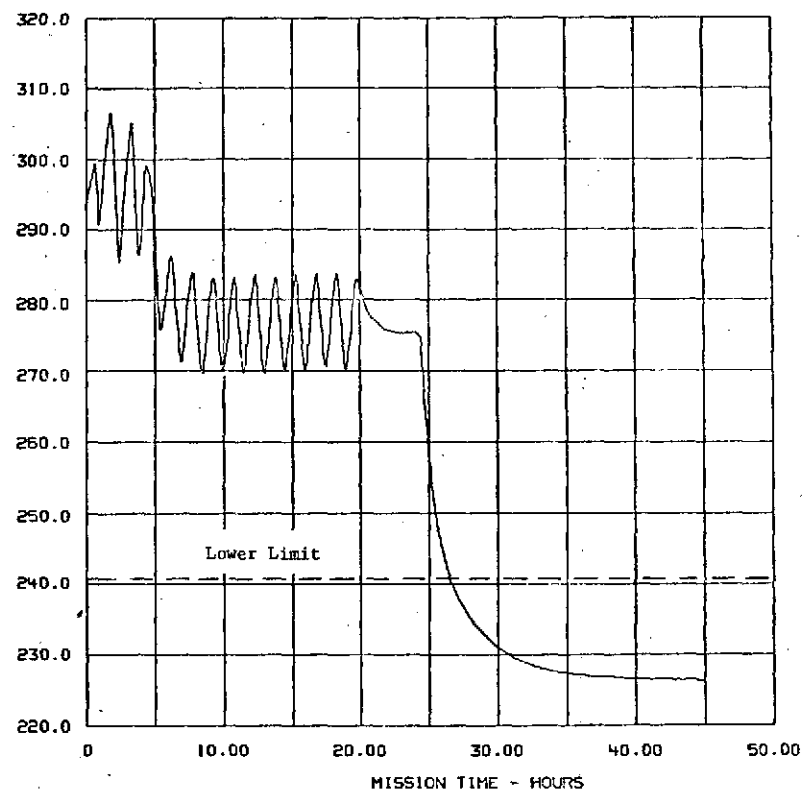
TEMP NODE NO.   570 Telemetry Formatter, Sec
MIN TEMP OF   248.844 OCCURRED AT TIME   48.900
MAX TEMP OF   327.169 OCCURRED AT TIME   101.900

FIGURE 5-81 . ANALYSIS OF TUG FWD. COMP. STATIONED AT GEO. SHADOW PT.

TEMP NODE NO.   570 Telemetry Formatter, Sec
MIN TEMP OF   226.329 OCCURRED AT TIME   45.000
MAX TEMP OF   306.568 OCCURRED AT TIME   1.800
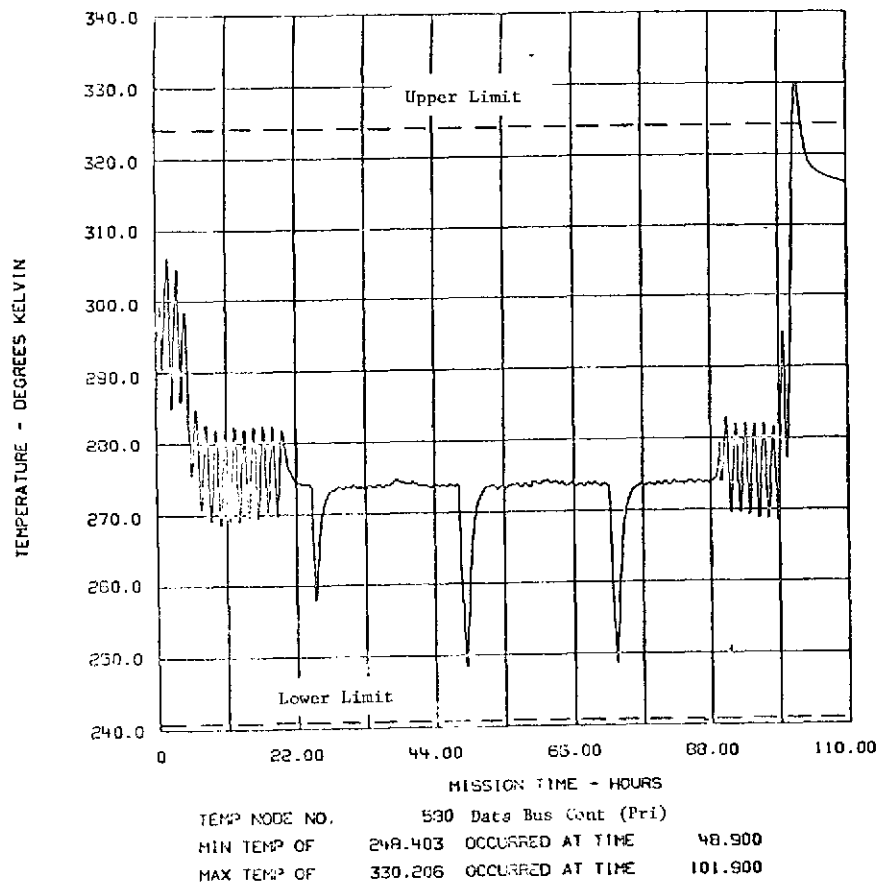
FIGURE 5-82. ANALYSIS OF TUG FWD. COMP. + COMPONENTS WITH HEAT PIPES

TEMP NODE NO.	530 Data Bus Cont (Pri)		
MIN TEMP OF	248.403	OCCURRED AT TIME	48.900
MAX TEMP OF	330.206	OCCURRED AT TIME	101.900
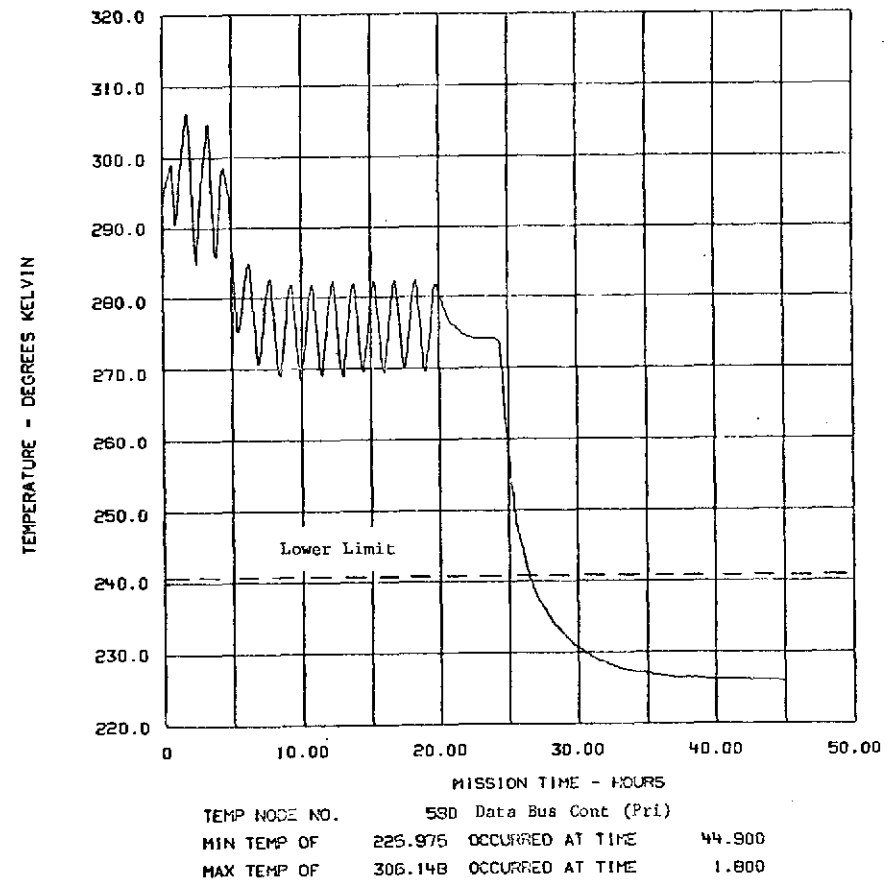
FIGURE 5-83. ANALYSIS OF TUG FWD. COMP. STATIONED AT GEO. SHADOW PT.

TEMP NODE NO.	530 Data Bus Cont (Pri)		
MIN TEMP OF	226.976	OCCURRED AT TIME	44.900
MAX TEMP OF	306.148	OCCURRED AT TIME	1.800

TEMPERATURE - DEGREES KELVIN

Upper Limit

Lower Limit

MISSION TIME - HOURS

TEMP NODE NO.	590	Data Bus Cont (Sec)	
MIN TEMP OF	248.914	OCCURRED AT TIME	48.900
MAX TEMP OF	330.143	OCCURRED AT TIME	102.000
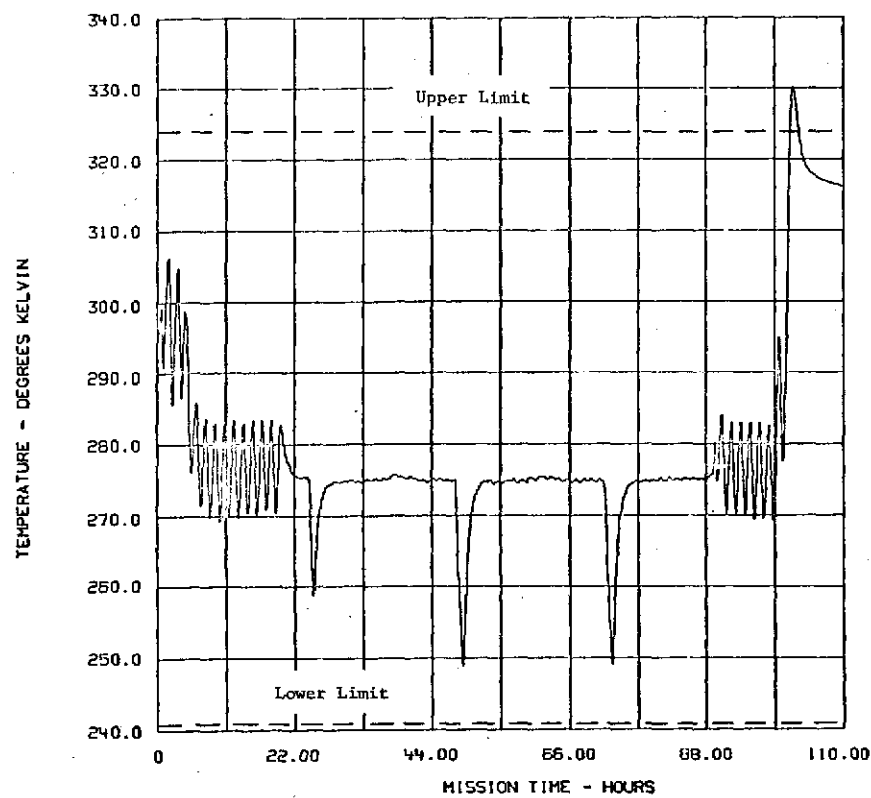
FIGURE 5-84. ANALYSIS OF TUG FWD. COMP. + COMPONENTS WITH HEAT PIPES

TEMPERATURE - DEGREES KELVIN

Lower Limit

MISSION TIME - HOURS

TEMP NODE NO.	590	Data Bus Cont (Sec)	
MIN TEMP OF	226.149	OCCURRED AT TIME	45.000
MAX TEMP OF	306.261	OCCURRED AT TIME	1.800
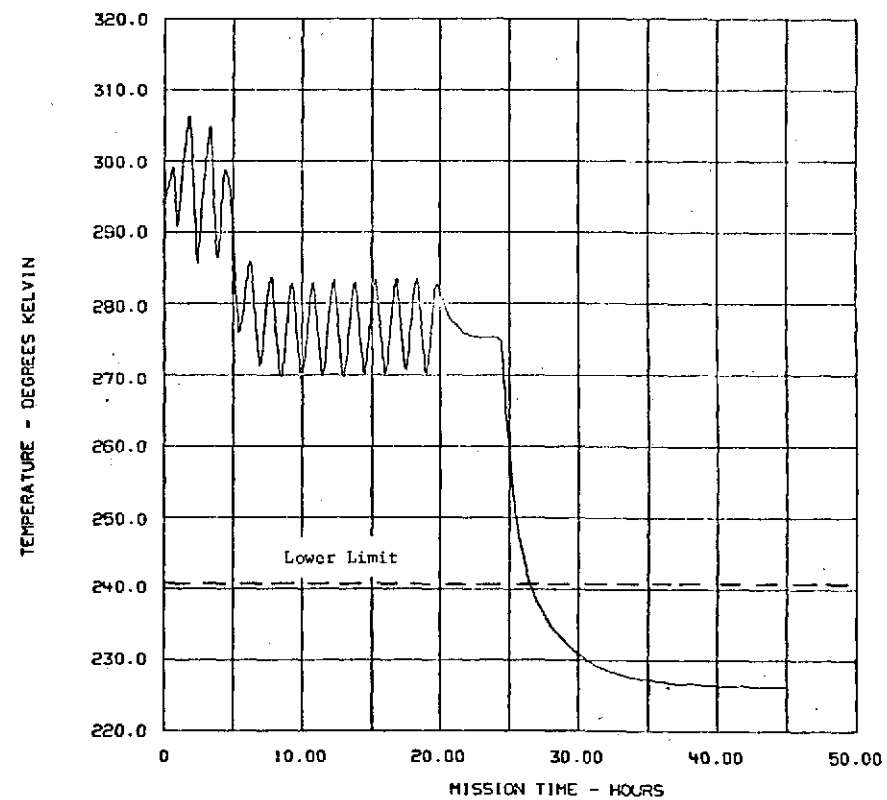
FIGURE 5-85. ANALYSIS OF TUG FWD. COMP. STATIONED AT GEO. SHADOW PT.

TEMPERATURE – DEGREES KELVIN

MISSION TIME – HOURS

TEMP NODE NO.   490 Tape Recorder
MIN TEMP OF   265.873 OCCURRED AT TIME   49.100
MAX TEMP OF   314.953 OCCURRED AT TIME   104.100
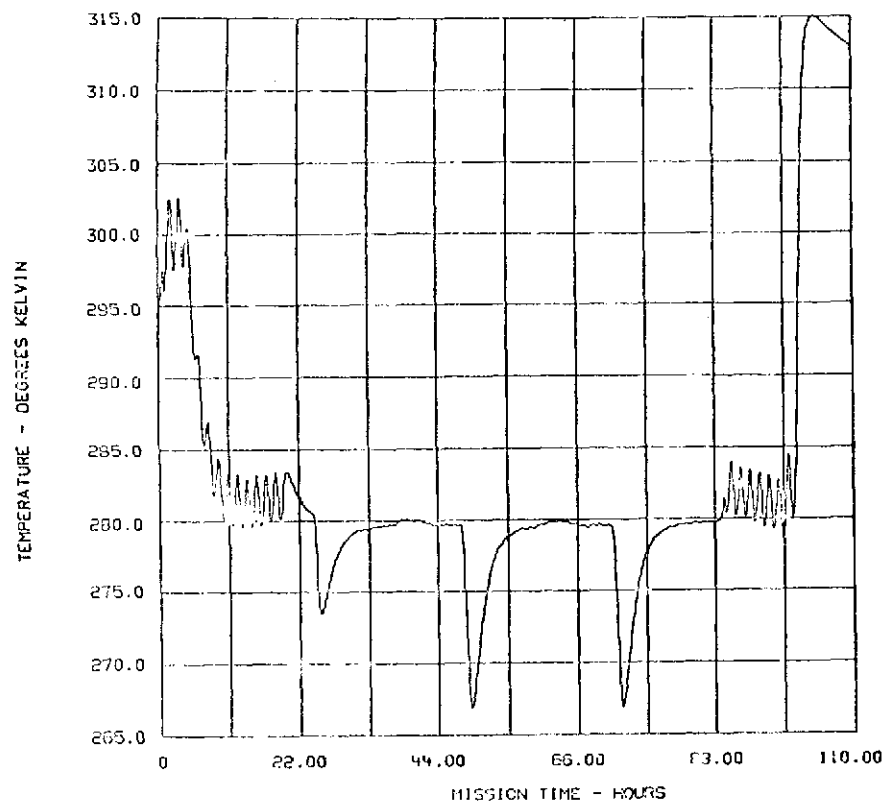
FIGURE 5-86   ANALYSIS OF TUG FWD. COMP. + COMPONENTS WITH HEAT PIPES

TEMPERATURE – DEGREES KELVIN

MISSION TIME – HOURS

TEMP NODE NO.   490 Tape Recorder
MIN TEMP OF   231.823 OCCURRED AT TIME   45.000
MAX TEMP OF   302.025 OCCURRED AT TIME   3.300
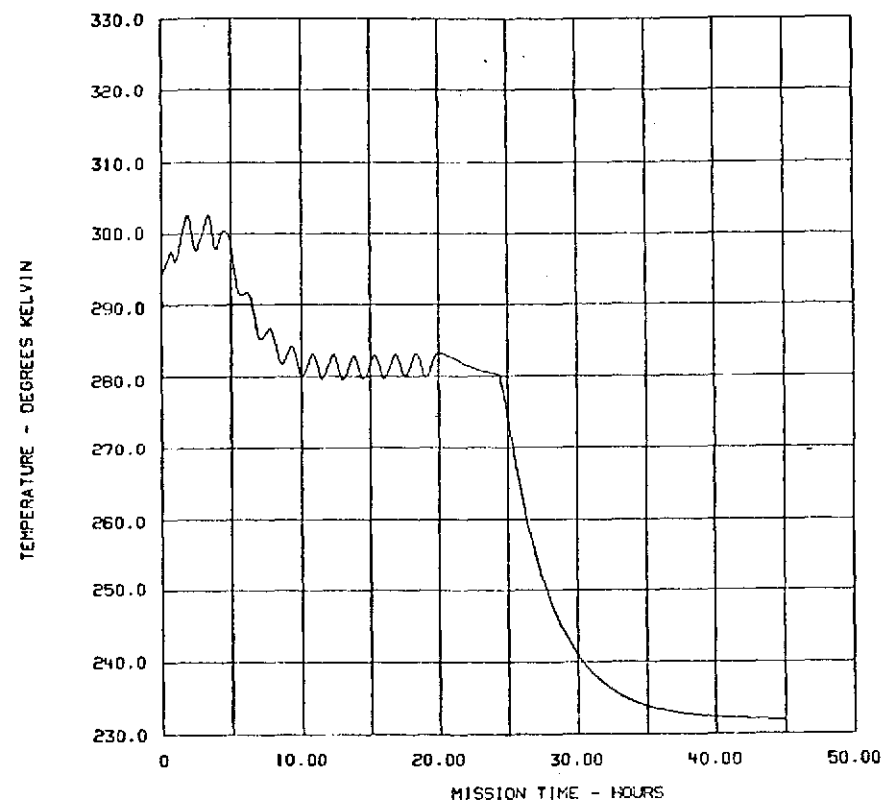
FIGURE 5-87 .   ANALYSIS OF TUG FWD. COMP. STATIONED AT GEO. SHADOW PT.

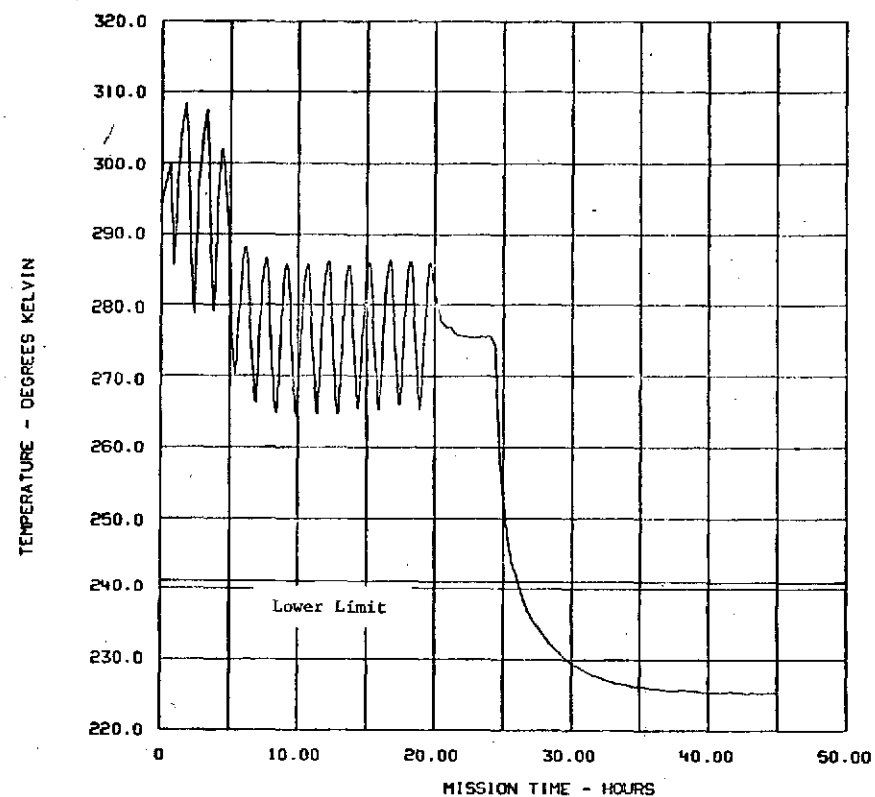FIGURE 5-88. ANALYSIS OF TUG FWD. COMP. + COMPONENTS WITH HEAT PIPES
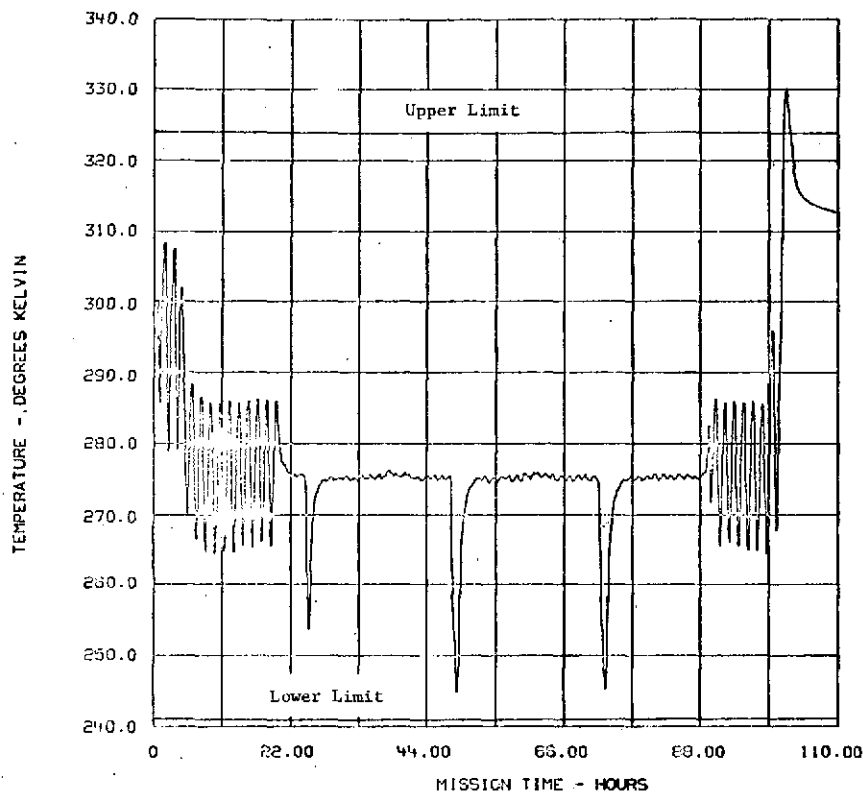
TEMP NODE NO.   430 Transponder, PM Pri
MIN TEMP OF   244.731   OCCURRED AT TIME   48.800
MAX TEMP OF   330.203   OCCURRED AT TIME   101.700

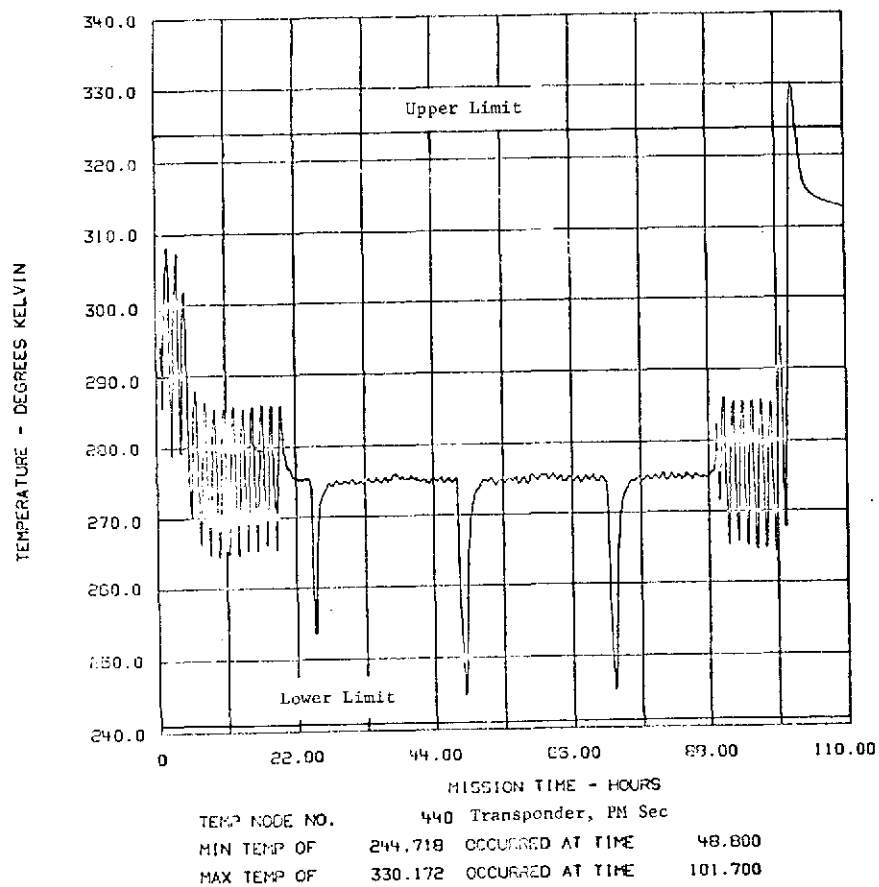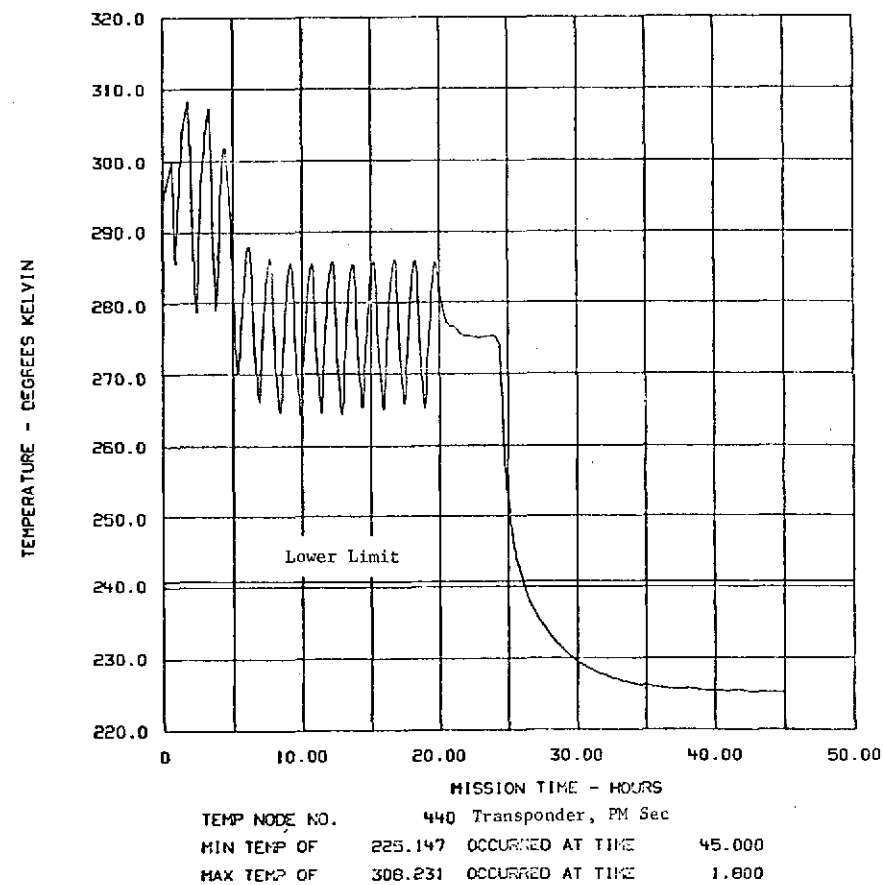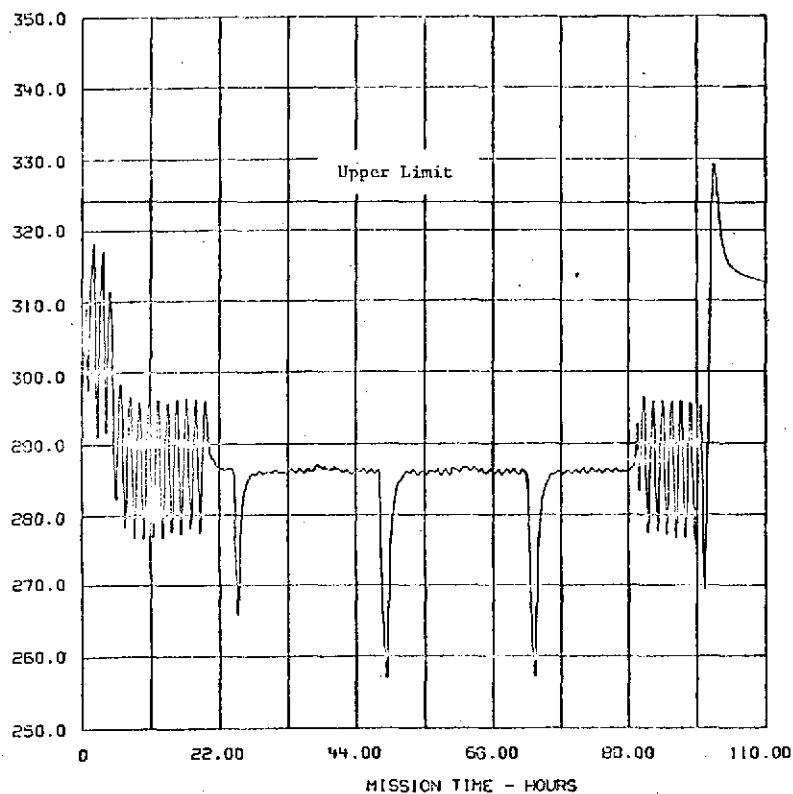FIGURE 5-89. ANALYSIS OF TUG FWD. COMP. STATIONED AT GEO. SHADOW PT.

TEMP NODE NO.   430 Transponder, PM Pri
MIN TEMP OF   225.125   OCCURRED AT TIME   45.000
MAX TEMP OF   308.395   OCCURRED AT TIME   1.800

TEMPERATURE - DEGREES KELVIN

MISSION TIME - HOURS

TEMP NODE NO.   440 Transponder, PM Sec
MIN TEMP OF   244.718 OCCURRED AT TIME   48.800
MAX TEMP OF   330.172 OCCURRED AT TIME   101.700

FIGURE 5-90 . ANALYSIS OF TUG FWD. COMP. + COMPONENTS WITH HEAT PIPES

TEMPERATURE - DEGREES KELVIN

MISSION TIME - HOURS

TEMP NODE NO.   440 Transponder, PM Sec
MIN TEMP OF   225.147 OCCURRED AT TIME   45.000
MAX TEMP OF   308.231 OCCURRED AT TIME   1.800

FIGURE 5-91 . ANALYSIS OF TUG FWD. COMP. STATIONED AT GEO. SHADOW PT.

FIGURE 5-92 . ANALYSIS OF TUG FWD. COMP. + COMPONENTS WITH HEAT PIPES
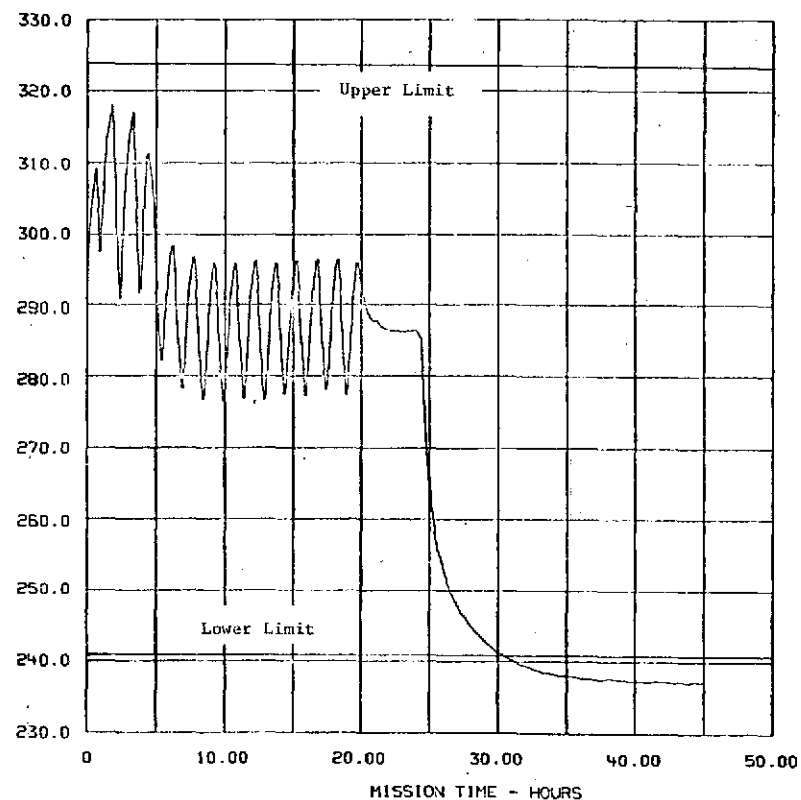
TEMP NODE NO.   450 Transmitter, FM Pri
MIN TEMP OF   256.787 OCCURRED AT TIME   48.800
MAX TEMP OF   329.284 OCCURRED AT TIME   101.700

FIGURE 5-93 . ANALYSIS OF TUG FWD. COMP. STATIONED AT GEO. SHADOW PT.
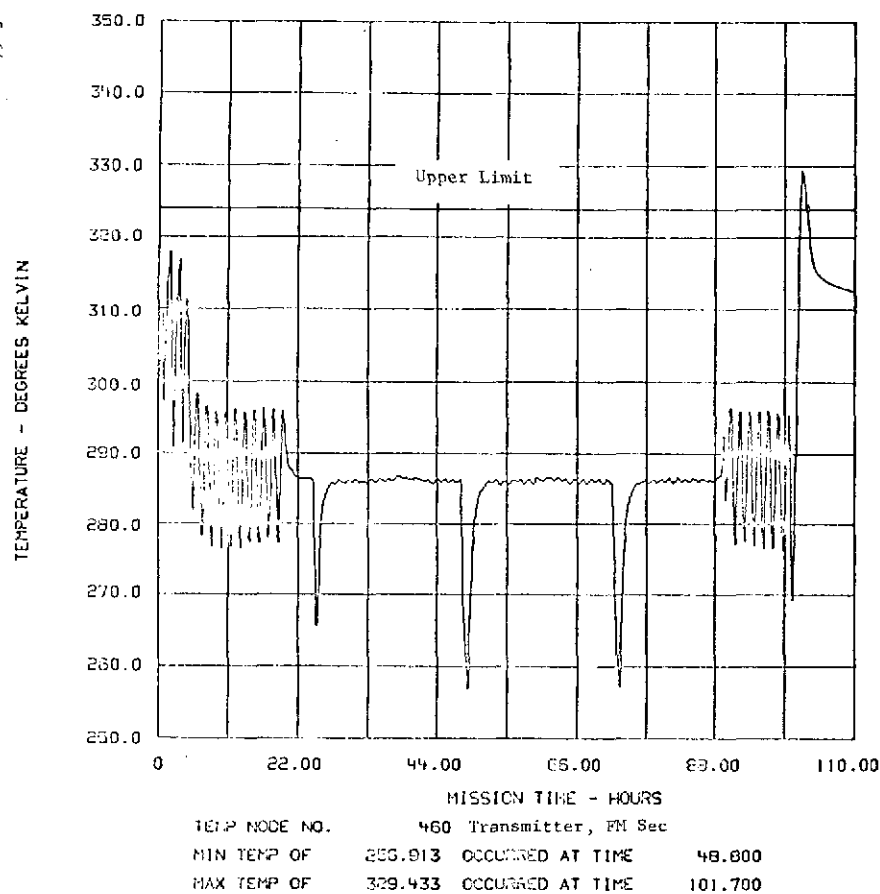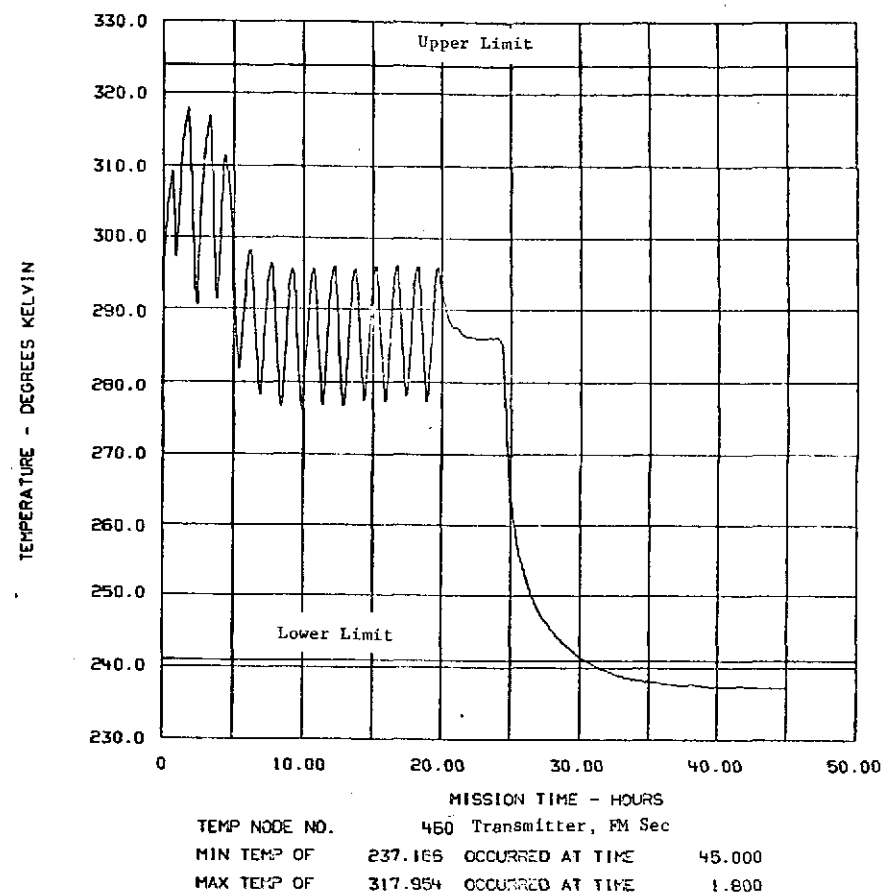
TEMP NODE NO.   450 Transmitter, FM Pri
MIN TEMP OF   236.993 OCCURRED AT TIME   45.000
MAX TEMP OF   318.028 OCCURRED AT TIME   1.800

5-63

FIGURE 5-94.   ANALYSIS OF TUG FWD. COMP. + COMPONENTS WITH HEAT PIPES

TEMP NODE NO.   460 Transmitter, FM Sec
MIN TEMP OF   255.913 OCCURRED AT TIME   48.800
MAX TEMP OF   329.433 OCCURRED AT TIME   101.700

FIGURE 5-95   ANALYSIS OF TUG FWD. COMP. STATIONED AT GEO. SHADOW PT.

TEMP NODE NO.   460 Transmitter, FM Sec
MIN TEMP OF   237.165 OCCURRED AT TIME   45.000
MAX TEMP OF   317.954 OCCURRED AT TIME   1.800

FIGURE 5-96   ANALYSIS OF TUG FWD. COMP. + COMPONENTS WITH HEAT PIPES
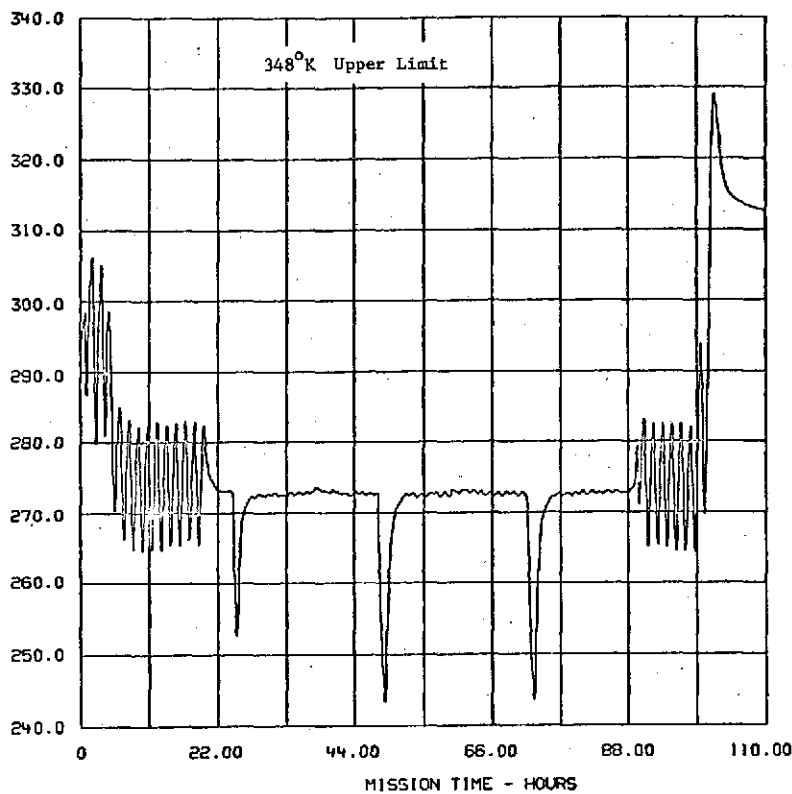
TEMP NODE NO.   470 Decoder Pri
MIN TEMP OF   243.359 OCCURRED AT TIME   48.900
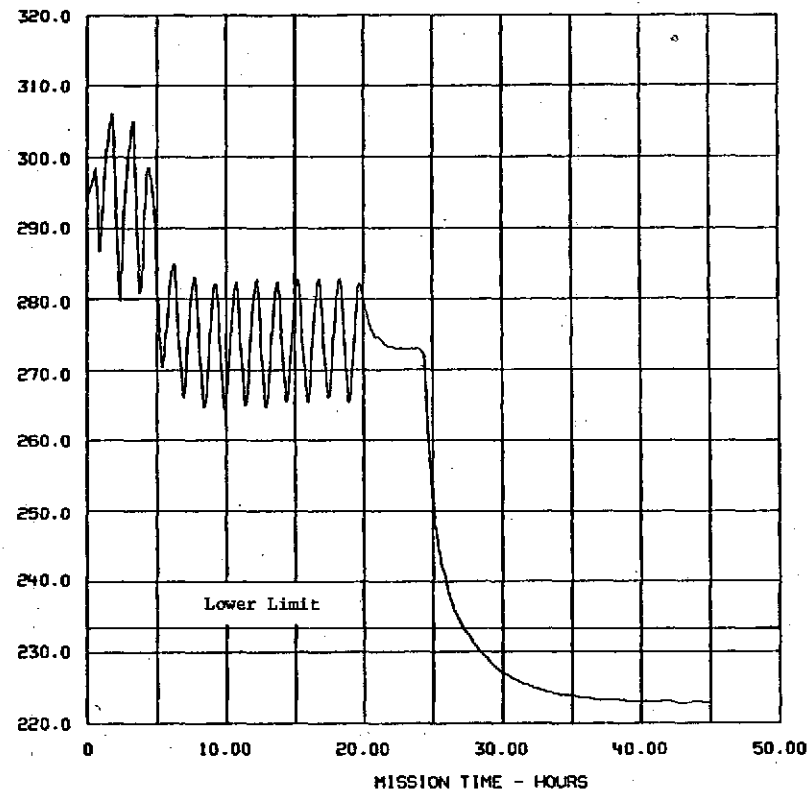MAX TEMP OF   329.000 OCCURRED AT TIME   101.800

FIGURE 5-97   ANALYSIS OF TUG FWD. COMP. STATIONED AT GEO. SHADOW PT.
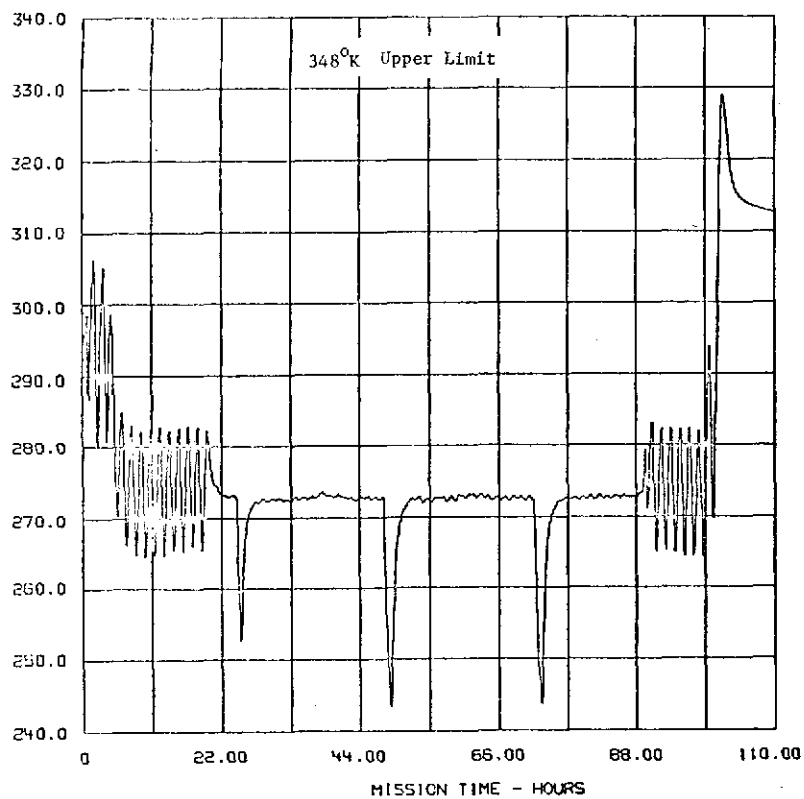
TEMP NODE NO.   470 Decoder Pri
MIN TEMP OF   222.786 OCCURRED AT TIME   45.000
MAX TEMP OF   306.209 OCCURRED AT TIME   1.800

TEMPERATURE - DEGREES KELVIN

MISSION TIME - HOURS

TEMP NODE NO.		480 Decoder Sec	
MIN TEMP OF	243.354	OCCURRED AT TIME	48.900
MAX TEMP OF	329.004	OCCURRED AT TIME	101.800

FIGURE 5-98   ANALYSIS OF TUG FWD. COMP. + COMPONENTS WITH HEAT PIPES

348°K Upper Limit

TEMPERATURE - DEGREES KELVIN

MISSION TIME - HOURS

Lower Limit

TEMP NODE NO.		480 Decoder Sec	
MIN TEMP OF	222.782	OCCURRED AT TIME	45.000
MAX TEMP OF	306.209	OCCURRED AT TIME	1.800

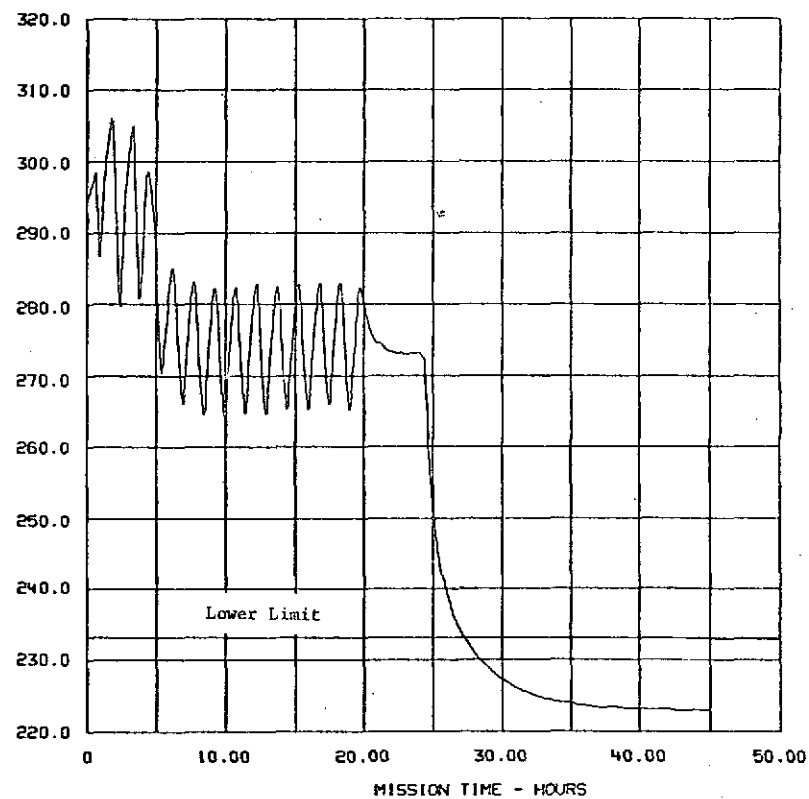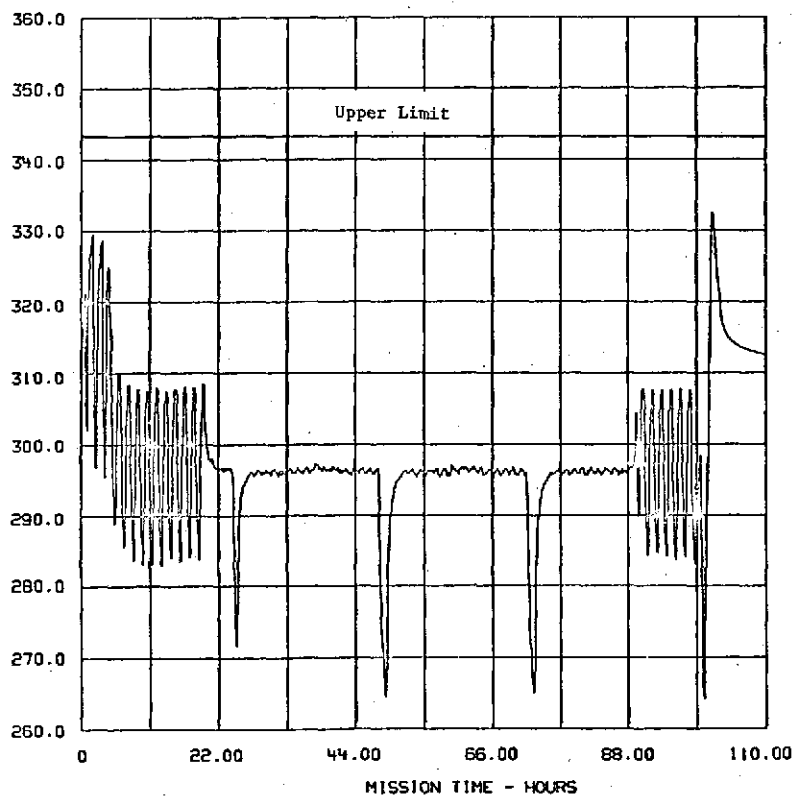FIGURE 5-99   ANALYSIS OF TUG FWD. COMP. STATIONED AT GEO. SHADOW PT.

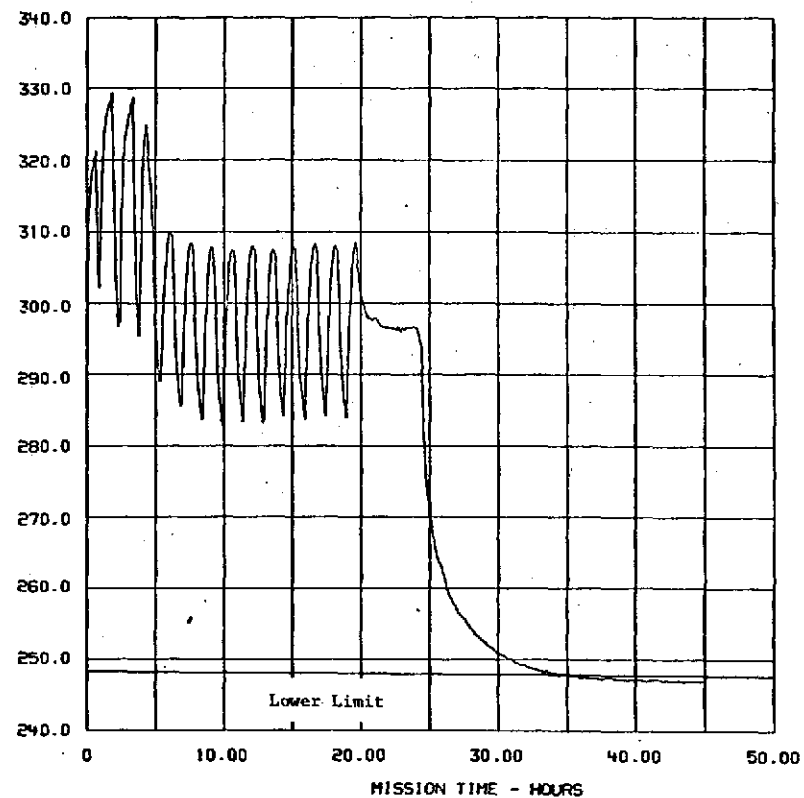FIGURE 5-100   ANALYSIS OF TUG FWD. COMP. + COMPONENTS WITH HEAT PIPES

TEMP NODE NO.   500 Power Amplifier Pri
MIN TEMP OF   264.171   OCCURRED AT TIME   100.200
MAX TEMP OF   332.426   OCCURRED AT TIME   101.500
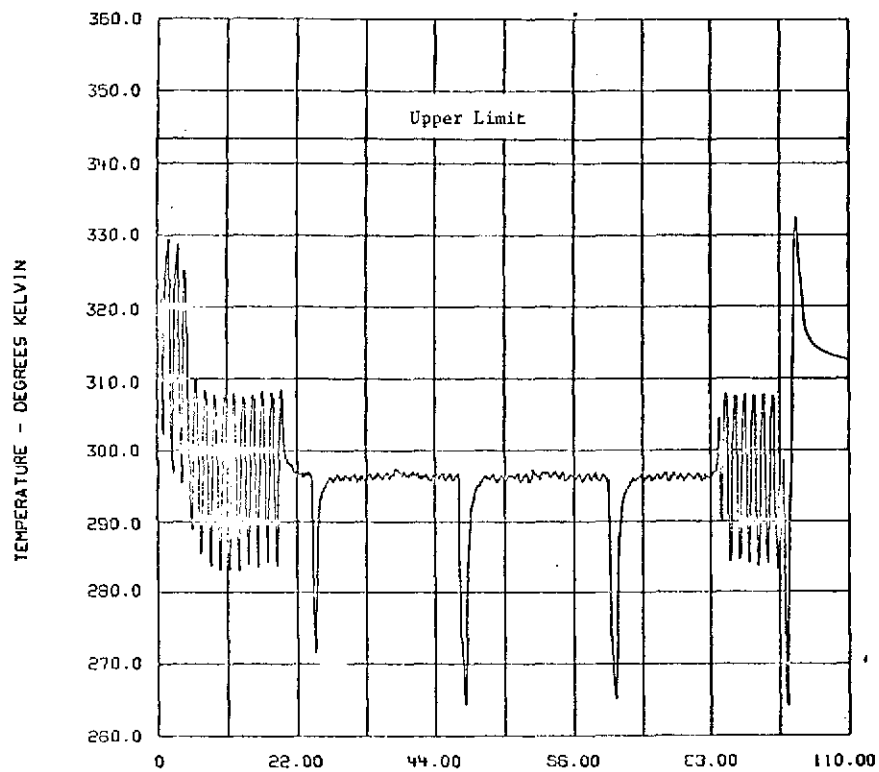

FIGURE 5-101   ANALYSIS OF TUG FWD. COMP. STATIONED AT GEO. SHADOW PT.
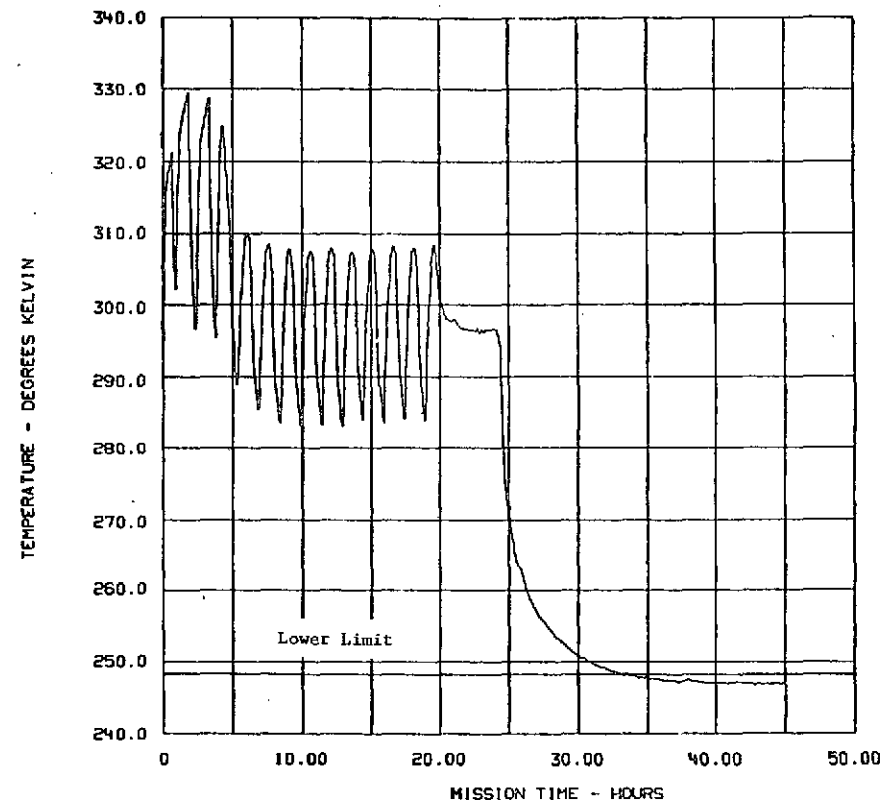
TEMP NODE NO.   500 Power Amplifier Pri
MIN TEMP OF   246.795   OCCURRED AT TIME   42.800
MAX TEMP OF   329.452   OCCURRED AT TIME   1.800

FIGURE 5-102   ANALYSIS OF TUG FWD. COMP. + COMPONENTS WITH HEAT PIPES

FIGURE 5-103   ANALYSIS OF TUG FWD. COMP. STATIONED AT GEO. SHADOW PT.

Left chart labels:

TEMPERATURE - DEGREES KELVIN

MISSION TIME - HOURS

Upper Limit

TEMP NODE NO.	510 Power Amplifier, Sec		
MIN TEMP OF	264.143	OCCURRED AT TIME	100.200
MAX TEMP OF	332.457	OCCURRED AT TIME	101.500

Right chart labels:

TEMPERATURE - DEGREES KELVIN

MISSION TIME - HOURS

Lower Limit

TEMP NODE NO.	510 Power Amplifier, Sec		
MIN TEMP OF	246.765	OCCURRED AT TIME	42.800
MAX TEMP OF	329.495	OCCURRED AT TIME	1.800

TEMP NODE NO.   520 RF Multiplexer
MIN TEMP OF   248.261 OCCURRED AT TIME   48.900
MAX TEMP OF   326.480 OCCURRED AT TIME   102.000

FIGURE 5-104 .   ANALYSIS OF TUG FWD. COMP. + COMPONENTS WITH HEAT PIPES

TEMP NODE NO.   520 RF Multiplexer
MIN TEMP OF   240.331 OCCURRED AT TIME   45.000
MAX TEMP OF   303.814 OCCURRED AT TIME   1.800

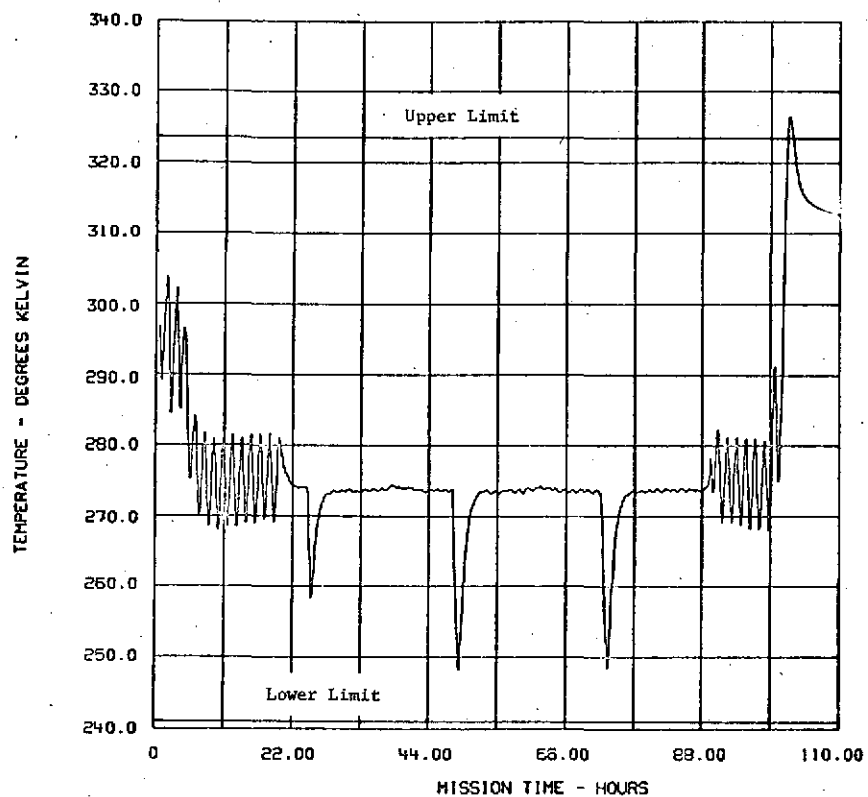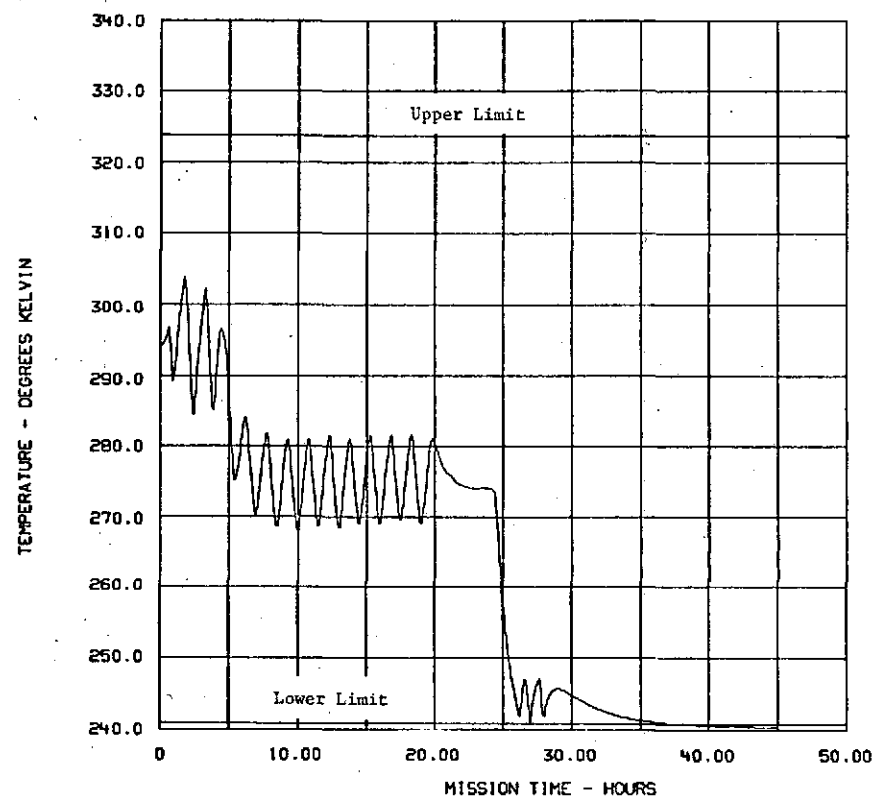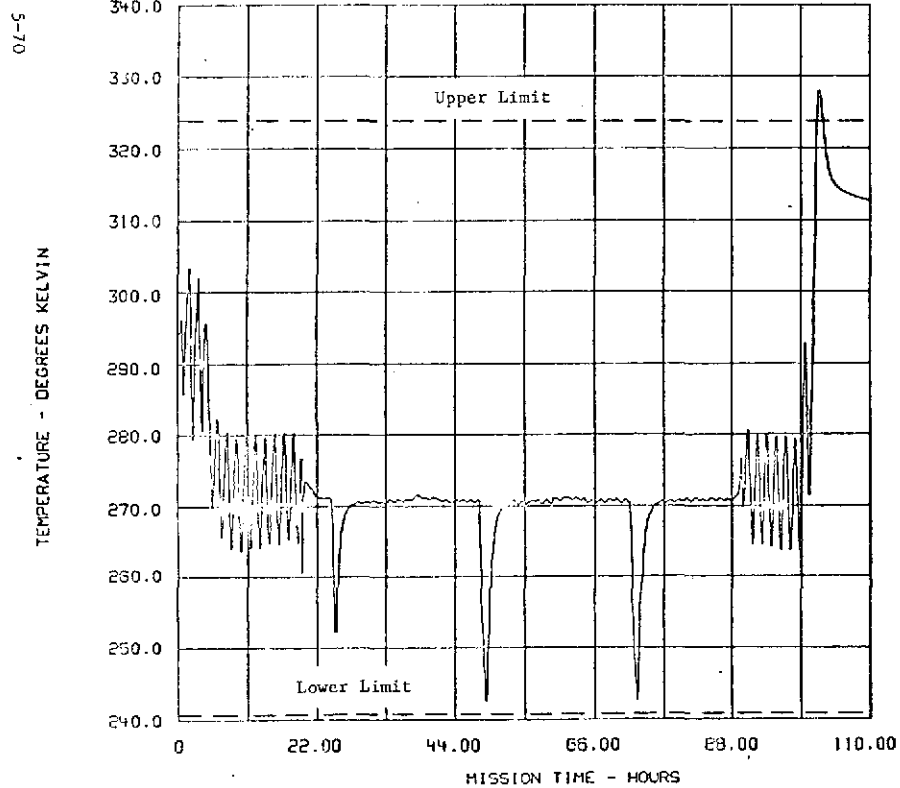FIGURE 5-105   ANALYSIS OF TUG FWD. COMP. STATIONED AT GEO. SHADOW PT.

FIGURE 5-106   ANALYSIS OF TUG FWD. COMP. + COMPONENTS WITH HEAT PIPES

TEMP NODE NO.   600 Hybrid Junction
MIN TEMP OF   242.424 OCCURRED AT TIME   48.900
MAX TEMP OF   328.030 OCCURRED AT TIME   101.900

FIGURE 5-107   ANALYSIS OF TUG FWD. COMP. STATIONED AT GEO. SHADOW PT.

TEMP NODE NO.   600 Hybrid Junction
MIN TEMP OF   220.944 OCCURRED AT TIME   45.000
MAX TEMP OF   303.395 OCCURRED AT TIME   1.800

FIGURE 5-108   ANALYSIS OF TUG FWD. COMP. + COMPONENTS WITH HEAT PIPES

TEMP NODE NO.   610 Filter
MIN TEMP OF   242.390 OCCURRED AT TIME   48.900
MAX TEMP OF   327.729 OCCURRED AT TIME   101.900

FIGURE 5-109   ANALYSIS OF TUG FWD. COMP. STATIONED AT GEO. SHADOW PT.
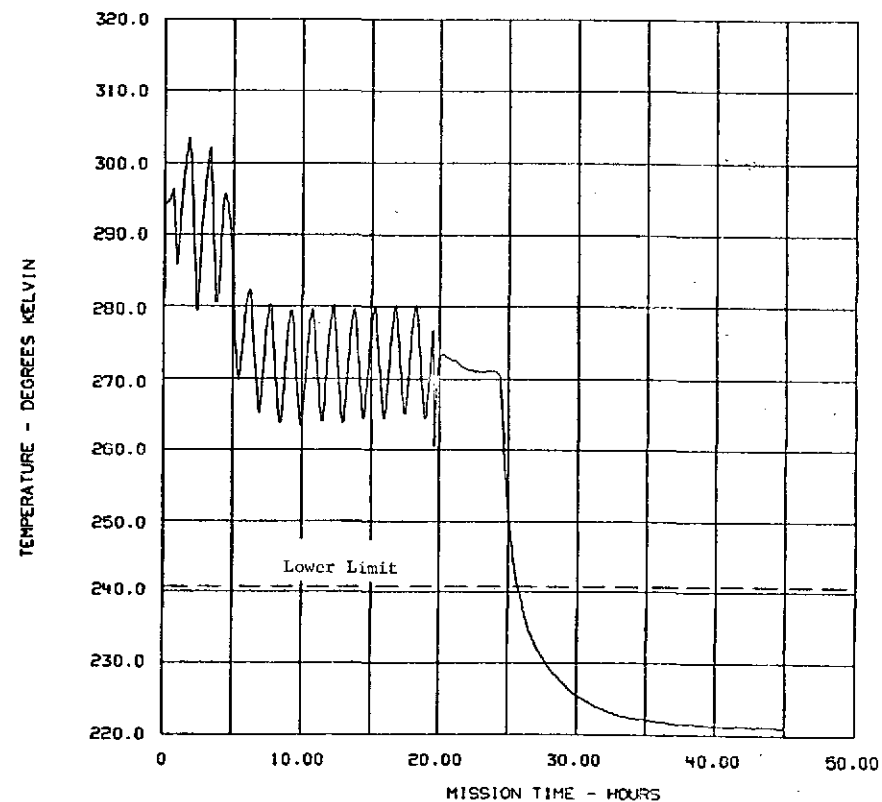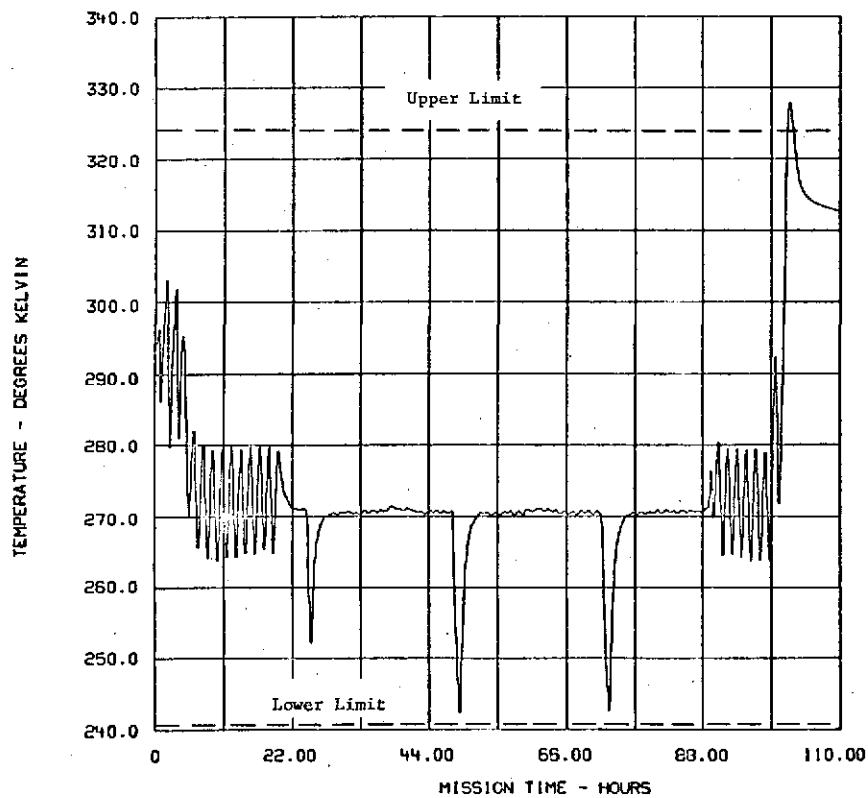
TEMP NODE NO.   610 Filter
MIN TEMP OF   220.751 OCCURRED AT TIME   45.000
MAX TEMP OF   303.135 OCCURRED AT TIME   1.800

FIGURE 5-110   ANALYSIS OF TUG FWD. COMP. + COMPONENTS WITH HEAT PIPES

TEMP NODE NO.   620 Modulation Proc. Pri
MIN TEMP OF   251.299 OCCURRED AT TIME   48.900
MAX TEMP OF   323.418 OCCURRED AT TIME   102.300

FIGURE 5-111   ANALYSIS OF TUG FWD. COMP. STATIONED AT GEO. SHADOW PT.
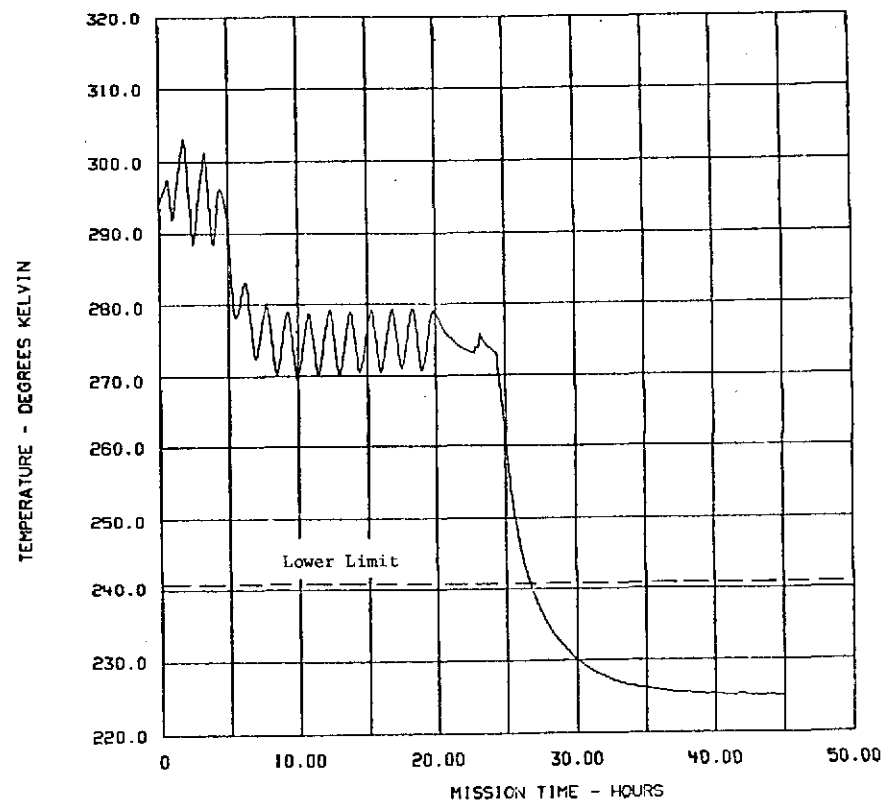
TEMP NODE NO.   620 Modulation Proc. Pri
MIN TEMP OF   224.925 OCCURRED AT TIME   44.900
MAX TEMP OF   303.094 OCCURRED AT TIME   1.800

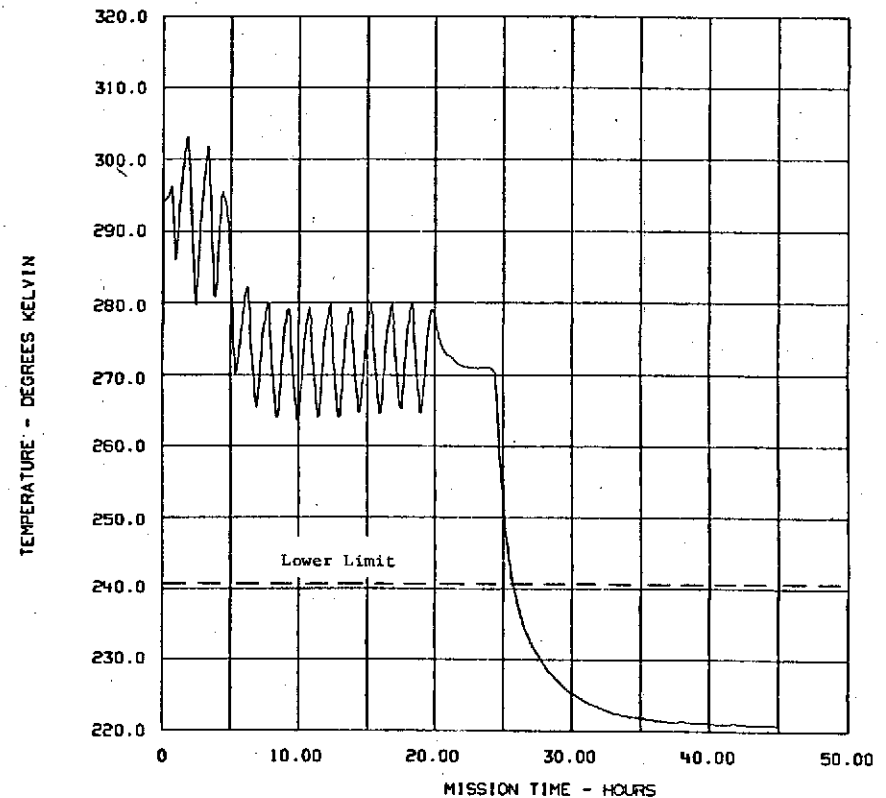FIGURE 5-112   ANALYSIS OF TUG FWD. COMP. + COMPONENTS WITH HEAT PIPES

TEMP NODE NO.   630 Modulation Proc. Sec
MIN TEMP OF   251.415   OCCURRED AT TIME   48.900
MAX TEMP OF   323.412   OCCURRED AT TIME   102.300

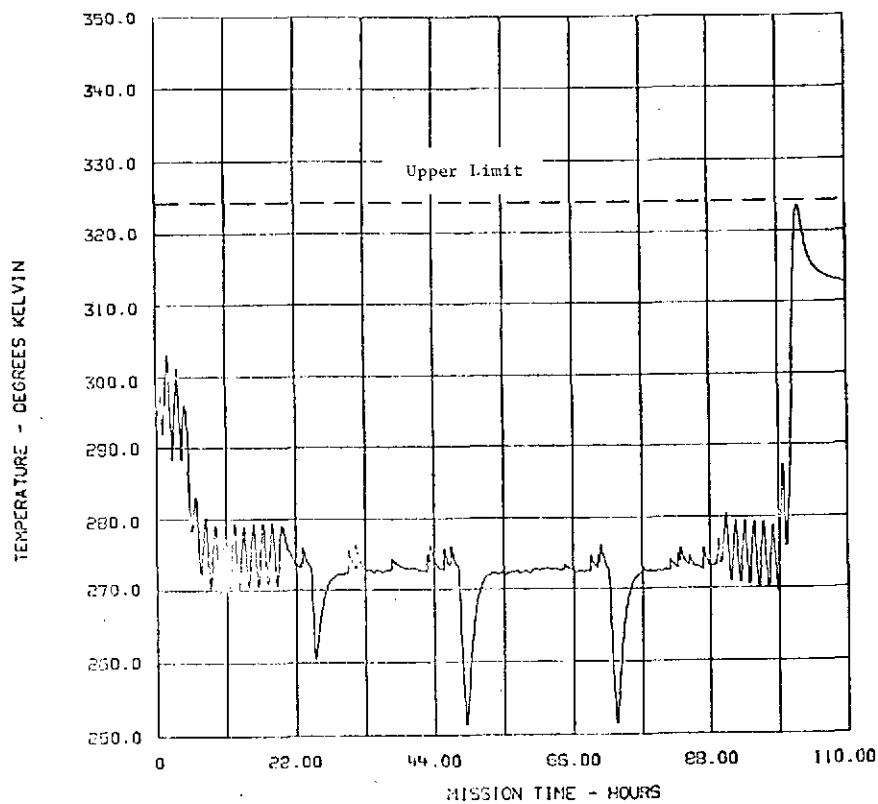FIGURE 5-113   ANALYSIS OF TUG FWD. COMP. STATIONED AT GEO. SHADOW PT.

TEMP NODE NO.   630 Modulation Proc. Sec
MIN TEMP OF   225.041   OCCURRED AT TIME   44.900
MAX TEMP OF   303.085   OCCURRED AT TIME   1.800

POWER - WATTS

MISSION TIME - HOURS

NODE NO.		113	Star Tracker Pri	Heater Power
MIN	OF	0.	OCCURRED AT TIME	110.000
MAX	OF	68.260	OCCURRED AT TIME	73.500
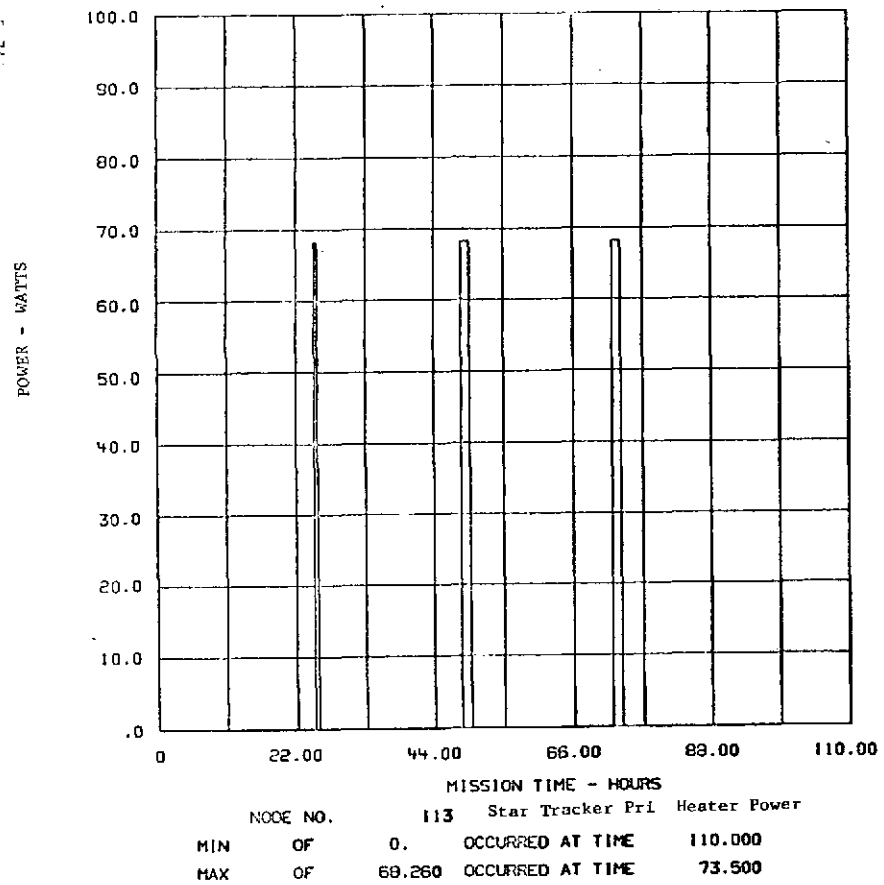
FIGURE 5-114   ANALYSIS OF TUG FWD. COMP. + COMPONENTS WITH HEAT PIPES

POWER - WATTS

MISSION TIME - HOURS

NODE NO.		113	Star Tracker Pri	Heater Power
MIN	OF	0.	OCCURRED AT TIME	24.900
MAX	OF	68.260	OCCURRED AT TIME	45.000
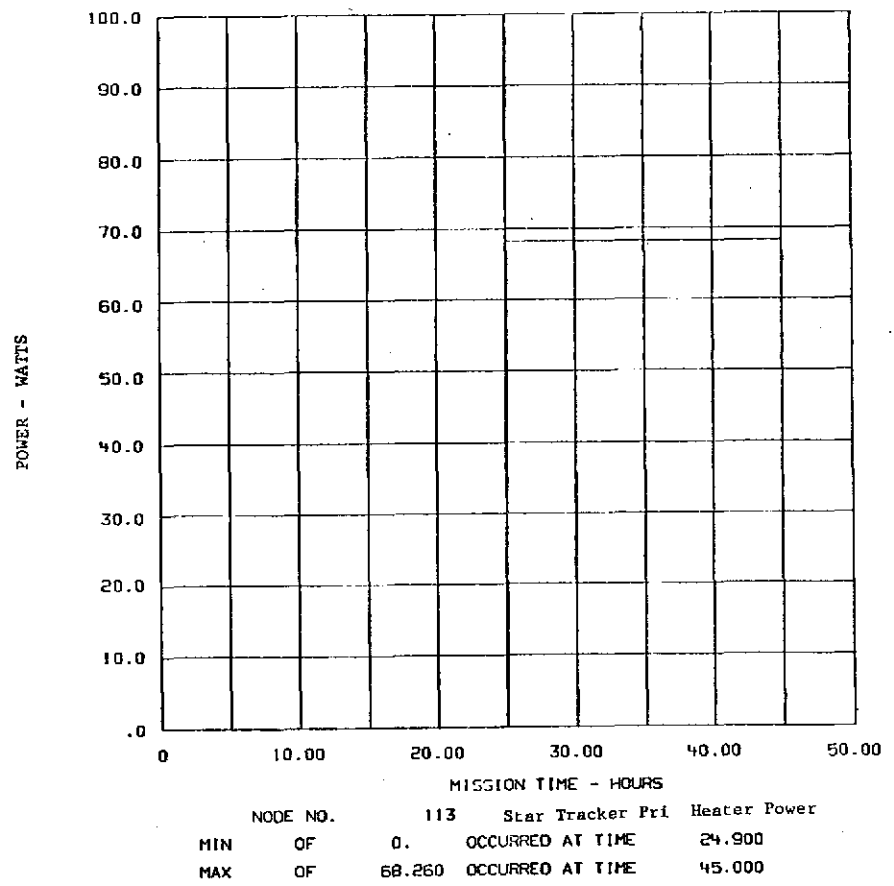
FIGURE 5-115   ANALYSIS OF TUG FWD. COMP. STATIONED AT GEO. SHADOW PT.
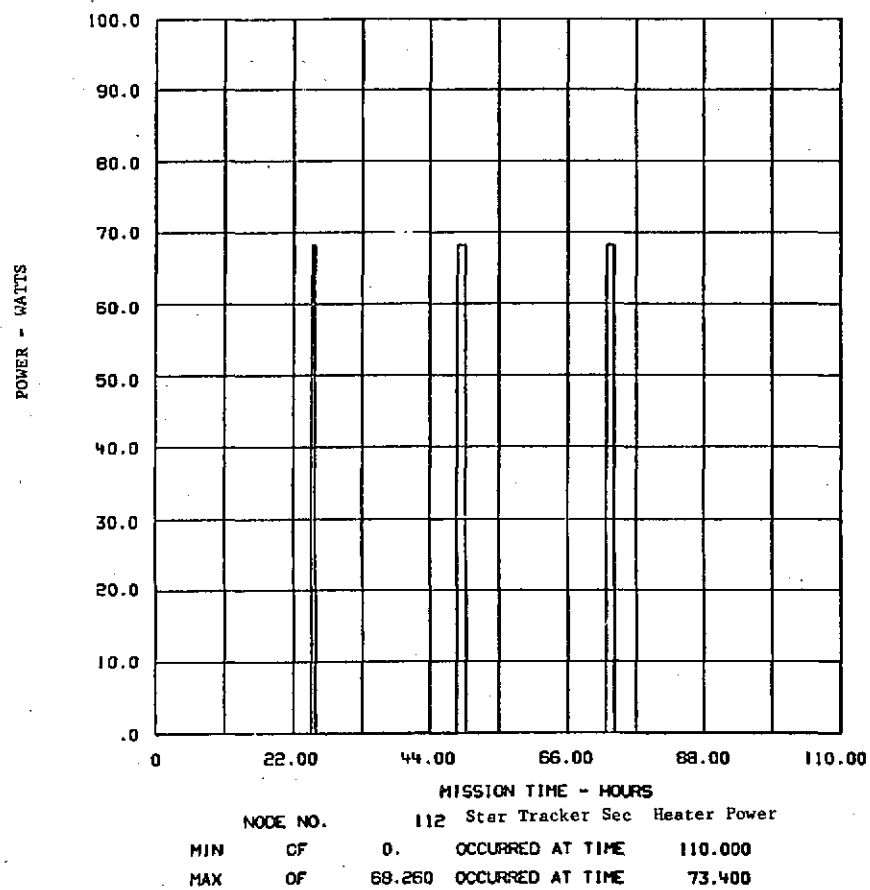
FIGURE 5-116 ANALYSIS OF TUG FWD. COMP. + COMPONENTS WITH HEAT PIPES

NODE NO.   112 Star Tracker Sec Heater Power
MIN   OF   0.   OCCURRED AT TIME   110.000
MAX   OF   68.260 OCCURRED AT TIME   73.400
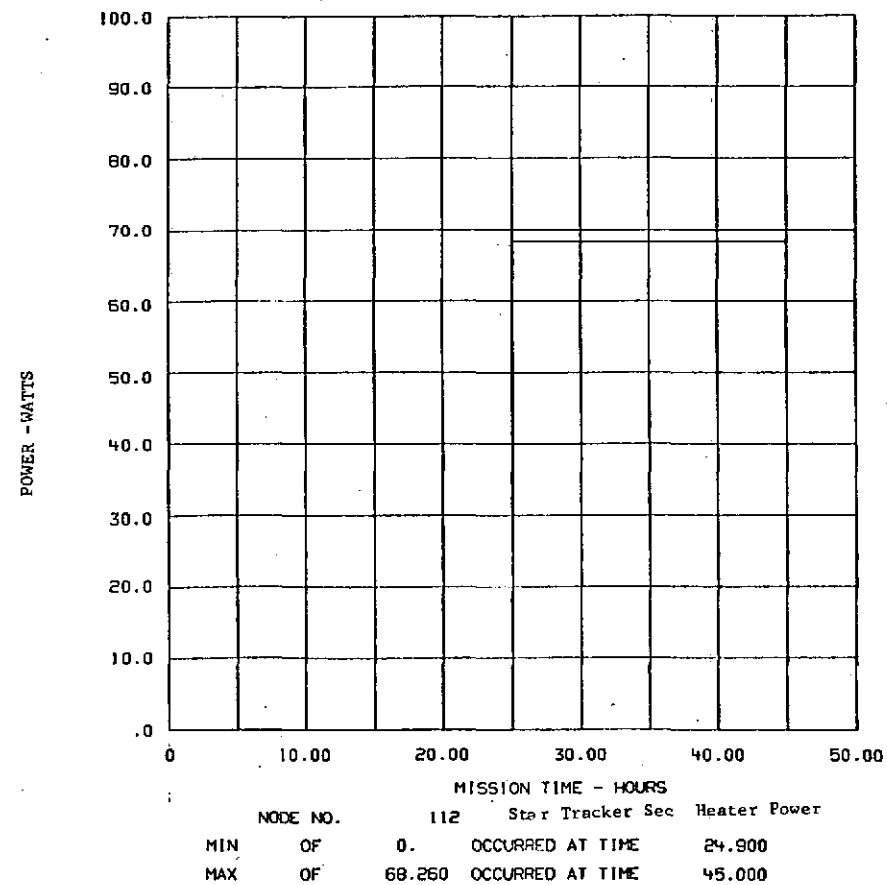
FIGURE 5-117 ANALYSIS OF TUG FWD. COMP. STATIONED AT GEO. SHADOW PT.
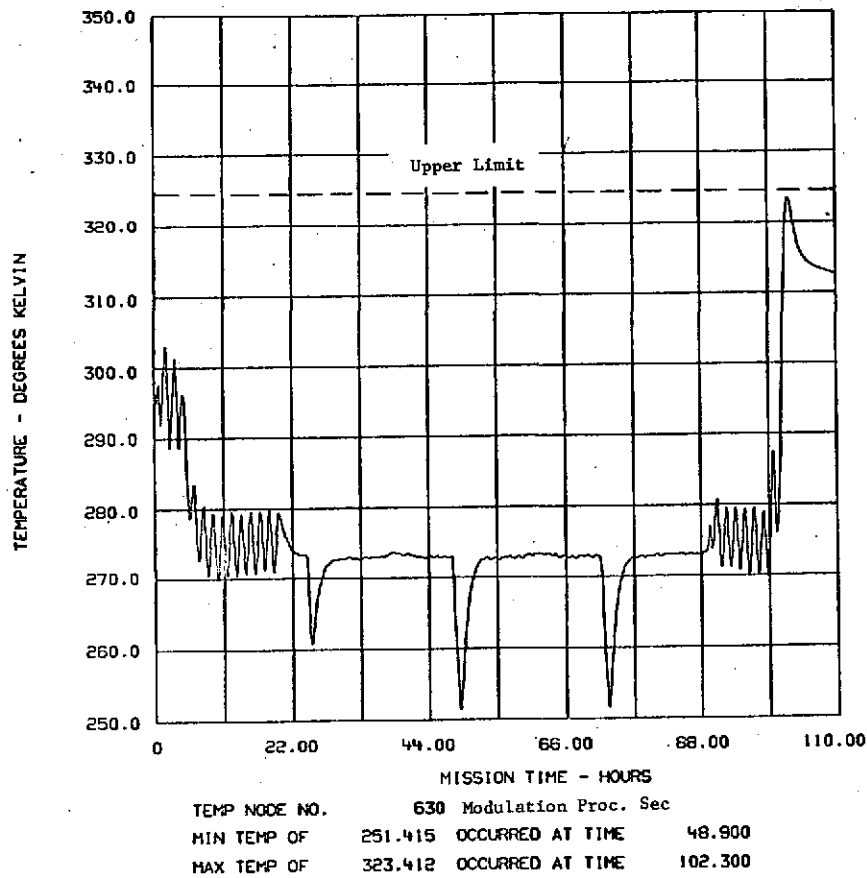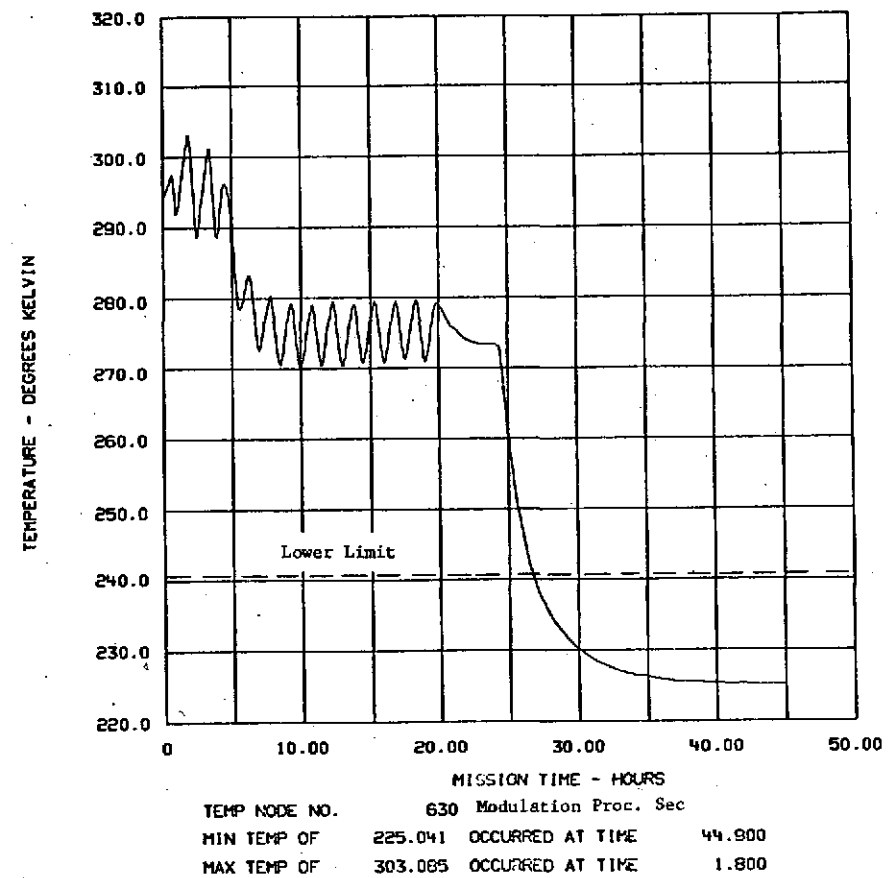
NODE NO.   112   Star Tracker Sec Heater Power
MIN   OF   0.   OCCURRED AT TIME   24.900
MAX   OF   68.260 OCCURRED AT TIME   45.000

POWER – WATTS

100.0
90.0
80.0
70.0
60.0
50.0
40.0
30.0
20.0
10.0
.0

0   22.00   44.00   66.00   88.00   110.00

MISSION TIME – HOURS

	NODE NO.		111 Horizon Scanner	Heater Power
MIN	OF	0.	OCCURRED AT TIME	110.000
MAX	OF	51.195	OCCURRED AT TIME	73.300
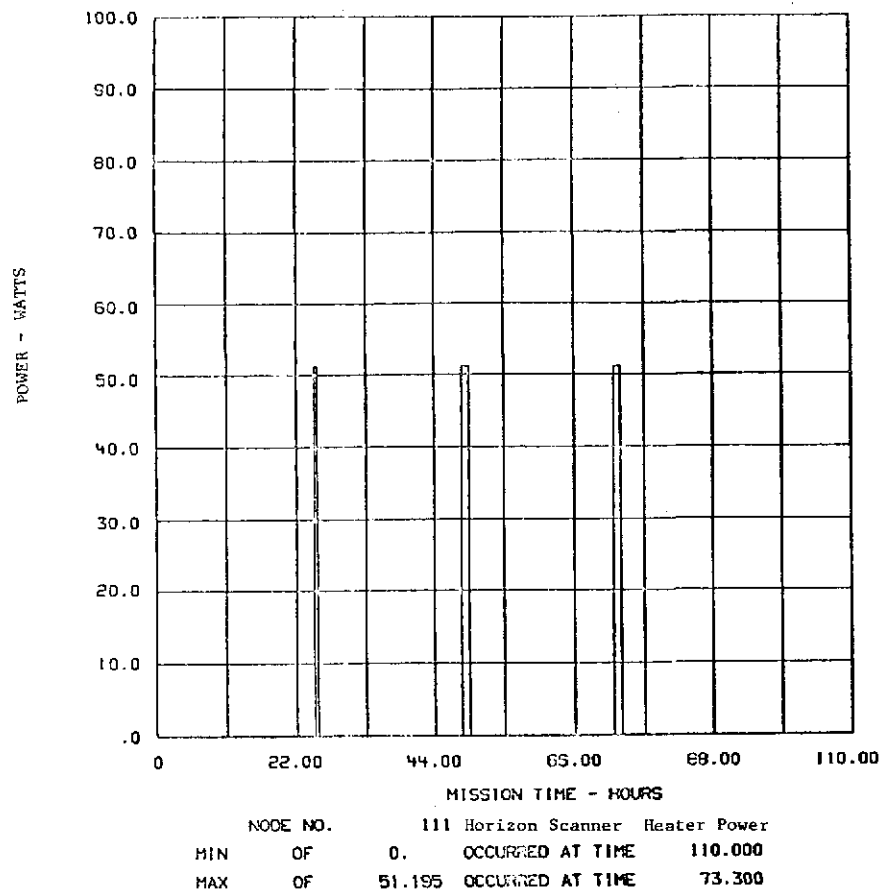
FIGURE 5-118   ANALYSIS OF TUG FWD. COMP. + COMPONENTS WITH HEAT PIPES

POWER – WATTS

100.0
90.0
80.0
70.0
60.0
50.0
40.0
30.0
20.0
10.0
.0

0   10.00   20.00   30.00   40.00   50.00

MISSION TIME – HOURS

	NODE NO.		111 Horizon Scanner	Heater Power
MIN	OF	0.	OCCURRED AT TIME	24.900
MAX	OF	51.195	OCCURRED AT TIME	45.000
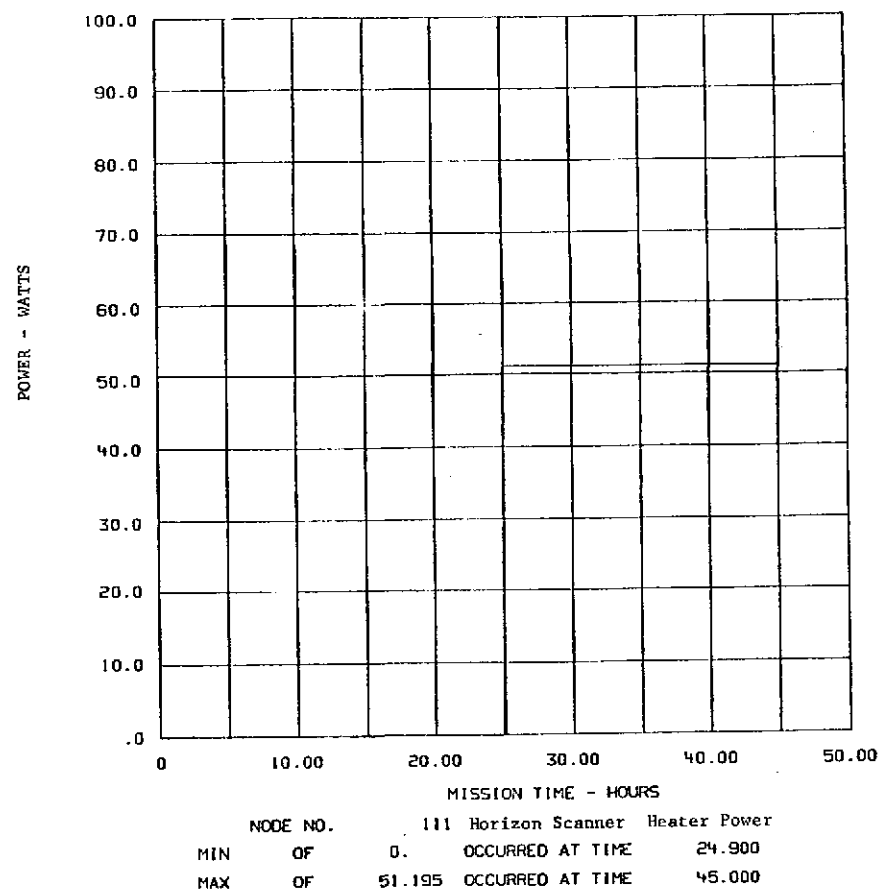
FIGURE 5-119   ANALYSIS OF TUG FWD. COMP. STATIONED AT GEO. SHADOW PT.

POWER - WATTS

MISSION TIME - HOURS

	NODE NO.		110 Horizon Scanner Electronics Heater Power	
MIN	OF	0.	OCCURRED AT TIME	110.000
MAX	OF	85.325	OCCURRED AT TIME	73.700

FIGURE 5-120   ANALYSIS OF TUG FWD. COMP. + COMPONENTS WITH HEAT PIPES

POWER - WATTS

MISSION TIME - HOURS

	NODE NO.		110 Horizon Scanner Electronics Heater Power	
MIN	OF	0.	OCCURRED AT TIME	25.400
MAX	OF	85.325	OCCURRED AT TIME	45.000

FIGURE 5-121   ANALYSIS OF TUG FWD. COMP. STATIONED AT GEO. SHADOW PT.
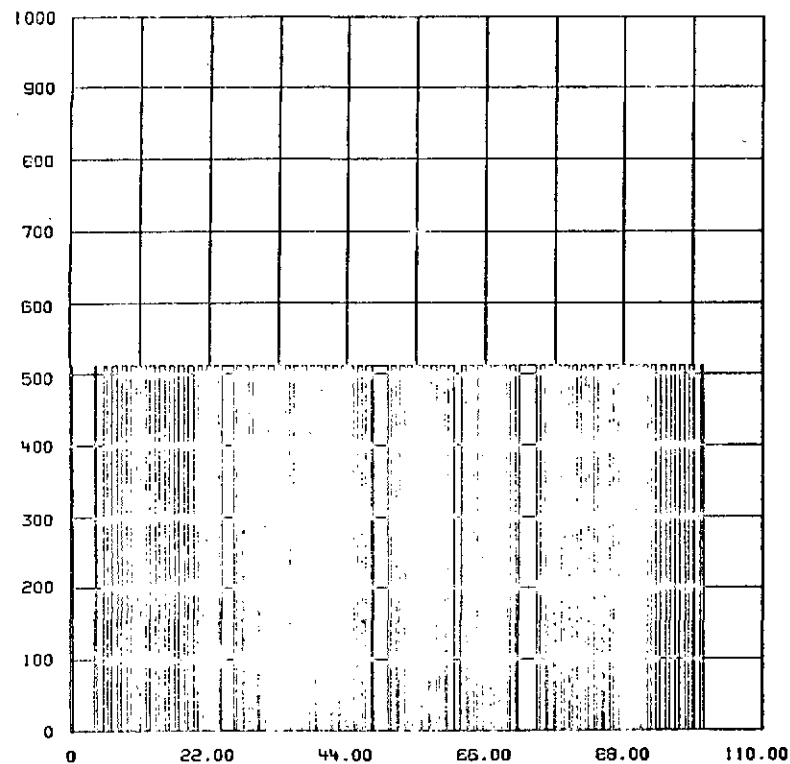
POWER - WATTS

1000
900
800
700
600
500
400
300
200
100
0

0   22.00   44.00   66.00   88.00   110.00

MISSION TIME - HOURS

NODE NO.	109 Laser Radar Pri Heater Power
MIN	OF	0.	OCCURRED AT TIME	110.000
MAX	OF	511.950	OCCURRED AT TIME	100.600

FIGURE 5-122   ANALYSIS OF TUG FWD. COMP. + COMPONENTS WITH HEAT PIPES
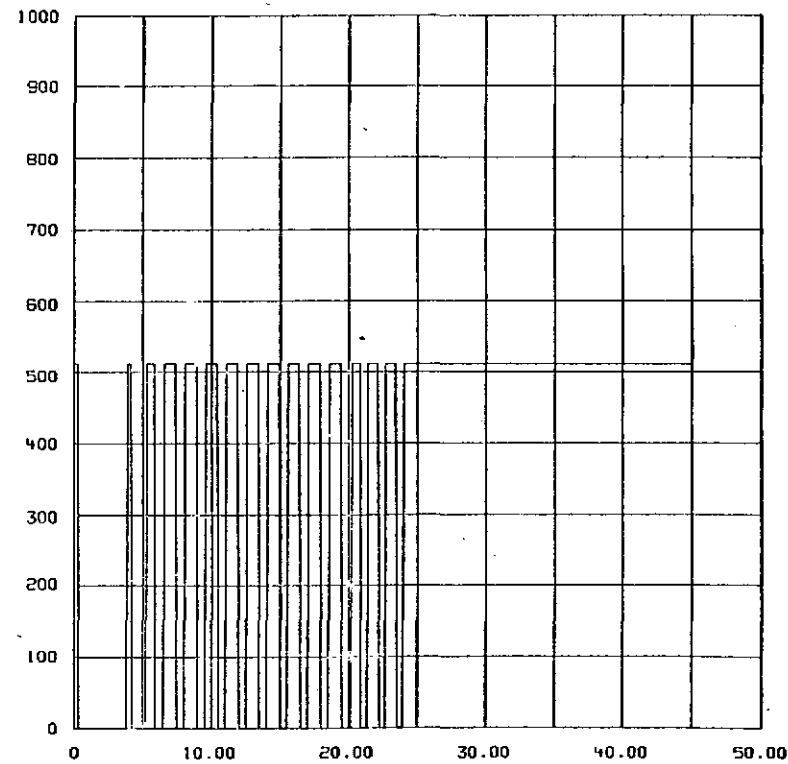
POWER - WATTS

1000
900
800
700
600
500
400
300
200
100
0

0   10.00   20.00   30.00   40.00   50.00

MISSION TIME - HOURS

NODE NO.	109 Laser Radar Pri Heater Power
MIN	OF	0.	OCCURRED AT TIME	23.900
MAX	OF	511.950	OCCURRED AT TIME	45.000

FIGURE 5-123   ANALYSIS OF TUG FWD. COMP. STATIONED AT GEO. SHADOW PT.
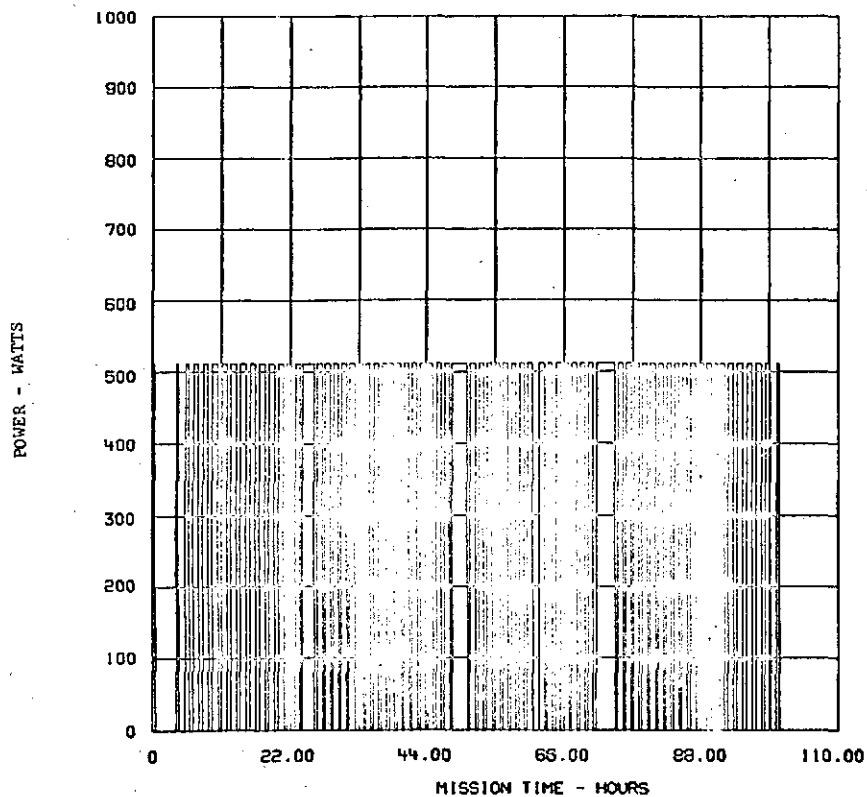
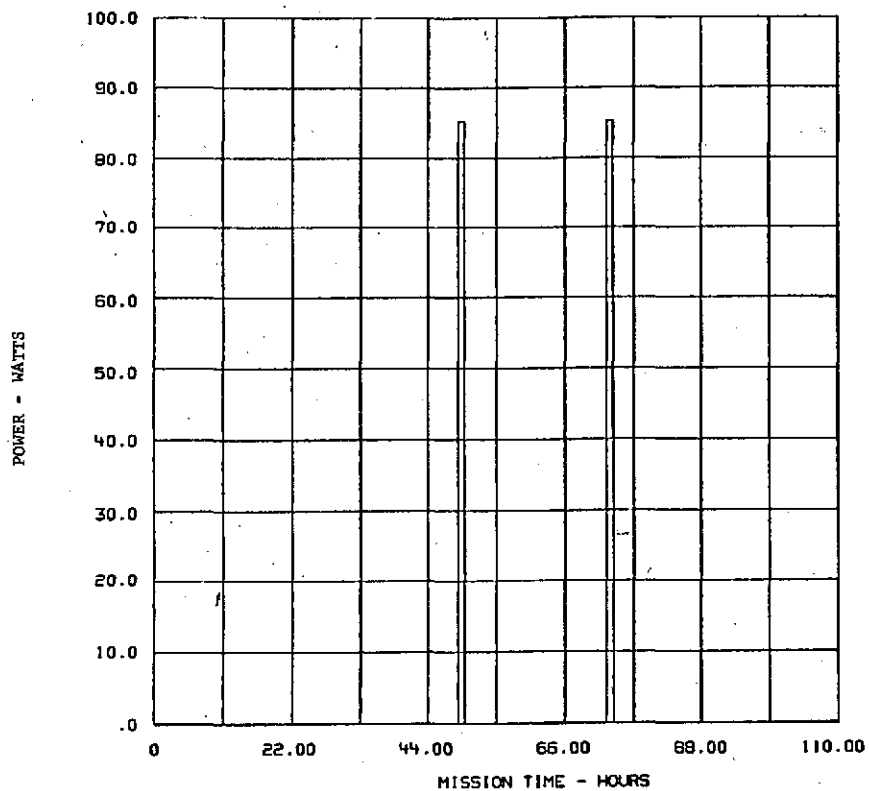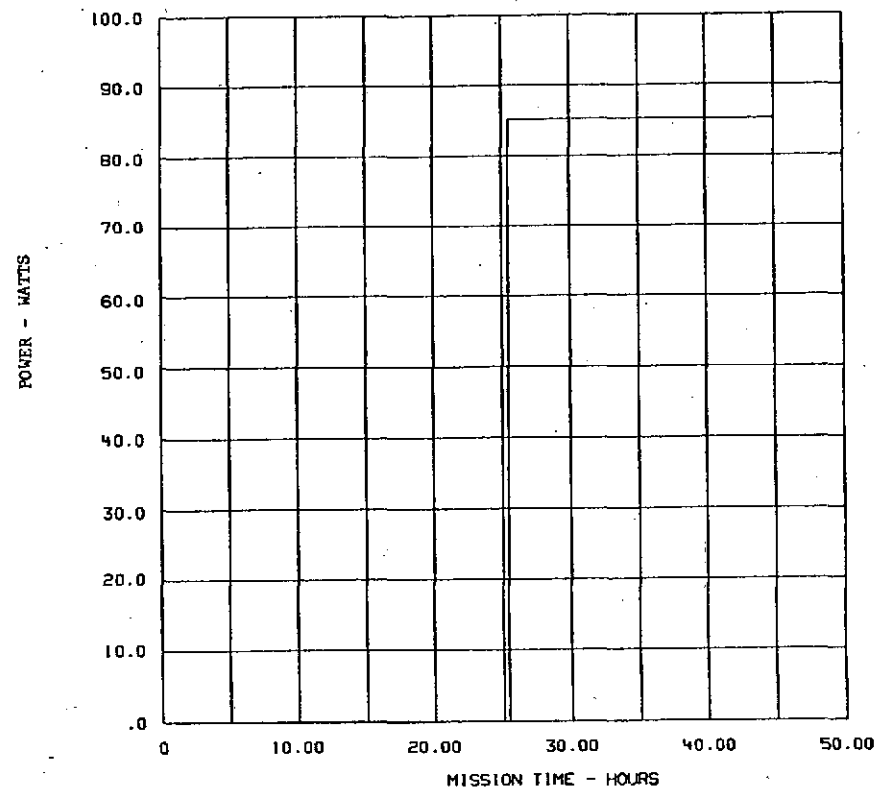FIGURE 5-124   ANALYSIS OF TUG FWD. COMP. + COMPONENTS WITH HEAT PIPES

NODE NO.		108 Laser Radar Sec	Heater Power
MIN	OF	0.	OCCURRED AT TIME	110.000
MAX	OF	511.950	OCCURRED AT TIME	100.600

FIGURE 5-125   ANALYSIS OF TUG FWD. COMP. STATIONED AT GEO. SHADOW PT.

NODE NO.		108 Laser Radar Sec	Heater Power
MIN	OF	0.	OCCURRED AT TIME	23.900
MAX	OF	511.950	OCCURRED AT TIME	45.000

POWER - WATTS

MISSION TIME - HOURS

	NODE NO.		107	Laser Radar Electronics Pri Heater Power	
MIN	OF	0.	OCCURRED AT TIME	110.000	
MAX	OF	511.950	OCCURRED AT TIME	100.300	

FIGURE 5-126   ANALYSIS OF TUG FWD. COMP. + COMPONENTS WITH HEAT PIPES

POWER - WATTS

MISSION TIME - HOURS

	NODE NO.		107	Laser Radar Electronics Pri Heater Power	
MIN	OF	0.	OCCURRED AT TIME	25.100	
MAX	OF	511.950	OCCURRED AT TIME	45.000	

FIGURE 5-127   ANALYSIS OF TUG FWD. COMP. STATIONED AT GEO. SHADOW PT.

POWER - WATTS

MISSION TIME - HOURS

NODE NO.   106 Laser Radar Electronics Sec Heater Power

MIN   OF   0.   OCCURRED AT TIME   110.000

MAX   OF   511.950 OCCURRED AT TIME   100.300

FIGURE 5-128   ANALYSIS OF TUG FWD. COMP. + COMPONENTS WITH HEAT PIPES
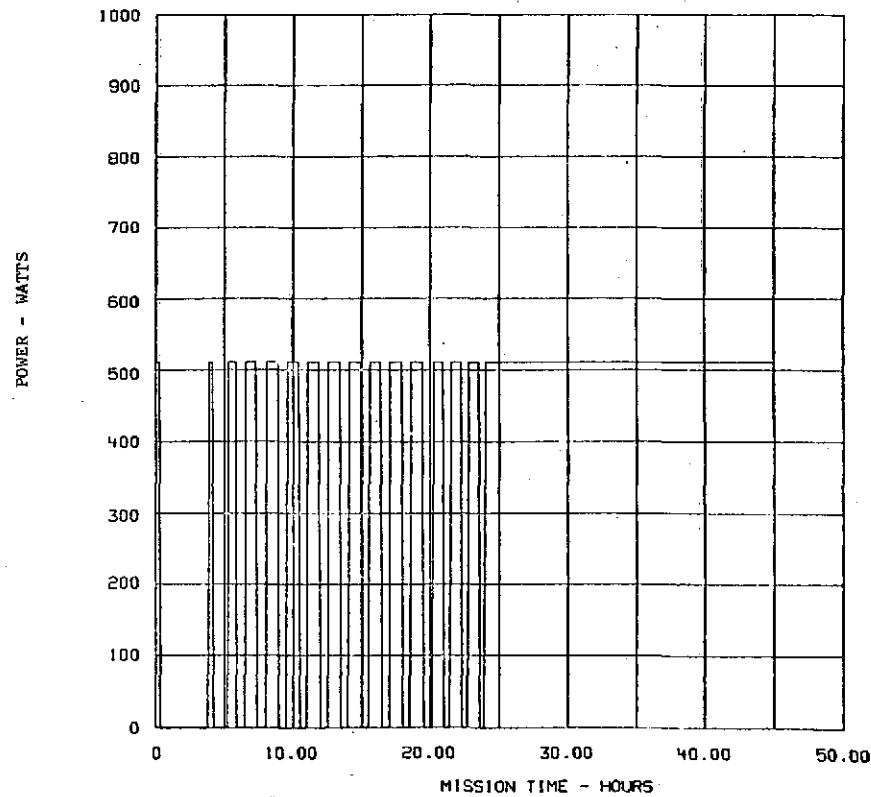

POWER - WATTS

MISSION TIME - HOURS

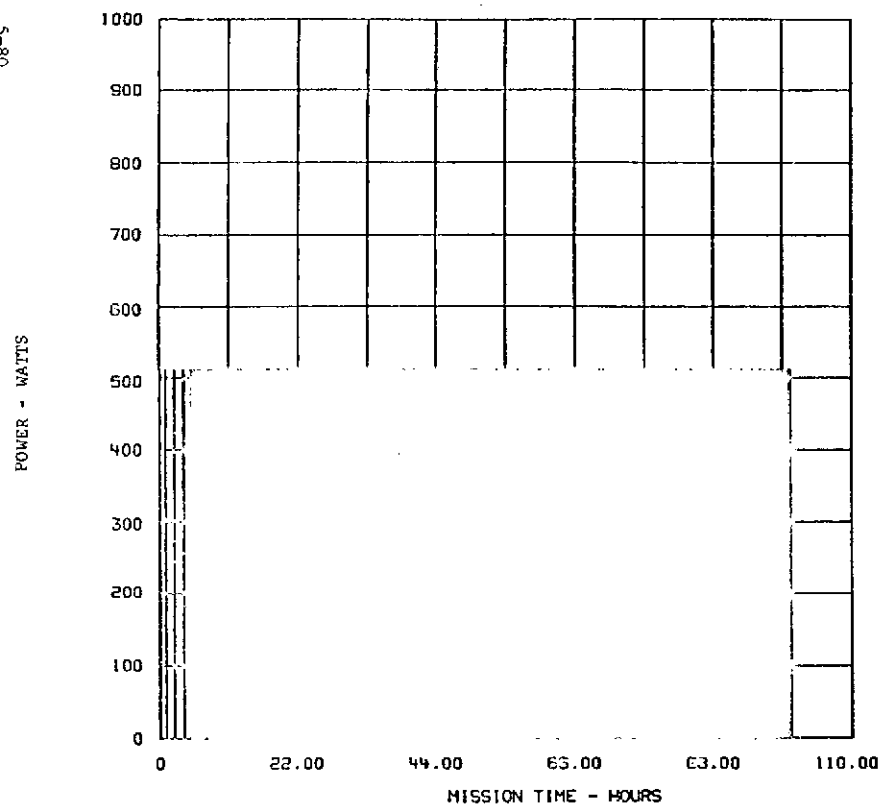NODE NO.   106 Laser Radar Electronics Sec Heater Power

MIN   OF   0.   OCCURRED AT TIME   24.600

MAX   OF   511.950 OCCURRED AT TIME   45.000

FIGURE 5-129   ANALYSIS OF TUG FWD. COMP. STATIONED AT GEO. SHADOW PT.

POWER - WATTS

MISSION TIME - HOURS

NODE NO. 105 Television Pri Heater Power

MIN   OF   0.   OCCURRED AT TIME   110.000

MAX   OF   69.260 OCCURRED AT TIME   73.600

FIGURE 5-130   ANALYSIS OF TUG FWD. COMP. + COMPONENTS WITH HEAT PIPES

POWER - WATTS

MISSION TIME - HOURS

NODE NO. 105 Television Pri Heater Power

MIN   OF   0.   OCCURRED AT TIME   24.900

MAX   OF   68.260 OCCURRED AT TIME   45.000

FIGURE 5-131   ANALYSIS OF TUG FWD. COMP. STATIONED AT GEO. SHADOW PT.

FIGURE 5-132   ANALYSIS OF TUG FWD. COMP. + COMPONENTS WITH HEAT PIPES

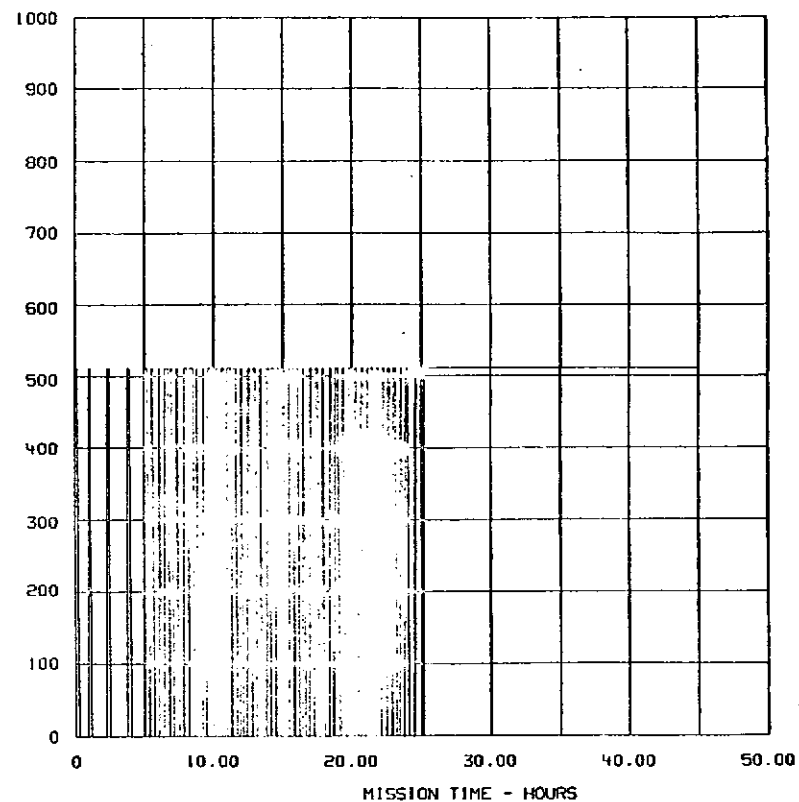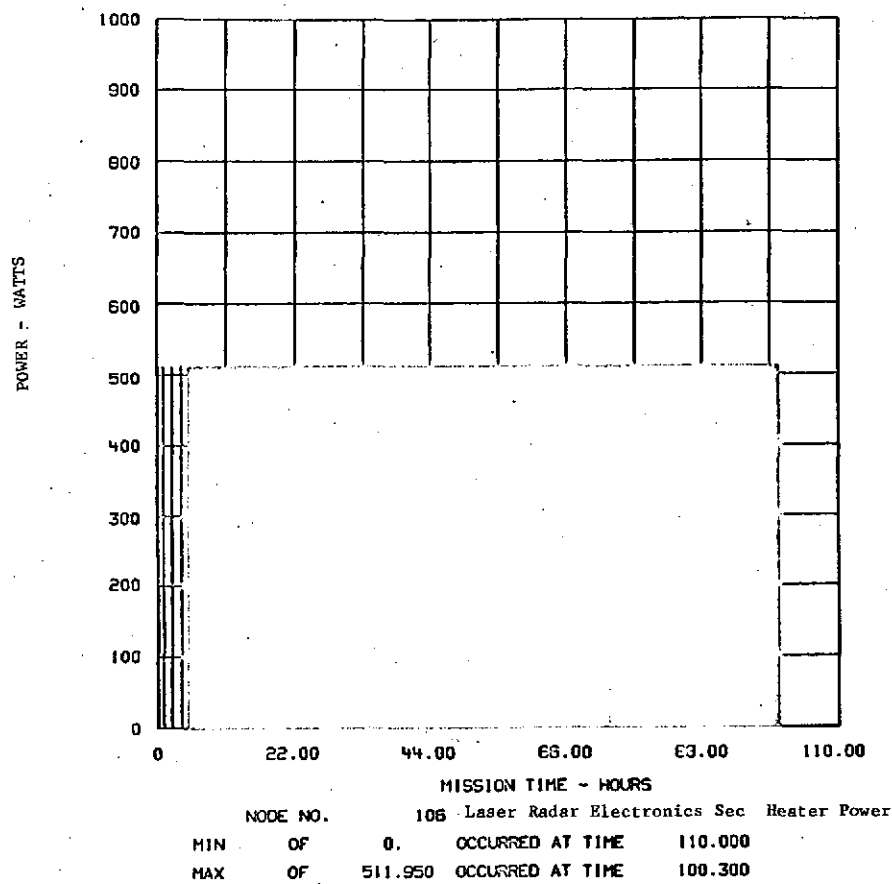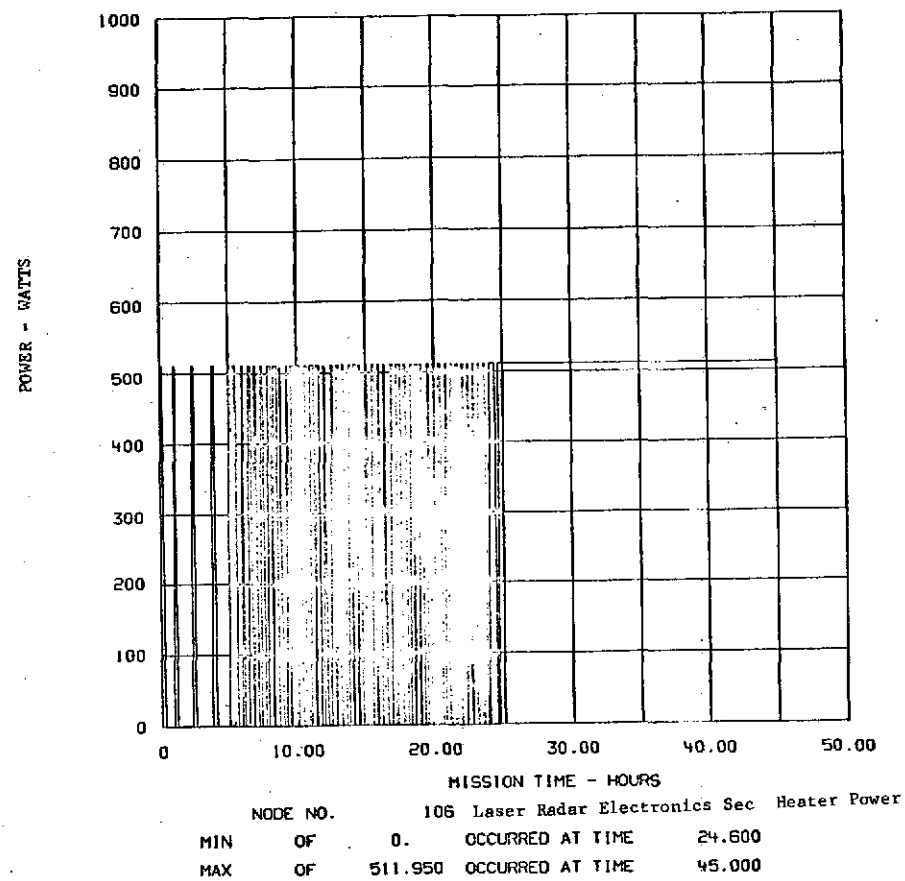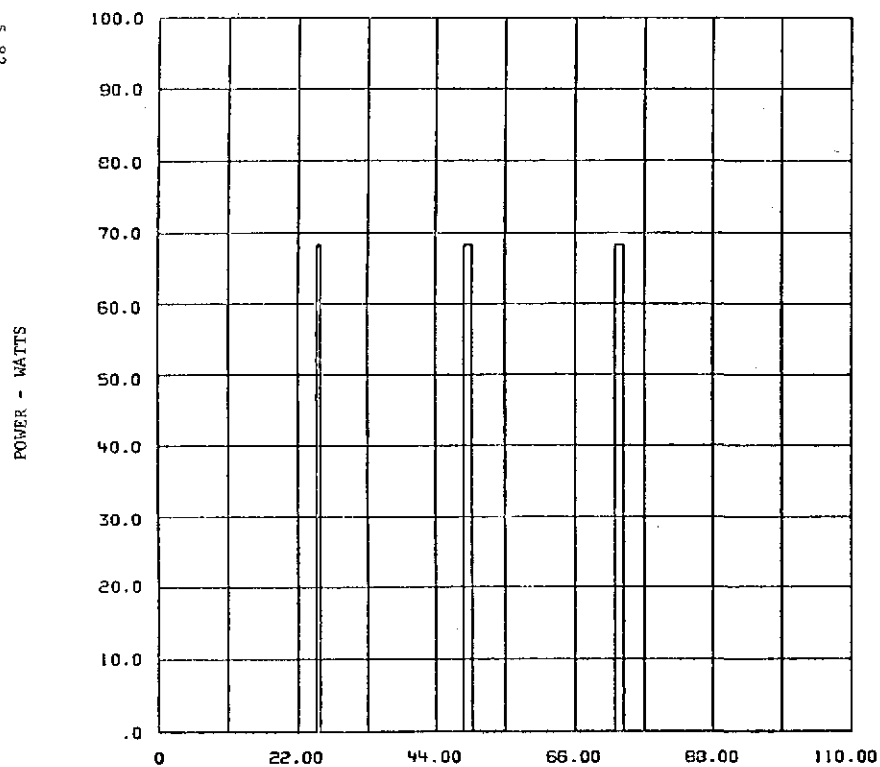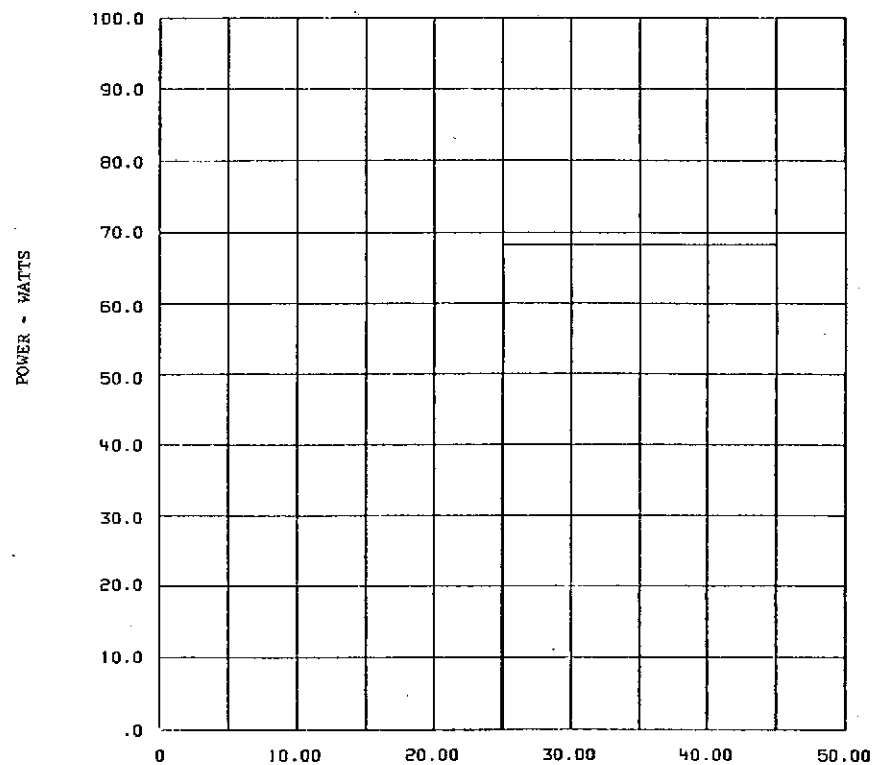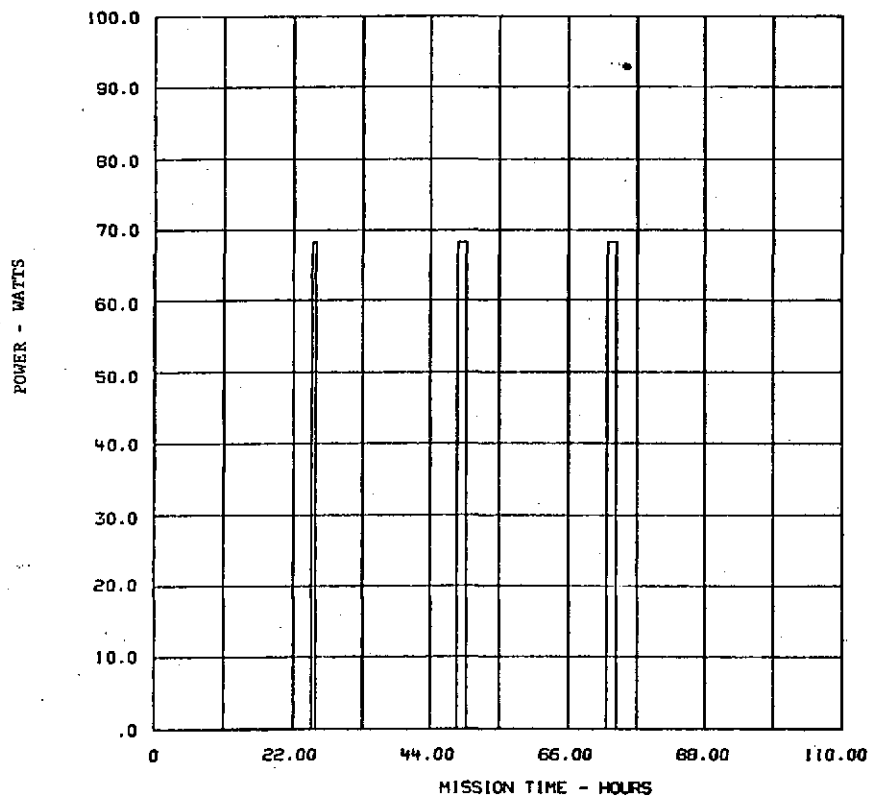FIGURE 5-133   ANALYSIS OF TUG FWD. COMP. STATIONED AT GEO. SHADOW PT.

POWER - WATTS

MISSION TIME - HOURS

	NODE NO.		102 Computer Pri Heater Power	
MIN	OF	0.	OCCURRED AT TIME	110.000
MAX	OF	0.	OCCURRED AT TIME	0.

FIGURE 5-134   ANALYSIS OF TUG FWD. COMP. + COMPONENTS WITH HEAT PIPES

POWER - WATTS

MISSION TIME - HOURS

	NODE NO.		102 Computer Pri Heater Power	
MIN	OF	0.	OCCURRED AT TIME	25.900
MAX	OF	68.260	OCCURRED AT TIME	45.000

FIGURE 5-135   ANALYSIS OF TUG FWD. COMP. STATIONED AT GEO. SHADOW PT.

POWER – WATTS

5.0
4.0
3.0
2.0
1.0
.0
-1.0
-2.0
-3.0
-4.0
-5.0

0   22.00   44.00   66.00   88.00   110.00

MISSION TIME – HOURS

NODE NO.   103 Computer Sec Heater Power

MIN   OF   0.   OCCURRED AT TIME   110.000
MAX   OF   0.   OCCURRED AT TIME   0.

FIGURE 5-136   ANALYSIS OF TUG FWD. COMP. + COMPONENTS WITH HEAT PIPES

POWER – WATTS

100.0
90.0
80.0
70.0
60.0
50.0
40.0
30.0
20.0
10.0
.0

0   10.00   20.00   30.00   40.00   50.00
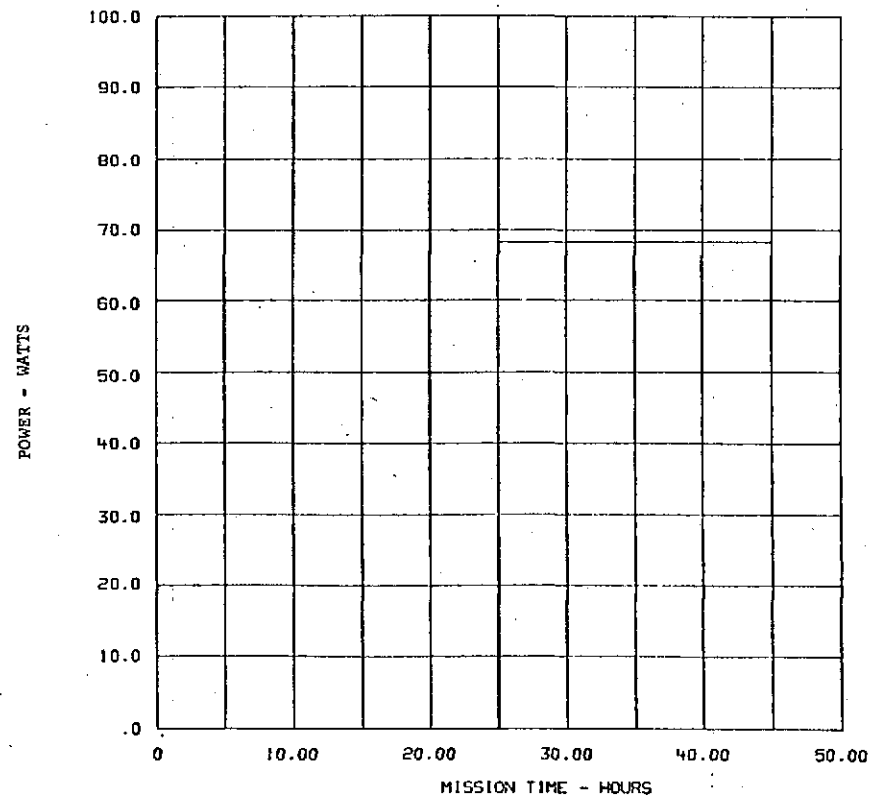
MISSION TIME – HOURS
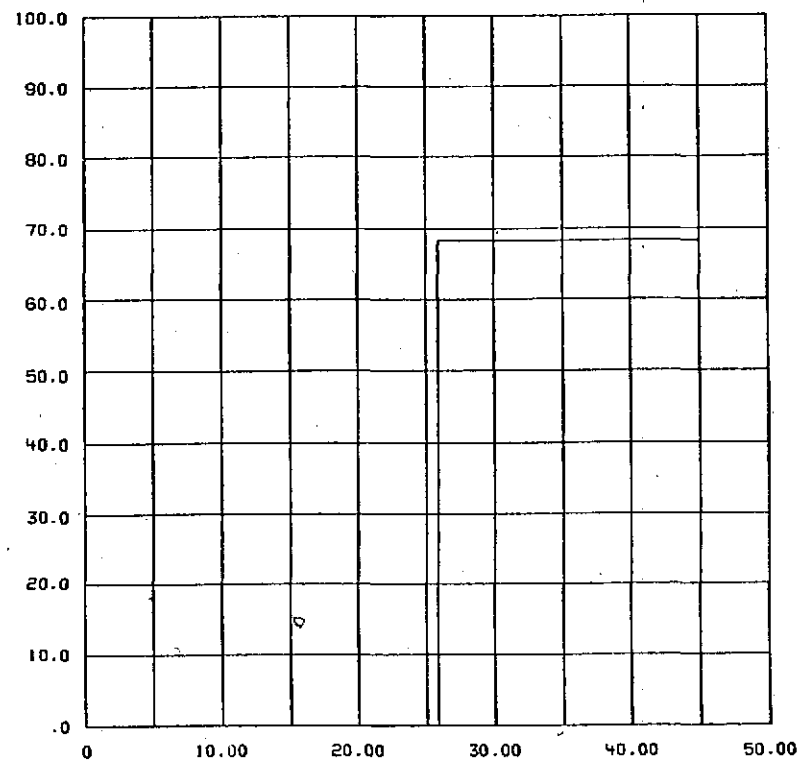
NODE NO.   103 Computer Sec Heater Power

MIN   OF   0.   OCCURRED AT TIME   25.800
MAX   OF   68.260   OCCURRED AT TIME   45.000

FIGURE 5-137   ANALYSIS OF TUG FWD. COMP. STATIONED AT GEO. SHADOW PT.
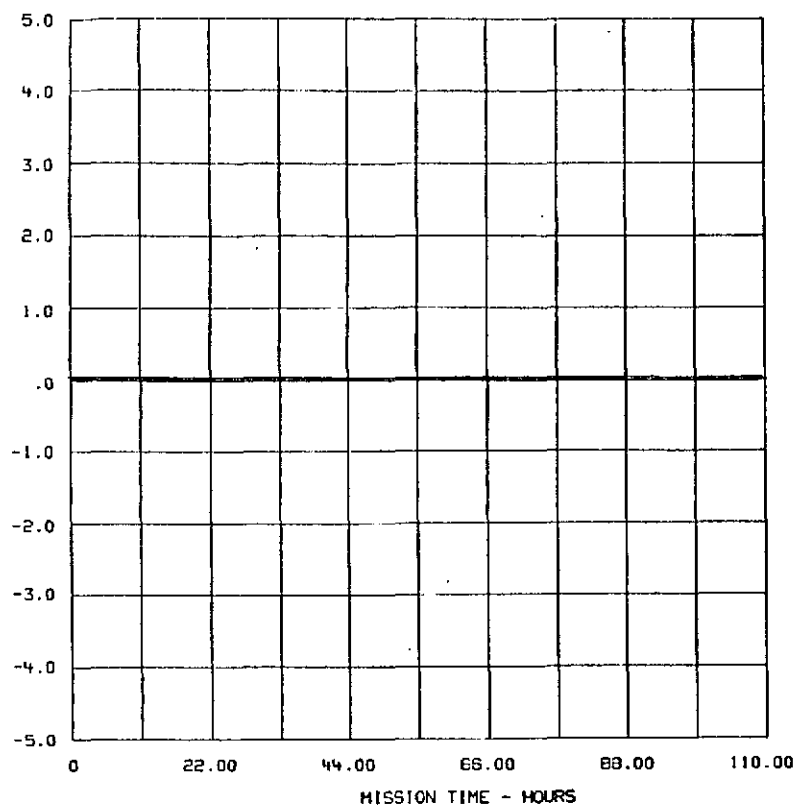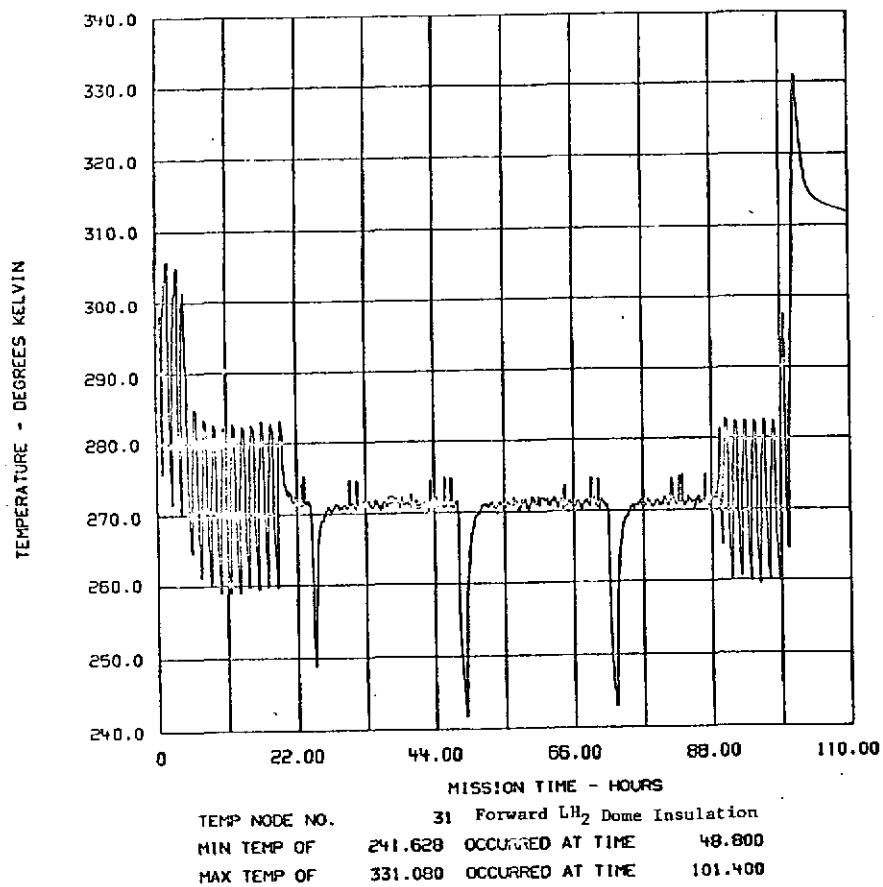
FIGURE 5-138   ANALYSIS OF TUG FWD. COMP. + COMPONENTS WITH HEAT PIPES

FIGURE 5-139   ANALYSIS OF TUG FWD. COMP. STATIONED AT GEO. SHADOW PT.
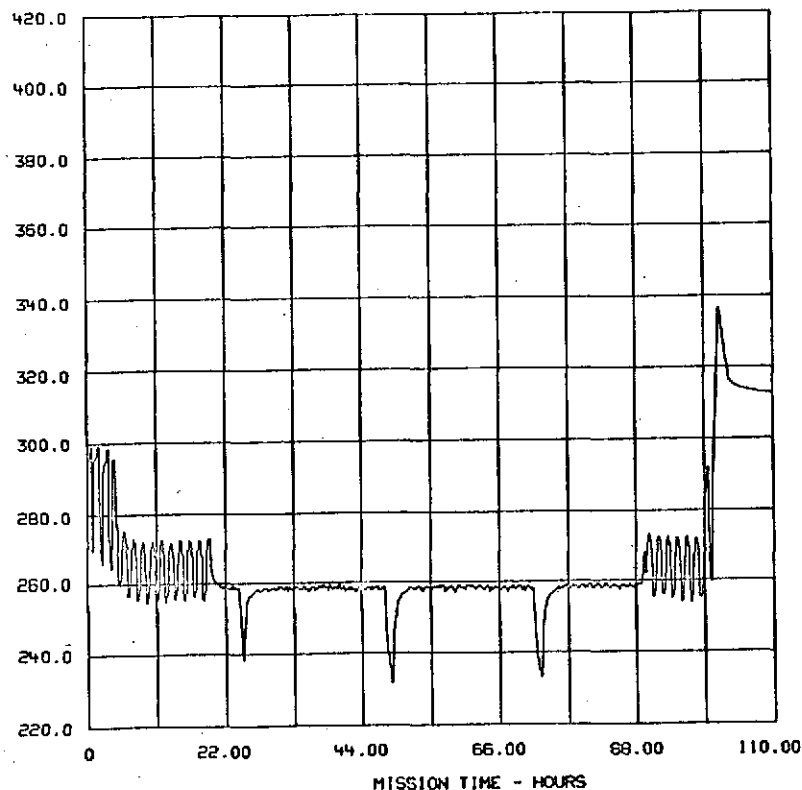
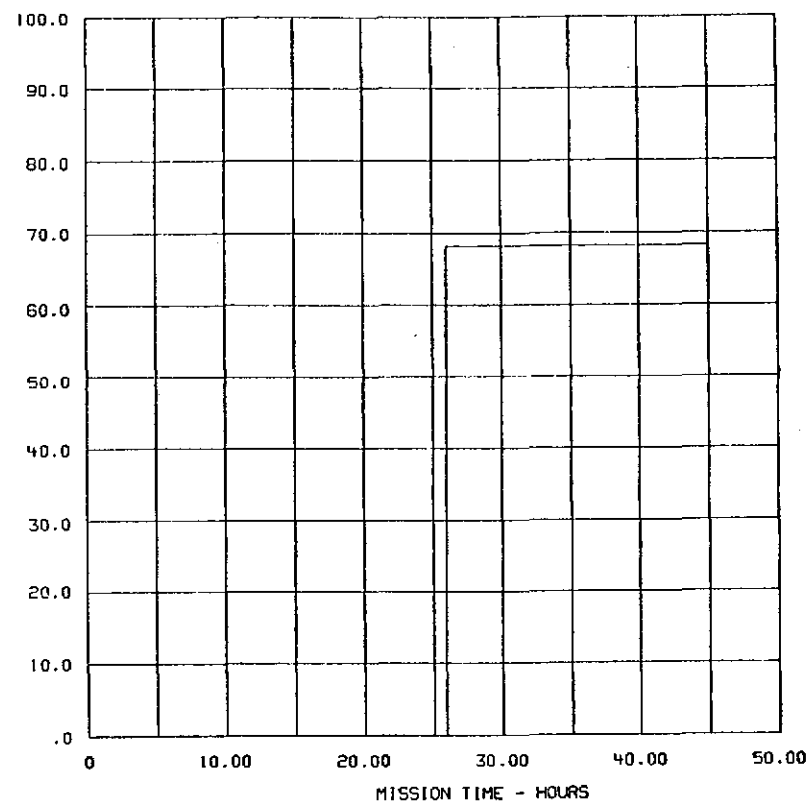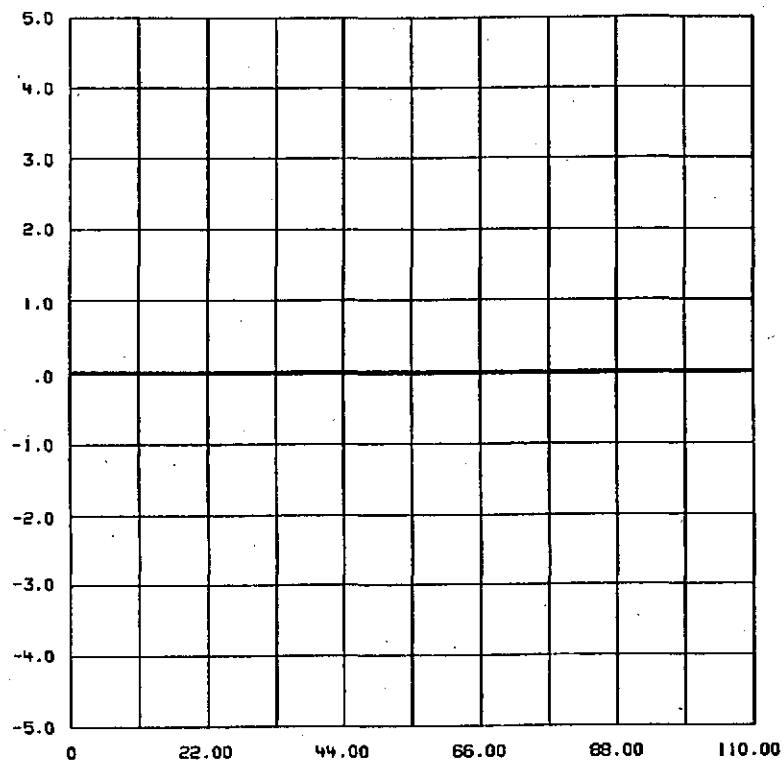FIGURE 5-140   ANALYSIS OF TUG FWD. COMP. + COMPONENTS WITH HEAT PIPES

TEMP NODE NO.   33 Forward Shield Inner Surface
MIN TEMP OF   231.671   OCCURRED AT TIME   48.800
MAX TEMP OF   336.627   OCCURRED AT TIME   101.400
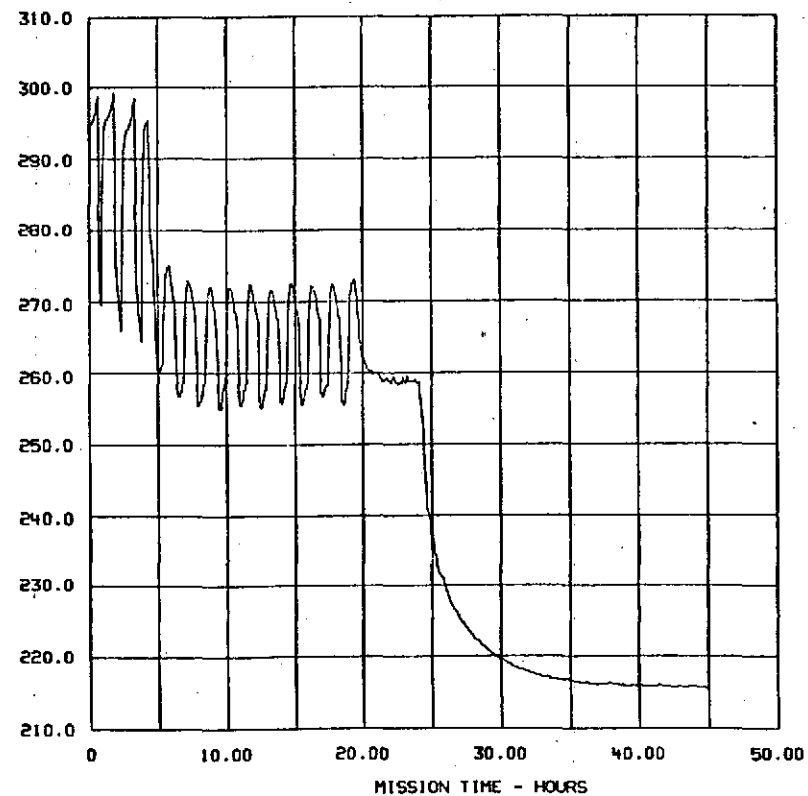
FIGURE 5-141   ANALYSIS OF TUG FWD. COMP. STATIONED AT GEO. SHADOW PT.

TEMP NODE NO.   33 Forward Shield Inner Surface
MIN TEMP OF   215.648   OCCURRED AT TIME   44.900
MAX TEMP OF   299.253   OCCURRED AT TIME   1.800

TEMP NODE NO. 35 Forward Shield Outer Surface - Beta Cloth
MIN TEMP OF 56.627 OCCURRED AT TIME 47.900
MAX TEMP OF 359.712 OCCURRED AT TIME 101.300
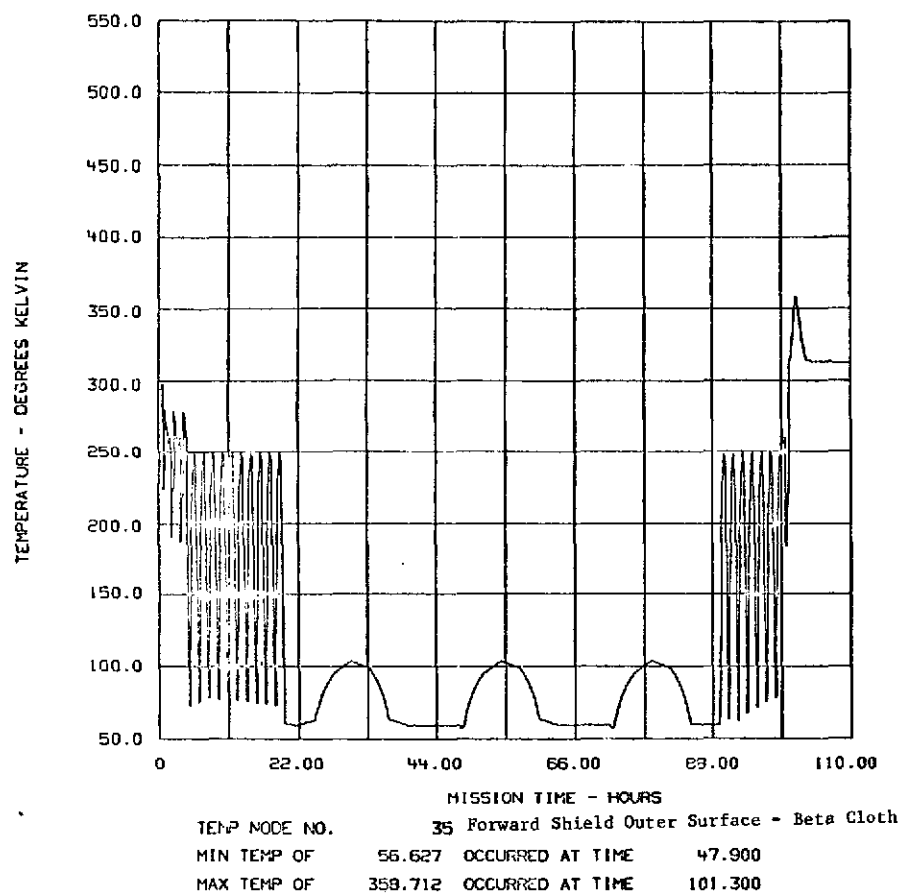
FIGURE 5-142   ANALYSIS OF TUG FWD. COMP. + COMPONENTS WITH HEAT PIPES

TEMP NODE NO. 35 Forward Shield Outer Surface - Beta Cloth
MIN TEMP OF 49.328 OCCURRED AT TIME 44.900
MAX TEMP OF 299.138 OCCURRED AT TIME .600
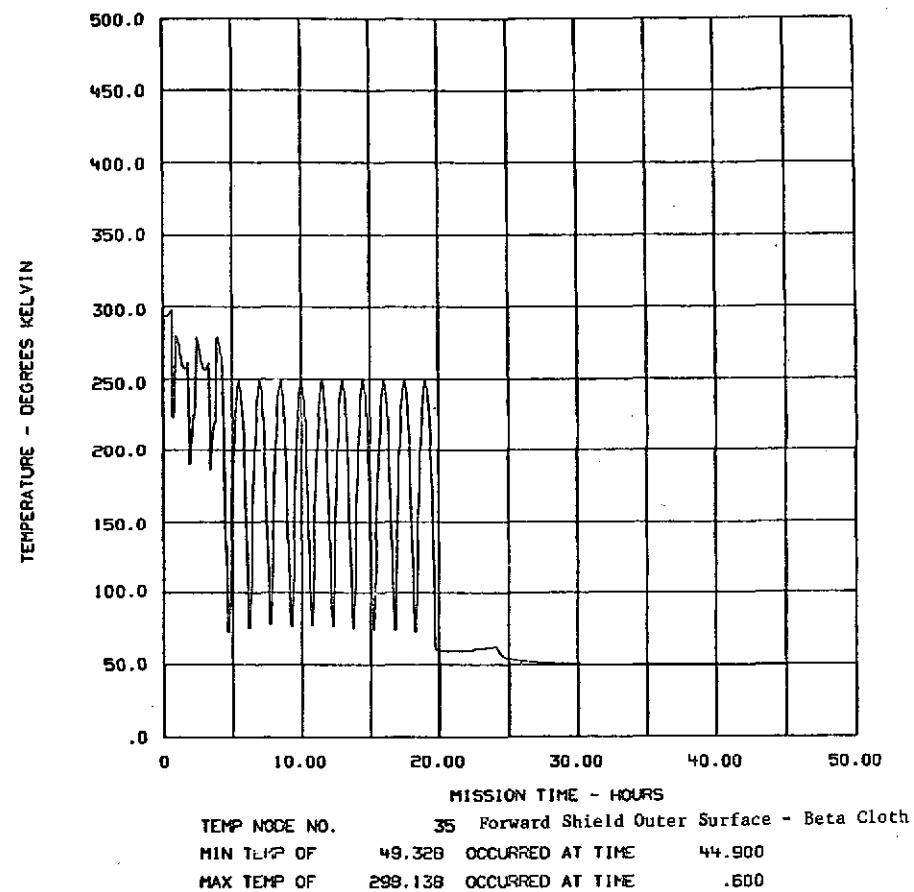
FIGURE 5-143   ANALYSIS OF TUG FWD. COMP. STATIONED AT GEO. SHADOW PT.

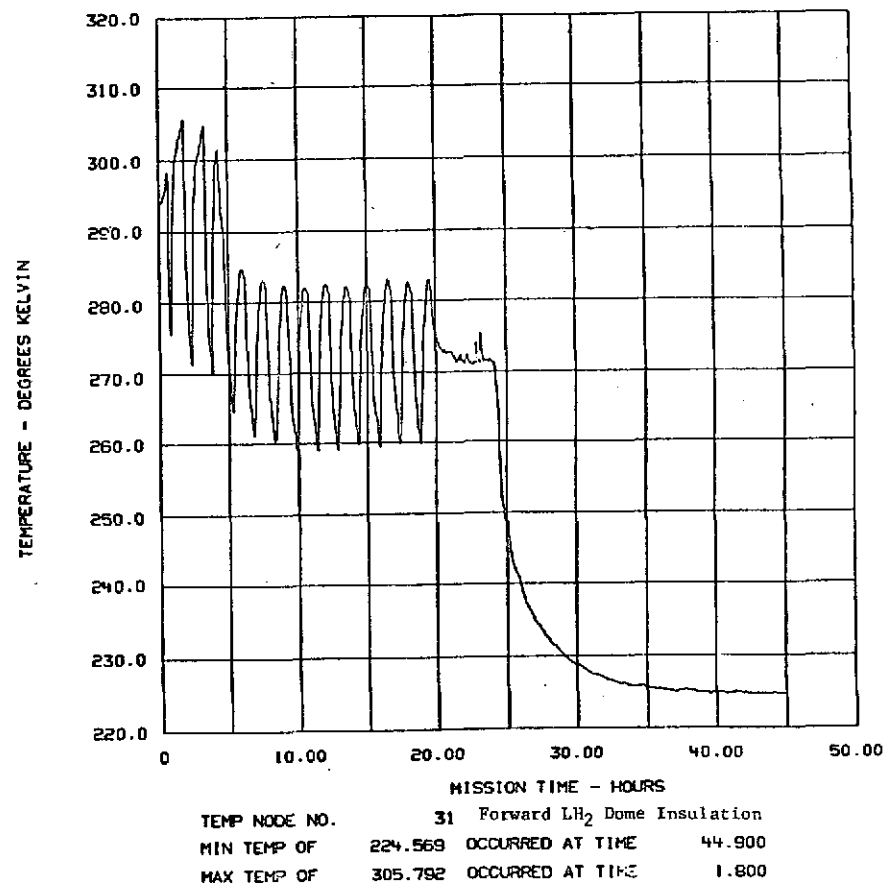FIGURE 5-144   ANALYSIS OF TUG FWD. COMP. + COMPONENTS WITH HEAT PIPES
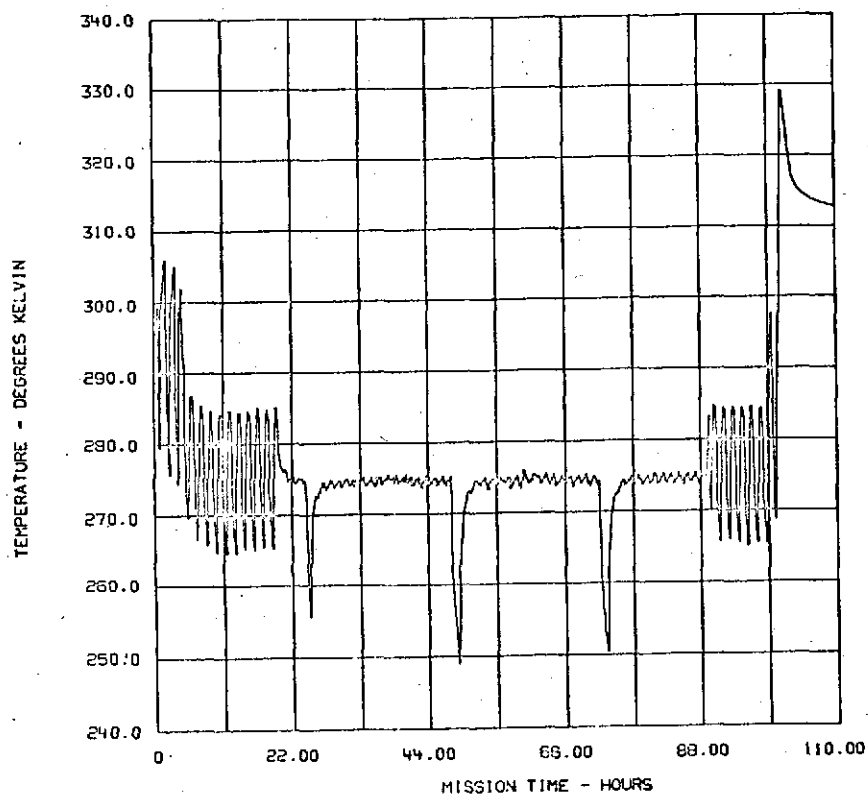
TEMP NODE NO.   34 Forward Compartment Internal Sink Temperature
MIN TEMP OF   249.007 OCCURRED AT TIME   48.800
MAX TEMP OF   329.158 OCCURRED AT TIME   101.400

FIGURE 5-145   ANALYSIS OF TUG FWD. COMP. STATIONED AT GEO. SHADOW PT.
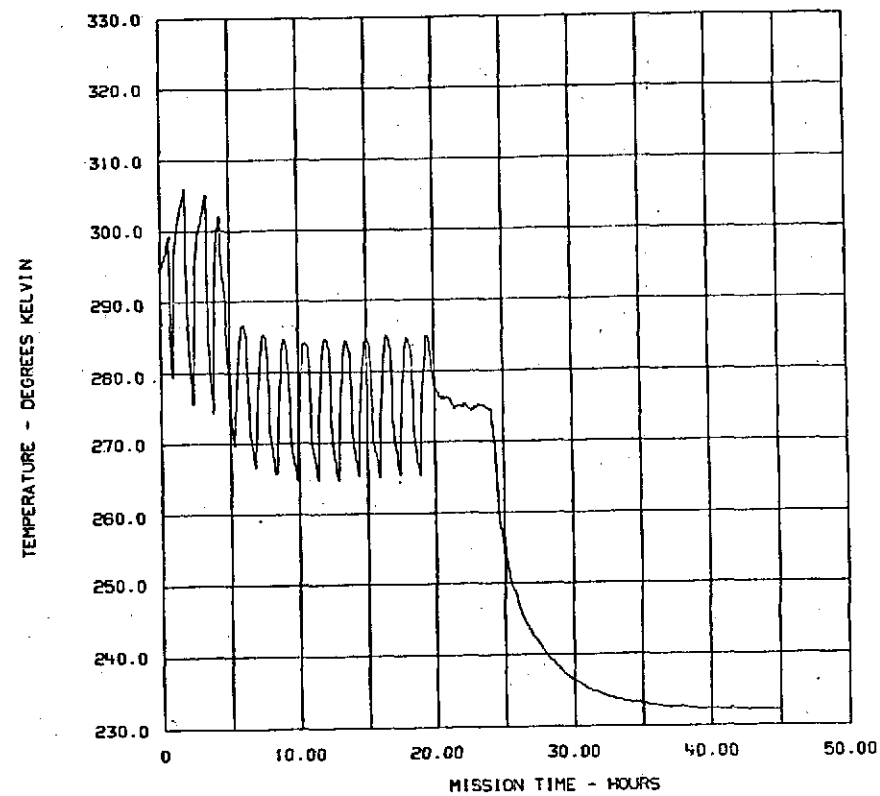
TEMP NODE NO.   34 Forward Compartment Internal Sink Temperature
MIN TEMP OF   232.049 OCCURRED AT TIME   44.900
MAX TEMP OF   306.022 OCCURRED AT TIME   1.800

FIGURE 5-146   ANALYSIS OF TUG INT. COMPARTMENT + COMPONENTS NO HEAT PIPE
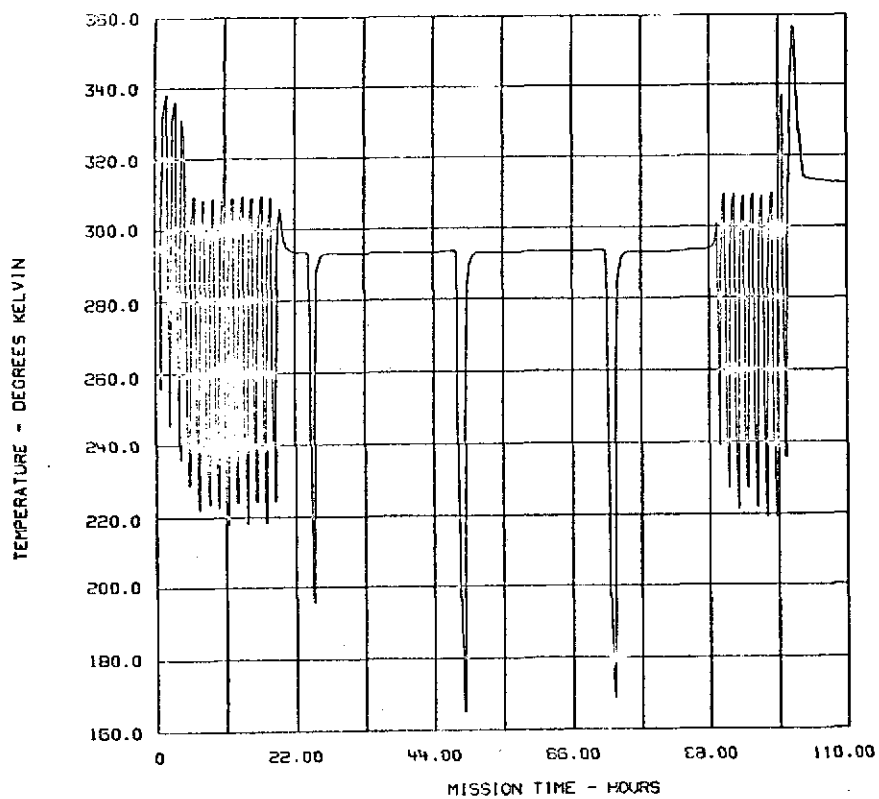
TEMP NODE NO.   81 Outer Skin
MIN TEMP OF   104.830 OCCURRED AT TIME   48.800
MAX TEMP OF   356.314 OCCURRED AT TIME   101.400

FIGURE 5-147   ANALYSIS OF TUG INT. COMP. STATIONED AT GEO. SHADOW PT.
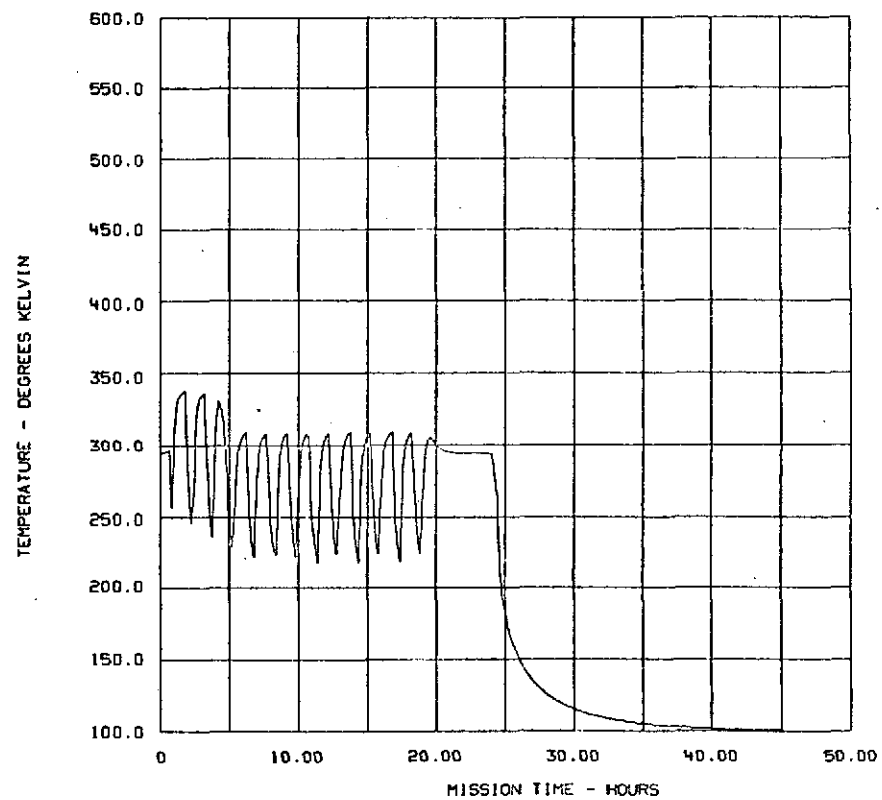
TEMP NODE NO.   81 Outer Skin
MIN TEMP OF   100.201 OCCURRED AT TIME   45.000
MAX TEMP OF   338.364 OCCURRED AT TIME   1.800

FIGURE 5-148   ANALYSIS OF TUG INT. COMPARTMENT + COMPONENTS NO HEAT PIPE

TEMP NODE NO.   9 Inner Skin
MIN TEMP OF   165.000 OCCURRED AT TIME   48.800
MAX TEMP OF   356.295 OCCURRED AT TIME   101.400
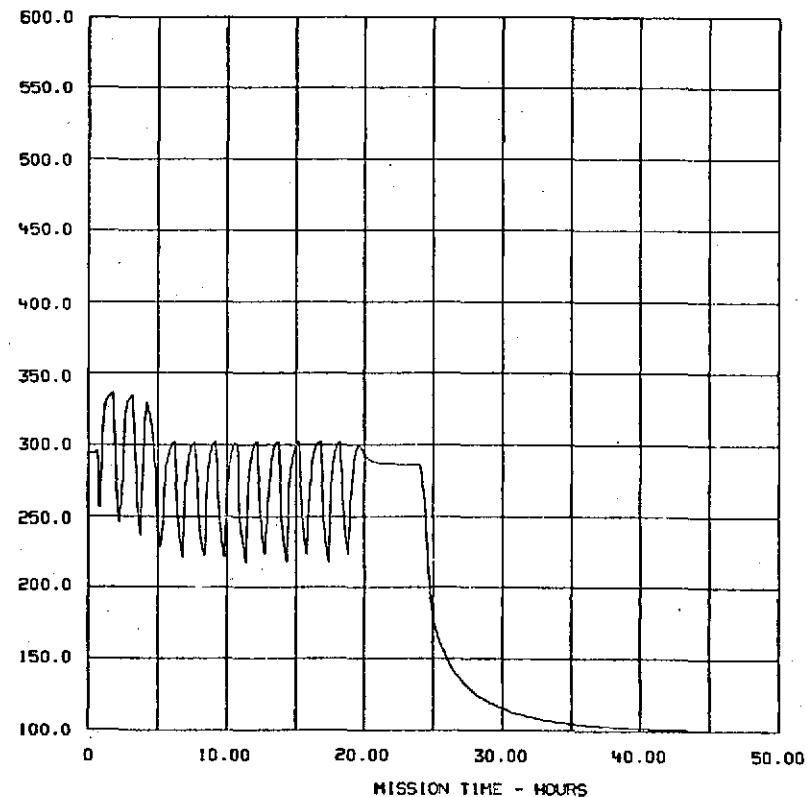
FIGURE 5-149   ANALYSIS OF TUG INT. COMP. STATIONED AT GEO. SHADOW PT.

TEMP NODE NO.   9 Inner Skin
MIN TEMP OF   100.406 OCCURRED AT TIME   45.000
MAX TEMP OF   336.514 OCCURRED AT TIME   1.800

MISSION TIME – HOURS

TEMP NODE NO.	82 Outer Skin		
MIN TEMP OF	163.699	OCCURRED AT TIME	48.800
MAX TEMP OF	356.359	OCCURRED AT TIME	101.400
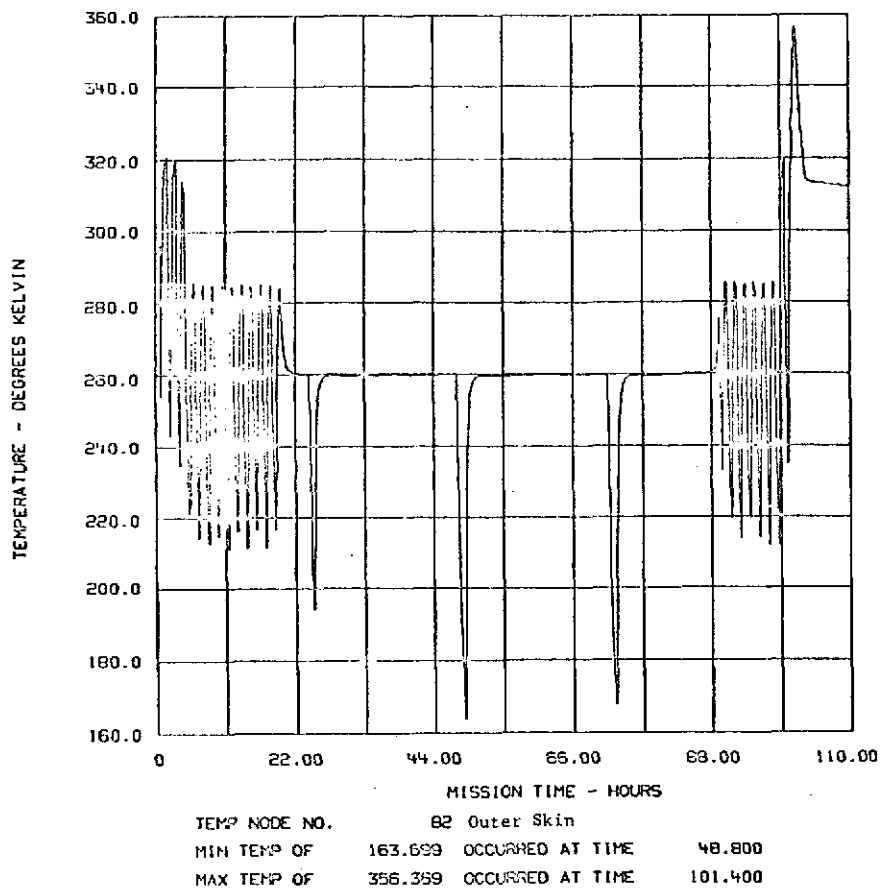
FIGURE 5-150   ANALYSIS OF TUG INT. COMPARTMENT + COMPONENTS NO HEAT PIPE

MISSION TIME – HOURS

TEMP NODE NO.	82 Outer Skin		
MIN TEMP OF	99.944	OCCURRED AT TIME	45.000
MAX TEMP OF	320.824	OCCURRED AT TIME	1.800

FIGURE 5-151   ANALYSIS OF TUG INT. COMP. STATIONED AT GEO. SHADOW PT.

TEMPERATURE - DEGREES KELVIN

MISSION TIME - HOURS

TEMP NODE NO.   10 Inner Skin
MIN TEMP OF   163.923 OCCURRED AT TIME   48.800
MAX TEMP OF   356.357 OCCURRED AT TIME   101.400

FIGURE 5-152   ANALYSIS OF TUG INT. COMPARTMENT + COMPONENTS NO HEAT PIPE

TEMPERATURE - DEGREES KELVIN

MISSION TIME - HOURS

TEMP NODE NO.   10 Inner Skin
MIN TEMP OF   100.146 OCCURRED AT TIME   45.000
MAX TEMP OF   324.199 OCCURRED AT TIME   1.800

FIGURE 5-153   ANALYSIS OF TUG INT. COMP. STATIONED AT GEO. SHADOW PT.

5-93

TEMPERATURE – DEGREES KELVIN

MISSION TIME – HOURS

TEMP NODE NO.	83 Outer Skin		
MIN TEMP OF	160.389	OCCURRED AT TIME	72.800
MAX TEMP OF	357.182	OCCURRED AT TIME	101.400

FIGURE 5-154   ANALYSIS OF TUG INT. COMPARTMENT + COMPONENTS NO HEAT PIPE

TEMPERATURE – DEGREES KELVIN

MISSION TIME – HOURS

TEMP NODE NO.	83 Outer Skin		
MIN TEMP OF	98.365	OCCURRED AT TIME	45.000
MAX TEMP OF	330.778	OCCURRED AT TIME	1.800

FIGURE 5-155   ANALYSIS OF TUG INT. COMP. STATIONED AT GEO. SHADOW PT.

TEMP NODE NO.   11 Inner Skin
MIN TEMP OF   161.245 OCCURRED AT TIME   72.800
MAX TEMP OF   356.939 OCCURRED AT TIME   101.400
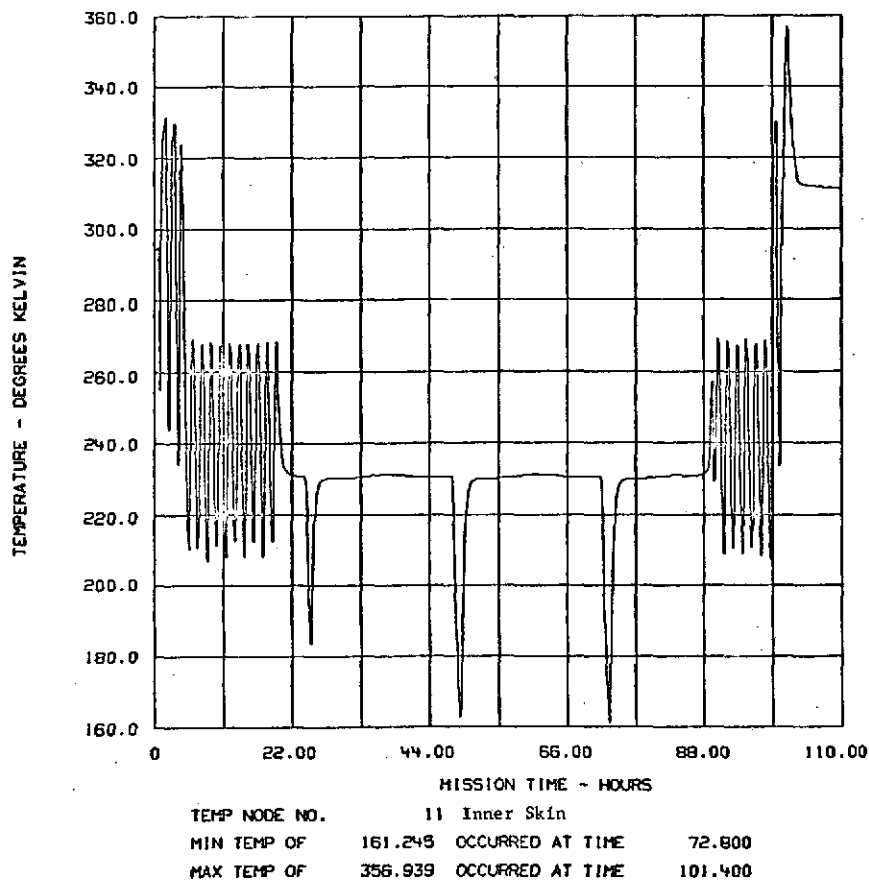
FIGURE 5-156   ANALYSIS OF TUG INT. COMPARTMENT + COMPONENTS NO HEAT PIPE

TEMP NODE NO.   11 Inner Skin
MIN TEMP OF   98.555 OCCURRED AT TIME   45.000
MAX TEMP OF   331.274 OCCURRED AT TIME   1.800

FIGURE 5-157   ANALYSIS OF TUG INT. COMP. STATIONED AT GEO. SHADOW PT.
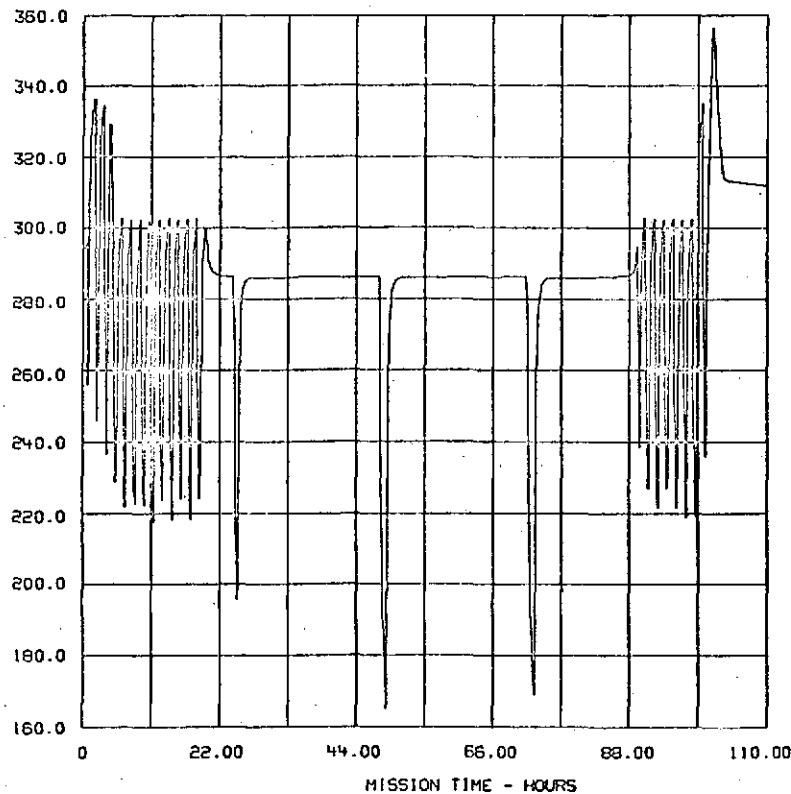
TEMPERATURE - DEGREES KELVIN

MISSION TIME - HOURS

TEMP NODE NO.		84	Outer Skin	
MIN TEMP OF	160.133	OCCURRED AT TIME		72.800
MAX TEMP OF	357.233	OCCURRED AT TIME		101.400
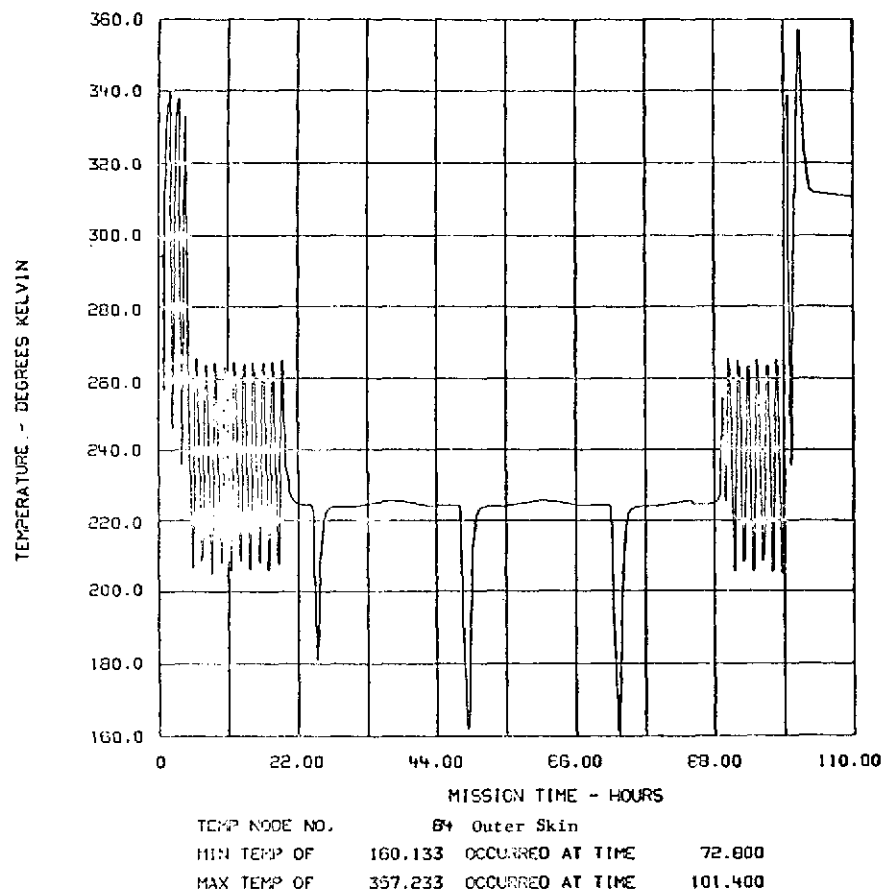
FIGURE 5-158   ANALYSIS OF TUG INT. COMPARTMENT + COMPONENTS NO HEAT PIPE

TEMPERATURE - DEGREES KELVIN

MISSION TIME - HOURS

TEMP NODE NO.		84	Outer Skin	
MIN TEMP OF	97.839	OCCURRED AT TIME		45.000
MAX TEMP OF	339.705	OCCURRED AT TIME		1.800

FIGURE 5-159   ANALYSIS OF TUG INT. COMP. STATIONED AT GEO. SHADOW PT.

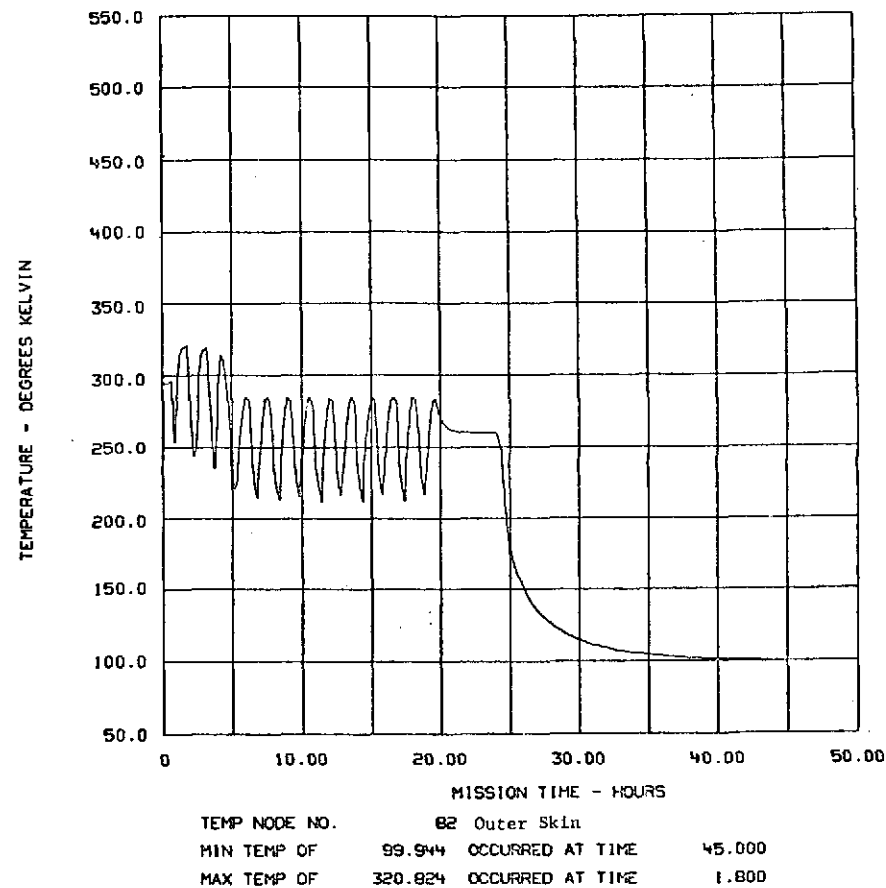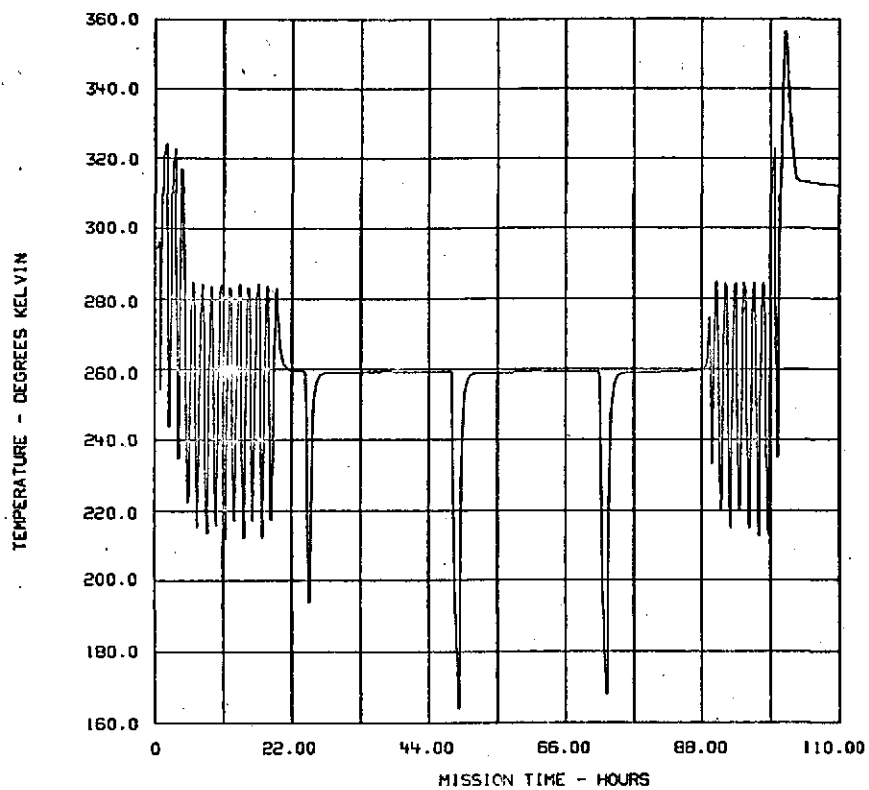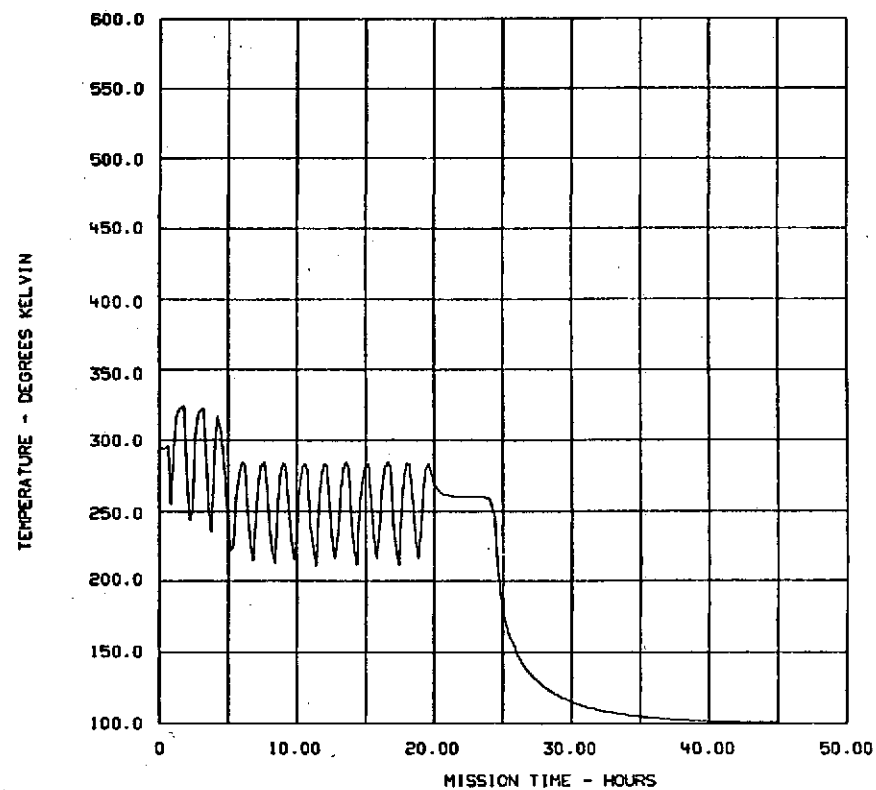FIGURE 5-160   ANALYSIS OF TUG INT. COMPARTMENT + COMPONENTS NO HEAT PIPE

TEMP NODE NO.   12 Inner Skin
MIN TEMP OF   160.910   OCCURRED AT TIME   72.800
MAX TEMP OF   356.991   OCCURRED AT TIME   101.400

FIGURE 5-161   ANALYSIS OF TUG INT. COMP. STATIONED AT GEO. SHADOW PT.

TEMP NODE NO.   12 Inner Skin
MIN TEMP OF   98.025   OCCURRED AT TIME   45.000
MAX TEMP OF   337.589   OCCURRED AT TIME   1.800

TEMP NODE NO.   85 Outer Skin
MIN TEMP OF   160.255 OCCURRED AT TIME   72.800
MAX TEMP OF   357.260 OCCURRED AT TIME   101.400

FIGURE 5-162   ANALYSIS OF TUG INT. COMPARTMENT + COMPONENTS NO HEAT PIPE

TEMP NODE NO.   85 Outer Skin
MIN TEMP OF   98.444 OCCURRED AT TIME   45.000
MAX TEMP OF   339.787 OCCURRED AT TIME   1.800

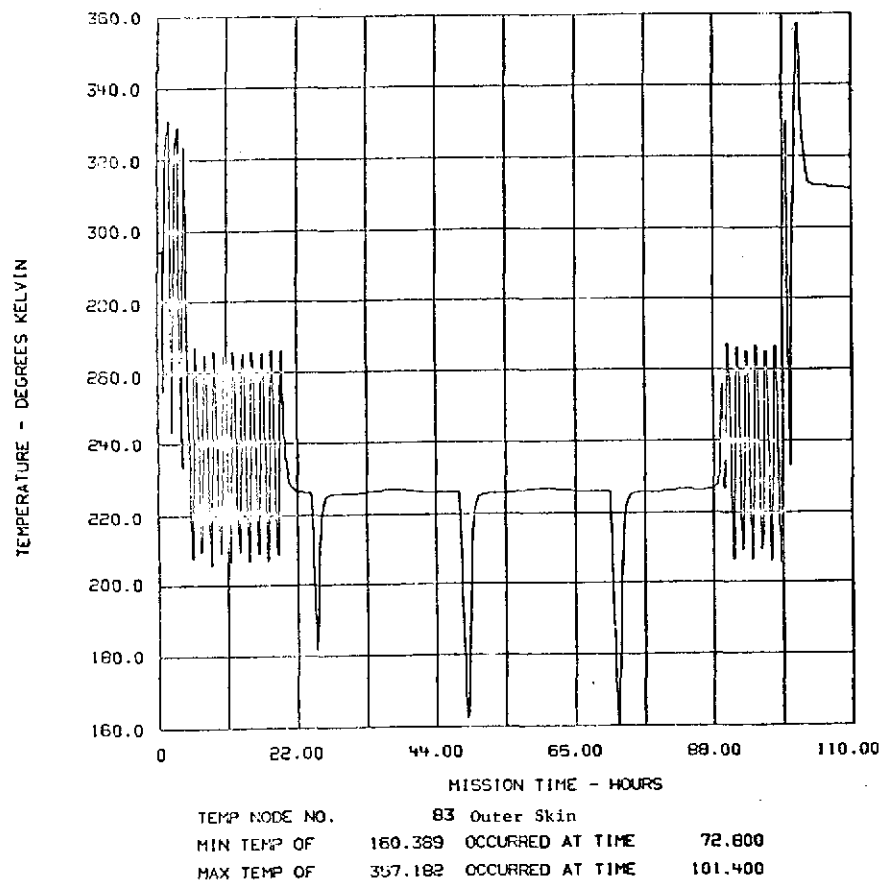FIGURE 5-163   ANALYSIS OF TUG INT. COMP. STATIONED AT GEO. SHADOW PT.

FIGURE 5-184   ANALYSIS OF TUG INT. COMPARTMENT + COMPONENTS NO HEAT PIPE
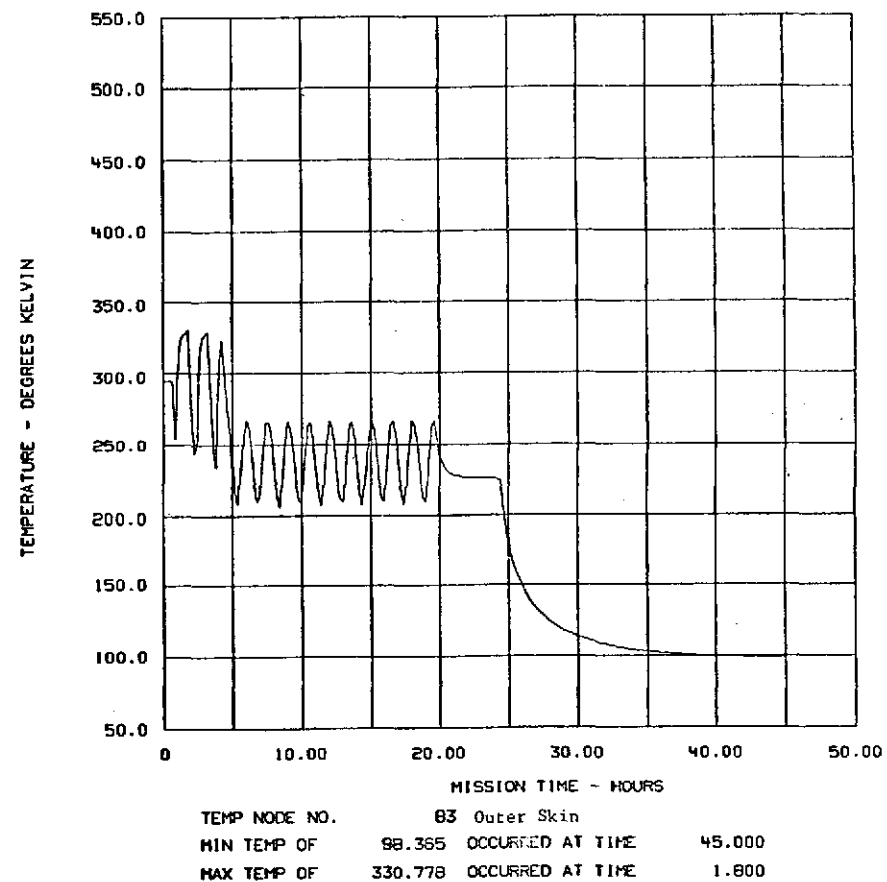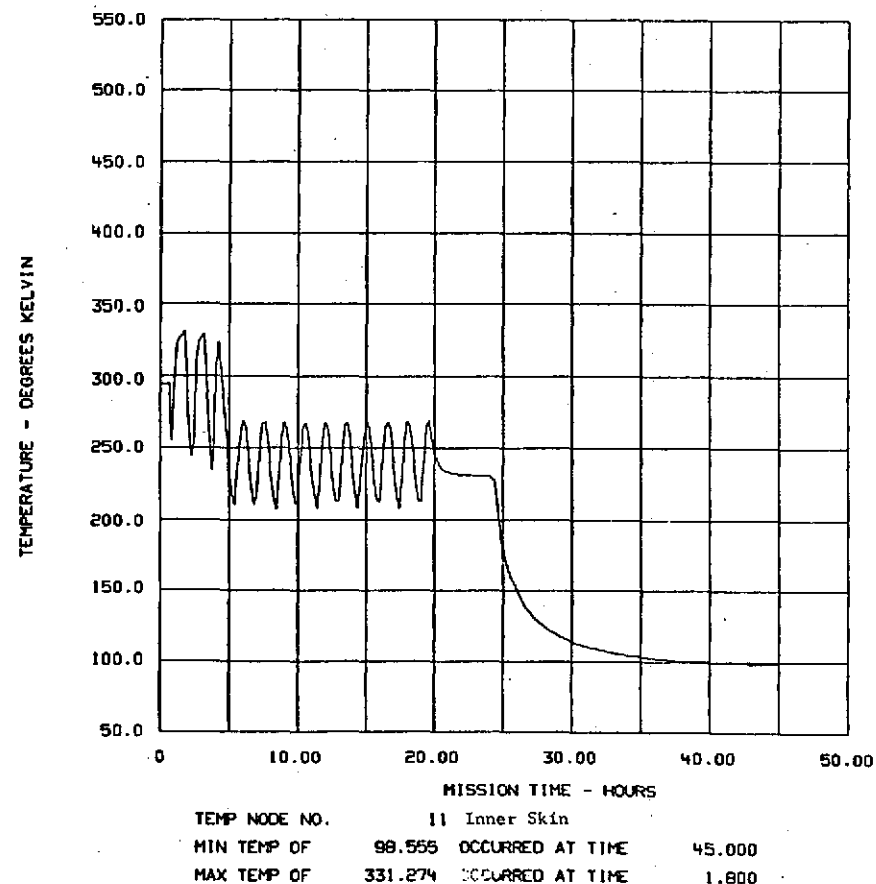
TEMP NODE NO.   13 Inner Skin
MIN TEMP OF   161.068 OCCURRED AT TIME   72.800
MAX TEMP OF   357.006 OCCURRED AT TIME   101.400

FIGURE 5-185   ANALYSIS OF TUG INT. COMP. STATIONED AT GEO. SHADOW PT.

TEMP NODE NO.   13 Inner Skin
MIN TEMP OF   98.635 OCCURRED AT TIME   45.000
MAX TEMP OF   337.692 OCCURRED AT TIME   1.800

TEMP NODE NO.   86 Outer Skin
MIN TEMP OF   160.583 OCCURRED AT TIME   72.800
MAX TEMP OF   357.272 OCCURRED AT TIME   101.400

FIGURE 5-166   ANALYSIS OF TUG INT. COMPARTMENT + COMPONENTS NO HEAT PIPE

TEMP NODE NO.   86 Outer Skin
MIN TEMP OF   99.698 OCCURRED AT TIME   45.000
MAX TEMP OF   330.855 OCCURRED AT TIME   1.800

FIGURE 5-167   ANALYSIS OF TUG INT. COMP. STATIONED AT GEO. SHADOW PT.
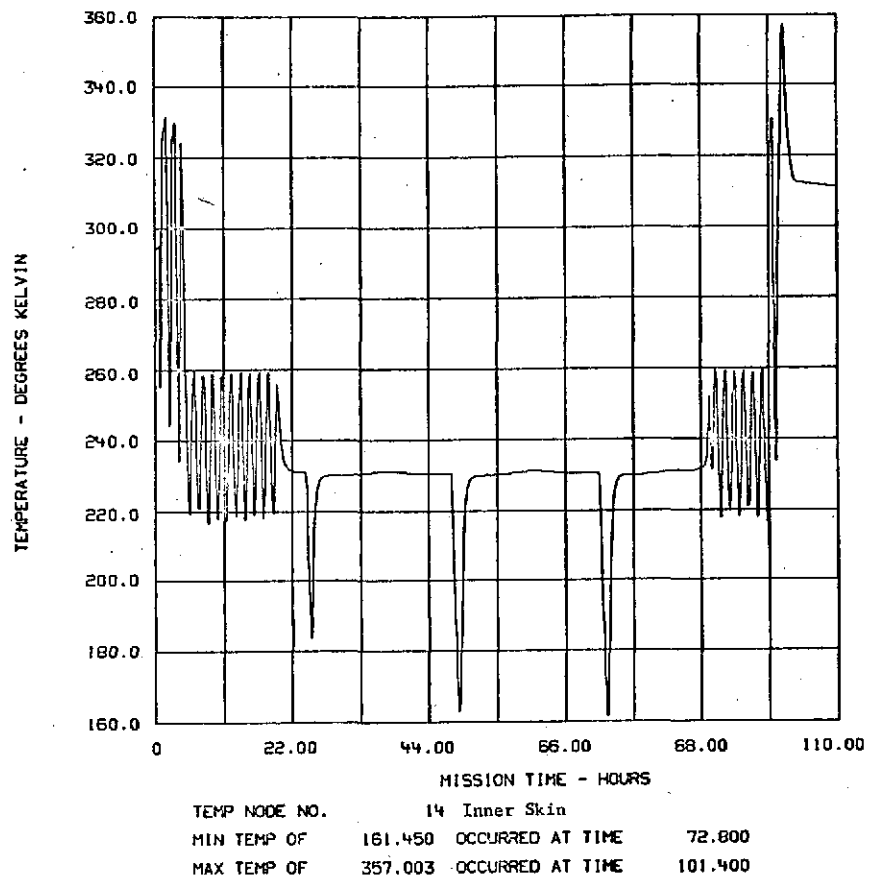
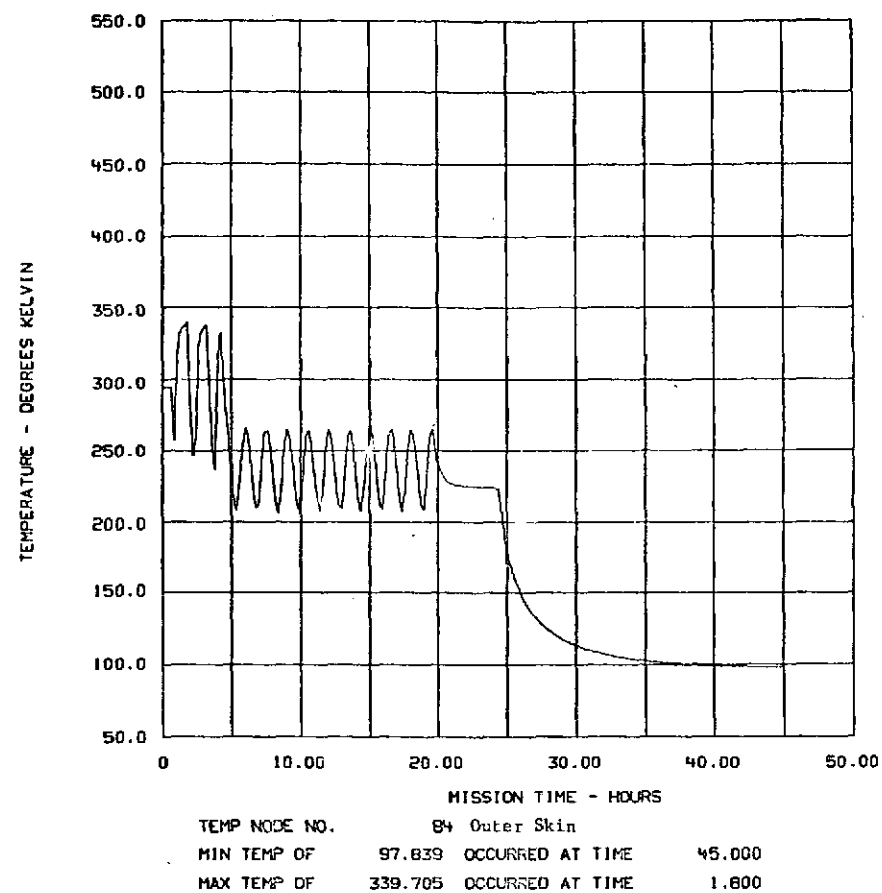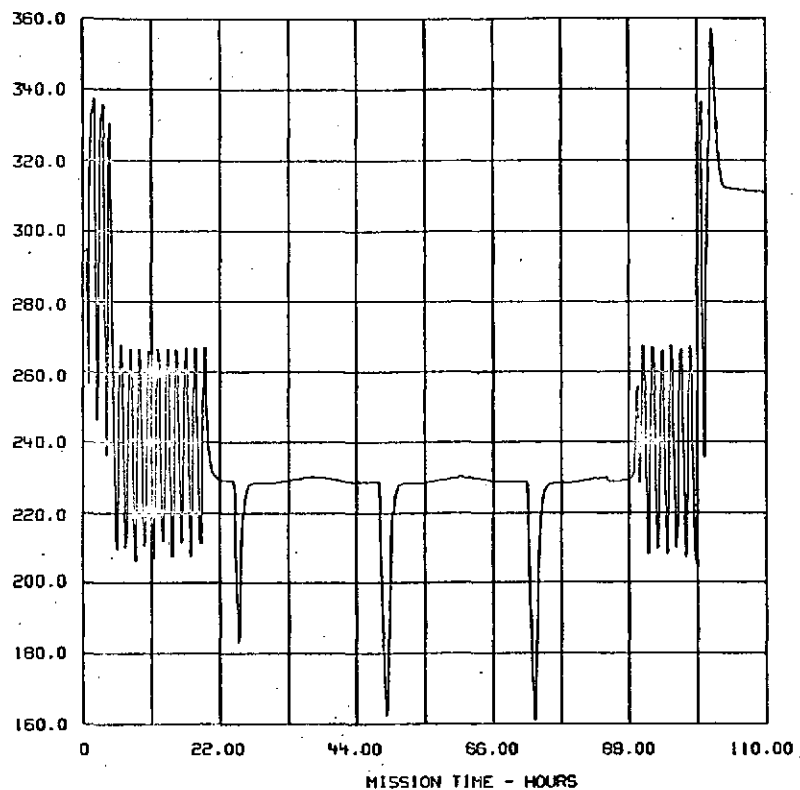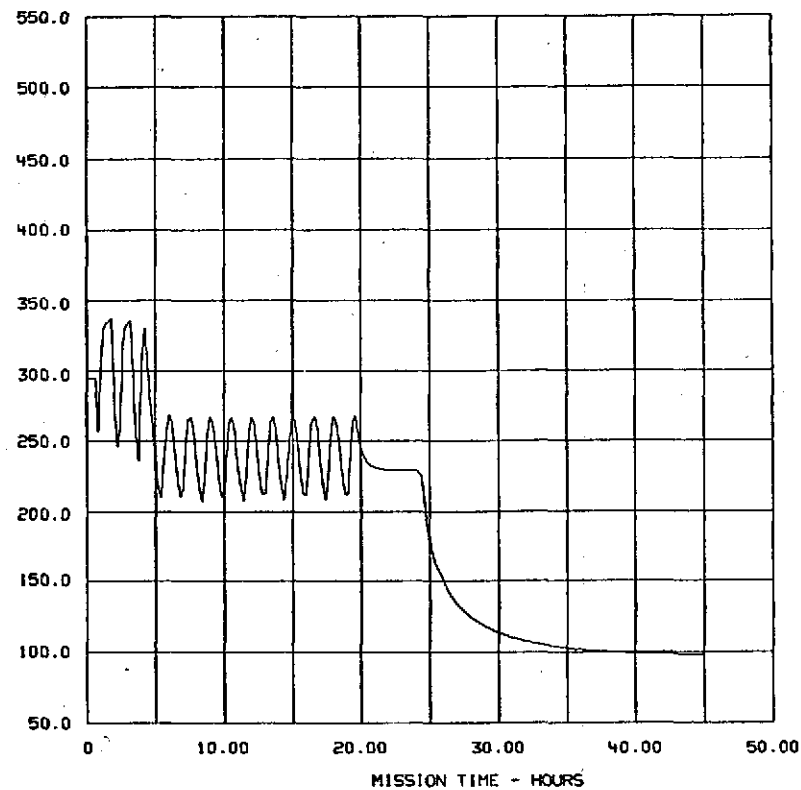FIGURE 5-168   ANALYSIS OF TUG INT. COMPARTMENT + COMPONENTS NO HEAT PIPE

TEMP NODE NO.   14 Inner Skin
MIN TEMP OF   161.450 OCCURRED AT TIME   72.800
MAX TEMP OF   357.003 OCCURRED AT TIME   101.400

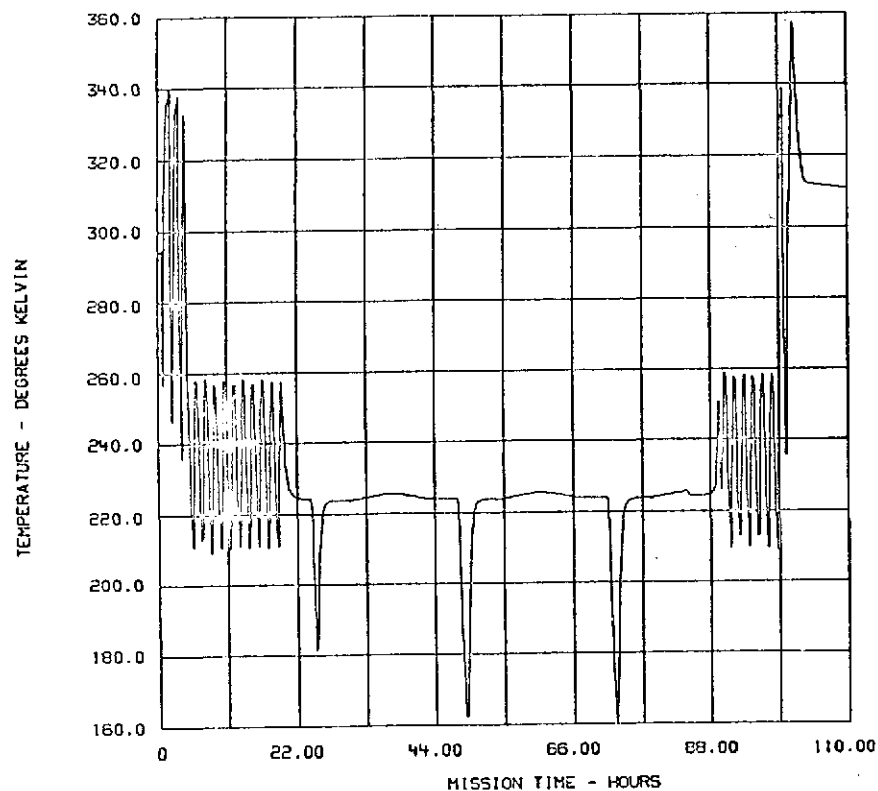FIGURE 5-169   ANALYSIS OF TUG INT. COMP. STATIONED AT GEO. SHADOW PT.

TEMP NODE NO.   14 Inner Skin
MIN TEMP OF   99.899 OCCURRED AT TIME   45.000
MAX TEMP OF   331.384 OCCURRED AT TIME   1.800

TEMPERATURE - DEGREES KELVIN

MISSION TIME - HOURS

TEMP NODE NO.	87 Outer Skin		
MIN TEMP OF	175.399	OCCURRED AT TIME	48.800
MAX TEMP OF	356.320	OCCURRED AT TIME	101.400

FIGURE 5-170   ANALYSIS OF TUG INT. COMPARTMENT + COMPONENTS NO HEAT PIPE

TEMPERATURE - DEGREES KELVIN

MISSION TIME - HOURS

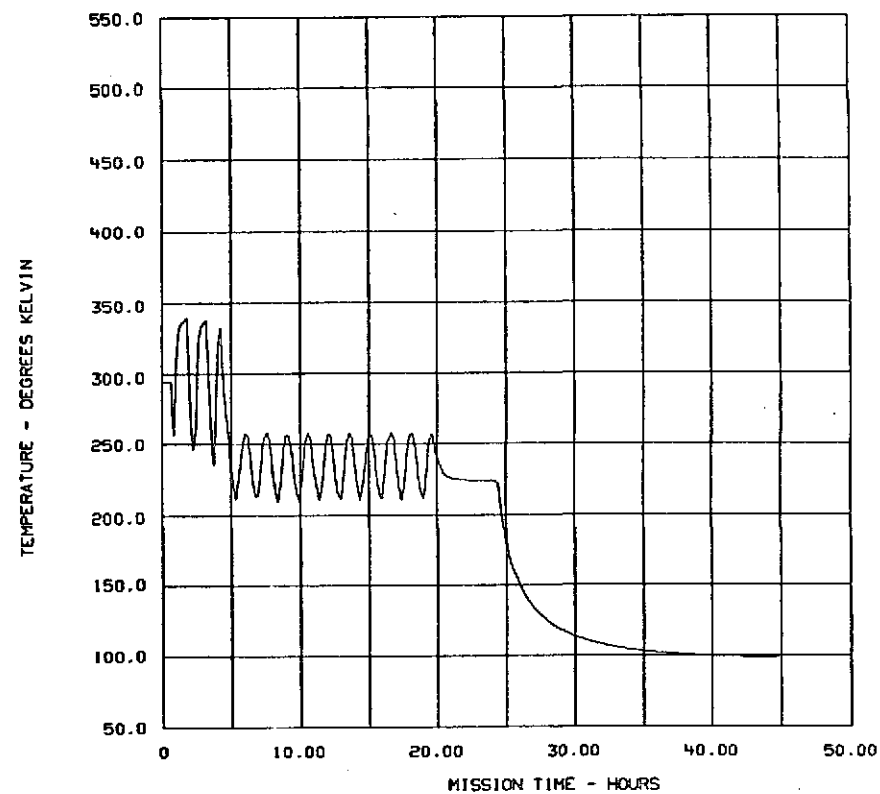| TEMP NODE NO.	87 Outer Skin		
MIN TEMP OF	141.459	OCCURRED AT TIME	44.600
MAX TEMP OF	321.582	OCCURRED AT TIME	1.800
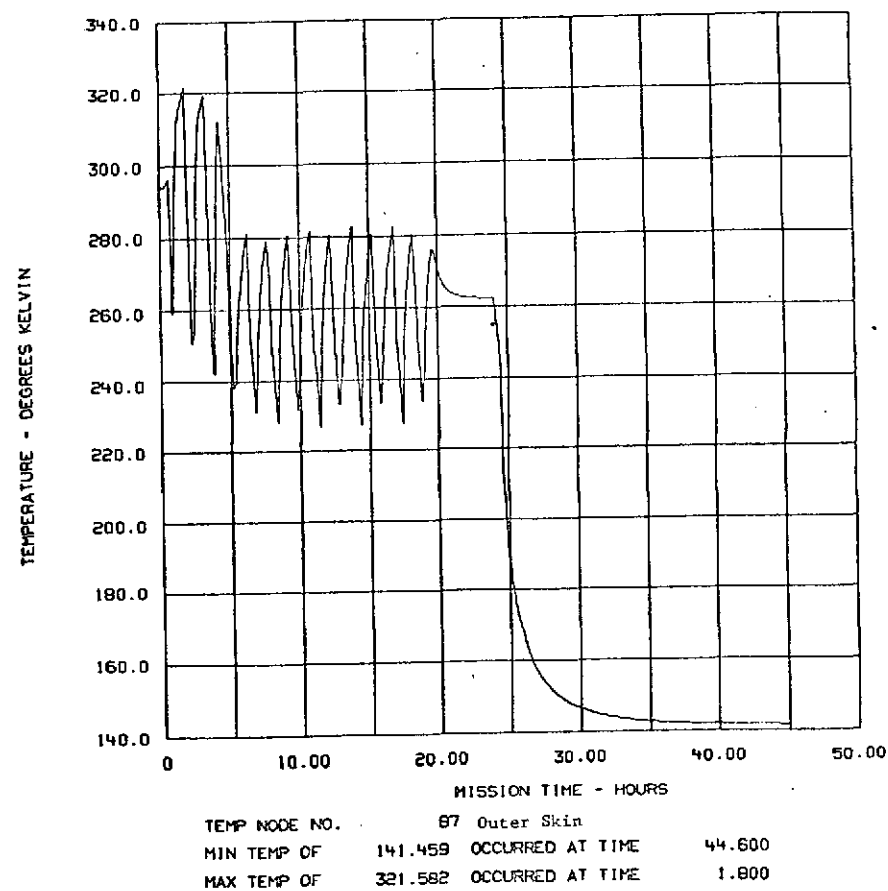
FIGURE 5-171   ANALYSIS OF TUG INT. COMP. STATIONED AT GEO. SHADOW PT.
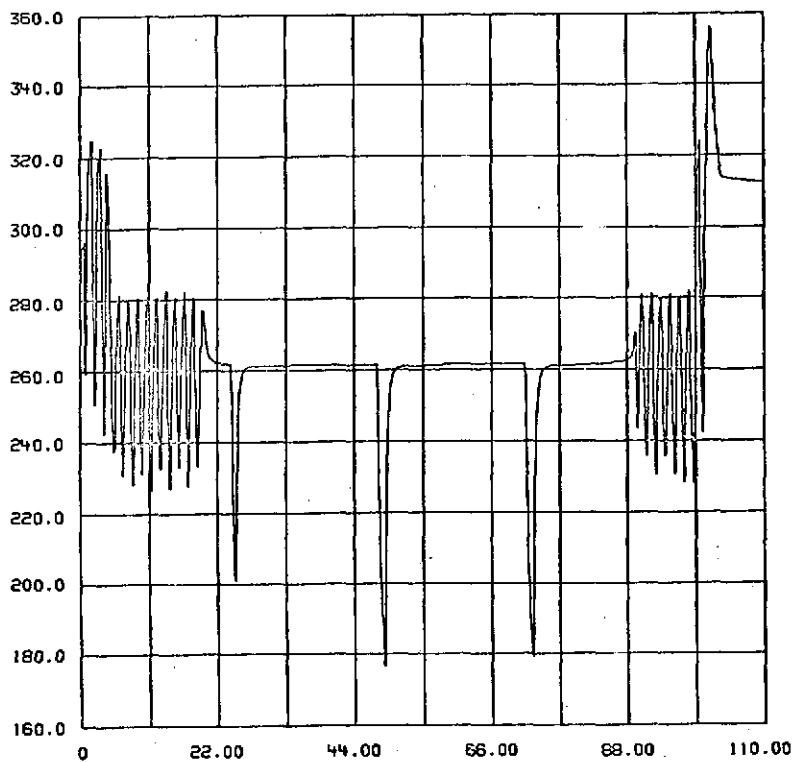
TEMP NODE NO.   15 Inner Skin
MIN TEMP OF   176.341 OCCURRED AT TIME   48.800
MAX TEMP OF   356.227 OCCURRED AT TIME   101.400

FIGURE 5-172   ANALYSIS OF TUG INT. COMPARTMENT + COMPONENTS NO HEAT PIPE

TEMP NODE NO.   15 Inner Skin
MIN TEMP OF   142.275 OCCURRED AT TIME   44.600
MAX TEMP OF   324.817 OCCURRED AT TIME   1.800

FIGURE 5-173   ANALYSIS OF TUG INT. COMP. STATIONED AT GEO. SHADOW PT.

FIGURE 5-174 ANALYSIS OF TUG INT. COMPARTMENT + COMPONENTS NO HEAT PIPE
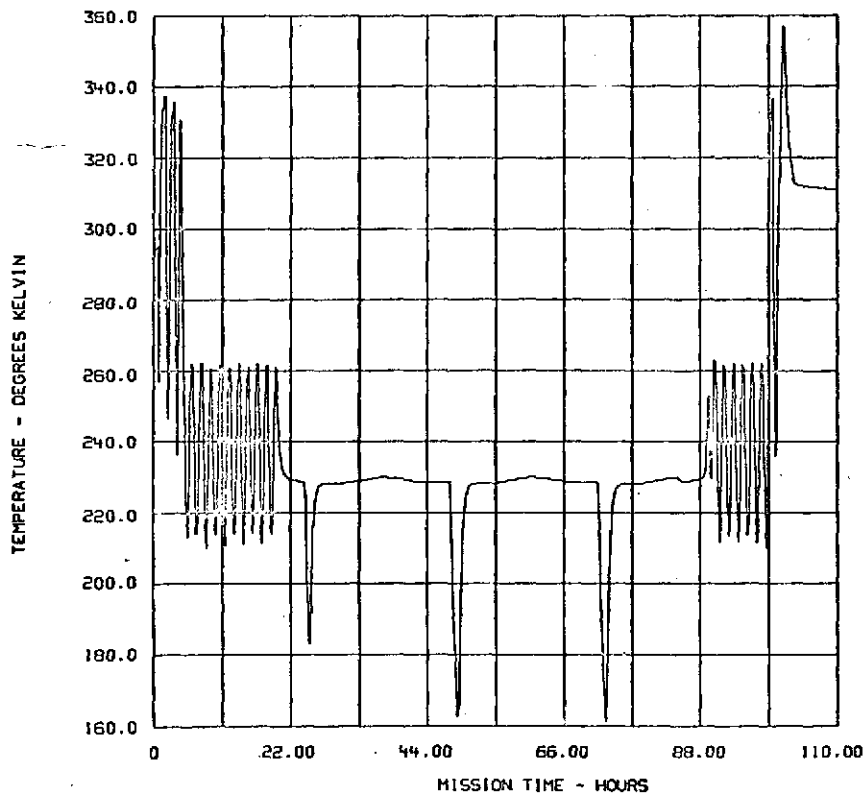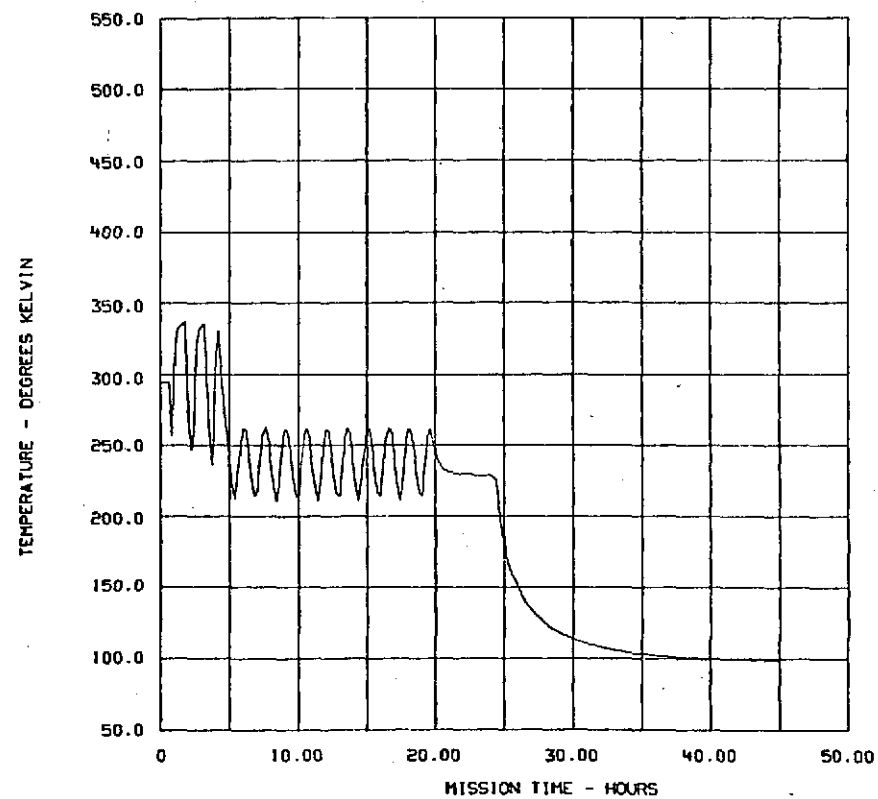
TEMP NODE NO. 83 Outer Skin
MIN TEMP OF 101.699 OCCURRED AT TIME 48.800
MAX TEMP OF 355.051 OCCURRED AT TIME 101.400
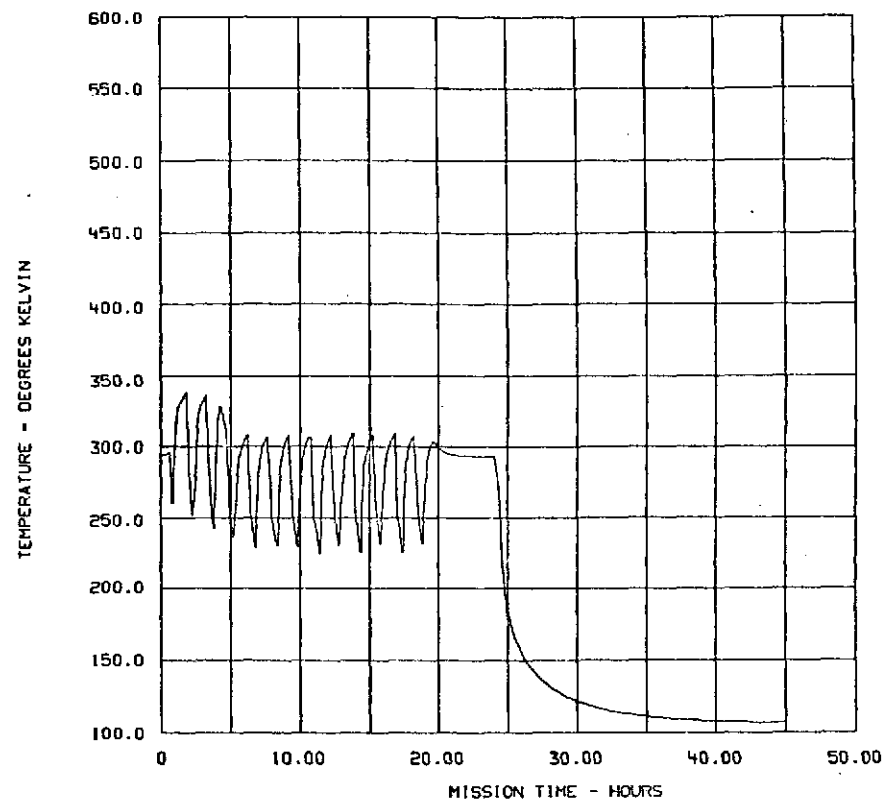
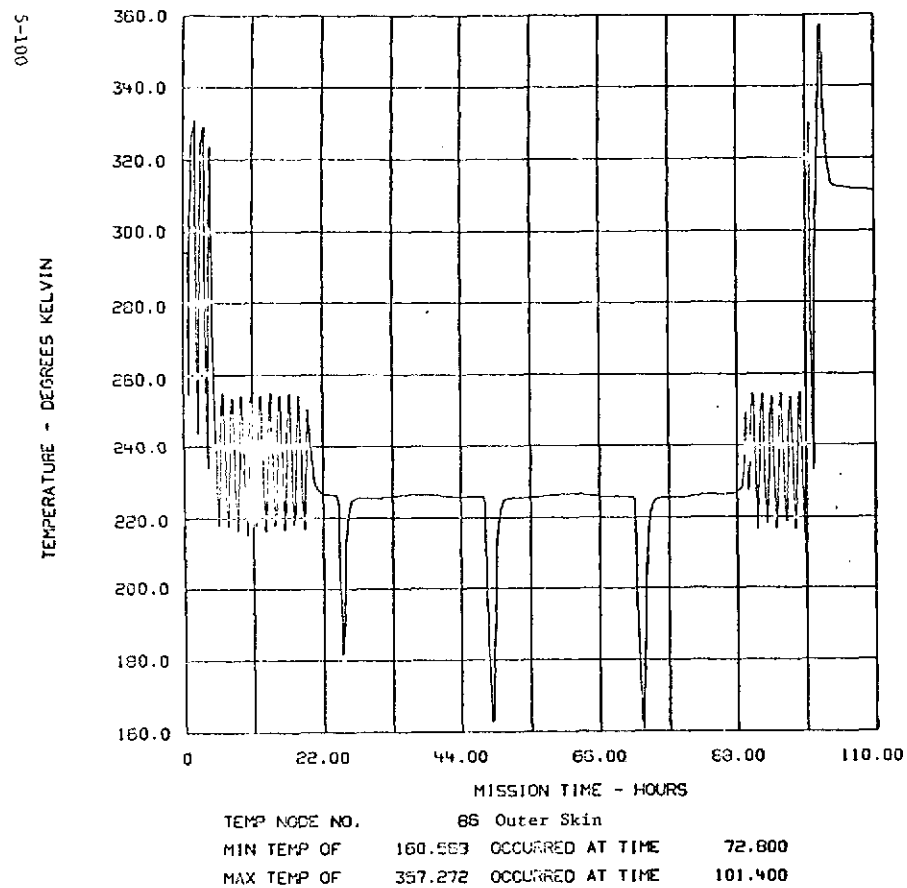FIGURE 5-175 ANALYSIS OF TUG INT. COMP. STATIONED AT GEO. SHADOW PT.

TEMP NODE NO. 83 Outer Skin
MIN TEMP OF 106.446 OCCURRED AT TIME 45.000
MAX TEMP OF 338.717 OCCURRED AT TIME 1.800

TEMP NODE NO.   16 Inner Skin
MIN TEMP OF   169.093   OCCURRED AT TIME   48.800
MAX TEMP OF   355.940   OCCURRED AT TIME   101.400

FIGURE 5-176   ANALYSIS OF TUG INT. COMPARTMENT + COMPONENTS NO HEAT PIPE

TEMP NODE NO.   16 Inner Skin
MIN TEMP OF   106.704   OCCURRED AT TIME   45.000
MAX TEMP OF   336.715   OCCURRED AT TIME   1.800
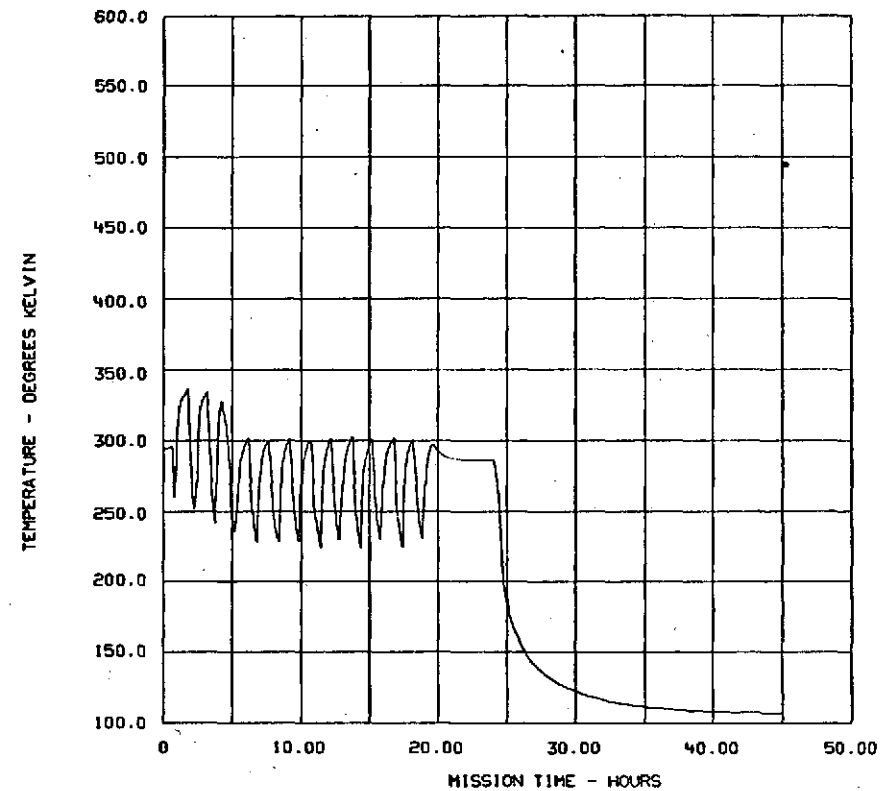
FIGURE 5-177   ANALYSIS OF TUG INT. COMP. STATIONED AT GEO. SHADOW PT.

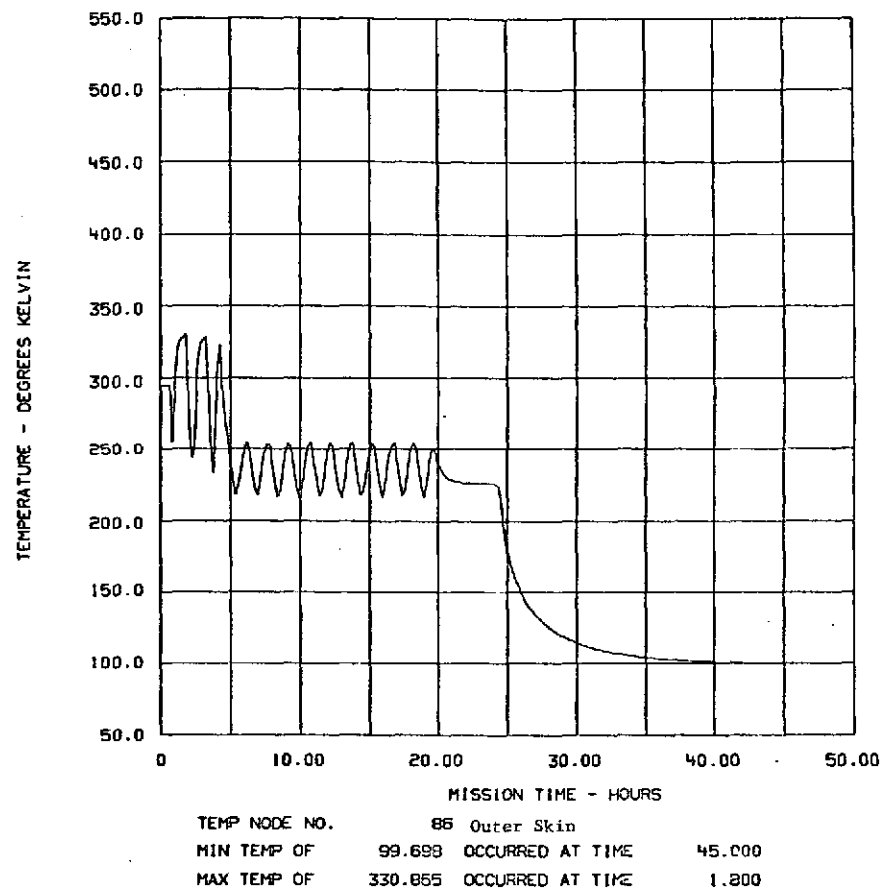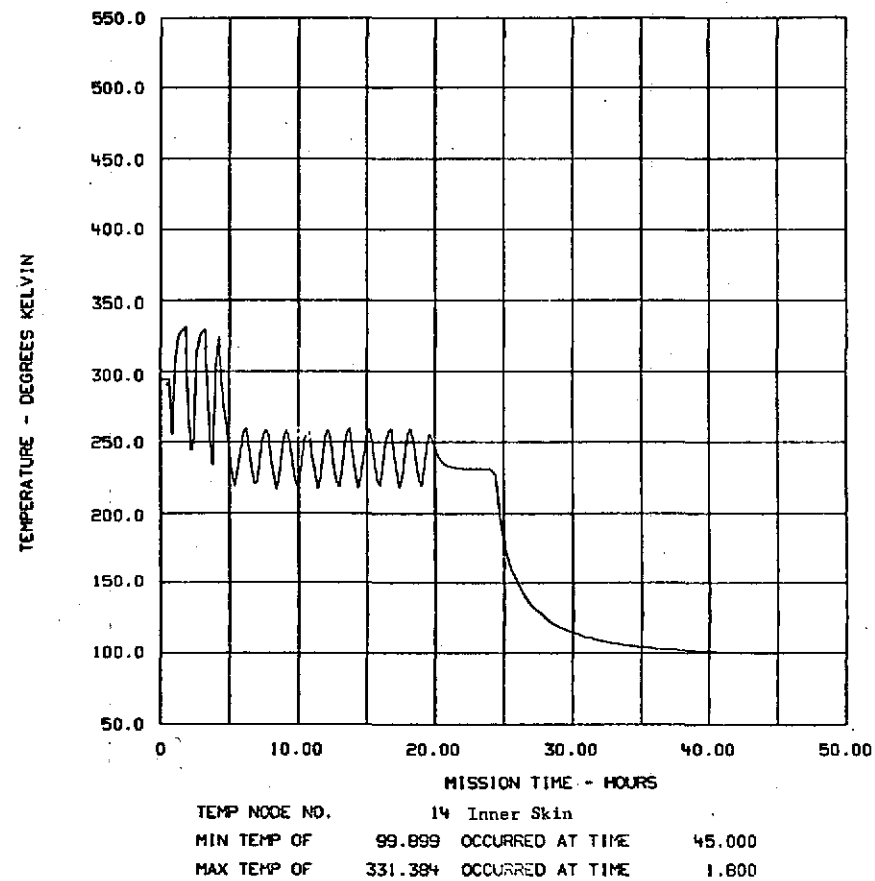FIGURE 5-178   ANALYSIS OF TUG INT. COMPARTMENT + COMPONENTS NO HEAT PIPE
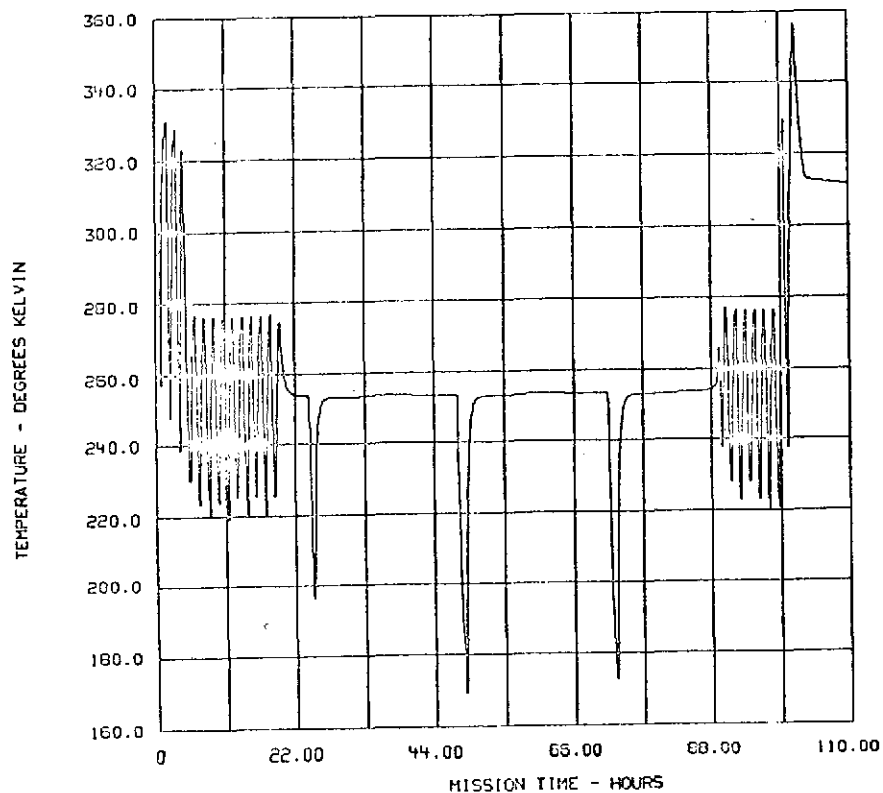
TEMP NODE NO.	201	APS Tank Insulation
MIN TEMP OF	169.293	OCCURRED AT TIME	48.800
MAX TEMP OF	356.367	OCCURRED AT TIME	101.400

FIGURE 5-179   ANALYSIS OF TUG INT. COMP. STATIONED AT GEO. SHADOW PT.

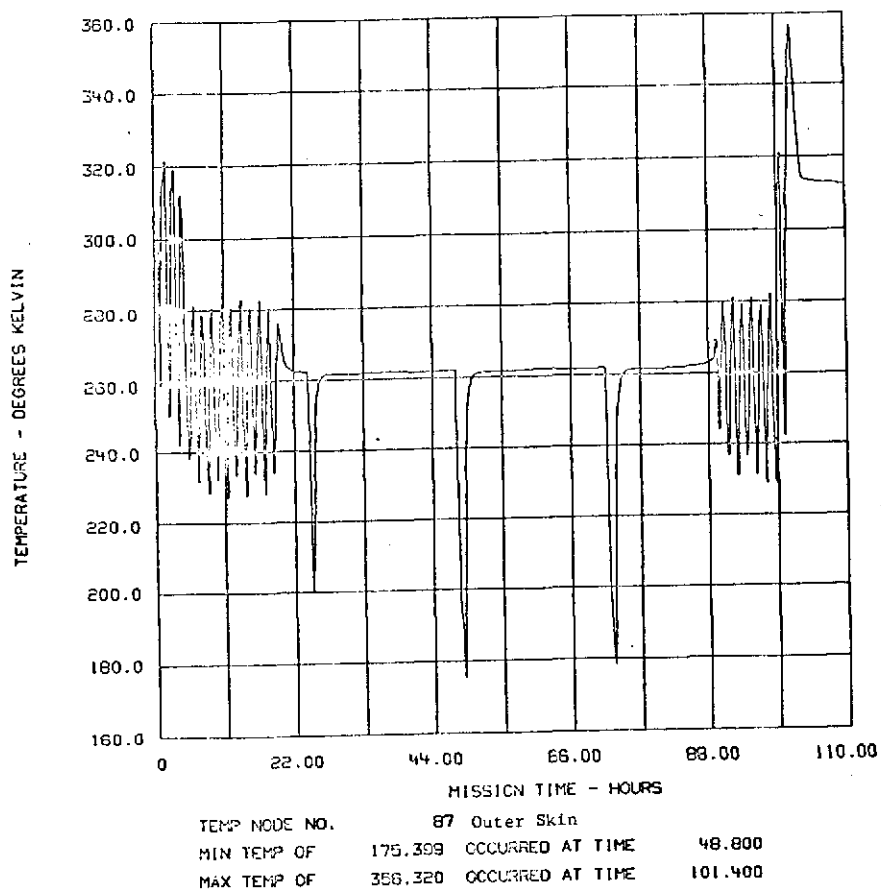| TEMP NODE NO. | 201 | APS Tank Insulation |
| MIN TEMP OF | 121.052 | OCCURRED AT TIME | 45.000 |
| MAX TEMP OF | 330.957 | OCCURRED AT TIME | 1.800 |

FIGURE 5-180 ANALYSIS OF TUG INT. COMPARTMENT + COMPONENTS NO HEAT PIPE

FIGURE 5-181 ANALYSIS OF TUG INT. COMP. STATIONED AT GEO. SHADOW PT.
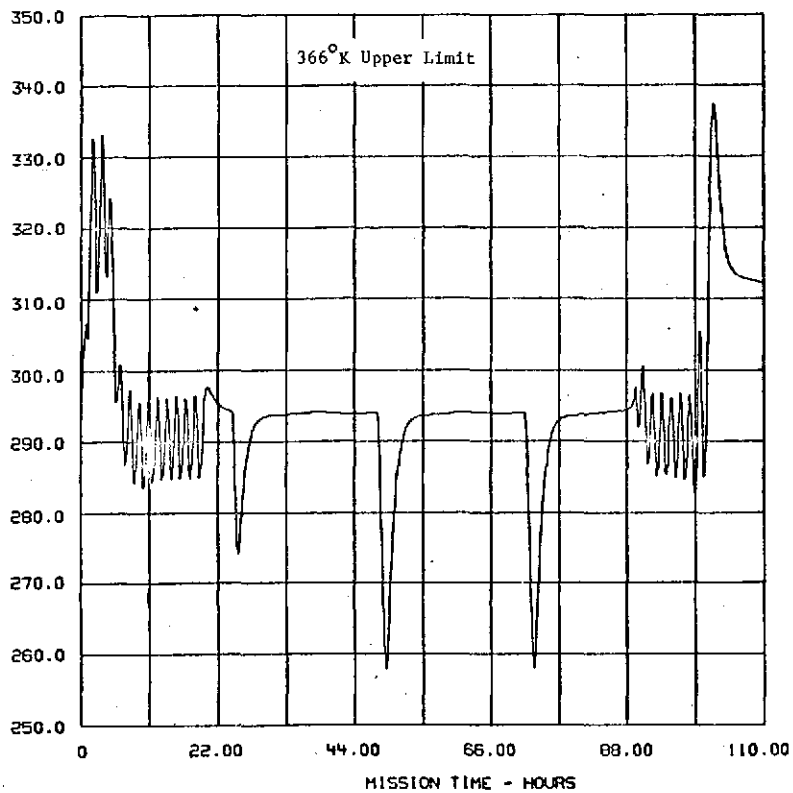
TEMP NODE NO.	290 Valve Amplifier		
MIN TEMP OF	257.667	OCCURRED AT TIME	49.000
MAX TEMP OF	337.378	OCCURRED AT TIME	101.950

TEMP NODE NO.	290 Valve Amplifier		
MIN TEMP OF	201.373	OCCURRED AT TIME	45.000
MAX TEMP OF	333.119	OCCURRED AT TIME	3.400

FIGURE 5-182   ANALYSIS OF TUG INT. COMPARTMENT + COMPONENTS NO HEAT PIPE

TEMP NODE NO.   231 Helium Press. Sphere
MIN TEMP OF   164.665 OCCURRED AT TIME   48.800
MAX TEMP OF   356.601 OCCURRED AT TIME   101.400
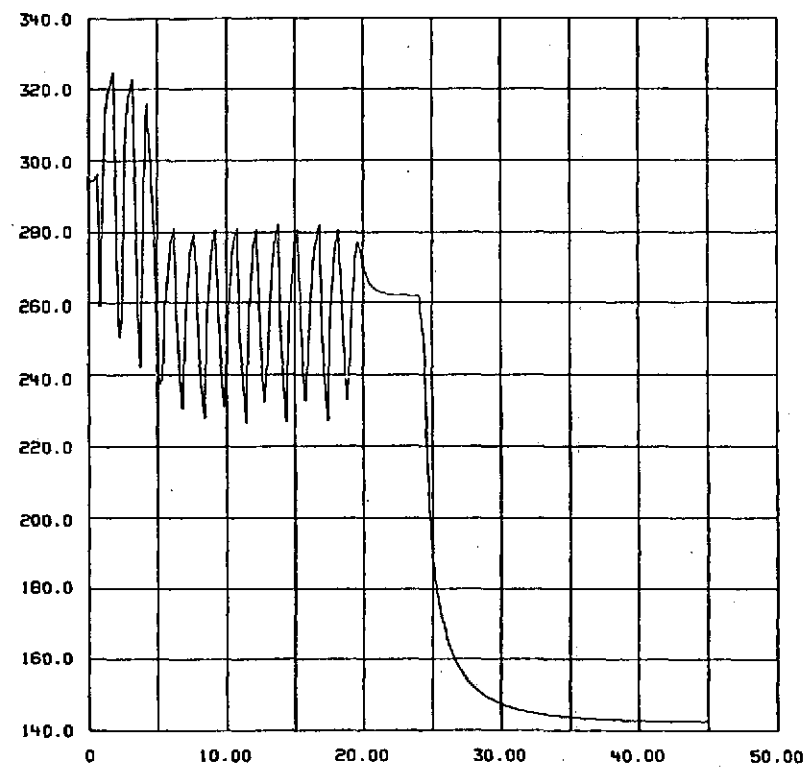

FIGURE 5-183   ANALYSIS OF TUG INT. COMP. STATIONED AT GEO. SHADOW PT.

TEMP NODE NO.   231 Helium Press. Sphere
MIN TEMP OF   104.752 OCCURRED AT TIME   45.000
MAX TEMP OF   333.893 OCCURRED AT TIME   1.800

FIGURE 5-184   ANALYSIS OF TUG INT. COMPARTMENT + COMPONENTS NO HEAT PIPE

TEMP NODE NO.   280   Data Acc. Unit
MIN TEMP OF   249.321   OCCURRED AT TIME   49.000
MAX TEMP OF   334.591   OCCURRED AT TIME   102.300

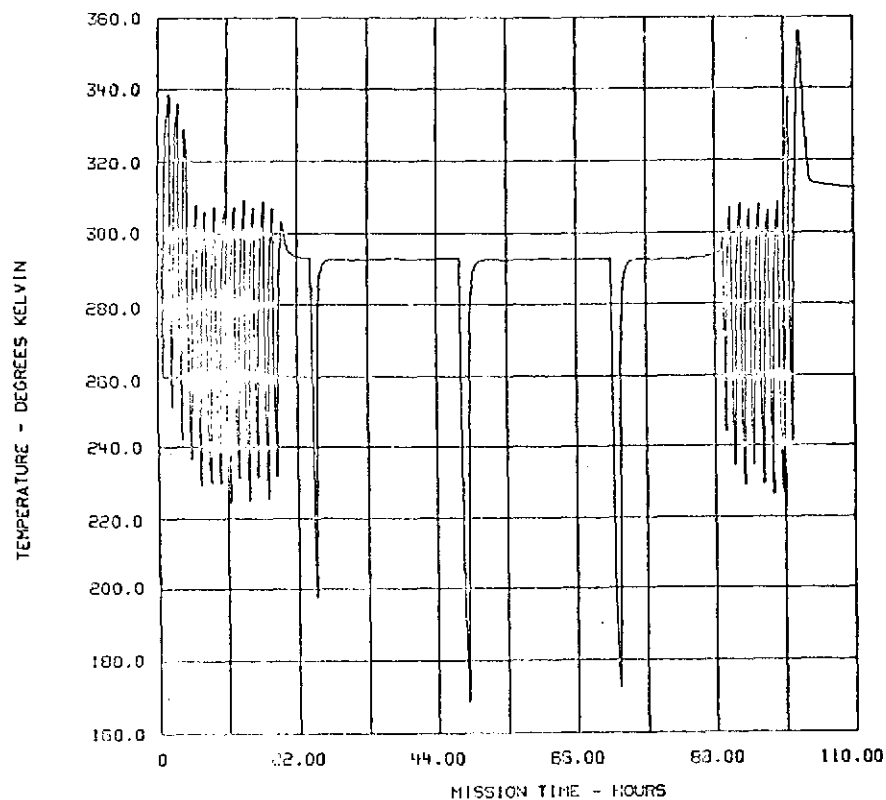FIGURE 5-185   ANALYSIS OF TUG INT. COMP. STATIONED AT GEO. SHADOW PT.
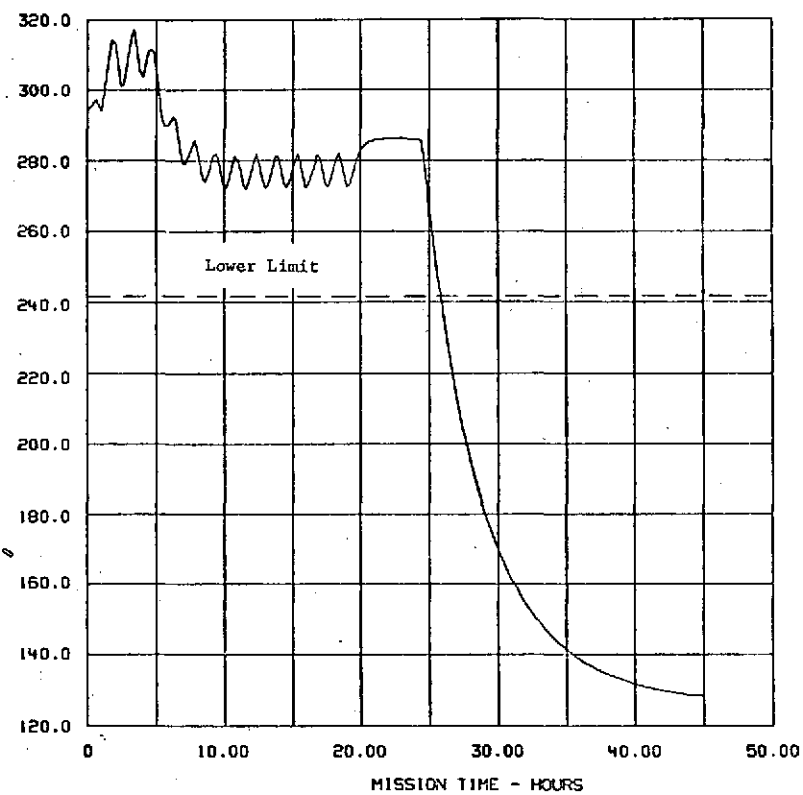
TEMP NODE NO.   280   Data Acc. Unit
MIN TEMP OF   128.229   OCCURRED AT TIME   45.000
MAX TEMP OF   317.204   OCCURRED AT TIME   3.400

FIGURE 5-186   ANALYSIS OF TUG INT. COMPARTMENT + COMPONENTS NO HEAT PIPE

TEMP NODE NO.   211 LH$_2$ Sphere
MIN TEMP OF   164.320 OCCURRED AT TIME   48.800
MAX TEMP OF   356.322 OCCURRED AT TIME   101.400

FIGURE 5-187   ANALYSIS OF TUG INT. COMP. STATIONED AT GEO. SHADOW PT.

TEMP NODE NO.   211 LH$_2$ Sphere
MIN TEMP OF   104.626 OCCURRED AT TIME   45.000
MAX TEMP OF   332.288 OCCURRED AT TIME   1.800
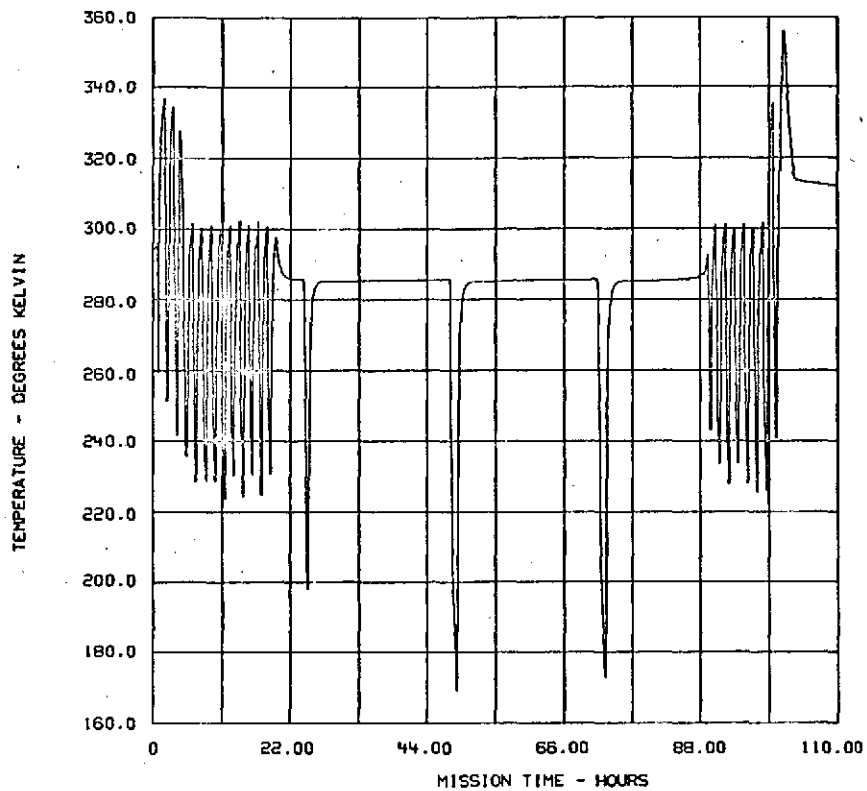
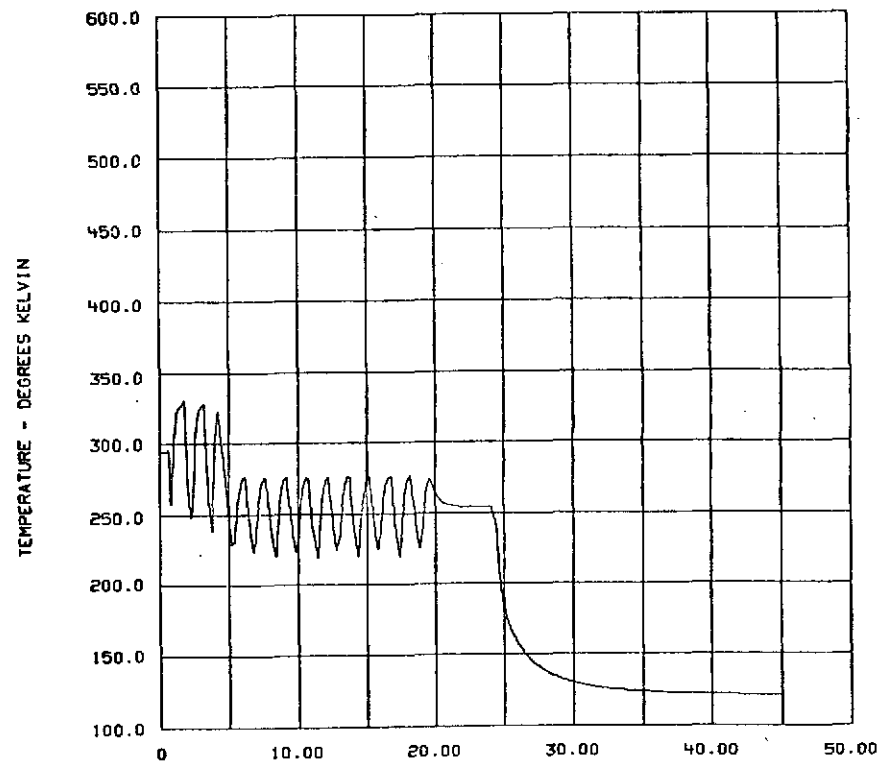FIGURE 5-188   ANALYSIS OF TUG INT. COMPARTMENT + COMPONENTS NO HEAT PIPE

FIGURE 5-189   ANALYSIS OF TUG INT. COMP. STATIONED AT GEO. SHADOW PT.

TEMPERATURE - DEGREES KELVIN

MISSION TIME - HOURS
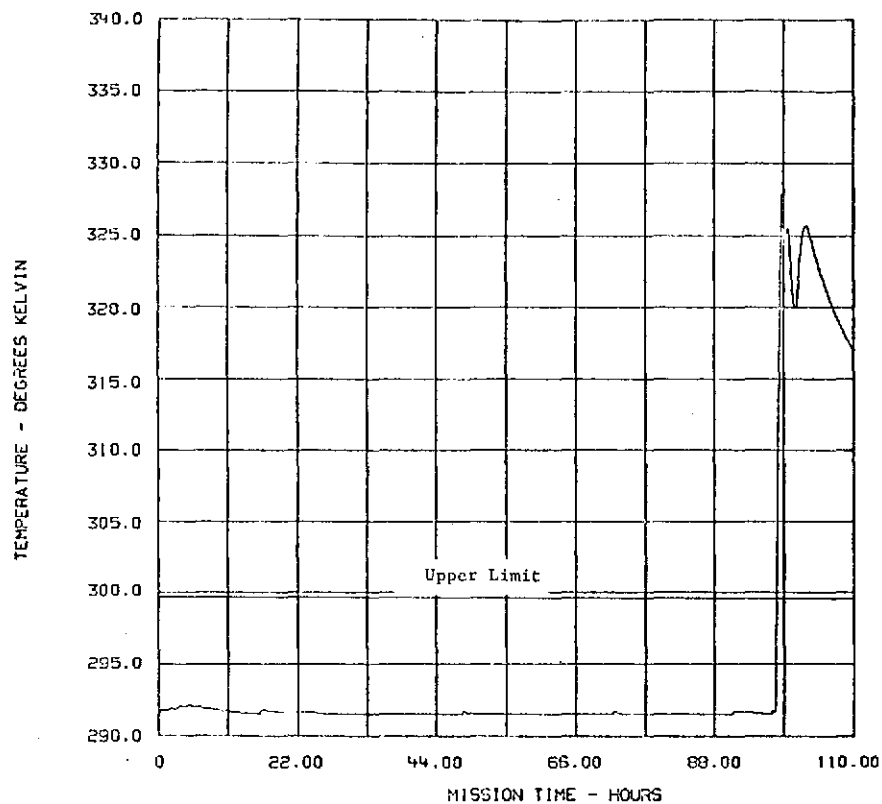
TEMP NODE NO.	275 Battery		
MIN TEMP OF	291.479	OCCURRED AT TIME	97.100
MAX TEMP OF	327.834	OCCURRED AT TIME	98.650

FIGURE 5-190   ANALYSIS OF TUG INT. COMPARTMENT + COMPONENTS NO HEAT PIPE

TEMPERATURE - DEGREES KELVIN

283°K Lower Limit

MISSION TIME - HOURS
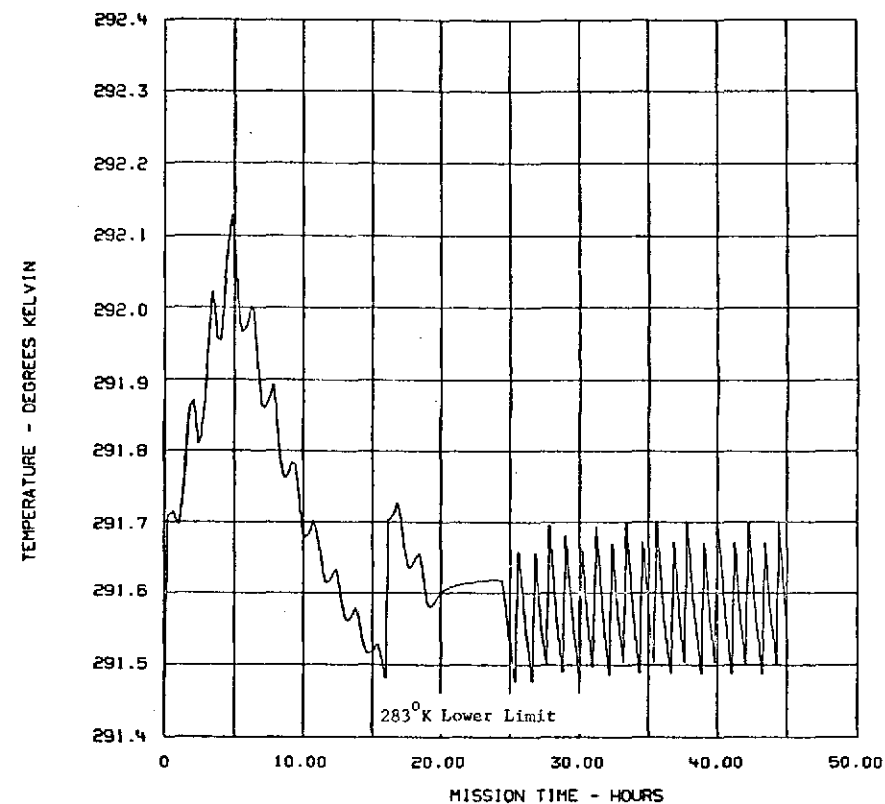
TEMP NODE NO.	275 Battery		
MIN TEMP OF	291.476	OCCURRED AT TIME	25.400
MAX TEMP OF	292.128	OCCURRED AT TIME	4.800

FIGURE 5-191   ANALYSIS OF TUG INT. COMP. STATIONED AT GEO. SHADOW PT.

FIGURE 5-192   ANALYSIS OF TUG INT. COMPARTMENT + COMPONENTS NO HEAT PIPE
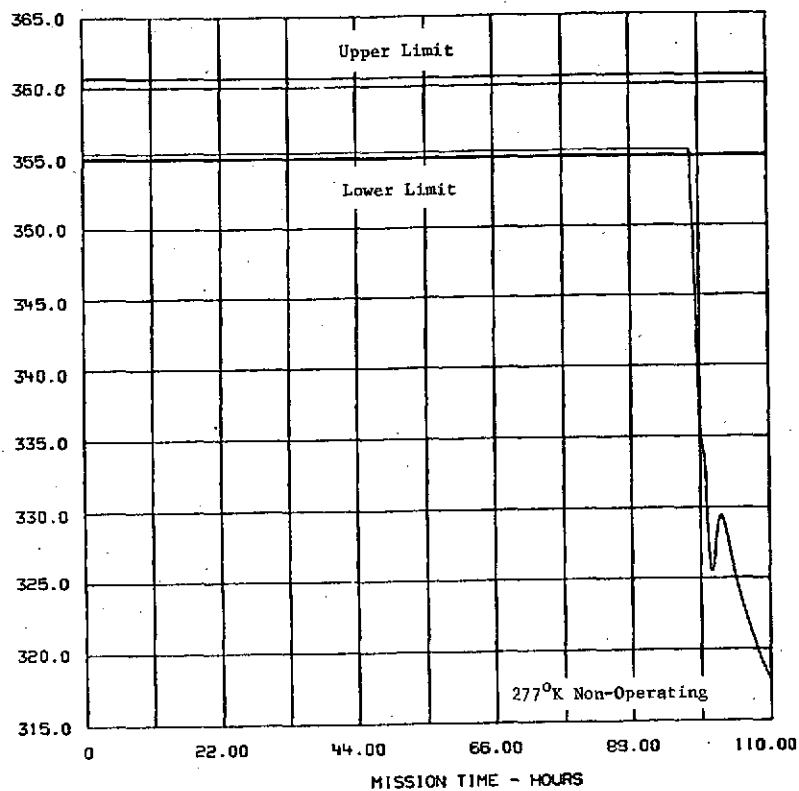
TEMP NODE NO.   433 Fuel Cell
MIN TEMP OF   317.841 OCCURRED AT TIME   110.000
MAX TEMP OF   355.371 OCCURRED AT TIME   0.

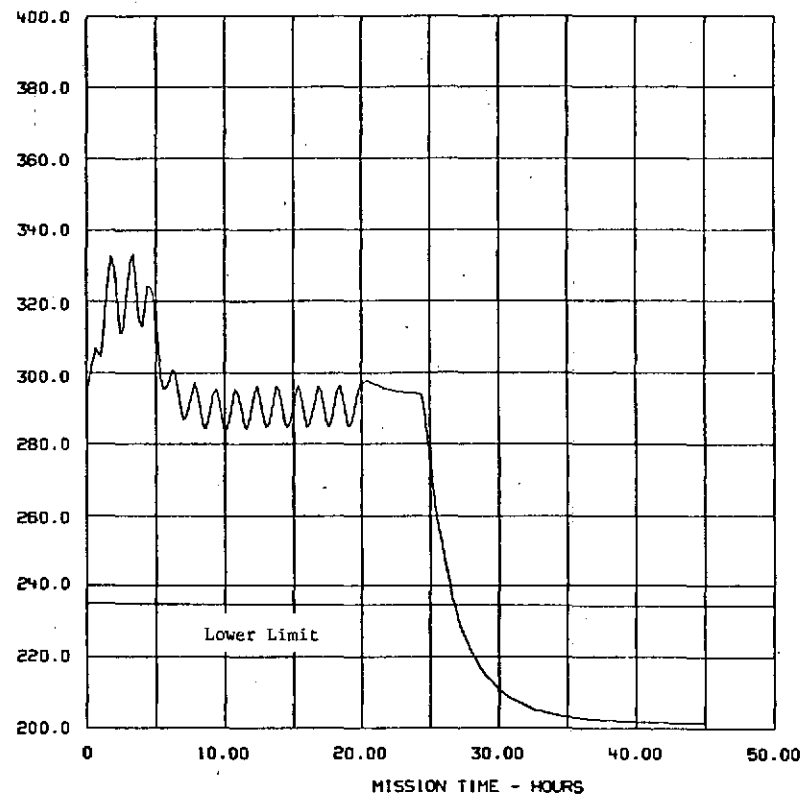FIGURE 5-193   ANALYSIS OF TUG INT. COMP. STATIONED AT GEO. SHADOW PT.

TEMP NODE NO.   433 Fuel Cell
MIN TEMP OF   355.371 OCCURRED AT TIME   45.000
MAX TEMP OF   355.371 OCCURRED AT TIME   0.

5-113

POWER - WATTS

MISSION TIME - HOURS
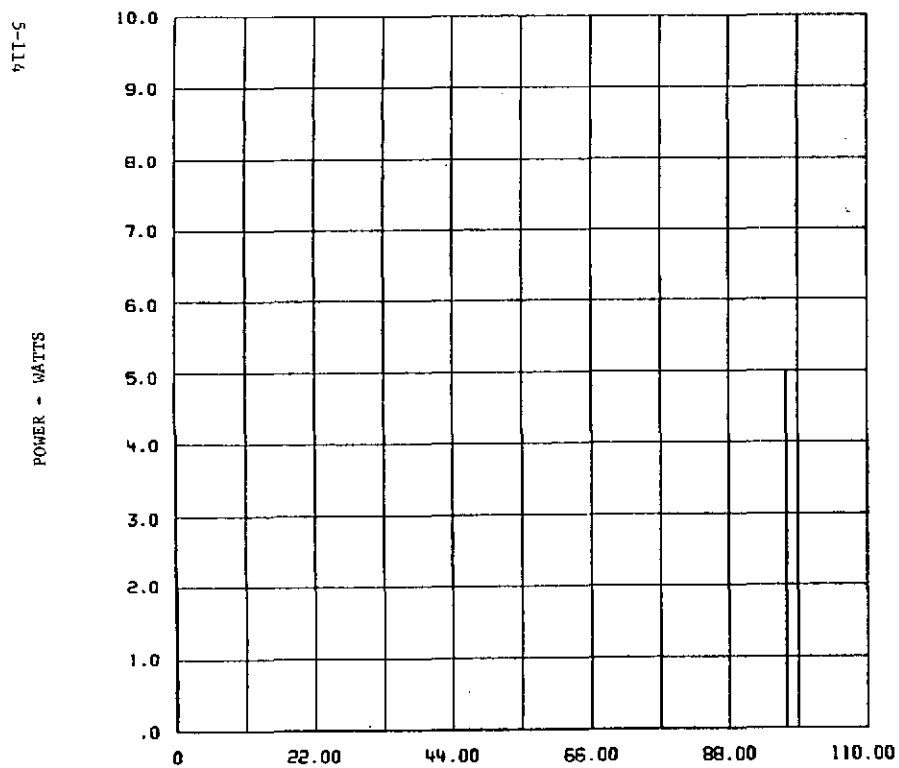
NODE NO. 402 Battery Heater Power

MIN OF 0. OCCURRED AT TIME 110.000

MAX OF 5.000 OCCURRED AT TIME 97.150

FIGURE 5-194 ANALYSIS OF TUG INT. COMPARTMENT + COMPONENTS NO HEAT PIPES

POWER - WATTS

MISSION TIME - HOURS
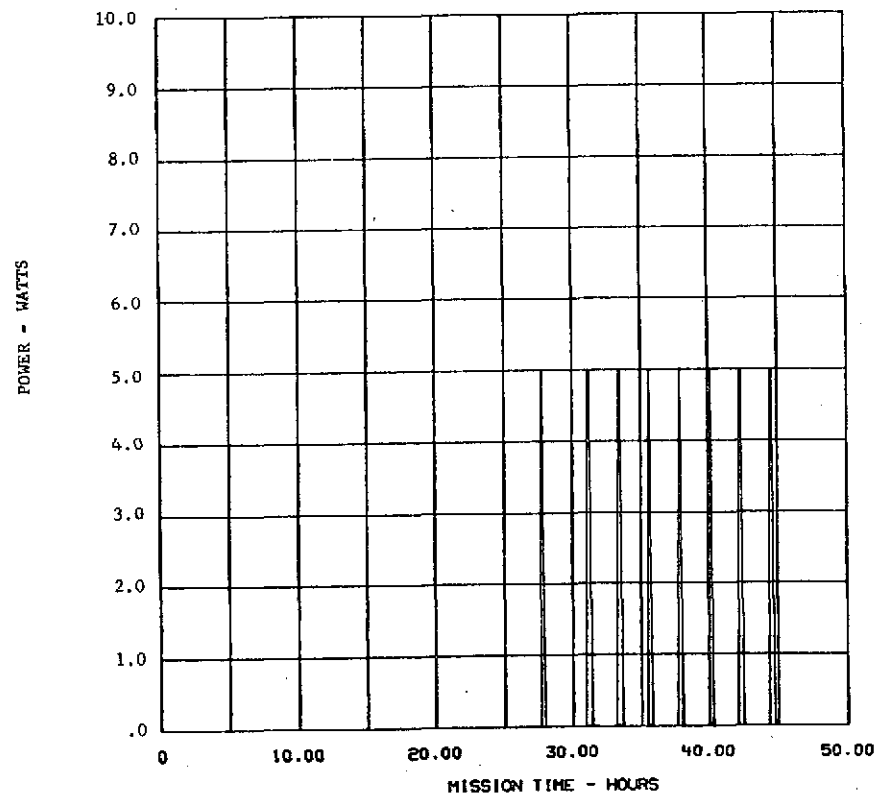
NODE NO. 402 Battery Heater Power

MIN OF 22.035 OCCURRED AT TIME 45.000

MAX OF 22.035 OCCURRED AT TIME 0.

FIGURE 5-195 ANALYSIS OF TUG INT. COMP. STATIONED AT GEO. SHADOW PT.
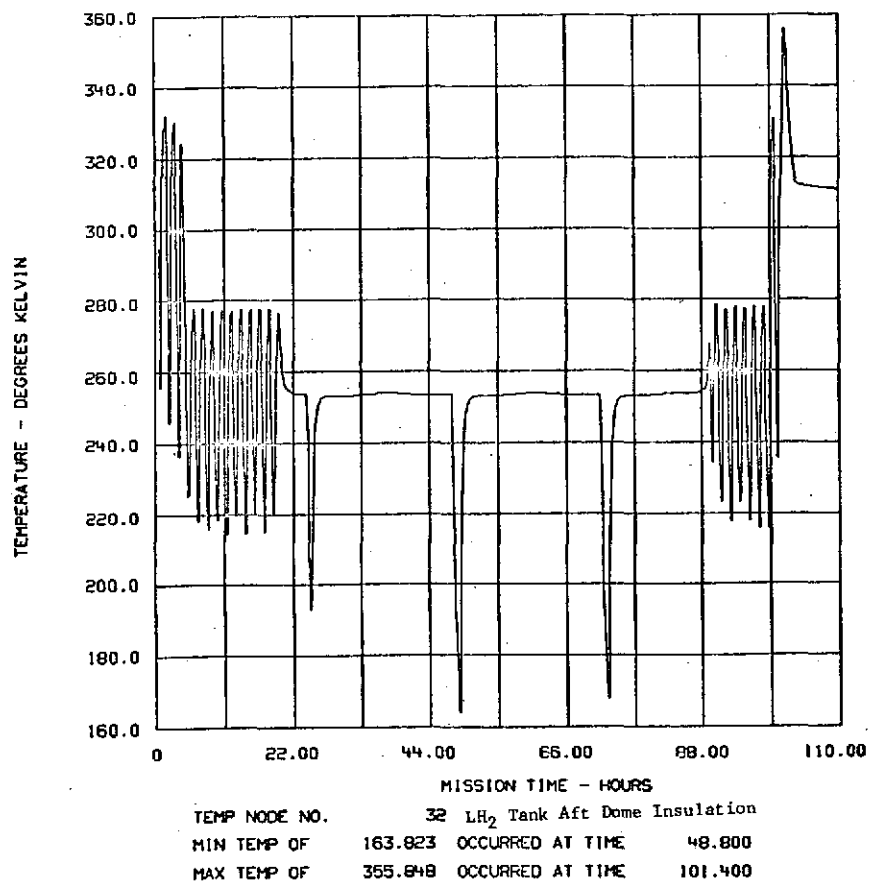
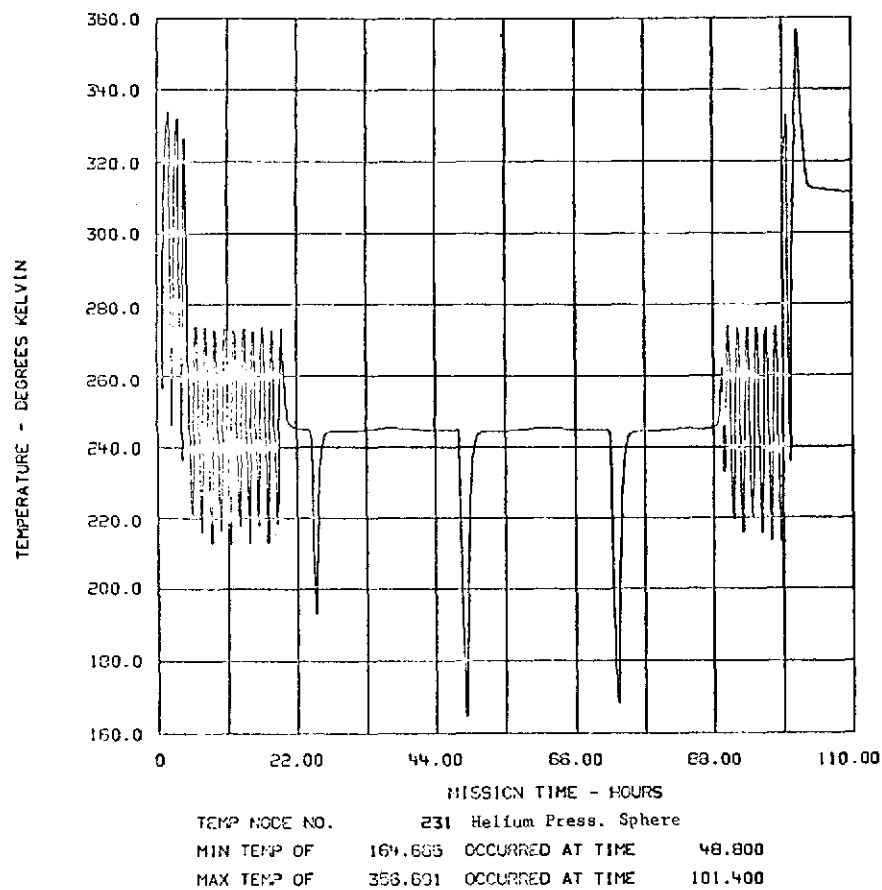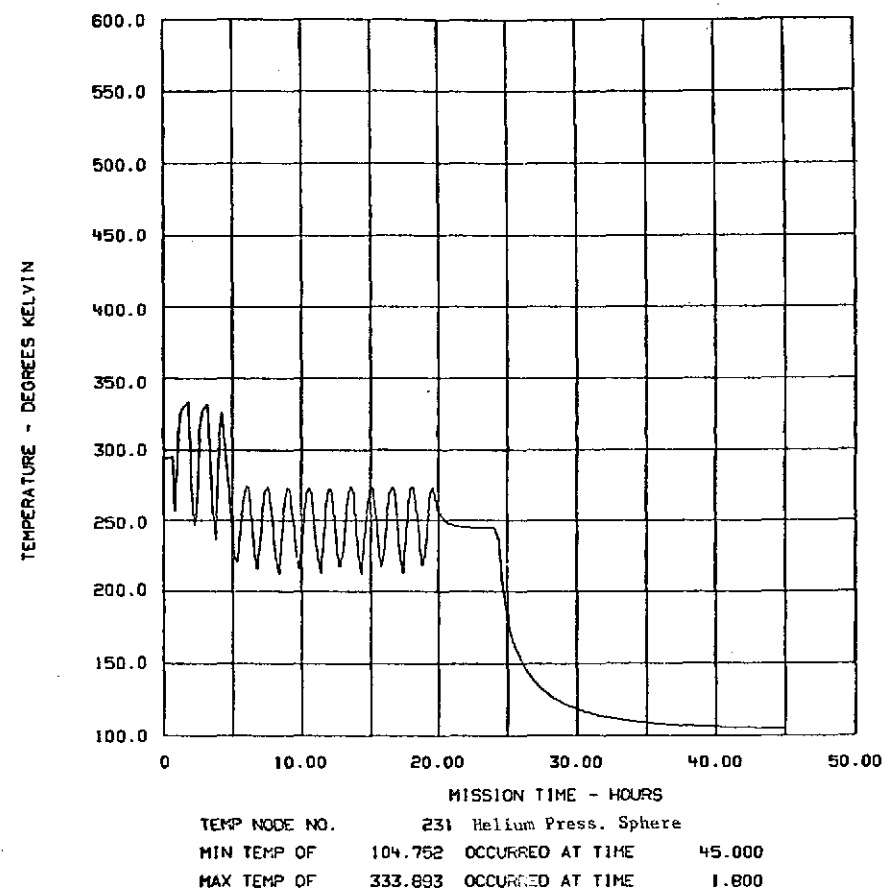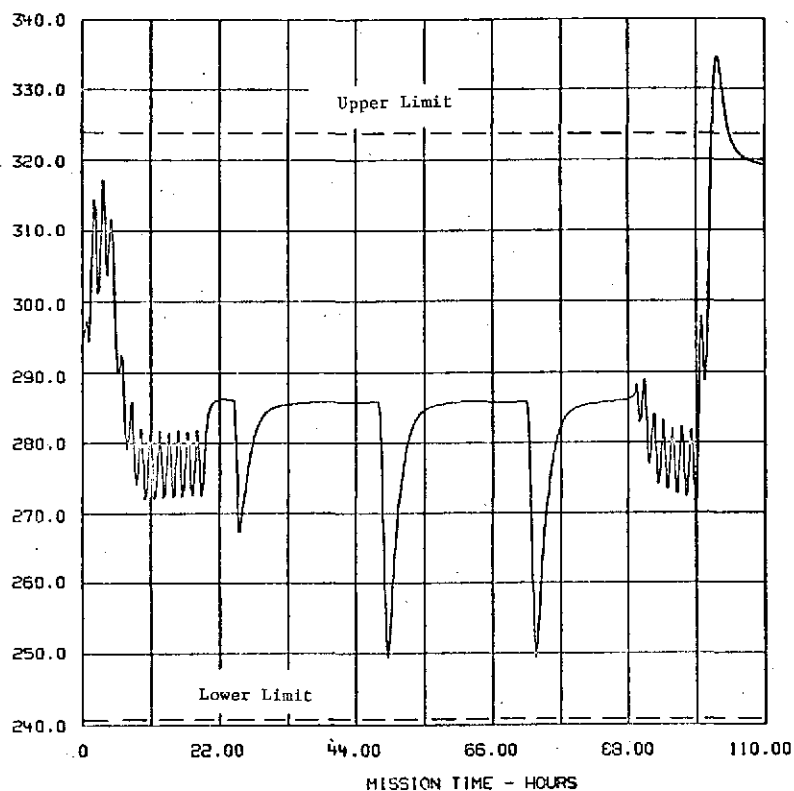FIGURE 5-196   ANALYSIS OF TUG INT. COMPARTMENT + COMPONENTS NO HEAT PIPE

TEMP NODE NO.   32 LH₂ Tank Aft Dome Insulation
MIN TEMP OF   163.823 OCCURRED AT TIME   48.800
MAX TEMP OF   355.848 OCCURRED AT TIME   101.400
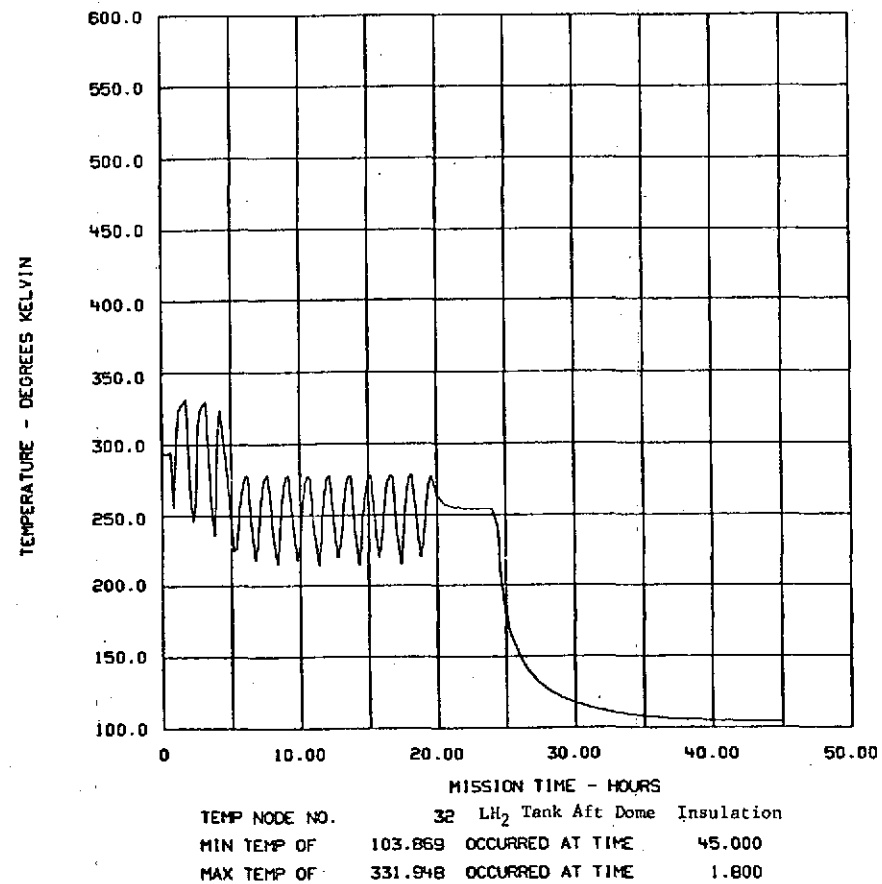
FIGURE 5-197   ANALYSIS OF TUG INT. COMP. STATIONED AT GEO. SHADOW PT.

TEMP NODE NO.   32 LH₂ Tank Aft Dome Insulation
MIN TEMP OF   103.869 OCCURRED AT TIME   45.000
MAX TEMP OF   331.948 OCCURRED AT TIME   1.800

TEMPERATURE - DEGREES KELVIN

MISSION TIME - HOURS

TEMP NODE NO.	41 LOX Tank Forward Dome Insulation	
MIN TEMP OF	165.026 OCCURRED AT TIME	48.800
MAX TEMP OF	355.950 OCCURRED AT TIME	101.400
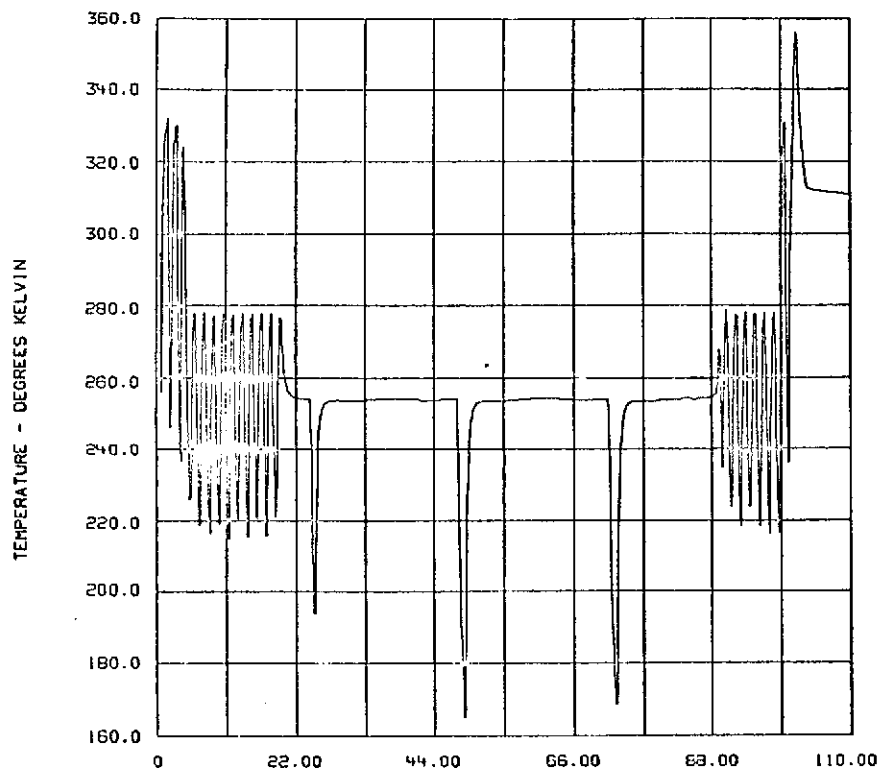
FIGURE 5-198   ANALYSIS OF TUG INT. COMPARTMENT + COMPONENTS NO HEAT PIPE

TEMPERATURE - DEGREES KELVIN

MISSION TIME - HOURS

TEMP NODE NO.	41 LOX Tank Forward Dome Insulation	
MIN TEMP OF	107.942 OCCURRED AT TIME	45.000
MAX TEMP OF	332.002 OCCURRED AT TIME	1.800
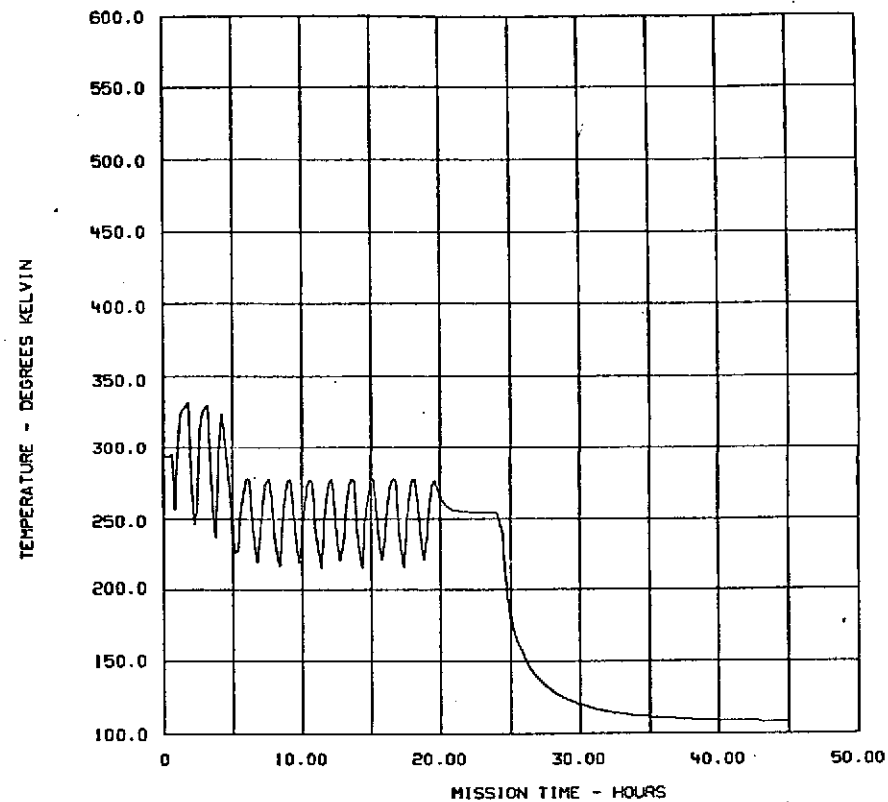
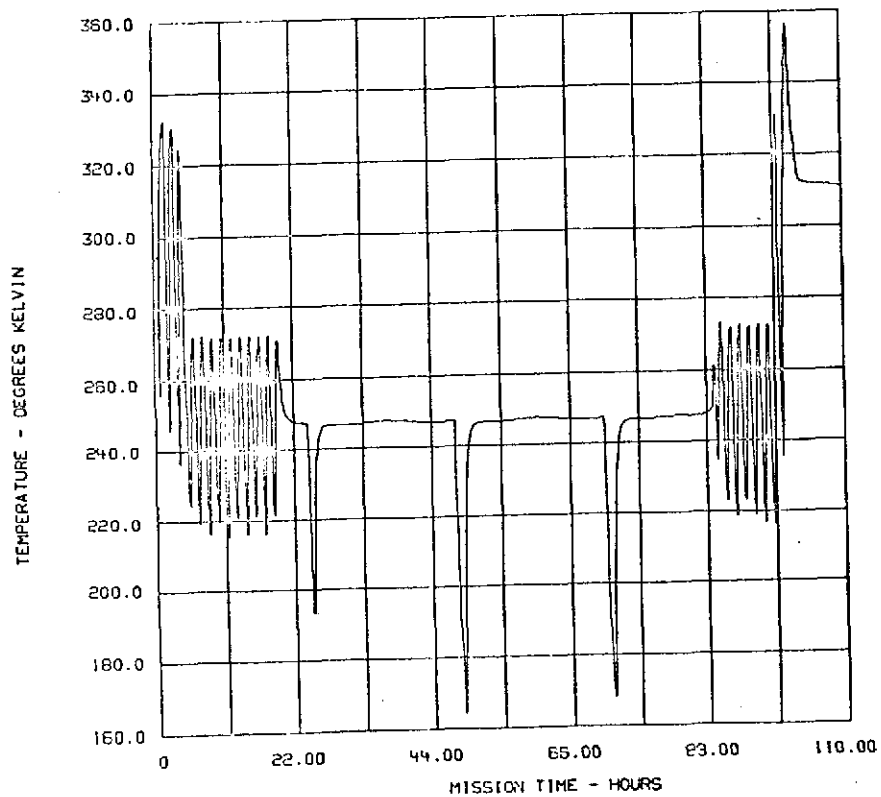FIGURE 5-199   ANALYSIS OF TUG INT. COMP. STATIONED AT GEO. SHADOW PT.

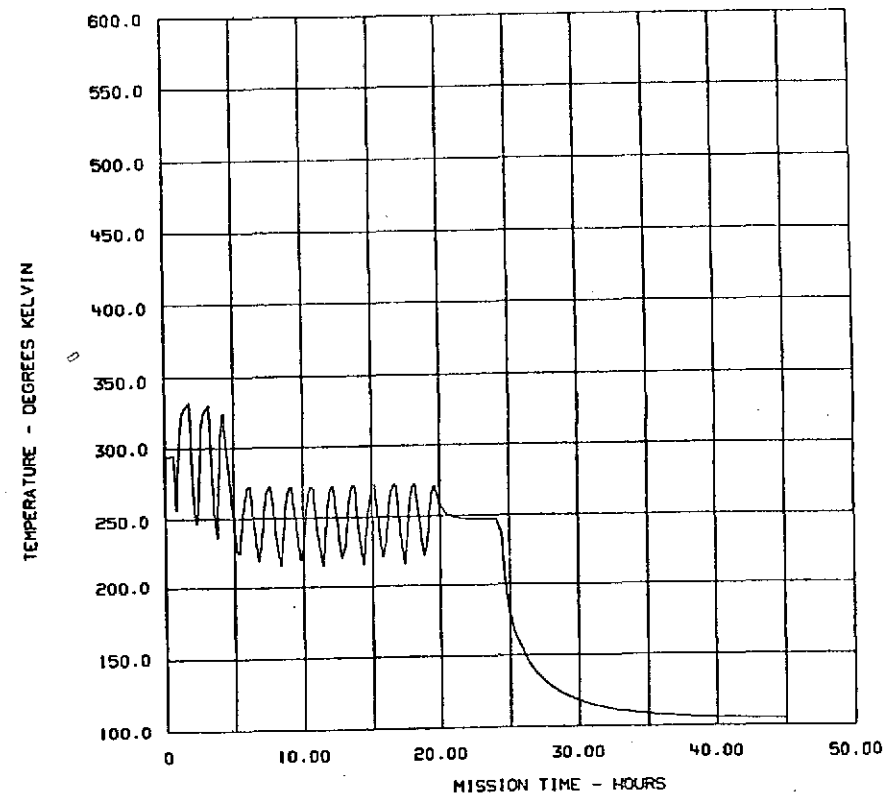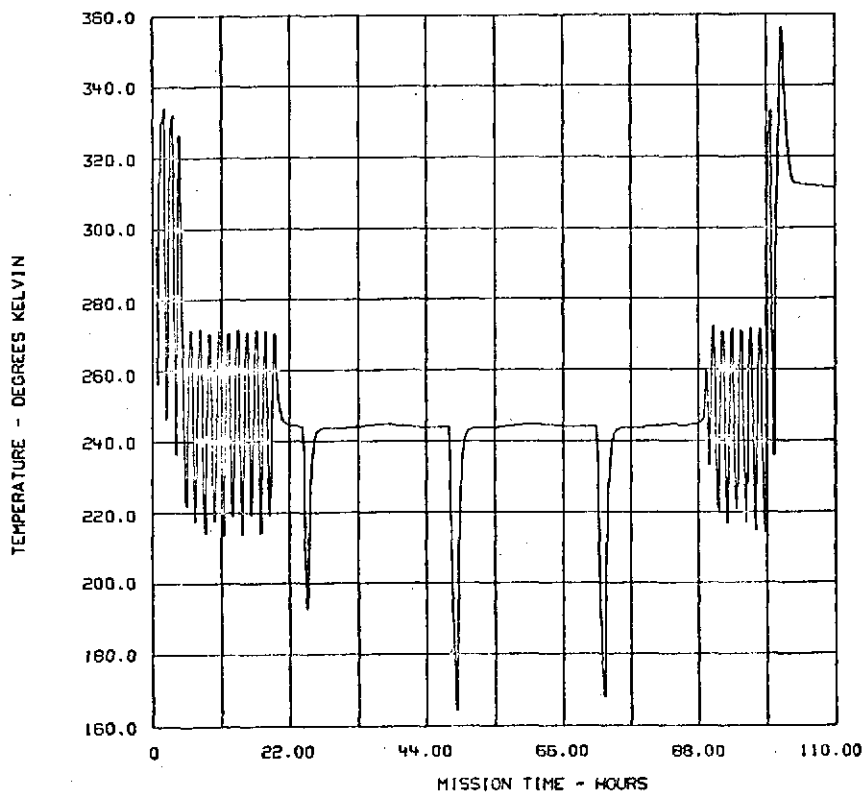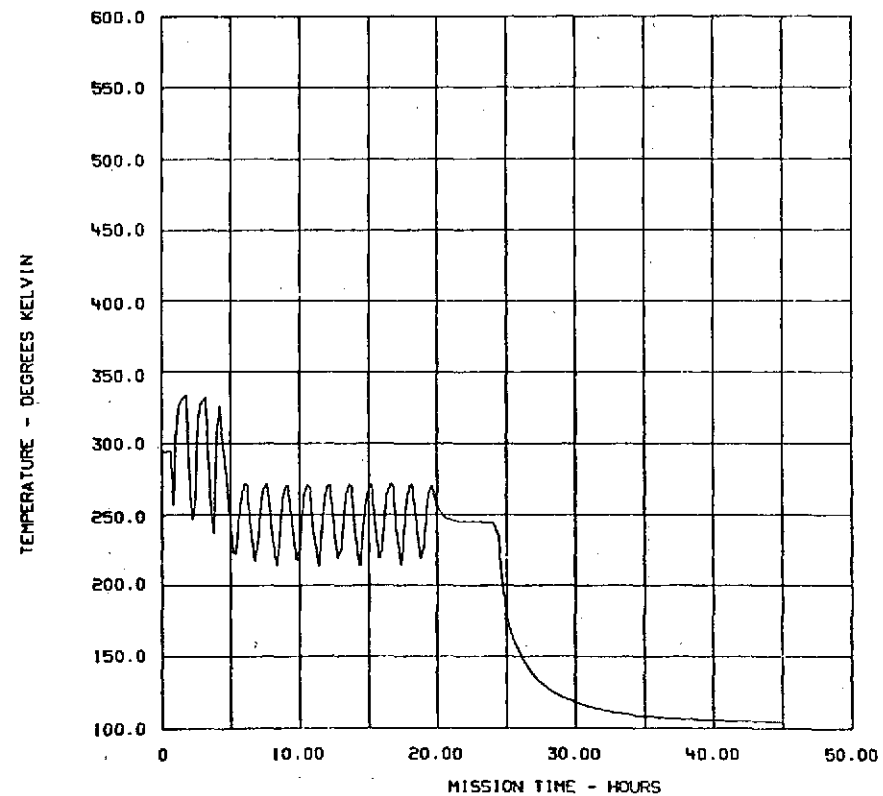FIGURE 5-200   ANALYSIS OF TUG INT. COMPARTMENT + COMPONENTS NO HEAT PIPE
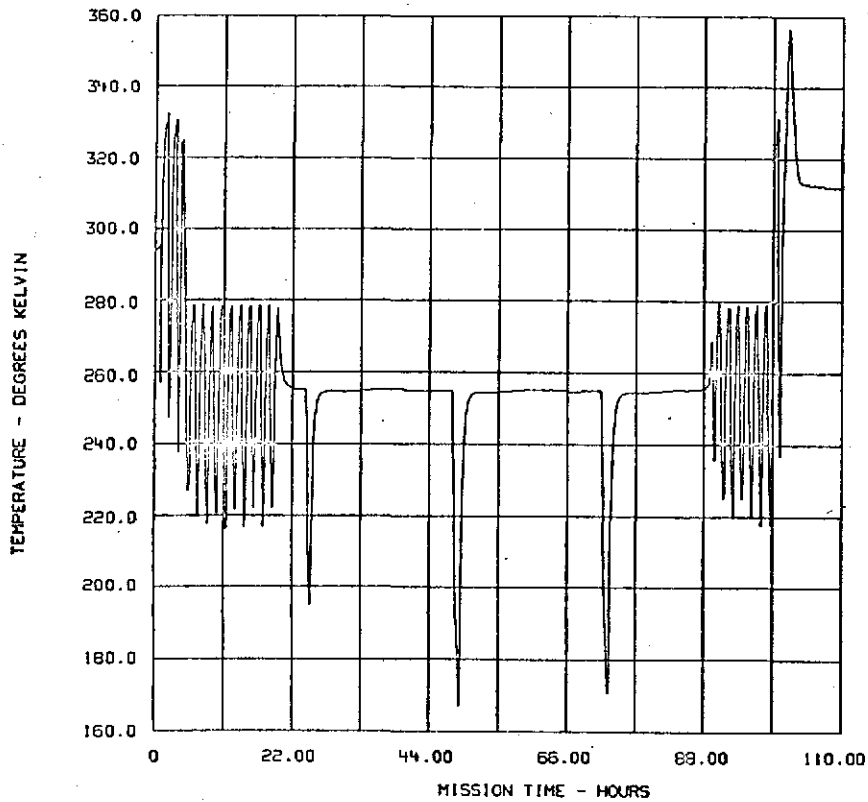
TEMP NODE NO.   44 Inner Tank Compartment Sink Temperature
MIN TEMP OF   166.973 OCCURRED AT TIME   48.800
MAX TEMP OF   356.392 OCCURRED AT TIME   101.400

FIGURE 5-201   ANALYSIS OF TUG INT. COMP. STATIONED AT GEO. SHADOW PT.
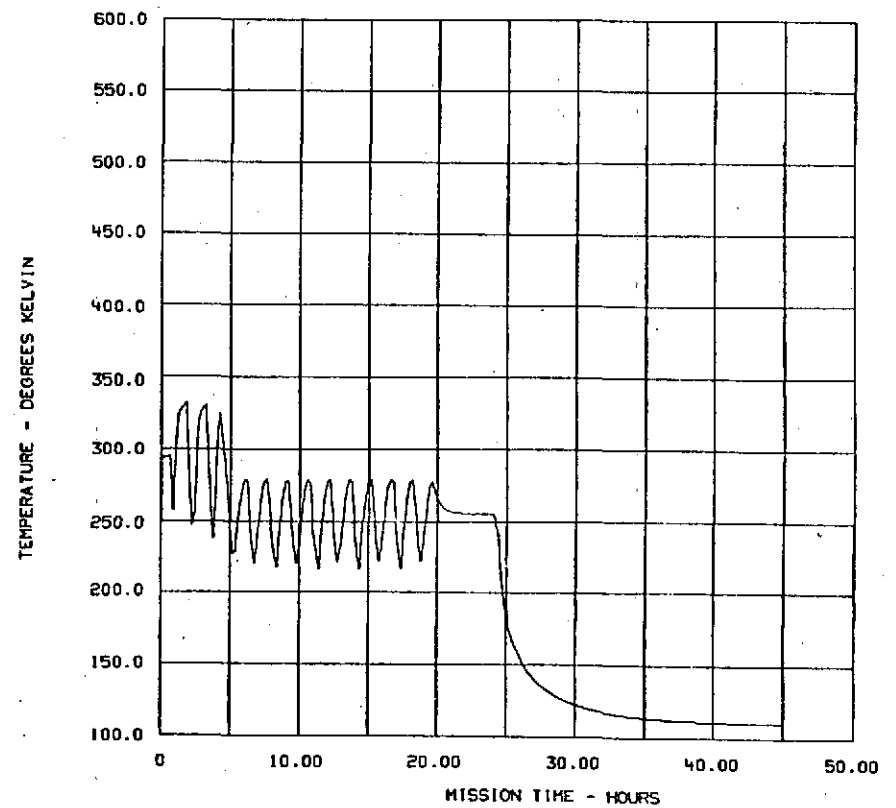
TEMP NODE NO.   44 Inner Tank Compartment Sink Temperature
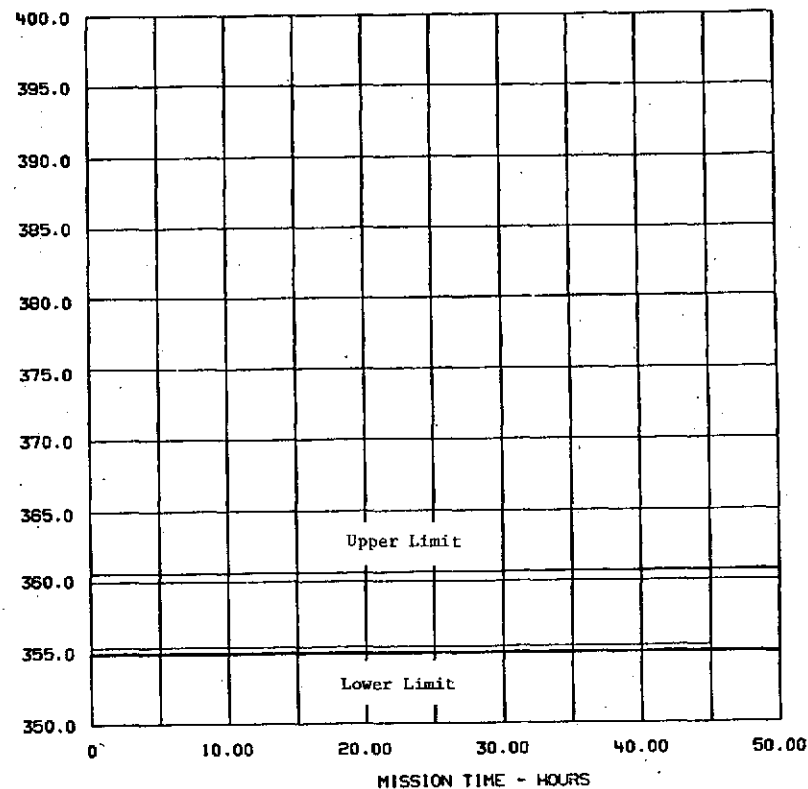MIN TEMP OF   110.037 OCCURRED AT TIME.   45.000
MAX TEMP OF   332.589 OCCURRED AT TIME   1.800

5.4 DISCUSSION OF RESULTS

Thermal control of the forward and intertank compartments for hot-case missions was achieved with the need of heater power. The heater power was concentrated in the low duty cycle components, namely, the primary and secondary laser radars and their electronics packages. Increasing the external coating α/ε ratio would reduce the amount of heater power required by increasing the internal compartmental sink temperature; however, the cold-case heater power consumption would likely remain high. The cold-case simulation resulted in all components except the fuel cell and battery dropping below the allowable lower temperature limits. Fifteen of the components were 10°K or less below limits while 31 were 10 to 20°K below and seven were 20 to 30°K below limits. Out of the latter group, the IMU heater power curve was 50% of expected, which would eliminate its cold problem. Several methods are available to solve the cold-case problems, reduce the lower limit qualifications temperature, add heater power, increase conduction isolation, change component coatings, and add insulation. All of these would rely upon heater power however, and some of the components would be affected in the hot case. In any event the hot case would still require heater power which ideally should not require any heat.

An alternative forward compartment layout would be prudent to solve the cold case problems while reducing the need of heater power. The components should be grouped to allow mounting of active and inactive components on the same mount. Mounting high and low duty cycle components on thermal conditioning panels (highly conductive panels) would be a desirable configuration from a thermal point of view. The configuration considered here is shown in Figure 5-202. As shown, louvers are mounted to the skin side of the panel. The louvers provide the means of reducing panel heat losses in the cold case, while the thermal conditioning panel distributes heat between components, thus reducing the heater power required by low duty cycle components. Figures 5-203 and 5-204 present the results of a study to determine the heat flux required to maintain various panel temperatures as a function of skin temperature and internal compartmental sink temperature (TE).

Referring to the hot case curve, Figure 5-203, and assuming the skin and internal sink temperatures at 294.4°K (70°F), the panel flux range would vary from 56.7 to 179.7 watts/meter^2 (18 to 57 Btu/hr-ft^2). This corresponds to a panel temperature range of 300 to 311°K (80 to 100°F). For the 600-watt heat load a total panel area of 3.34 meters^2 (36 feet^2) would result in a panel flux of 179.4 watts/meter^2, yielding a panel temperature of 311°K. The advantage in using this configuration is apparent when the cold-case data for a 200°K (-100°F) skin and internal sink temperature are considered. The flux required to maintain a 272°K (30°F) panel temperature is 220.8 watts/meter^2 (70 Btu/hr-ft^2). Comparing

the hot and cold case values results in a heater requirement of 41.4 watts/meter^2 to maintain the selected panel temperature. Scaling this up to the assumed panel area, 138.3 watts would be required. This compares with the amount of heat required in the hot case and reduces the cold-case heater power by more than 600 watts. Increasing the total panel area by 1/3 increases the heater power significantly to 101.4 watts/meter^2 or a total of 508 watts. This would still yield a savings in excess of 275 watts for the cold case.

As shown, a significant reduction in heater power can be achieved using this method. Several other advantages are derived from this approach. As the Tug design evolves, the forward compartment power level will probably change. This method of thermal control provides a means of reducing the sensitivity of steady-state power on heater power requirements by maintaining preselected panel heat fluxes. Minimum cable weight can be achieved by properly grouping components on individual panels while satisfying thermal requirements. The structural design would be simplified by reducing the number of component structural interfaces to a minimum. One tradeoff would be required to determine if the reduced cable and consumable weights would offset the added weight of the louvers and thermal conditioning panels. Other tradeoffs concerning cost and design flexibility would also be in order.

The intertank compartment suffers from the lack of heat dissipated to maintain acceptable internal sink and skin temperatures. Coatings, thermal standoffs, and heaters could be used as a solution. Due to number of components expected in this compartment the louver/ thermal conditioning panel concept appears to be too heavy for appli cation.

Heat Pipes

Louvers

MOUNTING SURFACE

Thermal Conditioning Panel
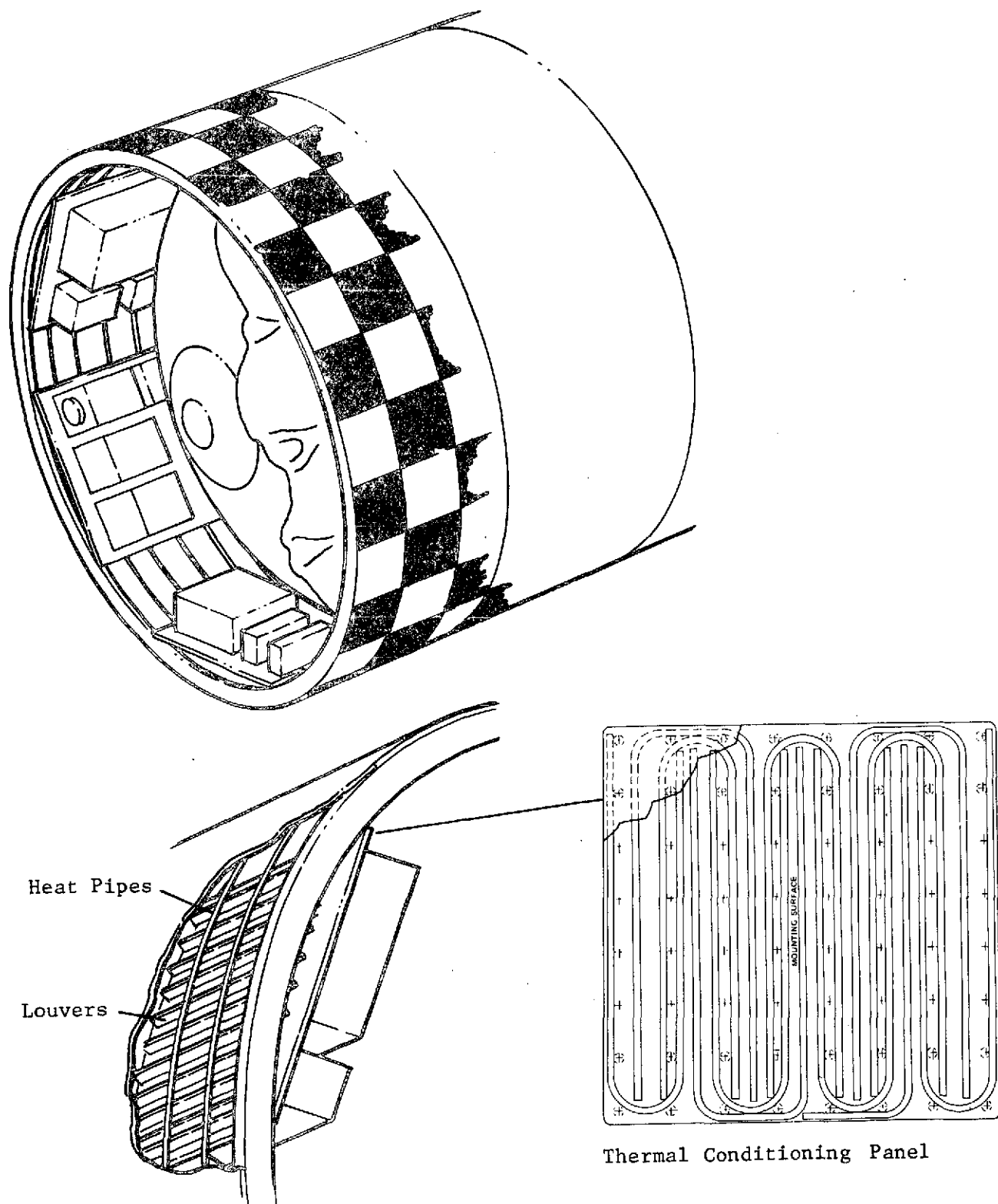
Figure 5-202   Forward Compartment Component Mounting
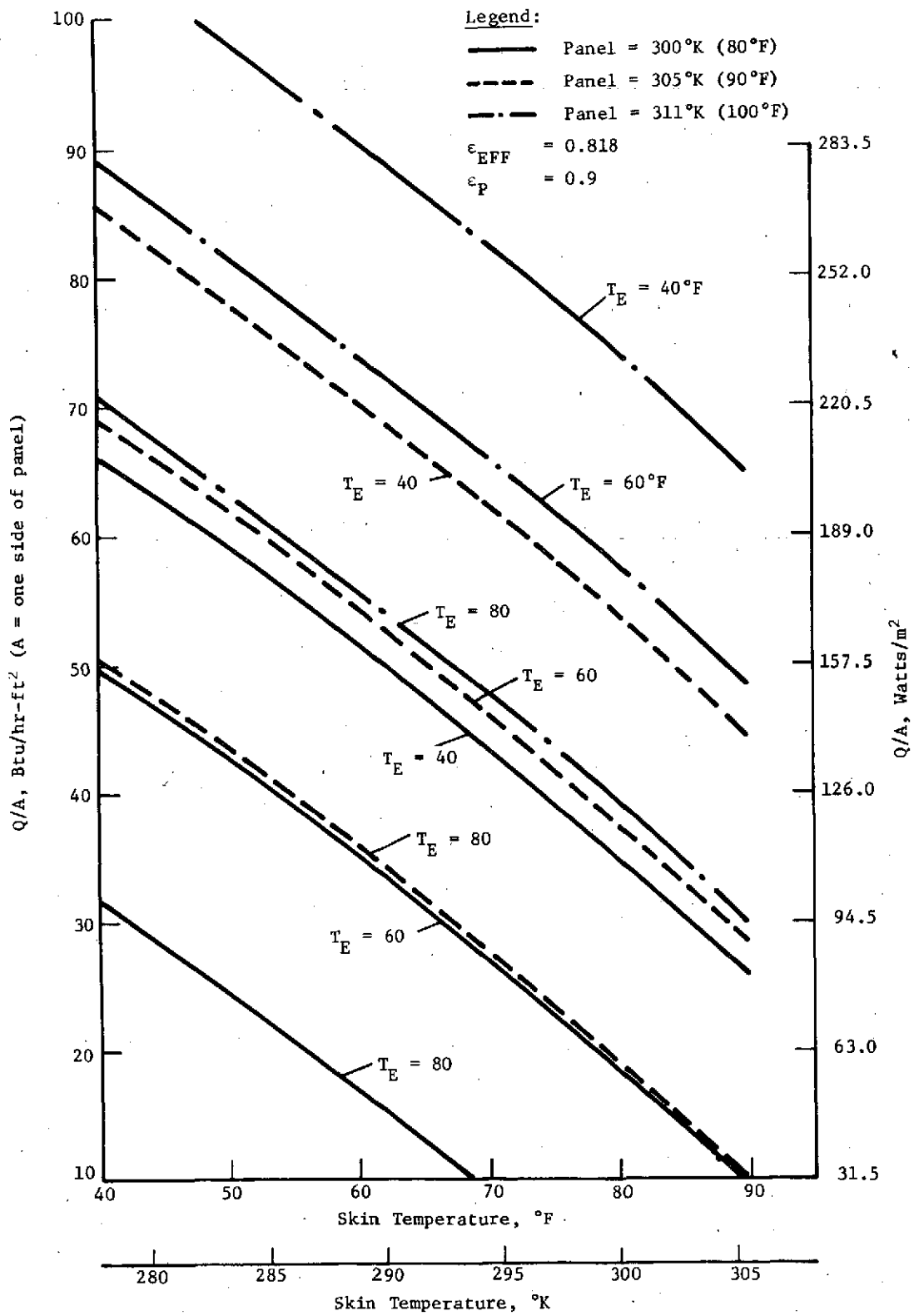
Figure 5-203 Hot-Case Mounting Panel Heat Fluxes, Louvers Open
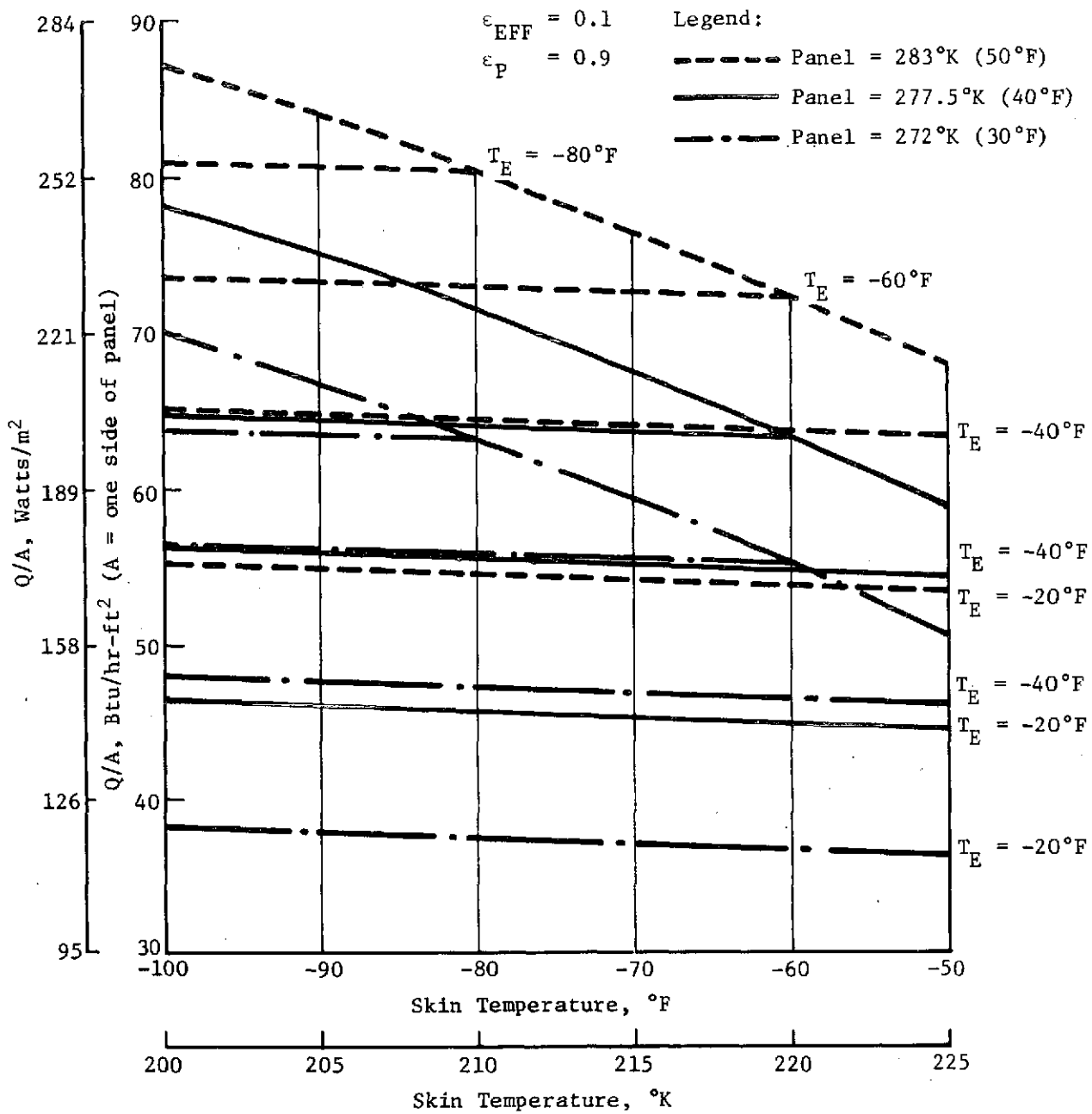
Figure 5-204 Cold-Case Mounting Panel Heat Fluxes, Louvers Closed

6. FUEL CELL HEAT REJECTION SYSTEM

Thermal control of the fuel cell electrical power subsystem represents a critical design consideration because a failure in this area could result in failure to achieve the specific mission objectives and the loss of a Tug. Two approaches were explored in this area; each used radiators. The approaches differed only in how the heat was transported from the fuel cell to the radiators. The system chosen was a redundant pumped fluid system using series-series bypassed radiators. The pumped fluid system was chosen over variable conductance (VC) heat pipes because of the current state of the art of pumped fluid systems and the current problems with VC heat pipes. The Tug is penalized in power and weight by this choice. As VC heat pipe technology expands in the future, the use of VC heat pipes in this part of the Tug design should be possible with less risk.

The fuel cell in this study was based upon design data obtained from Pratt and Whitney (Ref 13). The fuel cell heat rejection system is required to maintain the fuel cell internal fluid loop within an acceptable temperature range 349.67 to 355.2°K (170 to 180°F) independent of heat load. The baseline for the study included a single fuel cell which, when coupled with the components used in the study, resulted in an electrical load that varied from 600 to 1500 watts. The radiator design was based on rejecting resultant waste heat loads plus the fuel cell pump and radiator pump power.

Four equally sized radiator panels were assumed consistant with the baseline. The four radiators were located in each quadrant of the intertank compartment forward of and clocked 45° from the APS modules. The four panels, located as shown in Figure 6-1 reduce the effects of plume heating from the APS modules and minimize attitude influences from external heating. The apparent choice of a hydrazine APS configuration provides one of the more significant changes from earlier configurations (Ref 8), and will reduce the plume heating on the radiators to levels experienced on the Titan IIIC Transtage vehicle. These levels did not impair the radiator performance in seven flights of that vehicle.

The thermal environments were evaluated to determine the worst-case design environments for use in the radiator design. The cold-case design conditions were obvious, because at synchronous altitude the earth emitted and albedo is near zero and the Tug could be aligned with the sunline to result in no heat being applied to the radiator panels. The case 4 park orbit, $\beta = 52°$, resulted in slightly higher incident fluxes than the other cases studied and was chosen for the hot case. The vehicle orientation maximized absorbed heating when two radiators were exposed to the sun and when the included angle between the center of each radiator and the sun line was 45° as shown in Figure 6-1.
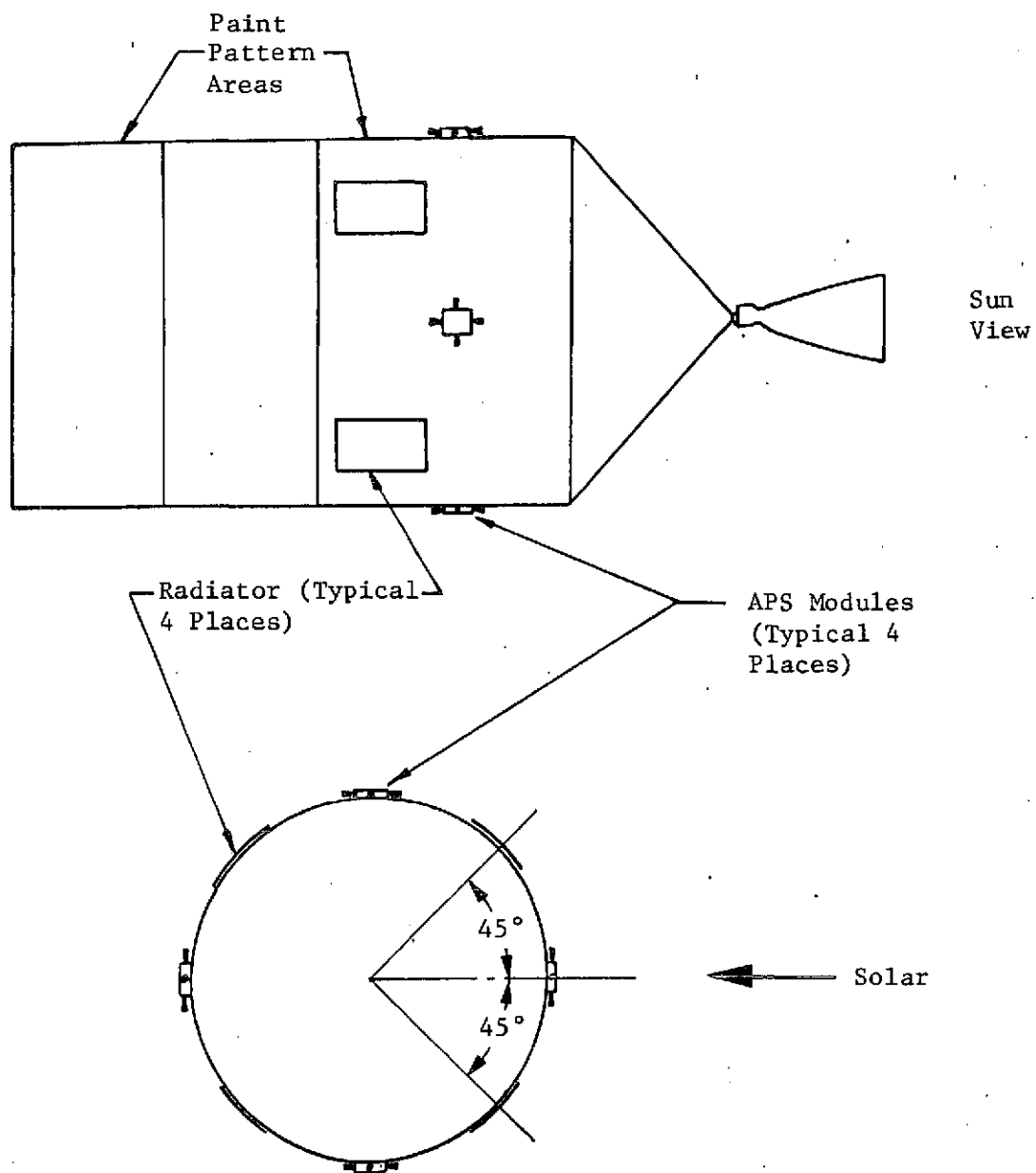
Figure 6-1 Tug Exterior

The maximum heat load to be rejected was used with the hot-case thermal environment and minimum heat load to be rejected was used with the cold-case environment to obtain the thermal design conditions. These conditions are consistent with orbital altitude requirements of 296 to 35,750 km (160 to 19300 n mi) with no attitude constraints.

Operationally the fuel cell was assumed to be activated in orbit before the Tug and payload were released by the orbiter. The fuel cell was also assumed to be deactivated before the Tug was remated to the orbiter. This sequence of events was sufficient to permit the fluid system to be designed without interfacing with the orbiter for thermal control. The potential for a fluid loop failure during a 7-day mission was considered sufficient for adding a redundant fluid loop. Each loop was designed to carry the full heat load. In addition, the radiators were used to provide micrometeorite protection for the fluid lines.

The fuel cell system shown in Figure 6-2 was obtained from Reference 13. The fuel cell generates waste heat, which is removed by a fluid loop. The coolant temperature control valve, pump, and interconnecting lines are an integral part of the system. Cell performance is predicated on maintaining the coolant through the fuel cell in a narrow temperature range independent of the electrical load. The primary parameters are control of the inlet temperature to 355.4°K (180°F) $\pm^0_3$°K and limiting the temperature rise through the cell to 5.6°K (10°F) under maximum load conditions. Figure 6-3 presents the waste heat rejection as a function of electrical load with the design conditions shown. The warmup heater shown in Figure 6-2 is used to heat the fluid and the cell to the operating temperature level during the activation period and is not used during the normal operational period. Pratt and Whitney suggests the use either water or FC-43 as the working fluid on the fuel cell side of the interface. FC-43 was used in the simulations; however, water could have been used because the interface temperatures chosen in the study will not result in freezing temperatures.

The reactants, H_2 and O_2, enter the cell as low-pressure gases and exit as slightly superheated steam at 355°K. The reactant consumption is presented in Figure 6-4. For this study the water vapor was assumed to be dumped continuously. However, payload contamination requirements could require a different approach. For example, the water could be stored in a tank after being condensed and dumped overboard during main engine burns, thus reducing the water vapor around the Tug during coast periods.

Flow Schematic
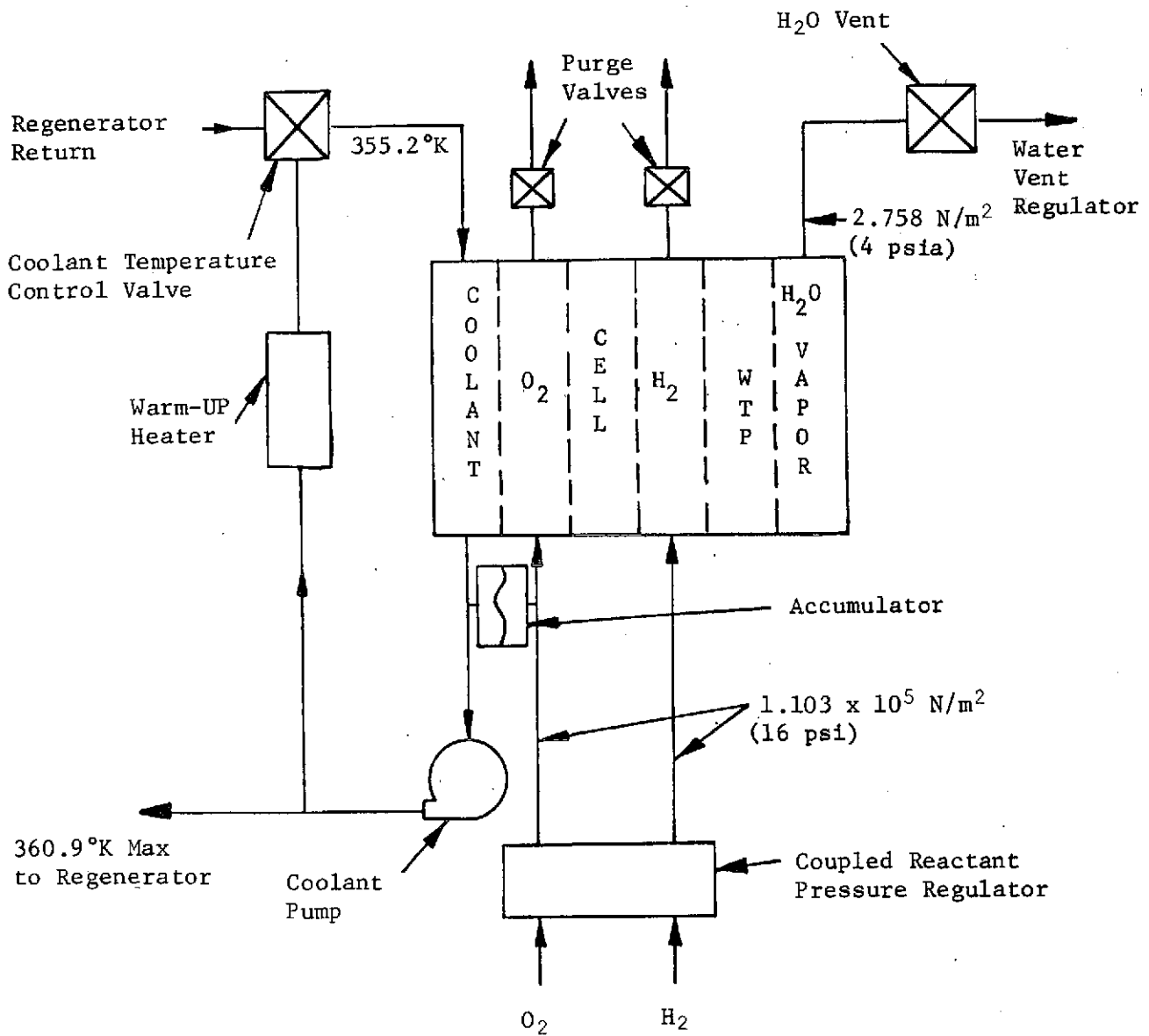
Figure 6-2   Fuel Cell Flow Schematic
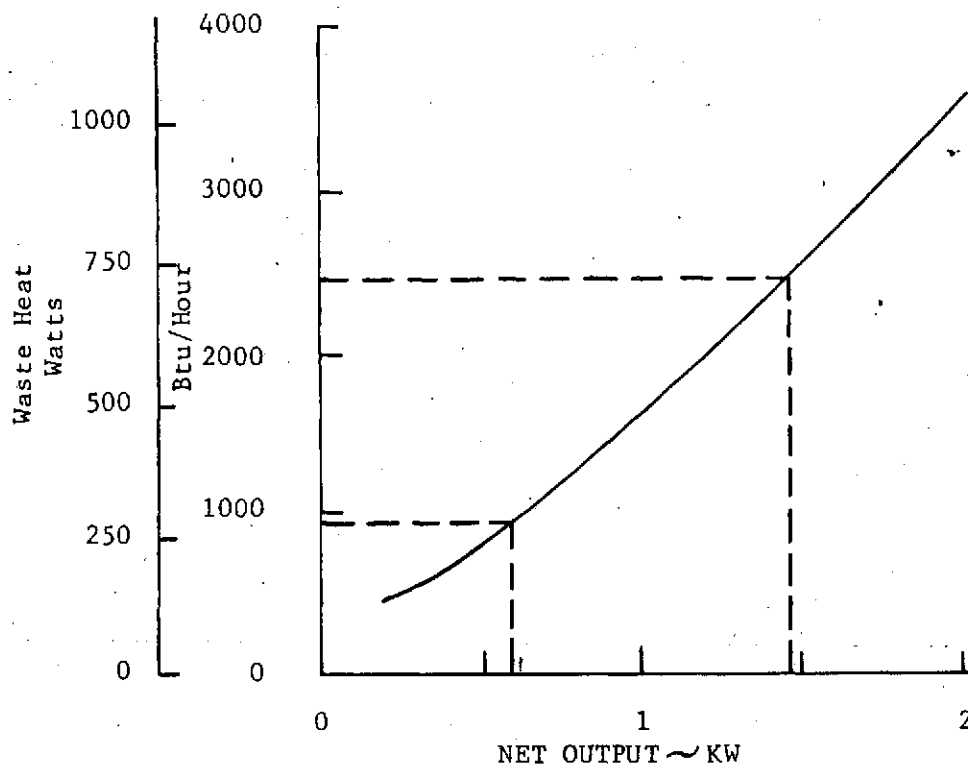
Figure 6-3   Waste Heat Rejection
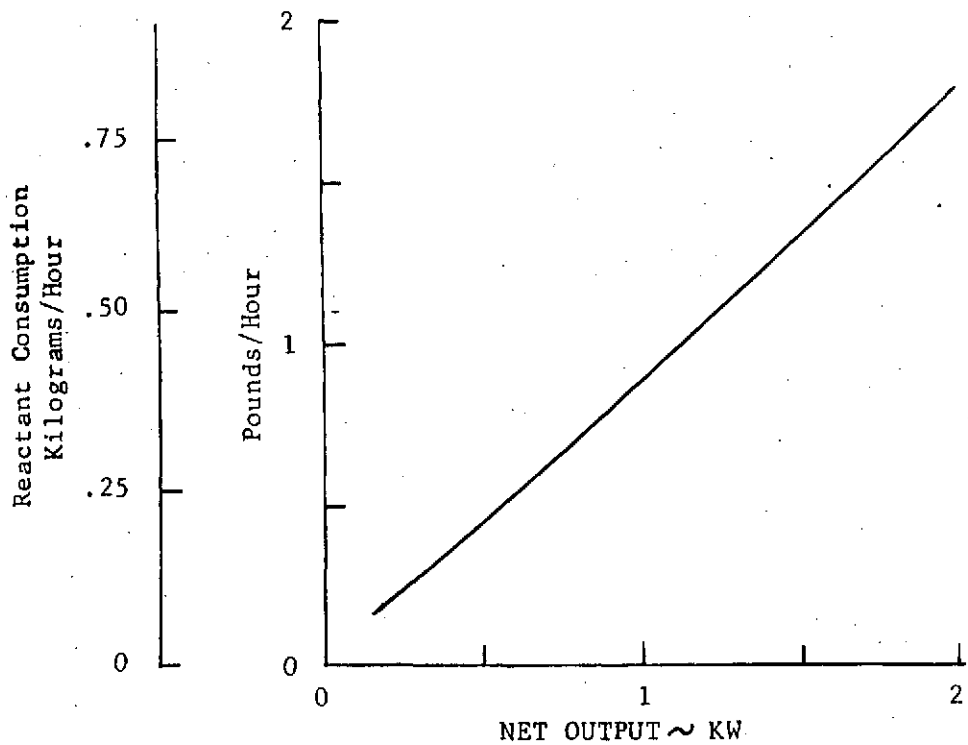
Figure 6-4   Reactant Consumption

The fuel cell heat rejection fluid loop is presented in Figure 6-5, which shows a single fluid loop through the thermal control valve and the radiators. The schematic is presented in this manner for clarity purposes only, and should be interpreted as having a redundant loop. The regenerator was considered to be a single unit with a redundant secondary loop.

The four radiator panels are in series with tubes on each panel in series, thus the series-series description. The radiators are similar in design to the Transtage radiator using the P-tube rail concept, Figures 6-5 and 6-6, details A and B, which allows two P-tubes to be attached to a single rail. Each panel has two continuous P-tubes from inlet to outlet with the flange removed in the bend and rail crossover areas. This concept minimizes the number of fluid connections and potential leakage points. The concept also provides micrometeorite protection.

The fluid is bypassed around the radiators, Figure 6-5, as the return fluid temperature drops below a predetermined level, 333°K (140°F). The thermal control valve was envisioned as a mechanically actuated valve using an electronic controller that senses the mixed fluid temperature going to the regenerator, T_3, and controls 333°K (140°F). This temperature was selected to meet the heat rejection requirements while minimizing radiator area. A lower temperature would also result in lower flowrates through the radiator in the cold case coupled with lower fluid temperatures. The pump was located on the outlet side of the regenerator to maximize the fluid temperature entering the radiators in the cold case. Freon E-1, the chosen working fluid, was developed primarily to yield heat transport properties similar to Freon 21 while eliminating the compatibility problems of that fluid. The cold-case results, discussed later, indicate that a heater is not required to avoid excessively cold fluid temperatures.

The system results in a relatively constant headrise requirement on the pump because the system pressure drop should remain relatively constant. Flow trimming problems experienced on parallel flow systems are avoided with the series configuration. One concern with this design is the confirmation of the transitional flow characteristics of a single panel. Although past radiator designs have been based on a turbulent or laminar operation, the Tug radiator was designed to operate through the transition region with Reynolds numbers ranging from 27,000 in the hot case to 600 in the cold case.

Two advantages of the bypass radiator design are the limited pressure drop and reduction in heat transfer coefficient as the fluid is cooled. The maximum pressure drop through the radiators occurs at full flow when the fluid is at its high temperature and is reduced as flow is bypassed around the panels.

6-6

RADIATORS

DETAIL B

DETAIL A

THERMAL CONTROL UNIT

RADIATOR DISCONNECTS

P_3 T_2

T_1

THERMAL CONTROL VALVE

P_2

T_3

P_5

P_4

ACCUMULATOR

FILL DISCONNECT

F_1 PUMP

P_1

REGENERATOR

FUEL CELL DISCONNECTS
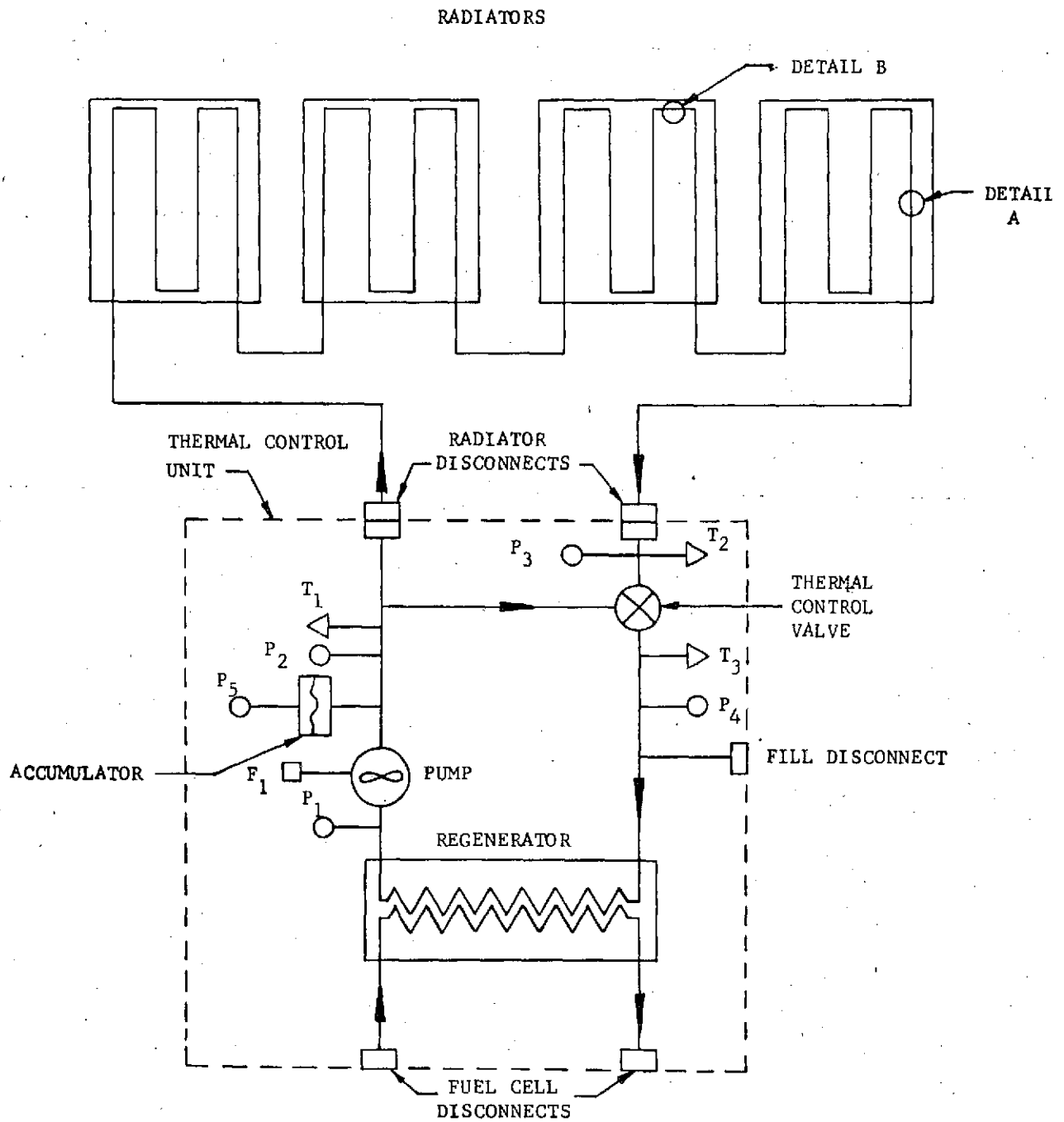
Figure 6-5   Fuel Cell Heat Rejection

Detail A
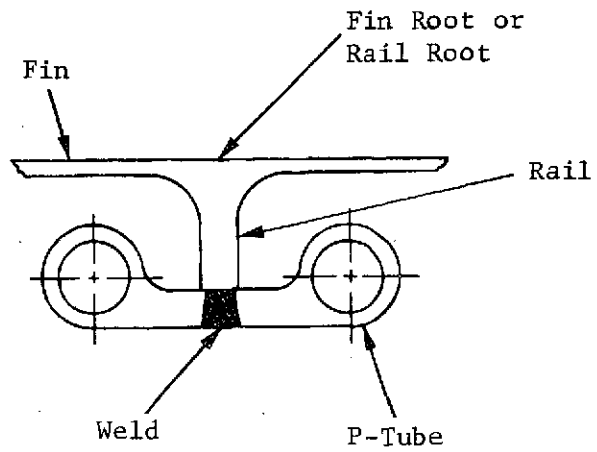
Detail B
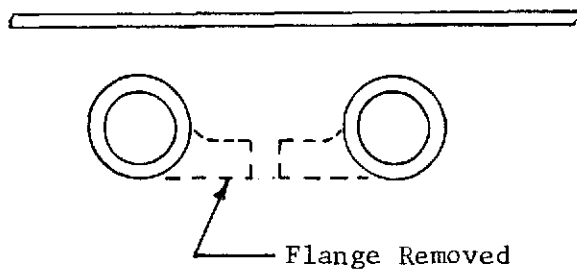
Figure 6-6   Radiator Details

Ideally, the radiator designer desires high heat transfer coefficients at maximum heat load conditions and minimum coefficients at minimum heat load conditions. This allows the total panel area to be minimized while limiting the minimum fluid temperature. The transitional flow design permits the designer to accomplish this.

This design assumes predictable operation over the above Reynolds number range using data Colburn presented in 1936 (Ref 12). The Transtage radiator was designed to operate down to Reynolds numbers of 7000 however, the complete transition region was not explored. Successful Skylab Airlock Module radiator operation was demonstrated up to Reynolds numbers of 2500. A verification test of a single panel is needed to confirm the design philosophy considered here. A further discussion follows in the cold case results discussion.

6.1 RADIATOR MODELING TECHNIQUES

A 79-node thermal model using variable material and fluid properties to evaluate the system performance was developed. Heat transfer coefficients were evaluated for each individual radiator tube. Classical heat exchanger theory was applied in evaluating the regenerator performance.

The tube heat transfer coefficients were obtained using the Colburn J-Factor method discussed in Reference 12. Figure 6-7 was obtained from Reference 12, page 394, which relates the Colburn J-Factor to Reynolds number. The Colburn J-Factor is related to the heat transfer coefficient by the equation:

$$J = \left(\frac{h_c}{\rho C_p V}\right) N_p^{2/3} \left(\mu_f/\mu_w\right)^{0.14}$$

where

C_p = fluid specific heat

V = fluid velocity in tube

ρ = bulk fluid density

N_p = Prandtl Number

μ_f = bulk fluid viscosity

μ_w = fluid viscosity at the tube wall
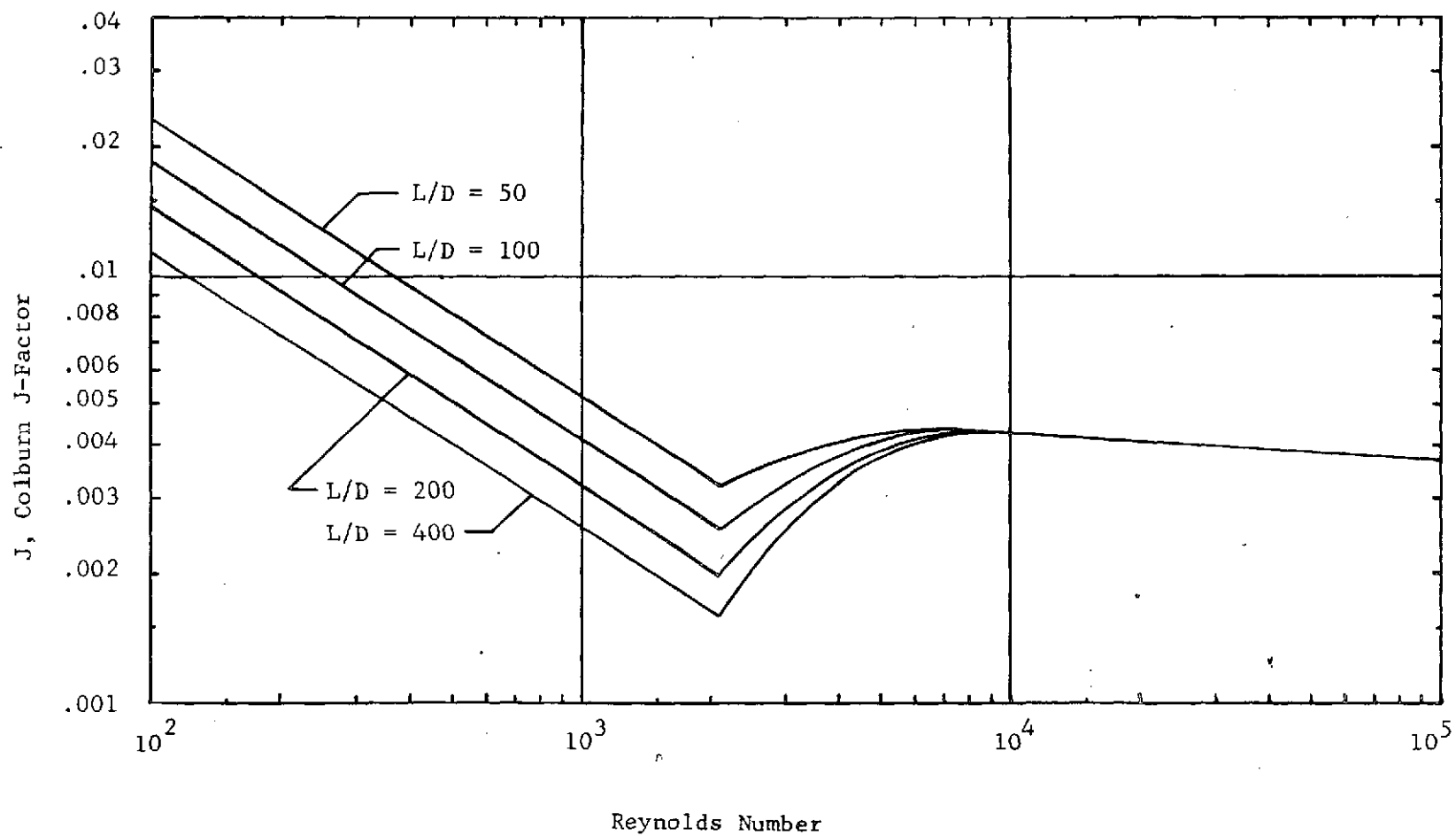
Figure 6-7 Colburn J-Factor vs Reynolds Number

J = Colburn J-Factor

k = fluid conductivity

N_R = Reynolds number

D = tube internal diameter

h_c = heat transfer coefficient to tube

Solving for h_c

$$h_c = Jk \, N_R \, N_p^{1/3} \left(\mu_w / \mu_f \right)^{0.14} / D$$

A subroutine with this equation was used in calculating the heat transfer equation and applying it to the model. Inherent in the subroutine was another technique used in evaluating radiator designs at the Denver Division for several years. This technique is directly adaptable to the finite differencing technique used by most thermal analyzer programs. Consider fluid flowing through a single tube and further consider this to be a part of a parallel flow heat exchanger.

The heat balance on the tube is governed by the following equations:

$$\text{fluid } Q = \dot{\omega} \, C_p \left(T_{in} - T_{out} \right)$$

$$\text{tube } Q = \varepsilon \dot{\omega} \, C_p \left(T_{in} - T_w \right)$$

$$\dot{\omega} \, C_p \left(T_{in} - T_{out} \right) = \varepsilon \dot{\omega} \, C_p \left(T_{in} - T_w \right)$$

where

Q = heat rate

$\dot{\omega}$ = mass flow rate

C_p = specific heat of the fluid

T_{in} = fluid inlet temperature

T_{out} = fluid outlet temperature

T_w = tube wall temperature

ε = heat exchanger effectiveness

solving for T_{out}

[1] $\quad T_{out} = (1-\varepsilon)\, T_{in} + T_w$

For a parallel flow heat exchange the effectiveness is

$$\varepsilon = \frac{1 - e^{-NTU\left(1 + \frac{C_{min}}{C_{max}}\right)}}{1 + C_{min}/C_{max}}$$

where

$C \qquad = \dot{\omega} C_p$

$C_{min} \quad$ = the minimum enthalpy flow

$C_{max} \quad$ = the maximum enthalpy flow

NTU $\quad$ = number of heat exchanger units = $h_c\, A/C_{min}$

If the tube wall were assumed to be a constant temperature, the enthalpy flow outside the tube would approach infinity of $C_{max} \approx \infty$ hence $C_{min}/C_{max} = 0$. The above equation reduces to

[2] $\quad \varepsilon = 1 - e^{-h_c\, A/C_{min}}$

Having solved for T_{out} in terms of T_{in} and T_w and determined ε, the finite difference equation was reviewed.

$$T_A = \frac{\sum_{j=1}^{n} G_{j-A}\, T_j}{\sum_{j=1}^{n} G_{j-A}}$$

where

T_A = temperature of node A

G_{j-A} = conductance from node j to node A

T_j = temperature of node j

n = number of nodes conducted to node A

The finite differencing equations would therefore solve for T_{out} in the following manner:

[3]
$$T_{out} = \frac{(1 - \varepsilon) T_{in} + \varepsilon T_w}{1 - \varepsilon + \varepsilon}$$

which reduces to Equation [1].

The network for Equation [3] is:
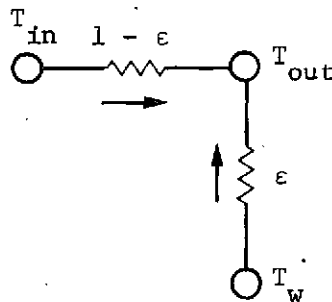
The tube equation is satisfied by adding the additional conductor to the network between T_{in} and T_w.
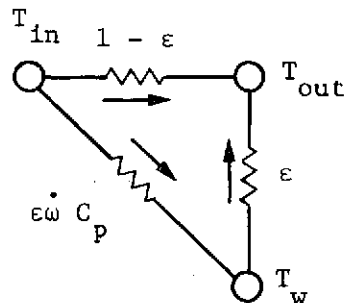
Hence the subroutine calculated the above network for each of the 16 radiator tubes, impressing the appropriate conductor values in the thermal network each iteration. In addition, the Reynolds numbers, Colburn J-Factors, and heat transfer coefficients were saved for printout purposes.

To complete the radiator evaluation, the fin effectiveness was evaluated by the following equation obtained from Reference 14.

$$\mu_F = \frac{\text{TANH } 2L_F \sqrt{\dfrac{\sigma\varepsilon T_R^3}{k\delta}}}{2 \ L_F \sqrt{\dfrac{\sigma\varepsilon T_R^3}{k\delta}}}$$

where

T_R = Fin root or rail root temperature

ε = Surface emissivity

k = Conductivity of the fin

δ = Fin thickness

L_F = fin width

σ = Stefan-Boltzman constant

Solving for the root temperature in the model the fin heat radiated is determined by

$$Q = \sigma \ A\varepsilon\mu_F \ T_R^4$$
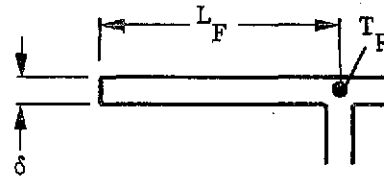
6.2 REGENERATOR SIZING

The regenerator was sized using the effectiveness approach described in Reference 15. For a counter flow heat exchanger, the effectiveness is defined as

$$\varepsilon = \frac{1 - e^{-NTU}\left(1 - C_{min}/C_{max}\right)}{1 - \left(C_{min}/C_{max}\right)e^{-NTU}\left(1 - C_{min}/C_{max}\right)}$$

6-14

where

NTU = number of heat transfer units = UA/C_{min}

C = $\dot{\omega} C_p$

C_{min} = minimum $\dot{\omega} C_p$

C_{max} = maximum $\dot{\omega} C_p$

A = heat transfer area

U = overall heat transfer coefficient

NTU was evaluated by assuming that on an individual iteration
basis the fuel cell fluid loop was at steady state. This agrees
with the use of arithmetic nodes to simulate the fluid. With that
assumption it follows that the heat dissipated by the fuel cell
must be transferred through the regenerator. Using the previous
iterations regenerator ΔT, the UA was calculated by the following
equation.

UA = $Q/\Delta T$

NTU was derived from the above equation after determining the min-
imum of the hot and cold side $\dot{\omega} C_p$ values.

6.3   RADIATOR PRESSURE DROP

Radiator pressure drop was evaluated directly from the following
equation which was obtained from References 12 and 16.

J = f/8

or

f = 8J

where

J = Colburn J-factor

f = friction factor

$$\Delta P = 8J \frac{L\rho}{D} \frac{V^2}{2g_c}$$

where

L = tube length

D = tube internal diameter

ρ = fluid density

V = average fluid velocity

g_c = gravity term

Substituting the velocity with the continuity equation

$$\Delta P = 8J \frac{L}{D} \frac{\rho}{2g_c} \left(\frac{\dot{\omega}}{\rho A}\right)^2$$

where

A = internal tube cross sectional area

$\dot{\omega}$ = fluid mass flow rate

Pressure drops for tube bends were evaluated using the above equation modified for equivalent L/D ratios obtained from Reference 16.

6.4   FUEL CELL MODEL

The fuel cell was modelled and integrated with the radiator model. The model schematic is shown in Figure 6-8.

Table 6-1 describes the nodes of the fuel cell model.

The conductor values used were temperature-dependent based upon FC-43 as the working fluid and were $\dot{\omega} C_p$ one-way conductors. The system mass flow was 5.75 kg/minute (12.67 lb/minute). The use of water in this loop would reduce the mass flow in proportion to the specific heat ratio.

Figure 6-8 Fuel Cell Model

Table 6-1 Fuel Cell Model Node Description
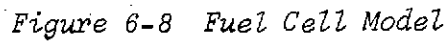
Node	Description
200	Fuel Cell
201	Pump
202	Fluid Node
203	Regenerator Inlet - Fluid
204	Regenerator Outlet - Fluid
205	Coolant Temperature Thermal Control Valve - Fluid
206	Bypass Fluid and Fast Warm-up Heater
207	Boundary Temperature
Heat	
Q 200	Fuel cell heat dissipation function of electrical load Figure 6-3
Q201	Pump heat dissipation - 30 watts constant.

The coolant temperature control valve was simulated by a linear curve assuming 100% flow through the regenerator at 356°K (181°F) and 10% flow at 353°K (176°F) regenerator outlet temperatures. The control range used was smaller than the 5.5°K (10°F) range obtained from Pratt and Whitney. The range was reduced to provide better control of the fuel cell and was based on experience with wax plug designs that tend to control in the range used. Pratt and Whitney also stated that the design of the valve is such that the minimum regenerator flow is 5 to 10% at the lower allowable fluid temperatures.

Node 207 was used as a boundary node to remove heat from the fluid using the regenerator equations and the following equations. The effectiveness is related to the heat flow by

$$\varepsilon = q/q_{max} = \frac{C_h \left(T_{h\ in} - T_{h\ out}\right)}{C_{min}\left(T_{h\ in} - T_{c\ in}\right)}$$

$$= \frac{C_c \left(T_{c\ out} - T_{c\ in}\right)}{C_{min}\left(T_{h\ in} - T_{c\ in}\right)}$$

where

q = heat flow from hot to cold side

q_{max} = maximum heat flow for $\varepsilon = 1$

C_h = $\dot{\omega} C_p$ for the hot side fluid (fuel cell)

C_c = $\dot{\omega} C_p$ for the cold side fluid (fuel cell heat rejection system)

C_{min} = minimum of C_h and C_c

$T_{h\ in}$ = fluid hot side inlet

$T_{h\ out}$ = fluid hot side outlet

$T_{c\ in}$ = fluid cold side inlet

$T_{c\ out}$ = fluid cold side outlet

solving for q

$$q = \varepsilon C_{min} \left(T_{h\ in} - T_{c\ in}\right)$$

6-18

Using arithmetic nodes to simulate the fluid implies that the heat generated must be removed from the system because the nodes are relaxed to steady state each iteration. The heat stored in the fuel cell and pump, nodes 200 and 201, was not considered due to expected small variations from one iteration to the next. The sum of Q200 and Q201 was used along with an assumed 5.6°K (10°F) temperature drop of the fuel cell fluid through the regenerator to calculate the UA term thus enabling the effectiveness to be calculated. Node 207 was set by the maximum temperature difference.

$$T_{207} = T_{204} - \left(T_{h\ in} - T_{c\ in} \right)$$

or

$$= T_{204} - \left(T_{203} - T_{34} \right)$$

where T_{34} was the cold side inlet temperature.

The above equation defining q was satisfied by substituting the individual temperatures.

$$q = \varepsilon\ C_{min} \left(T_{204} - T_{207} \right)$$

$$= \varepsilon\ C_{min} \left(T_{204} - T_{204} + \left(T_{h\ in} - T_{c\ in} \right) \right)$$

hence

$$q = \varepsilon\ C_{min} \left(T_{h\ in} - T_{c\ in} \right)$$

6.5   FUEL CELL HEAT REJECTION SYSTEM MODELING

The control portion of the fuel cell heat rejection system fluid loop was modelled as shown in Figure 6-9.

Table 6-2 presents a description of the nodes contained in Figure 6-9.
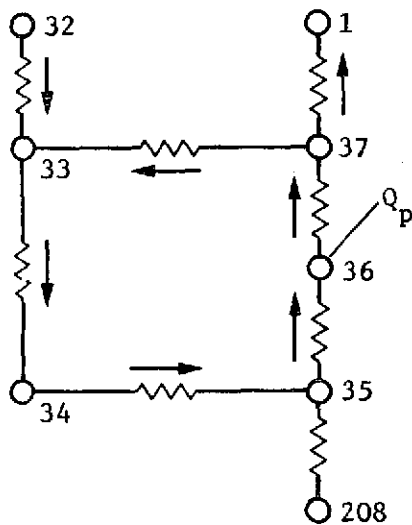
Figure 6-9
Fuel Cell Heat Rejection System
Flow Control Loop Model

Table 6-2   Radiator Control Loop

Node	Description
1	Radiator fluid inlet temperature
32	Radiator fluid outlet temperature
33	Thermal control valve outlet temperature
34	Regenerator inlet temperature
35	Regenerator outlet temperature
36	Pump outlet temperature
37	Fluid temperature
208	Boundary temperature

Heat was applied to node 36 as Q_p which was set at 51 watts. These data were derived from a Block II Apollo pump with Freon E-1 as the working fluid. The conductor values were obtained using temperature varying properties and represent the mass flow times specific heat. The pump flow was held constant at 1.81 kg/minute (4 lb/minute). Node 208 was used to add the heat removed from the fuel cell loop to the radiator loop and was evaluated by the following equation

$$T_{208} = T_{35} + \left(T_{h\ in} - T_{c\ in} \right)$$

$$= T_{35} + \left(T_{203} - T_{34} \right)$$

The conductor value between nodes 35 and 208 was set equal to $\varepsilon\ C_{min}$.

6-20

The radiator model is presented for a single panel. Each panel was modelled individually and integrated into the complete model. The first panel in the loop is shown in Figure 6-10.
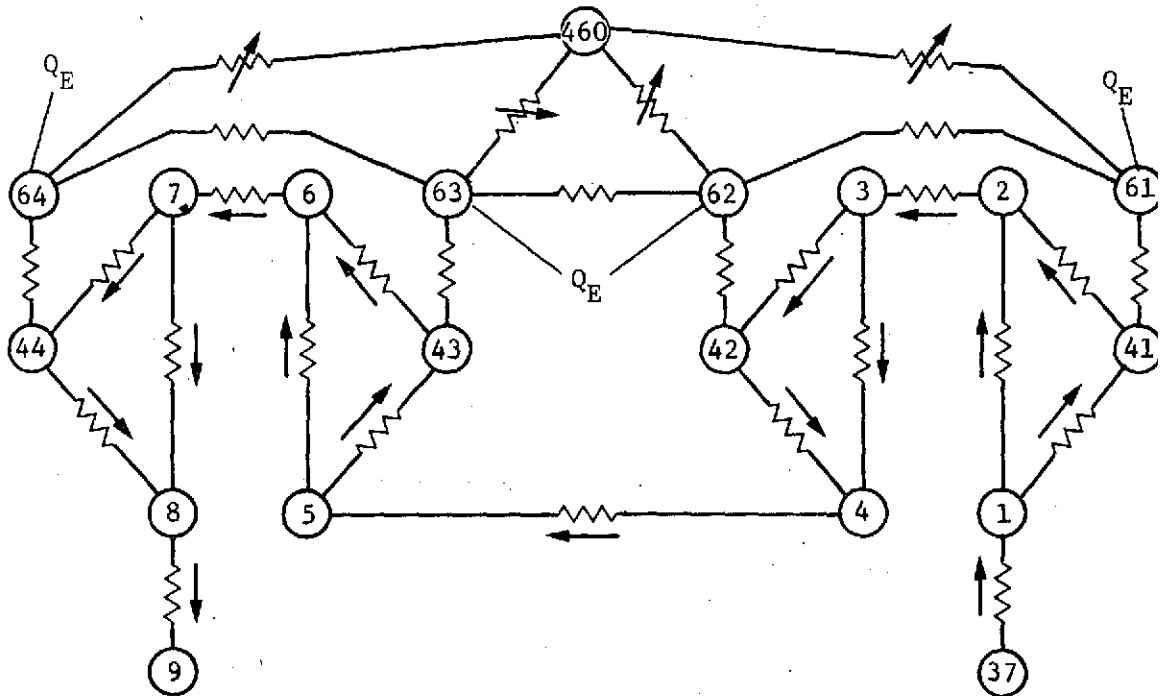
Q_E = External Heating

Figure 6-10 Radiator 1 Nodal Diagram

Nodes 1 through 9 and node 37 represent fluid nodes. Node 9 was equivalent to node 1 on panel number 2 with the entire numbering sequence contained. The series of nodes beginning with 41 were tube wall nodes while the nodes beginning with 61 were rail root nodes. Node 460 was the boundary node representing the space sink temperature of 0°K. The fluid conductors between radiator rails were $\omega\, C_p$ values. The tube-to-rail root and rail root-to-rail root conductors were handled as linear conductors. Q_E represents the application absorbed external heating.

6.6   HOT-CASE PERFORMANCE

The hot-case analysis was performed to size the area of the radiators and regenerator performance for the maximum external heating and maximum heat load condition. The results of the study

resulted in the radiator being sized to 8.05 m^2 (22 ft^2) or 2.01 m^2 (5.5 ft^2) per panel. The regenerator requirements derived from the analysis indicated that an effectiveness of 0.90 or greater was achievable. Table 6-3 presents the conditions used. As previously discussed, the maximum external environment was obtained from flux case 4 in park orbit and was a transient environment. The use of higher inclination angle orbits would require resizing the radiator area for a constant solar exposure in near-earth orbit.

Table 6-3 Hot-Case Radiator Design Conditions

Maximum External Heating	Flux Case 4 Park Orbit
Vehicle Attitude	Sun Normal to Tug Longitudinal Axis
	Two Radiators Exposed to Sun 45° from Sun Line
Maximum Electrical Load	1500 Watts
Maximum Heat Load	744 Watts Plus
	81 Watts for Pumps

A radiator coating selection study was pursued where primary requirements for screening were a low α/ε, demonstrated stability of the properties, ease of application, ease of maintenance, and durability. White paints were eliminated by most of the above considerations. Optical solar reflectors (OSR) were deleted due to anticipated problems with handling and maintenance. Silver-coated teflon tape was selected because of its fovorable optical property values, stability, ease of application, and maintenance. The properties used to represent silver Teflon in the analysis were $\alpha = 0.09$ and $\varepsilon = 0.76$, obtained from Reference 17.

Figures 6-11 thru 6-13 present key temperatures of the fuel cell loop, the regenerator inlet, regenerator outlet, and coolant temperature control valve outlet temperatures, respectively. The first temperature peak is due to the initial temperature in the radiators being set at 355.4°K (180°F). Hence, the first half hour of the simulation was used to gain control of the system. Most of this time was used to allow the control valve to respond; the valve was not allowed to change more than 0.5% of full flow from one iteration to the next. This logic was to limit the valve cycling. The same logic was also applied to the radiator loop thermal control valve. The resultant regenerator inlet temperature was 359.73°K (187.75°F), as shown in Figure 6-11, while the outlet of the regenerator was 344.54°K (160.5°F), as shown in Figure 6-12. The 0.1-hour output interval accounts for the seemingly jagged minor peaks in the curves indicating some minor cycling of the coolant control valve temperature at 353.7°K (177°F), as shown in Figure 6-13. Hence, the system was controlled within the desired temperature limits under maximum heating and load conditions.

6-22

TEMP NODE NO.   203 Fuel Cell Loop Regenerator Inlet
MIN TEMP OF   187.681 OCCURRED AT TIME   4.810
MAX TEMP OF   190.355 OCCURRED AT TIME   4.410
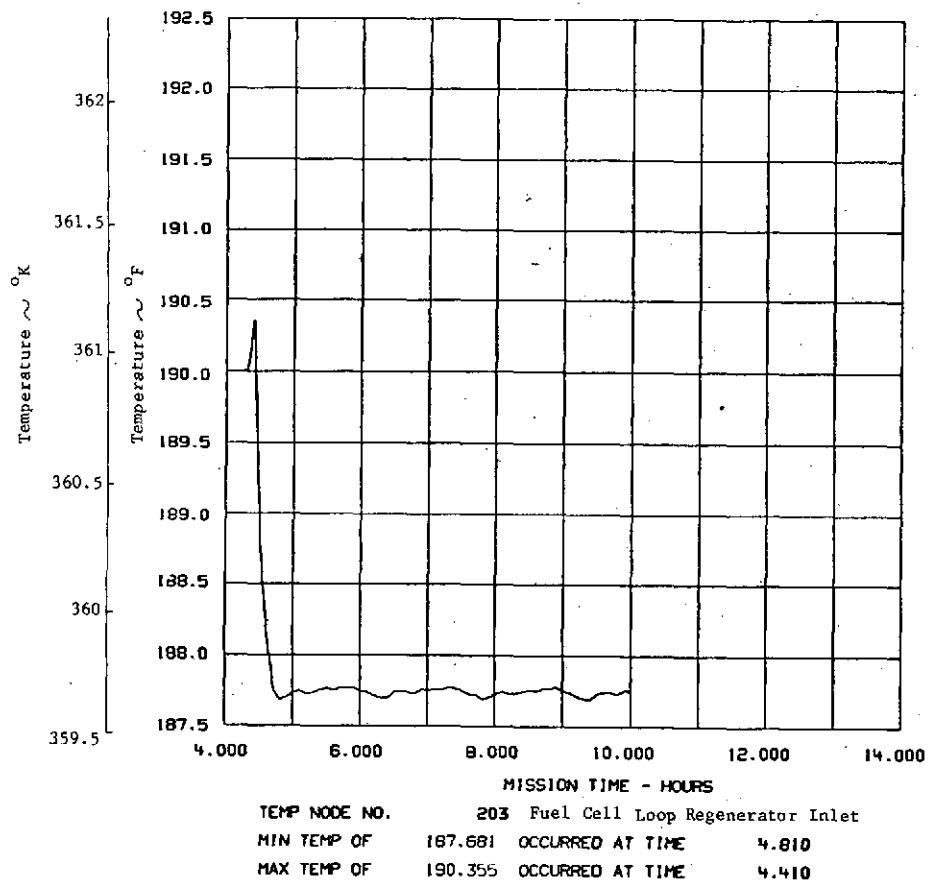
FIGURE 6-11   RADIATOR HOT CASE

TEMP NODE NO.   204   Fuel Cell Loop Regenerator Outlet
MIN TEMP OF   160.192 OCCURRED AT TIME   4.910
MAX TEMP OF   180.000 OCCURRED AT TIME   4.310
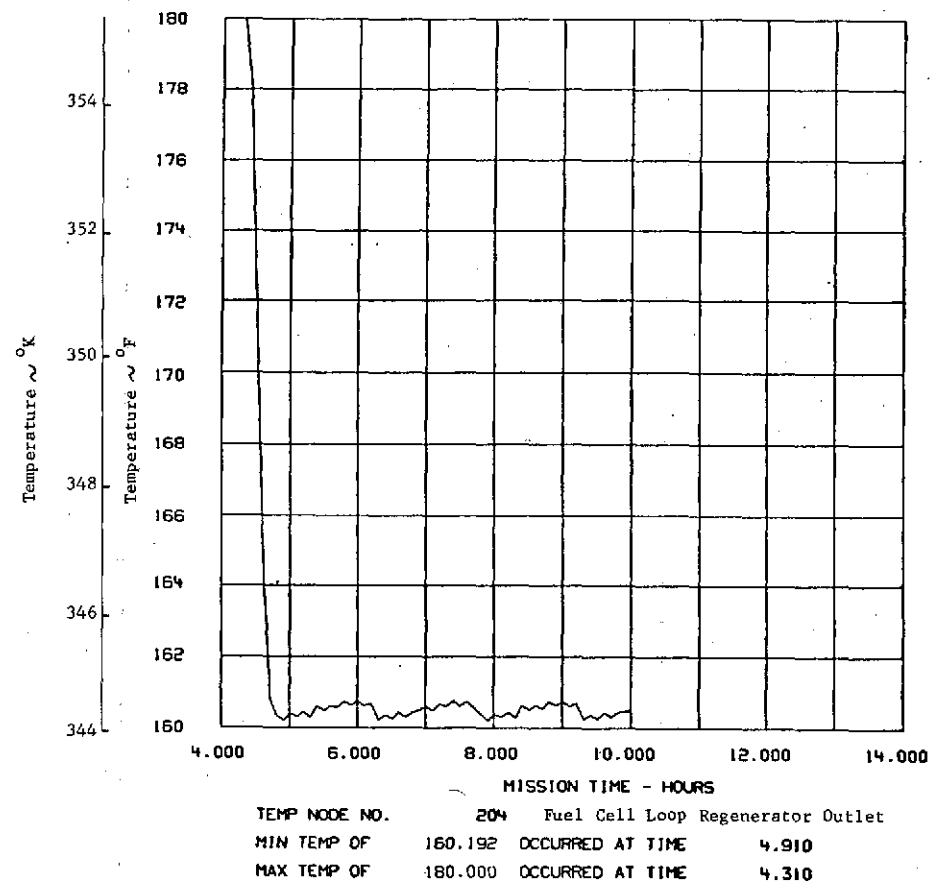
FIGURE 6-12 . RADIATOR HOT CASE

Figures 6-14 thru 6-16 represent the fluid inlet temperature to the radiators, fluid outlet temperature from the radiators, and the radiator loop thermal control valve outlet temperature, respectively. Figure 6-16 also represents the regenerator cold side inlet temperature and demonstrates control at the desired 333°K (140°F). Figure 6-17 presents the regenerator cold side outlet temperature. Figure 6-18 presents the heat rejected by the radiator fluid loop and Figure 6-19 presents the net heat radiated from the four radiator panels. The net heat rejected was evaluated by summing the total heat radiated from the panels and subtracting the summation of the absorbed heating rates. Figure 6-20 presents the radiator fluid mass flow, which ranged from 1.772 to 1.322 kg/minute (3.904 to 2.914 lb/minute). As shown the maximum system flow was 1.814 kg/minute (4 lb/minute. The maximum radiator flow of 1.772 kg/minute provides a 2% margin in flow in the hot case after the initial temperature transient.

Figure 6-21 presents the heat flow across the regenerator, which averaged 809 watts (2763 Btu/hour). The fuel cell loop flow through the regenerator, Figure 6-22, averaged 2.31 kg/minute (5.1 lb/minute), while the system capability was 5.75 kg/minute (12.67 lb/minute) as recommended by Pratt and Whitney. Based upon these results, the fuel cell loop flow could be reduced to 2.72 kg/minute (6 lb/minute) with adequate margin maintained.

The Reynolds numbers, Colburn J-Factors, heat transfer coefficients, and radiator pressure drop in the hot case were influenced by the tube L/D chosen for cold-case performances. With an L/D of 200 the hot-case parameters varied as shown in Table 6-4.

The radiator fin effectiveness varied between 0.908 to 0.923 for rail root temperatures of 354.2 to 330.2°K (177.8 to 134.6°F) at the maximum flow condition and 0.909 to 0.929 for rail temperatures of 352.3 to 320.8°K (174.5 to 117.7°F) at minimum flow conditions.

In reality, the hot-case electrical load on the fuel cell would occur during a main engine burn, which would result in the vehicle being oriented to the proper attitude before the burn. This required burn attitude would probably result in external heating rates less than the hot-case environment, which would yield more radiator performance margin than indicated. Further, the maximum load would be a relatively short interval, on the order of 200 to 300 seconds.
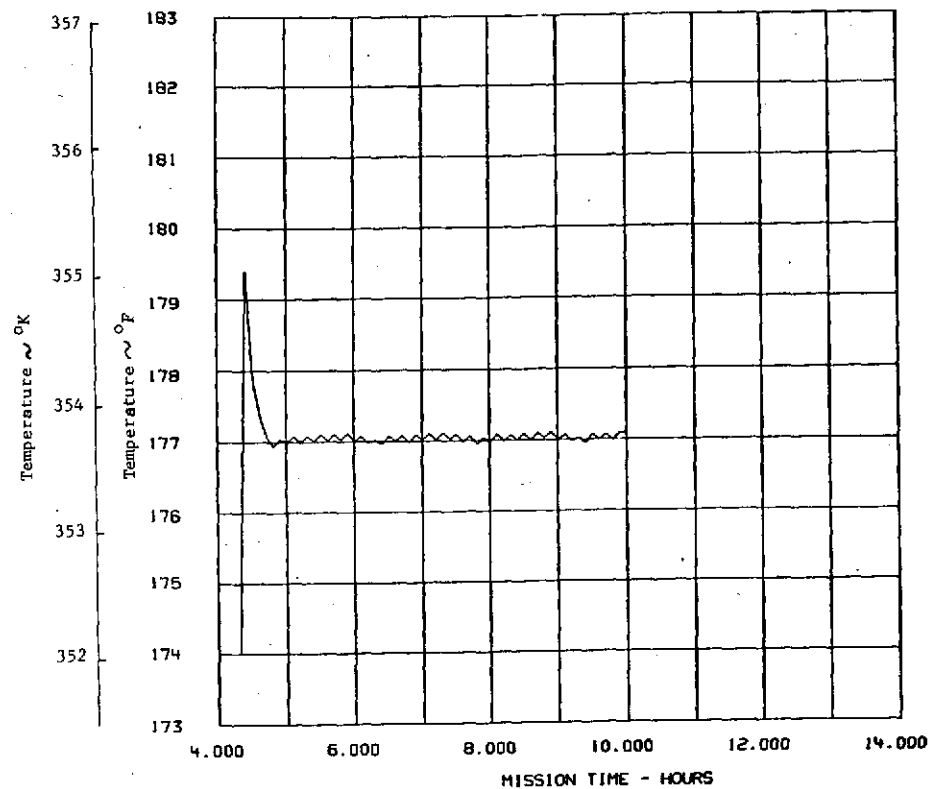
FIGURE 6-13 . RADIATOR HOT CASE

TEMP NODE NO.   205 Fuel Cell Coolant Temperature Control Valve
MIN TEMP OF   174.000 OCCURRED AT TIME   4.310
MAX TEMP OF   179.403 OCCURRED AT TIME   4.410
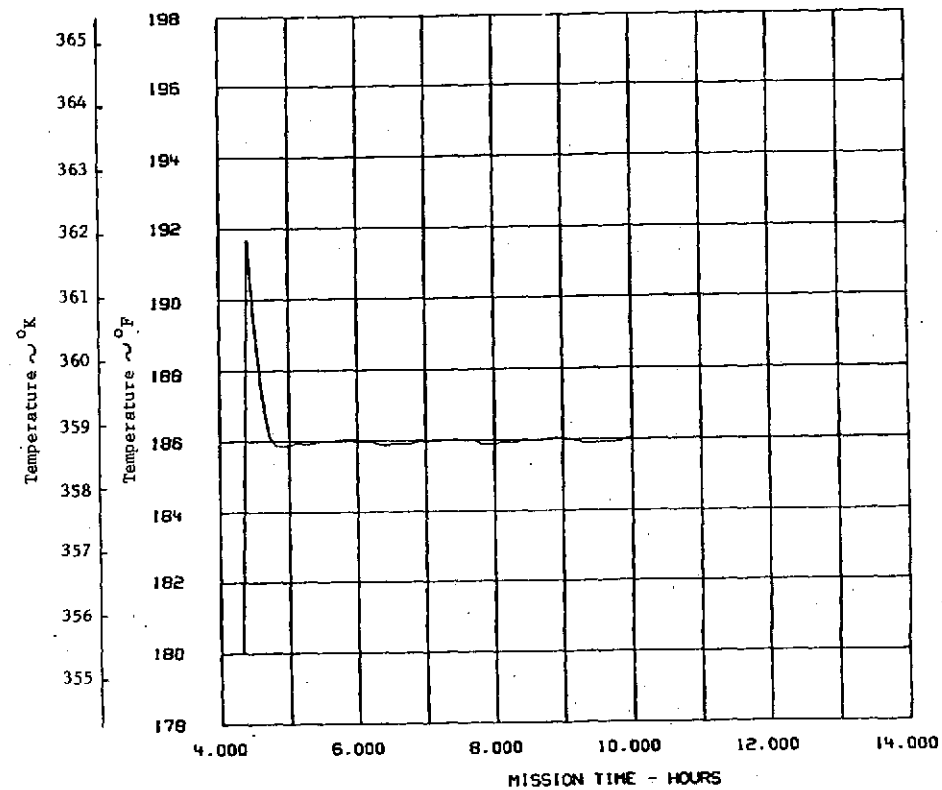
FIGURE 6-14 . RADIATOR HOT CASE

TEMP NODE NO.   1 Radiator Fluid Inlet Temperature
MIN TEMP OF   180.000 OCCURRED AT TIME   4.310
MAX TEMP OF   191.655 OCCURRED AT TIME   4.410

Temperature ~ °K

Temperature ~ °F

MISSION TIME - HOURS
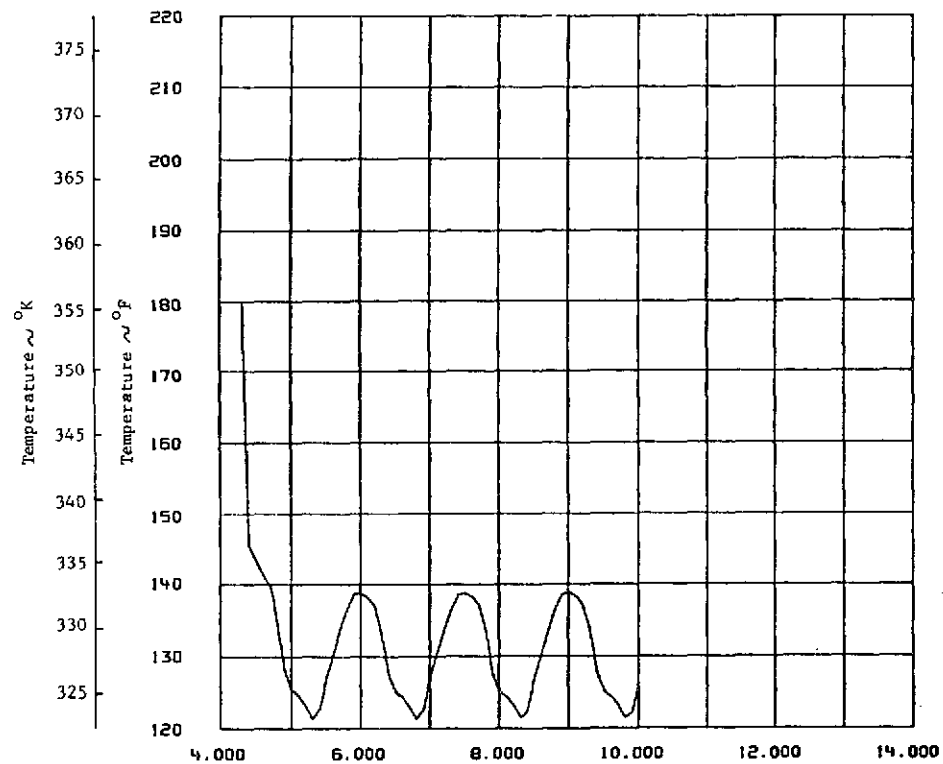
TEMP NODE NO.	32	Radiator Fluid Outlet Temperature
MIN TEMP OF	121.280	OCCURRED AT TIME	5.310
MAX TEMP OF	180.000	OCCURRED AT TIME	4.310

FIGURE 6-15 . RADIATOR HOT CASE

Temperature ~ °K

Temperature ~ °F

MISSION TIME - HOURS
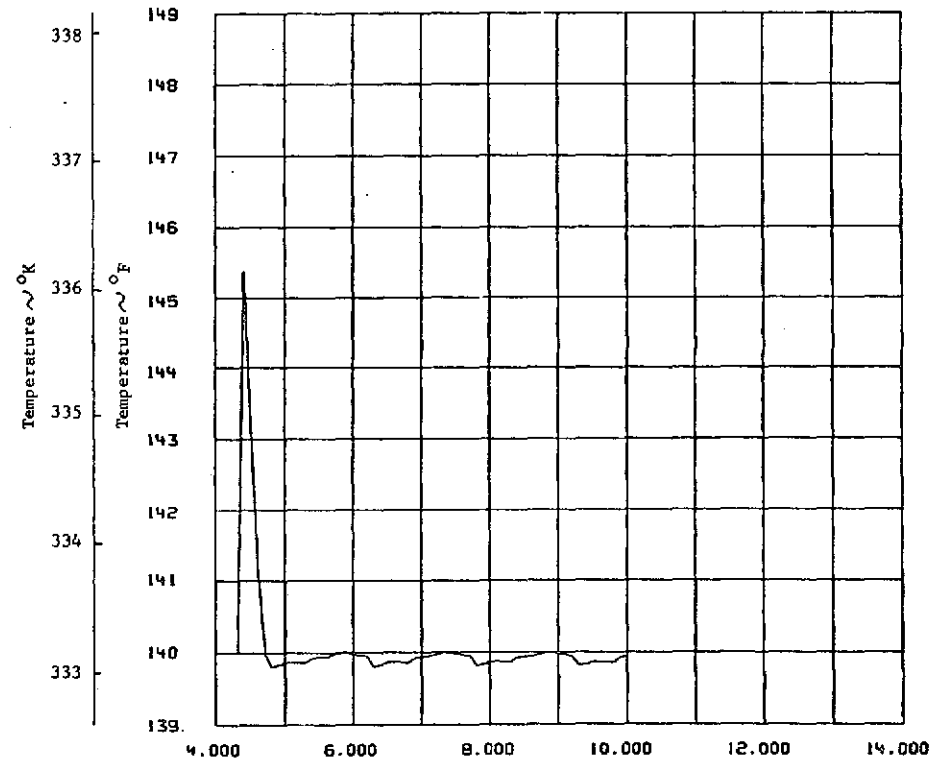
TEMP NODE NO.	33	Radiator Loop Thermal Control Valve Fluid Outlet Temperature
MIN TEMP OF	139.792	OCCURRED AT TIME	4.810
MAX TEMP OF	145.371	OCCURRED AT TIME	4.410

FIGURE 6-16   RADIATOR HOT CASE

FIGURE 6-17 . RADIATOR HOT CASE
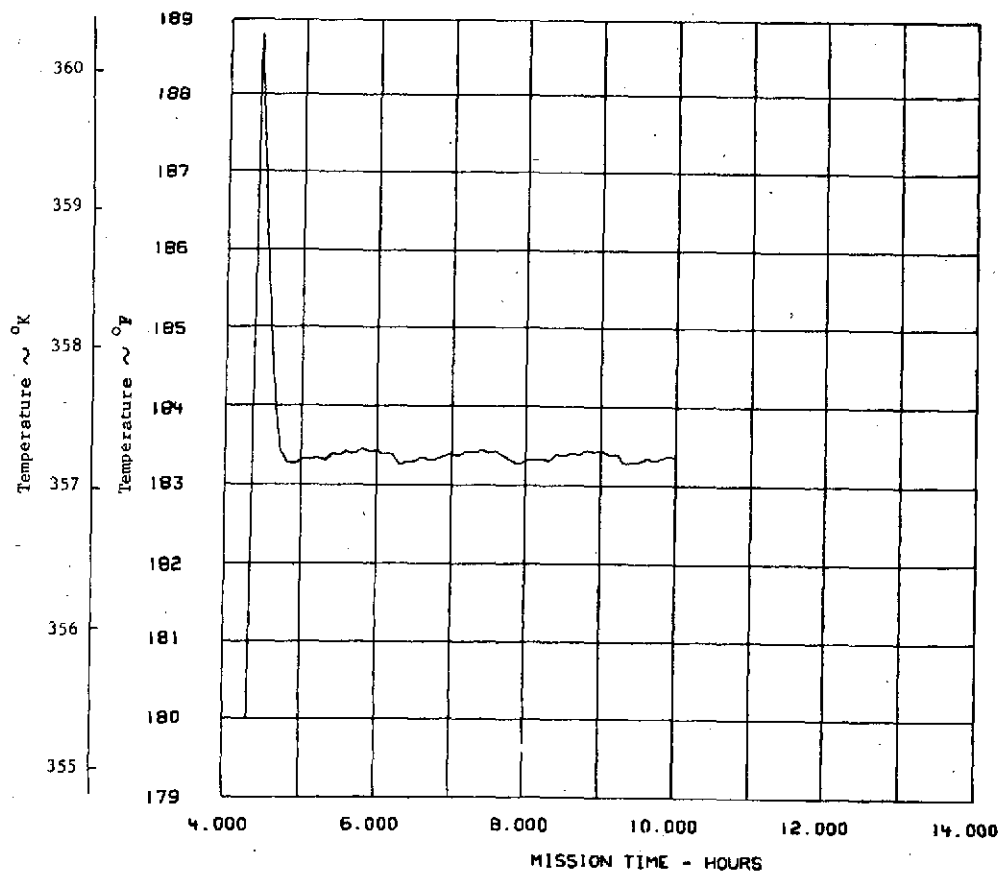
TEMP NODE NO.   35   *Regenerator Fluid Outlet Temperature*
MIN TEMP OF   180.000   OCCURRED AT TIME   4.310
MAX TEMP OF   189.801   OCCURRED AT TIME   4.410

FIGURE 6-18 RADIATOR HOT CASE
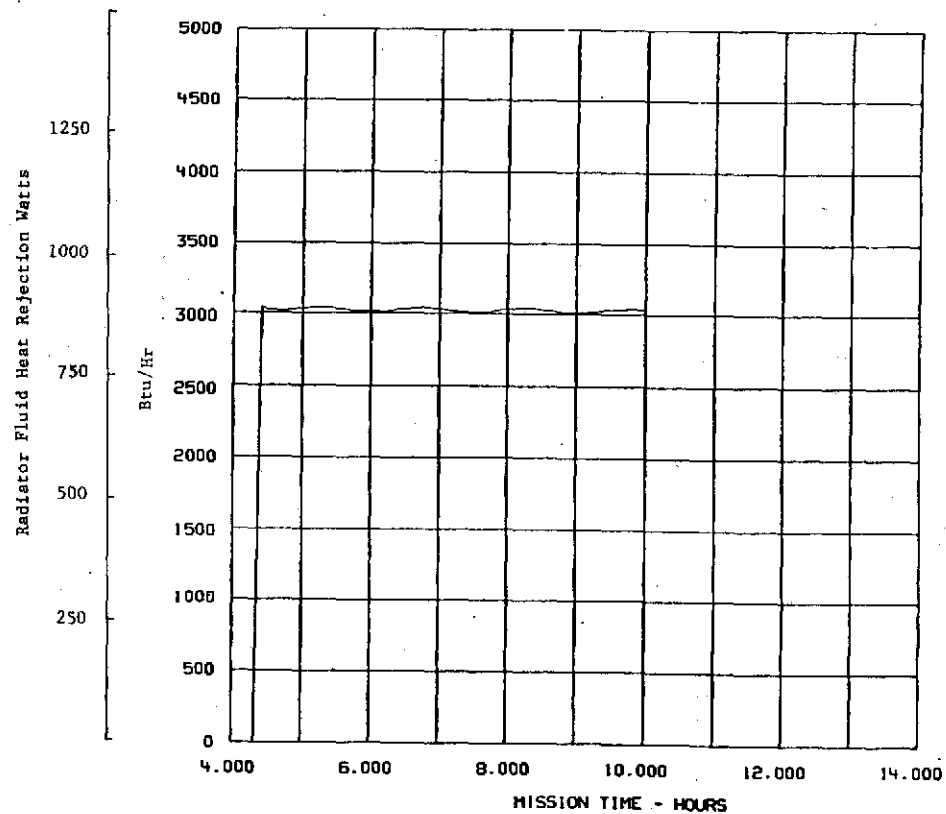
NODE NO.   300   *Radiator Fluid Heat Rejection*
MIN   OF   0.   OCCURRED AT TIME   4.310
MAX   OF   3047.005 OCCURRED AT TIME   4.410
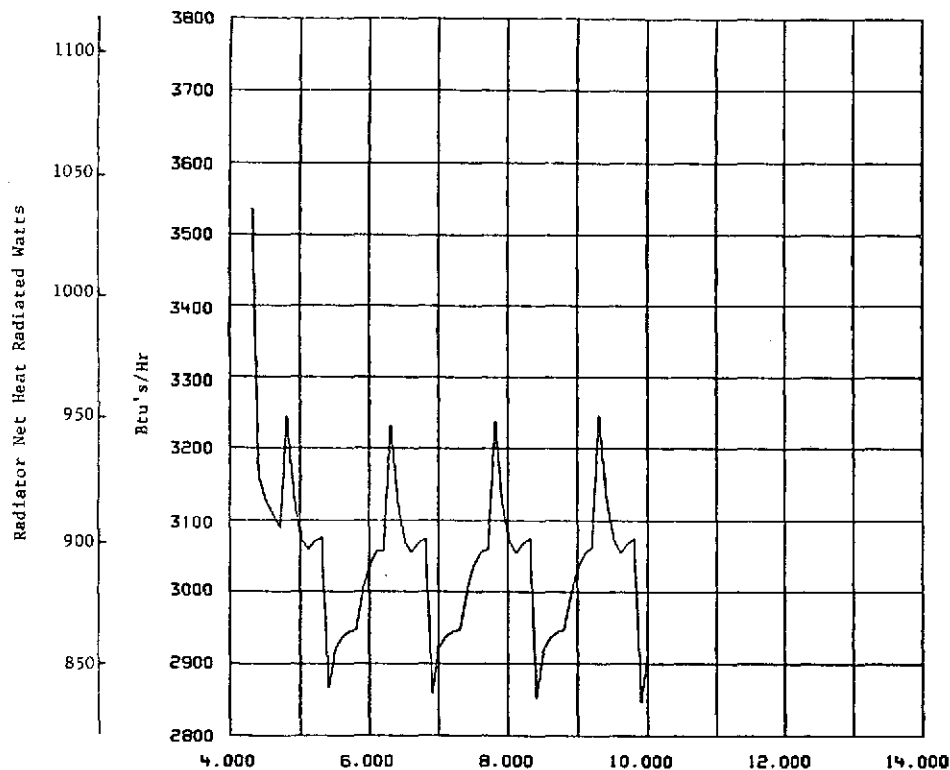
FIGURE 6-19   RADIATOR HOT CASE

TEMP NODE NO.   301   Radiator Net Heat Radiated

MIN TEMP OF   2846.932 OCCURRED AT TIME   9.910

MAX TEMP OF   3537.418 OCCURRED AT TIME   4.310
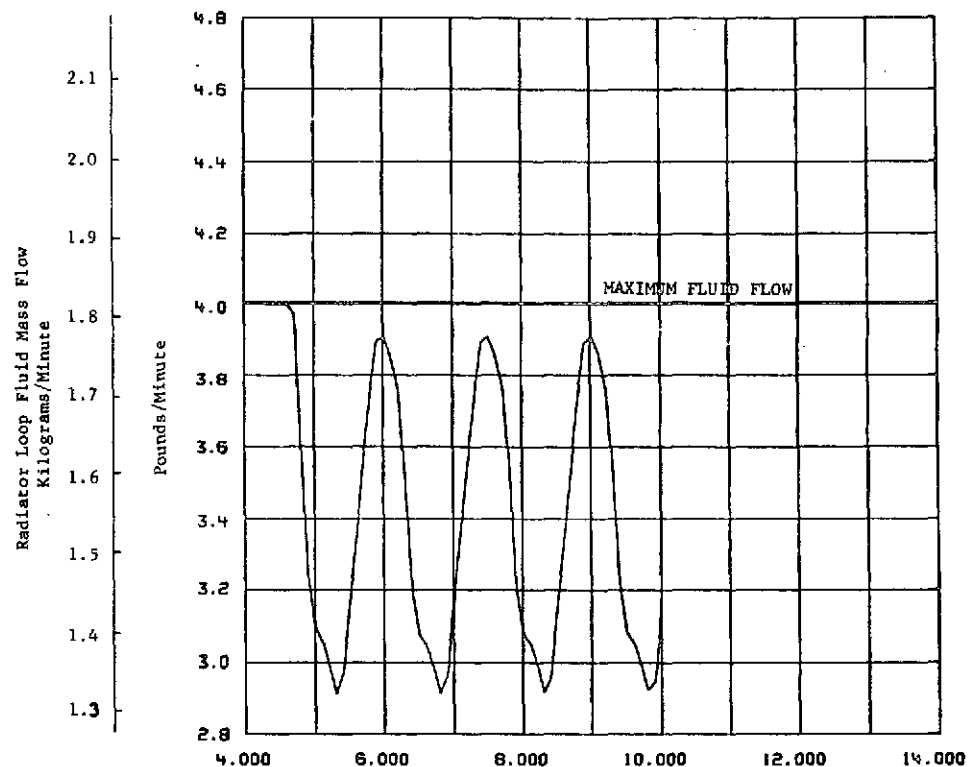
FIGURE 6-20   RADIATOR HOT CASE

TEMP NODE NO.   302   Radiator Loop Fluid Mass Flow

MIN TEMP OF   2.913   OCCURRED AT TIME   5.310

MAX TEMP OF   4.000   OCCURRED AT TIME   4.310
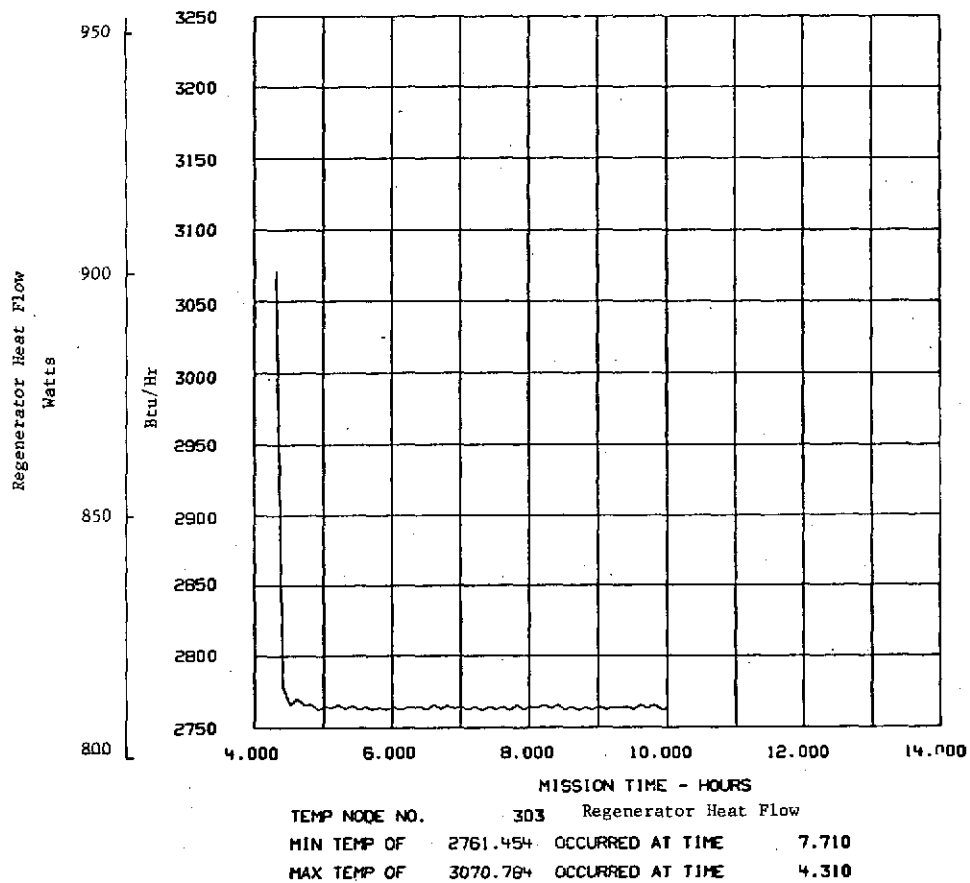
FIGURE 6-21 RADIATOR HOT CASE

TEMP NODE NO.   303   Regenerator Heat Flow

MIN TEMP OF   2761.454 OCCURRED AT TIME   7.710

MAX TEMP OF   3070.784 OCCURRED AT TIME   4.310
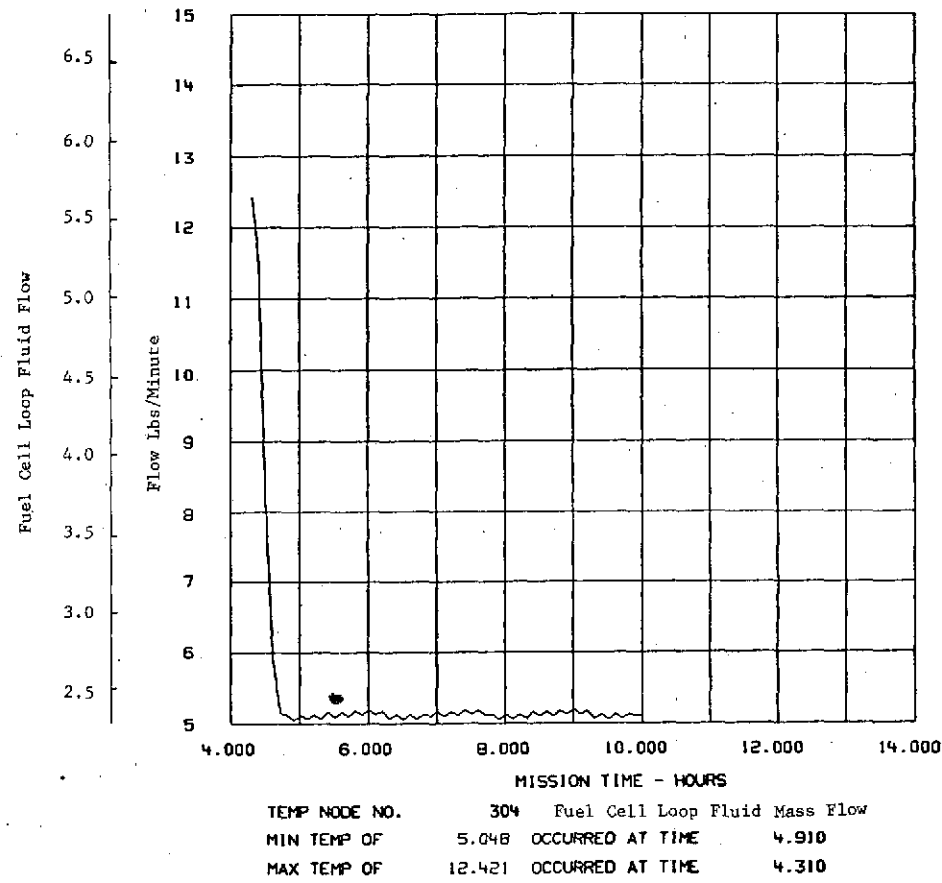
FIGURE 6-22 RADIATOR HOT CASE

TEMP NODE NO.   304   Fuel Cell Loop Fluid Mass Flow

MIN TEMP OF   5.048 OCCURRED AT TIME   4.910

MAX TEMP OF   12.421 OCCURRED AT TIME   4.310

Table 6-4 Radiator Parameters

Flow	Reynolds Numbers	J	Heat Transfer Coefficient	Pressure Drop
kg/minute (lb/minute)	inlet/ outlet	inlet/ outlet	inlet/outlet watt/m^2 °K (Btu/hr-ft^2-°F)	N/m^2 (psi)
1.772 (3.906)	27655/ 20561	0.00400 0.00407	1117/946 (680/576)	1.75058 x 10^5 (25.39)
1.322 (2.914)	20444/ 14553	0.00467/ 0.00418	842/705 (512/429)	9.84364 x 10^4 (14.277)

.7 COLD-CASE PERFORMANCE

The cold-case analysis was performed to verify that the radiator system performance was adequate in a minimum external heating environment with a minimum heat rejection requirement. For this case the heat load was reduced to 281 watts from the fuel cell, which results from a 600 watt electrical load. The external environment was reduced to no external heating being applied to the radiators, which would result from the vehicle longitudinal axis aligned to look at the sun.

The predicted radiator performance indicated that this environment could be flown under minimum heat load conditions without experiencing excessively cold fluid temperatures. The radiator flow was controlled at 12% of full flow.

Figures 6-23, 6-24, and 6-25 present the major fuel cell fluid temperatures. Figures 6-23 and 6-24 present the fluid inlet and outlet temperatures for the fuel cell side of the regenerator. Figure 6-25 presents the coolant temperature control valve outlet temperature. As discussed in the hot case, the high flow in this loop and the restricted response of the coolant temperature control valve resulted in the negative peak in fluid temperatures. The inlet to the fuel cell was maintained at 352.8°K (175.3°F).
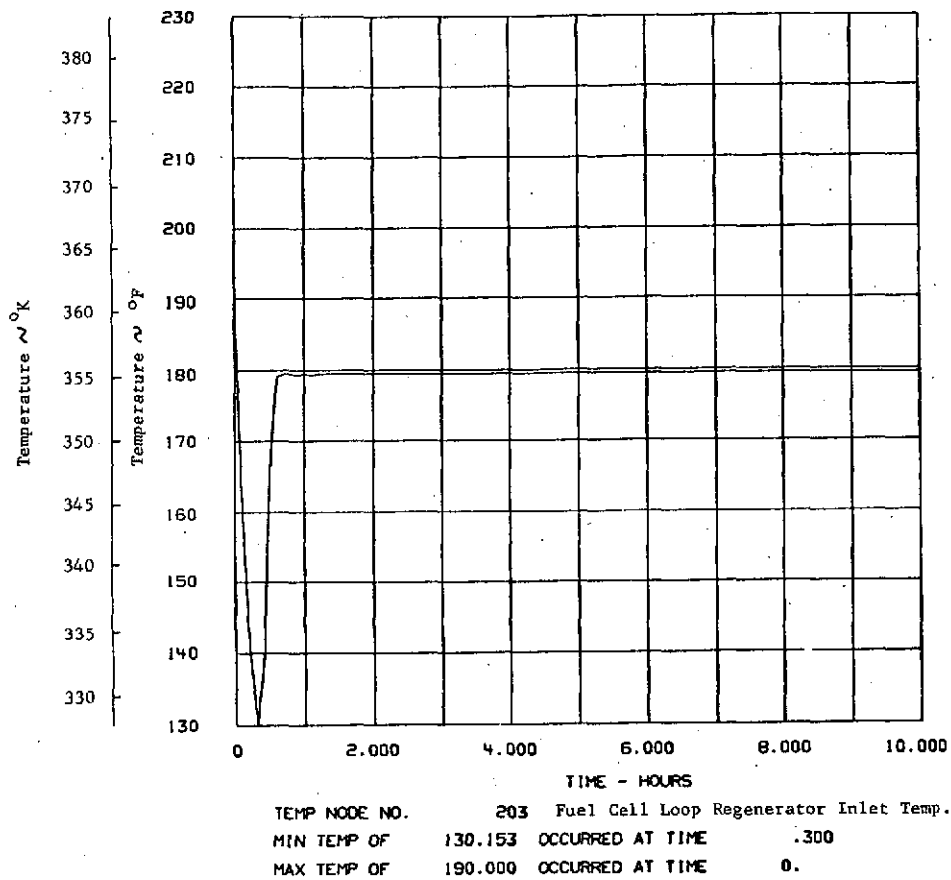
FIGURE 6-23 RADIATOR COLD CASE

TEMP NODE NO.   203   Fuel Cell Loop Regenerator Inlet Temp.
MIN TEMP OF   130.153 OCCURRED AT TIME   .300
MAX TEMP OF   190.000 OCCURRED AT TIME   0.
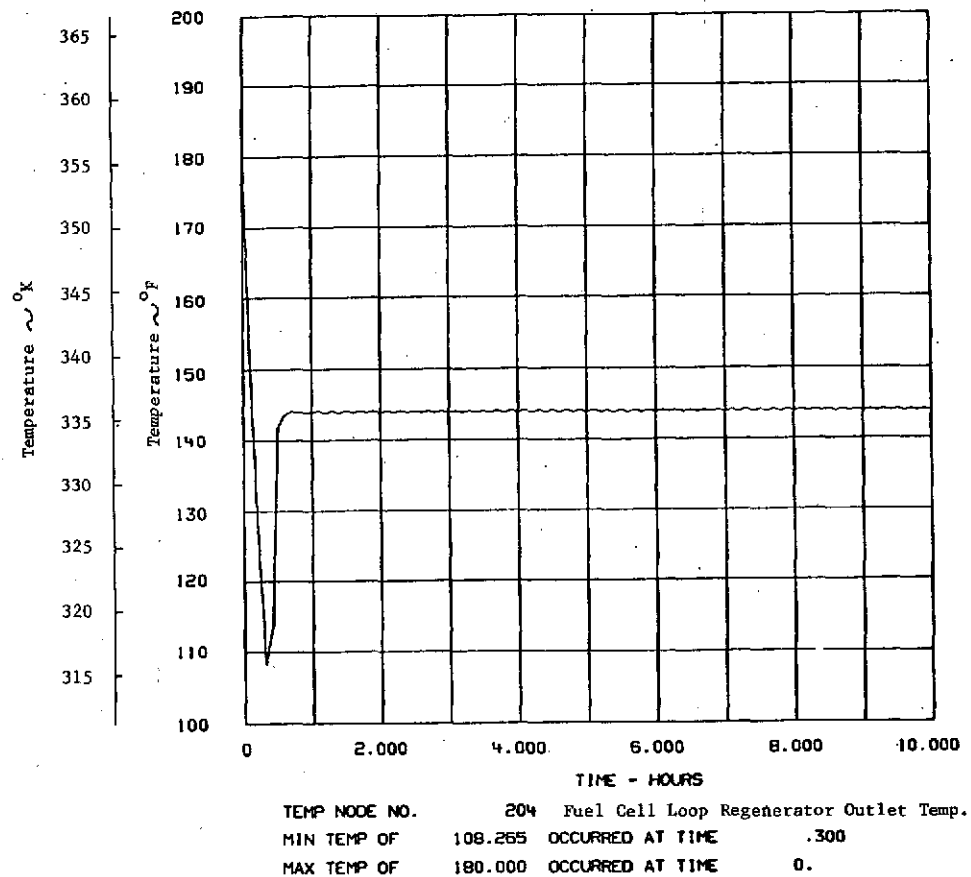
FIGURE 6-24 RADIATOR COLD CASE

TEMP NODE NO.   204   Fuel Cell Loop Regenerator Outlet Temp.
MIN TEMP OF   108.265 OCCURRED AT TIME   .300
MAX TEMP OF   180.000 OCCURRED AT TIME   0.

TEMP NODE NO.   205 Fuel Cell Loop Coolant Temperature Control
MIN TEMP OF   125.373 OCCURRED AT TIME   .300   Valve
MAX TEMP OF   175.316 OCCURRED AT TIME   2.000

FIGURE 6-25 RADIATOR COLD CASE

TEMP NODE NO.   1   Radiator Fluid Inlet Temperature
MIN TEMP OF   121.023 OCCURRED AT TIME   .300
MAX TEMP OF   180.000 OCCURRED AT TIME   0.

FIGURE 6-26 RADIATOR COLD CASE

The radiator inlet temperature showed a similar negative peak with
a resultant temperature of 344.3°K (160°F), Figure 6-26. Of major
interest in this run was the radiator outlet fluid temperature,
as shown in Figure 6-27, which leveled out at 227.6°K (-50°). For
the chosen fluid in the radiator loop, Freon E-1, this temperature
is well above the freezing temperature of 119°K (-246°F). Figure
6-28 presents the radiator thermal control valve outlet tempera-
ture and shows that control was achieved as desired at just under
333°K (140°F). The negative peak shown in the figure also resulted
from restricting the valve response. This figure also corresponds
to the regenerator cold side inlet temperature. Figure 6-29 shows
the regenerator outlet temperature was maintained at 343°K (158°F).

Figures 6-30 and 6-31 present the heat rejected from the radiator
loop fluid and by radiation from the radiators. Figure 6-32 pre-
sents the radiator mass flow with control maintained at 0.215 kg/
minute (0.474 lb/minute), which represents 12% of full flow.

Figure 6-33 presents the heat flow across the regenerator and Fig-
ure 6-34 presents the fuel cell mass flow through the regenerator.

The flow through the radiators resulted in Reynolds Numbers ranging
from 2554 at the inlet to 589 at the outlet. This represents flow
in the lower end of the transition region to fully developed laminar
flow. The Colburn J-Factors derived from Figure 6-7 ranged from
0.0024 at the inlet to 0.0084 at the outlet, with the minimum of
0.0021 achieved in the fourth tube of the first panel. Correspond-
ingly the heat transfer coefficients ranged from 238 $\frac{watts}{meter^2 \, °K}$ (42
Btu/hr-ft^2-°F) at the inlet to 324 $\frac{watts}{meter^2 \, °K}$ (57 Btu/hr-ft^2-°F) at
the outlet. The minimum coefficient, 173 $\frac{watts}{meter^2 \, °K}$ (30.5 Btu/
hr-ft^2-°F) was in the fourth tube. The pressure drop through the
radiators was 2096 N/m^2 (0.304 psi). The low pressure drop il-
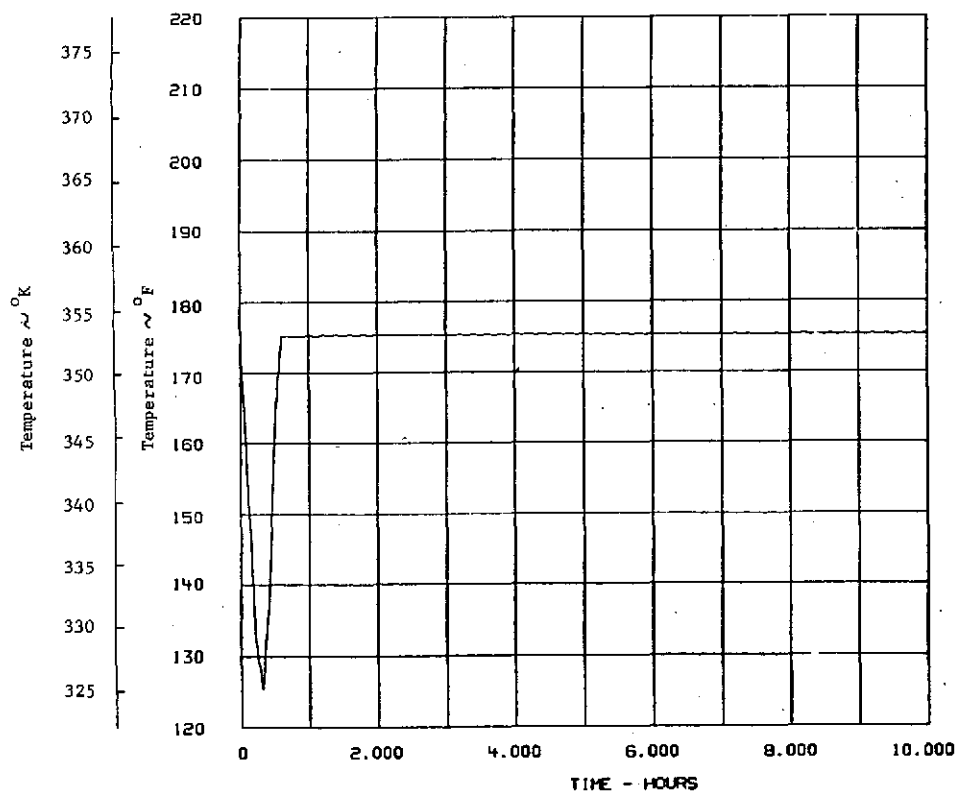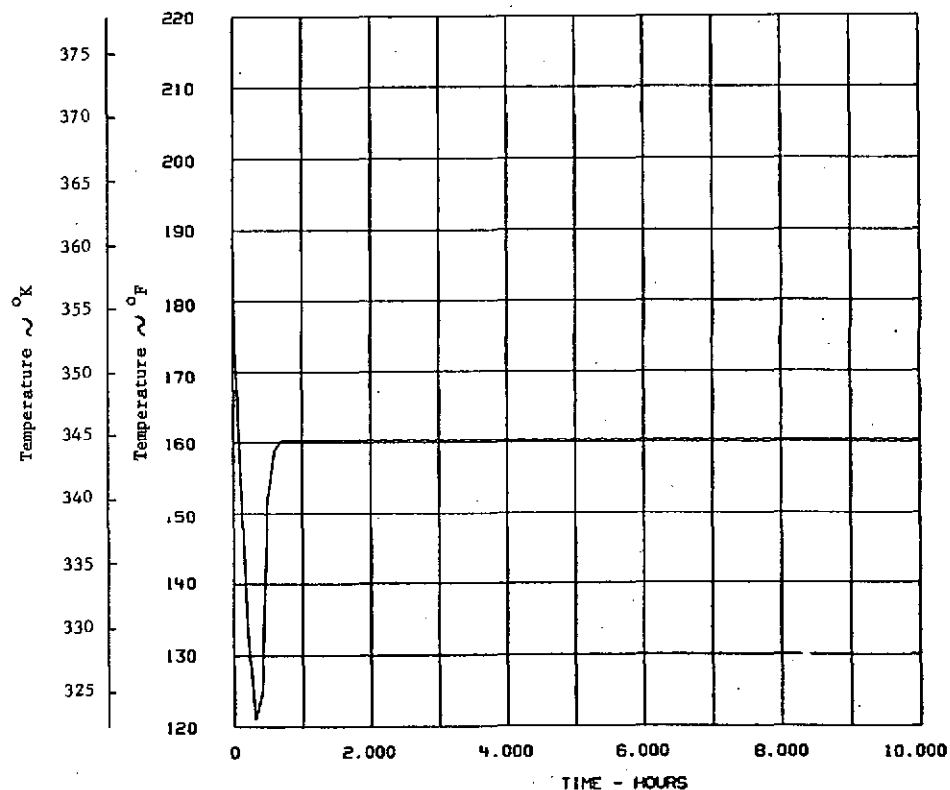lustrates one of the desirable features of the bypassed radiator
design, which allows low pressure drops in the radiator loop dur-
ing cold fluid conditions while achieving essentially a constant
pressure drop in the pump loop.

The transitional flow through the radiators permits the fluid to
be decoupled slightly from the radiators, thus allowing warmer
fluid temperatures and higher flow rates to be maintained. The
Colburn J-Factor approach to radiator design has not been pursued
to any great extent by the industry except on the Transtage ra-
diators, which have experienced seven successful flights. The
Transtage design did not, however, require the full transition
region to satisfy the design requirements operating down to Reynolds
numbers of 7000. The Airlock Module radiator on Skylab was suc-
cessfully and predictably operated at Reynolds numbers up to 2500.
Hence, before pursuing the radiator design further, it would be
desirable to conduct some breadboard level testing on a four-tube
panel to explore and verify the heat transfer and pressure drop
characteristics through the transition region.

TEMP NODE NO.   32 Radiator Fluid Outlet Temperature

MIN TEMP OF   -51.996 OCCURRED AT TIME   1.000

MAX TEMP OF   180.000 OCCURRED AT TIME   0.
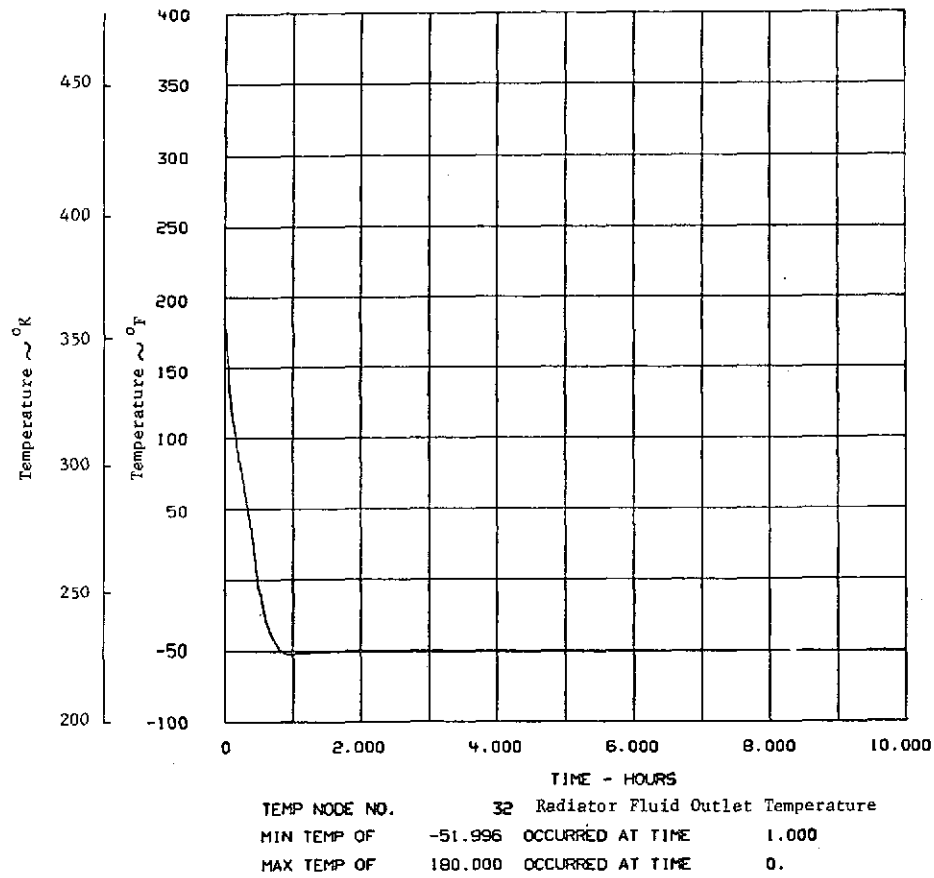
FIGURE 6-27 RADIATOR COLD CASE

TEMP NODE NO.   33 Radiator Loop Thermal Control Valve Fluid Outlet Temperature

MIN TEMP OF   99.216 OCCURRED AT TIME   .300

MAX TEMP OF   140.539 OCCURRED AT TIME   .600
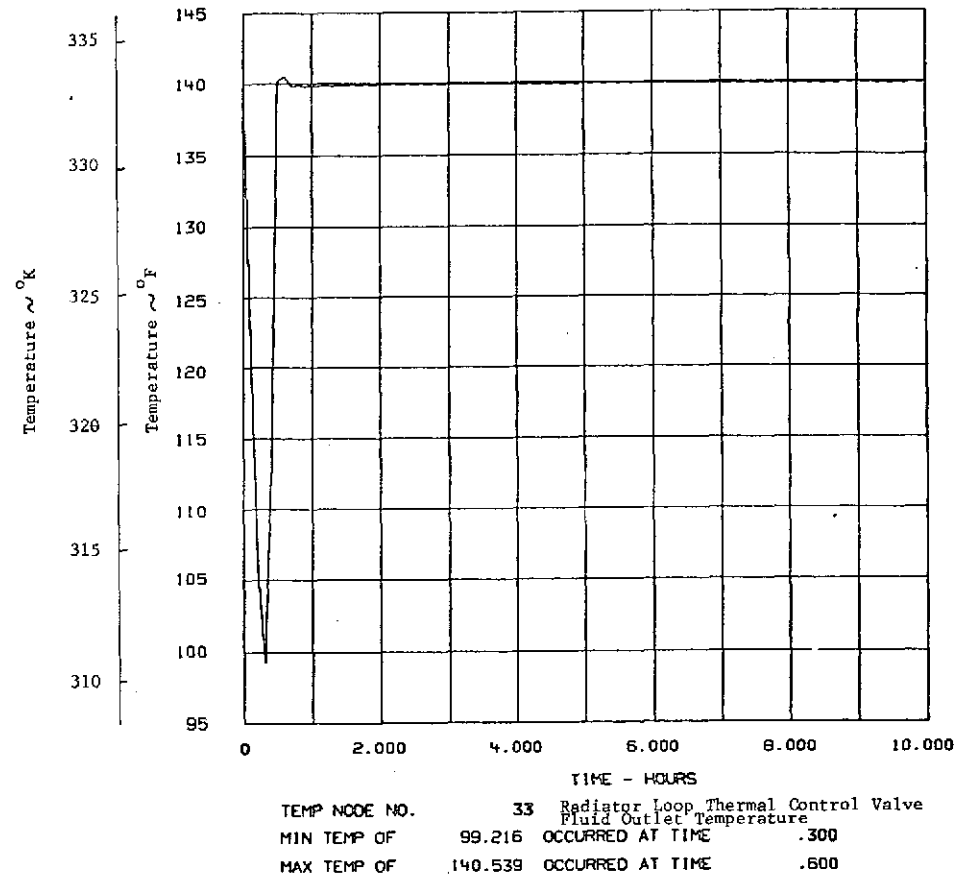
FIGURE 6-28 RADIATOR COLD CASE

TEMP NODE NO.   35   Radiator Loop Regenerator Outlet Temp.

MIN TEMP OF   117.921   OCCURRED AT TIME   .300

MAX TEMP OF   180.000   OCCURRED AT TIME   0.
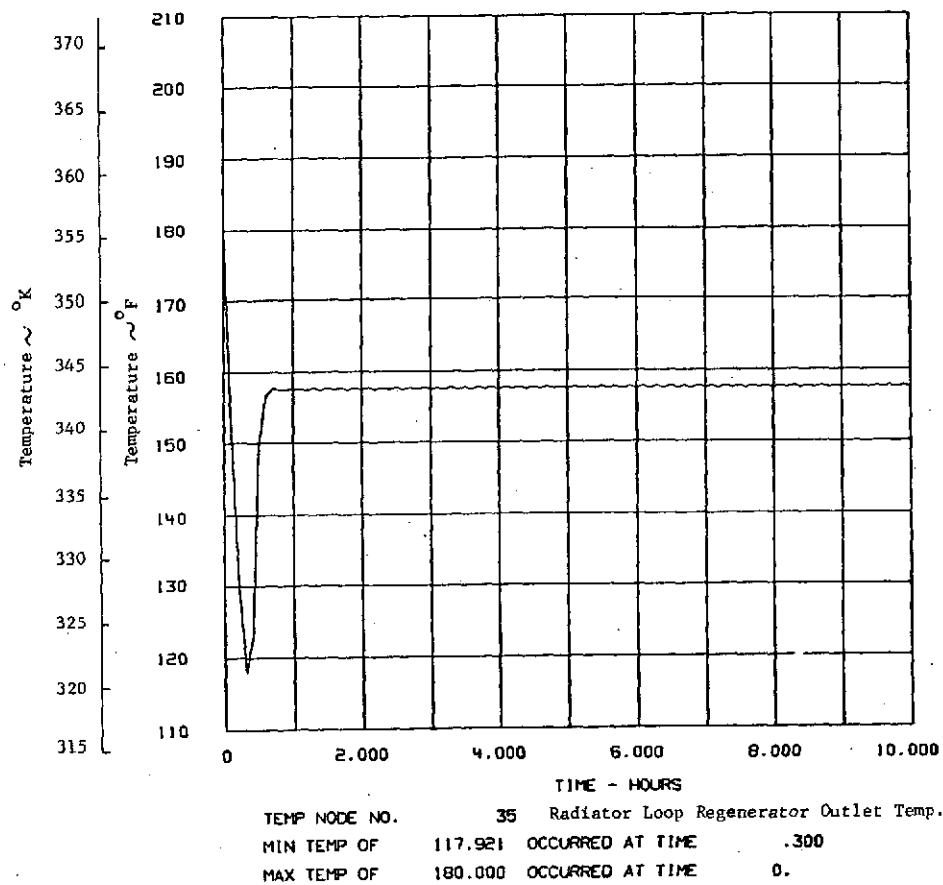
FIGURE 6-29 RADIATOR COLD CASE

NODE NO.   300   Radiator Fluid Heat Rejection

MIN   OF   0.   OCCURRED AT TIME   0.

MAX   OF   2102.452 OCCURRED AT TIME   .100
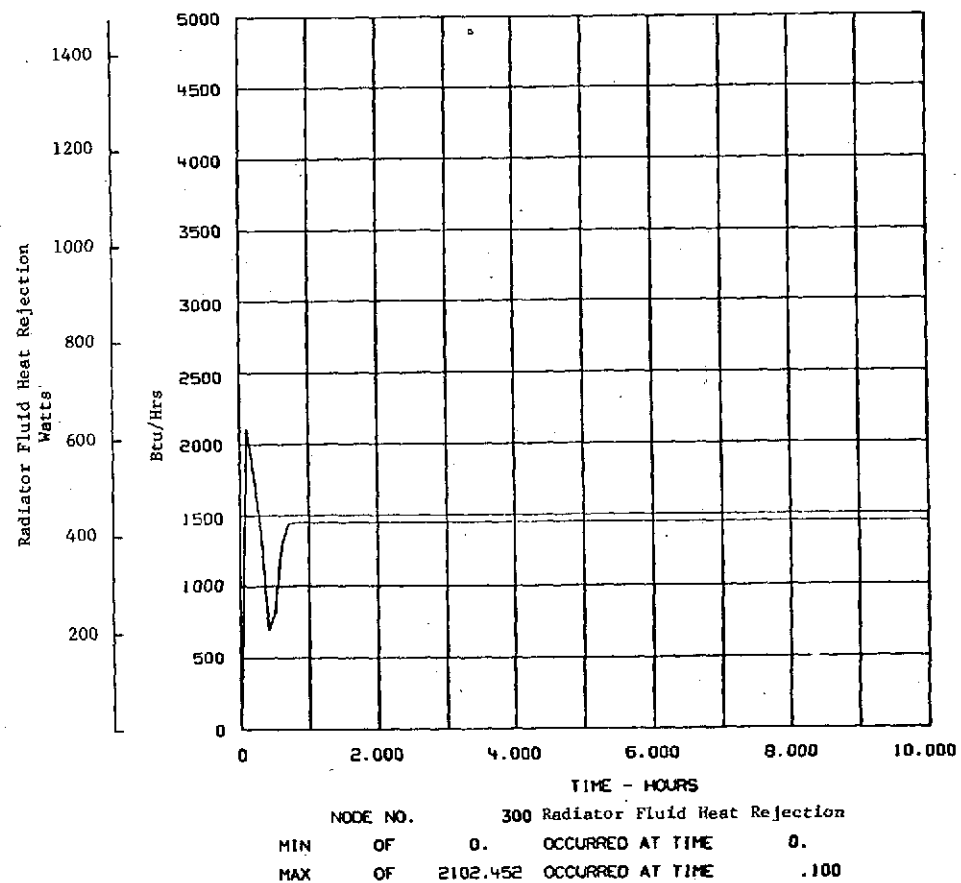
FIGURE 6-30   RADIATOR COLD CASE
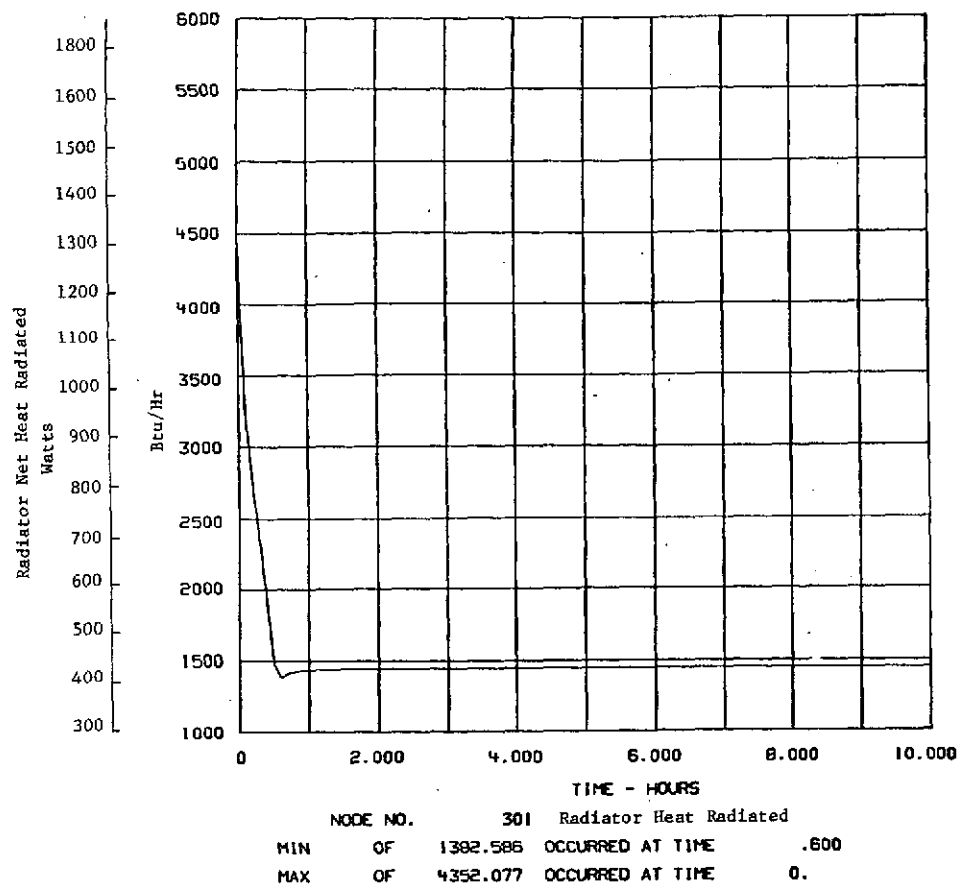
FIGURE 6-31   RADIATOR   COLD CASE
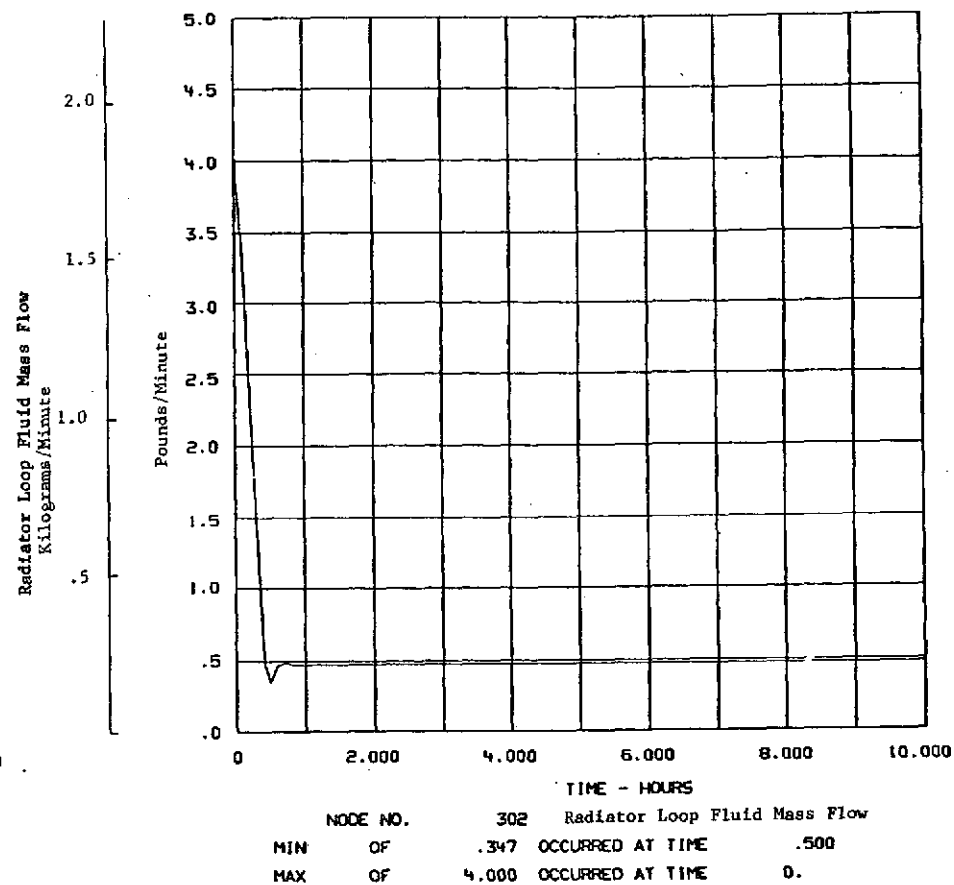
FIGURE 6-32   RADIATOR   COLD CASE

FIGURE 6-33   RADIATOR   COLD CASE
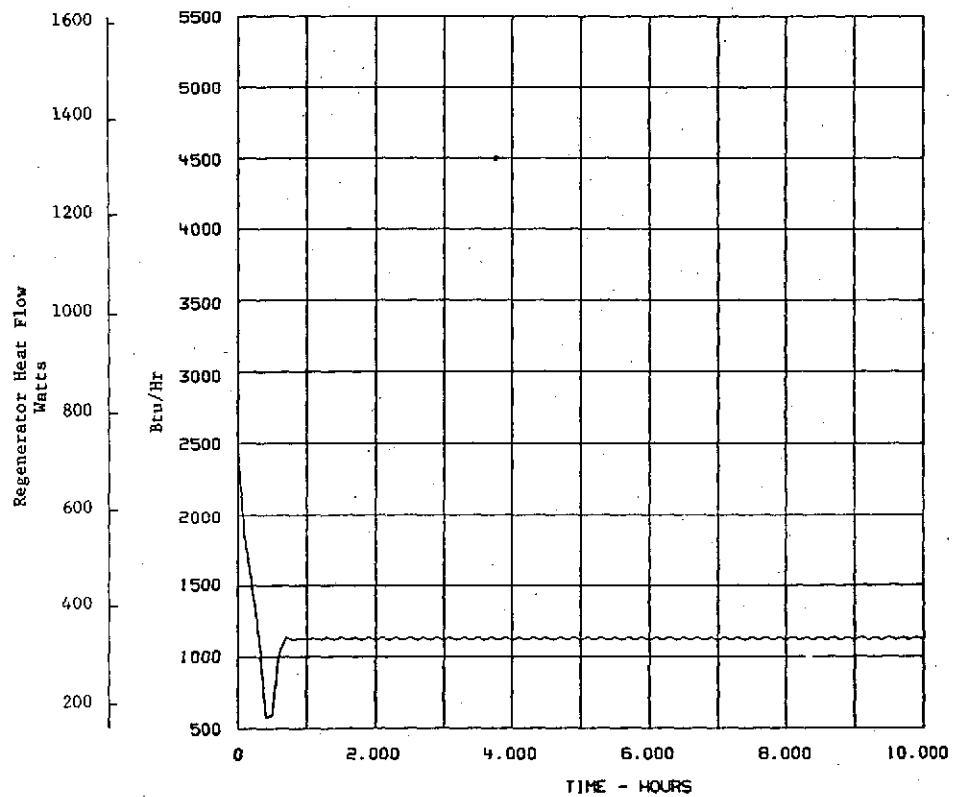
NODE NO.   303   Regenerator Heat Flow

MIN	OF	573.748	OCCURRED AT TIME	.400
MAX	OF	2442.045	OCCURRED AT TIME	0.

FIGURE 6-34   RADIATOR   COLD CASE
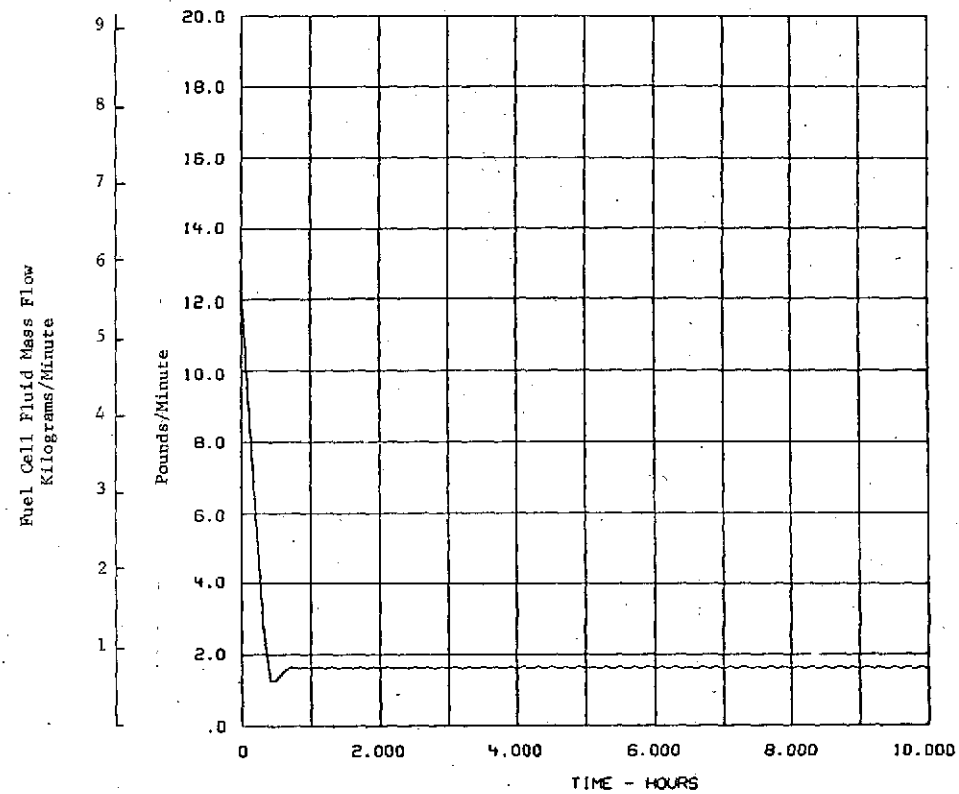
NODE NO.   304   Fuel Cell Fluid Mass Flow

MIN	OF	1.267	OCCURRED AT TIME	.500
MAX	OF	12.421	OCCURRED AT TIME	0.

8   SPECIFICATIONS

Design and performance parameters of the fuel cell heat rejection
system are documented in the form of a specification and are pre-
sented in Appendix I.

7. FURTHER CONSIDERATIONS

The Tug design confronts the state of the art in several areas. Inherent in the Tug mission is the goal of maximizing the payload delivery and retrieval capability. This has resulted in significant minimum weight requirements being placed on all systems. When designing the structural system, structural designers have been forced to explore the extensive use of composite structural designs aimed at a minimizing weight.

7.1 HONEYCOMB STRUCTURES

A honeycomb design for the forward skirt of Tug, for example, has been proposed by most investigators. While this appears to provide a minimum weight design, further tradeoffs are necessary before arriving at the preferred baseline. The past use of the aluminum skin stringer-longeron design, while being potentially heavier than the honeycomb design, has afforded the thermal designer a significant amount of flexibility. Use of the skin as a radiation skink for compartment heat dissipation was a simple and reliable means of achieving thermal control. However, the application of honeycomb designs in this area adds an unknown to the problem, and in some cases would result in significant thermal design problems.

Heat transfer through thin aluminum skin panels results in small temperature drops ($<<1°K$) and is usually considered to be zero. The honeycomb material represents two surfaces separated by a core material through which heat must be transferred. Depending on the core material and the bondline characteristics, large temperature drops can result when transferring the required heat. The use of high conductivity materials such as aluminum is required because the major mode of heat transfer through the honeycomb is via conduction. The use of fiberglass or other low conductivity materials would severely impact the internal compartmental temperature in the hot case and would require large holes in the skirt to allow heat to be dissipated in local areas. To achieve the required strength characteristics such a design would probably eliminate the weight advantages gained. Continued development of lightweight skirt structural concepts should include an evaluation of the thermal design impact that each concept might yield. One of the key requirements in a supporting thermal evaluation would be to determine experimentally the thermal characteristics of each candidate concept.

7.2   APS THERMAL DESIGN

The thermal design of the auxiliary propulsion system (APS) was not specifically investigated in this study. However, experience in the design and flight of the Transtage hydrazine attitude control system provides several guidelines. The selection of a hydrazine system for Tug will simplify the thermal design problem and will make it an integral part of limit cycling requirements of the system. The thruster module thermal design is the primary concern. Depending on the individual thruster design, heat is required to maintain the catalyst temperature at some minimum level to ensure that the desired minimum impulse can be delivered upon demand. The Transtage system used engine heat to maintain the catalyst bed temperatures above 450°K (350°F). Normal limit cycling of the engines required by the guidance system to maintain the required vehicle attitudes was sufficient to supply the major portion of required heat. Computer software was added to account for the fuel consumption over 10-minute periods, comparing that against predicted cold-case fuel consumption requirements. Shortage of the required cold-case fuel consumption in any 10-minute flight interval resulted in a burn of the required thruster to make up the difference. Hence, the design used the propellant consumption instead of heaters to satisfy module thermal design requirements. Further, definition of the Tug module and engine design will be required before a thermal design can be determined. Local application of high temperature fiberous insulation will be required.

The APS propellant storage and feed system will require insulation and thermostatically controlled heaters to eliminate propellant freezing. This should not represent a significant problem. In addition, the application of low conductance tank and feedline supports will be required.

8. THERMAL CONTROL SYSTEM SPECIFICATIONS AND DESIGNS

Thermal control system specifications were developed for those
problem areas that required the application of specific thermal
control devices. It was not considered necessary to develop a
specification for the use of insulation and/or heaters. The spec-
ifications are presented in the Appendixes to this report.

The fuel cell heat rejection system specification (Appendix I) out-
lines the basic system's thermal design requirements. Appendix
II presents the louver specification for application to the thermal
control of the battery.

Appendix III presents the specification for development of the
forward compartment thermal design using circumferential heat pipes,
louvers, and thermal conditioning panels. The panels will provide
a means to control those equipment items with low duty cycles,
such as the laser radar, its associated electronics, and the TV
cameras. Mounting these equipment items with other equipment which
operate throughout the mission will allow components to share
heat, thus reducing heat power requirements. This also provides
structural panels for mounting the equipment. The heat pipes avoid
excessively high or low skin temperature during constant attitudes
and further enable heat to be shared between the thermal condition-
ing panels.

9. FOLLOW-ON PLAN

Several areas were identified for future study and test to lead
to an orderly development of the Tug vehicle. In a study of this
nature as many questions are identified as are answered during
the course of the study.

9.1 STUDY AREAS

As the avionics system evolves in the future, the power dissipation
level is expected to change. This will require altering the paint
pattern and possibly revising heater power for some components.
Component placement and arrangement studies on the thermal con-
ditioning louver panels is warranted to further develop this tech-
niques. Parametric studies investigating panel Q/A, equipment
Q/A, component arrangement, matching of qualification requirements,
proper mix of high and low duty cycle, and environment temperature
ranges should be pursued to identify the capabilities and limita-
tions of this concept. The APS thermal control will require some
future investigations as that system evolves. The use of heater
power to maintain the catalyst temperature may be required; how-
ever, the limit cycle pulsing of that system will contribute sig-
nificantly to maintaining the desired temperatures. Early identi-
fication of timelines will be essential to develop the engine mod-
ule thermal design.

9.2 TESTING

Breadboard testing in several areas of the Tug thermal design is
warranted at this time. Two areas will be explored in the follow-
on to this contract. The application of louvers to the thermal
control of the battery is currently being examined along with the
performance of a thermal conditioning panel that will be coupled
with a heat pipe radiator. Thermal conditioning panel capabilities
will be further demonstrated. The design of a variable conductance
heat pipe radiator will be verified. The successful demonstration
of the radiator design will lend confidence in the credibility of
heat pipe systems to satisfy the fuel cell heat rejection system
requirements.

The pumped fluid system described here deserves further attention.
The proposed design requires some breadboard-level testing to veri-
fy the radiator's operation through the transition region. This
testing will verify the techniques used in the analytical models
for design and mission analysis.

Testing should also be performed to determine the effective thermal
conductance through honeycomb skin panels. The major unknown is
the influence of the two bondlines on the overall conductance.
The data generated in the study indicate that the forward compart-
ment thermal design is sensitive to this conductance. This could
have a severe impact on the compartment design concept.

The forward compartment heat pipes were envisioned as single closed
circular pipes. Current technology in heat pipes has generally
been limited to relatively short pipes. One 4.6-m-diameter pipe
has been built and tested (Ref 18). Continued development in this
area is warranted.

10. CONCLUSIONS

The analysis has shown that thermal control of Tug, exclusive of
the fuel cell, can be maintained through the use of surface coat-
ings, heat pipes, insulation, and louvers. Components can be
maintained within their temperature limits by using isolation
mounts, surface coatings, multilayer insulation, and in some
cases thermostatically controlled heaters. A second component
thermal control approach using thermal conditioning panels was
also investigated, which reduced the required heater power. Both
hot and cold environments for a simulated Tug mission were used
to analyze the thermal control techniques. The analysis was per-
formed for no orientation constraints during the Tug mission, thus
providing flexibility in satisfying future payload requirements.

The transient analysis of the forward compartment used a paint
pattern ($\alpha/\epsilon = 0.5$) derived from the steady-state parametric
studies using 800 watts of internal power. However, initial
transient analyses resulted in both hot and cold problems, with
a high power (187 watts) tape recorder which had a narrow operat-
ing range of 289°K to 314°K (60°F to 105°F). A tape recorder that
dissipated 8.4 watts was substituted. With the new power level
for the tape recorder, the actual average power dissipation for
the forward compartment was reduced to approximately 600 watts.
Based upon this power level a new value of $\alpha/\epsilon = 0.60$ is necessary
to maintain the temperature level of the forward compartment at
297°K (75°F). This would replace the original $\alpha/\epsilon = 0.2375/0.475 =
0.50$. An α/ϵ of 0.6 is obtainable using an α of 0.24 and $\epsilon = 0.40$.
This results in a paint pattern ratio of aluminum to white equal
to 75% to 25%.

In addition to the high-power tape recorder that was subsequently
replaced with a tape recorder of moderate power, other components
were marginally acceptable in regards to their temperature limits.
These include the laser radars and the laser radar electronics.
These components have a very high lower temperature limit in both
the operational and storage phases of the mission (operational
minimum = 293°K (68°F), maximum = 323°K (122°F); storage minimum =
288.7°K (60°F), maximum = 323°K (122_K)). A large amount of heater
power is required to maintain their temperatures, even in the hot
case. Heater power for these components for the hot case included
84 watts for each of the laser radars and 65 watts for each of
these four components while the rest of the components require
less than 5 watts for this case. This indicates that these par-
ticular components should be requalified to temperatures more in
line with the rest of the forward compartment components or ad-
ditional thermal design features incorporated into individual
components.

Many components exceeded their lower temperature limits in the cold-case simulation. However, this simulation used an unusually cold environment. This environment occurs only if the Tug longitudinal axis is maintained parallel to the solar vector and there is no significant planetary or albedo flux (i.e., Tug in a geosynchronous orbit). All of these component problems could be solved with additional heater power, further component isolation, and altering paint patterns. However, this reduces the flexibility of the design by making the component temperatures approach their upper limit in a hot case.

An alternative to the complex task of optimizing the isolation and heater power of each component is a new component mounting concept. In this concept, by grouping individual components with regard to electrical power output duty cycle and temperature limits on thermal conditioning panels, a reduction in heater power requirements in both hot and cold conditions can be obtained.

The thermal conditioning panels (see Appendix III) are mounting panels containing integral heat pipes and provide a means of obtaining an isothermal condition. Components are hard mounted to one side of the panel with a louver system on the other. The louvered side faces the compartment wall, which is maintained at a uniform temperature by circumferential heat pipes. The panel temperature is primarily controlled by the modulation of the temperature-sensitive louver blades. This concept offers a passive means of component control by allowing excess electrical power generation to be shared in maintaining other nonoperating components on the panel above their lower temperature limit.

11. REFERENCES

----

1. T. L. Ward: *Space Tug Thermal Control Equipment Thermal Requirements, Characteristics and Constraints Catalogue User's Guide*. MCR-74-144. Martin Marietta Corporation, Denver, Colorado, April 1974.

2. T. L. Ward: *Space Tug Thermal Control Equipment Thermal Requirements, Characteristics and Constraints Catalogue*. MCR-74-145. Martin Marietta Corporation, Denver, Colorado, April 1974.

3. "Space Shuttle and Spacelab Discussions. SSV73-58 (Contract NAS9-14000). Rockwell International Space Division, October 1973.

4. R. J. Conner, *et al.:* "Martin Interactive Thermal Analysis System (MITAS)." MDS-SPLPD-71-FD238. Martin Marietta Corporation, June 1971.

5. T. R. Scollon, Jr. and M. J. Carpitella: *Long Life High Reliability Thermal Control Systems Study Data Handbook*. (Contract NAS8-26252). Space Systems Organization, General Electric Company, Valley Forge Space Technology Center, December 1971.

6. G. A. Robinson: "Heat Pipe Technology Review. Presentation handouts for Marshall Space Flight Center, Huntsville, Alabama, August 1973.

7. J. P. Wright: *Thermal Investigation and Analytical Modeling of Heat Pipe Thermal Interface Techniques*. SD73-SA-086. Rockwell International Space Division, June 29, 1973.

8. "Baseline Tug Definition Document." National Aeronautics and Space Administration, Marshall Space Flight Center, Revision A, June 26, 1972.

9. C. L. Jensen, *et al.: Thermal Radiation Analyzer System (TRASYS)*. MCR-73-105. Martin Marietta Corporation, May 1973.

10. Dr. B. E. Lauer: "Heat Transfer Calculations." Reprinted from *Oil and Gas Journal*, 1953.

11. D. H. Elliott: "Thermal Conduction Across Aluminum Bolted Joints." ASME 65-HT-53, *American Society of Mechanical Engineers*, New York, August 1965.

12. Frank Dreith: *Principle of Heat Transfer*. Second Edition, International Text Book Company, Scranton, Pennsylvania, 1965.

13. L. M. Handley and R. C. Keifer: "Fuel Cells for Space Tug." Presentation handouts from Pratt & Whitney Aircraft Company, East Hartford, Connecticult, March 1973.

14. "Radiator Design for Space Vehicles." AiResearch Manufacturing Company, Los Angeles, California.

15. W. M. Kays, and A. L. Landon: *Compact Heat Exchangers.* Second Edition, McGraw Hill Book Company, New York, 1964.

16. "Flow of Fluids through Valves, Fittings and Pipe." Crane Technical Paper No. 410, Crane Company, Chicago, 1957.

17. James B. Heaney: *Evaluation of Commercially Supplied Silver Coated Teflon for Spacecraft Temperature Control Useage.* X-765-74-24. National Aeronautics and Space Administration, Goddard Space Flight Center, January 1974.

18. O. W. Clausen, B. D. Marcus, W. E. Piske, and R. C. Turner: *Final Report, Circumferential Heat Pipe Systems for Large Structures.* NASA-CR-114783. National Aeronautics and Space Administration, Manned Spacecraft Center, December 1970.

REVISIONS					
LTR	SH	DESCRIPTION		DATE	APPROVED

APPENDIX I

																	REV
																	SH
														REV	REV STATUS OF SHEETS	
														SH		

DRAWN BY T.R. Ward	DEPT 044	DATE	**MARTIN MARIETTA CORPORATION**
CHECKING			POST OFFICE BOX 179, DENVER, COLORADO
GROUP ENGR			
STRESS			
WEIGHT			SPACE TUG FUEL CELL HEAT REJECTION SYSTEM
CUSTOMER RPRSNTV			
PROGRAM RPRSNTV			

SIZE **A**	CODE IDENT NO. 04236	
SCALE	PAGE 1	SHEET

TABLE OF CONTENTS

SIZE	CODE IDENT NO.		
A	**04236**		
CHG			
SCALE		PAGE 2	SHEET

I-2 -68)

SYSTEM DESCRIPTION

The Space Tug fuel cell heat rejection system provides the means of maintaining the primary electrical power system, the fuel cell, within the desired operating temperature range during the tug mission. The fuel cell is activated in flight with power transfer occurring at $T + 3.877$ hours, and provides demand electrical power until $T + 97.634$ hours when power transfer to battery occurs.

During the mission the fuel cell rejects heat per Figure 1 and generates the byproduct water in the form of steam per Figure 2. Figure 3 is a simplified flow schematic of the fuel cell. Two major interfaces for the fuel cell heat rejection system are the internal fluid loop with the regenerator and the byproduct steam with the vent system.

The heat rejection system is comprised of the necessary plumbing and fittings, a redundant set of pumps, accumulators, thermal control valves, and controllers. The interface is accomplished with a single regenerator which has redundant secondary fluid loops. The 4 radiators are located in each quadrant around the intertank compartment with redundant fluid lines. Figures 4 through 6 schematically present the system.

The fuel cell fluid loop uses water or FC-40 Freon for a working fluid. The radiator system use E-1 Freon as the working fluid.

The fuel cell system is designed for a ΔT through the stack of $5.56^{\circ}K$ ($10^{\circ}F$) at electrical load of 1500 watts. This results in a heat rejection of 744.22 watts (2540 Btu/Hr). The coolant pump adds an additional 30 watts to the system. The coolant temperature control valve controls the stack inlet temperature within a nominal operating temperature range 349.67 to $355.2^{\circ}K$ ($170^{\circ}F$ to $180^{\circ}F$). The minimum flow to the regenerator at the lower temperature is 5 to 10% of full flow.

SIZE	CODE IDENT NO.		
A	**04236**		
CHG			
SCALE	PAGE 3		SHEET

FIGURE 1 - WASTE HEAT REJECTION

Waste Heat Watts / Btu/Hour vs NET OUTPUT ∼ KW
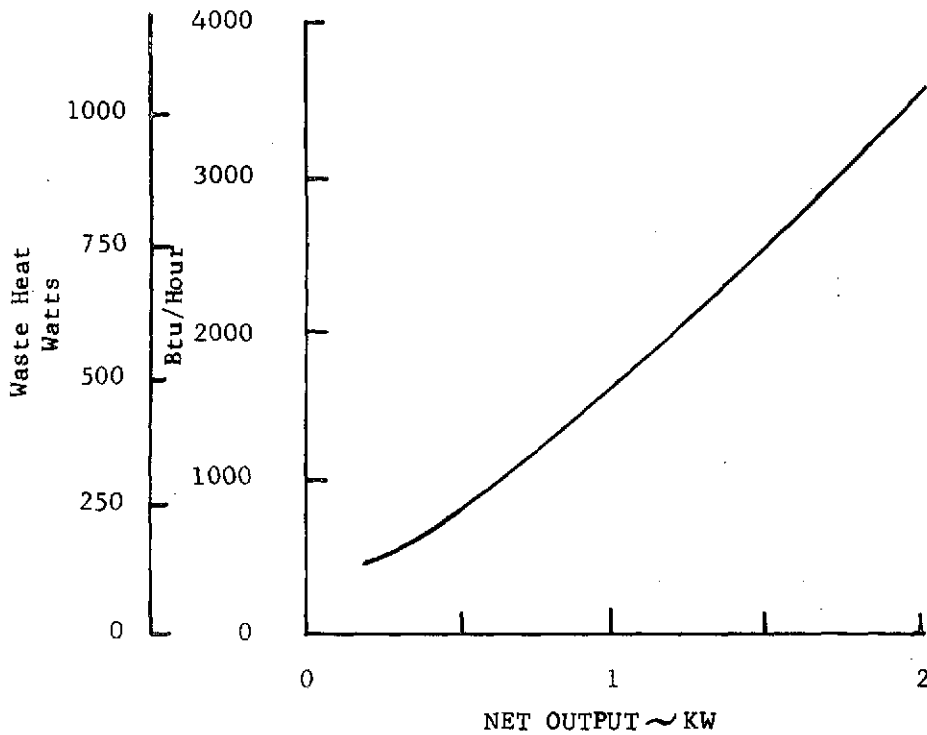
FIGURE 2 - REACTANT CONSUMPTION

Reactant Consumption Kilograms/Hour / Pounds/Hour vs NET OUTPUT ∼ KW
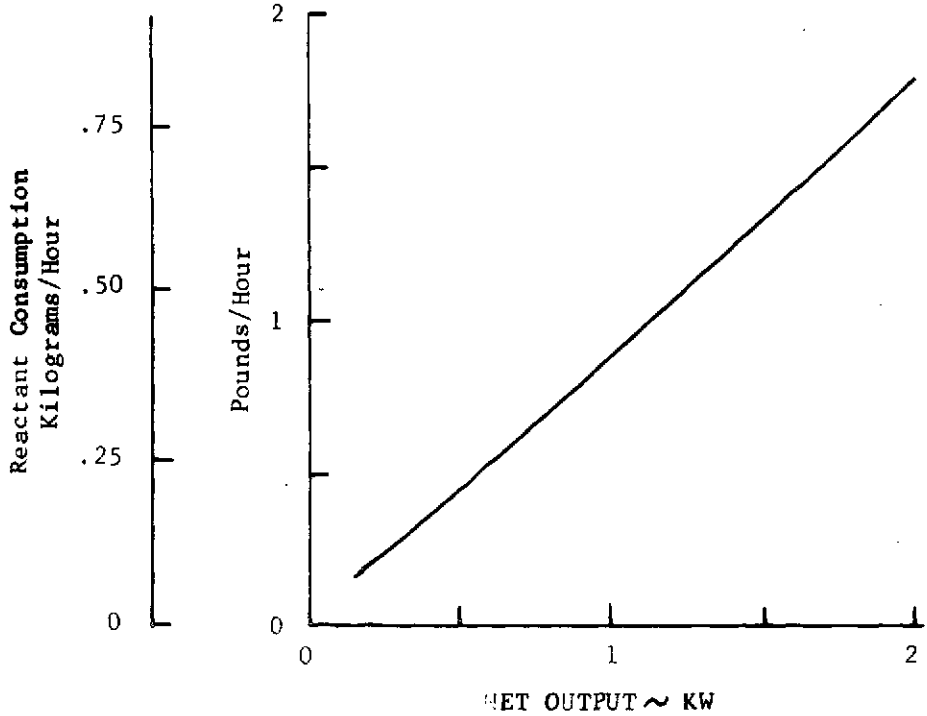
	SIZE	CODE IDENT NO.		
	A	**04236**		
CHG				
	SCALE	PAGE 4	SHEET	

FLOW SCHEMATIC

355.4°K

REGENERATOR
RETURN

COOLANT TEMP.
CONTROL VALVE

WARMUP HEATER

PURGE
VALVES

H_2O VENT

WATER VENT
REGULATOR

$2.758 \times 10^4 \dfrac{\text{NEWTONS}}{\text{METER}^2}$

4 PSIA

COOLANT O_2 CELL H_2 WTP H_2O VAPOR

ACCUMULATOR

1.103×10^5 NEWTONS/METER^2
16 PSI

360.9°K

TO REGENERATOR

COOLANT
PUMP

COUPLED REACTANT
PRESSURE REGULATOR

O_2 H_2
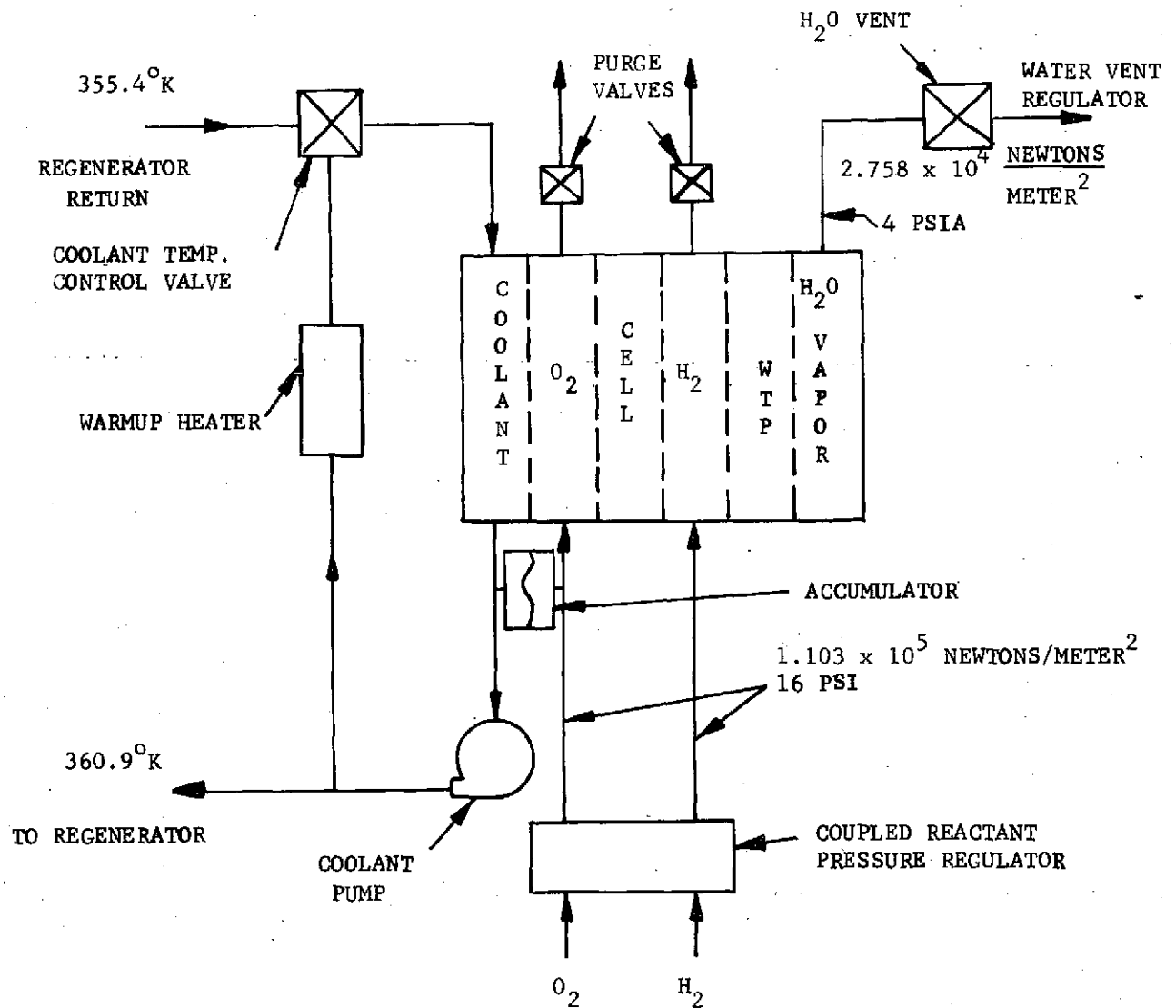
SIZE	CODE IDENT NO.	
A	**04236**	FIGURE 3 - FUEL CELL FLOW SCHEMATIC
CHG		
SCALE	PAGE 5	SHEET

PAINT PATTERN
AREAS

RADIATOR TYPICAL
4 PLACES

ACS MODULES
TYPICAL
4 PLACES

	SIZE	CODE IDENT NO.	
	A	**04236**	FIGURE 4 - TUG EXTERIOR
CHG			
	SCALE	PAGE 6	SHEET

RADIATORS

DETAIL B

DETAIL A

THERMAL CONTROL UNIT

RADIATOR DISCONNECTS

P_3 T_2

T_1

P_2

P_5

THERMAL CONTROL VALVE

T_3

P_4

ACCUMULATOR

F_1 PUMP

P_1

FILL DISCONNECT

REGENERATOR

FUEL CELL DISCONNECTS

SIZE	CODE IDENT NO.		
A	04236	FIGURE 5 — FUEL CELL HEAT REJECTION SYSTEM	
CHG			
SCALE	PAGE 7		SHEET

DETAIL A

.254 CM
(.1 IN)

.762 CM
(.3 IN)

.635 CM
(.25 IN)

.457 CM
(.18 IN)

.762 CM
(.3 IN)
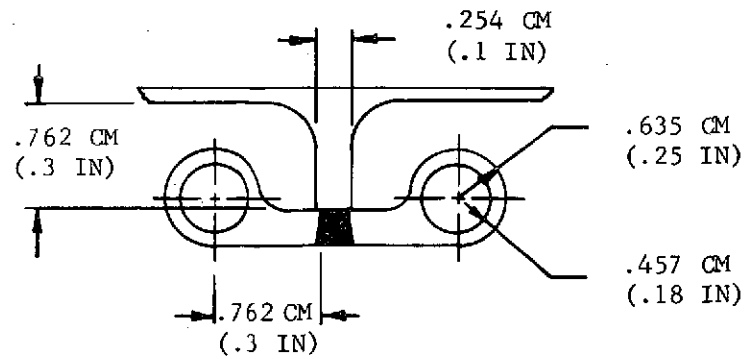
FLANGE THICKNESS

.254 CM
(.1 IN)

DETAIL B

FLANGE REMOVED
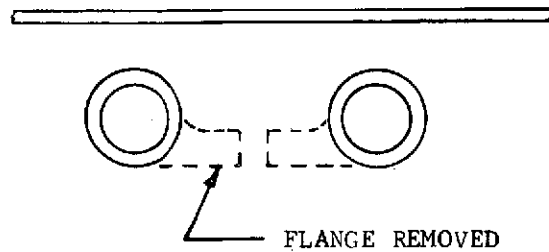
SCALE = 2/1

SIZE	CODE IDENT NO.	FIGURE 6 - RADIATOR DETAILS
A	04236	

CHG		
SCALE	PAGE 8	SHEET

The radiator system is a series - series-bypass flow system which has the radiators in series with flow through each radiator in series. The radiators are bypassed dependent upon the load by the thermal control valve which maintains a near constant fluid temperature to the regenerator of $333^{\circ}K$ ($140^{\circ}F$)

Micrometeorite protection is provided by using a redundant fluid loop and a P-tube rail concept as shown in Figure 6.

The regenerator, accumulators, pumps, thermal control valves, controls, and instrumentation will be packaged within a box designated as the Thermal Control Unit (TCU) as shown in Figure 5. The TCU and the Fuel Cell will be isolated from the inter-tank compartment by thermal washers and multi-layer insulation.

CHG	SIZE A	CODE IDENT NO. 04236		
	SCALE	PAGE 9	SHEET	

Fuel Cell Requirements:

1. Maintain the fuel cell radiant to the stack within the design operating temperature range of

   352.6 to 355.2 $^{\circ}$K (175 to 180°F) over the required heat load range.

2. The heat load range shall vary per Figure 1 with the 600 to 1500. The

   heat load is increased by 30 watts to account for the fuel cell pump heat

   dissipation.

Radiator System Requirements:

1. The system shall meet all fuel cell thermal requirements.

2. The system shall operate in earth orbit from 296 to 35750 kilometers (160 to

   19300 nautical miles) with no attitude constraints for an inclination of 28.5°.

3. The radiators shall provide micrometeorite protection for the fluid lines.

4. The fluid system shall have a redundant loop.

5. The regenerator inlet temperature shall be maintained at 333 $^{\circ}$K (140 $^{\circ}$F) $\pm$ TBD.

6. Regenerator flow shall be maintained at 1.814 kilograms/minute (4 lb$_{m}$/minute).

7. The working fluid shall be Freon E-1.

8. The regenerator (counter flow heat exchanger) shall exhibit a minimum effect-

   iveness of .900. The effectiveness (Eff) shall be defined as

$$
\text{Eff} = \frac{1 - e^{-NTU\ (1 - C_{min}/C_{max})}}{1 - \left(\frac{C_{min}}{C_{max}}\right) e^{-\ NTU\ (1 - C_{min}/C_{max})}}
$$

where:

$C = \dot{W}\,C_{P}$ W = mass flow rate

C_{min} = minimum enthalpy flow C_{P} = specific heat of fluid at constant pressure

C_{max} = maximum enthalpy flow

NTU = number of heat exchanger units

$= \dfrac{UA}{C_{min}}$

SIZE	CODE IDENT. NO.			
A	**04236**			
CHG				
SCALE		PAGE 10	SHEET	

U = overall heat exchanger conductance

A = heat exchanger area

9. Either fluid loop shall be capable of carrying the heat load to be dissipated.

10. The radiators shall be sized to dissipate the maximum heat load minimum altitude and maximum external absorbed heating.

11. The fluid shall not be permitted to freeze $119^{\circ}K$ ($-246^{\circ}F$) or reach highly viscous state.

12. The cold case shall be defined as the minimum heat load with no external flux on the radiators.

13. Radiator coating shall exhibit stable thermal properties.

14. Radiator shall be sized assuming an adabatic vehicle side.

SIZE	CODE IDENT NO.		
A	04236		
CHG			
SCALE		PAGE 11	SHEET

I-11

Predicted System Performance

Hot Case

Conditions:

1. Fixed attitude with respect to the sun. Normal sun to longitudinal axis
    with sun angle to center of 2 radiator panels of 45 degrees.

2. Attitude 296 kilometers (160 nautical miles).

3. $\beta = 52^O$ orbit.

4. Maximum electrical load 1500 watts.

5. Maximum heat dissipation is 744 watts plus 81 watts pump power.

Performance

See Figures 7 thru 10.

	SIZE	CODE IDENT NO.			
CHG	**A**	**04236**			
	SCALE		PAGE 12		SHEET

FIGURE 7

NET HEAT
REJECTED

Net Heat Rejected Watts

1000
950
900
850
800

Btu/Hr x 10^{-2}

34
32
30
28
26

Q RADIATED

Q FLUID

Mission Time - Hours
4   6   8   10

FIGURE 8

FLUID
FLOW

Fluid Flow Kilograms/Minute

2.0
1.5
1.0
.5

Pounds/Minute

4
3
2
1
0

Mission Time - Hours
4   6   8   10
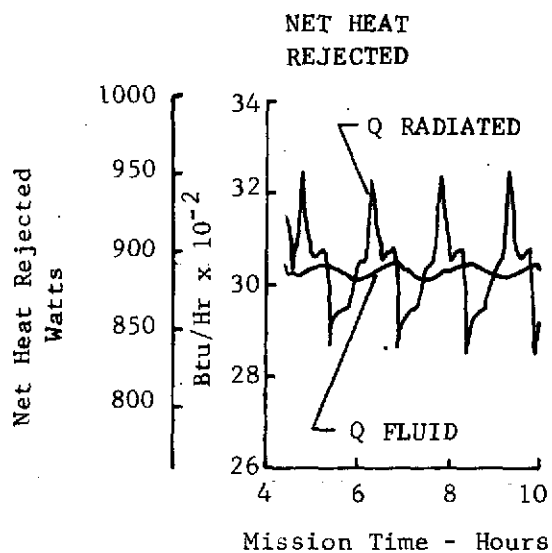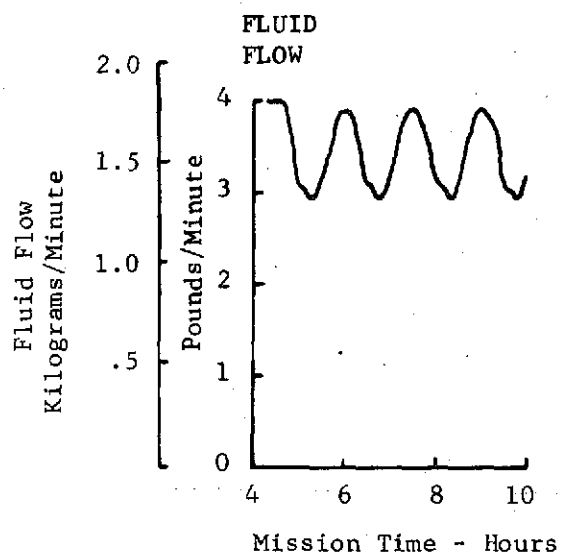
FIGURE 9 - RADIATOR FLUID TEMPERATURE

Fluid Temperature Degrees Kelvin

360
355
350
345
340
335
330
325

^{o}F

190
180
170
160
150
140
130
120

INLET

OUTLET

Mission Time - Hours
4   6   8   10

FIGURE 10

Radiator ΔP

Delta Pressure Newtons/Meter^2 x 10^{-3}

200
150
100
50
0

PSID

30
25
15
10
5
0

Mission Time - Hours
4   6   8   10
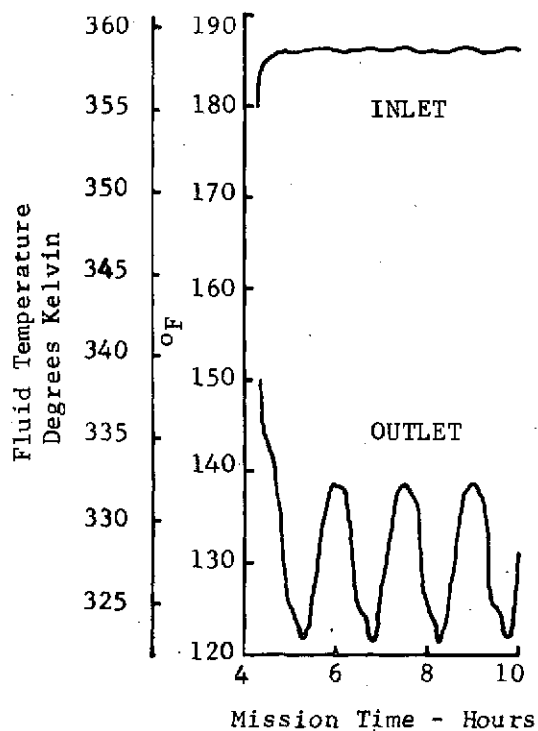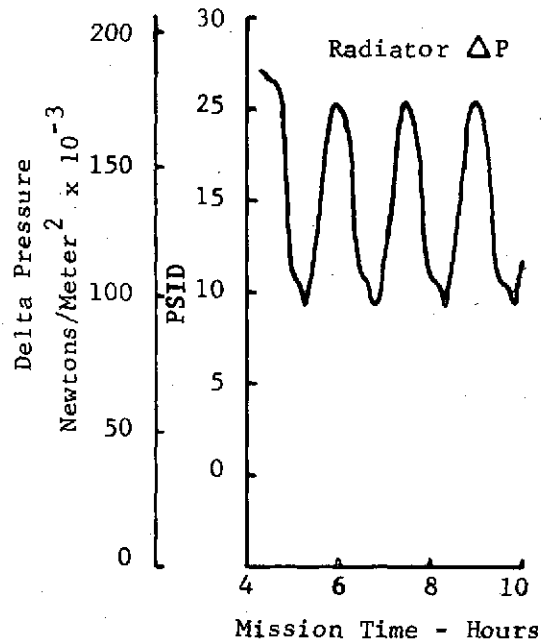
SIZE	CODE IDENT NO.		
A	04236	HOT CASE PERFORMANCE	
CAGE			
SCALE	PAGE 13		SHEET

a490(1-08)

I-13

Cold Case

Conditions:

1. Fixed attitude with respect to the sun (parallel to longitudinal axis).

2. Altitude 35750 kilometers (19300 nautical miles).

3. Minimum electrical load 600 watts.

4. Minimum heat load is 281 watts plus 81 watts pump power.

Performance   See Figures 11 thru 14.

Performance is based upon a transitional flow design where the fluid heat transfer

is based upon the Colburn J-Factor analogy per Figure 15.   The fluid heat

transfer coefficient is related to the J-Factor by the equation

$$h_c = J\ k\ N_R\ N_P^{1/3}\ (\mu_n/\mu_f)^{.14}/D$$

J   =   Colburn J Factor

k   =   Fluid Conductivity

N_R =   Reynolds Number

N_P =   Prandtl Number

μ_w =   Fluid Viscosity at the Tube Wall Temperature

μ_f =   Fluid Viscosity at the Average Fluid Temperature

D   =   Tube Internal Diameter

Performance is based upon an L/D per straight tube of 200.

	SIZE	CODE IDENT NO.	
CHG	A	04236	
	SCALE	PAGE 14	SHEET

FIGURE 11
RADIATOR FLUID TEMPERATURE

Inlet Temp.

Outlet Temp.

Time - Hours
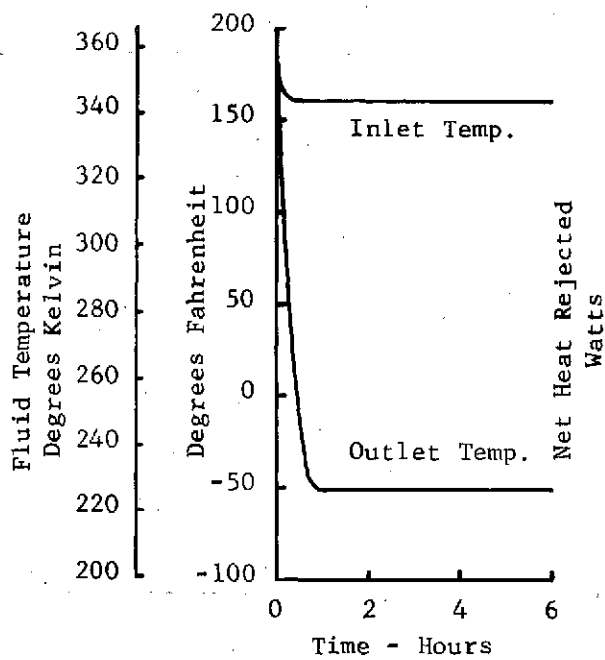
FIGURE 12
NET HEAT REJECTED

Q Radiated and Q Fluid

Time - Hours

FIGURE 13

Radiator ΔP

Time - Hours
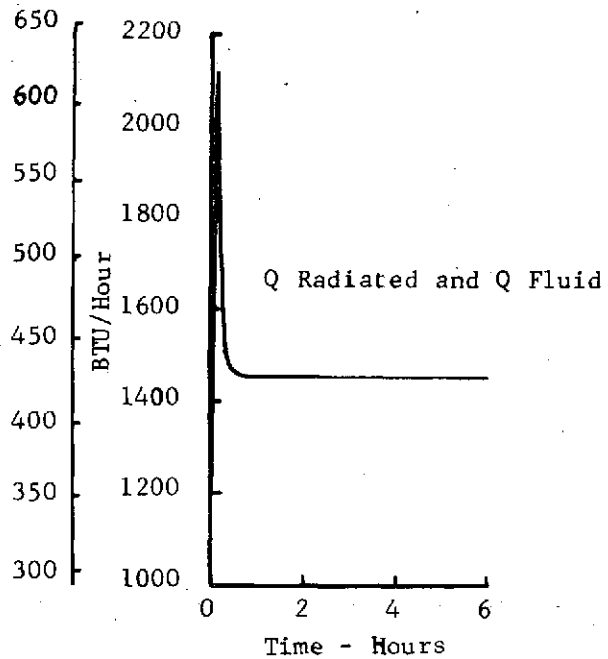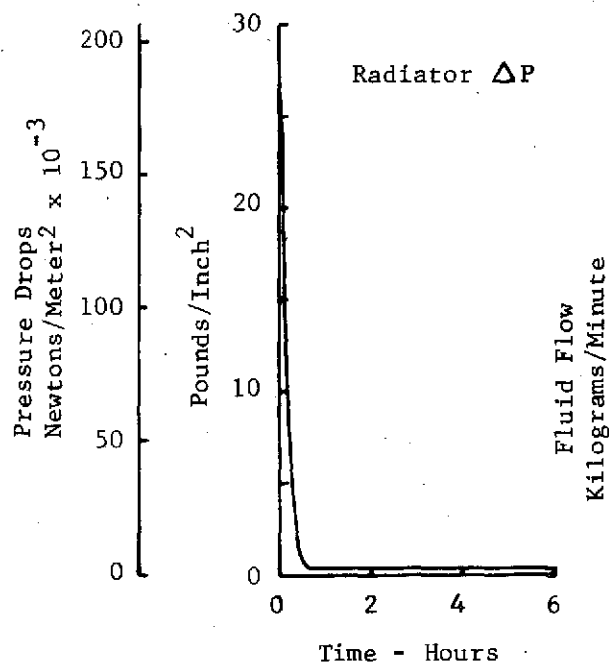
FIGURE 14
RADIATOR FLUID FLOW

Time - Hours
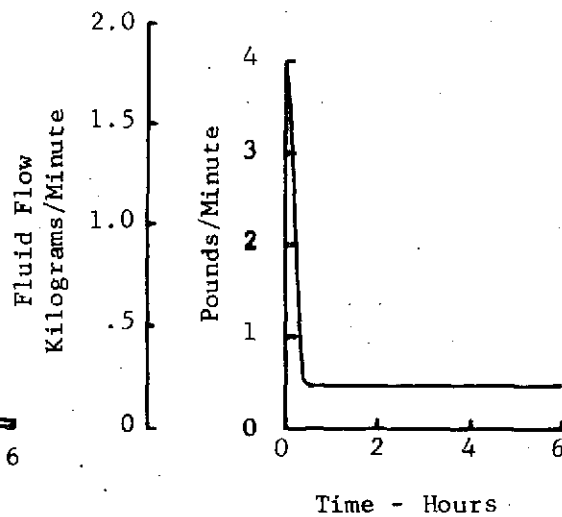
	SIZE	CODE IDENT NO.	
	A	**04236**	COLD CASE PERFORMANCE
CHG			
	SCALE	PAGE 15	SHEET

Colburn J-Factor vs Reynolds Number
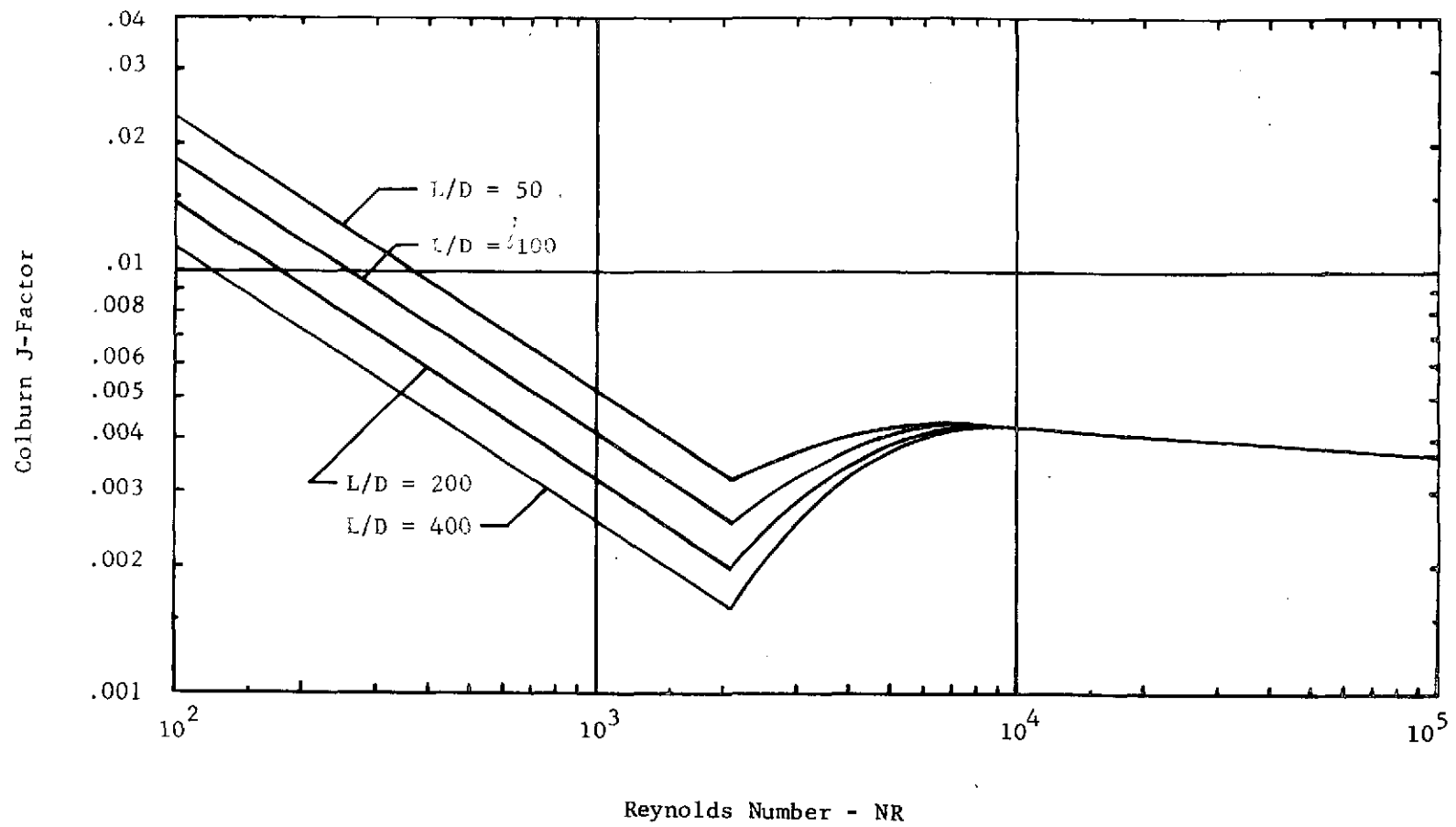
FIGURE 15 - COLBURN J-FACTOR

ITEM	QUANTITY	Thermal Control Unit

1   2   PUMP - Flow 1.59 to 2.04 KG/min. (3.5 to 4.5 lbs/min)

2   1   REGENERATOR - Redundant cold side loops approximately 1.379×10^5 Newtons/meter^2 (20 psi) pressure drop at 1.81 KG/min (4 lbm/min) flow/loop. Hot side loop pressure drop TBD.

3   2   ACCUMULATOR - Volume TBD. Pressure $\approx 3.447 \times 10^5$ Newton/meter^2 (50 Psi).

4   4   DISCONNECTS - Primary and secondary loops 2 each. Line size TBD. Pressure Drop $\leq 6.89 \times 10^3$ Newtons/meter^2 (1 psi).

5   2   THERMAL CONTROL VALVE - Maintain regenerator inlet temperature at 333°K (140°F) by mixing radiator return fluid with pump outlet fluid. Flow range 0 to 2.04 KG/minute 0 to 4.5 lbs/min. Pressure drop TBD.

6   2   FILL DISCONNECT - System fill and drain, zero leakage after dis- connect. Size - TBD.

7   10   PRESSURE TRANSDUCERS - Range 0 - 6.895×10^5 Newtons/meter^2 (0 - 100 Psia) Accuracy 1% of full scale.

8   6   TEMPERATURE SENSORS - Range 172 to 394°K (-150 to +250°F). Accuracy 1% of full scale.

9   2   FLOW MEASUREMENT - Range 0 - 2.04 kilograms/minute (0 - 4.5 pounds/minute) Accuracy 1% of full scale.

Radiators

10   4   Each panel with 4 integral rails, minimum fin efficiency = .9. P - tubes welded to rails per Figure 6 single tube L/D = 200. Size:

	Length	Width
	91.44 cm	55.88 cm
	(36 inches)	(22 inches)
Area	.511 meters^2	(5.5 feet^2)

Panel thickness 0.0762 cm (0.030 inches).
Tube ID 0.4572 cm (0.18 inches).

SIZE	CODE IDENT NO.	
A	**04236**	
CHG		
SCALE	PAGE 17	SHEET

Interconnecting Lines

11   10   ALUMINUM TUBING - Length as required: OD - .9525 CM (375 inches)
                                                                               ID - TBD

12   16   DISCONNECTS - Line size .9525 CM (.375 inches)
                                            Pressure Drop $\leq$ 6.89 Newtons/meter^2
                                            (1 Psi)

SIZE	CODE IDENT NO.		
A	04236		
CNG			
SCALE		PAGE 18	SHEET

REVISIONS					
LTR	SH	DESCRIPTION		DATE	APPROVED

APPENDIX II

																			REV
																			SH
																		REV	REV STATUS OF SHEETS
																		SH	

DRAWN BY T. Ward	DEPT 044	DATE
CHECKING		
GROUP ENGR		
STRESS		
WEIGHT		
CUSTOMER RPRSNTV		
PROGRAM RPRSNTV		

MARTIN MARIETTA CORPORATION
POST OFFICE BOX 179, DENVER, COLORADO

THERMAL CONTROL LOUVER SYSTEM

SIZE **A**	CODE IDENT NO. 04236	
SCALE	PAGE 1	SHEET

TABLE OF CONTENTS

SIZE	CODE IDENT NO.	
A	**04236**	
SCALE	PAGE 2	SHEET

CHG

SYSTEM DESCRIPTION

The louver system provides thermal control to the fuel cell primary battery which will be used when the fuel cell is deactivated at T + 97.634 hours. The battery will also function as an emergency backup power supply unit in the event of fuel cell failure. The battery is designed to provide 450 watts of electrical power for a time period of 0.5 hours. Based on the power output and a 90% efficiency of the battery, 45 watts of thermal energy will be generated within the battery.

The louver system will dissipate the 45 watts of thermal energy and maintain the battery operational temperature below the allowable limit temperature of $305.3^\circ K$ $(90^\circ F)$ for the required 0.5 hours of operation. The louver system will also add in controlling the non-operational temperature above $288.7^\circ K$ $(60^\circ F)$.

The louver thermal control system consists of a component mounting baseplate attached to a set of moveable aluminum louver blades by low conductance screws. The blades are automatically actuated by temperature sensitive bimetallic spiral wound springs radiatively coupled to the baseplate. The baseplate and louver blades are housed in a conductively isolated frame which is mounted on the interior side of the tug skin using minimum conductance fasteners. The louver assembly and mounting configuration are shown in Figure 1.

CODE IDENT NO.	SIZE	
38597	**A**	

| CHG. | | | |
| SCALE | PAGE 3 | | SHEET |

MULTILAYER
INSULATION
BLANKET

ACTUATOR HOUSING COVER
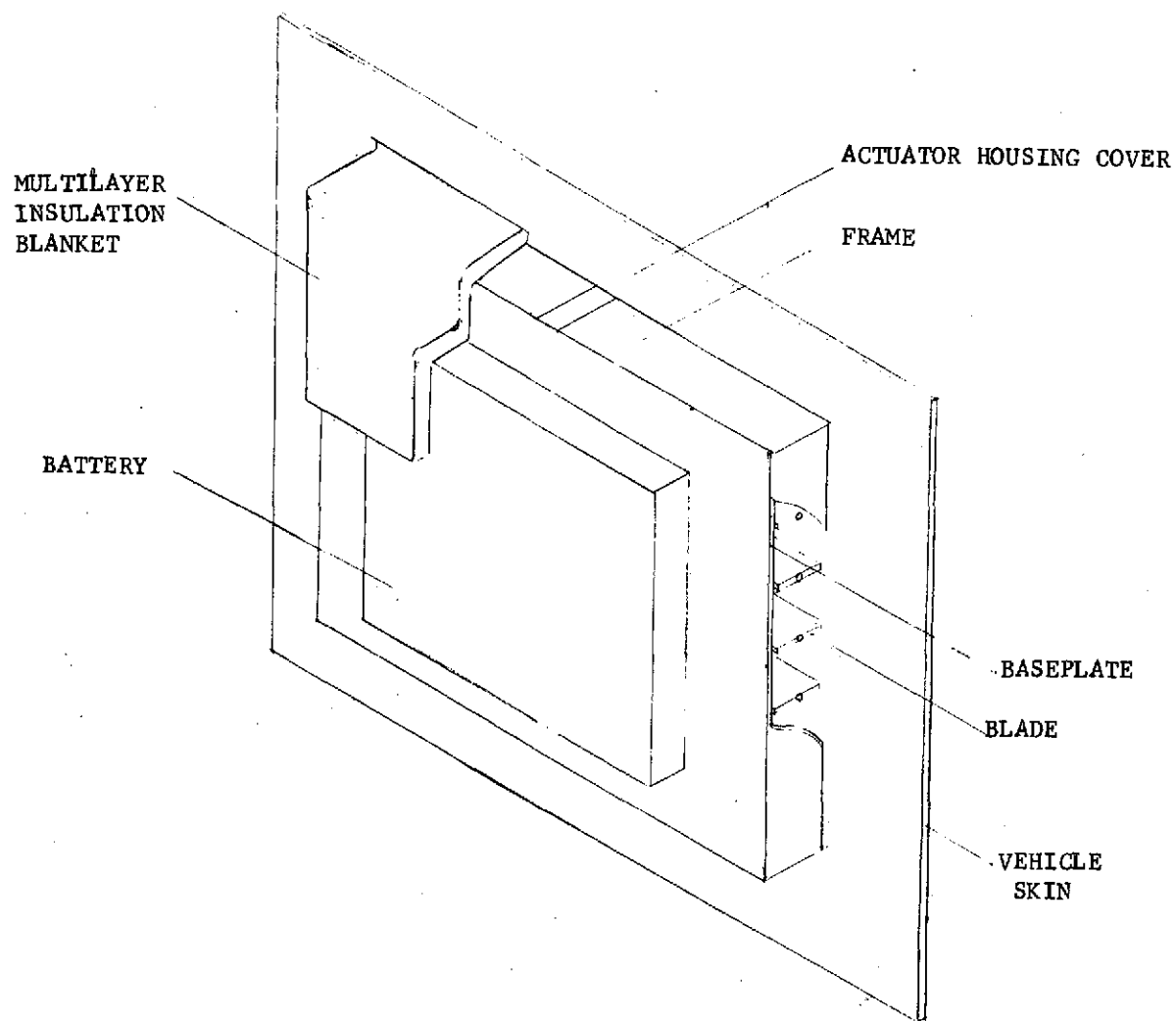
FRAME

BATTERY

BASEPLATE

BLADE

VEHICLE
SKIN

FIGURE 1 - LOUVER SYSTEM/MOUNTING CONFIGURATION

A thermal model of the louver system shown in Figure 1 was constructed for the MITAS thermal analyzer (Reference 1). The model was necessary because steady state, worst condition analysis tended to over design the system. The model accounts for the thermal characteristics of both the louver system and the emergency battery. A GFP absorbed heating environment was simulated in the model and is shown in Figure 2. This environment was calculated assuming an α/ϵ of the external skin equal to .2/.9. The thermal capacitance of the battery, baseplate and external skin along with a time line to adequately account for the battery power generation is included. Conduction through the multi-layer insulation and through the louver system standoffs is included as well as the contact resistance between the battery and the baseplate.

The louver system parameters used in the model correspond to a commercially available bimetallic actuated louver system (Reference 2). The blade angle is determined by the baseplate temperature (289°K (60°F) blades closed, 303°K (85°F) blades fully open). The effective emittance is then determined by the blade angle as shown in Table 1. The louvered area consists of 0.165 sq. m (1.78 sq. ft.) which was also used for the area of the baseplate and the external skin. The baseplate was assumed to be 0.32 CM (1/8 in.) thick aluminum and the external skin was assumed to be 0.25 CM (0.10 in.) thick aluminum. The emergency battery simulated was taken from the tug data bank (Reference 3) and had a thermal mass of 1.79 watt-hrs/$^\circ$K (3.39 btu/$^\circ$F). Also a 10 watt, thermostatically controlled, heater was incorporated in the battery to maintain temperature limits in the non-operating condition.

	SIZE	CODE IDENT NO.		
CHG	A	04236		
	SCALE	PAGE 5		SHEET

E-49011-001
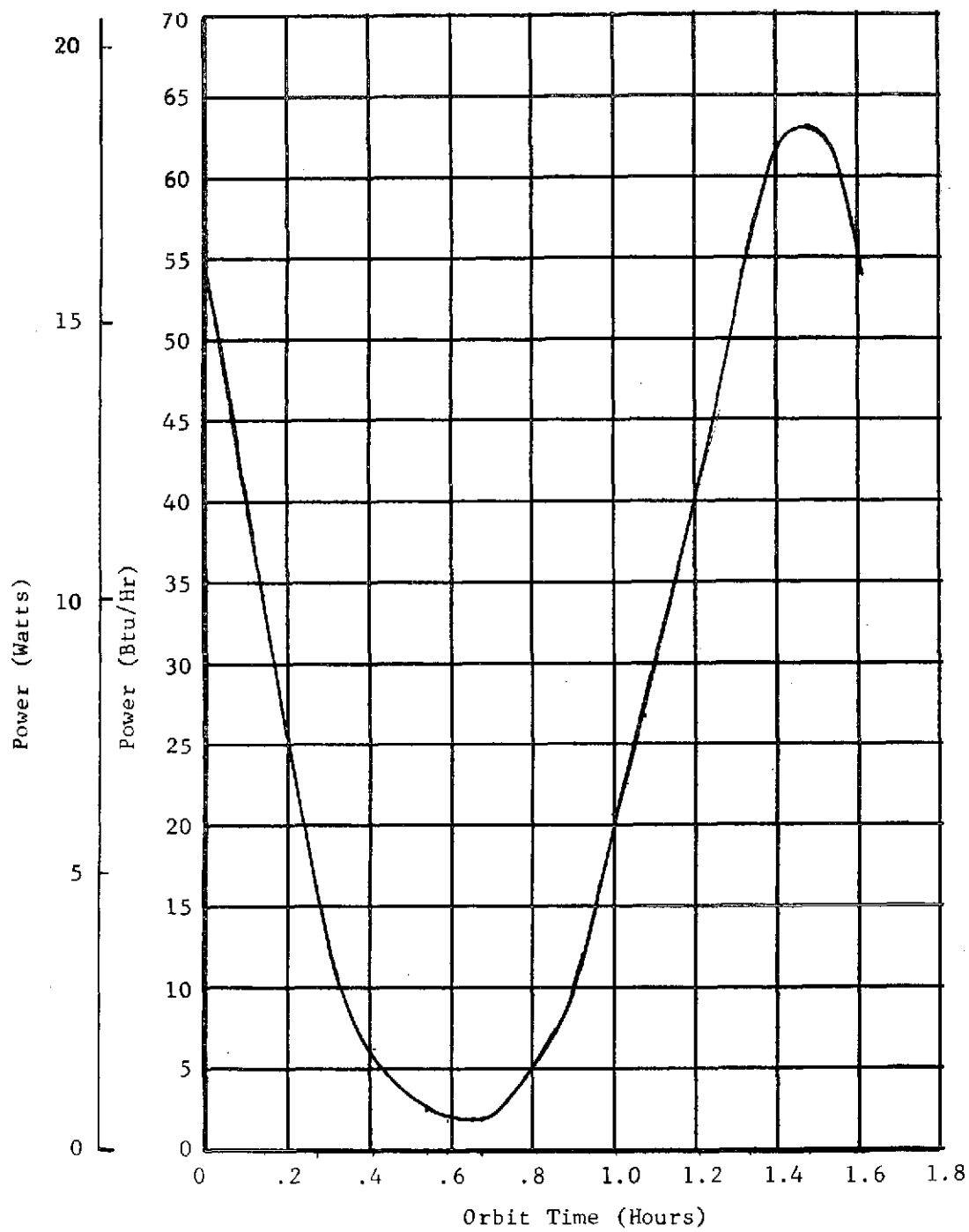
Figure 2 External Skin Absorbed Environmental Flux

SIZE	CODE IDENT NO.			
A	**04236**			
CMG				
SCALE		PAGE 6		SHEET

System Requirements and Performance Specifications

1. Maintain primary battery temperature below 305.4°K (90°F) for 0.5 hours of operation.

2. Provide means of dissipating 45 watts of thermal energy while battery is operating.

3. Control non-operational battery temperatures above 288.7°K (60°F).

4. Provide control of blade position as a function of baseplate temperature, 288.7°K (60°F) blades closed, 303.0°K (85°F) blade open.

CODE IDENT NO.	SIZE		
CHG.	**38597**	**A**	
SCALE	PAGE 7		SHEET

Predicted System Performance

Two cases were simulated using the previously described math model and the absorbed environment shown in Figure 2. In both cases the initial temperatures were started at $294.4^{\circ}K$ ($70^{\circ}F$) and the problem was simulated for 5 orbits approximately 8 hours corresponding to the heating rate in Figure 2. In the middle of the third orbit (approximately 4 hours) the battery was activated for 0.5 hours. The two cases differ in that the second case uses only 10 percent of the absorbed heating rate shown in Figure 2. This case demonstrates the adequacy of the 10 watt heater to maintain temperature control. The results of the first case are shown in Figures 3 through 7. The results of the second case are shown in Figure 8 through 12.

Figure 3, Case 1 Emergency Battery Temperature History
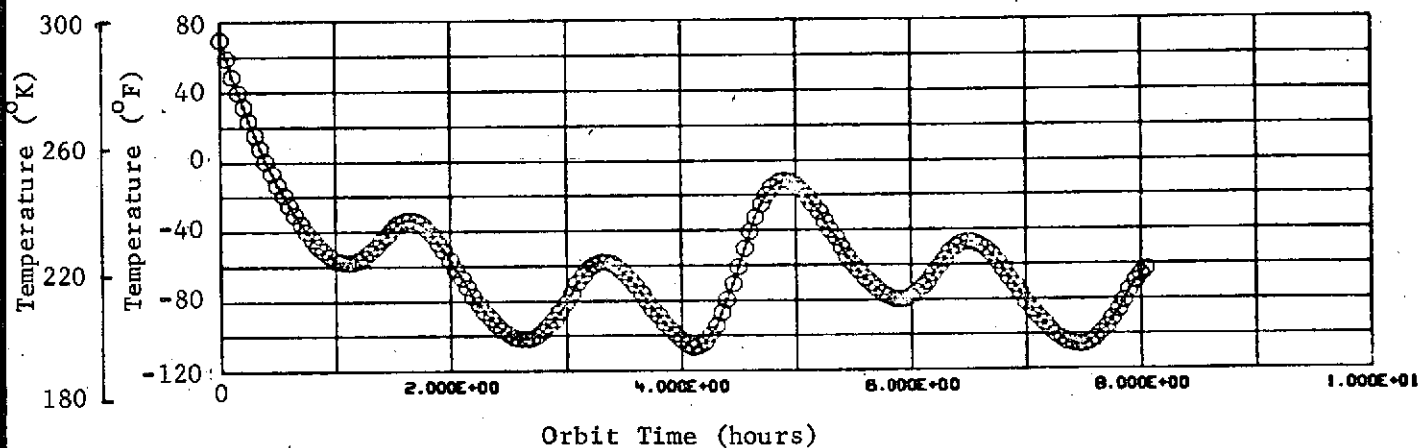
Figure 4, Case 1 Louver Cover Temperature History
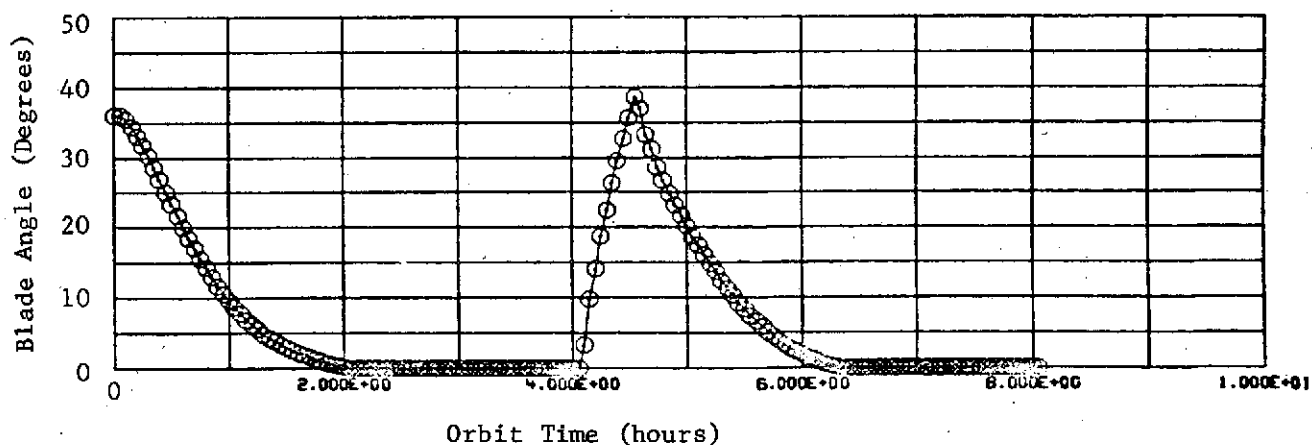
Figure 5, Case 1 Louver Blade Angle History

	SIZE	CODE IDENT NO.		
CHG	A	04236		
	SCALE	PAGE 9	SHEET	

Orbit Time (hours)
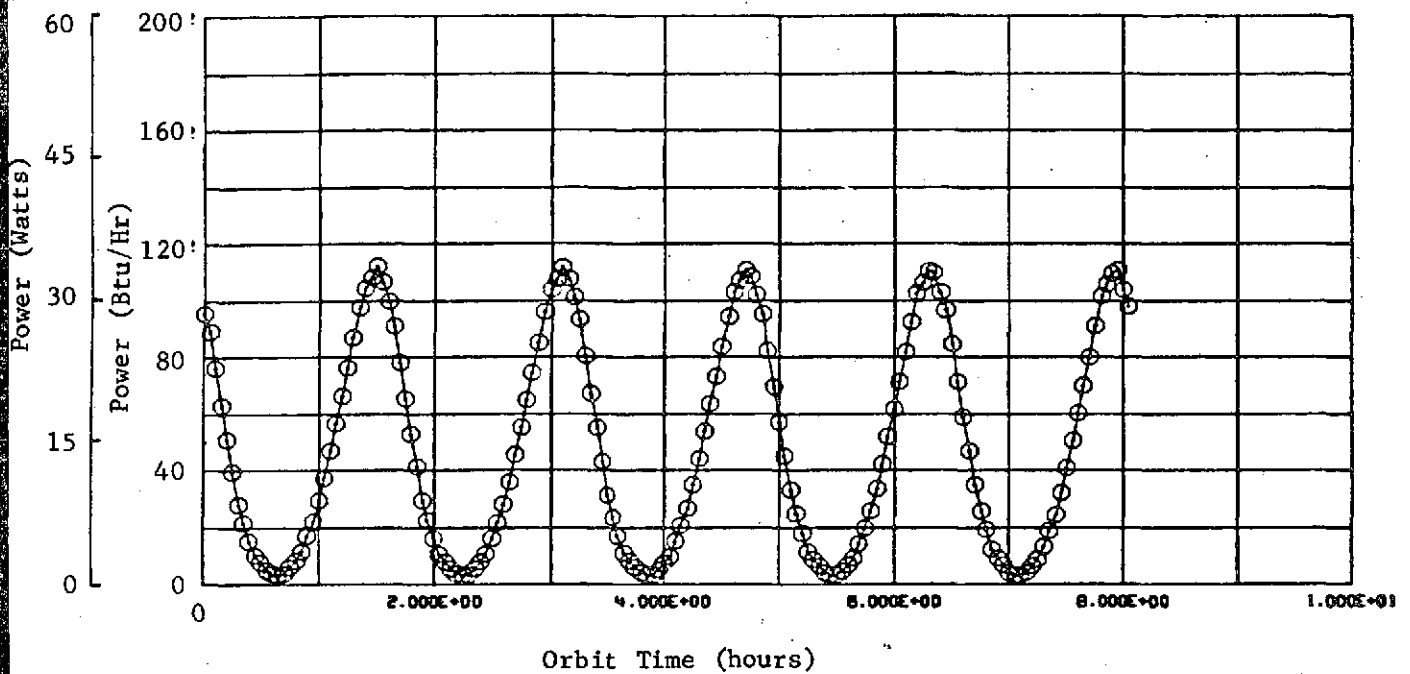
Figure 6, Case 1 Louver Cover Absorbed Heating

Orbit Time (hours)
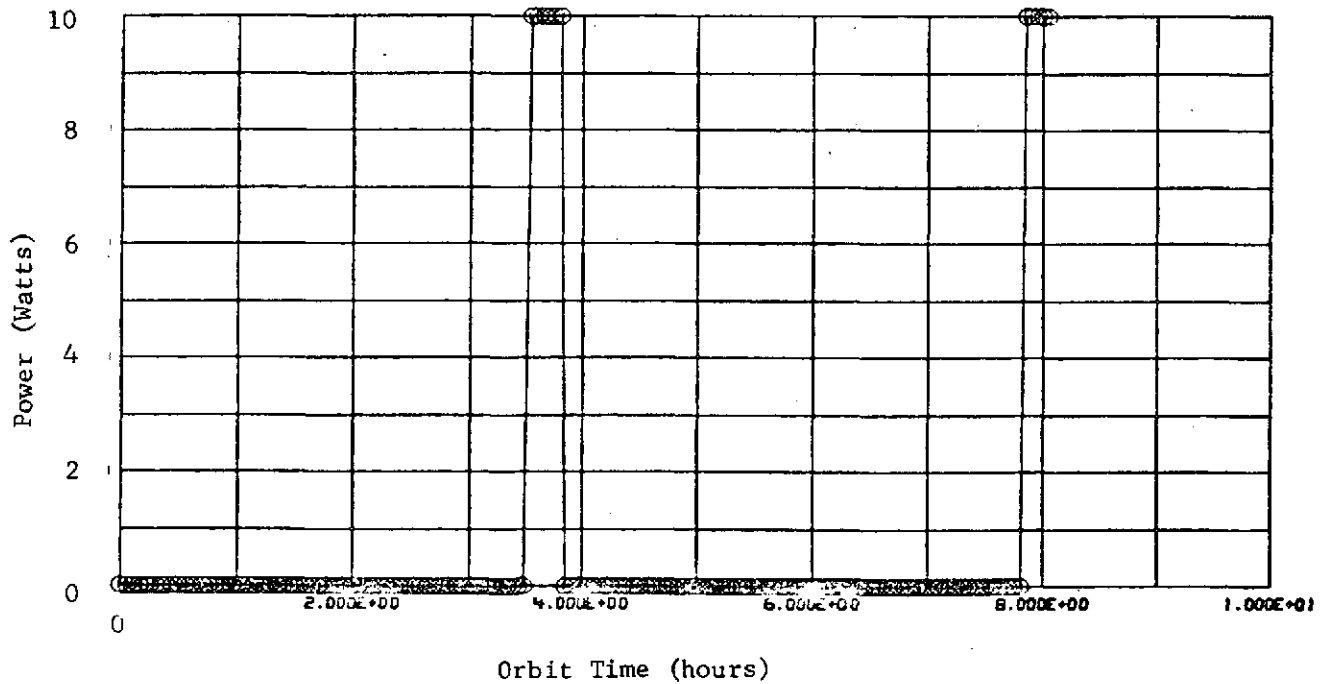
Figure 7, Case 1 Instantaneous Heater Power

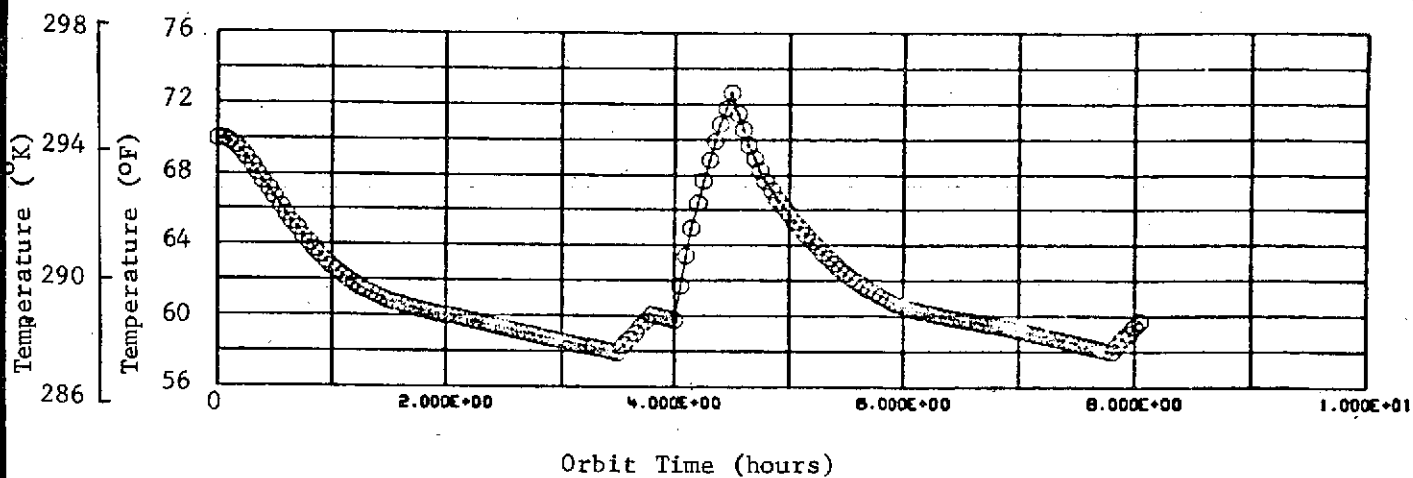|	SIZE	CODE IDENT NO.		
	A	04236		
CHG				
	SCALE		PAGE 10	SHEET
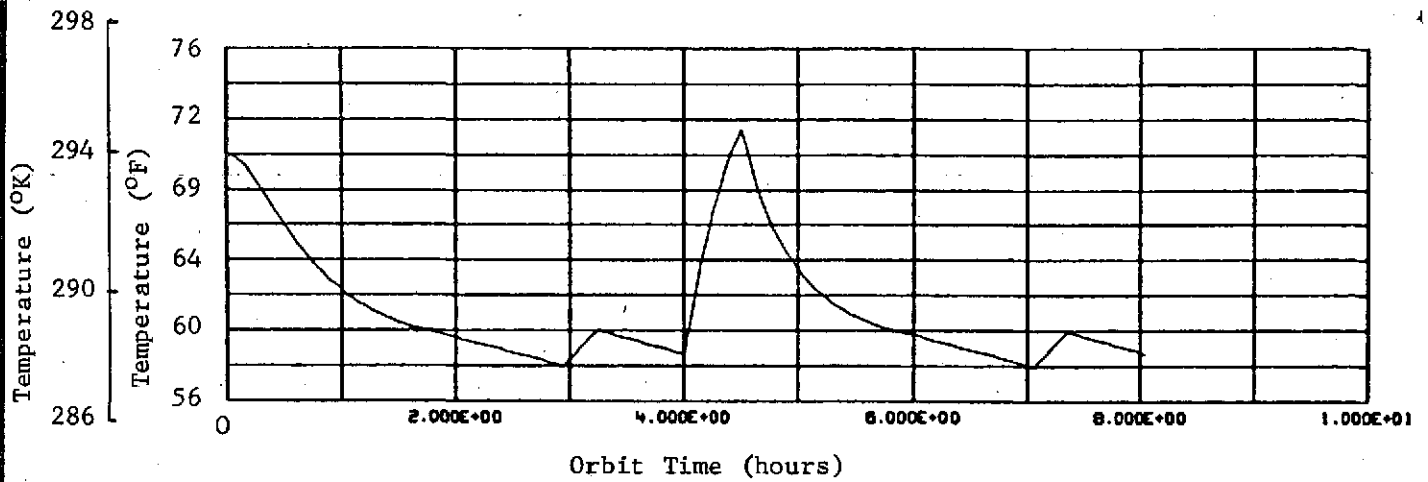
Figure 8, Case 2 Emergency Battery Temperature History
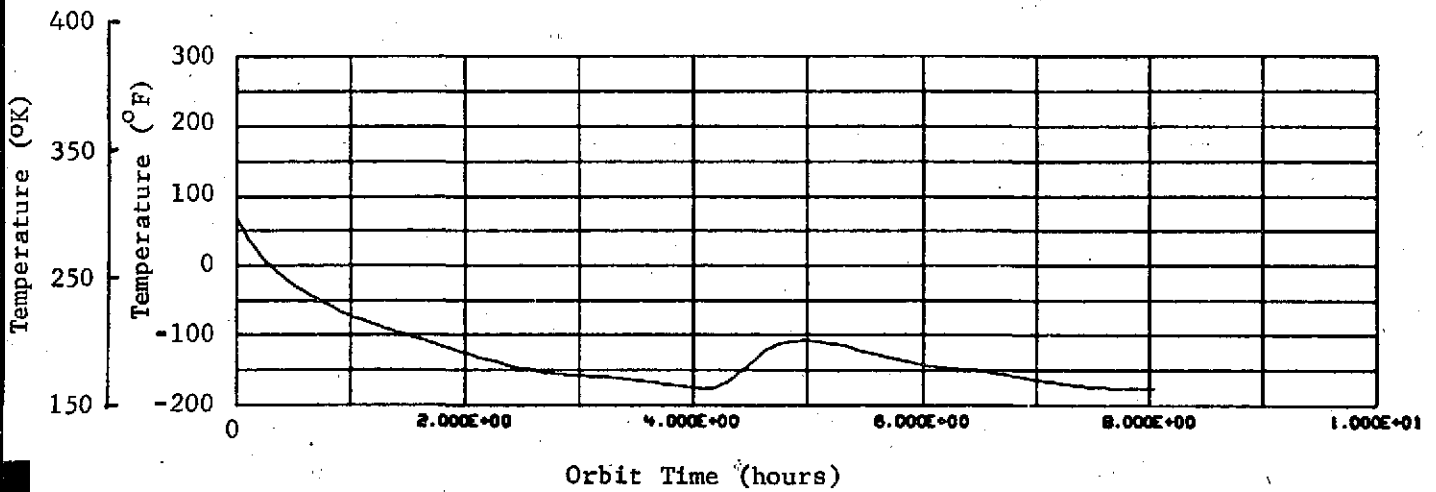
Figure 9, Case 2 Louver Cover Temperature History
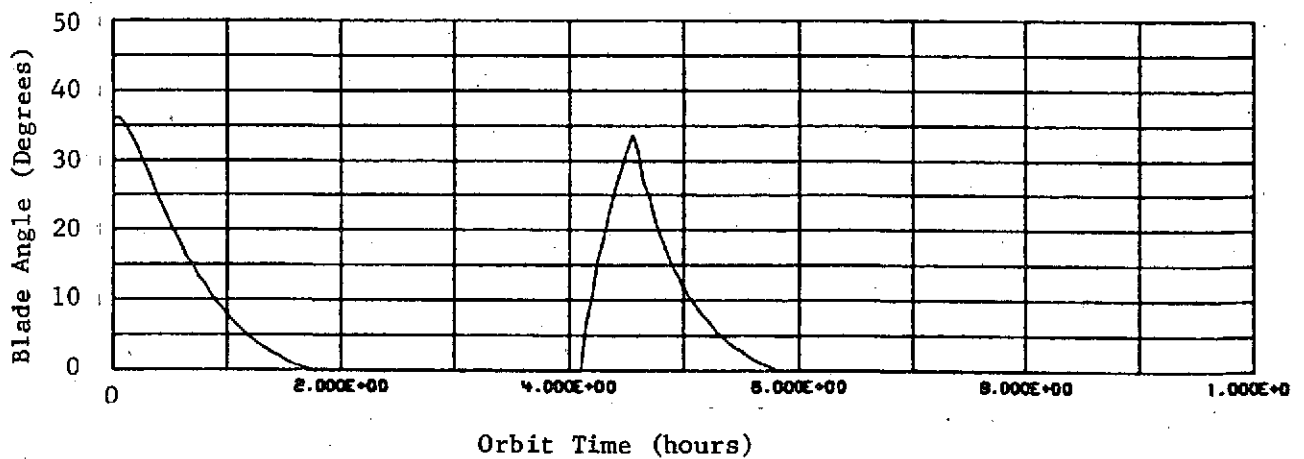
Figure 10, Case 2 Louver Blade Angle History

	SIZE	CODE IDENT NO.			
	A	**04236**			
CHG					
	SCALE		PAGE 11		SHEET

E-490(1-60)

Orbit Time (hours)
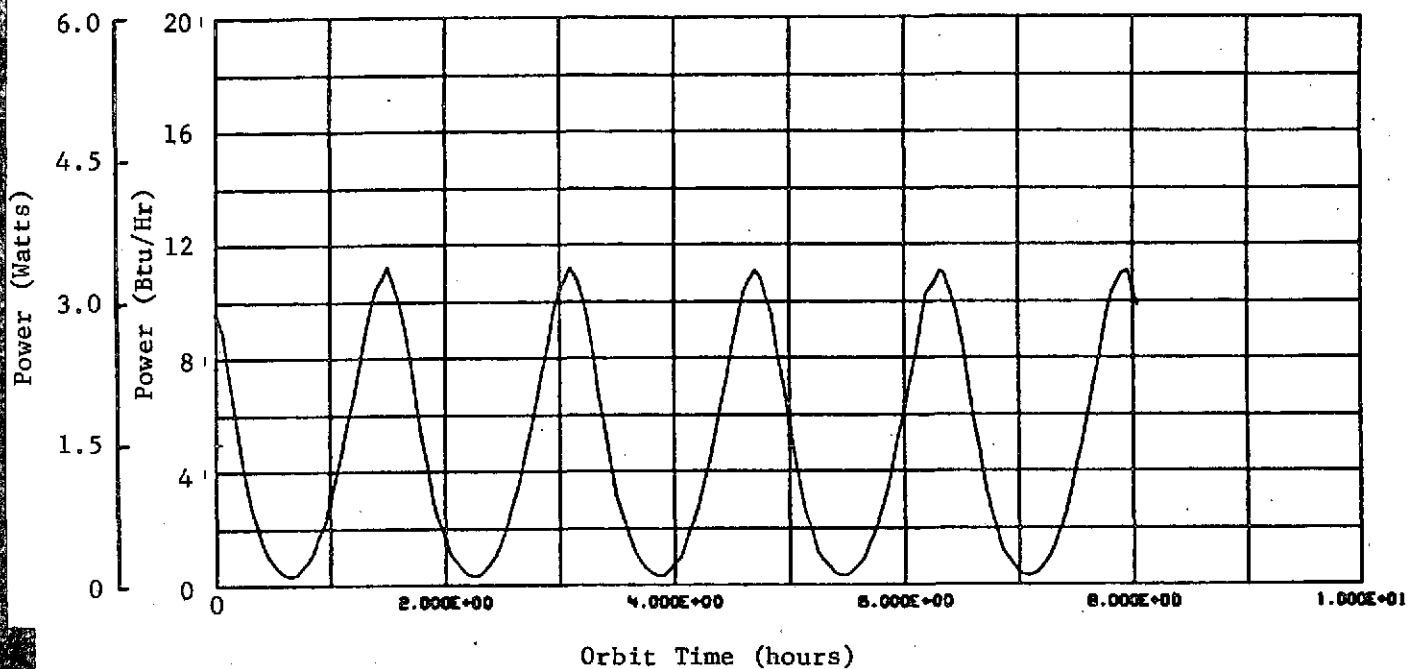
Figure 11, Case 2 Louver Cover Absorbed Heating

Orbit Time (hours)
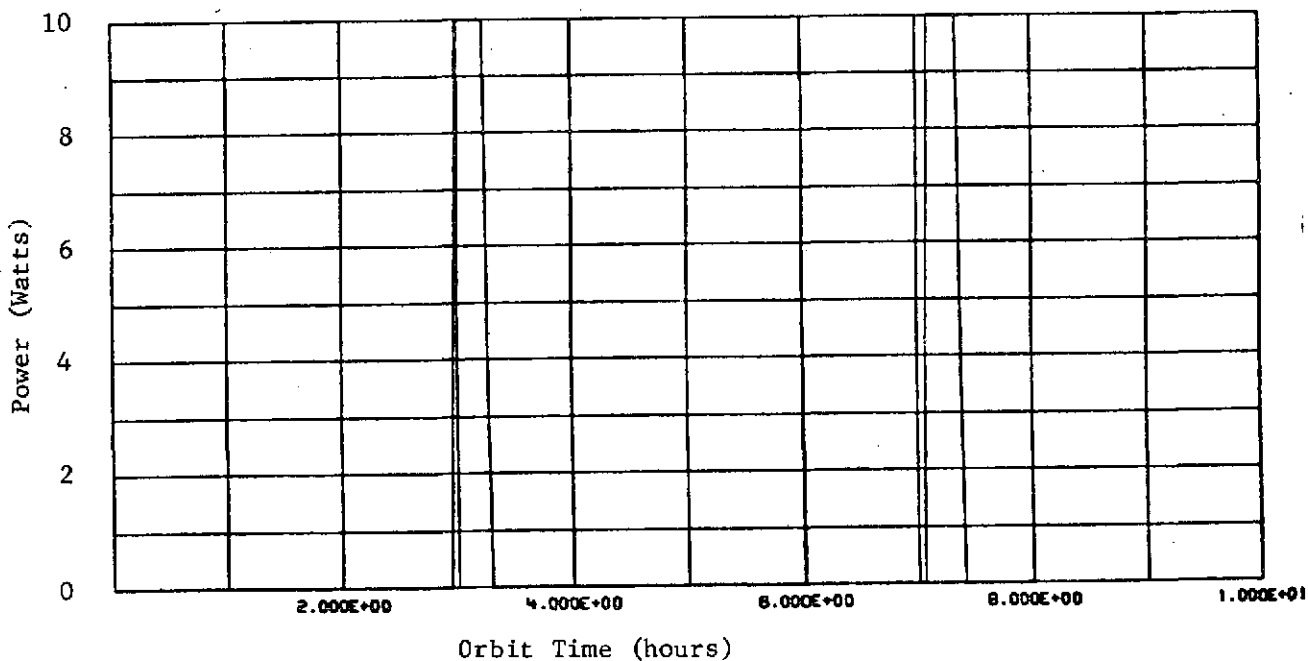
Figure 12, Case 2 Instantaneous Heater Power

SIZE	CODE IDENT NO.		
A	04236		
CHG			
SCALE		PAGE 12	SHEET

. TABLE 1 - EFFECTIVE EMITTANCE $\bar{\epsilon}$ FOR COVERED LOUVER SYSTEM

BLADE ANGLE DEG	EFFECTIVE EMITTANCE $\bar{\epsilon}$
90 (Full Open)	0.818
75	0.790
60	0.742
45	0.660
30	0.543
15	0.379
0 (Full Closed)	0.035

(for a covered louver system assuming a diffuse wall

and a diffuse baseplate ϵ = 0.9)

CODE IDENT NO.	SIZE	
38597	**A**	
SCALE	PAGE 13	SHEET

CHG.

E-49D(12-61)

Hardware List & Description

Item	Quantity	
1	1	Louver frame and blade assembly - minimum covered area of 0.17 M^2 (1.78 ft^2). Complete with temperature sensitive bimetallic actuators. Blades are specular and have an $\epsilon \le 0.5$.
2	1	Component mounting baseplate - 0.318 cm (0.125 in.) thick aluminum plate with a minimum surface area of 0.49 M^2 (5.30 ft^2).
3	1	Multilayer insulation blanket - 20 alternate layers of perforated aluminized mylar and tissue glass.
4	1	Interior thermal control coatings - radiating surface of component baseplate and interior of louver cover/skin, painted with a high emittance ($\epsilon \ge 0.9$) diffuse coating.
5	1	Exterior thermal control coatings - a minimum area of 0.17 M^2 (1.78 ft^2) of the external cover/skin should be covered with second surface mirrors.
6	TBD	Mounting panel thermal isolators-low conductance screws, washers, standoffs, etc. for the purpose of mounting the louver assembly to the cover/skin.

CODE IDENT NO.	SIZE	
CHG.	**38597**	**A**
SCALE	PAGE 14	SHEET

REFERENCES

1. Conner, R. J. et al, "Martin Interactive Thermal Analysis System (MITAS)" MDS-SPLPD-71-FD238, Martin Marietta Corporation, June 1971.

2. "Space Vehicle Thermal Controllers" Technical Description, Northrop Corporation Electronics Division Report, NORT 73-306, October 1973.

3. T. L. Ward, "Space Tug Thermal Control Equipment Thermal Requirements, Characteristics and Constraints Catalogue". MCR-74-145, Martin Marietta Corporation, April 1974.

SIZE	CODE IDENT NO.	
A	**04236**	
CHG		
SCALE	PAGE 15	SHEET

		REVISIONS		
LTR	SH	DESCRIPTION	DATE	APPROVED

DRAWING NO.

APPENDIX III

																			REV
																			SH
																	REV	REV STATUS
																	SH	OF SHEETS

DRAWN BY	DEPT	DATE
T.J. Ward 0/44		
CHECKING		
GROUP ENGR		
STRESS		
WEIGHT		
CUSTOMER RPRSNTV		
PROGRAM RPRSNTV		

MARTIN MARIETTA CORPORATION

POST OFFICE BOX 179, DENVER, COLORADO

SPACE TUG FORWARD COMPARTMENT THERMAL DESIGN

SIZE	CODE IDENT NO.		
A	04236		
SCALE		PAGE	SHEET

TABLE OF CONTENTS

Page

Figures

	SIZE	CODE IDENT NO.		
	A	**04236**		
CHG				
	SCALE		PAGE 2	SHEET

III-2

SYSTEM DESCRIPTION

The tug forward compartment is designed thermally to operate over a range of worst case environments which include a fixed attitude with respect to the sun in near earth orbit and a zero heating attitude at geosynchrous attitude. The design incorporates several thermal devices whose purposes is to provide temperature control of the avionics components.

The basic concept is to mount the components on thermal conditioning panels which are mounted to the structure with louver assemblies attached to the skin side of panels as shown in Figure 1. Heat pipes are mounted on the interior surface of the honeycomb skin to provide a relatively uniform temperature around the forward skirt.

The thermal conditioning panels are honeycomb panels with integral heat pipes. The panels are designed to permit two-dimensional heat flow, thus approaching an isothermal plate concept. Mounting of high and low duty cycle components on each panel permits distribution of heat between components thus reducing if not eliminating the need of component heaters. The skin side louvers provide the means to reduce radiation losses from the panel as the panel temperature begins to drop in cold environments by closing the blades. This permits the panel temperature to be passively controlled to a relatively narrow range thus simplifying the component thermal design problems as well as heater power requirements.

The heat pipes on the internal surface of the skin act to isothermalize the skin dependent upon the external and internal heating on the skin. Heat is transferred from the hot side of the vehicle to the cold side thus providing

SIZE	CODE IDENT NO.	
CHG	**A**	**04236**
SCALE	PAGE 3	SHEET

Heat Pipes
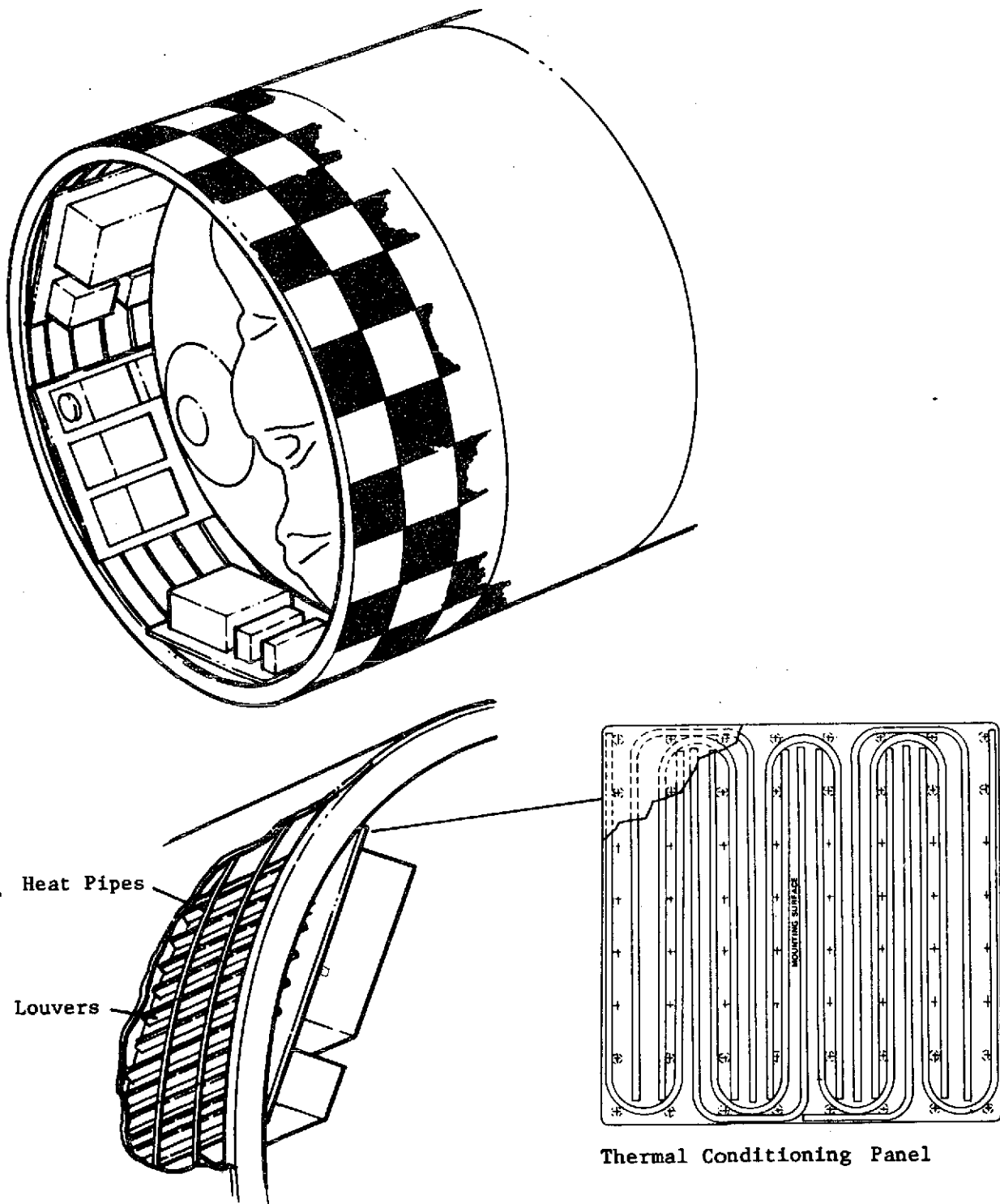
Louvers

Thermal Conditioning Panel

Figure 1   Forward Compartment Thermal Control Concept

a more uniform environment for the panels and the components.

System Requirements and Performance Specifications

The primary purpose of this system is to maintain the tug avionics components within acceptable temperature limits during the tug mission. To achieve this objective each of the major elements shall meet the following requirements.

Thermal Conditioning Panel

Non-Operating Temperature Range	255 to 367°K
	0 to 200°F
Operating Temperature Range	272 to 311°K
	30°F to 100°F
Maximum Component Heat Load	300 Watts
Maximum Gradient Across Panel Surface	2.77°K
	5°F
Maximum Thermal Load Density	.31 Watts/Cm^2
	2 Watts/in^2
Size As Required	
Bolt Pattern	.1 x .1 Meters
	4 x 4 inches
Panel Mass	$\leq$ 13.8 KG/m^2
Maximum Component Mass	45.4 KG
	100 Pounds

SIZE	**CODE IDENT NO.**	
A	**04236**	
CNB		
SCALE	**PAGE** 5	**SHEET**

*49D(1-88)

LOUVERS

Size   40.64 x 20.32 x 4.9 CM
(16 x 8 x 1.93 inches)

Weight   .27 KG   .6 Pounds

Blade Operating Temp. Range   288.7 to 302.6°K (closed to open)
(60 to 85°F)

End Point Adjustment $\pm$5.6°K ($\pm$10°F)

Blade Emissivity $\leq$ 0.1

Temperature Survivability   199.8 to 394.3°K
(-100 to 250°F)

Effective Emissivity of
Baseplate   Open $\geq$ .8

Closed $\leq$ .1

SKIN HEAT PIPES

Number/Spacing   6 Pipes One Every 5 Inches in Longitudinal Direction

Length   14.77M, (45.03 ft.) Circumferential

Diameter   1.27 CM, (0.5 in.) (Nominal)

Non-operating Temperature Range   144 to 366°K
-200 to 200°F

Operating Temperature Range   172 to 311°K
-150 to 100°F

Heat Flux Capability   60 Watts/M Per Pipe

at 300°K (80°F)   (19.7 Watts/Ft) Per Pipe

Evaporator to Condenser $<$5.6°K

Maximum $\triangle$T at 300°K (80°F)   (10°F)

Heat Transport Capability   TBD

SIZE	CODE IDENT NO.	
A	**04236**	
CHG		
SCALE	PAGE 6	SHEET

PREDICTED PERFORMANCE

Mounting panel heat fluxes are given in Figures 2 and 3 for hot and cold
conditions respectively. These curves were generated from the following
equation:

$$Q/A = \sigma_{eff} (T_p^4 - T_s^4) + \sigma \epsilon_p (T_p^4 - T_e^4)$$

where

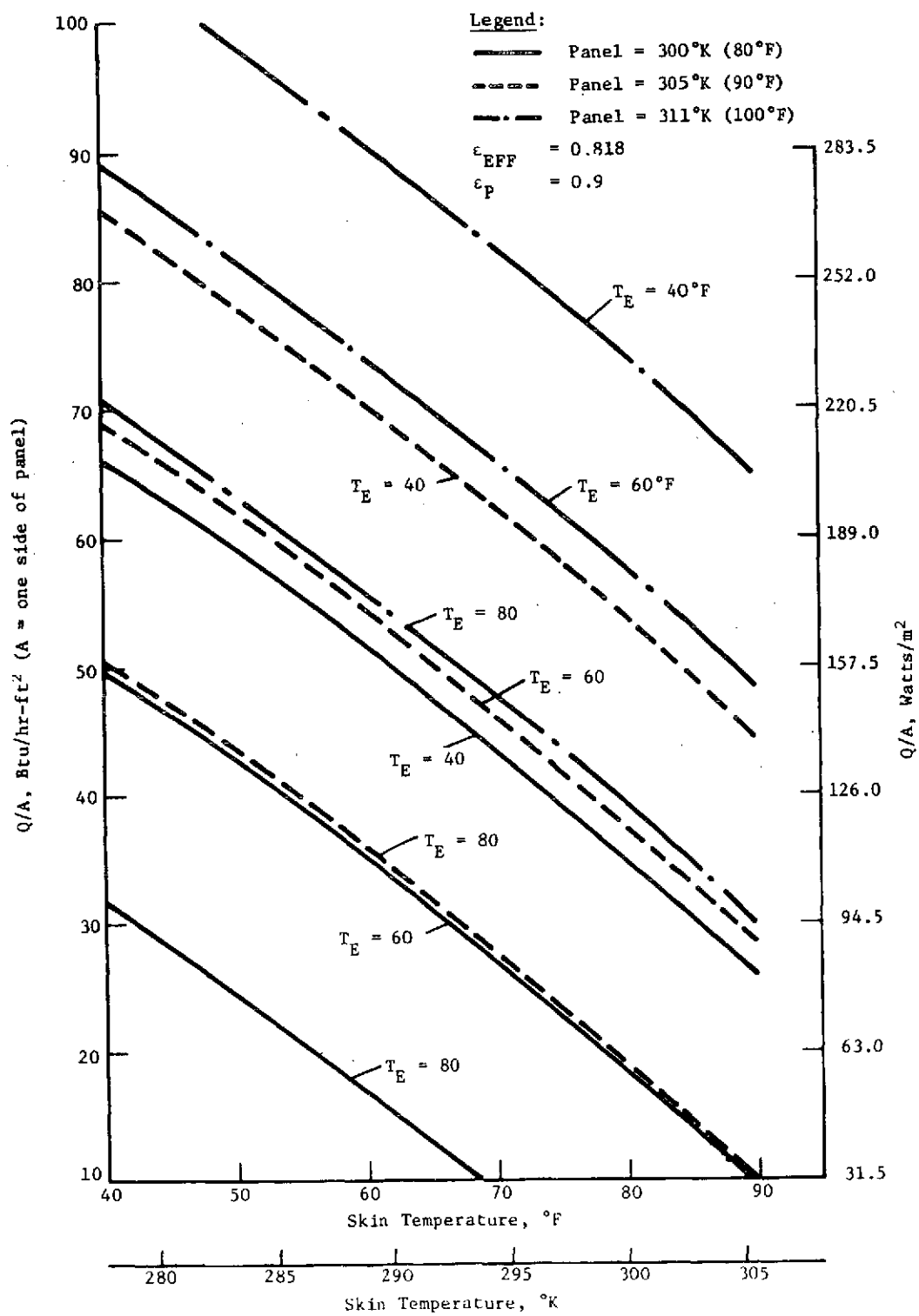|		
Q/A	=	Panel Net Heat Transfer
σ	=	Stefan-Boltzmann Constant
ϵ_{eff}	=	Louver System Effective Emissivity
T_p	=	Mounting Panel Temperature
T_s	=	Skin Temperature
T_e	=	Interior Environmental Temperature
ϵ_p	=	Emissivity of Mounting Panel

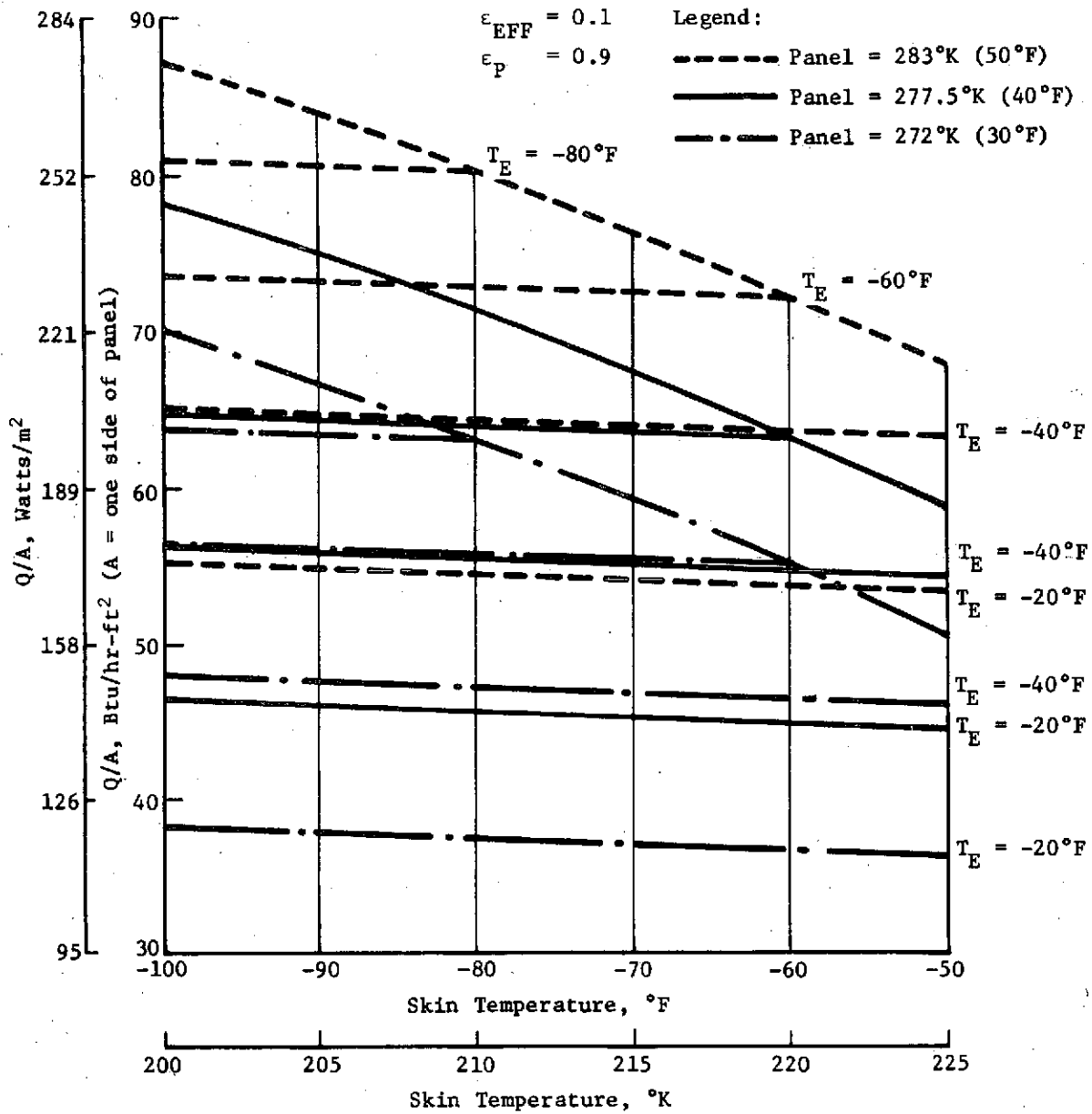*Figure 2 Hot-Case Mounting Panel Heat Fluxes, Louvers Open*

Figure 3 Cold-Case Mounting Panel Heat Fluxes, Louvers Closed

HARDWARE LIST

6 - Circumferential Heat Pipes and Mounting Brackets

5 to 6 Thermal Conditioning Panels - Number and Size Dependent Upon Component
Groupings

Thermal Control Louver Assemblies One for Each Thermal Conditioning Panel

SIZE	CODE IDENT NO.		
A	04236		
CHG			
SCALE		PAGE 10	SHEET